

The Role of UGT Enzymes as Novel Modulators of Lipid Biosynthesis in Breast Cancer

By

Jai Meyers

Thesis
Submitted to Flinders University
for the degree of

Doctor of Philosophy

College of Medicine and Public Health
February 2025

TABLE OF CONTENTS

SUMMARY.....	ix
DECLARATION	xi
ACKNOWLEDGEMENTS.....	xii
CONFERENCE PROCEEDINGS	xiii
AWARDS IN SUPPORT OF THIS THESIS.....	xiv
LIST OF ABBREVIATIONS	xv
List of Tables	xvi
List of Figures	xvii
1. CHAPTER 1 - LITERATURE REVIEW.....	19
1.1 Cancer: A Brief Overview	20
1.2 Steroid-Dependent Cancers	20
1.2.1 The Prostate and Prostate cancer	20
1.2.2 The Breast and Breast Cancer.....	21
1.3 Drug Metabolising Enzymes and Cancer.....	23
1.4 Uridine 5'-diphosphate-glycosyltransferases (UGTs)	24
1.4.1 UGT Structure and Function	27
1.4.2 UGT Expression	29
1.5 UGT2B11 and UGT2B28	29
1.5.1 UGT2B11 and UGT2B28 Substrate Preferences.....	30
1.5.2 UGT2B11 and UGT2B28 Variants.....	32
1.5.3 SNPs and Somatic Mutations in UGT2B11 and UGT2B28	35
1.5.4 Non-canonical Functions	36
1.5.5 Regulation of UGT2B11 and UGT2B28 Expression.....	36
1.5.6 UGT2B11 and UGT2B28 in Cancer.....	38
1.5.7 Summary of UGT2B11 and UGT2B28 roles in cancer.....	41

1.6	Lipid Metabolism.....	41
1.6.1	Regulation of Lipid Metabolism by SREBP	43
1.6.2	Dysregulation of Lipid Metabolism in Cancer.....	45
1.7	The SREBP-AR Axis	46
1.8	The role of UGT2B11 and UGT2B28 in Lipid Metabolism Dysregulation	47
1.9	Aims and Hypotheses.....	48
2.	CHAPTER 2 - MATERIALS AND METHODS.....	50
2.1	Materials	51
2.1.1	Chemicals and Reagents and Buffers.....	51
2.1.2	General Buffers	51
2.1.3	Bacterial and Mammalian Cell Lines.....	51
2.1.4	Mammalian reporter and expression vectors	51
2.1.5	Oligonucleotides	53
2.2	Methods	53
2.2.1	Mammalian Cell culture.....	53
2.2.1.1	Cell Culture Maintenance	53
2.2.1.2	Cryopreservation	54
2.2.1.3	Transfection.....	54
2.2.2	Gene Expression Analysis	55
2.2.2.1	RNA Extraction.....	55
2.2.2.2	Generation of cDNA.....	55
2.2.2.3	Quantitative RT-PCR	55
2.2.3	Crystal Violet assays.....	56
2.2.4	Protein Co-expression and Co-immunoprecipitation (Co-IP) analysis	57
2.2.4.1	Lysate Preparation.....	57
2.2.4.2	Co-immunoprecipitation	57
2.2.5	Western Blotting.....	58

2.2.5.1	Lysate Preparation.....	58
2.2.5.2	Polyacrylamide Gel Electrophoresis (PAGE), Transfer and Imaging.....	58
2.2.6	Luciferase Assays	59
2.2.7	Molecular Cloning and Associated Methods.....	60
2.2.7.1	Polymerase Chain Reaction (PCR)	60
2.2.7.2	Restriction Digests.....	60
2.2.7.3	Ligation and Transformation	60
2.2.7.4	Bacterial Culture and Plasmid Preparation	61
2.2.7.5	Agarose Gel Electrophoresis.....	61
2.2.7.6	Site-Directed Mutagenesis	61
2.2.7.7	Competent Cell Preparation.....	62
2.2.7.8	Sequencing	63
2.2.7.9	Nucleic Acid Quantification	63
2.3	Statistics	64
3.	CHAPTER 3 - ASSOCIATION OF UGT2B11 AND UGT2B28 EXPRESSION LEVELS WITH CLINICAL AND BIOCHEMICAL PARAMETERS IN BREAST CANCER PATIENT COHORTS	65
3.1	INTRODUCTION	66
3.1.1	The Cancer Genome Atlas (TCGA)	67
3.1.2	The Molecular Taxonomy of Breast Cancer International Consortium (METABRIC) project	67
3.1.3	UGTs correlate with Lipid Metabolism Gene Signatures.....	68
3.1.4	Aims	70
3.2	METHODS.....	71
3.2.1	Gene Expression Analysis	71
3.2.2	Survival Analysis.....	71
3.2.3	Pathway Analysis	71
3.3	RESULTS.....	72

3.3.1	UGT2B11 and UGT2B28 expression is associated with HER2 enrichment and an ER-negative status	72
3.3.2	The relationship between UGT2B11 and UGT2B28 expression and survival outcomes in different breast cancer molecular subtypes	83
3.3.3	High UGT2B11 and UGT2B28 expression is associated with worse survival outcomes for ER- tumours	90
3.3.4	High UGT2B11 and UGT2B28 expression correlates with worse survival outcomes for patients with Stage 1 Breast Cancers	94
3.3.5	UGT2B11 and UGT2B28 associate with gene signatures for lipid metabolism	96
3.4	Discussion.....	97
3.4.1	Conclusion.....	101
4.	CHAPTER 4 - UGT2B11 AND UGT2B28 PROMOTE SREBP ACTIVATION	103
4.1	INTRODUCTION	104
4.1.1	Dysregulation of Lipid Biosynthesis	104
4.1.2	UGTs and Lipid Metabolism.....	104
4.1.3	CRISPR Inhibition (CRISPRi).....	108
4.1.4	Aims	109
4.2	METHODS	110
4.2.1	Plasmids	110
4.2.2	Oligonucleotides	112
4.2.3	Generation of UGT2B11 and UGT2B28 stable overexpression cell lines	113
4.2.4	Fluorescence SREBP-2 Localisation Assay.....	114
4.2.5	GAL4-VP16 C-SREBP-2 Luciferase Assays.....	114
4.2.6	Delipidation of serum	114
4.2.7	Cell Fractionation.....	115
4.2.8	Enzyme Assays	115
4.3	RESULTS.....	115

4.3.1	Characterising the effect of UGT2B11 and UGT2B28 overexpression	115
4.3.2	Construction and analysis of MDA-MB-453 cell lines carrying UGT2B11 and UGT2B28 CRISPRi knockdown vectors	126
4.3.3	Generation of SREBP-2 constructs.....	127
4.3.4	Effect of UGT overexpression on activation of an SREBP target gene promoter 130	
4.3.5	Assessment of SREBP processing via immunoblotting.....	131
4.3.6	Development of a fluorescent SREBP processing assay	136
4.3.7	Development of a reporter based SREBP processing assay	139
4.3.8	Overexpression of UGT2B11 and UGT2B28 variants induces processing of GAL4-VP16 C-SREBP-2	142
4.3.9	Specificity of UGT Domains.....	148
4.3.10	UGT2B11 and UGT2B28 interact with components of the lipid sensing complex 151	
4.4	DISCUSSION	154
4.4.1	Effect of UGT overexpression on MDA-MB-453 cells.....	154
4.4.2	Attempts to knockdown UGT expression in MDA-MB-453 cells.....	157
4.4.3	UGTs mediate increased SREBP activation.....	158
4.4.4	Novel interactions between UGTs and the lipid sensing complex.....	162
4.4.5	Conclusion.....	166
5.	CHAPTER 5 - REGULATORY MECHANISMS OF SREBP ACTIVITY AND UGT EXPRESSION 168	
5.1	INTRODUCTION	169
5.1.1	Lipotoxicity.....	169
5.1.2	Regulation of nuclear SREBP protein levels by UGTs	169
5.1.3	Crosstalk between SREBPs, UGTs, and Androgen Receptor signalling.....	174
5.1.4	Tet-On Inducible System.....	175
5.1.5	Aims	176

5.2	METHODS	177
5.2.1	Plasmids	177
5.2.2	Oligonucleotides	178
5.2.3	Luciferase Assays	178
5.2.4	Protein Co-expression.....	179
5.2.5	Co-immunoprecipitation.....	179
5.2.6	Fluorescence Microscopy	180
5.2.7	Generation of Tet-On Cell lines	180
5.2.8	Quantitative PCR.....	180
5.3	Results	181
5.3.1	UGT2B11 and UGT2B28 reduce the levels of nSREBP-2 protein.....	181
5.3.2	UGT2B11 and UGT2B28 also modulate levels of nSREBP-1a protein	184
5.3.3	UGT2B11 and UGT2B28 variants affect the level of nSREBP proteins in MDA-MB-453 cells	185
5.3.4	Attempted knock down of FBW7 in HEK-293T cells.....	188
5.3.5	The UGT-mediated degradation of nSREBP isoforms is independent of GSK-3 β	194
5.3.6	nSREBPs repress the transactivation of UGT2B11 and UGT2B28 promoters	201
5.3.7	nSREBPs induce toxicity when stably overexpressed.....	204
5.3.8	Validation of Doxycycline Inducible nSREBP stable lines	204
5.3.9	Inducible nSREBP-1a stable lines show reduction of UGT2B28 promoter transactivation.....	206
5.3.10	nSREBP-1a overexpression does not reduce UGT2B28 mRNA Levels	210
5.4	Discussion.....	213
5.4.1	nSREBP signal termination by UGTs	213
5.4.2	nSREBP regulation of UGT2B11 and UGT2B28.....	216

5.4.3	Conclusion.....	219
6.	CHAPTER 6 - GENERAL DISCUSSION AND OVERALL SIGNIFICANCE OF FINDINGS	221
7.	APPENDICES.....	232
6.1	Appendix 1: Materials and Buffer Compositions	233
6.2	Appendix 2: Plasmid Maps and Sequences.....	236
8.	References	262

SUMMARY

The human UDP-glycosyltransferase (UGT) superfamily is comprised of 22 enzymes across four families (UGT1, UGT2, UGT3 and UGT8) that catalyse the covalent addition of sugars to a broad range of small lipophilic molecules. This process not only plays a critical role in the inactivation and elimination of exogenous chemicals but also controls the level and distribution of numerous endogenous signalling molecules, such as steroid hormones, which modulate both breast and prostate cancer progression. Several UGTs are also transcriptionally regulated by such steroids, thus creating a feedback loop to control steroid signalling. Unlike other UGTs, the biological activities of UGT2B11 and UGT2B28 are not well characterised. UGT2B11 and UGT2B28 are frequently overexpressed in cancer, particularly those arising in the breast and prostate. Furthermore, recent data shows that both UGT2B11 and UGT2B28 are dramatically induced by androgens in breast and prostate cancer cells. Although their expression has been linked to pathogenic features of breast and prostate cancers, their precise biological functions remain poorly understood. These enzymes lack well-defined high activity substrates and are often referred to as 'orphan' enzymes. This thesis sought to mechanistically explore the functional role of UGT2B11 and UGT2B28 in breast cancer models.

Analysis of RNAseq and microarray data from The Cancer Genome Atlas breast cancer (TCGA-BRCA) dataset and the Molecular Taxonomy of Breast Cancer International Consortium (METABRIC) dataset revealed a clear association between the expression of both *UGT2B11* and *UGT2B28* isoforms. Increased expression of these UGTs was observed in breast cancer patients with tumours that were estrogen receptor alpha negative (ER-), human epidermal growth factor receptor 2 (HER2) enriched and had high expression of the androgen receptor (AR). Interestingly, breast cancers with this expression profile are broadly consistent with molecular apocrine tumours and are similar to prostate cancers in many ways. Within the ER- subsets of breast cancer, high expression of either *UGT2B11* or *UGT2B28* was associated with significantly worse survival outcomes. In these patients, functional pathway analysis identified enrichment of gene signatures associated with lipid biosynthesis, particularly those involved in Sterol Regulatory Element Binding Protein (SREBP) mediated lipid biosynthetic pathways.

SREBPs are the master regulators of lipid metabolism. When cellular lipid levels are low, an endoplasmic reticulum (ER)-based lipid-sensing mechanism induces trafficking of SREBP

from ER to Golgi, where proteolytic processing generates the mature transcription factor form that enters the nucleus to drive lipogenic gene expression. The roles of UGT2B11 and UGT2B28 in lipid metabolism were assessed in the molecular apocrine MDA-MB-453 breast cancer cell line. Stable overexpression was associated with increased proliferation and increased expression of SREBP-target genes. Moreover, transient UGT2B11 and UGT2B28 expression triggered ER processing events that lead to increased nuclear accumulation of nSREBPs. These effects were also recapitulated with a series of naturally occurring truncated variants of UGT2B11 and UGT2B28 lacking critical domains for catalytic activity, suggesting a non-catalytic mechanism. HEK-293T co-expression models demonstrated physical interactions between UGT2B11 and all components of the ER-based lipid sensing complex; SCAP (SREBP cleavage activating protein), INSIG (Insulin induced gene product) and the SREBP precursor. Together these data support a model whereby, through novel functional interactions, UGT2B11 and UGT2B28 can increase SREBP activation and lead to increased SREBP target gene expression.

Finally, as excessive lipogenesis can result in lipotoxicity and cellular death, mechanisms by which cancerous cells can prevent this whilst still maintaining a proliferative advantage were examined. Intriguingly, UGT2B11 and UGT2B28 were able to promote the turnover of transcriptionally active nSREBPs in MDA-MB-453 breast cancer cells. This appeared to be independent of the canonical glycogen synthase kinase-3 β (GSK-3 β) phosphorylation, which is generally required for nSREBP turnover. As an alternative mechanism for preventing lipotoxicity, the capacity for nSREBPs to reduce expression of UGTs through reducing AR transcriptional activity was examined. Whilst UGT promoter constructs showed reduced transactivation following transient overexpression of nSREBPs, this did not translate to a significant change in UGT mRNA levels in doxycycline-inducible nSREBP overexpression cell lines.

Overall, the findings of this thesis demonstrate that UGT2B11 and UGT2B28 can modulate the activation of SREBPs, leading to enhanced proliferative capacity of breast cancer cells and to worse survival outcomes for patients with increased UGT expression. Additionally, UGT2B11 and UGT2B28 may also modulate nSREBP transcriptional activity by inducing nSREBP turnover, suggesting an important role for these enzymes in preventing toxic hyperactivation of lipogenesis. This research highlights the need for further studies on the enigmatic UGT2B11 and UGT2B28 'orphan' enzymes.

DECLARATION

I certify that this thesis:

1. does not incorporate without acknowledgment any material previously submitted for a degree or diploma in any university
2. and the research within will not be submitted for any other future degree or diploma without the permission of Flinders University; and
3. to the best of my knowledge and belief, does not contain any material previously published or written by another person except where due reference is made in the text.

Jai Meyers

September 2024

ACKNOWLEDGEMENTS

I would like to acknowledge and thank all of the people who have provided their invaluable support and encouragement throughout my PhD project, and I would like to express my utmost appreciation to all of those involved.

Firstly, I would firstly like to thank my supervisor, Professor Robyn Meech for her support and guidance throughout this project. I would also like to thank my co-supervisor Dr. Julie-Ann Hulin for her invaluable assistance and consistent support. You have both been an inspiration as well as incredible examples of scientists and I am forever grateful for the opportunities and expertise you have shared with me.

I would like to also thank all of the research staff and students within the Clinical Pharmacology department, not only for their assistance and support, but for making my time in the laboratory such a fantastic experience, it has been a pleasure to work with you all.

I would like to thank all of my friends and colleagues from across Flinders for their continual support throughout my time at Flinders University, whose encouragement and friendship I could not do without.

I would also like to thank my family for the immense support they gave from afar that kept me going throughout all of these past years.

Finally, I would like to thank my phenomenal partner Claire, who's support throughout my PhD I am incredibly grateful for.

CONFERENCE PROCEEDINGS

Oral Presentations

Meyers, J., Hulin, J.A., Mubarokah, S., Mackenzie, P., McKinnon, R. & Meech, R. 'The role of UGT enzymes as novel modulators of lipid biosynthesis and SREBP signalling in breast cancer', Oral Presentation, Australasian Society of Clinical and Experimental Pharmacologists and Toxicologists (ASCEPT) Student Symposium, Online 2020.

Meyers, J., Hulin, J.A., Mubarokah, S., Mackenzie, P., McKinnon, R. & Meech, R. 'The role of UGT enzymes as novel modulators of lipid biosynthesis and SREBP signalling in breast cancer', Oral Presentation, Australasian Society of Clinical and Experimental Pharmacologists and Toxicologists and Australasian Pharmaceutical Science Association (ASCEPT-APSA) Scientific Meeting, Online 2020.

Meyers, J., Hulin, J.A., Mubarokah, S., Mackenzie, P., McKinnon, R. & Meech, R. 'UGT enzymes as novel modulators of lipid biosynthesis in breast cancer', Oral Presentation, Adelaide Pharmacology Group, Adelaide 2021.

Meyers, J., Hulin, J.A., Mubarokah, S., Mackenzie, P., McKinnon, R. & Meech, R. 'UGT enzymes as novel modulators of lipid biosynthesis in breast cancer', Oral Presentation, Flinders University College of Medicine and Public Health Emerging Leaders Showcase, Adelaide 2022.

Poster Presentations

Meyers, J., Hulin, J.A., Mubarokah, S., Mackenzie, P., McKinnon, R. & Meech, R. 'The role of UGT enzymes as novel modulators of lipid biosynthesis and SREBP signalling in breast cancer', Poster Presentation, Australasian Society of Clinical and Experimental Pharmacologists and Toxicologists and Australasian Pharmaceutical Science Association (ASCEPT-APSA) Scientific Meeting, Online 2020.

Meyers, J., Hulin, J.A., Mubarokah, S., Mackenzie, P., McKinnon, R. & Meech, R. 'The role of UGT enzymes as novel modulators of lipid biosynthesis and SREBP signalling in breast cancer', DocFest, Adelaide, 2020.

Mackenzie, P., **Meyers, J.,** Hulin, J.A., Hu, D.G., Mubarokah, S., Mackenzie, P., McKinnon, R. & Meech, R. 'Potential Novel Role of UDP Glucuronosyltransferases 2B11 and 2B28 in Crosstalk Between Androgen and Lipid Signalling' Federation of American Societies for Experimental Biology (FASEB) Scientific Meeting, Online 2020. <http://dx.doi.org/10.1096/fasebj.2020.34.s1.04907>

AWARDS IN SUPPORT OF THIS THESIS

Australian Government Research Training Program Scholarship (AGRTPS) – 2020-2023

Playford Trust PhD Scholarship – 2020-2023

Australasian Society of Clinical and Experimental Pharmacologists and Toxicologists (ASCEPT) Student Conference Grant to attend and present at the ASCEPT-ASPA Scientific Meeting, Online 2020.

ASCEPT Drug Disposition and Response Special Interest Group Prize, Online 2020.

Flinders University College of Medicine and Public Health Emerging Leaders Showcase Best HDR Student Presentation, Adelaide, 2021

LIST OF ABBREVIATIONS

ATCC	American Type Culture Collection
bp	Base Pairs
cDNA	Complementary DNA
CRISPR	Clustered Regularly Interspaced Short Palindromic Repeats
CRISPRi	CRISPR Interference
Ct	Cycle Threshold
DMEM	Dulbecco's Modified Eagle's Medium
DMSO	Dimethyl Sulfoxide
DNA	Deoxyribonucleic Acid
dNTP	Deoxynucleotide Triphosphate
<i>E. coli</i>	<i>Escherichia coli</i>
ER	Endoplasmic Reticulum
EDTA	Ethylenediaminetetraacetic Acid
FBS	Fetal Bovine Serum
GFP	Green Fluorescent Protein
gRNA	Guide RNA
HRP	Horseradish Peroxidase
kDa	Kilodaltons
LB	Luria-Bertani
mRNA	Messenger RNA
Mut	Mutant
ns	Not Significant
OD	Optical Density
PAGE	Polyacrylamide Gel Electrophoresis
PBS	Phosphate Buffered Saline
PCR	Polymerase Chain Reaction
PIC	Proteinase Inhibitor Cocktail
qRT-PCR	Quantitative Reverse Transcription PCR
RNA	Ribonucleic Acid
RPMI 1640	Roswell Park Memorial Institute Medium
SDM	Site-directed Mutagenesis
SDS	Sodium Dodecyl Sulfate
SF	Serum Free
SNP	Single Nucleotide Polymorphism
TCGA	The Cancer Genome Atlas
Tr	Truncated
UDP	Uridine Diphosphate
WT	Wild Type
ER	Estrogen Receptor
AR	Androgen Receptor
S1P/S2P	Site 1/2 protease
SREBP	Sterol Regulatory binding protein
SCAP	SREBP Cleavage activating protein
INSIG	Insulin induced gene product

List of Tables

Table 1.1: Breast cancer molecular subtypes as defined by expression of nuclear receptors.....	23
Table 2.1: qRT-PCR cycling conditions	56
Table 2.2 Commonly used Sequencing Primers.....	63
Table 3.1: R values for Pearson's correlation of UGT2B enzymes with SREBP Target* and Lipid Metabolism** Gene signatures in TCGA-BRCA breast cancer RNAseq gene expression database (patient samples, n=981). Gene signatures sourced from Reactome Database (Fabregat et al., 2017) and assessed using GEPIA2 (Tang et al., 2019). Statistical significance ($p < 0.05$) was observed for UGT2B7, UGT2B10, UGT2B11 and UGT2B28 only.....	69
Table 3.2: Comparison of broadly similar molecularly based groupings used in TCGA-BRCA and METABRIC databases	73
Table 3.3: Top 25 enriched pathways in METABRIC Dataset for UGT2B11 or UGT2B28 high expression groups for ER- breast cancer patients. High UGT2B11 or UGT2B28 expressing groups were defined within the TCGA-BRCA and METABRIC ER-negative patient cohorts, and the 500 highest expressed genes within these groups were analysed using Reactome to assess enrichment of gene pathways. Statistical significance was assessed with a Binomial test where the false discovery rate was controlled using the Benjamini-Hochberg method.	97

List of Figures

Figure 1.1: Anatomy of the human breast.....	22
Figure 1.2: UDP-Glycosyltransferases	26
Figure 1.3: UGT Exon structure	28
Figure 1.4: UGT2B11 and UGT2B28 Domain structure	30
Figure 1.5: Exon and domain structure of UGT2B11 and UGT2B28.	34
Figure 1.6: UGT2B11 and UGT2B28 Promoter structure.....	37
Figure 1.7: Schematic overview of Lipid Biosynthesis	42
Figure 1.8: Schematic of SREBP activation and degradation	45
Figure 3.1: UGT2B11 and UGT2B28 mRNA expression in different TCGA-BRCA molecular subtypes and METABRIC 3-gene identifier subtypes	74
Figure 3.2: UGT2B11 and UGT2B28 mRNA expression in METABRIC integrative clusters	76
Figure 3.3: UGT2B11 and UGT2B28 mRNA expression does not correlate with estrogen receptor status in breast tumours	78
Figure 3.4: Correlation of UGT2B11 and UGT2B28 mRNA expression with HER2 status and androgen receptor expression in METABRIC cohort.....	80
Figure 3.5: Correlation of UGT2B11 and UGT2B28 mRNA expression with HER2 status and androgen receptor expression in TCGA-BRCA cohort.....	81
Figure 3.6: Correlation of UGT2B11 and UGT2B28 mRNA expression	82
Figure 3.7: Association between <i>UGT2B11</i> and <i>UGT2B28</i> mRNA expression and survival outcomes in all tumours	83
Figure 3.8: Association between <i>UGT2B11</i> and <i>UGT2B28</i> mRNA expression and survival outcomes in TCGA-BRCA molecular subtypes.....	85
Figure 3.9: Association between UGT2B11 and UGT2B28 mRNA expression and survival outcomes in METABRIC 3-gene classifier mRNA expression subtypes	86
Figure 3.10: Association between UGT2B11 mRNA expression and survival outcomes in METABRIC Integrative clusters	88
Figure 3.11: Association between UGT2B28 mRNA expression and survival outcomes in METABRIC integrative clusters	89
Figure 3.12: UGT2B11 and UGT2B28 mRNA expression and associated survival outcomes in HER2+ tumours	91
Figure 3.13: UGT2B11 and UGT2B28 mRNA expression and associated survival outcomes in ER-tumours.....	92
Figure 3.14: Association between UGT2B11 and UGT2B28 mRNA expression and survival outcomes in ER- tumours	93
Figure 3.15: Association between UGT2B11 and UGT2B28 mRNA expression and survival outcomes in METABRIC Tumour Stages	95
Figure 4.1: Preliminary results showing effects of UGT2B11 or UGT2B28 overexpression on SREBP target gene expression and proliferation.....	106
Figure 4.2: Preliminary results showing interaction between UGTs and SCAP.....	107
Figure 4.3: Characterisation of UGT2B11 and UGT2B28 MDA-MB-453 overexpression lines....	118
Figure 4.4: Effect of UGT2B11 and UGT2B28 overexpression in MDA-MB-453 cell lines on SREBP target genes	120
Figure 4.5: Characterisation of MDA-MB-453 overexpression lines of UGT2B11 and UGT2B28 truncated (Tr) isoforms	122
Figure 4.6: Characterisation of MDA-MB-453 overexpression lines of UGT2B28 His365 SNP isoform.....	124

Figure 4.7: Effect of over-expression of UGT2B11 and UGT2B28 truncated (Tr) and His365 SNP variants on SREBP target gene expression in MDA-MB-453 cell lines	125
Figure 4.8: UGT2B11 and UGT2B28 CRISPRi does not affect proximal promoter luciferase construct activity	127
Figure 4.9: Development and validation of SREBP-2 plasmid constructs	129
Figure 4.10: UGT2B11 increases transactivation of DHCR24 luciferase reporter	131
Figure 4.11: Effect of SCAP overexpression and delipidation of media on SREBP processing ...	133
Figure 4.12: Cellular fractionation to assess SREBP processing.....	135
Figure 4.13: Development of a fluorescence based SREBP-2 processing assay	138
Figure 4.14: Development of GAL4-VP16 SREBP-2 Processing Assay.....	141
Figure 4.15: UGT2B11 and UGT2B28 promote activation of GAL4-VP16 C-SREBP-2	144
Figure 4.16: UGT2B11 and UGT2B28 do not conjugate cholesterol or its derivatives.....	146
Figure 4.17: UGT mediated SREBP processing is inconsistently affected by sterols.....	148
Figure 4.18: UGT mediated SREBP processing by fragments of UGT2B15	150
Figure 4.19: UGT2B11 physically interacts with members of the lipid sensing complex in HEK-293T cells	152
Figure 4.20: UGT2B11 Expression does not affect interaction between SCAP and INSIG	153
Figure 4.21: Proposed role of UGTs in SREBP activation	167
Figure 5.1: Schematic of nSREBP degradation.....	170
Figure 5.2: UGT2B11 destabilises GSK-3 β -target proteins.....	173
Figure 5.3: UGT2B11 and UGT2B28 isoforms reduce protein levels of nSREBP-2	182
Figure 5.4: UGT2B11 reduces the transactivation activity of nSREBP-2.....	183
Figure 5.5: UGT2B11 and UGT2B28 reduces the nuclear abundance of nSREBP-1.....	184
Figure 5.6: UGT2B11 and UGT2B28 reduce the transactivation of a GAL4-VP16 nSREBP-1a fusion protein	187
Figure 5.7: Transient FBW7 CRISPRi vector validation in HEK-293T cells.....	191
Figure 5.8: Decrease in nSREBP transactivation not altered by FBW7 CRISPRi	192
Figure 5.9: KRAB, Cas9 and FBW7 mRNA levels in stable CRISPRi HEK-293T cell lines.....	195
Figure 5.10: UGT2B11 does not co-immunoprecipitate GSK-3 β	196
Figure 5.11: UGT-mediated reduction in the activity of truncated nSREBP-1a (1-136).....	198
Figure 5.12: UGT-mediated reduction in the activity of mutated nSREBP-2 S436A	200
Figure 5.13: nSREBPs repress transactivation of the ARR3 promoter by AR.	202
Figure 5.14: nSREBPs repress transactivation of the UGT2B28 promoter by AR and AR-v7	203
Figure 5.15: Validation of doxycycline inducible nSREBP-1a stable MDA-453 cells	205
Figure 5.16: UGT2B28 1kb Proximal promoter response in nSREBP-1a inducible MDA-MB-453 Cells.....	207
Figure 5.17: UGT2B28 1kb Proximal promoter response to bicalutamide in nSREBP-1a stable MDA-MB-453 cells.....	209
Figure 5.18: UGT2B28 mRNA induction by DHT in control GFP-expressing MDA-MB-453 stable cells	210
Figure 5.19: UGT2B28 mRNA induction by DHT in nSREBP-1a MDA-MB-453 stable cell lines... ..	212
Figure 6.1: Overall working model of UGT modulation of lipid metabolism	230

1. CHAPTER 1 - LITERATURE REVIEW

1.1 Cancer: A Brief Overview

Cancer is the malignant growth which results from the uncontrolled division of abnormal cells. It is a leading cause of death globally, accounting for approximately 10 million deaths per year since 2018 (Ferlay et al., 2021). This uncontrolled proliferation allows the cancerous cells to grow beyond the usual boundaries of their original cell type and also to disseminate throughout the body (metastasise). This can lead to the formation of new tumours in essential organs, ultimately leading to organ failure and thus death. The uncontrolled proliferative capacity of cancer cells can occur due to the accumulation of mutations in genes that control core, tightly-regulated pathways within normal tissue, particularly those associated with proliferation and apoptosis (Dai et al., 2016). Oncogenic mutations can arise due to stochastic errors in DNA replication, exposure to mutagenic or carcinogenic agents, or be inherited. Additionally, alteration of epigenetic processes can induce or promote cancer growth without direct modification of the genome (King et al., 2003; Rodríguez-Paredes & Esteller, 2011; Simpson et al., 2005).

1.2 Steroid-Dependent Cancers

Cancers are incredibly diverse and have been shown to arise within almost any tissue. The focus of this project was cancers of the breast and prostate, which are typically steroid-dependent and rely on steroid hormones to drive their initiation and growth. These two cancers are largely controlled by the sex steroids: estrogens and androgens. The steroid-responses of cells in the breast and prostate are dependent upon their expression of the cognate steroid sensing nuclear receptors: estrogen receptor (ER) and androgen receptor (AR) (Davey & Grossmann, 2016; Guillemette et al., 2004). These receptors are activated through direct binding to their respective steroid ligand, which drives the transcriptional regulation of target genes, many of which are involved in cellular proliferation and differentiation.

1.2.1 The Prostate and Prostate cancer

Normal prostate is comprised of a compact arrangement of glands and stromal tissue, with the majority of prostate cancers originating in the glands. Normal prostate tissue growth and development is controlled by androgens via the AR. AR is a nuclear receptor that undergoes activation through binding of androgen hormones (testosterone and

dihydrotestosterone (DHT)), leading to translocation from the cytoplasm to the nucleus, where it binds to androgen response elements (AREs) in the promoter regions of target genes (Gao et al., 2020). AR also possesses a number of DNA binding independent actions whereby it activates second messenger pathways (Davey & Grossmann, 2016).

Prostate cancers do not express ER alpha (which will be discussed further below), but almost all express AR. Prostate cancer cells expressing wildtype AR are responsive to androgens, and drugs that block production of androgens are generally first line therapeutics. However, under the selective pressure of androgen deprivation many prostate cancers lose androgen sensitivity and are then referred to as castration resistant prostate cancers (CRPC) (Perlmutter & Lepor, 2007). Most CRPC have greatly upregulated expression of AR, allowing them to respond to trace levels of androgens, and many also express constitutively active forms of AR generated by alternative splicing (Han et al., 2017).

1.2.2 The Breast and Breast Cancer

Normal breast is comprised primarily of the mammary gland, adipose tissue, and some supporting connective tissue (Figure 1.1). Growth and development of the mammary gland is controlled mainly by ovarian estrogens and progesterone (Arendt & Kuperwasser, 2015). This includes peri-pubertal growth and development, and lactation-associated remodelling (expansion and involution). Breast cancer can form along the ducts or within the lobule of the breast, this is the most common site for tumour occurrence and in this location these cancers are referred to as carcinomas. It can also occur within the connective tissues, which is defined as a sarcoma, but is much less common (Feng et al., 2018). Furthermore, these cancers can be subtyped into luminal or basal cancers, with luminal breast cancers arising in the lumen of the epithelial lining as opposed to distal tumours which are considered basal (Feng et al., 2018).

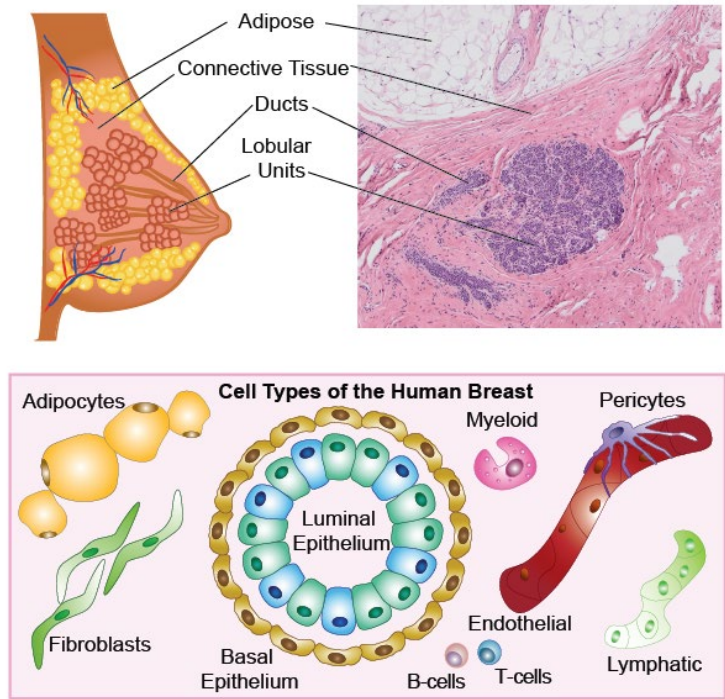


Figure 1.1: Anatomy of the human breast

Composition of the regular human breast with a pathological section stained with hematoxylin and eosin and depictions of major cell types. Image taken with permission from Human Breast Cell Atlas (n.d.).

In normal breast and prostate, steroids play complex and dynamic roles which vary by developmental stage and cell type. However, in cancers emerging from these tissues, these functions are dysregulated, in part because the tumours do not have the architectural organization nor diversity of cell types of the normal tissue. Breast and prostate tumours often originate from cell types that express these receptors (i.e. luminal epithelial cells) and are largely comprised of cells in which the expression of the receptors is elevated. The important steroid receptors in breast cancer and regular breast tissue are the estrogen receptor, progesterone receptor and HER2 (human epidermal growth factor receptor 2).

The estrogen receptor (ER) alpha functions as a transcription factor that once bound to estrogens binds estrogen response elements (EREs) in the genome, leading to target gene transcription through recruitment of co-regulators (Sherbet, 2011). Approximately 70% of breast cancers express estrogen receptor alpha (are ER+) with estrogen exposure promoting growth of these cells (Hickey et al., 2012). The expression of the progesterone receptor expression is regulated by ER and functions in much the same manner as ER as a

steroid hormone responsive transcription factor. HER2, encoded by the erythroblastic oncogene B2 (*ERBB2*) gene is a tyrosine kinase epidermal growth factor receptor that is expressed in many tissues throughout the body, including the breast (Iqbal & Iqbal, 2014). It is an oncogene, and it facilitates uncontrolled cell growth and tumorigenesis through an array of signal transduction pathways. It is frequently enriched through gene amplification, which occurs in 15-30% of breast cancers (Gutierrez & Schiff, 2011; Iqbal & Iqbal, 2014). Breast cancers can be characterised into molecular subtypes based on their expression of estrogen receptor, progesterone receptor and HER2 status, as summarised below in Table 1.1 (Dai et al., 2016; Russnes et al., 2017).

Table 1.1: Breast cancer molecular subtypes as defined by expression of nuclear receptors

	Estrogen Receptor	Progesterone Receptor	HER2 Expression
Luminal A	+	+	-
Luminal B	+	+	+
HER2-Enriched	-	-	+
Basal	-	-	-
Triple Negative	-	-	-

Of particular interest for this study are breast cancers that express high levels of AR, and therefore more likely to possess similarities to prostate cancers. The androgen receptor (AR) is important to consider in breast cancers, with approximately 80% of all breast cancers expressing the androgen receptor (are AR+) (Hickey et al., 2012). *In vitro*, ER+/AR+ positive breast cancer growth is promoted by estrogens and inhibited by androgens. Many ER negative breast cancers also express AR (ER-/AR+). These are not responsive to estrogens, and a subset of these may show growth stimulation in response to androgens (Doane et al., 2006; Moore et al., 2012).

1.3 Drug Metabolising Enzymes and Cancer

Drug metabolising enzymes (DMEs) regulate the metabolism of small molecules of both endogenous and exogenous origin. Phase I DMEs, primarily the family of cytochrome P450 enzymes (CYPs), are responsible for the reduction, oxidation, or hydrolysis of these molecules. Subsequently, Phase II DMEs (the main focus in this study), catalyse the conjugation of hydrophilic chemical groups (mainly sugars or sulphate) to these small

lipophilic bioactive substrates, thereby further increasing their water solubility and promoting excretion (Jancova et al., 2010; Josephy et al., 2005; Rowland et al., 2013). Whilst this is critical to the detoxification of xenobiotics, including pharmaceuticals, it is also essential for modulating the levels of many endogenous lipophilic signalling molecules, such as lipids and steroids. As conjugation generally renders the target molecule inactive (for example, making a steroid unable to interact with its receptor), this pathway can terminate signalling events. Thus Phase II DMEs are considered critical to maintaining the homeostatic control of essential signalling pathways (Allain et al., 2020; Jancova et al., 2010).

Due to the plethora of biological functions that phase II DMEs possess, any alterations in their function or catalytic activity, due to changes in gene expression or presence of mutations, can have a profound effect on the inactivation and excretion of any given bioactive substrate (Allain et al., 2020; Jancova et al., 2010). Such alterations have been widely shown to contribute to the risk and/or progression of cancer in three main ways. First, reduced expression or activity of DMEs can impair the detoxification of exogenous carcinogens, increasing the risk of carcinogenesis (Allain et al., 2020; Meech et al., 2019). Second, increased expression or activity of DMEs may increase the inactivation and clearance of anti-cancer drugs, thus reducing treatment efficacy and/or contributing to drug resistance. Thirdly, and of most relevance to this study, alteration of DME expression and function may promote cancer progression by altering levels of endogenous signalling molecules that are involved in cancer cell proliferation and survival.

There are several families of phase II DMEs, including: Uridine-5'-diphosphoglycosyltransferases (UDP-glycosyltransferases, UGTs), Sulfotransferases (SULTs), arylamine N-acetyltransferases (NATs), Glutathione-S-transferases (GSTs), and Methyltransferases. Of these, UGTs represent the largest gene family, which show the widest expression distribution, and are considered the most quantitatively important for inactivation and elimination of drugs (Ge et al., 2016).

1.4 Uridine 5'-diphosphate-glycosyltransferases (UGTs)

The human *UGT* superfamily comprises 22 genes (Meech et al., 2019) which are characterised into four distinct families based on sequence similarity: UGT1, UGT2, UGT3 and UGT8 (Figure 1.2A). All UGTs are type I transmembrane glycoproteins that reside within

the smooth endoplasmic reticulum (ER) and nuclear envelope, and have a predicted topology as shown in Figure 1.2B. UGTs catalyse the conjugation of UDP-sugars to a broad array of small lipophilic substrate molecules of both endogenous and exogenous origin, a process referred to as glycosylation (Figure 1.2C) (Rowland et al., 2013; Tukey & Strassburg, 2000). To be a suitable substrate for glycosylation, a lipophilic molecule must contain a stable nucleophilic functional group, such as aliphatic alcohols, carboxylic acids, phenols, thiols or amines (Guillemette et al., 2010; Meech et al., 2018). These groups may be pre-existing within a substrate molecule or have been generated by a Phase I DME reaction. The largely irreversible glycosylation of these substrate molecules increases their polarity, rendering them water soluble and generally functionally inert. This facilitates their excretion from cells, and ultimately from the body via urine or bile (Guillemette et al., 2014; Xu et al., 2005).

Of the 22 human UGTs, 19 use either exclusively or predominantly UDP-glucuronic acid as the sugar donor in their conjugation reactions; hence these enzymes are also conventionally referred to as UDP-glucuronosyltransferases (Mackenzie et al., 2003; Mackenzie et al., 2005; Senafi et al., 1994). The other 3 family members use alternate sugars, namely UDP-glucose or UDP-xylose (UGT3A1), UDP-*N*-acetylglucosamine (UGT3A1), and UDP-galactose (UGT8). UGT-mediated biotransformation has critical roles in regulating the levels of numerous exogenous compounds, including a significant fraction of commonly used drugs. In 2002 it was identified that 1 in 10 of the top 200 prescribed drugs were cleared via UGT mediated glucuronidation (Ge et al., 2016; Williams et al., 2004). In addition, UGTs control levels of a wide array of endogenous signalling molecules, including steroids, bile acids, fat soluble vitamins, and bioactive lipids (Rowland et al., 2013; Tukey & Strassburg, 2000). However, in general, the endogenous functions of UGTs are less well studied than their roles in drug metabolism.

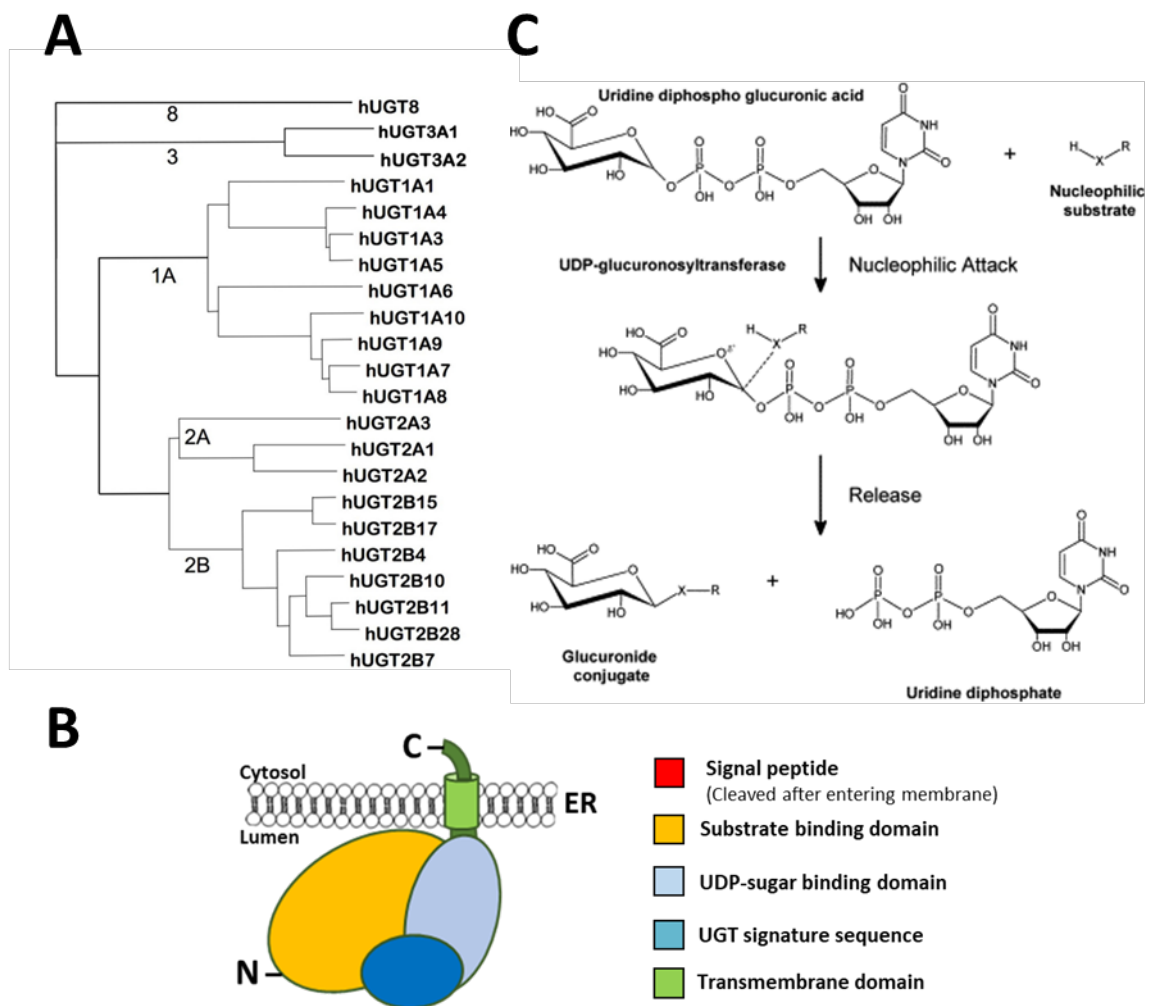


Figure 1.2: UDP-Glycosyltransferases

(A) Dendrogram depicting relationships between primary amino acid sequences of all human UGT enzymes, adapted from Meech et al. (2019) with copyright permission (4699510865156). **(B)** Topology of wildtype UGT (not to scale) **(C)** General reaction scheme for glycosylation by UGT enzymes, taken from Rowland et al. (2013) with copyright permission (4696380031896).

1.4.1 UGT Structure and Function

Each of the seven UGT2B family enzymes are encoded by six unique exons, this is unlike the UGT1 family enzymes which have an unusual exon sharing arrangement in which each UGT1 isoform is encoded by one unique and four shared exons (Figure 1.3A-B) (Guillemette et al., 2010). Consequently, there is a greater degree of homology between members of the UGT1 family, than between members of the UGT2B family (Figure 1.3C).

Individual UGT enzymes have broad substrate specificities; however, each enzyme shows a specific substrate preference profile, defined by the set of substrates conjugated, and the relative enzymatic efficiency with each substrate. The set of substrates that different UGTs can conjugate is largely overlapping, with only a few substrates (operationally called probe substrates) showing exclusive metabolism by one UGT isoform. When UGTs share substrates they typically show different pharmacokinetic properties (e.g. binding affinity and reaction rate) (Meech et al., 2012). Substrate preference is proposed to be largely specified by the N-terminal half of the UGT protein (a region of ~250 amino acids), while the C-terminal half of the protein contains the relatively well-defined UDP-sugar (cofactor) binding domain (Rowland et al., 2013). Consequently, high amino acid sequence homology, or relatedness, between UGTs typically correlates with more closely overlapping substrate profiles. To date, no complete, experimentally determined UGT protein structure exists; only a C-terminal portion of UGT2B7 has been crystallographically resolved, due to the difficulties associated with crystalizing membrane bound proteins (Fujiwara et al., 2016; Miley et al., 2007). There are however many full or partial (N-terminal or C-terminal) homology models for a range of human UGT isoforms (Fujiwara et al., 2016; Nair et al., 2015; Smith et al., 2020). Therefore, whilst speculations have been made regarding the structure of these enzymes, further research in this area is necessary, which may lead to a greater understanding of substrate preference.

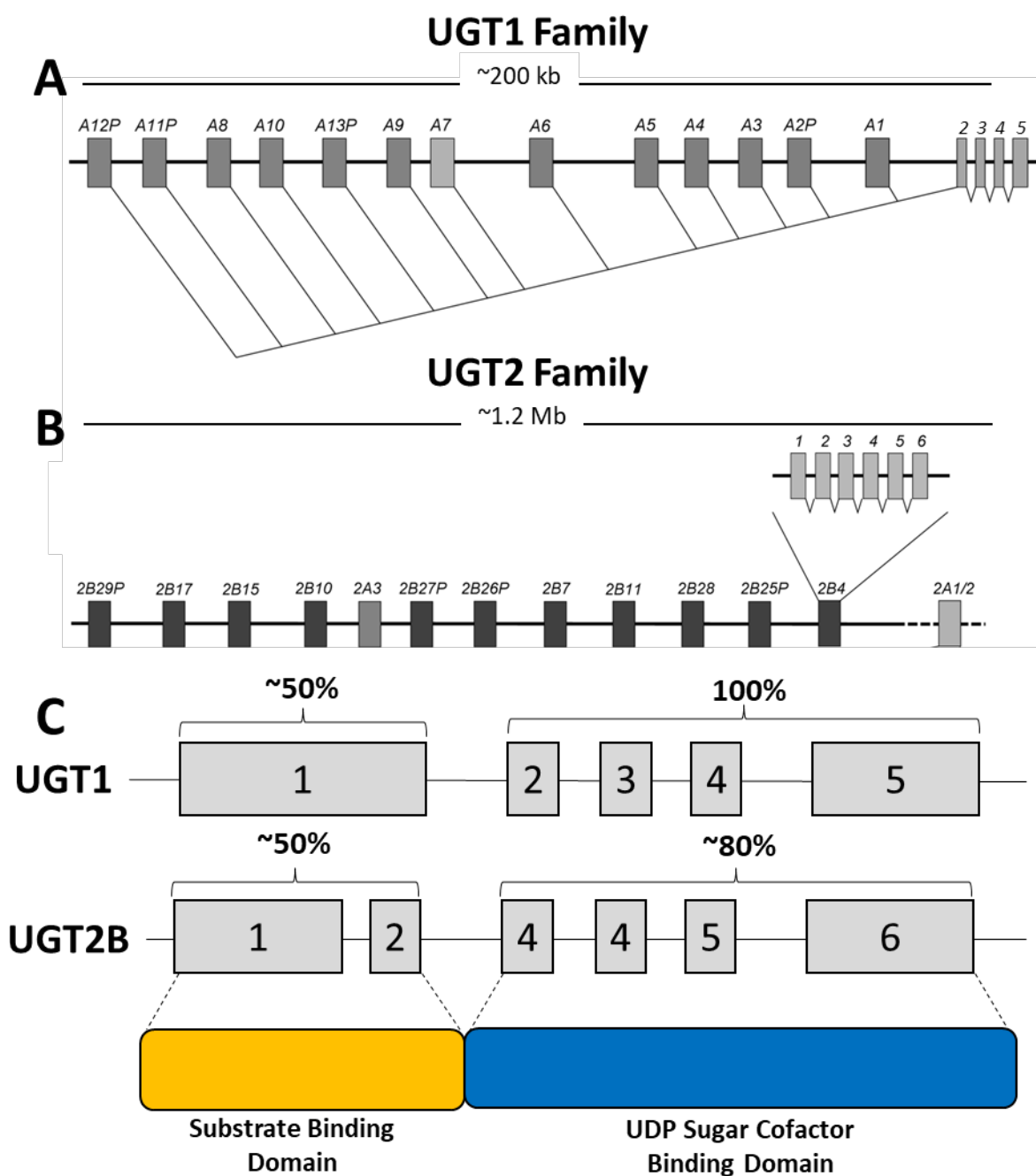


Figure 1.3: UGT Exon structure

Exon arrangement of **(A)** UGT1 and **(B)** UGT2 Family genes. P – indicates pseudogene. **(C)** Simplified exon structure of UGT1 and UGT2B family members are shown in relation to substrate and UDP-sugar cofactor binding domains. Approximate percentage conservation of amino acid sequence identity amongst family members indicated above each domain.

1.4.2 UGT Expression

The majority of UGT-mediated detoxification within the human body occurs in the liver, where almost all UGT genes are expressed to varying degrees. However, UGTs are also expressed extra-hepatically and are present and variably expressed within 28 tissues and organs throughout the body. The extra-hepatic tissues with the greatest UGT abundance are the gut (oesophagus, stomach, small intestine, colon) and kidney, with generally lower levels of expression (and a narrow range of expressed isoforms) found in airway tissues (nasal epithelium, trachea, bronchi, lungs), exocrine glands (salivary gland, pancreas, mammary and prostate glands), endocrine organs (adrenal gland, thyroid gland) connective tissues (skeletal muscle, heart, adipose tissue), hematopoietic and lymphoid tissue (thymus, bone marrow, spleen), reproductive tissues (ovary, testis, uterus, cervix, placenta), and the nervous system (brain and spinal cord) (Court et al., 2012; Fisher et al., 2001; Meech et al., 2019; Shuji & Shizuo, 2011; Tukey & Strassburg, 2000). Interestingly, a large body of literature has demonstrated that UGT expression within cancerous tissues is particularly variable relative to matched non-cancerous tissues (Allain et al., 2020; Angstadt et al., 2013; Belledant et al., 2016; Dates et al., 2015; Hu et al., 2020; Hu et al., 2021; Hu, Marri, et al., 2019; Wang et al., 2017).

1.5 UGT2B11 and UGT2B28

Although the functional roles of many UGTs are well characterised, the biological functions of two UGT2B family enzymes, UGT2B11 and UGT2B28, are poorly characterised (Meech et al., 2019). UGT2B11 and UGT2B28 were initially cloned and characterised by Beaulieu et al. (1998) and Lévesque et al. (2001), respectively. The genes encoding these UGTs are present on chromosomal band 4q13 in a cluster with the genes encoding the eight additional members of the UGT2A and UGT2B family enzymes, as previously discussed (Figure 1.3) (Mackenzie et al., 2005).

The full-length mRNA transcripts of the *UGT2B11* and *UGT2B28* genes encode 529 amino acid proteins with observed molecular weights of ~50 kDa (Beaulieu et al., 1998; Lévesque et al., 2001). Furthermore, as identified by Shuji and Shizuo (2011), these proteins are highly homologous, possessing 95% amino acid sequence identity, which is the highest degree of homology between any two UGT isoforms. As indicated in Figure 1.4 the wildtype full length proteins differ by only 27 amino acids (10 of which are considered conservative

replacements as the amino acids possess similar biochemical properties). These changes are not clustered within the N-terminal substrate recognition domain but distributed throughout the protein. Given this relatively high degree of conservation between the N-terminal domains of UGT2B11 and UGT2B28, it is speculated that these proteins may have somewhat similar substrate preferences and potentially a degree of cellular redundancy. UGT2B15 and UGT2B17 are highly homologous UGT isoforms, which possess a 95% identical nucleotide sequence identity (Beaulieu et al., 1996) and these isoforms possess an overlapping preference for steroidal substrates (Meech et al., 2019), providing support for this speculation of UGT2B11 and UGT2B28's cellular redundancy.

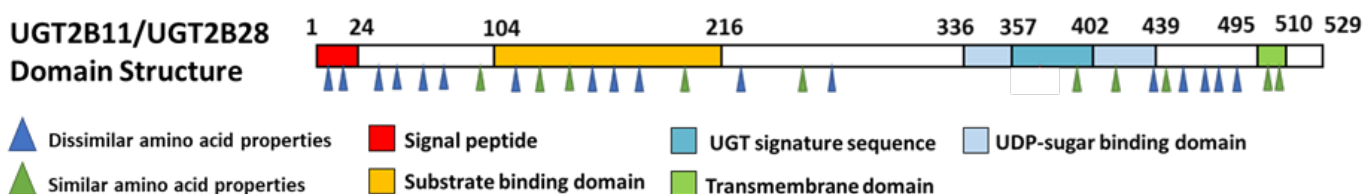


Figure 1.4: UGT2B11 and UGT2B28 Domain structure

Domain structure of UGT2B11 and UGT2B28 enzyme wildtype. Arrows indicate amino acid residues that differ between UGT2B11 and UGT2B28, with green and blue arrows representing strongly or weakly similar amino acid properties, respectively.

1.5.1 UGT2B11 and UGT2B28 Substrate Preferences

The substrate specificities of UGT2B11 and UGT2B28 have been the subject of limited research. Upon initial characterisation of UGT2B11, it was found to have no glycosylation activity with approximately 100 classical endogenous and exogenous UGT substrates tested (Beaulieu et al., 1998). Later work reported that UGT2B11 glucuronidates some fatty acid derivatives; hydroxylated arachidonic and linoleic acid metabolites, including the eicosanoids 12-hydroxyeicosatetraenoic acid, 15-hydroxyeicosatetraenoic acid and 13-hydroxyoctadecadienoic acid (Turgeon et al., 2003). No catalytic rates for these bioactive lipid substrates have been reported and hence the biological significance of these findings remains largely undefined. However, a study in prostate cancer cells by Chouinard et al. (2006) suggested that UGT2B11 is less efficient at glucuronidation of bioactive lipids than UGT2B10 and UGT2B17 isoforms. Hence it remains unclear if these enzymatic activities are the main cellular function of UGT2B11. Although they share significant homology, UGT2B28

was not found to conjugate eicosanoids when tested by Turgeon et al. (2003). UGT2B28 has been shown to conjugate the pregnanediol derivatives 5 α -pregnan-3 α ,20 α -diol and 5 α -pregnan-3 β ,20 α -diol, however, the significance of this does also require further research (Rouleau et al., 2022). Additionally, a genome-wide association study conducted by Thareja et al. (2022) suggested that UGT2B11 may be involved in acetaminophen glucuronidation, however, no experimental evidence yet exists to support this postulation.

During the initial characterisation of UGT2B28 (Lévesque et al., 2001), it was reported to glycosylate a number of classical UGT substrates: eugenol, 5 β -androstane 3 α -17 β -diol, etiocholanolone, 5 α -androstane 3 α -17 β -diol, 4-methylumbelliferone, 1-naphthol, estradiol, androsterone, testosterone, hyodeoxycholic acid and lithocholic acid. However, the enzymatic activity of UGT2B28 with these substrates was extremely low, and when compared to other UGTs that metabolise these substrates would be considered negligible (Turgeon et al., 2001). For example, the best substrate for glucuronidation by UGT2B28 as reported by Lévesque et al. (2001); eugenol, had a reaction velocity (V_{max}) of 2.18 pmol/min/mg of protein, whereas UGT2B4, UGT2B7, UGT2B15 and UGT2B17 have glucuronidation activity of eugenol between 39.7 - 347.3 pmol/min/mg of protein (Turgeon et al., 2001).

More recently, Rouleau et al. (2022) assessed the metabolic consequences of naturally occurring UGT2B28 germline deletions in prostate cancer patients. Whilst this does not directly assess which substrates UGT2B28 metabolises, it does indicate which metabolic pathways UGT2B28 activities may alter. This study revealed that levels of sphingolipid precursors (sphinganine and sphingosine) were increased in UGT2B28 null patients, suggesting that these sphingolipids might be substrates of UGT2B28. However, given that levels of sphingolipid-glucuronides were not reported, this remains a supposition. UGT2B11 deletions are very rare in humans, hence it is also possible that UGT2B11 activity could compensate for UGT2B28 deletion in this study. In addition to the increase in sphingolipid levels in UGT2B28 null patients, Rouleau et al. (2022) found that a vast array of other lipids were decreased in these individuals. As discussed further below, this is suggestive of UGT2B28 being involved in lipid metabolism (biosynthetic and/or biotransformation) pathways.

As is evident from these studies, the biological functions of UGT2B11 and UGT2B28 cannot be readily predicted based upon their very low or undefined catalytic activities. Hence, there is necessity for further research to be conducted in this area.

1.5.2 UGT2B11 and UGT2B28 Variants

As with all other UGT family members, a number of alternatively spliced transcripts have been identified or predicted in addition to the wildtype mRNA transcripts of UGT2B11 and UGT2B28 (Lévesque et al., 2001; Tourancheau et al., 2016) (Figure 1.5A). A recent study by Tourancheau et al. (2016) utilised RNA sequencing to characterise nine novel putative UGT2B11 transcripts, each caused by a combination of intronization of parts of exon 1, novel exons and splice shifts. Our laboratory has confirmed the existence of and cloned UGT2B11_n2 from cDNA of the prostate cancer cell line LNCaP, which encodes a truncated protein of ~40 kDa (data not published). This truncated protein arises due to insertion of a novel exon, exon 5b, between exons five and six. This insertion causes a frameshift mutation such that the protein is prematurely truncated and has a novel 57 aa C-terminal peptide. Two alternatively spliced UGT2B28 transcript variants, UGT2B28_v2 and UGT2B28_v3, were characterised in the initial study that isolated UGT2B28 (Lévesque et al., 2001). UGT2B28_v2 and UGT2B28_v3 arise due to skipping of exons 4 and 5, or the insertion of an additional novel exon 2b (89 aa), respectively. Both variants encode proteins with novel truncated C-terminal peptides. Our laboratory previously cloned UGT2B28_v2 (also from cDNA from LNCaP cells) into an expression plasmid and confirmed that its expression in mammalian cells produces a ~35 kDa truncated protein (data unpublished). A further four putative UGT2B28 variants have been predicted by Tourancheau et al. (2016) using RNA-seq data. As shown in Figure 1.5B, the truncated UGT2B28 proteins encoded by each of these variants lack domains which are considered essential for catalytic activity. Specifically, the UDP-sugar binding domain and the transmembrane domain are missing, and thus the proteins are considered to be catalytically inactive (Lévesque et al., 2001; Ménard et al., 2013). Additionally, based on studies of C-terminally truncated UGT2B7 (Ménard et al., 2013), it is predicted that this lack of transmembrane domain may cause cellular localisation to be altered.

Due to the high sequence homology between the UGT2B11 and UGT2B28 variants and other UGT2B family members, it has not yet been possible to amplify and hence validate any other predicted putative transcripts. Consequently, the validation of existence and

subsequent exploration of the function of these putative variants remains an area to be explored.

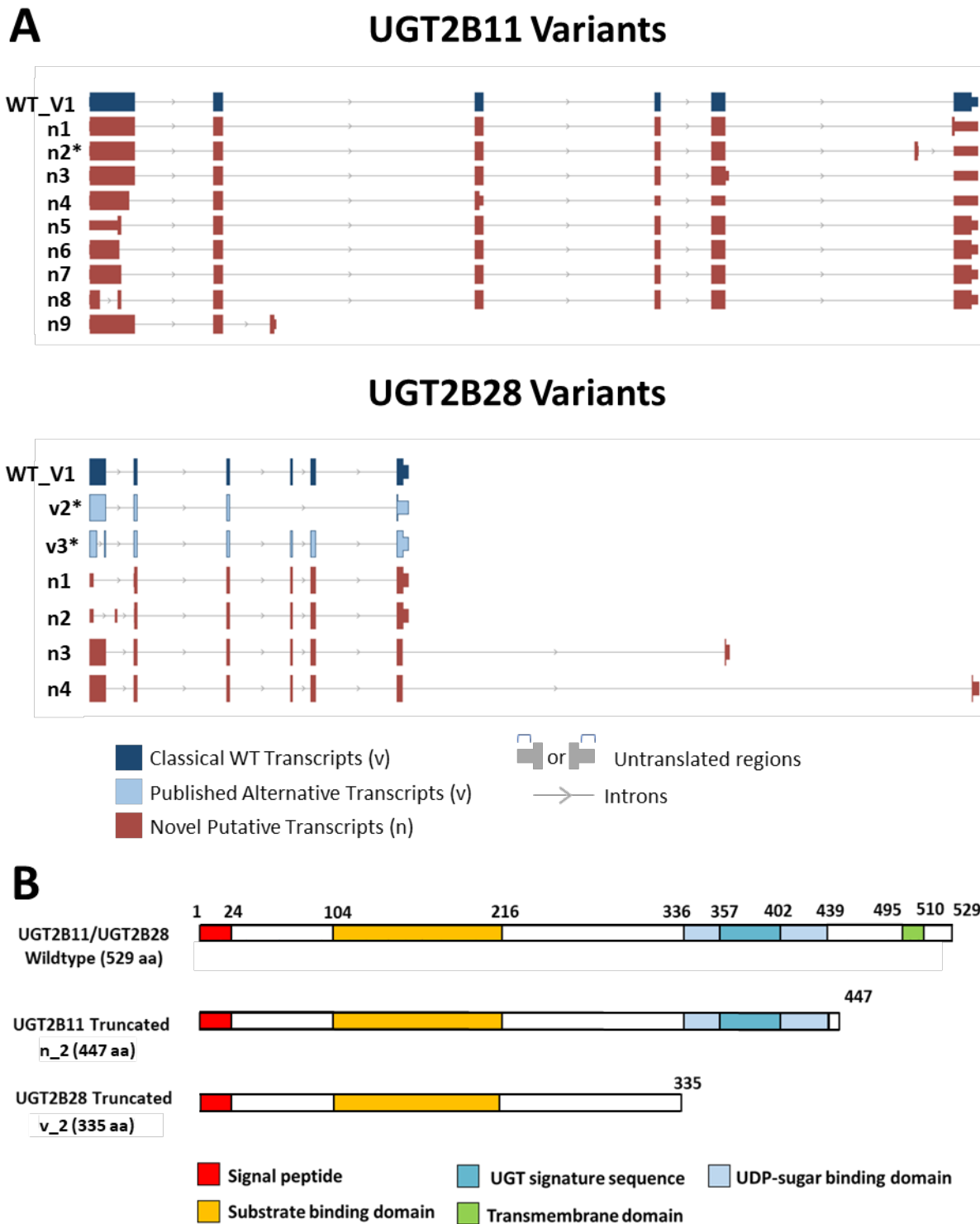


Figure 1.5: Exon and domain structure of *UGT2B11* and *UGT2B28*.

(A) Classical (Wildtype) transcripts are shown in dark blue. Alternative *UGT2B28* transcripts described by Lévesque *et al.* [1] are shown in light blue. Novel alternative transcripts described by Tourancheau *et al.* (2016) are depicted in red. Alternative transcripts independently and experimentally validated by our laboratory are labelled with * (data unpublished). Panel A adapted from Tourancheau *et al.* (2016). **(B)** Domain structure of wildtype and experimentally validated alternative *UGT2B11* and *UGT2B28* proteins used throughout this study.

1.5.3 SNPs and Somatic Mutations in UGT2B11 and UGT2B28

UGT2B28 is reported to be the second most frequently deleted gene in the human genome, with 13-35% of people, depending on ancestry, possessing no functional copies (homozygous nulls) of this gene (McCarroll et al., 2006; Ménard et al., 2009). No such copy number variations (CNVs) have been reported for *UGT2B11*. As discussed later, there is conflicting evidence whether these germline CNVs of *UGT2B28* are associated with cancer risk.

The *UGT2B28* missense single-nucleotide polymorphisms (SNP) variant (rs4235127) results in a Leu365>His365 substitution in the sugar binding domain of the protein. Notably, the His365 residue is conserved in all other human UGT enzymes and was found to be important for the catalytic activity of *UGT1A6* based on an alanine substitution experiment (Ouzzine et al., 2000). Therefore, the His>Leu substitution found in the wildtype isoform might be functionally disruptive (Grantham, 1974). Whilst there are numerous SNPs in *UGT2B* enzymes, this *UGT2B28* SNP variant is of particular interest as the designated wildtype isoform (*UGT2B28* Leu365) has a population frequency of 0.5475 (as per the NCBI Allele Frequency Aggregator), only slightly higher than that of the *UGT2B28* SNP His365 variant (0.4525) (Sherry et al., 2001). To date, only the Leu365 form of the *UGT2B28* enzyme has been assessed for enzymatic activity where no significantly conjugated substrates were identified. It is possible that the wildtype Leu365 *UGT2B28* allele is less active than the His365 SNP variant, which is currently untested and should be examined in future studies.

In addition to *UGT* variation that is encoded in the germline (e.g. SNPs and INDELS), our laboratory has shown widespread somatic mutations of *UGT* genes in an array of different cancers (Hu et al., 2022). *UGT2B11* and *UGT2B28* were found to be mutated at a rate equivalent to that of other *UGT2B* family genes in these studies. Approximately 60% of mutations present were missense mutations, with ~60% of missense mutations encoding deleterious amino substitutions. A further 15% of total mutations led to premature stop codons, frequently leading to truncated polypeptide chains. A mutation hotspot within a 31 bp region of *UGT2B28* between nucleotides 1153-1183 (relative to the ATG) was also identified. In addition to mutations that have direct effects on the coding sequence in *UGT2B11* and *UGT2B28*, mutations were identified within the 5' untranslated region (UTR) Kozak sequence that may reduce translation efficiency; and in either donor or acceptor

splice sites which could affect splicing of exons within the nascent pre-mRNA. Whilst somatic mutations of *UGT* genes have not been considered to be driver mutations that initiate tumour formation (Alexandrov et al., 2013; Bailey et al., 2018; Consortium, 2020), somatic *UGT* mutations in these isoforms might be involved in modulating cancer cell growth through altering cellular metabolic processes.

1.5.4 Non-canonical Functions

As aforementioned, wildtype UGT2B11 appears to have a very narrow substrate profile (hydroxylated fatty acid derivatives), and UGT2B28 was not found to have significant activity with any substrate. However, recent evidence suggests that in addition to their catalytic activities, some UGTs may be able to perform non-canonical ‘moonlighting’ functions through physical interactions with other proteins (Hu, Hulin, et al., 2019). Although no such functions are currently defined for any UGT2B11 or UGT2B28 variant, our laboratory has evidence that both wildtype and validated truncated variants of these UGTs can interact with and inhibit two important androgen metabolising UGTs called UGT2B15 and UGT2B17.

1.5.5 Regulation of UGT2B11 and UGT2B28 Expression

UGT2B11 and *UGT2B28* are adjacent genes located approximately 70 kb apart and divergently transcribed (Figure 1.6A). The promoter structures of these genes have been examined in prior work by this laboratory (manuscript in preparation). As identified by both this laboratory and the work of others, *UGT2B11* and *UGT2B28* are highly inducible by androgens in breast and prostate cancers, both *in vitro* and *in vivo* (Chouinard et al., 2006; Moore et al., 2012; Moore et al., 2020; Ngan et al., 2009), and is discussed in more detail below.

The proximal -300 bp region upstream of the transcription start site is highly conserved (96% identical) between *UGT2B11* and *UGT2B28* and is considered to be the minimal promoter region, containing all of the core responsive elements necessary for androgen driven transcription (data unpublished). The promoter contains four predicted steroid responsive regulatory elements; two androgen response-like (ARE) and two estrogen response-like (ERE) elements, in addition to a consensus Forkhead Box A1 (FOXA1) binding motif (Figure 1.6B). The androgen responsiveness of these genes was found to be dependent on the presence of an intact FOXA1 motif. In addition to the regulatory element

contained within the proximal promoters of *UGT2B11* and *UGT2B28*, the first intron of each of these genes also contains an enhancer region with multiple AR binding elements. Moreover, the intergenic region between the two genes also contains an enhancer with both AR and FOXA1 binding sites. These distal enhancers are predicted to cooperate with the proximal promoters via long range interactions to mediate the high levels of transcription observed in response to androgen exposure. The intergenic region also contains structural maintenance of chromosome 3 (SMC3) and CCCTC binding factor (CTCF) binding sites which are involved in maintenance of the three-dimensional organisation of the genome and transcriptional regulation of UGT1 and UGT2 genes (Zheng et al., 2019).

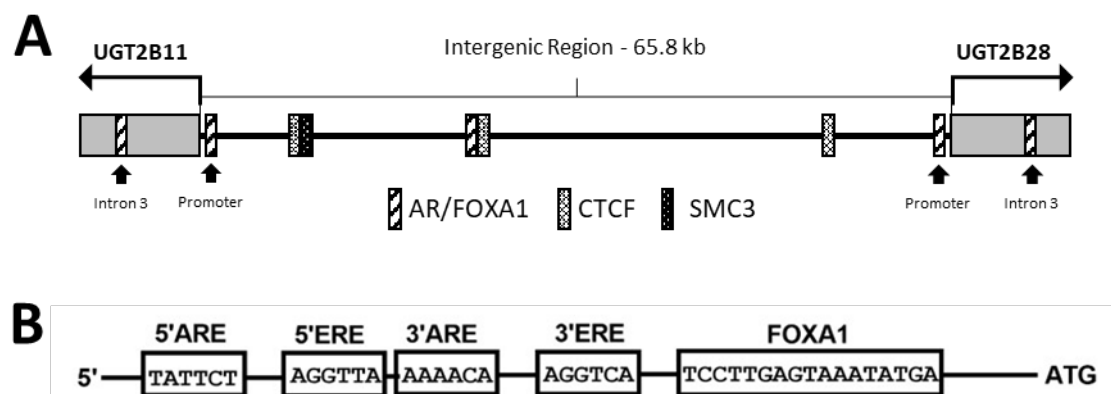


Figure 1.6: UGT2B11 and UGT2B28 Promoter structure

(A) Schematic of AR, FOXA1, CTCF and SMC3 binding loci within the *UGT2B11* and *UGT2B28* genomic locus as identified by analysis of ENCODE-ChIP data. **(B)** Schematic of predicted response units within the *UGT2B11* and *UGT2B28* -300 bp proximal promoter (Data unpublished).

The finding that *UGT2B28* can be transcriptionally induced by androgens in cell line models is consistent with several clinical studies where increased circulating levels of testosterone and dihydrotestosterone (DHT) in patients have been associated with increased *UGT2B28* expression (Belledant et al., 2016; Kaushik et al., 2013; Nadeau et al., 2011; Taylor et al., 2010). While only *UGT2B28* was measured in these studies, due to the conserved regulatory mechanism, it is likely that *UGT2B11* expression is also positively associated with high androgen levels *in vivo*.

In addition to regulation by transcription factors, UGTs are frequently post-transcriptionally regulated by miRNAs. Targetscan software analysis by Wijayakumara et al. (2015) predicted binding sites for an array of miRNAs in the 3'-UTRs of both *UGT2B11* and *UGT2B28*, however, there was no experimental validation of the role of these miRNAs in their regulation. Dluzen et al. (2016) showed that a binding site for miR-216b-5p is present in the 3'-UTR of *UGT2B28* but not *UGT2B11*. A luciferase reporter construct containing the 3'-UTR of *UGT2B28* was found to be repressed by miR-216b-5p (Margaillan et al., 2016). While there was no experimental validation of this miRNAs effect on *UGT2B28*, it was shown that it significantly repressed mRNA and protein levels for *UGT2B7* in hepatic cell lines and hence it is likely to have the same effect on *UGT2B28* due to the presence of the miR-216b-5p binding site (Dluzen et al., 2016).

1.5.6 UGT2B11 and UGT2B28 in Cancer

The expression of *UGT2B11* and *UGT2B28* is variable between individuals and between different tissues within the body, and furthermore, there is immense variability within cancerous tissues. This variation in cancer is proposed to be largely due to dysregulation of transcriptional control mechanisms but may also involve genetic variation such as somatic copy number variation (CNV). Aside from the somatic mutations, CNVs account for a large proportion of such genetic variation. *UGT2B28* is reported to be the second most frequently deleted gene in the human genome, while no such CNVs have been reported for *UGT2B11* (McCarroll et al., 2006; Ménard et al., 2009). In addition to copy number variations, the expression levels of *UGT2B11* and *UGT2B28* have been examined as risk factors in a variety of cancers.

Several studies have examined whether these copy number variations in *UGT2B28* are associated with cancer risk or progression. Through genotyping 665 Caucasian colorectal cancer (CRC) cases and 621 controls, Angstadt et al. (2013) determined that there is no significant association between any *UGT2B28* CNV and colorectal cancer risk. This conflicts with findings from Yoshida et al. (2010), where in 70 Japanese CRC patients, copy number decreases and reduced expression of *UGT2B28* were observed in patients with worse T classification, suggesting that repression of *UGT2B28* may have a potential role in CRC progression and tissue dedifferentiation. As these are the only two studies that examine these associations, further work is necessary to establish whether any association between *UGT2B28* CNV does exist, and if this is specific to particular populations.

In prostate cancer patients, several meta-analysis studies found no association with prostate cancer risk and *UGT2B28* germline CNVs (Habibi et al., 2017; Lee et al., 2016; Setlur et al., 2010). The populations studied by Setlur et al. (2010), Lee et al. (2016) and Habibi et al. (2017) consisted of 426 Austrian men (205 controls and 221 cases), 960 Korean Men (404 controls and 555 cases) and 360 Iranian Men (120 controls, 120 cases and 120 benign prostatic hyperplasia cases), respectively. This suggests strongly that reduced *UGT2B28* copy number does not affect prostate cancer risk across a range of populations. However, Nadeau et al. (2011) has linked deletion of *UGT2B28* with a significantly higher risk of biochemical relapse after prostatectomy in Caucasian and Asian populations. Whilst CNV of *UGT2B28* appears to have no effect on prostate cancer risk, a number of studies have reported that *UGT2B11* and/or *UGT2B28* expression is frequently upregulated in prostate cancer and likely associated with both an increased risk of prostate cancer development and progression (Beaulieu et al., 1998; Belledant et al., 2016; Dozmorov et al., 2009; Lévesque et al., 2001; Zhu et al., 2019). Specifically, *UGT2B28* expression is associated with a higher Gleason score; which is a grading system for prostate cancer, suggestive of cancers that are more likely to metastasise (Belledant et al., 2016; Grant et al., 2017). This has been proposed to occur as a result of modulation of steroidogenesis (Meech et al., 2019). Recent work by Lacombe et al. (2023) reports that the increased expression of *UGT2B28* in prostate tumours stabilises the AR/epidermal growth factor receptor proliferative pathways through HIP1 (endocytic adaptor protein huntingtin-interacting protein 1) an important AR cofactor, and hence it could be considered as an oncogene modulator during tumour progression.

Whilst not directly related to cancer, but can occur as a result of cancer induced adrenal gland infarction, there is an association between low *UGT2B28* copy number and development of Addison's disease (Brønstad et al., 2011).

Of the studies that have found an association between *UGT2B28* CNV and risk of disease, there has been a consistent trend of low expression or decreased copy number and increased risk. However, Joshi et al. (2006) reported that increased expression of *UGT2B28* is associated with progression of esophageal dysplasia in a cohort of 29 Chinese individuals, which can ultimately develop into esophageal cancer. This conflicts with Hu et al. (2015), where in 806 patients (404 cases and 402 controls), reduced copy number and mRNA

expression of *UGT2B28* was significantly associated with esophageal squamous cell carcinoma risk in a similar Chinese population.

In each of these studies, *UGT2B28* has been the focus due to the lack of any reported CNV for *UGT2B11*. There are, however, a small number of studies that have reported associations with increased cancer risk and elevated *UGT2B11* expression. In a single study on pancreatic ductal adenocarcinoma, *UGT2B11* was significantly upregulated in tumour samples when compared to matched pairs of adjacent non tumour tissue samples in 45 patient samples (He et al., 2019). Utilising the Cancer Genome Atlas (TCGA) hepatocellular carcinoma RNA-Seq dataset (50 matched cancerous and adjacent non tumour tissue), Hu, Marri, et al. (2019) reported that *UGT2B11* was upregulated in tumour samples. Whilst no further studies have attempted to directly repeat these analyses, it has been reported that the *UGT2B28* rs2132039 genomic SNP variant is associated with earlier age of presentation, earlier post-surgery recurrence, metastasis and death of hepatocellular carcinoma patients (Le et al., 2019).

Finally, the expression of these UGTs is associated with breast cancer risk or subtype. Marino et al. (2020) demonstrated an increase in *UGT2B11* mRNA expression in the early phase of carcinogenesis whilst Haakensen et al. (2010) reports that lower levels of *UGT2B11* are associated with high mammographic density in normal breast, a risk factor for breast cancer development. Wang et al. (2013) investigated differentially expressed genes in the contralateral unaffected breast of breast cancer patients in relation to the estrogen receptor (ER) status of the tumour in the affected breast. This showed that *UGT2B11* and *UGT2B28* had higher expression in patients with ER-negative (ER-) tumours than in those with ER-positive (ER+) tumours.

Interestingly, CRISPR-based gene-essentiality analysis reporter in the DepMap database indicates that *UGT2B11* is essential for cell survival in a number of cancer cell lines (26/1095), whilst *UGT2B28* is considered essential in only 5 cell lines (DepMap, 2019; Meyers et al., 2017). This is consistent with reports that *UGT2B28* is one of the most frequently deleted genes in the human genome (McCarroll et al., 2006; Ménard et al., 2009), whilst there is a lack of any reported CNVs for *UGT2B11*. Therefore, due to their significant amino acid sequence homology, this finding suggests a degree of functional redundancy, which appears not to be reciprocally equivalent.

1.5.7 Summary of UGT2B11 and UGT2B28 roles in cancer

In summary, most associations between UGT2B11 and UGT2B28 and cancer risk have been identified in gastrointestinal, breast and prostate cancers. Whilst this traditionally has been explained as being due to alteration of steroidogenesis, this literature supports a role of these UGTs in lipid metabolism.

Although UGT2B28 is often associated with higher androgen levels in prostate cancer (Belledant et al., 2016), UGT2B28 itself has no considerable role in altering androgen levels. This may be because high concentration of androgens drive expression of *UGT2B28* or alternatively/additionally that through increasing cholesterol synthesis, enhanced androgen production is possible. Furthermore, as Rouleau et al. (2022) identified, in UGT2B28 null individuals, lipid metabolite levels were significantly dysregulated. Which corroborates with the findings of Turgeon et al. (2003) that suggest UGT2B11 has a preference for some lipid substrates. This therefore strongly warrants the exploration of the role of these UGTs in regulating lipid biology rather than, or in addition to, their roles in modulation of steroids.

1.6 Lipid Metabolism

Lipid metabolism is the complement of synthesis, interconversion, and degradation of lipids in cells. For this study, the focus was upon the biogenesis of lipids and the regulation of this process. During fatty acid biosynthesis, a number of lipid classes are produced including: diacylglycerides, triacylglycerides, phosphoglycerides, sphingolipids, phosphoinositides and eicosanoids (refer to Figure 1.7) (Baenke et al., 2013). Although these lipid classes vary significantly in structure and cellular metabolic role, the generation of all lipids begins with the production of acetyl-CoA from citrate by ATP-citrate lyase and further converted to malonyl-CoA by acetyl-coA carboxylase (Zaidi et al., 2012). A majority of the citrate utilised in this process is generated from glucose catabolism, however, in cancerous tissue, glutamine is also a common source of citrate (Metallo et al., 2011; Mullen et al., 2011). Subsequent to their generation, acetyl-coA and malonyl-coA are coupled by fatty acid synthase, which through repetitive condensation produces the most basic fatty acid, palmitic acid (Baenke et al., 2013). Through various pathways, each of these lipid classes are synthesised from palmitic acid, with unsaturated fatty acids utilised to build these more complex lipids resulting from palmitic acid desaturation via stearyl-CoA

desaturase activity. Essential unsaturated fatty acids that cannot be formed from this process (linoleic acid and linolenic acid) are obtained directly from the diet (Santos & Schulze, 2012). As a direct consequence of this inability to synthesise essential fatty acids, the immense upregulation of *de novo* fatty acid biosynthesis in cancerous tissue is generally accompanied by an increase in fatty acid uptake (Swinnen et al., 2006; Tirinato et al., 2017). Also produced via lipid biosynthesis is cholesterol, the synthesis of which begins in the same manner as fatty acid biosynthesis yet utilises the mevalonate pathway for all subsequent steps beyond acetyl-CoA production (Horton et al., 2002; Rezen et al., 2011). Not only is cholesterol an integral component of lipid membranes, it is also utilised in the production of all steroid hormones; hence, as summarised in Figure 1.7, lipogenesis and steroidogenesis are intrinsically linked (Baenke et al., 2013; Stocco, 2001).

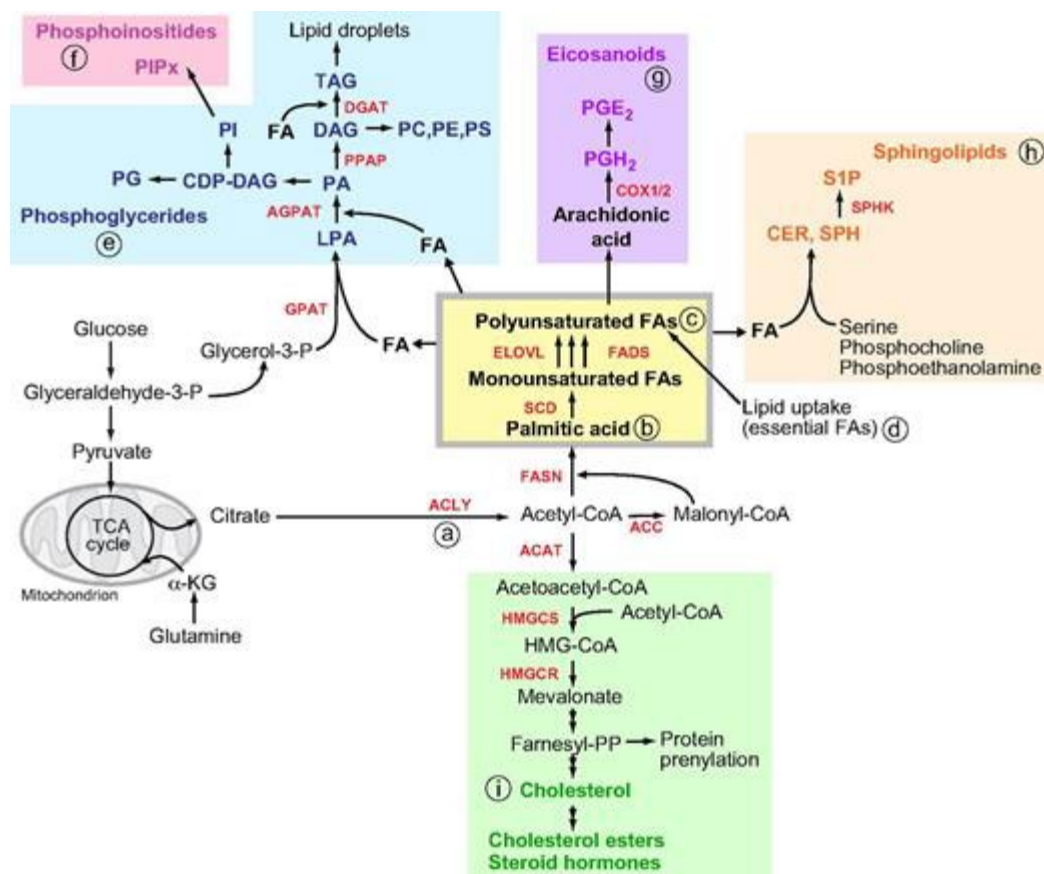


Figure 1.7: Schematic overview of Lipid Biosynthesis

Diagram taken from Baenke et al. (2013) with permission.

1.6.1 Regulation of Lipid Metabolism by SREBP

Lipid biosynthesis is tightly regulated by the sterol regulatory element binding protein (SREBP) transcription factor family, which is responsible for the transcriptional regulation of the majority of genes associated with lipid biosynthesis. The mammalian SREBP transcription factor family has three members: SREBP-1a, SREBP-1c and SREBP-2 (Eberlé et al., 2004; Horton et al., 2002; Weber et al., 2004). Both SREBP-1a and SREBP-1c proteins are produced from *sreb1* through alternative splicing and distinct promoters. They are both responsible, although with varying transcriptional strength, for the modulation of fatty acid and triglyceride biosynthetic genes (Xiaoping & Fajun, 2012). SREBP-2 is encoded by its own distinct gene, *sreb2*, and regulates the expression of cholesterologenic genes (Amemiya-Kudo et al., 2002; Baenke et al., 2013; Shimano, 2001).

Whilst there are a number of alternative pathways and cellular processes by which SREBPs are regulated in order to control cellular lipid biosynthesis, cellular sterol levels are considered to be the most significant controlling factor in regular cells. Inactive SREBP-precursors are ER-bound in a larger lipid sensing complex through interacting with the SREBP cleavage activating protein (SCAP) and insulin induced gene product (INSIG) (Goldstein et al., 2006; Gong et al., 2006). SCAP constitutively interacts with SREBP precursors through the presence of C-terminal regulatory domains in both proteins, whereas SCAP and INSIG interact in a sterol dependent manner. Under high cellular sterol conditions, a strong interaction between INSIG and SCAP anchors SREBP in the ER. Conversely, under low cellular sterol levels, conformational changes in SCAP occur leading to its dissociation from INSIG, allowing SCAP to interact with coat protein type II (COPII)-dependent vesicles that transport SREBP to the Golgi apparatus (Espenshade et al., 2002). There are two known mammalian variants of INSIG, INSIG-1 and INSIG-2, which appear to control the export of SCAP in an identical manner (Yabe et al., 2002; Yang et al., 2002). Within the Golgi, sequential proteolysis of the SREBP precursors by site 1 and 2 proteases (S1P and S2P) occurs. This cleaves the SREBP precursor into an N-terminal fragment and a C-terminal fragment. The N-terminal fragment (referred to as nSREBP) contains the basic-helix-loop-helix-leucine zipper (bHLHZ) transcriptional regulatory domains and is considered the mature form of SREBP (Sakai et al., 1996; Sakai et al., 1998). Mature nSREBP transcription factors translocate to the nucleus and bind to sterol regulatory elements (SREs) or enhancer box sequences on target lipogenic genes (Eberlé et al., 2004; Horton et

al., 2002). The C-terminal fragment of SREBP is believed to be degraded. The rationale for this complex mechanism is that it allows the sterol sensing complex (SCAP and INSIG) to rapidly and precisely control the amount of N-SREBP produced by post-translational processing of SREBP precursors.

Cellular fatty acid levels control SREBP-1 levels via an alternative mechanism to cholesterol; this mechanism involves transcriptional regulation rather than post-translational control. When cellular fatty acid levels are high, they inhibit activation of the liver X receptor (LXR); a nuclear hormone receptor necessary for transcription of SREBP-1 isoforms, ultimately preventing the transcription of SREBP-1 target genes (Amemiya-Kudo et al., 2002; Eberlé et al., 2004; Weber et al., 2004). However, when fatty acid levels are low, this inhibition does not occur, and SREBP-1 is robustly expressed. The conversion of SREBP-1 precursors into mature nSREBP-1 forms can then be regulated by cellular sterol levels via the post-translational processing mechanism described above.

Once in the nucleus, transcriptionally active nuclear nSREBPs undergo transcriptionally dependent degradation to prevent excessive transcription of lipogenic genes. This is controlled by the nuclear ubiquitin-proteasome pathway via a Cdc4 phosphodegron (CPD) motif within nSREBP (Hirano et al., 2001; Sundqvist et al., 2005; Sundqvist & Ericsson, 2003). Phosphorylation of the phosphodegron motif by glycogen synthase kinase-3 β (GSK-3 β) recruits a ubiquitin ligase called F-box and WD repeat domain-containing 7 (FBW7). FBW7 interacts with and confers specificity to the SKP1-cullin 1-F-box protein (SCF) E3 ligase complex (Krycer et al., 2012). In this context, FBW7 targets the SCF complex to nSREBP which is then polyubiquitinated. In the polyubiquitinated form, nSREBP is targeted to the proteasome for degradation (Sundqvist et al., 2005; Sundqvist & Ericsson, 2003). The regulation of SREBP activation and degradation is summarised in Figure 1.8.

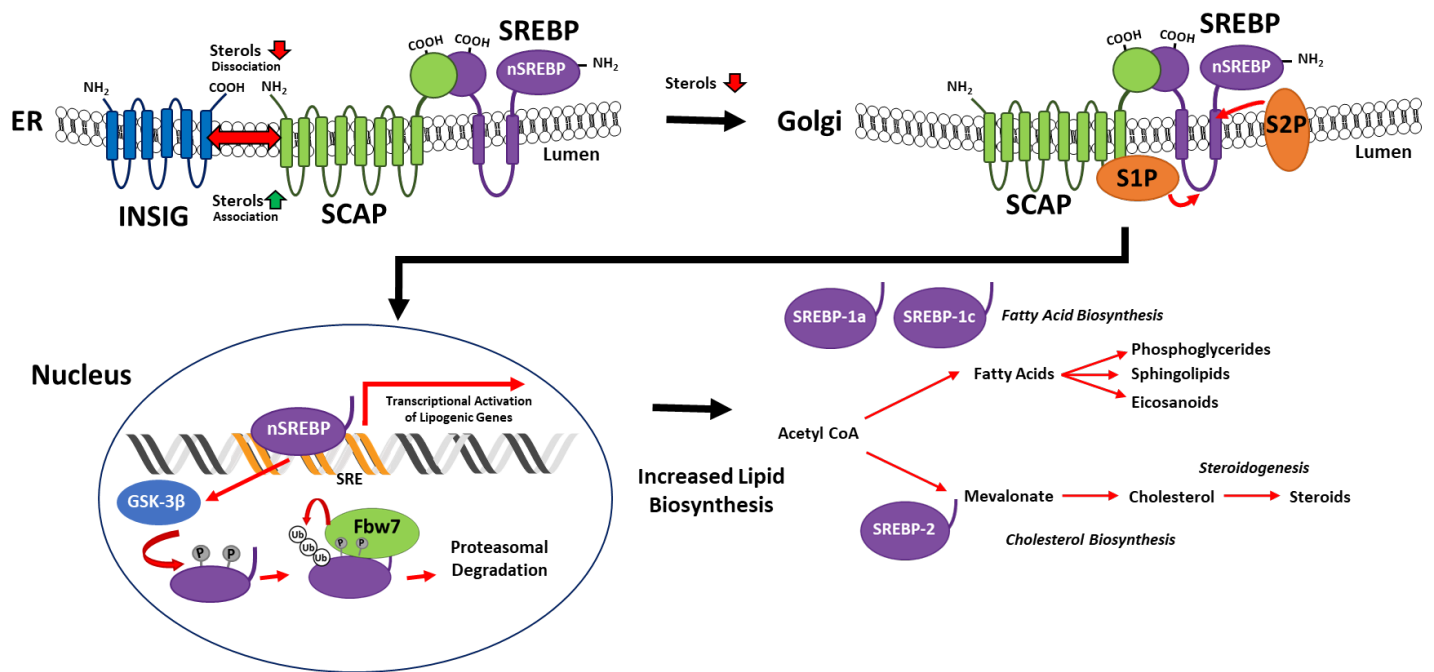


Figure 1.8: Schematic of SREBP activation and degradation

SREBPs exist as inactive precursors in the ER associated with SCAP, which interacts with INSIG. INSIG retains the SREBP: SCAP complex in the ER under high cellular sterol conditions, however, in low sterol conditions, INSIG dissociates from SCAP, which then chaperones SREBPs escort to the Golgi. In the Golgi, SREBP is cleaved by site-1 and -2 protease to release the active nuclear bHLHZ transcription factor domain (nSREBP). Active nSREBP translocates to the nucleus and binds to SRE sites within the promoters of lipogenic genes. Active SREBP-1a and -1c mediate transcription of fatty acid biosynthetic genes while SREBP-2 regulates cholesterol biosynthetic gene expression. nSREBP signal termination is promoted by GSK-3 β -mediated phosphorylation of a phosphodegron motif. This leads to recruitment of the FBW7 component of the SCF E3 ligase, polyubiquitination and proteasomal degradation.

1.6.2 Dysregulation of Lipid Metabolism in Cancer

Dysregulation of metabolic pathways is a hallmark of cancer, and the regulation of lipid metabolism is frequently perturbed in a vast array of different cancer types. Only a defined subset of normal tissues are capable of undertaking *de novo* lipid biosynthesis (mainly liver, adipose and secretory cells in the mammary glands), and thus most cells obtain all necessary lipids from the bloodstream (Menendez & Lupu, 2007; Walther & Farese, 2012). This, however, is not true for cancerous cells, where *de novo* lipid biosynthesis is regularly activated and dysregulated (Menendez & Lupu, 2007). Due to the variety of lipids that can be generated in this biosynthetic pathway, there are numerous proposed explanations for the role of increased lipid biosynthesis in cancer. The rapid proliferation of cancer cells

requires an increased rate of lipid synthesis for phospholipid formation to fuel membrane growth. Hence, it has been suggested that cancerous cells may rely upon lipid biosynthesis because the amount of lipid that can be obtained from dietary uptake is insufficient to fuel their high growth demands (Rysman et al., 2010). Furthermore, increased *de novo* lipid biosynthesis increases the intra-cellular concentrations of saturated fatty acids, consequently resulting in an increased saturation of the phospholipids from which cellular membranes are composed. Lipid membranes are primary targets of oxidative stress, with unsaturated, fluid membranes particularly susceptible to peroxidation (Naudí et al., 2013). Hence, such an increase in membrane saturation allows for increased proliferation whilst preventing oxidative stress induced death via unsaturated lipid peroxidation (Rysman et al., 2010; Santos & Schulze, 2012). In addition to increased membrane components, increased lipid synthesis has been demonstrated to also sustain the rapid proliferation of cancerous cells through the provision of additional cellular fuel by Liu (2006) and Vander Heiden et al. (2009). Furthermore, as cholesterol is an essential component in steroidogenesis, and steroid hormones are required for growth of breast and prostate cancer cells, the dysregulation of cholesterol biosynthesis is also associated with steroid-dependent cancer risk and progression (Krycer & Brown, 2011; Krycer et al., 2009). Finally, as identified by Tirinato et al. (2017), the accumulation of lipids in vesicles (referred to as lipid droplets) is an area in which a significant amount of research is currently being conducted. As increased storage allows lipids to be readily utilised for each of the aforementioned purposes, the accumulation of lipid droplets is a common characteristic of cancerous cells, and thus could be considered a biomarker. It has however, been indicated that the abundance of lipid droplets in cancerous tissues is in part dependent on the activity of SREBP-1 (Takahashi et al., 2013).

1.7 The SREBP-AR Axis

Many studies have reported an increased rate of SREBP transcription and proteolytic activation in cancerous tissues, particularly in steroid sensitive cancer types (Huang et al., 2012; Swinnen et al., 2004). Thus, it is suggested that altered SREBP signalling is an important cause of the dysregulation of lipid metabolism observed in cancerous tissues. Moreover, as described by Han et al. (2017) lipid metabolism dysregulation is often observed alongside aberrant AR signalling in such tissues. The SREBP and AR signalling systems are tightly interconnected and the mechanistic basis of this crosstalk is presented

in more detail in Chapters 4 and 5. As a brief summary: the *AR* gene is transcriptionally regulated by SREBP-1 (Huang et al., 2010); while AR increases the proteolytic activation of SREBPs by upregulating SCAP expression (Butler et al., 2016). This titrates out INSIG which anchors the SCAP-SREBP complex in the ER (Han et al., 2017; Heemers et al., 2005; Krycer & Brown, 2011; Krycer et al., 2009). Via this reciprocal regulatory network, intracellular sterol levels can increase AR activity, and androgen/AR signalling can increase nSREBP-1 levels. Furthermore, multiple gene promoters (including those of lipid metabolism genes) have been shown to bind both AR and nSREBPs, suggesting coordinate regulation by both factors (Heemers et al., 2001). Taken together, it is apparent that there are multiple layers of crosstalk between androgen and lipid signalling in cancer, which has recently been termed an SREBP-AR axis (Huang et al., 2018).

1.8 The role of UGT2B11 and UGT2B28 in Lipid Metabolism Dysregulation

A question prompted by this literature review is whether metabolism of lipids by UGT2B11 and UGT2B28, demonstrated in a limited fashion for UGT2B11 by Turgeon et al. (2003) and predicted for UGT2B28 based on homology to UGT2B11, may alter SREBP signalling, and thus lipid metabolism as a whole. A small number of studies have demonstrated a link between *UGT2B11* and *UGT2B28* and dysregulation of lipid metabolism in a variety of different diseases. However, these findings do not suggest that this is through direct metabolism of lipids, and in most cases do not yet have molecular mechanisms for the observed dysregulation.

In non-alcoholic steatohepatitis (NASH), the most severe form of non-alcoholic fatty liver disease (NAFLD) in which the hepatic system builds up excessive fat deposits, *UGT2B28* mRNA levels were significantly increased (Mathur et al., 2020). *UGT2B28* was also shown to be a key regulator of fatty acid metabolism in rat models of hepatic fibrosis (Yan-qin et al., 2022). Proteomic analysis of leukocytes has identified the presence of UGT2B11 within lipid rafts (Cayrol et al., 2008). Pathological lipid rafts have been associated with pathogenesis of a variety of diseases, including cancer, and can be formed from physiologically normal rafts by alterations in the lipid and cholesterol type and content, which could potentially be caused by aberrant UGT activity (Sviridov et al., 2020).

Gene expression analysis of co-culture spheroids demonstrated that cancer associated fibroblasts induced a significant upregulation *UGT2B11* mRNA levels in prostate cancer cells, and this this was associated with upregulation of cholesterol and steroid biosynthesis pathways (Neuwirt et al., 2020). Furthermore, in prostate cancer patients, *UGT2B28* null individuals were found to have an overall lower level of steroids, fatty acid carnitines, dicarboxylates and oxylipins than gene-proficient individuals (Rouleau et al., 2022). The latter is consistent with *UGT2B28* having a role in the SREBP-AR axis. Consistent with these findings, Bidgood et al. (2024) recently demonstrated that in prostate cancer cell lines 3-hydroxyisobutyryl-CoA hydrolase (HIBCH) null lines, *UGT2B11* and *UGT2B28* mRNA levels were significantly reduced, which was associated with a reduction in lipid biosynthesis. This again suggests that they are important in regulating lipid production in prostate cancers and further that HIBCH may be involved in their regulation.

Finally, these two UGTs have been associated with lipid metabolism in breast cancer. Following from Wang et al. (2013) where *UGT2B11* and *UGT2B28* were more highly expressed in patients with ER-negative (ER-) tumours, Wang et al. (2017) designated *UGT2B11* and *UGT2B28* as part of a 'lipid-signature' in breast, and suggested that high levels of these UGTs might contribute to the development of ER- breast tumours.

While the mechanistic details remain undefined, the observation that these UGTs are frequently mis-expressed in cancer and are likely to modulate lipid and steroid pathways which are drivers of cancer progression, prompts further research into their functions.

1.9 Aims and Hypotheses

As described herein, a small but compelling body of research suggests that *UGT2B11* and *UGT2B28* may be involved in the development and progression of cancer through association with both lipid metabolism and steroid signalling pathways; however, the mechanistic basis of this association is still poorly defined. This has thus identified numerous areas in which further research is necessary to elucidate the true functional role of these UGTs in both cancerous and normal tissues and to understand their association with cancer risk and progression. A priority area of study identified is the likely role that these enzymes possess in modulating lipid biosynthetic signalling pathways. It was hypothesised that *UGT2B11* and *UGT2B28* may alter the SREBP signalling pathway and

hence their mis-expression may contribute to the dysregulation of lipid metabolism in cancerous tissues.

Therefore, this project had three specific aims:

- 1. Identification of associations of UGT2B11 and UGT2B28 expression levels with clinical and biochemical parameters in breast cancer patient cohorts*
- 2. Defining the role of UGT2B11 and UGT2B28 in modulating SREBP activation*
- 3. Defining the role of UGT2B11 and UGT2B28 in mediating crosstalk between SREBP and AR signalling*

2. CHAPTER 2 - MATERIALS AND METHODS

2.1 Materials

2.1.1 Chemicals and Reagents and Buffers

All chemicals and reagents used during this project were of analytical grade. The chemicals and reagents along with their suppliers used throughout this project are listed in Table S1 (Appendix 1). The composition of all the buffers used in this project are listed in Table S2 (Appendix 1).

2.1.2 General Buffers

The composition of all buffers used is listed in Table S2 (Appendix 1). The following buffer formulae were used to make up general buffers:

Phosphate buffered saline (PBS): 137 mM NaCl, 2.7 mM KCl, 10 mM Na₂HPO₄ and 2 mM KH₂PO₄, pH 7.4

Tris-acetate EDTA electrophoresis buffer (TAE): 40 mM Tris pH 8, 20 mM acetic acid, 1 mM EDTA

SDS-PAGE running buffer: 25 mM Tris pH 8.3, 192 mM glycine, 0.1% SDS

SDS-PAGE transfer buffer: 25 mM Tris pH 8.3, 192 mM glycine, 20% methanol

Tris-buffered saline (TBS): 50 mM Tris pH 7.4, 150 mM NaCl

2.1.3 Bacterial and Mammalian Cell Lines

The DH5α *Escherichia coli* (*E. coli*) strain was originally purchased from the American Type Culture Collection (ATCC; Manassas, Virginia, USA). The breast cancer cell lines MDA-MB-453 and MDA-MB-231, and the human embryonic kidney cell line HEK-293T were also originally purchased from the ATCC.

2.1.4 Mammalian reporter and expression vectors

Prior to the commencement of this study, FLAG-tagged SLC35B4 (Solute Carrier Family 35 Member B4), FLAG-tagged Oxidoreductase, and wildtype and FLAG-tagged versions of UGT2B11 and UGT2B28 were cloned into the pEF1-IRES-puro6 (pIRES) mammalian expression vector (Hobbs et al., 1998) by Dr Julie-Ann Hulin (Flinders University, South Australia, Australia). Similarly, UGT2B28 SNP rs4235127 (which causes the L364H variation)

and truncated versions of UGT2B11 and UGT2B28 were also previously cloned into pIRES and were available for use. The mCherry-2A-pcDNA3 plasmid encoding mCherry and the self-cleaving 2A peptide was also constructed prior to this study and has been described previously (Meech et al., 2010). UGT2B11 and UGT2B28 promoter-pGL3 luciferase reporter constructs were generated by amplifying varying regions of the gene promoters from human genomic DNA and cloning into the promoterless pGL3-Basic vector by Apichaya Chanawong (Flinders University, South Australia, Australia). AR-v7 was cloned into an expression vector by Dr Dong Gui Hu (Flinders University, South Australia, Australia) and described previously (Hu et al., 2009)

The KRAB-dCas9-PX459 CRISPRi plasmid was generated prior to this project by Professor Robyn Meech (Flinders University, South Australia, Australia). The Kruppel Association Box fused to catalytically dead Cas9 (KRAB-dCas9) fragment was amplified from the pHR-SFFV-KRAB-dCas9-P2A-mCherry vector and inserted into the SpCas92A-Puro-PX459 vector, both of which were obtained from Addgene (Plasmids #60954 and #62988) (Gilbert et al., 2014; Ran et al., 2013). The CRISPRi-FBW7 construct targeting FBW7 was generated by cloning guide RNAs (gRNAs), designed using CRISPR-ERA (Liu et al., 2015), that target the *FBW7* proximal promoter regions, into the *Bpil* cloning site of KRAB-dCas9-PX459. The FLAG-tagged mouse Notch intracellular domain (NICD) pCAGGS-NICD plasmid, and WT and mutant CBF1-responsive element luciferase reporter constructs (CBFRE-pTA-Luc and CBFRE-Mut-pTA-Luc) were obtained from Addgene (Plasmids #26891, #26897 and #26896) (Dang et al., 2006; Yu et al., 2008).

The SCAP-Myc-His(C)-pcDNA4 and nSREBP-2-HA(N)-pcDNA4 expression constructs, along with the *DHCR24*-300-pGL3-Basic luciferase reporter construct were kind gifts from Professor Andrew Brown (University of New South Wales, New South Wales, Australia) (Krycer et al., 2012; Zerenturk et al., 2012). The nSREBP-1a-pEPI expression construct was a kind gift from Professor David Jans and has been described previously (Hübner et al., 2006). The pMM043 EGFP-expression plasmid was a kind gift from Associate Professor Michael Michael (Flinders University, South Australia, Australia). The ER localised ER-RFP was a kind gift from Professor Erik Snapp (Snapp et al., 2006).

The vectors pGL3-Basic, pRL-Null, pRL-CMV and pcDNA3 were originally purchased from Promega (Wisconsin, USA) and Invitrogen (Massachusetts, USA). The vectors pM, pVP16 and pck-1 GAL4-UAS luciferase reporter were purchased from Takara Bio.

The construction of all other plasmids utilised within this study is described in the relevant chapters of this thesis. The plasmid maps and sequences of these plasmids are presented in [Appendix 2](#). For plasmids received dried on filter paper, DNA was dissolved in 50 µL of 10 mM Tris-HCl (pH 8.5) and used for transformation as per section 2.2.7.3 Ligation and Transformation.

2.1.5 Oligonucleotides

All oligonucleotides were of standard purification quality (desalted) and were purchased from Macrogen (Seoul, Korea) or Merck (NSW, Australia). Oligonucleotides for qRT-PCR and for site-directed mutagenesis were designed using NCBI Primer-BLAST (Ye et al., 2012) and WatCut (Palmer, 2007), respectively. The sequences of all oligonucleotides are listed within the relevant chapters of this thesis.

2.2 Methods

2.2.1 Mammalian Cell culture

2.2.1.1 Cell Culture Maintenance

MDA-MB-453 cells were cultured in Roswell Park Memorial Institute Medium 1640 (RPMI 1640) and supplemented with 10% foetal bovine serum (FBS). MDA-MB-231 and HEK-293T cells were cultured in Dulbecco's Modified Eagle medium (DMEM) supplemented with 10% FBS (foetal bovine serum). Supplemented RPMI 1640 and DMEM are designated 'complete medium'. All cells were cultured in an incubator that maintained a constant temperature of 37°C and a humidified atmosphere of 5% carbon dioxide (CO₂).

An Olympus CK2 microscope was regularly used to assess confluence. Upon reaching a confluence of approximately 80-90%, cells were passaged or harvested for experimental analysis. To passage cells, medium was aspirated, and cells were washed with sterile PBS to remove remaining medium. MDA-MB-453 and MDA-MB-231 cells were detached from the flask by the addition of 1-1.5 mL 0.5% trypsin/0.53 mM EDTA in PBS solution and incubated at 37°C for 3-5 minutes. To inactivate trypsin activity, complete medium (RPMI 1640 or DMEM as appropriate) was added. For HEK-293T cells, cells were detached from the flask by vigorous pipetting in complete DMEM. MDA-MB-453 and MDA-MB-231 cells were routinely passaged at a dilution of 1:5-1:10 while HEK-293T cells were passaged at dilutions of 1:10-1:20.

Cell density was determined by diluting the cell suspension 1:2 in 0.2% trypan blue to enable counting of viable cells. This was loaded onto a haemocytometer (Hausser Scientific) and the cells were counted to determine the volume of suspension required for the given experiment. Cell cultures were replaced from cryogenically preserved stocks (see Section 2.2.1.2 [Cryopreservation](#)) once reaching predefined 'high' passage numbers (i.e. passage 15-20). All cell culture manipulation was conducted in sterile conditions.

2.2.1.2 Cryopreservation

To maintain early passage cell lines for use, cryopreserved stocks were established. Cells were harvested, suspended in appropriate complete medium and pelleted gently by centrifugation at 1500 x *g* at room temperature (RT) for 5 minutes. Cell pellets were resuspended in freezing medium (FBS containing 10% DMSO) such that there were approximately 5.0×10^5 cells/mL. Approximately 1 mL of cell suspension was transferred into each cryotube vial (Nunc), which were stored at -80°C for short term storage, or in liquid nitrogen for long-term/indefinite storage.

On removal from cold storage, vials were rapidly thawed in a 37°C water bath (~1-2 minutes), and cells were transferred to a T75 flask containing appropriate prewarmed complete medium. Medium was replaced after 16-24 hours to remove residual DMSO and cells were subsequently cultured as aforementioned (Section 2.2.1.1 [Cell Culture Maintenance](#)).

2.2.1.3 Transfection

For luciferase assays, protein interaction and expression experiments, HEK-293T cells were reverse transfected using Lipofectamine 2000 (Thermo Fisher Scientific) using a modified version of the manufacturer's protocol with a 1:2 DNA to Lipofectamine ratio. To prepare complexes, the desired amount of plasmid DNA (as listed in each figure caption) and Lipofectamine reagent were each diluted separately in 100-500 µL serum free DMEM (approximately 50 µL per microgram of DNA). These mixtures were incubated separately for 5 minutes at RT, then combined and incubated for 20 minutes at RT to allow for DNA-Lipofectamine complex formation before adding to cells. Transfected cells were cultured as previously mentioned (Section 2.2.1.1 [Cell Culture Maintenance](#)) until harvest. MDA-MB-231 and MDA-MB-453 cells were transfected following the same experimental pipeline but with a 1:4 DNA to Lipofectamine ratio.

2.2.2 Gene Expression Analysis

2.2.2.1 RNA Extraction

Total RNA was extracted using TRIzol reagent (Invitrogen) from 80-90% confluent wells of a 6-well plate, as per the manufacturer's instructions. Briefly, cells were initially washed with PBS and subsequently harvested in 1 mL TRIzol reagent by incubating for 20 minutes at RT on a rocking platform. Lysates were transferred to microcentrifuge tubes, and 200 μ L of chloroform was added to each sample, followed by extensive mixing. Tubes were centrifuged at 12000 $\times g$ for 15 minutes at 4°C and the aqueous layer containing the RNA was transferred to a fresh tube. RNA was precipitated by the addition of 500 μ L isopropanol, followed by an incubation for 10 minutes at RT and centrifugation at 12000 $\times g$ for 10 minutes at 4°C. The RNA pellet was washed with 1 mL of 75% ethanol, re-pelleted by centrifugation and air dried before resuspension in 20 μ L of nuclease free water. RNA was quantified using a NanoDrop (Thermo Fisher), with quality assessed by OD260/280 ratio.

2.2.2.2 Generation of cDNA

To synthesise cDNA from extracted RNA, 2-4 μ g RNA (normalised for each experiment) was treated with DNase I (Life Technologies) in 15 μ L reactions as per the manufacturer's protocol and heat inactivated by the addition of 1.5 μ L of 2.5 mM EDTA and incubation at 75°C for 5 minutes. Reverse transcription of DNase-treated RNA was performed using NxGen[®] M-MuLV Reverse Transcriptase (Lucigen) as per manufacturer's protocol. To do so, 8 μ L of DNase treated cDNA was incubated for 5 mins at 65°C for 5 minutes with 1 μ L of 10 mM dNTPs, 1 μ L of random hexamers (50 ng/ μ L) and 6 μ L of nuclease free water. Subsequently, NxGen M-MuLV Reverse transcriptase and NxGen RNase inhibitor and 1x reverse transcriptase buffer were added to bring the total reaction volume to 20 μ L. This was incubated at 42°C for 1 hour followed by heat inactivation at 90°C for 10 minutes. Synthesised cDNA was diluted 1:5 in nuclease free water.

2.2.2.3 Quantitative RT-PCR

Quantitative real-time PCR (RT-PCR) was used to quantify levels of mRNA transcripts. and performed using qPCR Master Mix (Promega) as per manufacturer's protocol in 20 μ L reactions. Each reaction contained: 20 ng of cDNA, 1X GoTaq qPCR Master Mix (Promega) and 0.5 μ M forward and reverse primers for the target gene. Reactions were performed

using a Rotor-gene RG3000 (Qiagen) under the cycling conditions listed in Table 2.1. Primer sets used are detailed in the appropriate chapters. In order to calculate the fold change of gene expression relative to a defined control, the $2^{-\Delta\Delta Ct}$ method (Livak & Schmittgen, 2001) was utilised, as per the following equation:

$$\Delta\Delta Ct = (Ct_{TX} - Ct_{T_HKG}) - (Ct_{CX} - Ct_{C_HKG})$$

$$\text{Fold Change} = 2^{-\Delta\Delta Ct}$$

Ct_{TX} = Ct value for gene of interest in treatment condition

Ct_{T_HKG} = Ct value for House Keeping Gene in treatment condition

Ct_{CX} = Ct value for gene of interest in control condition

Ct_{C_HKG} = Ct value for House Keeping Gene in control condition

Table 2.1: qRT-PCR cycling conditions

PCR Step		Temperature	Duration
Activation		95°C	10 minutes
Cycling (40X)	Denaturation	95°C	10 seconds
	Annealing (Depended on primer set)	60-65°C	15 seconds
	Extension (Data acquisition of SYBR Green Fluorescence)	72°C	20 seconds
Melt		Ramp from 55-95°C at 1°C per second and hold for 3 minutes at 95°C	

2.2.3 Crystal Violet assays

Crystal violet assays were performed to assess the proliferative capacity of cell lines (Feoktistova et al., 2016). Using 96 well plates, 5.0×10^4 cells/well were seeded in 100 μ L of complete medium and cultured under aforementioned conditions (Section 2.2.1.1 [Cell Culture Maintenance](#)). To fix cells at each time, growth medium was removed, and cells

were fixed with 0.5% crystal violet in 50% methanol (50 μ L per well) and incubated for 20 minutes at RT on an orbital shaker. To remove excess crystal violet, plates were gently washed using tap water and air dried overnight. Crystal violet was solubilised in 100 μ L of 33% acetic acid per well and incubated on a rocking platform for 20 minutes at RT. The optical density was measured at 595 nm utilising a Beckman Coulter DTX 880 Multimode Detector with SoftMax Pro 7 Software. To assess the plating density, cells were incubated for 6 hours prior to cellular fixation, providing enough time for cells to adhere without proliferating. Optical density at each time point was normalised to the plating density and empty vector (pIRES) control. Significance was assessed via One-way ANOVA with post-hoc testing.

2.2.4 Protein Co-expression and Co-immunoprecipitation (Co-IP) analysis

2.2.4.1 Lysate Preparation

For protein co-expression and co-immunoprecipitation (co-IP) experiments, HEK-293T cells were reverse-transfected in two T25 flasks as previously described (Section 2.2.1.3 [Transfection](#)) with 5 μ g total plasmid DNA per condition. Cell lysates were prepared by harvesting cells 48 hours post transfection in 400 μ L of hypotonic lysis buffer (Table S2 - [Appendix 1](#)) per T25 flasks on ice with protease inhibitor cocktail, PhosSTOP(Roche) and glycerol-2-phosphate phosphatase inhibitors (Roche) included as per Klenova et al. (2002). Cell membranes were disrupted via passaging through a 30G needle 10 times and subsequently supplemented with NaCl to a concentration of 150 mM. Lysates were sonicated on ice using a Sonics Vibracell VCX130 (John Morris Scientific) with a 3 mm stepped microtip probe as follows: 25% amplitude, two 15 second pulses and one 10 second pulse, with a 60 second rest between pulses. Sonicated lysates were incubated for 1 hour at 4°C while rotating and cellular debris was removed via centrifugation for 15 minutes at 20,000 x *g* at 4°C. For co-expression experiments, samples were either used directly for immunoblotting (see Section 2.2.5.3 [Polyacrylamide Gel Electrophoresis \(PAGE\), Transfer and Imaging](#)) or stored at -20°C.

2.2.4.2 Co-immunoprecipitation

For co-immunoprecipitation (co-IP), cell lysates were initially pre-cleared with 20 μ L of Protein G Magnetic beads (Cell Signaling Technology) for 1 hour and then divided as

follows: 20 μL positive input control, 200 μL for immunoprecipitation and 200 μL for IgG pre-immune control. To the treatment lysates, 2.5 μg of specific antibody or normal IgG (same species) were added to the immunoprecipitation and IgG pre-immune control sample, respectively. Samples were incubated overnight while rotating at 4°C. Protein complexes were captured via incubation with 20 μL of Protein G Magnetic beads for 2-3 hours at 4°C and then washed three times for 10 minutes each with cold PBS. Complexes were captured between each wash using a magnetic stand. Finally, complexes were eluted with 20 μL of SDS sample dye (Table S2 - [Appendix 1](#)) and incubated for 10 minutes at RT before being resolved via SDS-PAGE for immunoblotting (Section 2.2.5.3 [Polyacrylamide Gel Electrophoresis \(PAGE\), Transfer and Imaging](#)).

2.2.5 Western Blotting

2.2.5.1 Lysate Preparation

For isolation of protein from stable overexpression lines, cultured cells were scraped from the flask in PBS and pelleted via centrifugation at 1500 $\times g$ for 10 minutes at 4°C. The cell pellet was resuspended in 20-100 μL Radioimmunoprecipitation assay (RIPA) buffer (Table S2 - [Appendix 1](#)) with proteinase inhibitor cocktail and passed through a 30G needle ten times to facilitate lysis. Lysates were incubated on ice for 20 minutes and insoluble material was removed via centrifugation at 10,000 $\times g$ for 10 minutes. All lysates were used directly for immunoblotting or stored at -20°C.

2.2.5.2 Polyacrylamide Gel Electrophoresis (PAGE), Transfer and Imaging

The total protein concentration of RIPA lysates was quantified using the Bio-Rad Protein Assay reagent (Bio-Rad, NSW, Australia) through the establishment of a BSA standard curve as per the manufacturer's protocol. Briefly, 200 μL of diluted Bio-Rad Protein Assay reagent was added to each sample and standard (0.1-1 mg/mL BSA) in duplicate in a 96-well plate and incubated for 20 minutes at RT prior to measurement of absorbance at 595nm in the multimode detector plate reader. Protein samples were normalised for each experiment (~20-50 μg) and diluted in SDS-PAGE loading buffer (Table S2 - [Appendix 1](#)) and incubated for 10 minutes at RT. Proteins were separated at RT by SDS-PAGE with 4% stacking and 10% resolving polyacrylamide gels, at 70 V and 120 V respectively, using Mini-Protean II Cell equipment (Bio-Rad). Protein lysates were resolved alongside a Precision Plus WesternC standards (Bio-Rad) molecular weight marker.

Resolved proteins were transferred onto Trans-blot nitrocellulose membrane (0.45 μm , Bio-Rad) in an ice-cooled Mini Trans-Blot Cell apparatus at 100 V for 1 hour at 4°C. Membranes were washed in TBST (Tris-buffered saline (TBS) with 0.2% Tween 20) and then blocked in 5% (w/v) non-fat milk powder in TBST blocking buffer for 90 minutes at RT. Appropriate primary antibodies (as detailed in Figure captions for specific experiments) were added at a dilution of 1:2000 in 2% blocking buffer and incubated on rocking platform overnight at 4°C. In all figures of immunoblots, the antibody used has been indicated as IB: antibody, for ease of reading. Membranes were washed in TBST three times for 10 minutes at RT prior to addition of secondary antibody HRP-conjugates in 2% blocking buffer, which were then incubated on a rocking platform for 2-3 hours at RT. Finally, membranes were washed in TBST prior to imaging. SuperSignal West Pico chemiluminescent (ECL) HRP substrate (Thermo Fisher Scientific) was used as per the manufacturer's instructions and blots were imaged using an ImageQuant LAS-4000 (Ge Healthcare Life Sciences). Where appropriate, ImageJ FIJI software was utilised to quantify relative band intensity via densitometry (Schindelin et al., 2012).

2.2.6 Luciferase Assays

HEK-293T, MDA-MB-231 and MDA-MB-453 cells were reverse transfected in triplicate as previously mentioned (Section 2.2.1.3 [Transfection](#)). Typically, cells were plated at 3.6×10^4 cells/well in 48-well plates and transfected with 8 ng of pRL-null and a total of 250 ng of appropriate plasmid DNA. At 48-hours post transfection, cells were harvested by the addition of 50 μL of Passive Lysis Buffer (Promega) to each well and incubated at RT on a rocking platform for 20 minutes. Lysates were either assayed immediately or stored at -20°C. Using the Dual-Luciferase reporter assay system (Promega), 20 μL of lysate was analysed as per the manufacturer's protocol, using either a TopCount NXT scintillation and luminescence counter (Packard, Australia) or an iD5 multi-mode microplate reader (Molecular Devices, California, USA), for firefly (*Photinus pyralis*) and *Renilla* (*Renilla reniformis*) luciferase activity. To minimise carry-over luminescence, lysates were analysed in alternate wells of a 96-well white opaque OptiPlate (PerkinElmer). Relative luciferase activities (firefly/*Renilla* luciferase activity) were calculated for each well and then averaged across triplicates.

2.2.7 Molecular Cloning and Associated Methods

2.2.7.1 Polymerase Chain Reaction (PCR)

PCR for generation of DNA fragments for cloning was performed with the high fidelity Phusion DNA polymerase (Thermo Fisher Scientific) in 50 μ L reactions as per the manufacturer's protocol. Phusion reactions consisted of the supplied Phusion HF buffer, 0.02 Units/ μ L *Phusion*, 200 μ M dNTPs and 0.5 μ M each primer. For PCR screening where fidelity was not essential, 20 μ L Phire Hot Start DNA polymerase (Thermo Fisher Scientific) was used. Reactions were performed as per the manufacturer's protocol and consisted of the supplied buffer, 0.02 Units/ μ L *Phire*, 200 μ M dNTPs and 0.5 μ M each primer. All amplification and incubation steps were conducted using a Bio-Rad iCycler™ thermal cycler with optimal annealing temperatures calculated based on primer melting temperature.

2.2.7.2 Restriction Digests

Restriction digests of PCR products and plasmid vectors for cloning and diagnostic analysis were performed using New England Biolab (NEB) enzymes in 50 μ L reactions with the supplied buffer. Reactions were performed with 15-20 μ L of PCR product or 5 μ g of plasmid DNA and incubated at 37°C for 3-5 hours. For cloning purposes, restriction digests of PCR products originating from plasmid DNA were treated with 1 μ L of DpnI for 1 hour at 37°C to remove template plasmid DNA. Digested vectors were treated with Antarctic phosphatase (NEB) for 30 minutes to prevent re-ligation of excised fragments during ligation. All products digested for cloning were subsequently purified using the Qiagen QIAquick PCR purification kit (Qiagen) as per the manufacturer's instructions.

2.2.7.3 Ligation and Transformation

Ligations were performed using the NEB quick ligation kit containing 2X quick ligation buffer and T4 DNA ligase. Reactions were prepared in a total 14 μ L with a 3-5 molar excess of insert DNA to vector DNA. The reaction mixture was incubated at RT for 10 minutes and subsequently stored at -20°C or chilled on ice for immediate use for transformation.

Transformations were performed using competent DH5 α *E. coli* cells (prepared as per Section 2.2.6.6 [Competent Cell Preparation](#)) via heat shock. Briefly, 2 μ L of ligation product was added to 50 μ L of competent cells (thawed on ice), mixed gently, and incubated on ice for 20-30 minutes. Cells were heat shocked for 45 seconds at 42°C to facilitate uptake of DNA, and then incubated on ice for 2 minutes. Heat shocked cells were then incubated with

450 µL of LB (Luria-Bertani) broth without antibiotics at 37°C with shaking for 1 hour. Transformed bacteria were then cultured on prewarmed LB-agar plates with appropriate selection (ampicillin 100 µg/mL or kanamycin 25 µg/mL) overnight at 37°C. If necessary, colonies were screened for the presence of appropriate inserts by PCR. Colonies were picked from the plate and transferred to PCR tubes containing 30 µL of nuclease free water. They were boiled for 10 minutes, after which 2 µL of the lysate was used as template DNA in a Phire PCR reaction, as previously described (2.2.6.1 [Polymerase Chain Reaction](#)).

2.2.7.4 Bacterial Culture and Plasmid Preparation

Colonies screened as positive via PCR screening were cultured in broth culture for plasmid extraction. Colonies were transferred via sterile pipette tip into 5 mL (Miniprep) or 100 mL (Midiprep) LB broth cultures containing appropriate antibiotics. Cultures were subsequently grown for 16-20 hours in an Innova 4330 incubator shaker at 37°C and shaken at 200 rpm. Qiagen MiniPrep or Midi Kits were utilised as per manufacturer's protocol for plasmid extraction.

Previously established bacterial freezer stocks were also used to establish broth cultures for plasmid extraction by scraping stock with a sterile pipette tip and using tip to inoculate an appropriate volume of LB broth and cultured under these same conditions. To establish bacterial freezer stocks, overnight broth cultures were combined with sterile glycerol to a concentration of 25% and stored at -80°C indefinitely.

2.2.7.5 Agarose Gel Electrophoresis

To analyse DNA products, agarose gel electrophoresis was performed. Agarose gels (1%) were prepared in TAE buffer (Table S2 - [Appendix 1](#)) with the addition of SYBR™ Safe DNA Gel Stain (1:25,000 dilution; Thermo Fisher Scientific). Samples were prepared in Gel Loading Dye and loading alongside an appropriate DNA ladder (100 bp or 1 kb; NEB). Samples were electrophoresed at 100-120V (constant ampere) and visualised in a GeneGenius bio-imaging system apparatus (Syngene, Cambridge, England) using GeneSnap version 6.04 software.

2.2.7.6 Site-Directed Mutagenesis

Oligonucleotides for site-directed mutagenesis (SDM) were purchased as standard (desalted) and were purified by polyacrylamide gel electrophoresis (PAGE) in the laboratory prior to use. Complementary primers were annealed in 50 µL reactions by combining 2250

μM of each primer in 1X NEBuffer 2 (10 mM Tris-HCl, 50 mM NaCl, 10 mM MgCl₂ and 1 mM DTT, pH 7.9; NEB), incubating at 99°C for 5 minutes in a thermocycler and then allowing the reaction to slowly cool in the open machine for 2 hours (until it reached RT). Annealed primers were resolved on a 10% polyacrylamide gel in 0.5X TBE (Table S2 - [Appendix 1](#)). They were visualised by staining with a 1:1000 dilution of SYBR Safe DNA Gel stain in 0.5X TBE and exposing to UV light. Primers were excised from the gel and eluted in 400 μL of 1X NEBuffer 2 (NEB) by rotating overnight at 4°C. The primers were then precipitated by the addition of 40 μL of 3 M sodium acetate and 800 μL of cold ethanol and centrifuged at 13,000 $\times g$ for 20 minutes. The DNA pellet was resuspended and washed in 1 mL of 70% ethanol, re-centrifuged and resuspended in 50 μL of TE buffer (Table S2 - [Appendix 1](#)).

Using 100 ng of plasmid DNA template and 2 μL of PAGE-purified primers, 50 μL Phusion PCR reactions were performed for a total of 18 amplification cycles. Post-amplification, the amplified vector was incubated with 10 units of DpnI at 37°C for 1 hour to degrade the wild-type parent vector, 1-2 μL of digested PCR product was then used for transformation of DH5 α competent *E. coli* as described (see Section 2.2.7.3 [Ligation and Transformation](#)). For Phire PCR screening of bacterial colonies for the desired mutation, an oligonucleotide was designed such that the mutated nucleotides were present on the 3' terminal end, allowing for amplification of only the mutated sequence. Colonies that screened positive were confirmed by sequencing for the desired mutation.

2.2.7.7 Competent Cell Preparation

Competent DH5 α *E. coli* were prepared using a modified version of the Hanahan protocol (Hanahan et al., 1991). Initially, a 5 mL DH5 α overnight culture was established from a glycerol stock (Section 2.2.6.4 [Bacterial Culture and Plasmid Preparation](#)), 1 mL of which was used to inoculate a 100 mL LB broth culture. This culture was incubated at 37°C with shaking until the OD₆₀₀ reached 0.25-0.30. The culture was centrifuged at 3000g at 4°C for 10 minutes and then the pellet was resuspended in 32 mL of cold CCMB80 buffer (Table S2 - [Appendix 1](#)) and incubated on ice for 20 minutes. The cells were centrifuged as previously and subsequently resuspended in 4 mL of cold CCMB80 buffer. Competent cells were aliquoted and stored at -80°C.

2.2.7.8 Sequencing

Sanger sequencing was conducted to validate DNA sequences. Sequencing reactions were performed by the Flinders Sequencing Facility (Genetics & Molecular Pathology Directorate, Flinders Medical Centre site, SA Pathology, South Australia) using Big Dye Terminator Cycle Sequencing Version 3.1 chemistry (Applied Biosystems, Foster City, CA) and an ABI 3130xl Genetic Analyser sequencer (Applied Biosystems). Results obtained from sequencing were analysed by aligning to expected sequence using the EMBL-EBI Pairwise Sequence Alignment Tool (Madeira et al., 2019). The commonly used standard sequencing primers are listed below (Table 2.2).

Table 2.2 Commonly used Sequencing Primers

Primer Name	Sequence (5'→3')
T7 F	TAATACGACTCACTATAGGG
SP6 F	ATTTAGGTGACACTATAG
M13 F (-20)	GTAAAACGACGGCCAG
M13 R	CAGGAAACAGCTATGAC
pBABE F	CTTTATCCAGCCCTCAC
pBABE R	ACCCTAACTGACACACATTCC
CMV F	CGCAAATGGGCGGTAGGCGTG

2.2.7.9 Nucleic Acid Quantification

To quantify DNA and RNA yield and purity, a NanoDrop™2000 (Thermo Fisher Scientific) or a GeneQuant II (Pharmacia Biotech) spectrophotometer was used to determine the OD₂₆₀. Absorbance data was given as 1 unit per 50 µg/ml and 40 µg/ml for DNA and RNA, respectively. Nucleic acid concentration was calculated as per the following equations:

$$DNA\ Concentration\ (ng/\mu L) = OD_{260} \times 50 \times Dilution\ Factor$$

$$RNA\ Concentration\ (ng/\mu L) = OD_{260} \times 40 \times Dilution\ Factor$$

The OD₂₆₀/OD₂₈₀ was used to determine the nucleic acid to protein ratio, and thus the samples purity, with a ratio of 1.8-2.0 deemed sufficient.

2.3 Statistics

Statistical analysis of all results presented in this thesis was performed using Microsoft Office Excel or IBM SPSS (Version 26.0) statistics package software. The statistical significance was determined by use of a Student's *t*-test or a one-way ANOVA with Tukey's post hoc testing, as appropriate. A change was deemed statistically significant if $p < 0.05$ and indicated as follows: $p < 0.05$ *, $p < 0.01$ **, $p < 0.001$ ***.

**3. CHAPTER 3 -
ASSOCIATION OF UGT2B11
AND UGT2B28 EXPRESSION
LEVELS WITH CLINICAL AND
BIOCHEMICAL
PARAMETERS IN BREAST
CANCER PATIENT COHORTS**

3.1 INTRODUCTION

As discussed in Chapter 1, UGT2B11 and UGT2B28 have been the subject of minimal research, and the research that has been conducted has been largely focused on their cellular functions with respect to prostate cancer. High *UGT2B28* mRNA expression has been associated with poor survival outcomes in prostate cancer patients, and it has been proposed that this is due to modulation of circulating androgen levels (Lacombe et al., 2023). The role of UGT2B11 has not been examined in these prostate cancer studies; however, it is widely considered to be a paralog of UGT2B28. As mentioned in Chapter 1, UGT2B11 and UGT2B28 share high amino acid sequence identity, and have very similar promoter sequences, including conserved regulatory elements involved in their androgen-dependent regulation. Thus, it is likely that these UGTs share overlapping functions in prostate cancer. Furthermore, given the frequent deletion of *UGT2B28*, the maintenance of the UGT2B11 gene may indicate a balancing selection mechanism, such that the genes possess the same cellular functions to allow for compensation in individuals with a homozygous null UGT2B28 genotype (Aqil et al., 2023). Whilst the majority of research on UGT2B11 and UGT2B28 expression and function has been conducted in prostate cancer, minimal research has been conducted in breast cancer.

The androgen receptor (AR) is expressed in ~80% of all breast tumours including both ER-positive and ER-negative disease states. In some ER-negative contexts, specifically molecularly defined luminal AR type triple negative breast cancers (LAR-TNBC) and the histologically defined molecular apocrine (MA) breast cancers, androgen signalling is proposed to promote growth (Proverbs-Singh et al., 2015). These cancers can show androgen-dependent gene expression programs similar to prostate cancers. In such breast cancer subtypes, UGT2B11 and UGT2B28 may have a similar role to that previously described in prostate cancer and associate with worse outcomes for patients.

Breast cancer is highly heterogeneous with subtypes defined by such extensive genetic, epigenetic and phenotypic variation that they could be described as different diseases. It is therefore vital to investigate the roles of UGTs in a subtype-specific manner. It was previously shown that UGT2B11 and UGT2B28 are highly inducible by androgens in the MDA-MB-453 breast cancer cell line (Moore et al., 2012), which is generally considered to represent the LAR/MA-type tumour type. This suggested that these UGTs may show higher expression in breast tumour subtypes that express a higher level of AR, and that they may

be most functionally relevant in this subtype. To examine relative UGT expression in various breast cancer subtypes, and associations between UGT expression and survival outcomes, databases such as The Cancer Genome Atlas (TCGA) and the Molecular Taxonomy of Breast Cancer International Consortium (METABRIC) are invaluable resources. In studies described in this Chapter, the cBio Cancer Genomics Portal (cBioPortal) web server was utilised to access both of these datasets. cBioPortal is an open-access resource which allows for gene expression analysis in predefined breast cancer subtypes and in biologically relevant user-defined groups (Cerami et al., 2012).

3.1.1 The Cancer Genome Atlas (TCGA)

The TCGA database was the result of a landmark cancer genomics program whereby 20,000 primary cancer and matched normal samples spanning 33 cancer types were subject to genomic, epigenomic, transcriptomic, and proteomic analyses (Tomczak et al., 2015). The TCGA breast cancer cohort (TCGA-BRCA) is comprised of 1098 tumour samples. Transcriptomic analysis was performed via RNA-sequencing, and whole genomic profiling was undertaken with Sanger DNA-sequencing. This data was paired with clinical data such as demographics, diagnosis and treatment information, and survival outcomes, allowing for comprehensive pan-cancer analyses.

3.1.2 The Molecular Taxonomy of Breast Cancer International Consortium (METABRIC) project

The METABRIC database is comprised of 1992 primary tumours for which long term patient outcomes have been integrated together with genomic and transcriptomic analyses (Curtis et al., 2012). METABRIC genomic profiling was performed using Affymetrix SNP 6.0 microarrays which contain markers including SNPs and probes for detection of copy number variation. Transcriptional profiling was performed by the microarray method using Illumina HT-12 v3 Expression BeadChips. Thus, inherited variants (copy number variants (CNVs) and single nucleotide polymorphisms (SNPs)) and acquired mutations and somatic copy number aberrations (CNAs), can be integrated with gene expression data and clinical outcomes. This genomic profiling ultimately allowed for the discovery of 10 novel biological subgroups of breast cancer, referred to as integrative clusters, which were stratified by well-defined copy number aberrations.

3.1.3 UGTs correlate with Lipid Metabolism Gene Signatures

Previously, our laboratory conducted a series of preliminary bioinformatic analyses to gain insight into potential cellular functions of UGT2B11 and UGT2B28 in breast cancer cells. These analyses were performed using the TCGA-BRCA cohort dataset and the Genotype-Tissue Expression (GTEx) dataset. To access and manipulate these data, the GEPIA2 (Gene Expression Profiling Interactive Analysis 2) platform was utilised. GEPIA provides access to TCGA and the GTEx data for gene expression analysis, and it also has a function that allows for a gene signature to be defined (Tang et al., 2019; Tang et al., 2017). Genes whose expression was robustly correlated ($R > 0.9$) with *UGT2B11* and *UGT2B28* expression in normal breast tissue samples ($n=112$) were initially identified using GEPIA2. These co-expressed genes were then subjected to pathway analysis using the Reactome pathway analysis web server, which is a manually curated bioinformatics platform that identifies gene signatures associated with functional cellular pathways (Fabregat et al., 2015; Fabregat et al., 2017). These analyses showed that the gene set most strongly correlated with *UGT2B11* and *UGT2B28* expression was enriched with genes associated with SREBP-mediated lipid metabolism pathways.

Next, core gene signatures associated with lipid metabolism (AACS, ALDH3B2, DHCR7, HMGCSI, HRASLS2, MOGAT2, ACSL3, ALOX15B, FDFTI, HMGCS2, HSD3B1, MSMOI, SRD5A1, AWAT2, GGTI, HPGD, IDII, MVK, PLA2G4E, FADS2, SCP2, APOD, PNLIPRP3) and SREBP signalling (DHCR7, IDI1, FDFTI, MVK, HMGCSI) were defined using GEPIA2. Correlation coefficients for all 22 UGT isoforms relative to these gene signatures were examined using the independent TCGA-BRCA dataset. The expression of all UGT1A and UGT2A family members (12 genes), plus UGT2B4, UGT2B15, and UGT2B17, were not significantly correlated with these gene signatures. In contrast, the expression of *UGT2B7*, *UGT2B10*, *UGT2B11*, and *UGT2B28* were significantly positively correlated with both signatures. The correlation coefficients were close to 1.0 (ranging 0.91 to 0.93) for *UGT2B11* and *UGT2B28* but were lower (ranging from 0.67 to 0.83) for *UGT2B7* and *UGT2B10* (Table 3.1). This suggests a strong relationship between UGT2B11 and UGT2B28, and lipid signalling pathways, and potentially more broadly with this group of homologous UGT2B enzymes. In further support of this conclusion, literature analysis uncovered two studies that found a correlation between the expression of *UGT2B11* and a lipogenic gene signature in the

contralateral unaffected breast of patients with ER- breast cancers (Wang et al., 2013; Wang et al., 2017).

Table 3.1: R values for Pearson's correlation of UGT2B enzymes with SREBP Target* and Lipid Metabolism** Gene signatures in TCGA-BRCA breast cancer RNAseq gene expression database (patient samples, n=981). Gene signatures sourced from Reactome Database (Fabregat et al., 2017) and assessed using GEPIA2 (Tang et al., 2019). Statistical significance ($p < 0.05$) was observed for UGT2B7, UGT2B10, UGT2B11 and UGT2B28 only.

	UGT2B4	UGT2B7	UGT2B10	<u>UGT2B11</u>	UGT2B15	UGT2B17	<u>UGT2B28</u>
SREBP Activation	-0.11	0.83	0.73	0.91	0.03	0.46	0.92
Lipid Metabolism	-0.14	0.72	0.67	0.93	0.12	0.44	0.93

*SREBP Gene Signature: DHCR7, IDI1, FDFTI, MVK, HMGCSI

**Lipid Metabolism Signature: AACS, ALDH3B2, DHCR7, HMGCSI, HRASLS2, MOGAT2, ACSL3, ALOX15B, FDFTI, HMGCS2, HSD3B1, MSMOI, SRD5A1, AWAT2, GGTI, HPGD, IDII, MVK, PLA2G4E, FADS2, SCP2, APOD, PNLIPRP3.

Although the bioinformatic analyses described above suggested a relationship between UGT2B11 and UGT2B28 and SREBP and lipid signalling pathways, the nature of the relationship was unclear. One possible explanation was that SREBP signalling was involved in regulating the expression of these *UGT* genes. However, no SRE sequences have been identified in the 5'-upstream promotor sequence of any human UGTs, and previous genome-wide studies of SREBP targets have not identified any UGTs (Hu et al., 2014). An alternative explanation considered was that these UGTs may be involved in mediating the effects of SREBP signalling. This hypothesis is broadly consistent with the known functions of UGTs in modulating signalling pathways involving small lipophilic ligands, for example, modulating steroid and bile acid signalling by altering ligand levels (Meech et al., 2019).

3.1.4 Aims

Based on the prior knowledge described above and the questions raised by it, the overall aim of this chapter was to interrogate the TCGA-BRCA and METABRIC datasets to define the expression profiles of *UGT2B11* and *UGT2B28* in breast cancers and characterizing their association with clinical variables including survival. The objective was to use this information to help refine the hypotheses underpinning the experiments undertaken in the subsequent chapters of this thesis. It would also provide insight into the potential for these UGTs to serve as diagnostic or prognostic biomarkers in breast cancer.

Specifically, the aims of this chapter were as follows:

1. Identify breast cancer subtypes that express the highest levels of *UGT2B11* and *UGT2B28*
2. Determine the relationship between survival outcomes and levels of *UGT2B11* and *UGT2B28* expression
3. Identify gene signatures and functional pathways associated with high *UGT* expression in breast cancer

3.2 METHODS

3.2.1 Gene Expression Analysis

Gene expression correlation analysis was performed using cBioportal for both the METABRIC and TCGA-BRCA datasets. Gene expression data in both of these datasets is presented as Z-scores. A z-score is a measure of how many standard deviations a gene's expression level is from the mean expression level in a reference population. The reference population for each dataset is based upon all samples in each relevant study. Tumours were stratified by subtype, classical histopathological gene markers, or user-defined mRNA expression profiles, the latter of which is described in the relevant figure caption. For the TCGA-BRCA dataset, the ER-negative patient group was defined using ER α protein level \leq 0, and HER2 status was stratified by *ERBB2* mRNA expression. Statistical analysis was performed using an independent two-tailed Student's *t*-test or one-way ANOVA with Tukey's post hoc test as appropriate.

3.2.2 Survival Analysis

For survival analysis, Kaplan-Meier plots were generated using the cBioportal platform. For the METABRIC dataset, the 502 patients recorded as 'Died of Other Causes' were excluded from analysis. These patients were included in the gene expression correlation analysis described above. In most instances, data were stratified by median *UGT* expression; however, in some cases, alternative optimised cut-points were utilised as indicated in the relevant figure captions. Median expression was used due to the presence of outliers where *UGT* expression was extremely high or low. Alternative optimised cut-points were determined by recursive partitioning to determine a cut point where a significant result was identified. Statistical significance for survival between groups was assessed via a logrank test.

3.2.3 Pathway Analysis

Reactome (version 85) was utilised for functional gene pathway analysis (Fabregat et al., 2017). High *UGT2B11* or *UGT2B28* expressing groups were defined within the TCGA-BRCA and METABRIC ER-negative patient cohorts, and the 500 differently highest expressed genes within these groups were analysed using Reactome to assess enrichment of gene pathways. Reactome performs over-representation analysis (hypergeometric distribution

test) to determine whether genes associated with functional pathways are over-represented or enriched within a given sample. Statistical significance was assessed with a Binomial test. The false discovery rate was controlled using the Benjamini-Hochberg method.

3.3 RESULTS

3.3.1 UGT2B11 and UGT2B28 expression is associated with HER2 enrichment and an ER-negative status

The expression of *UGT2B11* and *UGT2B28* has been largely understudied and hence this was examined in a range of different breast cancer groups using the METBRIC and TCGA-BRCA datasets. Initially, the mRNA expression of *UGT2B11* and *UGT2B28* was examined in different molecular breast cancer subtypes (Figure 3.1).

The TCGA-BRCA dataset stratifies data according to standard molecular subtypes (Luminal A, Luminal B, Basal, HER2-enriched, and Normal-like). It does not stratify by ER-alpha ($ER\alpha$) status based on standard methods such as immunohistochemistry (IHC), but does provide quantitative proteomic data that includes $ER\alpha$, allowing the user to define an ER-negative (ER-) group. The METABRIC dataset utilises a 3-gene classifier subtyping system based on ER and HER2 expression (ER+/HER2- low proliferation, ER+/HER2- high proliferation, ER-/HER2-, HER2+). Broadly equivalent subgroups are present in Table 3.2, noting however that ER-/HER2- (also referred to as TNBC) and Basal-like tumours are distinct molecular classes with only about 70-80% of TNBC also classified as Basal-like based on basal markers (Prat et al., 2013). The normal-like group in TCGA-BRCA dataset does not have an equivalent in the METABRIC dataset. Normal-like samples represent the smallest group in the TCGA-BRCA cohort (<5%) and are defined by low tumour cellularity; consequently they are often considered to be false negative biopsies and are excluded from analysis (Peppercorn et al., 2008; Wu et al., 2017). In both datasets, *UGT2B11* and *UGT2B28* expression was significantly different between subgroups: the HER2 enriched subgroups showed the highest expression of both *UGT2B11* and *UGT2B28* mRNA, while basal or TNBC subtypes showed the lowest expression of these *UGTs*. These associations were statistically significant for both genes in both datasets (Figure 3.1).

Table 3.2: Comparison of broadly similar molecularly based groupings used in TCGA-BRCA and METABRIC databases

TCGA-BRCA	Classical Subtyping	Luminal A	Luminal B	Basal-like	Her2-enriched
METABRIC	3-Gene Classifier	ER+/HER2- Low Proliferation	ER+/HER2- High Proliferation	ER-/HER2-	HER2+

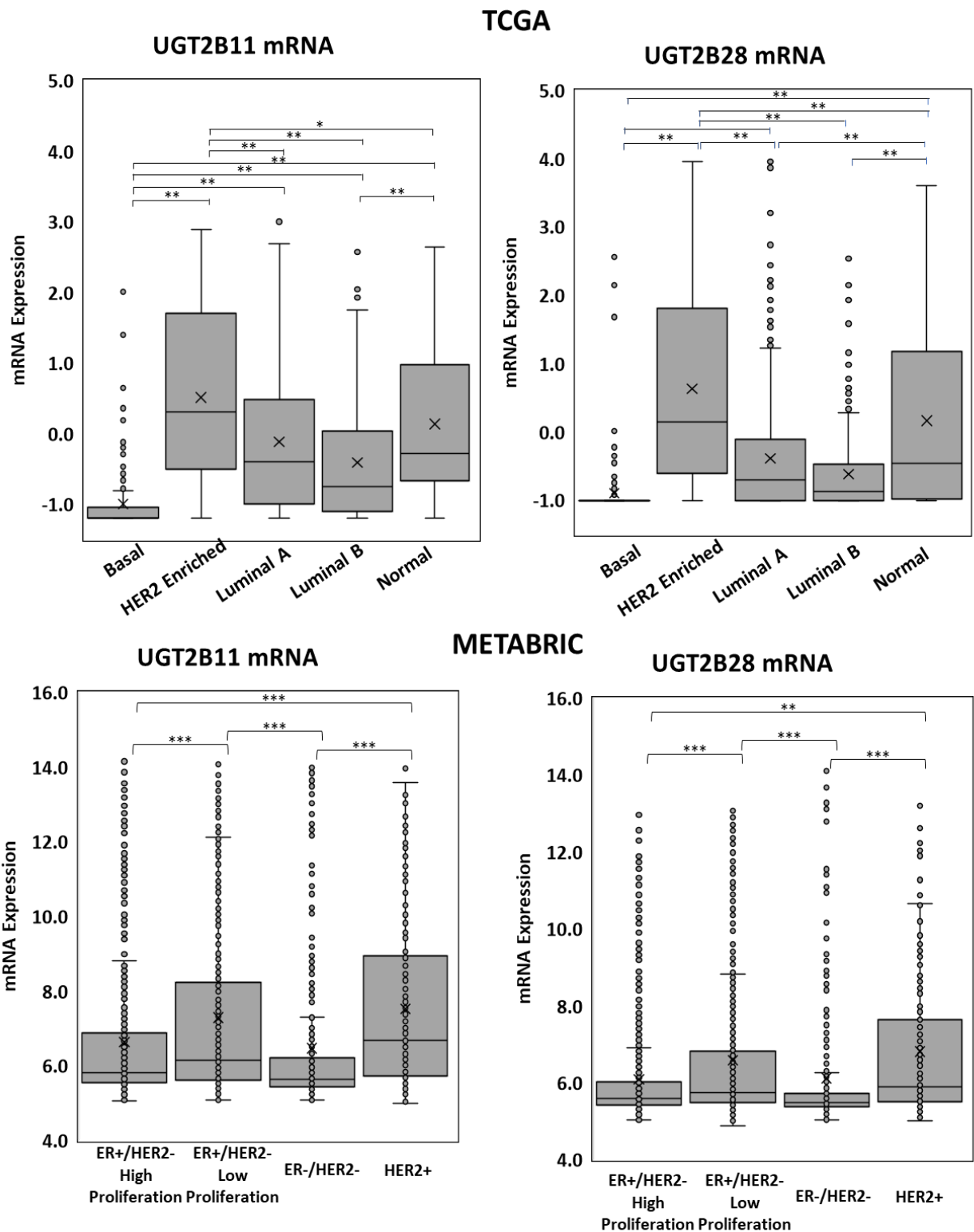


Figure 3.1: *UGT2B11* and *UGT2B28* mRNA expression in different TCGA-BRCA molecular subtypes and METABRIC 3-gene identifier subtypes

Expression of *UGT2B11* and *UGT2B28* in different breast cancer subtypes was analyzed using both the TCGA-BRCA (n=981) and METABRIC (n=1764) breast cancer and cohorts. Box and whisker plots represent the median, and interquartile range and outlier data points are shown, where X indicates mean of dataset. Statistical significance was assessed by one-way ANOVA followed by post-hoc testing and indicated as follows, p<0.05 *, p<0.01 **, p<0.001 ***.

Subsequently, the expression of *UGT2B11* and *UGT2B28* was stratified by molecularly defined Integrative Clusters (IntClust) in the METABRIC dataset (Figure 3.2). Whilst the TCGA-BRCA dataset does not have similar stratification categories, the integrative clusters do partly overlap with the aforementioned molecular subtypes. The highest mean expression of both *UGT2B11* and *UGT2B28* was observed in the integrative clusters IntClust3, 4ER+, 4ER-, 5 and 7 and 8, whose means were not significantly different from each other (ANOVA and Tukeys HSD).

Each of these clusters contains ER+ luminal A and B tumours except for 4ER- which comprises ER-negative tumours. Notably, IntClust5 encompassed the HER2 enriched cancers (Daemen & Manning, 2018) and historically showed the worst survival outcomes of the 10 integrative clusters (Curtis et al., 2012). The lowest *mean* expression levels were observed in IntClust 1, 2, 6 and 10, whose means were not significantly different from each other (ANOVA and Tukeys HSD). IntClust 1, 2 and 6 are comprised of different subsets of ER+ luminal A and B tumours, and IntClust10 is comprised entirely of basal cancers (Figure 3.2). These results are broadly concordant with those from the molecular subtype analyses which indicated that both *UGTs* show low expression in TNBC and basal-like cancers. The overall conclusion from these analyses is that high *UGT2B11* and *UGT2B28* expression is positively associated with HER2 enrichment and negatively associated with the basal subtype.

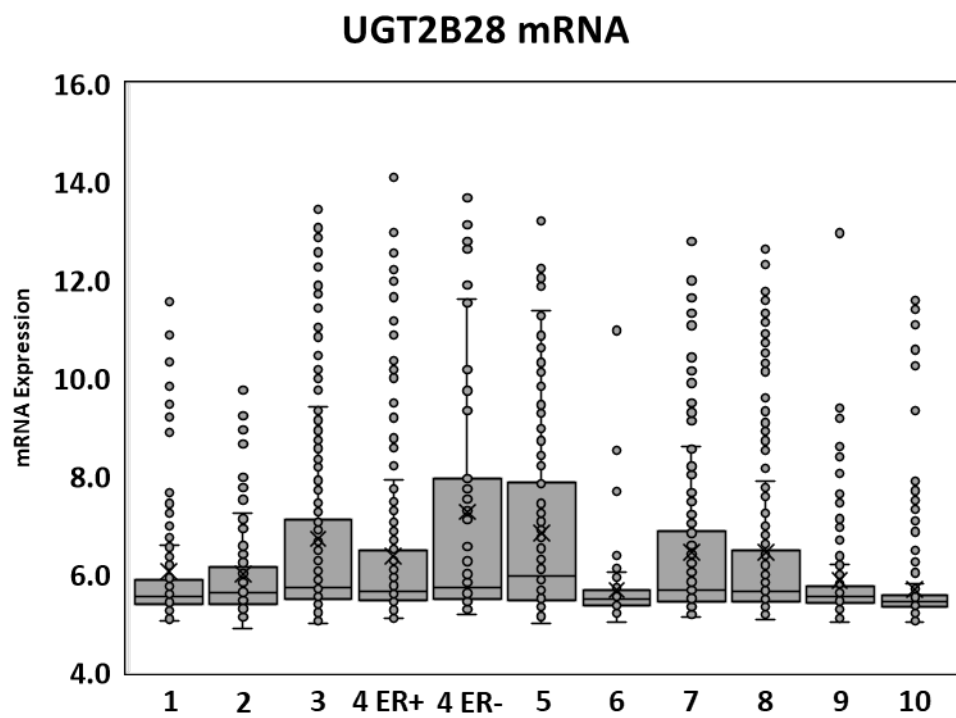
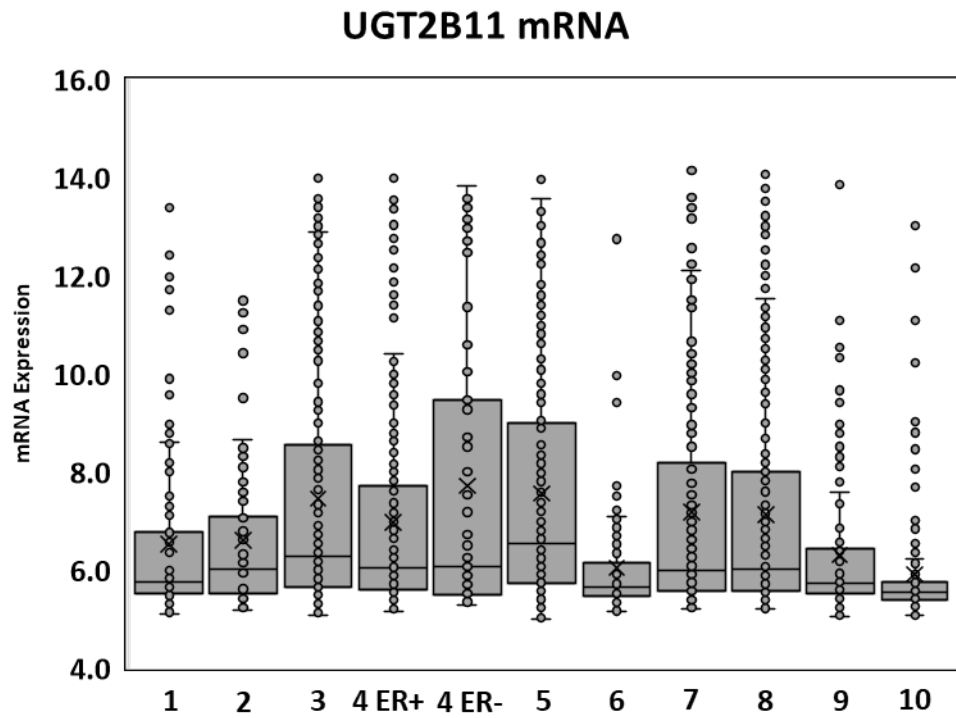


Figure 3.2: *UGT2B11* and *UGT2B28* mRNA expression in METABRIC integrative clusters

Expression of *UGT2B11* and *UGT2B28* mRNA in METABRIC integrative clusters (n=1980). Box and whisker plots represent the median and interquartile range and outlier data points are shown, where X indicates mean of dataset.

To better understand the relationship between *UGT2B11* and *UGT2B28* expression and ER expression status, tumours were stratified by ER expression. There was no statistically significant difference in *UGT* expression between ER-positive and ER-negative tumours in either the TCGA-BRCA or METABRIC dataset (Figure 3.3). This contradicts the findings of Wang et al. (2013), where *UGT2B11* expression was significantly higher in ER- breast tumours compared to ER+, however, this may be due to the small sample size of their study (n=24).

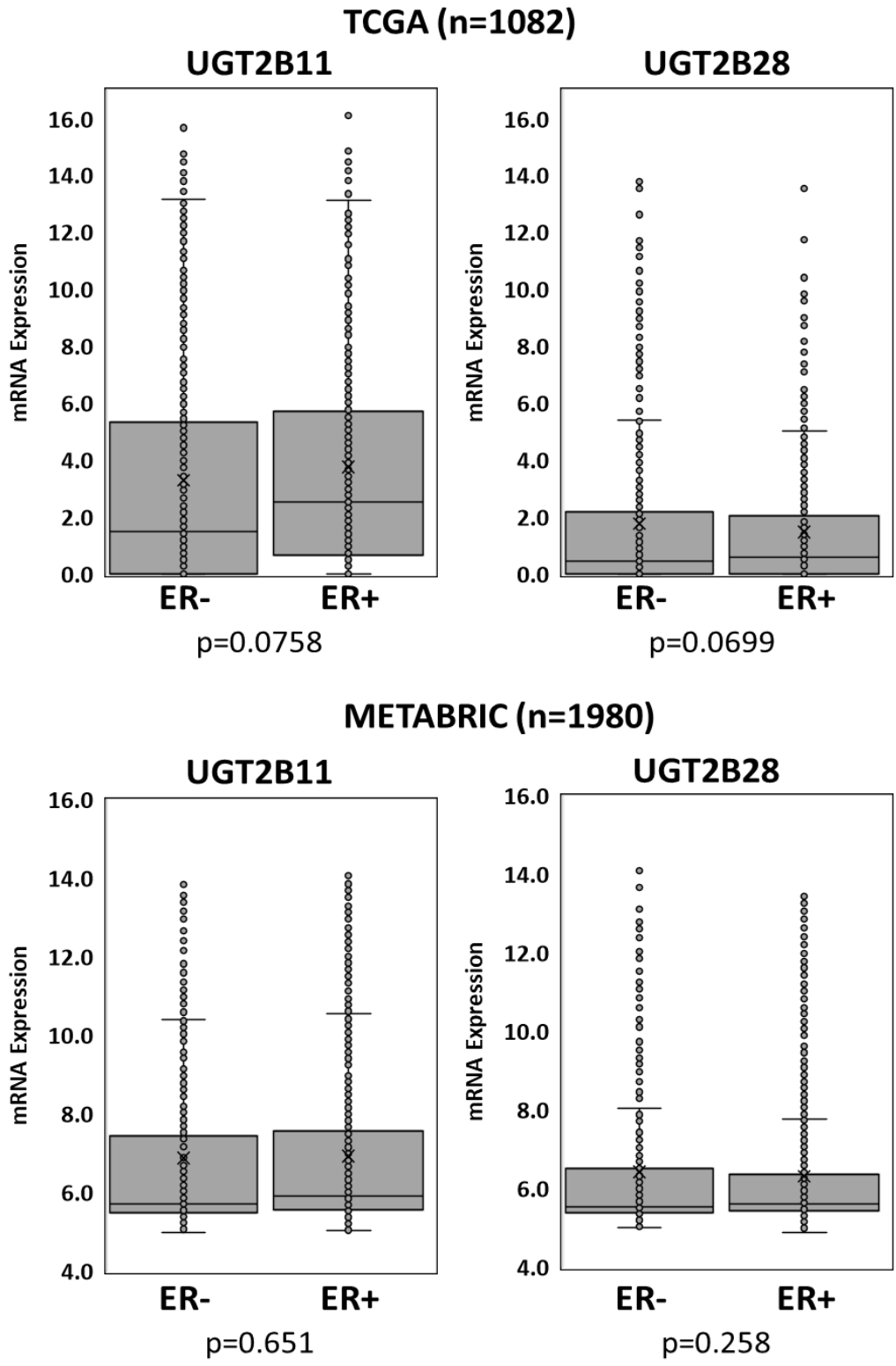


Figure 3.3: *UGT2B11* and *UGT2B28* mRNA expression does not correlate with estrogen receptor status in breast tumours

UGT2B11 and *UGT2B28* mRNA expression z-scores were correlated with estrogen receptor expression status in TCGA-BRCA and METABRIC cohorts. Box and whisker plots represent the median, and interquartile range and outlier data points are shown, where X indicates mean of dataset. Statistical significance assessed via Student's *t*-test.

The relationship between *UGT* expression and HER2 status was further examined by stratifying the entire cohort in each database by HER2 status. For the METABRIC cohort the HER2- group (n = 1782) was obtained by subtracting the HER2+ group (n = 198) from the whole cohort (n = 1980). For the TCGA-BRCA cohort the non-HER2-enriched group (n = 1004) was obtained by subtracting the HER2+ group (n = 78) from the whole cohort (n = 1082). *UGT2B11* and *UGT2B28* showed significantly higher expression in tumours that were HER2+/HER2-enriched (Figure 3.4A and Figure 3.5A). To further explore the relationship between *UGT2B11* and *UGT2B28* expression and both ER and HER2 status, the cohorts were first stratified by ER status and then stratified the ER- and ER+ groups by HER2 status as described above. Interestingly, the positive association between *UGT2B11* and *UGT2B28* expression and HER2 enrichment was only observed in ER- cancers, with no significant relationship observed in ER+ positive cancers (Figure 3.4 and Figure 3.5). These results were similar in both TCGA-BRCA and METABRIC datasets. This suggests that whilst ER- status may not correlate with *UGT* expression, there is enrichment of these *UGTs* in ER-/HER2+ tumours.

Next, the relationship between *UGT2B11* and *UGT2B28* expression and *AR* expression was examined. Tumours were stratified into AR high and low groups based on median AR mRNA expression in both the METABRIC and TCGA-BRCA cohorts. *UGT2B11* and *UGT2B28* expression was strongly positively correlated with *AR* expression in all tumours (Figure 3.4A and Figure 3.5A). When tumours were first stratified by ER status, and then by AR expression, the positive association between *UGT* expression and *AR* expression remained for both ER+ and ER- cohorts, but the association was strongest in ER- cancers (Figure 3.4B-C and Figure 3.5B-C).

The *UGT2B11* and *UGT2B28* expression patterns were extremely similar in each of the above analyses, prompting analysis of the expression correlation between these two genes. There was a very strong correlation between *UGT2B11* and *UGT2B28* expression in both TCGA-BRCA and METABRIC datasets, with a Pearson correlation coefficient of 0.97 in the METABRIC cohort (Figure 3.6). As identified by Meech et al (manuscript in preparation), these genes possess highly homologous proximal and distal promoter elements, which could explain these similar expression patterns. The highly overlapping expression patterns supports the hypothesis that these genes may possess overlapping functions in tumours.

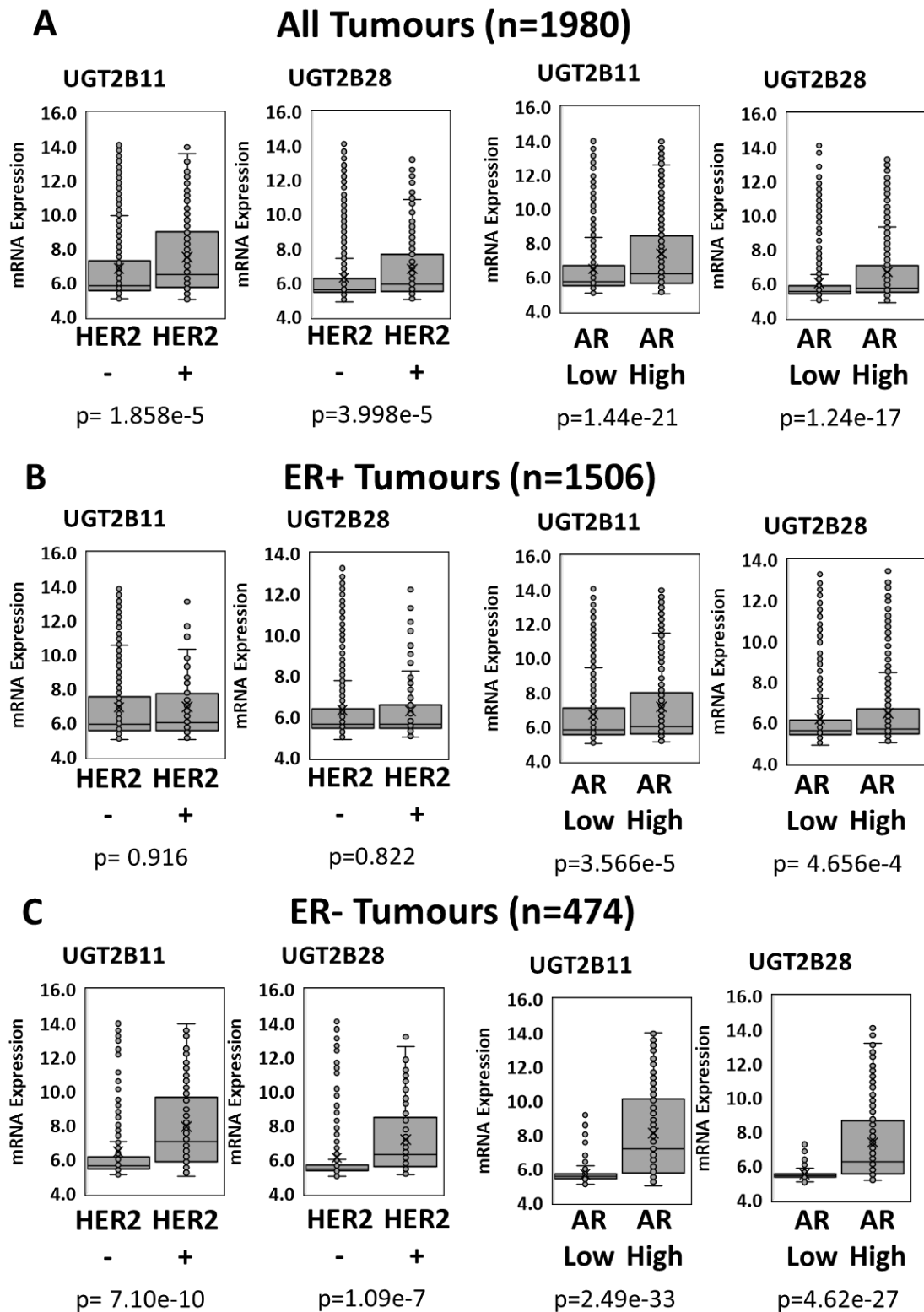


Figure 3.4: Correlation of UGT2B11 and UGT2B28 mRNA expression with HER2 status and androgen receptor expression in METABRIC cohort

UGT2B11 and UGT2B28 mRNA expression z-scores were correlated with HER2 status and androgen receptor expression (high and low were defined by median AR expression) (A) all tumours, (B) ER+ and (C) ER- tumours. Box and whisker plots represent the median, and interquartile range and outlier data points are shown, where X indicates mean of dataset. Statistical significance assessed via Student's t-test.

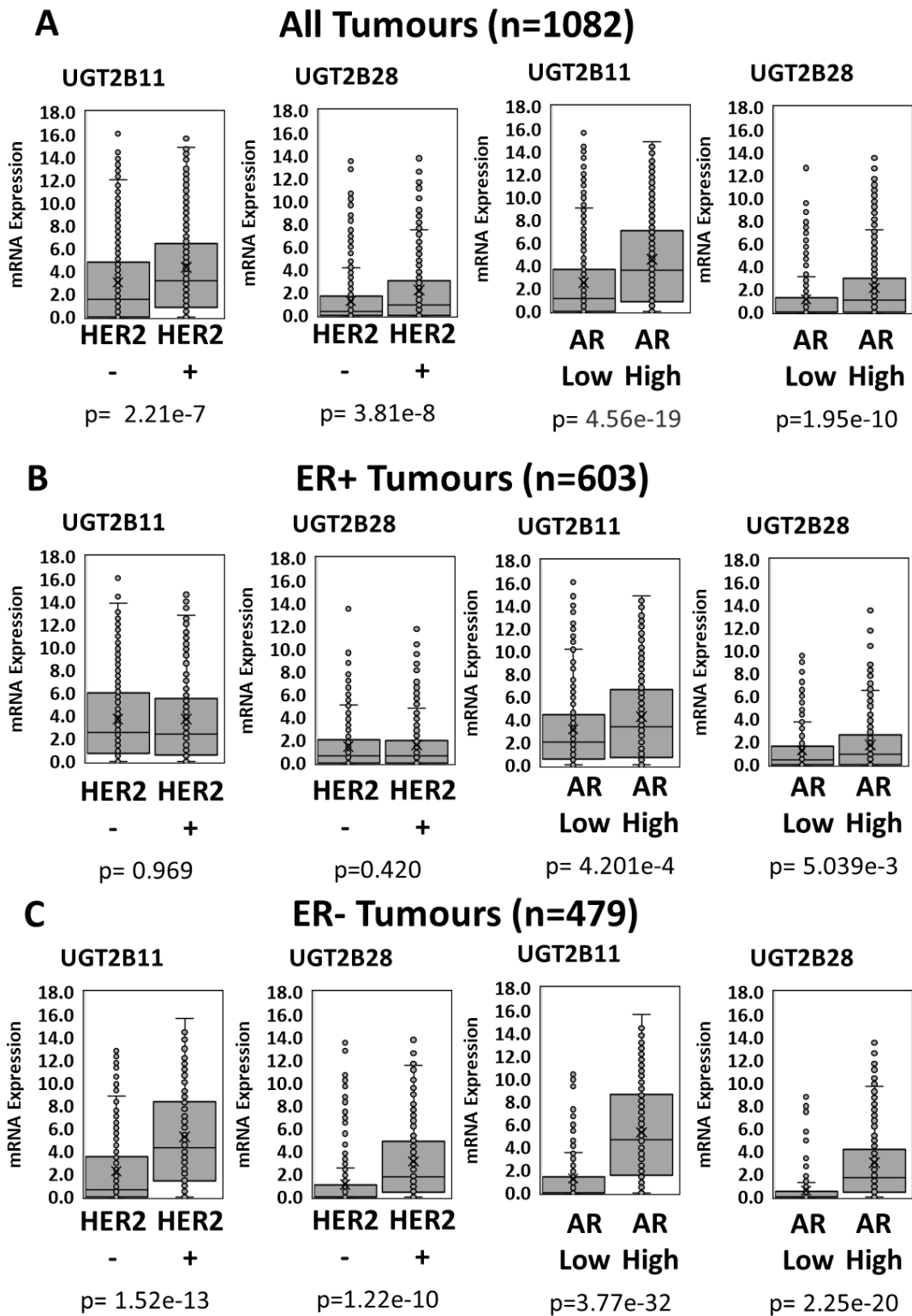
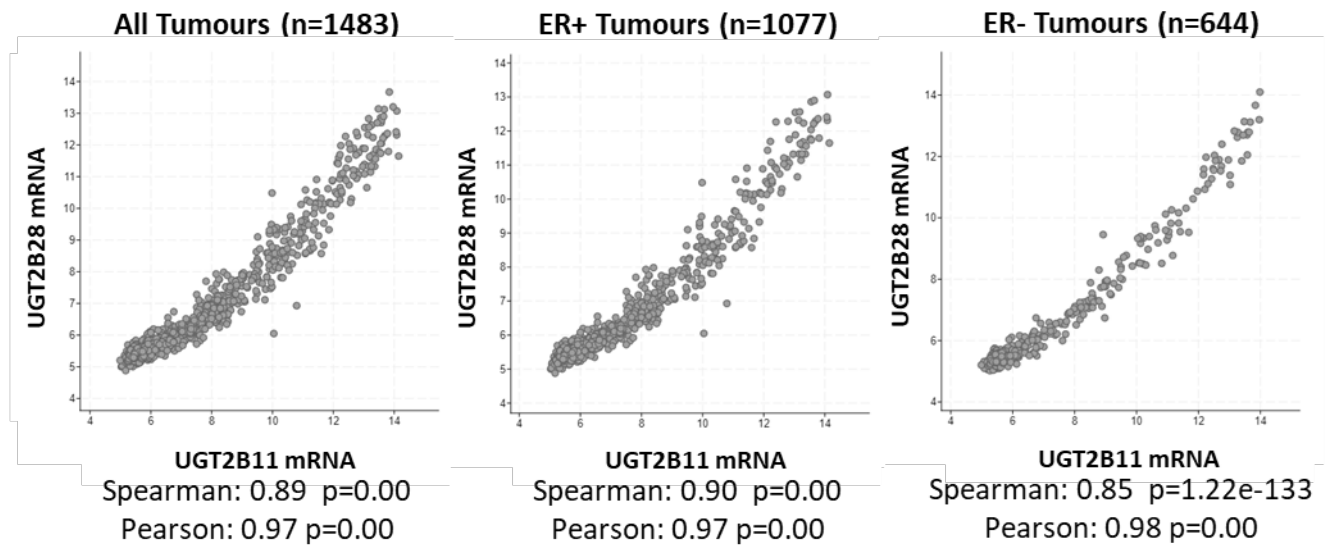


Figure 3.5: Correlation of *UGT2B11* and *UGT2B28* mRNA expression with HER2 status and androgen receptor expression in TCGA-BRCA cohort

UGT2B11 and *UGT2B28* mRNA expression z-scores were correlated with HER2 status and androgen receptor expression (high and low were defined by median AR expression) (A) all tumours, (B) ER+ and (C) ER- tumours. Box and whisker plots represent the median, and interquartile range and outlier data points are shown, where X indicates mean of dataset. Statistical significance assessed via Student's *t*-test.

METABRIC Cohort



TCGA Cohort

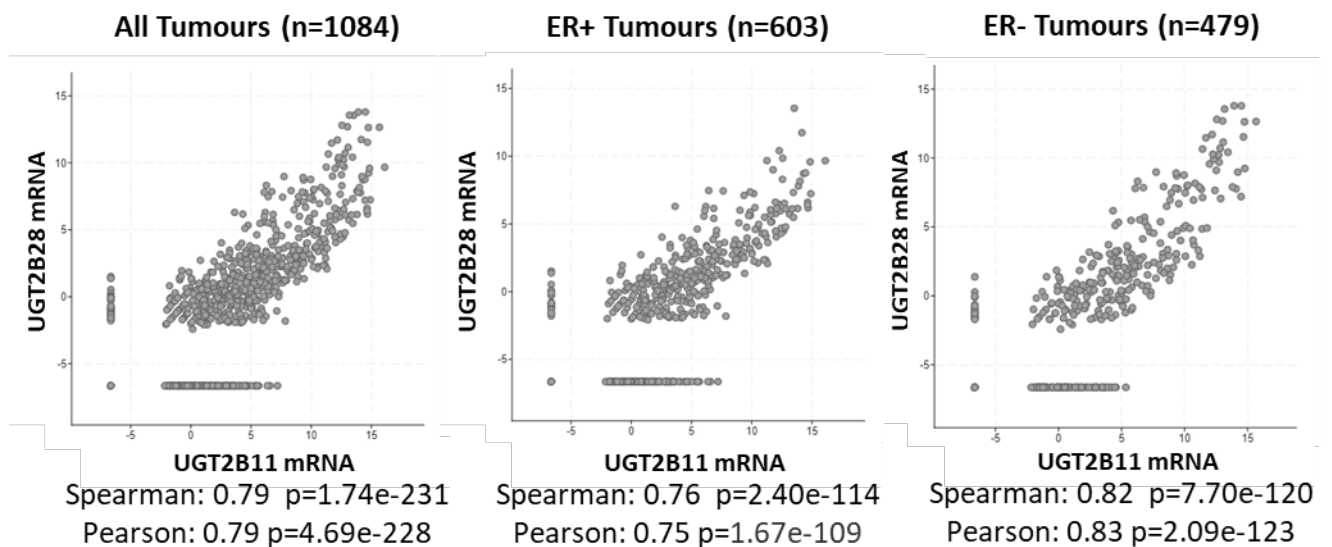


Figure 3.6: Correlation of *UGT2B11* and *UGT2B28* mRNA expression

UGT2B11 and *UGT2B28* mRNA expression z-scores were correlated with each other in all tumours, ER+ tumours and ER- tumours in METABRIC and TCGA-BRCA datasets. Spearman's and Pearson's correlation coefficients are indicated, with statistical significance calculated via 2-sided *t*-test.

3.3.2 The relationship between *UGT2B11* and *UGT2B28* expression and survival outcomes in different breast cancer molecular subtypes

The findings described in the previous section (Section 3.3.1), suggest that *UGT2B11* and *UGT2B28* mRNA expression is associated with ER-negative status, HER2 enrichment, and AR expression level. The analyses presented in this section examine the relationship between *UGT2B11* and *UGT2B28* expression (parsed by median mRNA level) and survival outcomes. When examining all tumours in both TCGA-BRCA and METABRIC datasets, there was no significant association between *UGT2B11* or *UGT2B28* expression when parsed by either median expression (Figure 3.7) or expression quartile and survival (data not shown). The analyses were repeated using a recursive partitioning approach and again there was no significant association (not shown).

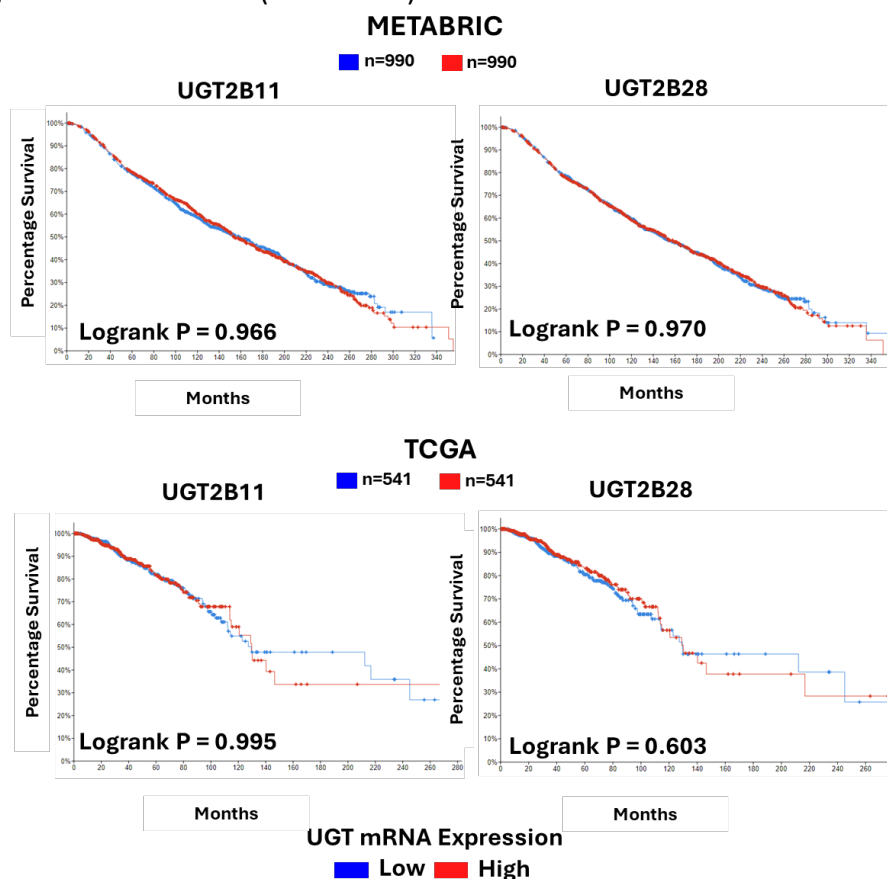


Figure 3.7: Association between *UGT2B11* and *UGT2B28* mRNA expression and survival outcomes in all tumours

Correlation of *UGT2B11* and *UGT2B28* high and low mRNA expression with survival outcomes in all tumours from METABRIC and TCGA-BRCA datasets. High and low expression bins were based on median expression values in the cohort, hence there are an approximately equal number of patients in each expression group. Statistical significance was assessed via logrank test.

Next, the relationship between UGT expression and survival was examined within each of the groups defined by TCGA-BRCA molecular subtyping. When stratifying *UGT2B11* and *UGT2B28* expression by median mRNA level, there were no significant associations between UGT expression and overall survival in any of these groups (Figure 3.8). The analysis was repeated using a recursive partitioning approach and again there was no significant association (not shown).

These analyses were repeated with the METABRIC dataset examining each of the 3-gene classifier subtypes. When stratifying *UGT2B11* and *UGT2B28* expression by median mRNA level, there was no significant difference in survival outcomes for the high and low *UGT* expression groups for any subtype (Figure 3.9).

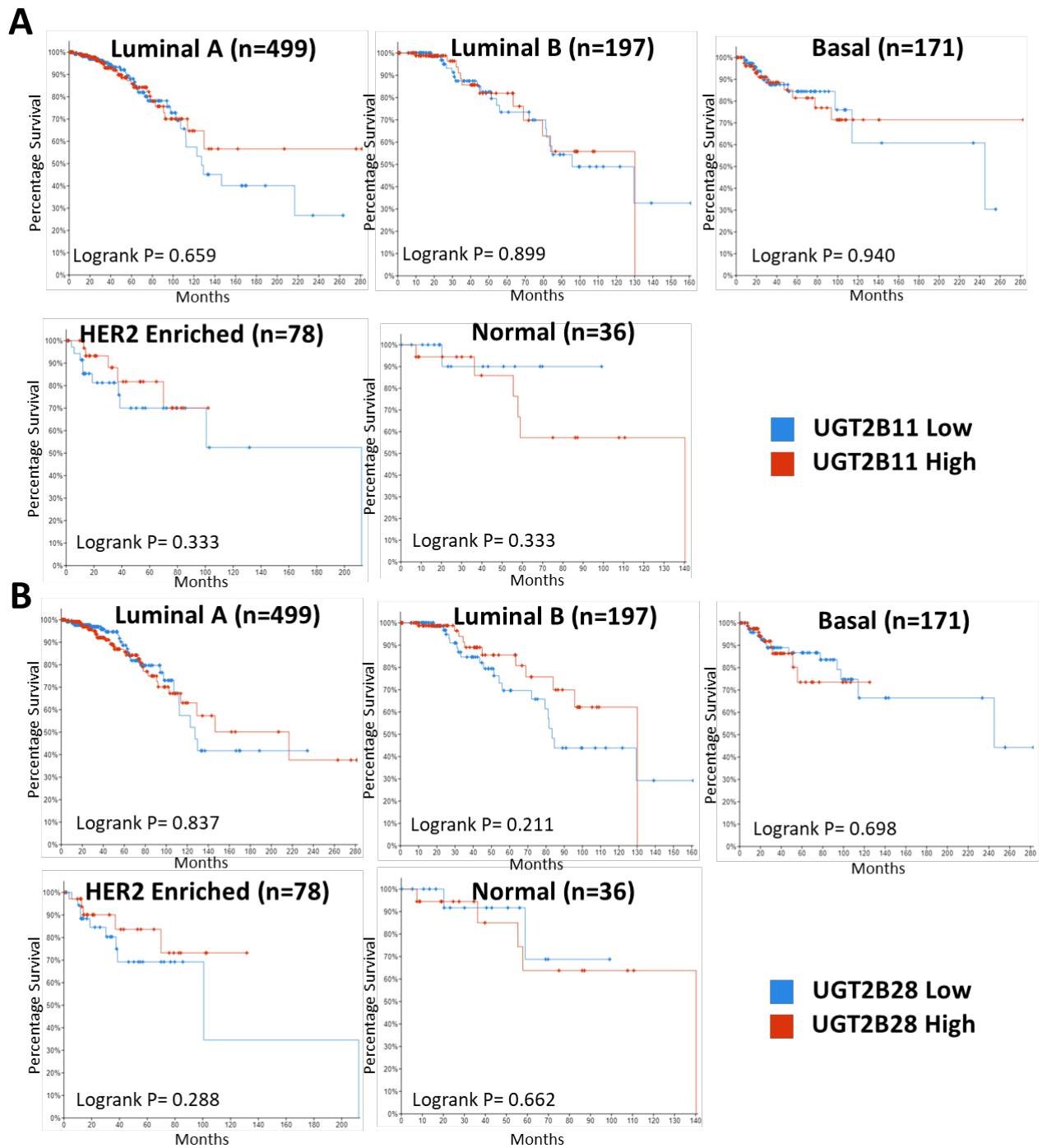


Figure 3.8: Association between *UGT2B11* and *UGT2B28* mRNA expression and survival outcomes in TCGA-BRCA molecular subtypes

Correlation of *UGT2B11* (A) or *UGT2B28* (B) mRNA expression z-scores with survival outcomes in cancer subtypes from TCGA-BRCA database. High and low expression bins were based on median expression values in the cohort, hence there are an approximately equal number of patients in each expression group. Statistical significance was assessed via logrank test.

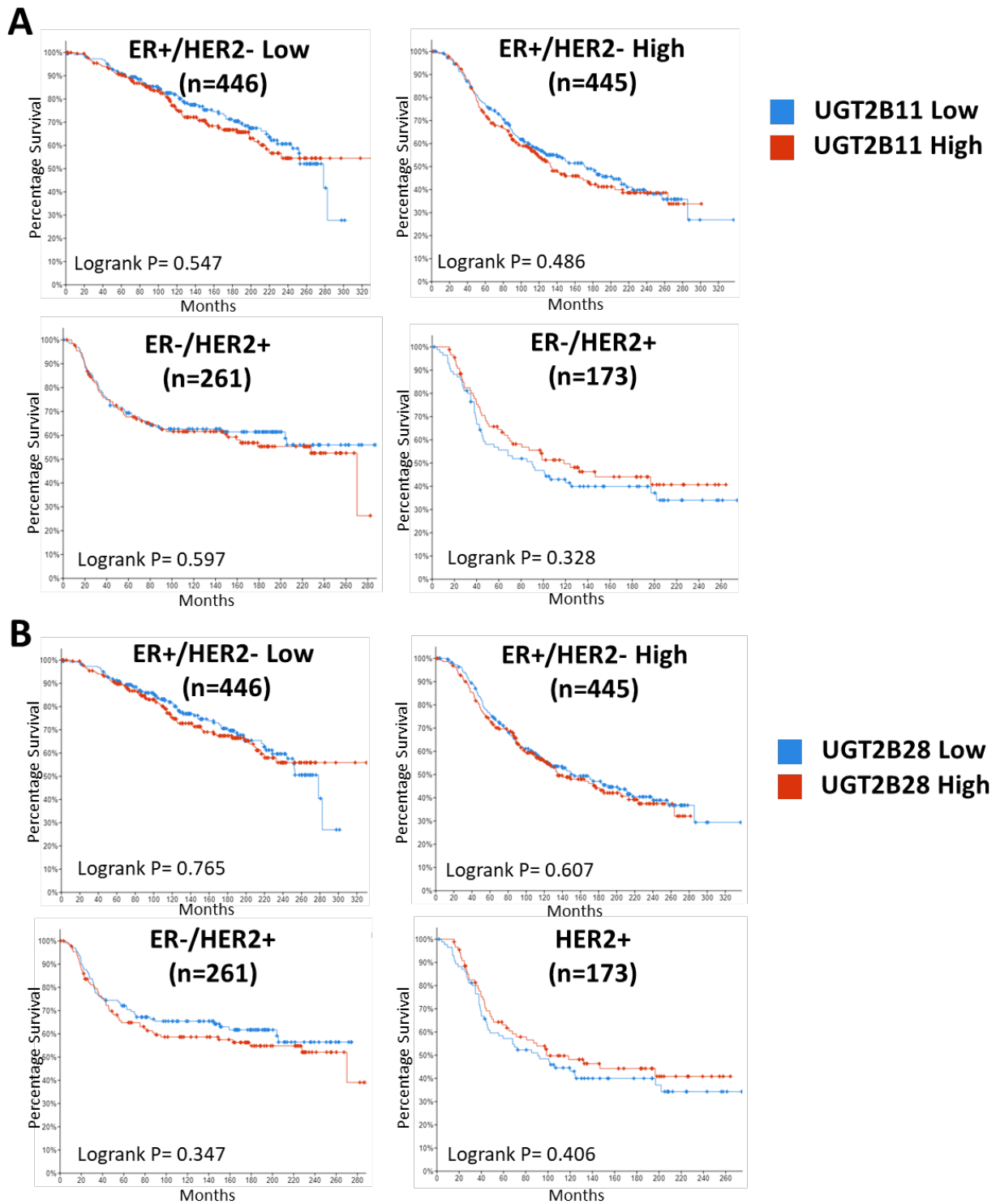


Figure 3.9: Association between *UGT2B11* and *UGT2B28* mRNA expression and survival outcomes in METABRIC 3-gene classifier mRNA expression subtypes

Correlation of *UGT2B11* (A) or *UGT2B28* (B) mRNA expression z-scores with survival outcomes in cancer subtypes from METABRIC database. High and low expression bins were based on median expression level within the cohort. Statistical significance was assessed via logrank test. HER2 low/high refers to low proliferation and high proliferation respectively.

The association between survival outcomes and *UGT2B11* (Figure 3.10) and *UGT2B28* (Figure 3.11) mRNA expression was then examined in the 10 METABRIC integrative clusters. For both genes, higher expression was associated with significantly worse survival outcomes in IntClust2. This cluster had relatively low average *UGT2B11* and *UGT2B28* mRNA expression (see Figure 3.2) and comprised largely ER+ tumours that showed poor prognosis due to chemotherapy resistance. Lower *UGT2B11* expression was associated with significantly poorer survival in IntClust7; no such association was observed for *UGT2B28*. IntClust 4ER-, the subgroup with the highest mean expression of *UGT2B11* and *UGT2B28*, showed a trend towards worse survival outcomes for those patients expressing higher levels of both *UGT2B11* and *UGT2B28*. This was not significant, potentially due to the small sample size (n=68).

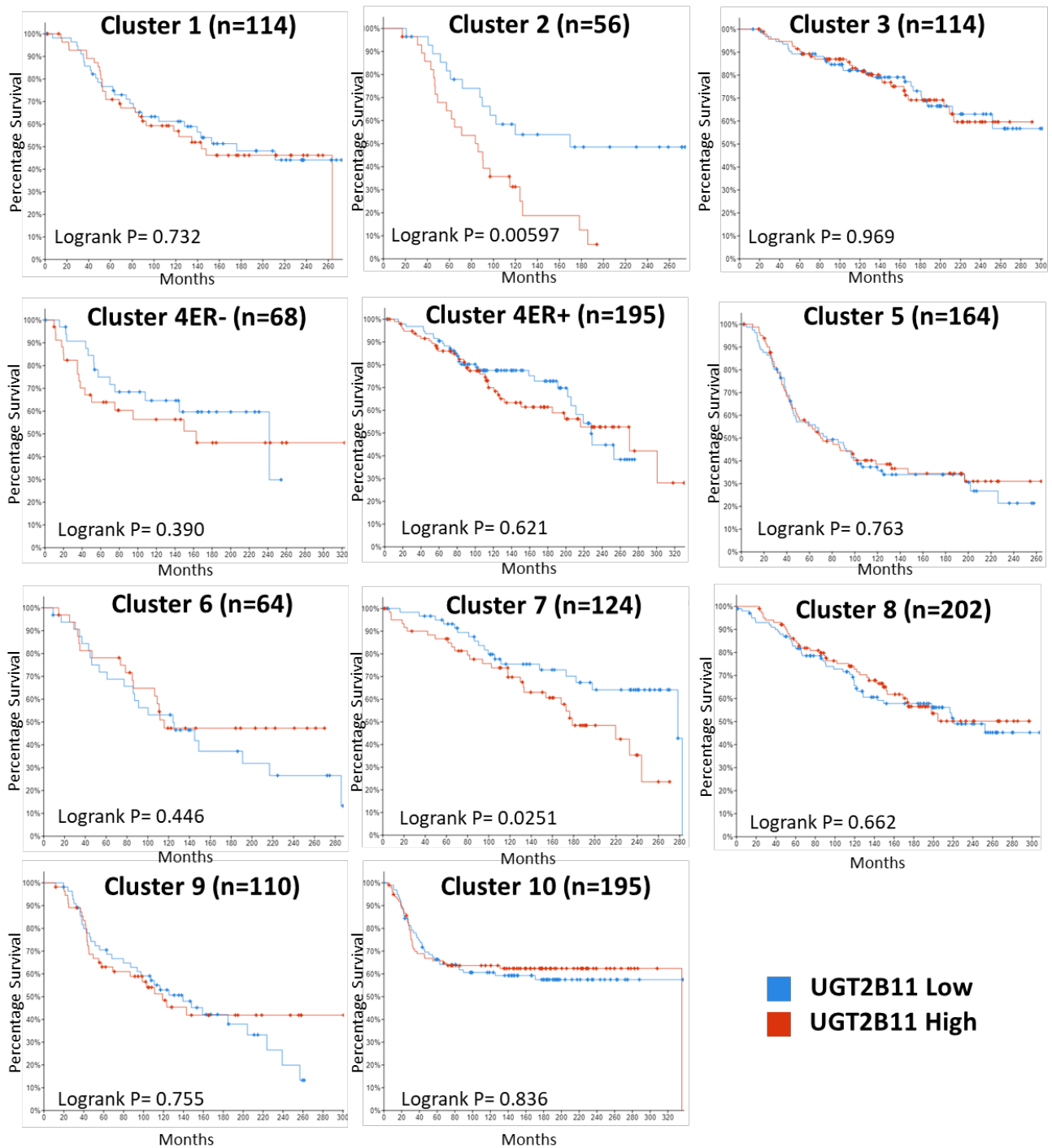


Figure 3.10: Association between *UGT2B11* mRNA expression and survival outcomes in METABRIC integrative clusters

Correlation of *UGT2B11* mRNA expression z-scores with survival outcomes in integrative clusters from METABRIC database. High and low expression bins were based on median expression values in the cohort. Statistical significance was assessed via logrank test.

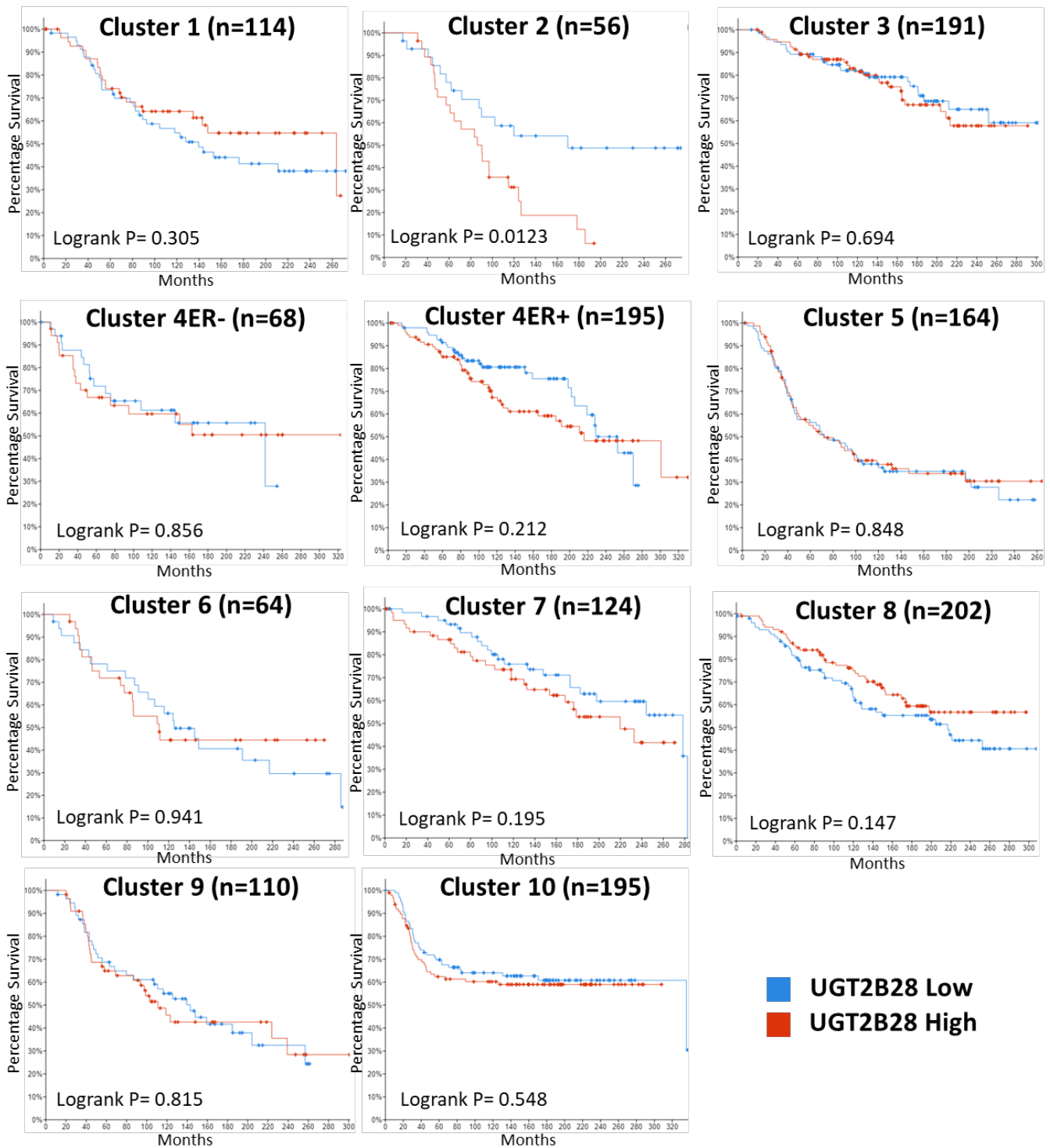


Figure 3.11: Association between *UGT2B28* mRNA expression and survival outcomes in METABRIC integrative clusters

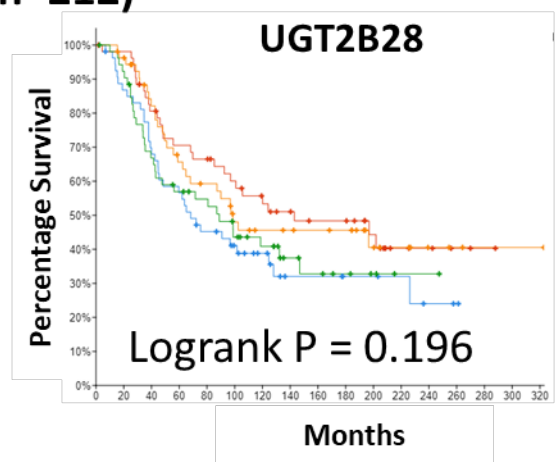
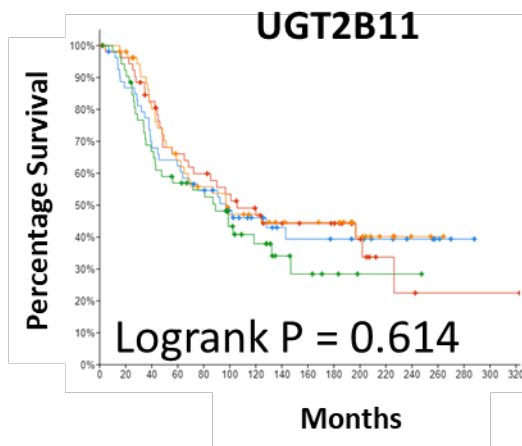
Correlation of *UGT2B28* mRNA expression z-scores with survival outcomes in integrative clusters from METABRIC database. High and low expression bins were based on median expression values in the cohort. Statistical significance was assessed via logrank test.

3.3.3 High UGT2B11 and UGT2B28 expression is associated with worse survival outcomes for ER- tumours

There were only a small number of breast cancer subtypes for which there was an association between survival outcomes (overall survival) and *UGT2B11* or *UGT2B28* expression when the latter was parsed by median expression. When using a recursive partitioning approach, additional significant associations were found in some cohorts. However, caution should be applied when using the latter approach with small cohorts because it can result in partitions with very small numbers of patients in individual leaves, which often results in poor generalizability to the overall biological effect of these enzymes.

To create larger molecularly meaningful groups for analysis, patient groups were stratified by ER and HER2+ status by IHC in both the TCGA-BRCA and METABRIC cohorts. For the HER2+ cohort, when parsed by either expression quartile (Figure 3.12) or median expression (data not shown) there was no significant association between higher UGT expression and poorer survival outcomes. When parsed by UGT expression quartile in the METABRIC ER- cohort, there was a significant difference in survival outcomes for *UGT2B28* high expressing quartiles, and a distinct trend towards worse survival outcomes for *UGT2B11* higher expressing quartiles (Figure 3.13). These trends were entirely absent in the TCGA-BRCA ER- cohort when data was stratified by either median (data not shown) or expression quartile, which could be attributed to a smaller sample size. Therefore, the ER- cohorts for both the TCGA-BRCA and METABRIC cohorts were recursively partitioned such that there was a statistically significant difference in survival outcomes. This showed that patients with the top 23-31% of *UGT2B11* or *UGT2B28* mRNA expression had much poorer survival outcomes than those with lower expression. For both datasets this was statistically significant for *UGT2B28*, but for *UGT2B11*, was only significant in the METABRIC dataset, (Figure 3.14). Therefore, from these analyses, it can be concluded that high *UGT2B11* and *UGT2B28* mRNA expression in ER- breast cancers are associated with worse survival outcomes, and that whilst HER2 enrichment is associated with higher expression of these UGTs, it does not appear to associate with poorer survival outcomes.

METABRIC HER2+ Cohort (n=212)



TCGA HER2+ Cohort (n=407)

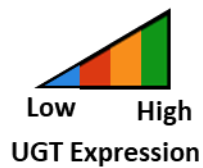
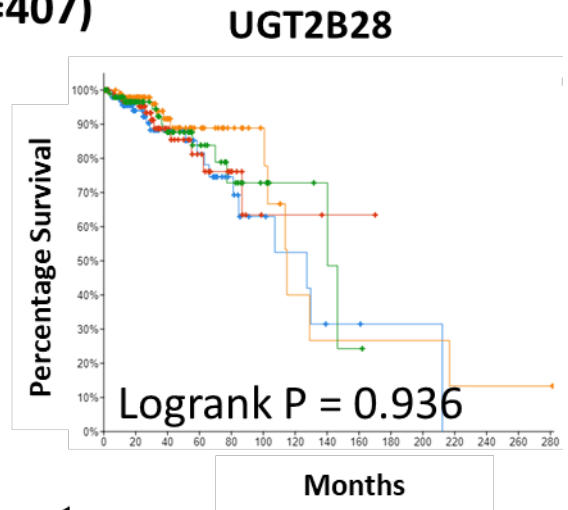
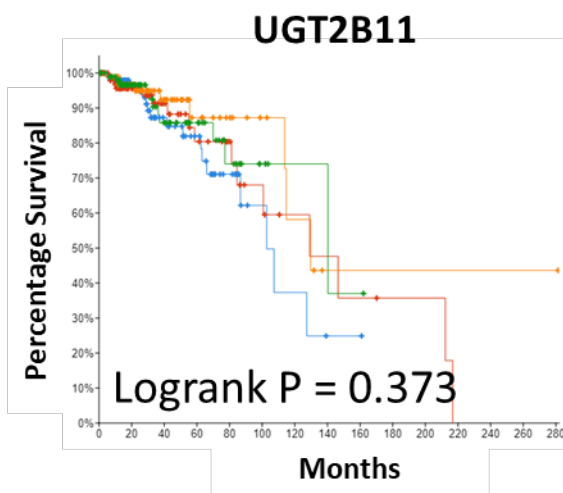
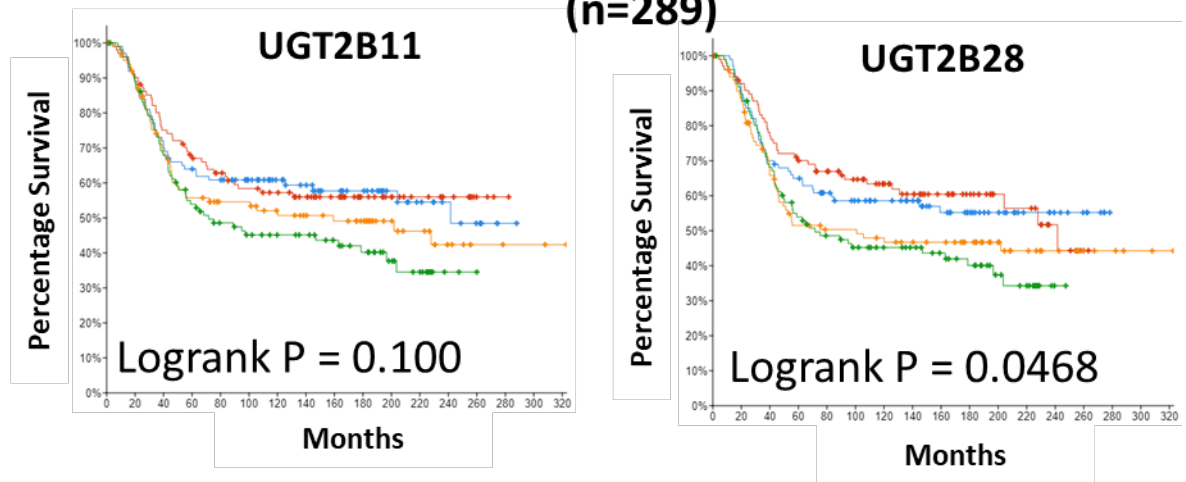


Figure 3.12: *UGT2B11* and *UGT2B28* mRNA expression and associated survival outcomes in HER2+ tumours

Correlation of *UGT2B11* and *UGT2B28* mRNA expression quartiles with survival outcomes in HER2+ tumours from TCGA-BRCA and METABRIC cohorts. Statistical significance assessed via logrank test.

METABRIC ER- Cohort

(n=289)



TCGA ER- Cohort

(n=252)

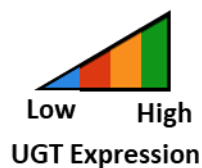
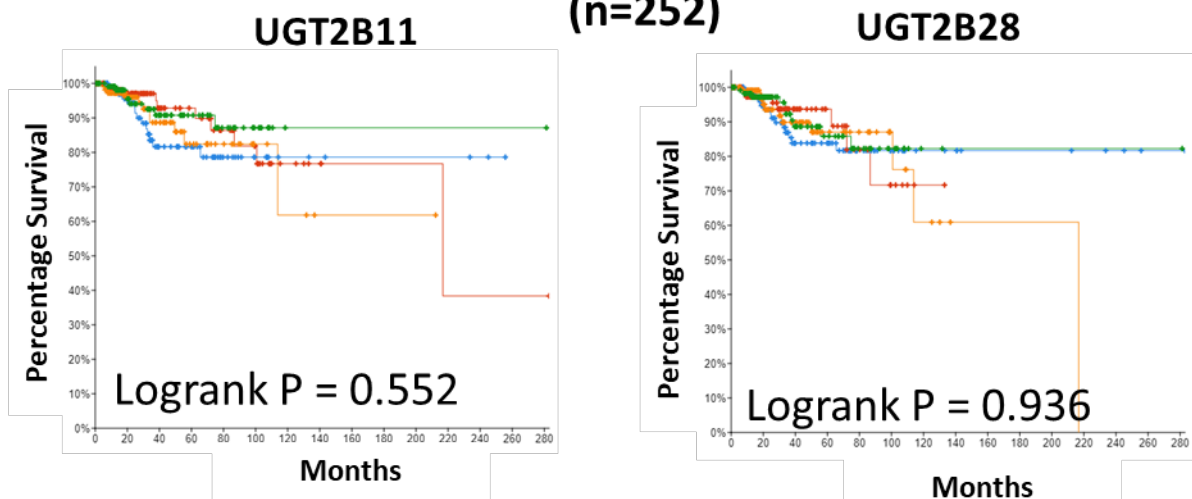
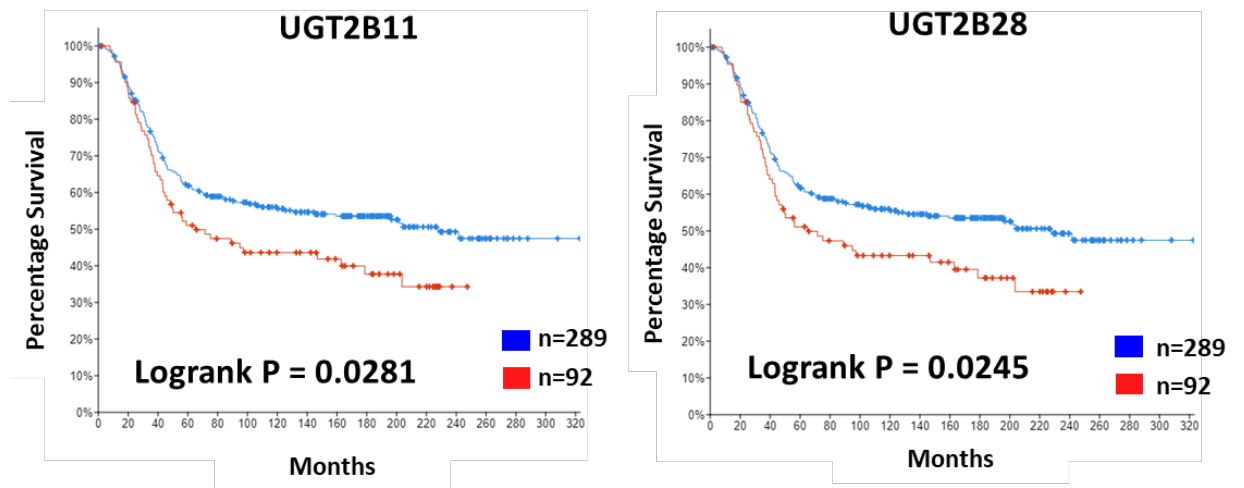


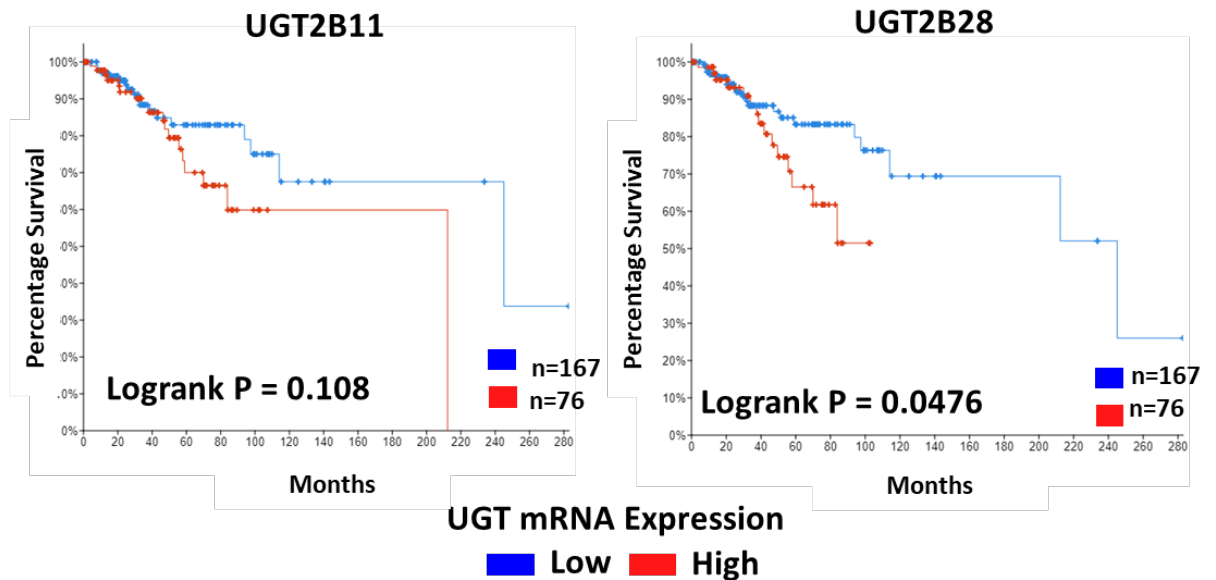
Figure 3.13: *UGT2B11* and *UGT2B28* mRNA expression and associated survival outcomes in ER- tumours

Correlation of *UGT2B11* and *UGT2B28* mRNA expression quartiles with survival outcomes in ER- tumours from TCGA-BRCA and METABRIC cohorts. Statistical significance assessed via logrank test.

METABRIC Cohort



TCGA Cohort



UGT mRNA Expression

■ Low ■ High

Figure 3.14: Association between *UGT2B11* and *UGT2B28* mRNA expression and survival outcomes in ER- tumours

Correlation of *UGT2B11* and *UGT2B28* mRNA expression with survival outcomes in ER- tumours from TCGA-BRCA and METABRIC cohorts. High and low expression was binned such that the top 23-31% of *UGT* expressing patients comprise the UGT High expression group. Statistical significance assessed via logrank test.

3.3.4 High UGT2B11 and UGT2B28 expression correlates with worse survival outcomes for patients with Stage 1 Breast Cancers

In addition to the molecularly defined subtypes of breast cancer, the effect of *UGT* mRNA expression on survival outcomes of patients in each of the four stages of cancer was examined in the METABRIC dataset. This analysis could not be repeated with the TCGA-BRCA dataset as this information is not provided for this cohort. When *UGT* mRNA was stratified by median expression, there was significantly poorer survival outcomes for patients with tumours graded as stage 1 for both *UGT2B11* and *UGT2B28* (Figure 3.15). For *UGT2B28* only, there was significantly worse survival outcome associated with higher expression in Stage 3, with a similar non-significant trend observed for *UGT2B11*. There were no significant differences for patients with tumours graded as stage 2. Patients with stage 4 tumours (n = 10) were excluded from the analysis due to small sample size. When examining the expression of these UGTs across these four stages, there was no significant difference in mRNA levels (Figure 3.15). The finding that Stage 1 cancers with high expression of these UGTs is associated with poorer outcomes for patients suggests that the UGTs might influence the trajectories of these cancers.

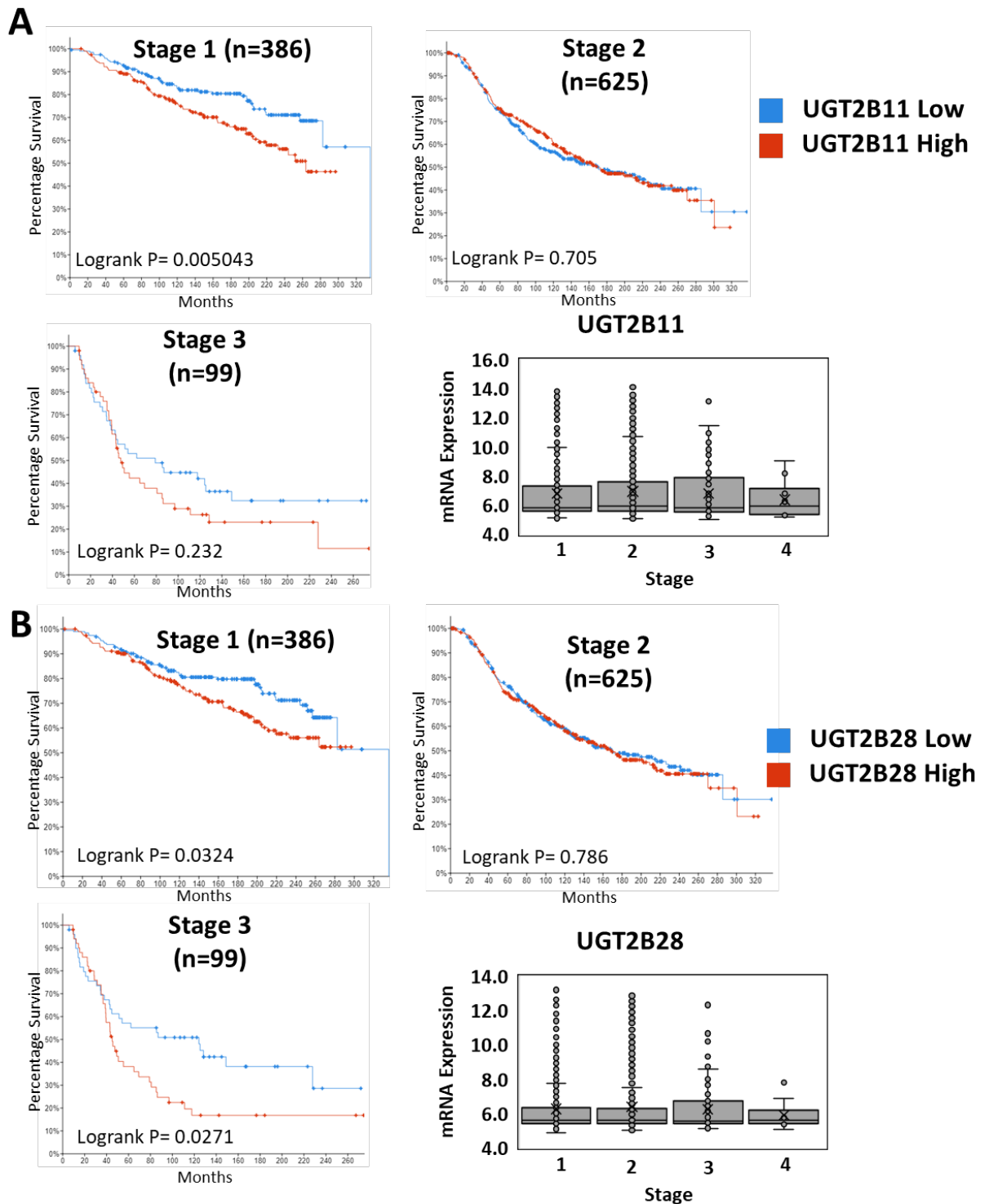


Figure 3.15: Association between *UGT2B11* and *UGT2B28* mRNA expression and survival outcomes in METABRIC Tumour Stages

Correlation of *UGT2B11* (A) or *UGT2B28* (B) mRNA expression with survival outcomes in cancer stages from the METABRIC database. High and low expression bins were based on median expression values in the cohort. Statistical significance assessed via logrank test. For expression levels in each stage, box and whisker plots represent the median and interquartile range and outlier data points are shown.

3.3.5 UGT2B11 and UGT2B28 associate with gene signatures for lipid metabolism

As shown, *UGT2B11* and *UGT2B28* expression is associated with worse survival outcomes in ER- breast cancers (see Figure 3.14). To determine what metabolic pathways may be altered in this subset of patients with worse survival outcomes, the top 500 genes showing increased expression in the *UGT2B11* or *UGT2B28* high expression groups for the ER-negative METABRIC dataset was analysed using REACTOME (Fabregat et al., 2017) to assess enrichment of functional gene signatures.

In the METABRIC dataset, lipogenic gene pathways were consistently identified as the top 5 most enriched pathways for both *UGT2B11* and *UGT2B28* isoforms in the UGT high expression patient cohort (Table 3.3). In particular, SREBP mediated lipid biosynthetic pathways were robustly correlated with high UGT expression. This result is concordant with that described in Section 3.1.3 (Table 3.1), in which genes whose expression correlated strongly with *UGT2B11* and *UGT2B28* expression were identified in the GTEx and TCGA-BRCA normal tissue datasets. Similar findings in tumour samples suggests that these UGTs are associated with a lipogenic tumour phenotype which could contribute to poorer outcomes.

Table 3.3: Top 25 enriched pathways in METABRIC Dataset for UGT2B11 or UGT2B28 high expression groups for ER- breast cancer patients. High UGT2B11 or UGT2B28 expressing

UGT2B11		UGT2B28	
Pathway Name	p-value	Pathway Name	p-value
NR1H2 & NR1H3 regulate gene expression linked to lipogenesis	4E-06	Aspirin ADME	2.10E-04
Activation of gene expression by SREBF (SREBP)	2E-05	Activation of gene expression by SREBF (SREBP)	3.34E-04
Regulation of cholesterol biosynthesis by SREBP (SREBF)	0.0001	NR1H2 & NR1H3 regulate gene expression linked to lipogenesis	4.40E-04
Aspirin ADME	0.0009	Glucuronidation	1.31E-03
Glucuronidation	0.0014	Regulation of cholesterol biosynthesis by SREBP (SREBF)	1.54E-03
Sema4D induced cell migration and growth-cone collapse	0.0025	Sema4D induced cell migration and growth-cone collapse	2.39E-03
NR1H2 and NR1H3-mediated signalling	0.0048	Sphingolipid de novo biosynthesis	3.83E-03
Sema4D in semaphorin signalling	0.0062	Phase II - Conjugation of compounds	3.98E-03
Formation of the nephric duct	0.0062	Sema4D in semaphorin signalling	5.89E-03
RHO GTPases Activate Rhotekin and Rhophilins	0.0063	RHO GTPases Activate Rhotekin and Rhophilins	6.05E-03
Phase II - Conjugation of compounds	0.0095	Tyrosine catabolism	6.46E-03
Peroxisomal protein import	0.0129	Antagonism of Activin by Follistatin	9.55E-03
Metabolism of steroids	0.0143	Proline catabolism	1.49E-02
Proline catabolism	0.0154	CD28 dependent PI3K/Akt signalling	1.99E-02
GRB7 events in ERBB2 signalling	0.021	GRB7 events in ERBB2 signalling	2.05E-02
Kidney development	0.0223	Regulation of TP53 Activity through Association with Co-factors	2.47E-02
Transport of inorganic cations/anions and amino acids/oligopeptides	0.0226	Signalling by Activin	3.28E-02
Protein localisation	0.0255	Signalling by MAPK mutants	3.47E-02
Regulation of TP53 Activity through Association with Co-factors	0.0255	Formation of lateral plate mesoderm	3.47E-02
Beta-oxidation of pristanoyl-CoA	0.0285	Stimuli-sensing channels	3.48E-02
Fatty acyl-CoA biosynthesis	0.0337	PTK6 Regulates RHO GTPases, RAS GTPase and MAP kinases	3.70E-02
Signalling by MAPK mutants	0.0355	SUMOylation of transcription factors	3.70E-02
Formation of lateral plate mesoderm	0.0355	NR1H2 and NR1H3-mediated signalling	3.70E-02
Stimuli-sensing channels	0.0371	Signalling by ERBB2	3.90E-02
PTK6 Regulates RHO GTPases, RAS GTPase and MAP kinases	0.0384	Glutathione conjugation	3.90E-01

groups were defined within the TCGA-BRCA and METABRIC ER-negative patient cohorts, and the 500 highest expressed genes within these groups were analysed using Reactome to assess enrichment of gene pathways. Statistical significance was assessed with a Binomial test where the false discovery rate was controlled using the Benjamini-Hochberg method.

3.4 Discussion

The aim of this chapter was to acquire new data regarding *UGT2B11* and *UGT2B28* expression in breast cancer patient samples from the METABRIC and TCGA-BRCA datasets,

and to use this information to refine hypotheses underpinning the *in vitro* studies described in the subsequent chapters of this thesis.

UGT2B11 and *UGT2B28* were more highly expressed in breast cancer subtypes that expressed high levels of HER2 (generally due to *ERBB2* amplification, thus possessing HER2+ status). While there was no significant difference in expression of *UGT2B11* and *UGT2B28* between ER-positive and ER-negative tumours, it was notable that when tumours were stratified by ER status, the association between higher UGT expression and HER2+ status was only significant in the ER-negative group (Figure 3.4B and Figure 3.5B). There was no significant association with increased *UGT* expression and survival in the HER2 enriched molecular subtype. Any association between survival and *UGT* expression may be masked by the already poor survival outcomes of this group. The majority of individuals within this subtype had died by 100 months, which is much quicker than the other molecular subtypes, however, this is consistent with HER2 enriched cancers characterised by being aggressive with faster growth and often worse prognosis (Daemen & Manning, 2018). *UGT2B11* and *UGT2B28* were most highly expressed in tumours that expressed high levels of AR (Figure 3.4C and Figure 3.5C).

There is no conventional molecular subtype associated with an ER-, HER2+ and AR-enriched molecular/transcriptional profile. However, it is consistent with molecular apocrine (MA) tumours which are defined as ER- with AR expression and activation of an AR-dependent expression program, with or without HER2 overexpression (Bonnetfoi et al., 2019). In particular, Lehmann-Che et al. (2013) characterised a cohort of MA tumours via IHC staining and reported the marker frequency to be 93% ER-, 58% AR+, 90% FOXA1+, and 67% HER2+ (the latter reported as 3+ staining level). All MA tumours analysed in this report showed high AR expression by qRT-PCR, even though not all stained positive for AR by IHC. Clinically, MA tumours were considered aggressive, with poor prognostic features. The potential association of these UGTs with the MA phenotype may warrant further study.

As previously discussed, these two UGT isoforms are highly androgen regulated at a transcriptional level, and hence their positive association with AR expression is not unexpected. In fact, when examining the ER-negative cohort, AR and its co-factor FOXA1 were within the top 20 genes most highly correlated with *UGT2B28* and *UGT2B11* (Meech, manuscript in preparation).

The association of *UGT2B11* and *UGT2B28* expression with HER2 status in breast cancer patients was a new finding (Figure 3.4 and Figure 3.5). However, concurrent with these studies, two reports appeared in the literature showing that HER2 expression is associated with increased *UGT2B28* mRNA expression via RNAseq (Atallah et al., 2023; Yam et al., 2023). To date no molecular mechanism for these associations has been investigated. Orrù et al. (2022) has shown that there is a high prevalence of AR expression in HER2+ breast cancers, so there may be an intrinsic relationship between these two hormone receptors. In addition, AR signalling can promote HER2 phosphorylation and upregulates HER3, leading to enhancement of signalling by HER2/HER3 dimers (Ni et al., 2011; Redmond et al., 2019). More recently, it was shown that FOXA1 is required for ERBB2 gene expression in breast cancer through direct binding to its promoter (Jeong et al., 2024). Thus, it is possible that the correlation between UGT and HER2 expression reflects their co-regulation by FOXA1/AR-mediated pathways. HER2 has also been reported to bind to chromatin, hence another possible explanation for the observed co-expression is direct transcriptional regulation of the *UGT* genes by HER2 (He et al., 2017). Overall, the relationship between HER2 and UGT expression remains an area that requires further research but was outside of the scope of the current study.

High *UGT2B11* and *UGT2B28* expression was associated with poorer survival outcomes in patients with ER-negative breast tumours (Figure 3.14). This shows for the first time the prognostic value of these UGT isoforms for breast cancer patients. Previous data showed an association between high *UGT2B28* expression and poorer survival outcomes in prostate cancer (Belledant et al., 2016), but there are no previous studies examining *UGT2B11* and *UGT2B28* in a subtype-specific manner in breast cancer. Previous work has shown association of other UGTs, namely *UGT2B15* and *UGT2B17*, with poorer outcomes in specific ER+ breast cancer patient subsets (Hu et al., 2016B). *UGT2B11* and *UGT2B28* expression did not associate with worse survival outcomes in patients with HER2+ tumours (Figure 3.12). This may be due to the small subgroup of patients that possess this classification (n = 72 in the TCGA-BRCA cohort and n = 173 in the METABRIC cohort). As shown by our laboratory (manuscript in preparation), higher expression of either *AR* or *ERBB2* (HER2) is associated with poorer survival in ER-negative tumour cohorts in the METABRIC dataset. It is possible that a relationship between survival and UGT expression

is masked by the poor survival outcomes characteristic of this small patient subgroup (Bonnefoi et al., 2019).

Although the association between *UGT2B11* and *UGT2B28* expression and survival outcomes in ER- patients was clearly identified within two independent datasets, there were limitations of the analyses conducted within this chapter. Further stratification of the ER- subsets by other markers was limited by the small sample sizes. Recursive partitioning created very small sub-groups in some analyses. It is also known that UGT genes produce variant transcripts in a range of tissues, and these generally give rise to non-functional proteins (Lévesque et al., 2001). The datasets analysed here are unable to distinguish between truncated and full-length variants of UGT isoforms. To date there has been no analysis of the relative abundance of UGT2B transcript variants in breast cancer. Additional studies using other clinical datasets that include gene expression and clinical data would add robustness and potentially corroborate the present analyses. RNA and protein levels are not always well correlated (Vogel & Marcotte, 2012), thus obtaining datasets that include UGT protein expression data would also be very valuable. The TCGA-BRCA dataset does contain some protein expression data, however, it is not comprehensive and does not include any data for UGTs.

Subsequent to finding that higher *UGT2B11* or *UGT2B28* expression is associated with poorer survival outcomes in ER- patients, gene enrichment and pathway analysis of this cohort was performed (Table 3.3). The top 25 most enriched pathways were involved in SREBP target gene expression and *de novo* lipid and cholesterol biosynthetic pathways. The functional pathways enriched in both *UGT2B11* and *UGT2B28* high expression groups are very similar, which is consistent with their high expression correlation (Figure 3.6). These results are consistent with findings from Wang et al. (2017) that UGTs are co-enriched with lipogenic genes in ER-negative breast cancer patients. However, potential mechanisms underpinning the association between UGT expression and SREBP signalling remain to be investigated. One intriguing hypothesis is that these UGTs help to promote lipogenic signalling and that this could be involved in driving a more aggressive phenotype.

Pathways designated as signalling by ERBB2 (HER2) were also significantly enriched in the *UGT2B28* high expressing group of tumours, further supporting the association between HER2+ status and increased UGT expression in this study. These findings are corroborated

by Yam et al. (2023), who found that breast tumours with high HER2 expression show elevated levels of *UGT2B28* and of genes involved in fatty acid metabolism.

Interestingly, similar analyses of the ER-negative tumour subset in the TCGA-BRCA database did not produce clear enrichment of SREBP signalling pathways (not shown). This was unexpected as a previous analysis of the GTEx normal tissues and cancerous tissues from the TCGA-BRCA cohort (Table 3.1) showed a significant association between high *UGT2B11* and *UGT2B28* expression and enrichment of SREBP signalling and lipogenic pathways. This highlights the value of obtaining further breast cancer expression datasets to corroborate the findings from METABRIC analyses; however, due to time constraints and the goal of pursuing more mechanistic studies, this avenue was not pursued.

3.4.1 Conclusion

Throughout this chapter, the TCGA-BRCA and METABRIC breast cancer databases were explored to develop an understanding of *UGT2B11* and *UGT2B28* expression in breast cancer. These UGT isoforms showed highest expression in breast cancers that showed a molecular apocrine-like profile with high expression of HER2 and AR, and ER-negative status. Moreover, high levels of *UGT2B11* and *UGT2B28* mRNA expression correlated with worse survival outcomes in patients with ER-negative tumours. In the METABRIC dataset, ER-negative tumours showing high expression of *UGT2B11* or *UGT2B28* were enriched for expression of genes involved in SREBP signalling and lipid biosynthetic pathways. A speculative proposal is that these UGTs may play a role in enhancing lipid signalling in these tumours. Increasing the provision of lipids to cancer cells (either by uptake or *de novo* synthesis) can enhance their proliferation and is also associated with other cellular processes that make cancers more aggressive. These included promoting cell migration, epithelial-to-mesenchymal transition (EMT), and drug resistance (De Piano et al., 2020; Germain et al., 2020; Yang et al., 2016). These pathways have been well defined in prostate cancer where the lipogenic phenotype is strongly associated with AR activity and with more aggressive cancer (Lounis et al., 2020; Zeković et al., 2023). It would be of interest to examine whether the expression of *UGT2B11* and *UGT2B28* also correlates with lipogenic gene expression in prostate cancer patient datasets; however, this is outside of the scope of this project.

Overall, these studies prompted the development of new hypotheses regarding the relationship between these UGTs and the SREBP signalling pathway, which are explored in the subsequent chapters of this thesis via experimental work in breast cancer cell lines.

4. CHAPTER 4 -
UGT2B11 AND UGT2B28
PROMOTE SREBP
ACTIVATION

4.1 INTRODUCTION

4.1.1 Dysregulation of Lipid Biosynthesis

Lipid metabolism is a tightly regulated cellular process. *De novo* lipogenesis, which produces lipids from acetyl-coA, mainly occurs in normal adipocytes and hepatocytes, but may be induced in cancer cells as a mechanism to enhance growth and survival. Like many aspects of lipid metabolism, *de novo* lipogenesis is controlled by the sterol regulatory element-binding proteins (SREBP) transcription factor family. There are three SREBP isoforms, SREBP-1a, SREBP-1c and SREBP-2. As described in Chapter 1 (see Section 1.6), cellular sterol levels are the most significant factor controlling SREBP activation in normal cells. Briefly, the inactive SREBP precursor is anchored in the ER via direct association with the SCAP-INSIG sterol sensing complex. When cholesterol levels decrease within the cell, this ER localised complex detects the decrease and subsequently undergoes conformation changes leading to dissociation of SCAP from INSIG. SCAP then interacts with COPII proteins on ER-Golgi transport vesicles, facilitating translocation of SCAP-SREBP complexes to the Golgi (Goldstein et al., 2006; Gong et al., 2006). In the Golgi, proteolytic cleavage of the SREBP precursor occurs to release the mature N-terminal fragment from the membrane. This fragment, referred to as nSREBP, travels to the nucleus where it induces transcription of lipogenic genes (Eberlé et al., 2004; Horton et al., 2002). For a summary of this process, refer to Figure 1.8 (see Chapter 1, Section 1.6.1).

Dysregulation of lipid metabolism occurs in various types of cancerous cells, and it frequently involves *de novo* lipid biosynthesis. This increased provision of lipids can provide cells with an energy source, phospholipids for membrane production, protection from reactive oxygen species (ROS), and cholesterol for steroidogenesis, ultimately resulting in an increase in the proliferative capacity of cancerous cells (Liu, 2006; Rysman et al., 2010; Santos & Schulze, 2012; Vander Heiden et al., 2009).

4.1.2 UGTs and Lipid Metabolism

As presented in Chapter 3, bioinformatic analyses of the METABRIC and TCGA-BRCA datasets showed that high *UGT2B11* and *UGT2B28* expression levels were correlated with poor outcomes in breast cancer patients with ER-negative tumours. These poor survival outcomes were associated with increased expression of SREBP target genes. Both of these findings are consistent with Wang et al. (2013), where *UGT2B11* and *UGT2B28* showed

higher expression in patients with ER-negative tumours, and Wang et al. (2017) where both *UGT2B11* and *UGT2B28* were designated as part of a 'lipid-signature' in breast tumours. To date, no other published studies report a link between these UGTs and lipid metabolism in a breast cancer context. Prior to the start of this project, recent work by our laboratory produced experimental data that complements these results and suggests that these UGTs might be involved in mediating the activation of SREBPs in breast cancer cells.

This work involved the generation of MDA-MB-453 breast cancer cell lines that stably overexpress *UGT2B11* or *UGT2B28*. The MDA-MB-453 cell line was chosen for this overexpression model due to its high expression of AR and the previously defined ability for these UGTs to be expressed at extremely high levels after androgen exposure (Meech, manuscript in preparation). However, as now identified in Chapter 3, the MDA-MB-453 cell line is also considered a model of a molecular apocrine-like tumour type: it is ER-negative, shows moderately elevated HER2 expression, and high expression of AR (Moore et al., 2012). Molecular apocrine-like tumours show the highest expression of *UGT2B11* and *UGT2B28* based on analyses shown in Chapter 3.

The MDA-MB-453 cell lines engineered to stably overexpress *UGT2B11* or *UGT2B28* were subjected to preliminary RNA analysis. This data showed increased expression of a small set of SREBP target genes (Figure 4.1A). Data from these pilot studies showed that the cell lines overexpressing *UGT2B28* possessed an increased proliferative capacity (Figure 4.1B). Taken together, this was suggestive that increased UGT expression led to increased SREBP activity, providing the first evidence for a functional connection between these factors.

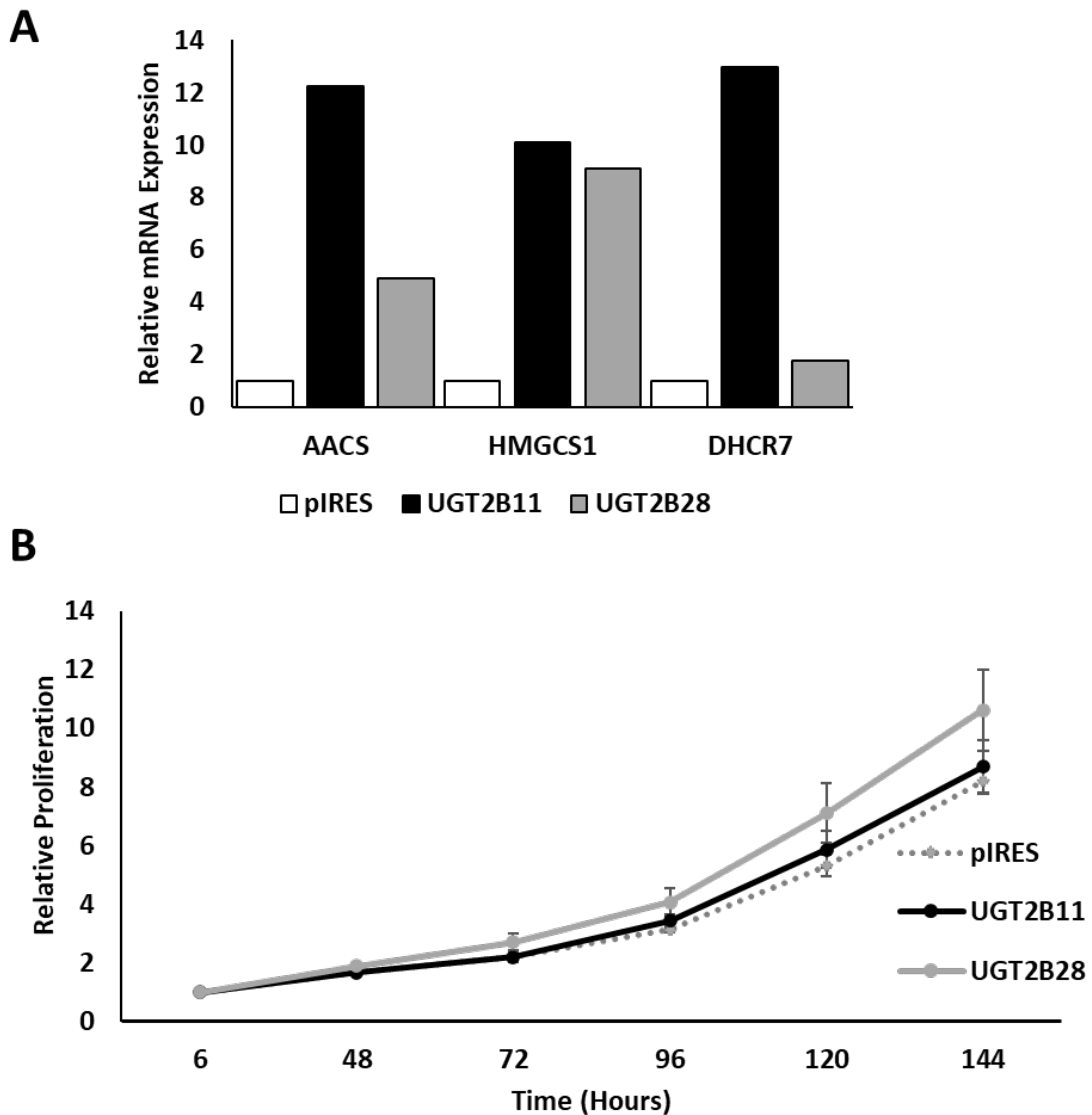


Figure 4.1: Preliminary results showing effects of UGT2B11 or UGT2B28 overexpression on SREBP target gene expression and proliferation

A) mRNA expression of SREBP-target genes in control (pIRES) and UGT2B11 and UGT2B28 MDA-MB-453 stable overexpression cell lines were measured via qRT-PCR (n=1). **B)** Cellular proliferation was assessed via crystal violet staining for control (pIRES empty vector) and UGT2B11 and UGT2B28 MDA-MB-453 stable overexpression cell lines (n=3 independent experiments).

Further preliminary studies were undertaken to assess a possible physical association between UGTs and members of the sterol sensing complex in the ER. As shown in Figure 4.2, when Myc-tagged SCAP and FLAG-tagged UGT2B11 or FLAG-tagged UGT2B28 were co-expressed in HEK-293T cells, SCAP was able to co-immunoprecipitate both UGT2B11 and UGT2B28. This assay did not confirm a direct interaction between these proteins, as it was

possible that the interaction involved third party proteins. However, if UGTs are capable of interacting with SCAP, other members of the lipid sensing complex, or other as yet undefined accessory proteins, then they might be able to modulate lipid sensing and hence affect processing of SREBPs. This could thus potentially increase the provision of lipids to cancer cells.

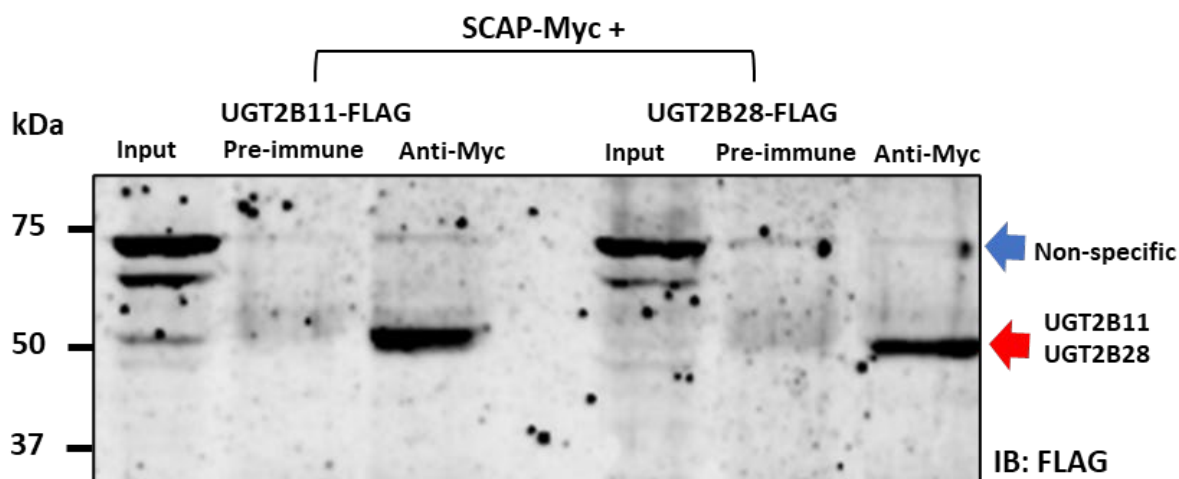


Figure 4.2: Preliminary results showing interaction between UGTs and SCAP

Myc-tagged SCAP was co-immunoprecipitated via magnetic bead-based co-immunoprecipitation with FLAG-tagged UGT2B11 and FLAG-tagged UGT2B28 using anti-Myc antibody. Immunoblot was probed with anti-Flag antibody. Lysates for co-immunoprecipitation were prepared from HEK-293T cells transfected 48 hours prior to harvest with indicated plasmids.

As reviewed previously, a small body of literature has suggested a link between UGT2B11 and UGT2B28 and dysregulation of lipid metabolism in a variety of different diseases (Bidgood et al., 2024; Cayrol et al., 2008; Mathur et al., 2020; Wang et al., 2013; Wang et al., 2017; Yan-qin et al., 2022). However, these studies have not suggested that this is through direct metabolism of lipids, and generally have not proposed any molecular mechanisms for the observed associations. In prostate cancers, which share many similarities with molecular apocrine breast cancers, increased expression of these UGTs has been shown to be associated with increased lipogenesis (Neuwirt et al., 2020). Conversely, individuals with the naturally occurring UGT2B28 deletion have lower circulating levels of steroids, fatty acid carnitines, dicarboxylates and oxylipins, compared to gene-proficient

individuals (Rouleau et al., 2022). The mechanisms underlying these metabolic changes remains unclear, in part because substrates for UGT2B28 remain poorly defined.

4.1.3 CRISPR Inhibition (CRISPRi)

CRISPR and CRISPRi methods are established approaches for gene perturbation in the context of functional genomics. The generation of knock out cell models using CRISPR (Clustered regularly interspaced short palindromic repeats) can induce off-target genome modifications (Stojic et al., 2018). Moreover, it typically requires the clonal selection of a homogenous population of cells with identical genome modifications, for which it is difficult to develop a suitable isogenic control (Panda et al., 2023). Clonal selection can also enrich aberrant cellular phenotypes which in some instances can be caused by heterogeneity in the parental population (McGranahan & Swanton, 2017).

CRISPR interference (CRISPRi) is a more recent adaption of the CRISPR-Cas9 genome modification system and possesses the benefits of CRISPR and that of a knock down system. In this system, catalytically deactivated or dead Cas9 (dCas9) is fused to the Kruppel Association Box (KRAB) repressor domain. The dCas9 containing a specific guide allows for the targeting of KRAB to a specific genomic locus, whereby KRAB recruits KAP-1 (KRAB-associated protein 1), a co-repressor and forms a repression complex that regulates histone modifications that ultimately reduces transcriptional activity on chromatin at the desired location (Gilbert et al., 2014; Sripathy et al., 2006; Stoll et al., 2022). In a recent study, Stojic et al. (2018) suggested that using CRISPRi in a heterologous pool provides the fewest off-target effects as compared to RNA interference approaches that use short interfering RNA (siRNA) or antisense oligonucleotides, which can cause repression of non-target genes through non-specific interactions (Jackson et al., 2003; Sigoillot et al., 2012). CRISPRi was utilised in this Chapter to attempt to generate knock down models of UGT2B11 and UGT2B28 expression in breast cancer cells.

4.1.4 Aims

The bioinformatic results of Chapter 3, together with preliminary data collected prior to this project, led to the hypothesis that *UGT2B11* and *UGT2B28* play a role in regulating the activities of SREBPs, either by direct or indirect mechanisms. The goal of this Chapter was to confirm the previous preliminary data, and to test the above core hypothesis.

The specific aims of this chapter were therefore to:

1. Generate *UGT2B11* and *UGT2B28* stable overexpression and knock down cell lines in MDA-MB-453 cells and assess the effects of these perturbations on proliferation.
2. Determine if *UGT2B11* and *UGT2B28* can alter SREBP activation.
3. Assess potential molecular mechanisms of UGT-mediated SREBP modulation.

4.2 METHODS

4.2.1 Plasmids

The KRAB-dCas9-PX459 CRISPRi plasmid was generated by cloning the Kruppel Association Box fused to catalytically dead Cas9 (KRAB-dCas9) fragment from the pHR-SFFV-KRAB-dCas9-P2A-mCherry vector into the SpCas92A-Puro-PX459 vector, both of which were obtained from Addgene (Plasmids #60954 and #62988) (Gilbert et al., 2014; Ran et al., 2013). To create the CRISPRi *UGT2B11* and *UGT2B28* targeting constructs, guide RNAs (gRNAs) were designed using the CRISPR-ERA program (Liu et al., 2015) to target the proximal promoter regions of these genes. Oligonucleotides corresponding to these gRNAs were cloned into the *P*il restriction site of KRAB-dCas9-PX459.

The dual epitope tagged (N-terminal myc and C-terminal HA) SREBP-1a (Y335R) vector ([SREBP-1a-Y335R-myc\(N\)-HA\(C\)-pcDNA3](#)); referred to as SREBP-1a (Mut) throughout for simplicity, was generated by subcloning the SREBP-1a gene from the SREBP-1a(Y335R)-HA(N)-myc(C)-pBABE-puro expression plasmid (Yuan et al., 2019); which was a kind gift from Dr Jonas Dehairs (KU Leuven, Flanders, Belgium), into pcDNA3. This was achieved by amplifying SREBP-1a from the plasmid template by PCR and cloning the resultant product between the *M*feI/*E*coRI-*X*baI restriction sites of pcDNA3 already containing an N-terminal myc-tag. The vector containing transcriptionally inactive nSREBP-1a ([nSREBP-1a-myc\(N\)\(Y335R\)-pcDNA3](#)); referred to as nSREBP-1a (Mut), was generated by amplifying the sequence corresponding to amino acids 1-460 from the SREBP-1a (Mut) plasmid and cloning into pcDNA3 as aforementioned.

The C-terminal HA epitope tagged SREBP-2 vector ([SREBP-2-myc\(N\)-pcDNA3](#)) was generated using a multi-step approach due to the difficulty associated with amplifying the entire ~3.5 kb SREBP-2 cDNA sequence. Initially, the first 48-1700 bp was amplified from nSREBP-2-HA(N)-pcDNA4 plasmid DNA (Krycer et al., 2012), while the sequence corresponding to 1670-3634 bp was amplified from cDNA isolated from MDA-MB-453 cells. The two fragments were ligated together using a silent *S*all restriction site incorporated via site-directed mutagenic cloning primers and cloned into the Zero Blunt PCR vector (Thermo Fisher). The resulting full-length C-terminally HA-tagged SREBP-2 insert was then subcloned into the *M*feI/*E*coRI-*X*baI sites of pcDNA3 already containing an N-terminal myc-tag. It should be noted that this product has a 48 bp deletion in the N-terminal region

corresponding to amino acid 5-21, which is similar in size and location to that of the deletion found in the nSREBP-2-HA(N) pcDNA4 construct used in this study (Krycer et al., 2012). Extensive attempts to generate a full length SREBP-2 construct without this deletion were unsuccessful, however, as the protein produced by this construct was functional in this study, and in the study described by Krycer et al. (2012), it is likely that this deletion is functionally inert.

To generate transcriptionally inactive nuclear (nSREBP-2 (Mut)-HA(N)-pcDNA4) and full length SREBP-2 ([SREBP-2 \(Mut\)-myc\(N\)-pcDNA3](#)) expression plasmids (referred to as nSREBP-2 (Mut) and SREBP-2 (Mut), respectively), tyrosine 342 (equivalent to tyrosine 335 in SREBP-1a numbering) was mutated to arginine (Y342R) in the nSREBP-2 pcDNA4 and SREBP-2 pcDNA3 constructs via site-directed mutagenesis. No map is provided for nSREBP-2 (Mut)-HA(N)-pcDNA4 because details regarding the parent vector construction were unavailable.

Variants of SREBP-2 with higher transactivation capacity were generated by fusing SREBP-2 with the VP16 activation domain. This fusion protein was designed to increase the sensitivity of luciferase reporter assays. To make the fusion construct, the region encoding residues 14-478 of nSREBP-2 (Mut) was amplified by PCR and cloned into pVP16 between the EcoRI-Sall sites to generate [nSREBP-2 \(Mut\)-HA\(N\)-pVP16](#). To generate the plasmid containing full length SREBP2 fused to VP16, designated [SREBP-2 \(Mut\)-HA\(N\)-pVP16](#), the SREBP C-terminal domain was amplified and fused to the N-terminal domain as described previously.

To generate a fluorescently tagged SREBP-2 precursor ([mCherry SREBP-2\(Mut\)-HA\(N\)-pcDNA3](#)), SREBP-2 (Mut) pVP16 was first digested with EcoRI-XbaI to generate two fragments (EcoRI-EcoRI and EcoRI-XbaI). The EcoRI-XbaI fragment was cloned into mCherry-2A-pcDNA3 (Meech et al., 2010) EcoRI-XbaI, followed by the EcoRI-EcoRI fragment.

The C-terminally HA epitope tagged INSIG1 and INSIG2 plasmids ([INSIG1-HA\(C\)-pcDNA3](#) and [INSIG2-HA\(C\)-pcDNA3](#), respectively) were generated by two rounds of PCR amplification of INSIG1 and INSIG2 from cDNA isolated from HEK-293T cells; first with INSIG specific primers (INSIG1/2 EcoR1 F and INSIG1/2 R) and subsequently with primers specific for the INSIG isoform and containing the HA epitope tag (INSIG1 HA XbaI R and INSIG 2 HA

NheI R), and cloning of the resultant PCR products via EcoRI-XbaI or EcoRI/NheI-XbaI sites, respectively into pcDNA3.

A GAL4-UAS luciferase reporter system was developed to estimate the nuclear accumulation of SREBP-VP16 fusion proteins. This assay was one of a number of methods used to assess SREBP processing to its nuclear form. Initially, a GAL4 DNA binding domain and VP16 activation domain fusion construct ([GAL4-VP16-pM](#)) was generated by Phusion amplification of the VP16 activation domain corresponding to amino acids 404-490 from the pVP16 vector and cloned EcoRI/MfeI-SalI into pM. Subsequently, the sequence corresponding to amino acids 477-1141 was digested from SREBP-2 (Mut)-HA(N)-pVP16 and cloned SalI/XbaI downstream to form [GAL4-VP16-C-SREBP-2-pM](#).

For all plasmids constructed in this Chapter, refer to [Appendix 2](#) for sequences and plasmid maps. All other plasmids have been previously described in Chapter 2.

4.2.2 Oligonucleotides

Table 3.1: Primers utilised during this chapter.

For cloning primers restriction sites are shown in bold and epitope tags are underlined. For site-directed mutagenesis, mutated bases are shown in bold.

Primer Name	Sequence (5'→3')
Cloning	
SREBP-2 MfeI F	GCG CAATTG GACGACAGCGGCGAGCTG
SREBP-2 XbaI R	TAAT CTAGAG AAATCGAGAGAGAGGTGGAGGG
nSREBP-2 SalI R	GGT CGACC ATGCCAGCG
C-SREBP-2 SalI F	CATGG TCGACC GCTCACGGA
INSIG1 EcoRI F	GCG GAATTC ATGCCAGATTGCACGACCAC
INSIG1 R	ATCACTATGGGGCTTTTCAGGAACA
INSIG1 HA XbaI R	TAAT CTAGAT CAAGCGTAATCTGGAACATCGTATGGGTAATCACTATGGGGCTT
INSIG2 EcoRI F	GCG GAATTC ATGGCAGAAGGAGAGACAGAGTCA
INSIG2 R	TTCCTGATGAGATTTTTCTGCGATAACTTTA
INSIG2 HA NheI R	TAAG CTAGCT CAAGCGTAATCTGGAACATCGTATGGGTATTCCTGATGAGATT
VP16 MfeI F	GCG CAATTG ATGGGCCCTAAAAGAAGCGTA
VP16 SalI R	CGC GTCGACC CCACCGTACTCGTCAATTC
Site-Directed Mutagenesis	
SREBP-1a R335Y F	ATTGAGAAGCGCT ACCG CTCCT
SREBP-1a R335Y R	AGGAGCGGT AGCG CTTCTCAAT
SREBP-1a SDM screening F	ACAACGCCATTGAGAAGCG CTA
SREBP-2 Mut Y342R F	GAGAAACGAC GTCG CTCTCCAT
SREBP-2 Mut Y342R R	ATGGAGGAGCGAC GTCG TTTCTC

SREBP-2 SDM screening F	CCCATAATATCATTGAGAAACGACG		
Sequencing & Screening			
SREBP-2 Sequencing F	ATCCATCTGACTGCTGCCAT		
SREBP-2 Sequencing R	AGTCAGGGGGTTAAAGGAGA		
pM Sequencing F	CTGGATATGGCCGACTTCGAGTTT		
pVP16 Sequencing F	CTGGATATGGCCGACTTCGAGTTT		
pM/pVP16 Sequencing R	TTTAAAGCAAGTAAAACCTCTACAAATGTG		
qRT-PCR			
Gene	Accession Number	Primer	Sequence (5' → 3')
UGT2B11	NM_001073.3	Forward	CTTCCATTCTTTTGGATCCCAAT
		Reverse	TAAGCGGAGACTGTACACAAC
UGT2B28	NM_053039.2	Forward	TGAAGACAATCCTGAAAGA
		Reverse	AATGTCTGACCATCTCTTAA
18srRNA	M10098.1	Forward	CGATGCTCTTAGCTGAGTGT
		Reverse	GGTCCAAGAATTTACCTCT

4.2.3 Generation of UGT2B11 and UGT2B28 stable overexpression cell lines

Stable MDA-MB-453 cells that overexpress variants of UGT2B11 and UGT2B28 were generated during and immediately prior to this study. The wildtype UGT-overexpressing stable lines generated prior to this study were generated using electroporation. Initially, 5×10^6 cells were electroporated (230 V, 950 mF, time constant ~ 20 ms) with 10 μ g of appropriate plasmid DNA in serum free (SF) RPMI 1640 using a Gene Pulser Xcell apparatus (Bio-Rad). The wildtype, truncated, and SNP UGT variant overexpressing stable lines generated during this study were generated using lipofectamine LTX (Invitrogen) as per the manufacturer's protocol. Briefly, 5×10^6 cells were transfected in T25 flasks using 5 μ g plasmid DNA with a 1:1 DNA: Plus reagent ratio and 1:4 DNA: lipofectamine ratio. To select for cells overexpressing integrated plasmid, 48 hours post transfection, transfected cells were treated with increasing puromycin up to a final 0.55 μ g/mL. This was based on a previously established killing curve for MDA-MB-453 cells (data not shown). This process resulted in a heterologous non-clonal population of cells that overexpress the desired integrated plasmid. Once established, cells were maintained under regular growth conditions with consistent puromycin exposure.

4.2.4 Fluorescence SREBP-2 Localisation Assay

In order to assess the nuclear localisation of nSREBP-2, the mCherry N-terminally tagged SREBP-2 plasmid ([mCherry SREBP-2\(Mut\)-HA\(N\)-pcDNA3](#)) generated in this study was utilised. For transfection, 5×10^4 MDA-MB-231 cells were seeded, and reverse transfected in a 24-well plate with a total of 850-1700 ng of plasmid DNA per well. Lipofectamine LTX (1:4 DNA to lipofectamine ratio) was used as per the manufacturers protocol, and cells were subsequently cultured for 48 hours. Cells were then washed with PBS and fixed with 3.7% formaldehyde in PBS for 10 minutes at RT, prior to membrane permeabilization with 0.5% Triton-X in PBS for 5 minutes. Nuclei were stained with DAPI (1 μ g/mL in PBS) for 5 minutes at RT and cells were stored in PBS at 4°C until imaging. Wells were imaged using an EVOS M5000 microscope at 40X magnification with excitation wavelengths of 357/444 nm for DAPI and 585/629 for mCherry-SREBP-2. ImageJ FIJI software (Schindelin et al., 2012) was used to quantify nuclear and cytoplasmic fluorescence, with DAPI staining utilised to determine bounds of nuclei. Entire nuclei and cytoplasm imaged for 20 cells per condition for each biological experiment.

4.2.5 GAL4-VP16 C-SREBP-2 Luciferase Assays

In order to assess proteolytic activation of SREBP precursors, the GAL4-VP16 fusion C-SREBP-2 plasmid ([GAL4-VP16-C-SREBP-2-pM](#)) constructed in this study was utilised. In 48 well plates, 3×10^4 HEK-293T or MDA-MB-231 cells were seeded, and reverse transfected with 2 ng of GAL4-VP16 C-SREBP2, 50 ng of pck-1 GAL4-UAS luciferase reporter, 5 ng of pRL-null Renilla and indicated amounts of additional plasmid constructs with Lipofectamine 2000 (1:4 DNA to lipofectamine ratio) as per standard manufacturers protocol. Cells were cultured under indicated conditions for 48 hours, then lysed in passive lysis buffer and assayed for luciferase activity as aforementioned (Chapter 2, Section 2.2.6 [Luciferase Assays](#)).

4.2.6 Delipidation of serum

To delipidate serum for use in culture media, the protocols from Agnese et al. (1983) and Brovkovich et al. (2019) were adapted as follows. PBS was used to dilute 50 mL of FBS to 100 mL, to which 2 g of fumed silica (Sigma, S5130) was added. This mixture was rotated at 4°C for 3 hours and then centrifuged at 5100 g at 4°C for 30 minutes to remove lipid bound silica. A further 2 g of fumed silica was added to the supernatant, and the mixture

was rotated for 16 hours, followed by centrifugation and filter sterilisation through a 0.22 μ M filter.

4.2.7 Cell Fractionation

Cell fractionation was performed as per Suzuki et al (2010) to generate nuclear and membrane fractions. Briefly, cells were harvested in cold PBS with 0.1% NP40, centrifuged for 10 seconds in a table-top centrifuge. The supernatant was removed, pelleted cells were washed and centrifuged again for 10 seconds. The remaining nuclear pellet was resuspended in RIPA buffer and harvested as previously described for protein lysates.

4.2.8 Enzyme Assays

Autoradiographs of TLC plates were performed determining UGT cholesterol and cholesterol derived substrates. UGT containing lysates for enzymatic reactions were prepared by transiently transfecting HEK-293T cells with either empty pIRES vector (control) or UGT2B11 and UGT2B28 encoding plasmids. A pool of HLM of unknown origin was also utilised. All glycosidation reactions were performed in a final volume of 100 μ l containing 100 mM phosphate buffer, pH 7.5, 4 mM magnesium chloride, enzyme source (100 μ g cell lysate), 250 μ M aglycone substrate, and 2 mM [C-14] UDP sugar (0.1 μ Ci/mmol). The reactions were performed at 37 °C for 1 hour and were terminated with 200 μ l of ethanol. After centrifugation to remove denatured protein, aliquots of supernatant were subjected to thin layer chromatography on silica gel plates (Baker Si250F) in chloroform: methanol: water: acetic acid, in the v/v ratio of 65:25: 4:2. Radioactive products were visualized and quantified by exposure to a Phosphor Screen, which was scanned with a Typhoon 9400 scanner (GE Healthcare).

4.3 RESULTS

4.3.1 Characterising the effect of UGT2B11 and UGT2B28 overexpression

To determine the effects of UGT2B11 or UGT2B28 overexpression on molecular apocrine-like breast cancer cells, two sets of UGT-over-expressing MDA-MB-453 cell lines were independently generated. Both sets of cell lines were generated by stable integration of pIRES vectors encoding wild type UGT2B11, UGT2B28, or the empty vector, and each line comprised a polyclonal pool of cells with multiple plasmid integration sites. These

polyclonal 'lines' reduce the impact of integration artefacts that may occur in monoclonal lines. The overexpression of UGT2B11 or UGT2B28 in these lines was assessed by qRT-PCR (Figure 4.3). The levels of overexpression of each isoform varied significantly between the two independent sets of stable lines, with late Ct values of 32-35 in the control cell lines for each isoform and much earlier Ct values of 15-20 in each of the stable overexpression lines. In the UGT2B11 overexpression lines, *UGT2B11* mRNA was significantly increased by ~3,500 (line 1) and 107,000-fold (line 2) relative to the control cell line (Figure 4.3A). Similarly, in the UGT2B28 lines, *UGT2B28* mRNA was increased by ~14,000-16,000-fold relative to the control cell line but only significantly different for line 2 due to the variability between biological experiments in line 1 (Figure 4.3B).

Western blotting was performed to confirm that these stable lines overexpress UGT2B11 and UGT2B28 proteins (Figure 4.3C). The antibody used for this analysis was raised to the UGT2B7 protein (anti-UGT2B7) but was previously shown to cross-react with UGT2B11 and UGT2B28. This antibody detected bands at ~50 kDa in the UGT2B11 and UGT2B28 overexpressing lines and detected no comparable bands in the control empty vector lines (Figure 4.3C). This result was interpreted as indicating heterologous overexpression of the UGT2B11 and UGT2B28 proteins, as it is consistent with the increase in UGT mRNA levels in these lines, and endogenous expression of UGT2B proteins is very low in this cell line and not detectable under these conditions. Relative overexpression could not be quantified due to this lack of detectable protein in the control cell lines.

To determine whether UGT overexpression alters cell behaviour, the proliferation of each stable line was quantified using a crystal violet assay (Figure 4.3D). Relative to the control line, both overexpression lines demonstrated a modest increase in proliferative capacity. Both sets of three independent biological experiments for each set of stable lines showed a similar result; hence the data shown in Figure 4.3D is the six independent experiments combined. The UGT2B11 overexpression line showed a trend towards increased proliferation after 72 hours, which was followed by a statistically significant increase in proliferation for all time points beyond 96 hours. The UGT2B28 overexpression line demonstrated a statistically significant increase in proliferative capacity at all time points. The different magnitude of the effect of UGT2B11 and UGT2B28 on proliferation may indicate that they have different effects on proliferation-associated pathways or may relate to the different levels of relative overexpression. These data suggest that the UGTs could

enhance tumour growth, which is consistent with the observations in Chapter 3 that the subset of patients with ER-negative tumours that have high UGT2B11 or UGT2B28 expression show poorer survival outcomes (see Chapter 3, Figure 3.14).

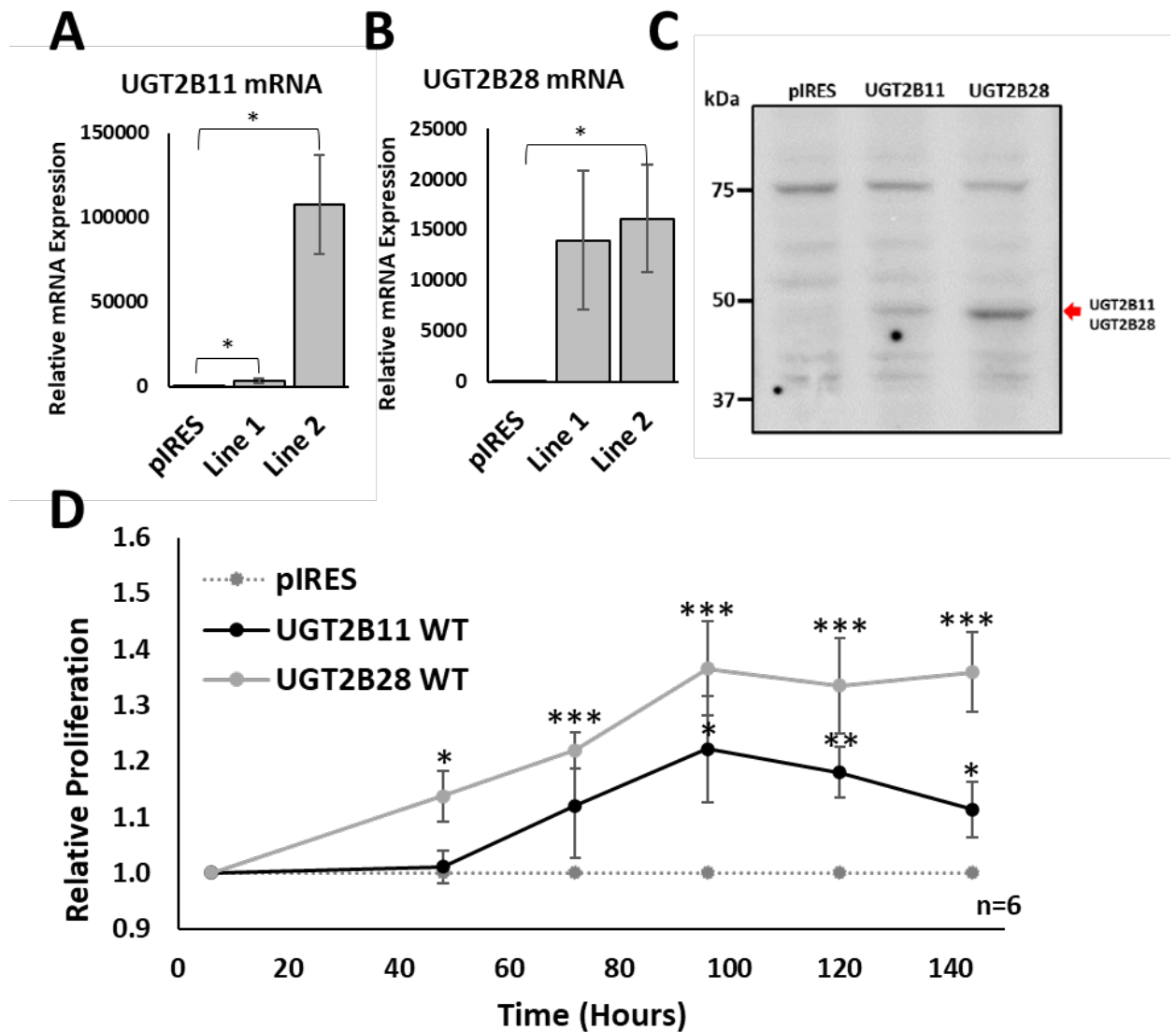


Figure 4.3: Characterisation of UGT2B11 and UGT2B28 MDA-MB-453 overexpression lines

UGT mRNA expression was quantified for two independent UGT2B11 (**A**) and UGT2B28 (**B**) MDA-MB-453 overexpression cell lines via qRT-PCR. Mean \pm SEM of three biological experiments normalised to 18s rRNA housekeeping gene and then expressed relative to pIRES control cell line. Statistical significance was assessed by Student's *t*-test. (**C**) Representative immunoblot of at least two independent experiments showing UGT overexpression in stable overexpression lines. Protein lysates were harvested as described in methods, 30 μ g of which was subjected to SDS-PAGE and Western blotting. Membranes were probed with anti-UGT2B7 polyclonal antibody. (**D**) Proliferative capacity of stable lines was quantified using the crystal violet assay. Mean \pm SEM of six biological replicates from two independently derived sets of lines (each consisting of 24 averaged technical replicates) is presented, normalised to cellular density at 6 hours and to the pIRES control stable line at each time point. Statistical significance was assessed by one-way-ANOVA and Dunnett's post hoc testing and indicated as follows: * $p < 0.05$, ** $p < 0.01$, *** $p < 0.001$.

As bioinformatic analysis of RNAseq data implicated UGT2B11 and UGT2B28 in SREBP-dependent lipid biosynthetic pathways in breast tissue (see Chapter 3), it was hypothesised that a UGT-mediated increase in SREBP activity might underlie the observed increase in proliferation in MDA-MB-453 cells. Consequently, the mRNA levels of an array of previously defined SREBP-1 and SREBP-2 gene targets were assessed in the second generated set of UGT-overexpressing lines (Figure 4.4).

There was a marked increase in the expression of multiple SREBP-1 (-1a and -1c) and SREBP-2 gene targets in both overexpression lines (Figure 4.4). Of the 19 SREBP-targets that were amplified in MDA-MB-453 cells, 15 showed increased expression in either the UGT2B11 line, UGT2B28 line, or both, relative to the control line. This data is consistent with the hypothesis that UGT overexpression results in perturbation of lipid biosynthetic pathways. As SREBP-1 targets are primarily involved in fatty acid biosynthetic pathways and SREBP-2 targets typically mediate cholesterologenic pathways, these data suggest that UGT2B11 and UGT2B28 may be able to influence both pathways through altering the functions of multiple SREBP isoforms.

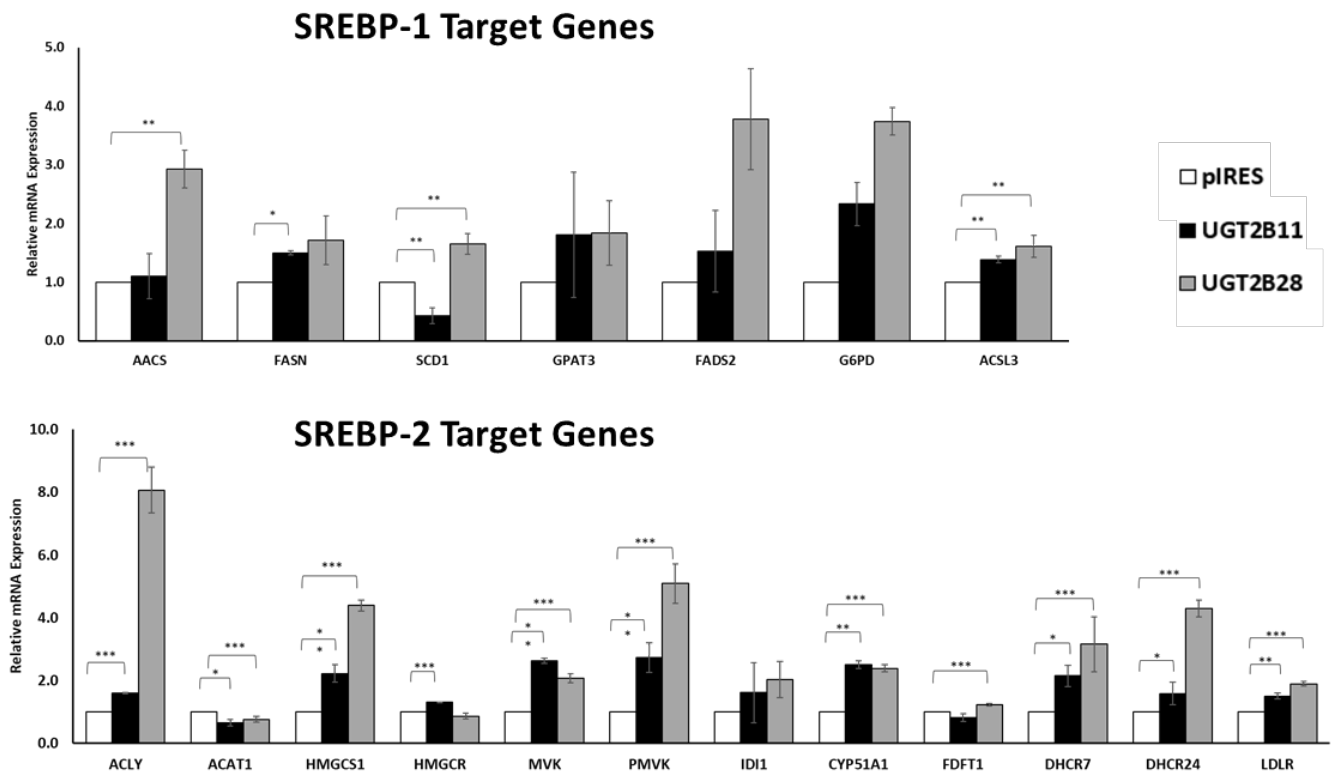


Figure 4.4: Effect of UGT2B11 and UGT2B28 overexpression in MDA-MB-453 cell lines on SREBP target genes

The mRNA expression levels of SREBP-1 and SREBP-2 gene targets were quantified in one set of pIRES, UGT2B11 and UGT2B28 MDA-MB-453 overexpression stable lines using qRT-PCR. Mean \pm standard deviation is shown from three independent biological experiments (each with two averaged technical replicates). Data is normalised to the average of the 18s housekeeping gene and then expressed relative to pIRES control line. Statistical significance was assessed by One-way ANOVA and Dunnett's post hoc testing and is indicated as follows: * $p < 0.05$, ** $p < 0.01$, *** $p < 0.001$.

The mechanism by which UGT2B11 and UGT2B28 might modify expression of SREBP targets remains unknown. UGT enzymes transform lipophilic chemicals into less active and more readily eliminated glucuronide metabolites. The most efficiently glucuronidated substrates of UGT2B11 are hydroxylated fatty acid metabolites, while UGT2B28 has no well-defined substrates. This knowledge prompted a hypothesis that these UGTs might modulate SREBP signalling by altering levels of specific lipid species. *UGT* genes produce transcript variants that encode truncated, inactive variants; it was reasoned that these inactive variants could be used to assess whether the UGTs modulate SREBP function by a catalytic mechanism. To this end, new stable lines were generated that express natural variants that encode truncated proteins designated UGT2B11 Tr and UGT2B28 Tr, along with cognate empty vector line. Heterologous expression of the variant UGT2B11 Tr and UGT2B28 Tr transcripts was assessed by qRT-PCR, revealing a very high abundance relative to the endogenous expression level e.g. ~23,000 and ~53,500 fold, respectively (Figure 4.5A-B).

The proliferative capacity of these cell lines was assessed as described previously (Figure 4.5C). Both UGT2B11 Tr and UGT2B28 Tr overexpression lines showed increases in proliferative capacity relative to the control line. This difference was only statistically significant at a subset of timepoints, which may be due to intra-experimental variability (n = 3 independent experiments); however, despite the greater variability in the proliferation data, there was a consistent overall trend towards increased proliferation that was similar to that conferred by overexpression of wild type UGT2B11 and UGT2B28 transgenes. This may suggest that the pro-proliferative effect of overexpression UGT2B11 and UGT2B28 variants may be non-catalytic in nature.

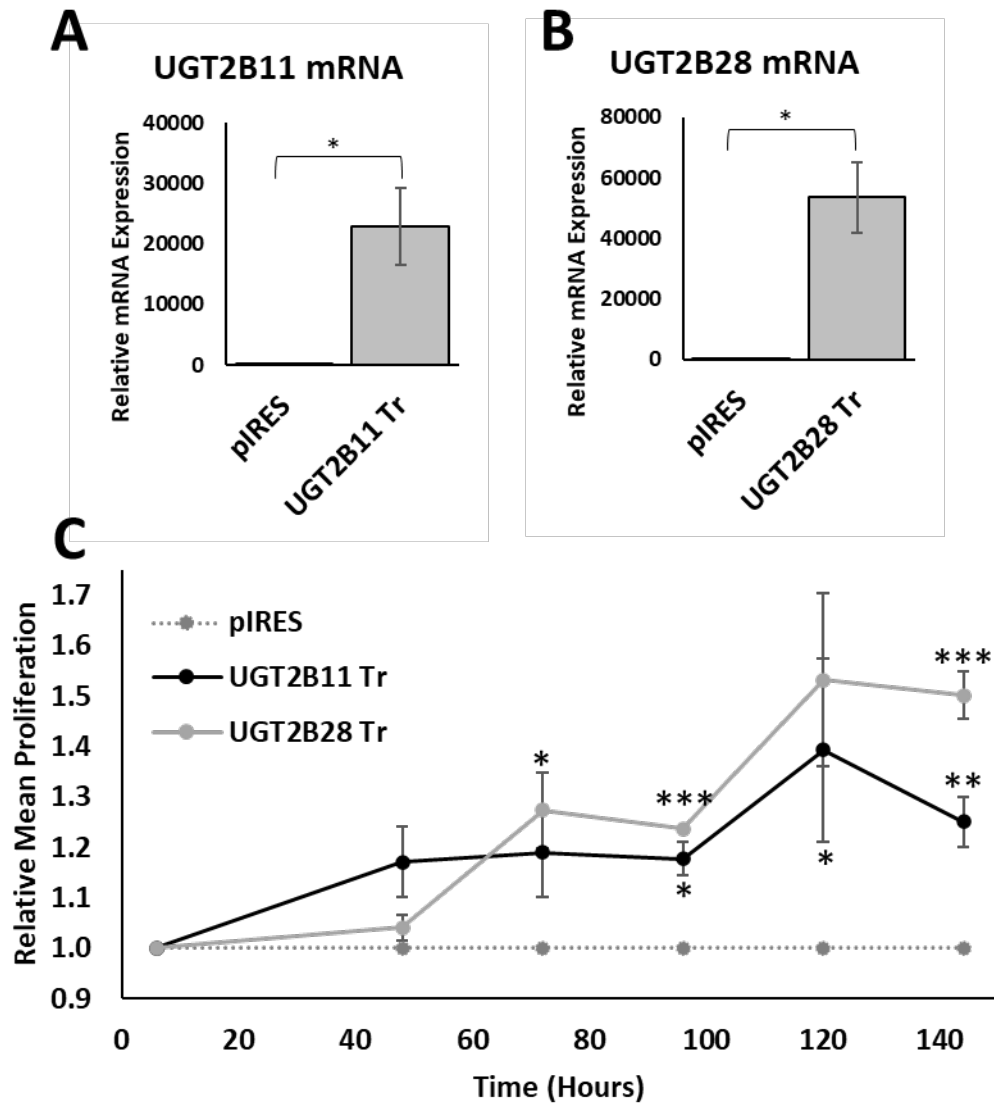


Figure 4.5: Characterisation of MDA-MB-453 overexpression lines of UGT2B11 and UGT2B28 truncated (Tr) isoforms

UGT mRNA expression was quantified for UGT2B11 Tr (**A**) and UGT2B28 Tr (**B**) MDA-MB-453 overexpression cell lines via qRT-PCR. Mean \pm SEM of three biological replicates normalised to 18s rRNA housekeeping gene and then expressed relative to pIRES control cell line depicted. (**C**) Proliferative capacity of stable lines was quantified using the crystal violet assay. Mean \pm SEM of three biological replicates (each consisting of 24 averaged technical replicates) is presented normalised to cellular density at 6 hours and to the pIRES control stable line at each time point. Statistical significance was assessed via Student's *t*-test and indicated as follows: * $p < 0.05$, ** $p < 0.01$, *** $p < 0.001$.

In addition to wildtype and truncated UGT2B28, the effect of overexpressing the common UGT2B28 SNP variant (SNP rs4235127) in MDA-MB-453 cells was also examined (Figure 4.6). This UGT2B28 SNP variant results in a Leu365>His365 substitution in the sugar binding domain of the UGT. Notably, this His365 residue is conserved in all other 21 human UGT enzyme isoforms and has previously been found to be important for the catalytic activity of UGT1A6 based on an alanine substitution experiment (Ouzzine et al., 2000). Therefore, as per the correlation coefficients derived by Grantham (1974), the His>Leu substitution found in the wildtype isoform may be functionally disruptive in UGT2B28. Although it is designated as the reference allele, *UGT2B28* encoding Leu365 has only a slightly higher population frequency (0.502) to that of the *UGT2B28* His365 SNP variant (0.498) (Sherry et al., 2001). To date, only the Leu365 form of the UGT2B28 enzyme has been assessed for enzymatic activity, and no highly conjugated substrates have been found (Lévesque et al., 2001; Turgeon et al., 2003). It is therefore possible that the UGT2B28 protein containing Leu365 is less active than the His365 variant and that overexpression of the latter may result in different effects on cellular function. It should be noted that truncated UGT2B28 lacks residues beyond 335 and thus this SNP is not relevant to studies performed using the UGT2B28 Tr construct.

An MDA-MB-453 cell line stably over-expressing the UGT2B28 His365 variant was generated using the previously described methods. Expression of the transgene was assessed by qRT-PCR using UGT2B28 primers that do not differentiate between the wildtype and SNP isoform transcripts. The data is presented as fold change relative to the level of the endogenous *UGT2B28* reference allele transcript (Figure 4.6A). The UGT2B28 His365 SNP transcript was expressed at levels ranging from ~1,000 to 60,000-fold over the endogenous transcript in three independent experiments. This variance in fold change was likely due to variation in the low baseline levels of wildtype UGT2B28 in the pIRES control line, which could be affected by the cell cycle stage at which the cells were at when plated and harvested for RNA extraction, or minor differences in cell culture parameters (Dolatabadi et al., 2017; Guo et al., 2016; Neumann et al., 2010).

As shown in Figure 4.6B, the UGT2B28 His365 SNP over-expressing cell line showed increased proliferation relative to the control line. The result was similar to that observed in both the UGT2B28 WT (Leu365) and UGT2B28 Tr overexpression lines. The similar

findings in each of these lines suggested that the function of these UGTs with respect to SREBP activity may be non-enzymatic.

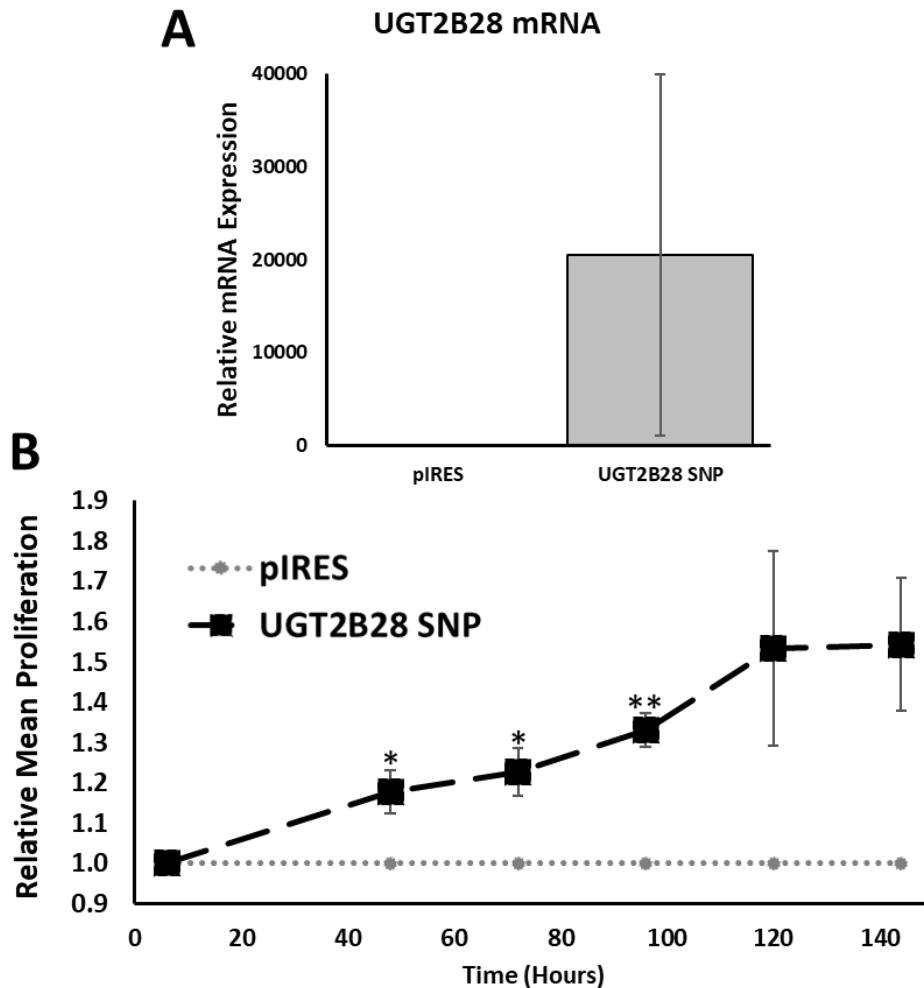


Figure 4.6: Characterisation of MDA-MB-453 overexpression lines of UGT2B28 His365 SNP isoform

(A) UGT mRNA expression was quantified for the UGT2B28 His365 SNP MDA-MB-453 overexpression cell line via qRT-PCR. Mean \pm SEM of three biological replicates normalised to 18s rRNA housekeeping gene and to pIRES control cell line. **(B)** Proliferative capacity of stable lines was quantified using the crystal violet assay as described in methods. Mean \pm SEM of three biological replicates (each consisting of 24 technical replicates) is presented normalised to cellular density at 6 hours and to the pIRES control stable line at each time point. Statistical significance was assessed by Student's *t*-test and indicated as follows: * $p < 0.05$, ** $p < 0.01$.

The UGT2B11 Tr, UGT2B28 Tr, and UGT2B28 His365 SNP MDA-MB-453 stable lines were further characterised by gene expression analysis of lipogenic genes via qRT-PCR (Figure 4.7). Representative SREBP-1 target genes: FASN, G6PD and HMGCS1, and SREBP-2 target genes: DHCR7 and DHCR24, were selected for analysis. There was an overall trend towards increased expression of these lipogenic genes in each of the UGT over-expressing cell lines relative to the control line; although, for some targets, UGT2B28 Tr overexpression did not confer an increase. The variability may be due to different levels of expression of each UGT variant, or other factors that could alter the baseline levels of these genes such as variation in cell density or the relative number of proliferating cells in the population within each experiment. This consistent trend towards increased expression of lipogenic gene targets like that observed for the WT variants could therefore suggest that any affect mediated by the WT variants of these UGTs may be non-catalytic in nature.

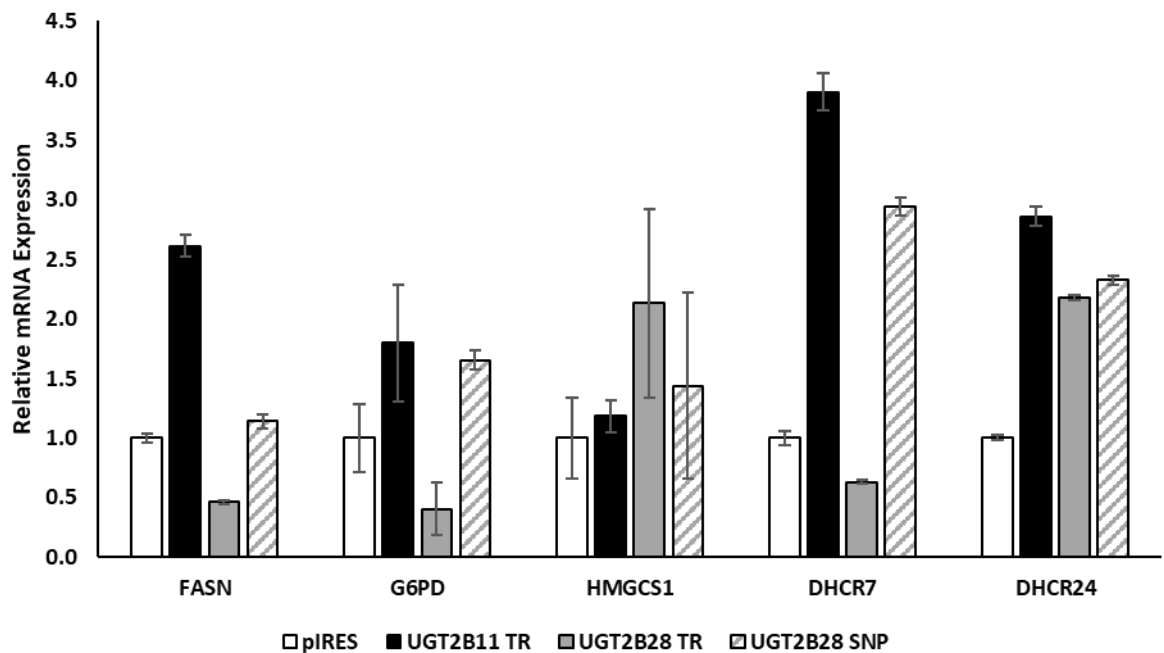


Figure 4.7: Effect of over-expression of UGT2B11 and UGT2B28 truncated (Tr) and His365 SNP variants on SREBP target gene expression in MDA-MB-453 cell lines

The mRNA expression levels of SREBP-1 and SREBP-2 gene targets were quantified in pIRES, UGT2B11 Tr, UGT2B28 Tr and UGT2B28 His365 SNP MDA-MB-453 overexpression stable lines using qRT-PCR. Mean \pm standard deviation is shown from two independent biological experiments (each with two technical replicates). Data is normalised to the average of a 18s housekeeping gene and then expressed relative to pIRES control line.

4.3.2 Construction and analysis of MDA-MB-453 cell lines carrying UGT2B11 and UGT2B28 CRISPRi knockdown vectors

To corroborate the findings from the UGT2B11 and UGT2B28 stable overexpression MDA-MB-453 cell lines, attempts were made to generate knock-down lines using CRISPR inhibition (CRISPRi). A pX459 CRISPRi vector system was generated, with constructs containing gRNAs targeting the proximal promoters of either *UGT2B11* or *UGT2B28*. The CRISPRi vector expresses a KRAB-dCas9 fusion protein that binds to the targeted promoter sequence to effect transcriptional inhibition. The expression of KRAB-dCas9 from the vector was validated by qRT-PCR after transient transfection in HEK-293T cells (data not shown).

Before generating stable MDA-MB-453 cell lines carrying the CRISPRi constructs, attempts were made to test their ability to reduce transactivation from the UGT promoters using a luciferase-reporter assay approach. Luciferase constructs containing the proximal promoter regions of both *UGT2B11* and *UGT2B28* were co-transfected into MDA-MB-453 cells with CRISPRi vectors expressing UGT2B11 or UGT2B28 gRNAs, or the empty vector. None of the vectors altered luciferase activity (Figure 4.8A & B). This indicates that the gRNAs selected do not effectively target the CRISPRi complexes to the promoters. However, it is also possible that the CRISPRi complexes are not effective on non-chromatinised episomal plasmid DNA. This is possible given that the KRAB domain functions by promoting formation repressive chromatin structures. Thus, despite this result, the development of CRISPRi knockdown cell lines was still pursued. It should be noted that there was no change in promoter activity with 1 nM DHT. This was expected as these experiments were performed in sterol replete conditions, which this synthetic reporter has been demonstrated not to respond under.

MDA-MB-453 cell lines stably expressing either the UGT2B11 or UGT2B28-targeted CRISPRi construct, or the control empty vector, were generated by transfection and puromycin selection. This process was performed twice, generating two independent sets of lines. The resulting pools of puromycin resistant cells carried integrated CRISPRi constructs as shown by genomic PCR analysis (data not shown). However, analysis of UGT2B11 or UGT2B28 mRNA levels in the CRISPRi lines showed no reduction in UGT mRNA relative to the empty vector control line (data not shown). Due to the lack of effectiveness of the CRISPRi constructs, and difficulties achieving CRISPRi-mediated knockdown of UGTs in other

projects ongoing within the laboratory, knockdown studies were ceased and remain an area for future investigation.

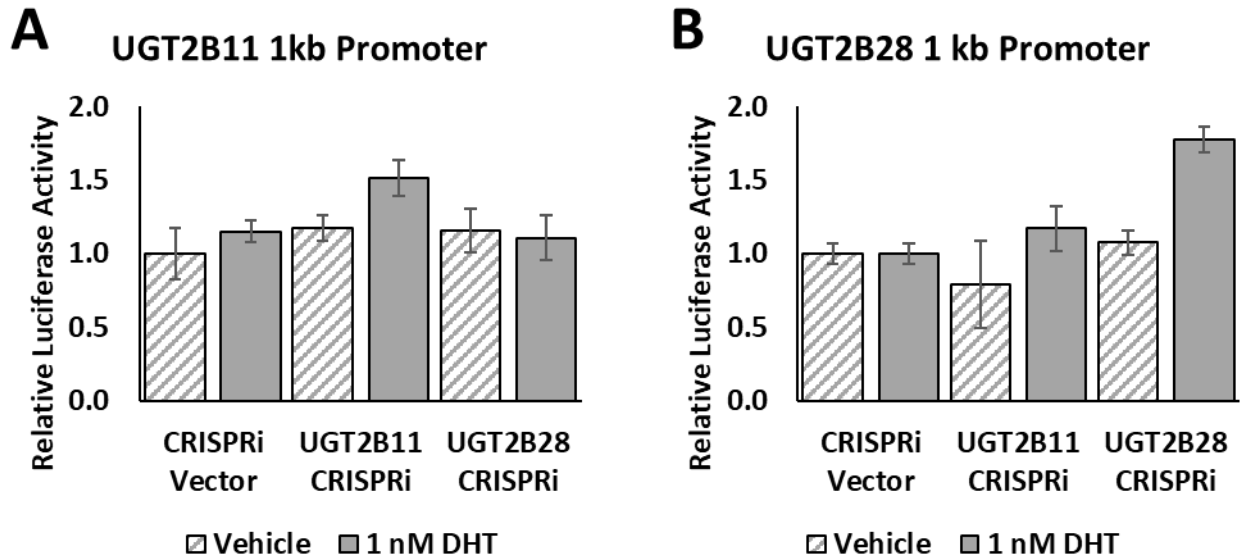


Figure 4.8: UGT2B11 and UGT2B28 CRISPRi does not affect proximal promoter luciferase construct activity

(A) UGT2B11 1 kb proximal promoter (50 ng) or (B) UGT2B28 1 kb proximal promoter (50 ng) luciferase construct was co-transfected with 150 ng of indicated CRISPRi construct and 5 ng pRL-Null. Luciferase activity was assayed 48 hours post transfection. All data normalised to *Renilla* luciferase and vehicle control condition. Mean \pm standard deviation depicted for one representative experiment (n=3 technical replicates).

4.3.3 Generation of SREBP-2 constructs

In order to assess the effect of UGT2B11 and UGT2B28 upon SREBP activity, it was first necessary to generate and validate SREBP-encoding plasmid constructs. Three constructs encoding full length SREBP-2 precursors were generated: Myc-WT SREBP-2, Myc-SREBP-2 S436A and VP16-HA SREBP-2 S436A (Figure 4.9A).

As wildtype nSREBPs undergo rapid proteasomal degradation upon nuclear translocation (Sundqvist & Ericsson, 2003), a variant of SREBP was made in which residue S436 in the phosphodegron was mutated to alanine (S436A), preventing proteasomal turnover (Sundqvist et al., 2005). The nSREBP domain of this variant (Myc SREBP-2 S436A) was predicted to accumulate in the nucleus and produce more transactivation than that of WT SREBP-2.

To generate an even more transcriptionally active variant of SREBP, the VP16 activation domain from the Herpes simplex virion protein 16 was appended to the N-terminus of the phospho-mutant S436A form of SREBP-2. This variant was designated VP16-HA-SREBP-2 S436A. The strong activating VP16 domain has been shown to increase potency of a number of transcription factors (Hirai et al., 2010), and hence when nSREBP accumulates in the nucleus due to the S436A mutation, it was predicted that transactivation would be further enhanced.

Immunoblot analysis showed that each of these three SREBP constructs expressed precursor proteins of the expected size when transfected in HEK293T cells (Figure 4.9B). The functionality of the expressed SREBP proteins was assessed using a transactivation assay using a *DHCR24* promoter-luciferase reporter construct. The *DHCR24* promoter contains a well-defined SREBP responsive element (SRE) (Zerenturk et al., 2012). An additional set of co-transfection conditions included SCAP to promote processing of SREBP into its active nSREBP form. The SREBP constructs alone induced minimal activation of the *DHCR24* reporter. However, co-expression of SCAP with the SREBPs led to a significant increase in promoter induction. This result is consistent with previous studies showing that co-expression of SCAP increases processing of SREBP into the transcriptionally active nuclear form by outcompeting the ER retention effect of endogenous INSIG (Figure 4.9C) (Yang et al., 2000).

Under SCAP co-expression conditions, wildtype SREBP-2 significantly increased reporter transactivation an average of 2.4-fold relative to control conditions. Similarly, under SCAP co-expression conditions the variant of SREBP-2 carrying the phosphodegron mutation (S436A), increased reporter transactivation by 3.4-fold. This greater transactivation capacity is presumed to be due to the stabilizing effect of the S436A mutation which allows nSREBP to accumulate in the nucleus. The version of the SREBP-2 S436A protein that was fused to the VP16 activation domain (VP16-SREBP-2 S436A) showed even greater capacity to transactivate the reporter, increasing activity by 4.3-fold under SCAP co-expression conditions (Figure 4.9C).

It should also be noted that SCAP co-expression in the empty vector control also significantly enhanced promoter transactivation, however, this activity increase is minimal (1.3-fold) and is likely due to it acting to increase processing of endogenous SREBP precursors (Figure 4.9C).

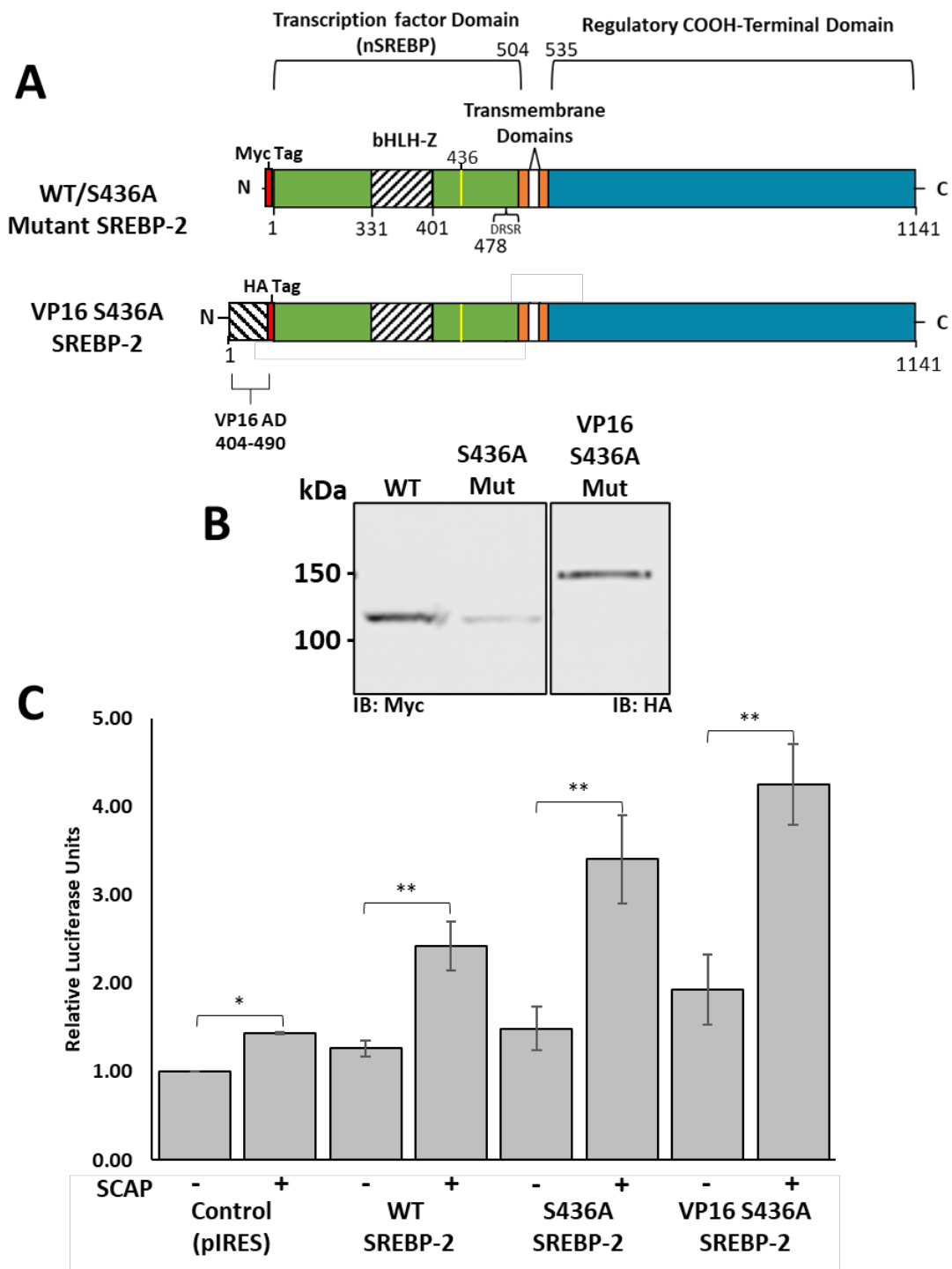


Figure 4.9: Development and validation of SREBP-2 plasmid constructs

(A) Domain structure of SREBP-2 plasmid constructs. **(B)** Immunoblot of HEK-293T lysates transiently transfected with SREBP-2 expression constructs, confirming expression of proteins of the expected sizes (IB indicates antibody used for each blot). **(C)** HEK-293T cells were co-transfected with 50 ng *DHCR24-300* SRE containing luciferase reporter construct, 5 ng pRL-Null and 100 ng of indicated plasmid DNA. Luciferase activity assayed 48 hours post transfection. All data were normalised to *Renilla* luciferase and control condition. Mean \pm SEM depicted of at least four independent biological experiments. Statistical significance was assessed by Student's *t*-test or one-way-ANOVA and Tukey post hoc testing as appropriate and indicated as follows: * $p < 0.05$, ** $p < 0.01$.

4.3.4 Effect of UGT overexpression on activation of an SREBP target gene promoter

The next set of experiments examined whether UGT2B11 or UGT2B28 could modulate the ability of SREBP-2 to transactivate the *DHCR24* reporter. The VP16 SREBP-2 S436A variant was used for these studies as it showed the greatest capacity to transactivate this reporter, both alone and with SCAP co-expression (as shown in Figure 4.9). As the effects of UGT2B11 and UGT2B28 appeared to be similar in previous studies, the UGT2B11 WT plasmid was used as a representative 'type isoform'. Co-transfection of the expression and reporter plasmids was performed under the same conditions shown in Figure 4.9.

The effect of UGT2B11 was compared to the effect of SCAP, both in the presence and absence of VP16 SREBP-2 S436A (Figure 4.10). Expression of SCAP alone caused a small but significant increase in the activity of the reporter gene, relative to the empty vector control. This is likely due to SCAP-induced processing of endogenous SREBPs, as observed previously (see Figure 4.9). Expression of UGT2B11 alone also slightly but significantly increased reporter activity. Expression of VP16 SREBP-2 S436A alone had minimal effect on the reporter activity. In contrast, co-expression of SCAP with VP16 SREBP-2 S436A induced a significant ~3.5-fold increase in reporter activity. Co-expression of VP16 SREBP-2 S436A with UGT2B11 led to a moderate increase in reporter transactivation (~1.7-fold) relative to the control condition (Figure 4.10). These data suggest that, while less effective than SCAP, UGT2B11 may increase the amount of the SREBP precursors that are processed into transcriptionally active nSREBP. Similarly, the slight yet statistically significant increase in luciferase activity (1.3-fold) observed when only UGT2B11 was transfected might be due to increased processing of endogenous SREBP precursors.

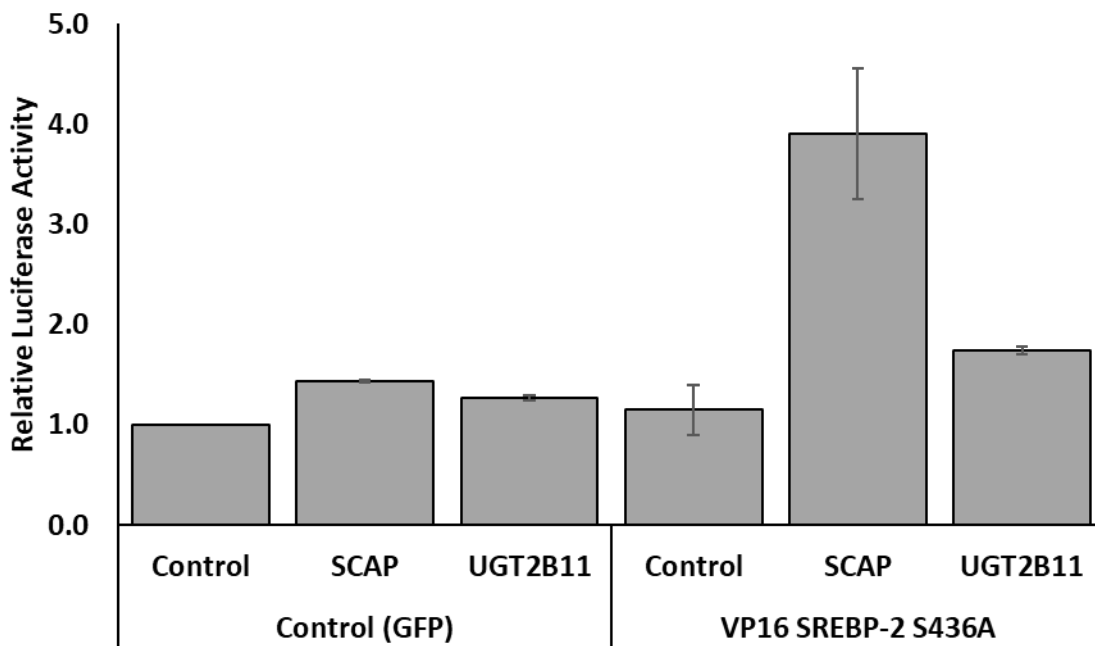


Figure 4.10: UGT2B11 increases transactivation of *DHCR24* luciferase reporter

HEK-293T cells were co-transfected with 50 ng *DHCR24*-300 luciferase reporter construct, 5 ng pRL-Null, 100 ng of VP16 SREBP-2 S436A and 100 ng indicated plasmid DNA. Luciferase activity was assayed 48 hours post transfection. All data were normalised to *Renilla* luciferase and control condition. Mean \pm SEM depicted of two independent biological experiments.

4.3.5 Assessment of SREBP processing via immunoblotting

As an orthogonal approach to study the effects of UGTs on SREBP processing, immunoblotting was used to assess the relative abundance of nSREBP produced after transfecting an epitope tagged SREBP-2 precursor into HEK-293T cells under various conditions. The SREBP-2 precursor is approximately 100 kDa, whereas the processed transcriptionally active nuclear nSREBP form is approximately 65 kDa. Due to the location of the epitope tag in the SREBP-2 construct, it is retained after processing, allowing both forms to be detected on a single immunoblot.

Assessment of processing by immunoblotting was attempted under a variety of different conditions. In the Myc-SREBP-2 and SCAP co-expression condition, processed nSREBP-2 could not be detected (Figure 4.11A). This was surprising because SCAP co-expression increased SREBP-2 activation based on the *DHCR24* reporter assays. Reasoning that the

amount of processed nSREBP-2 produced in HEK-293T cells under these conditions was below the sensitivity limit of the immunoblot assay, attempts were then made to enhance processing by culturing cells in lipid-deplete serum (Figure 4.11A-C). The medium was prepared as described in methods (Section 4.2.5) (Agnese et al., 1983; Brovkovich et al., 2019), and was validated via the *DHCR24* reporter assay (Figure 4.11B). The lipid-deplete culture condition increased the basal activity of the *DHCR24* promoter, and its capacity to be transactivated by exogenously expressed SREBP, both with and without SCAP co-expression. This result was consistent with previous studies reporting that sterol depletion causes conformational changes in SCAP that allow it to dissociate from INSIG, and chaperone SREBPs to the Golgi to initiate processing. Although the lipid-deplete culture condition only led to a modest increase in SREBP-2 processing as inferred from the transactivation assay, the immunoblotting experiments were repeated using this condition. Unfortunately, it was still not possible to detect processed nSREBP-2. Furthermore, an attempt was made to stabilise the processed nSREBP-2 form with the proteasomal inhibitor MG132 (Figure 4.11C). Transfected cells were treated with MG132 (25 μ M) for 4 hours prior to harvesting. This condition was insufficient to cause a detectable amount of nSREBP-2 protein to accumulate based on immunoblotting analysis. Increasing MG132 concentration beyond 25 μ M, or increasing the duration of treatment, led to cell death before harvesting.

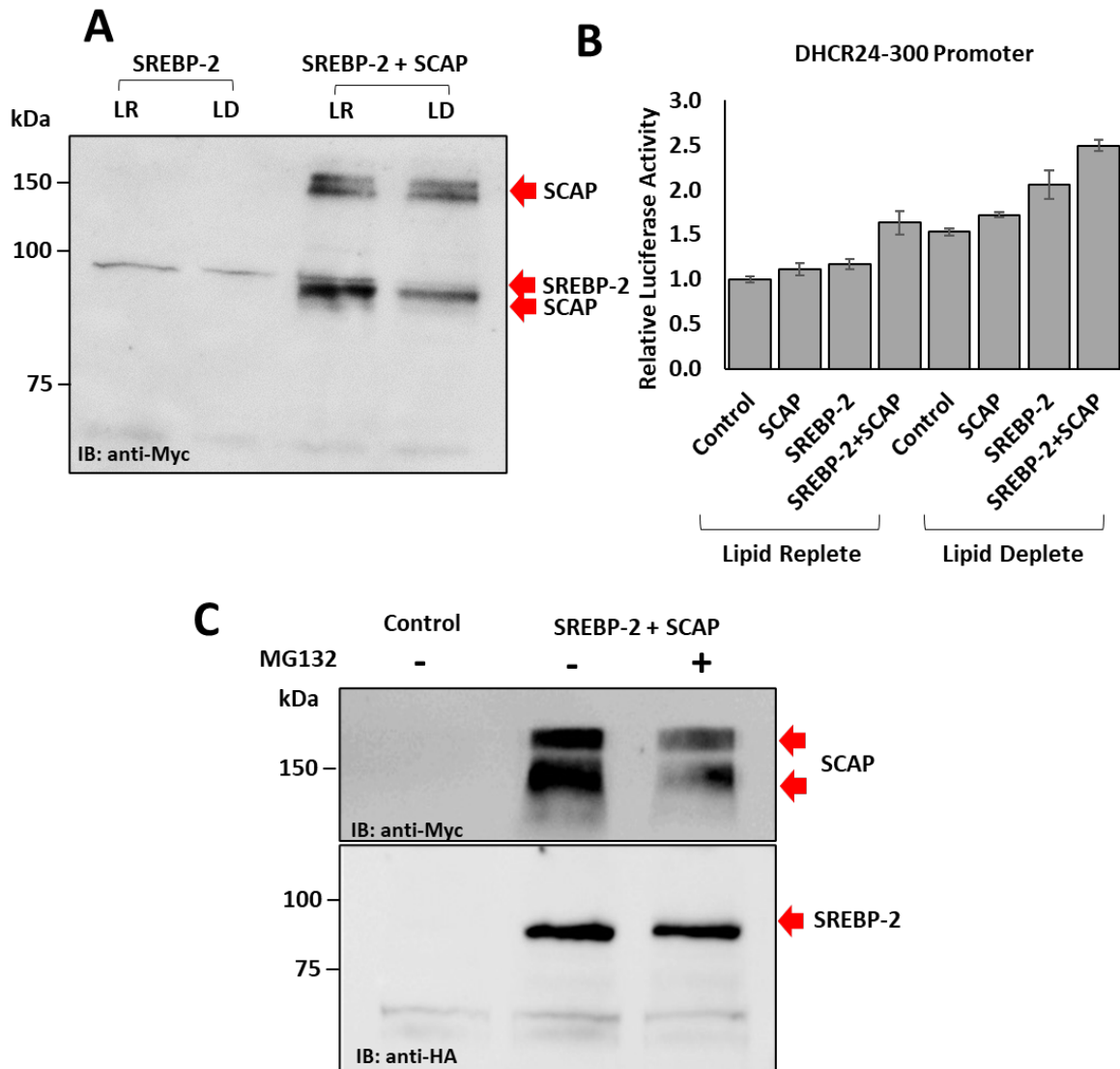


Figure 4.11: Effect of SCAP overexpression and delipidation of media on SREBP processing

(A) HEK-293T cells were co-transfected with Myc-SCAP and Myc-SREBP-2 and cultured for 48 hours in media containing lipid replete (LR) or lipid deplete (LD) serum. **(B)** HEK-293T cells cultured in indicated media were transfected with 50 ng of *DHCR24-300* luciferase promoter construct, 5 ng pRL-Null and 100 ng of SCAP or SREBP-2 expression plasmids. Transfections were normalised through the addition of GFP (control) expression plasmids. Luciferase activity assayed 48 hours post transfection. All data were normalised to *Renilla* luciferase and control condition. **(C)** HEK-293T cells were co-transfected with Myc-SCAP and HA-SREBP-2 and cultured for 48 hours in media containing lipid deplete serum, 4 hours prior to harvest cells were treated with MG132 (25 μ M) proteasome inhibitor.

Finally, an attempt was then made to enhance the sensitivity of the immunoblotting method by performing nuclear and membrane fractionation of lysates as per Suzuki et al. (2010) (Figure 4.12). However, in three independent experiments, nSREBPs could not be detected in the nuclear fractions after co-expressing HA-SREBP-2 and SCAP (Figure 4.12).

Ultimately, it was not possible to confirm the effect of SCAP or UGT2B11 co-expression on SREBP-2 processing in HEK-293T cells via immunoblotting. It is hypothesised that whilst co-expression of these factors can increase SREBP-2 processing based on enhanced transactivation of the *DHCR24* reporter, the absolute amount of nSREBP-2 produced remains below the detection limit of the immunoblot method. The greater sensitivity of the luciferase reporter assay may explain why this method was able to detect changes that could not be observed by measuring the protein directly.

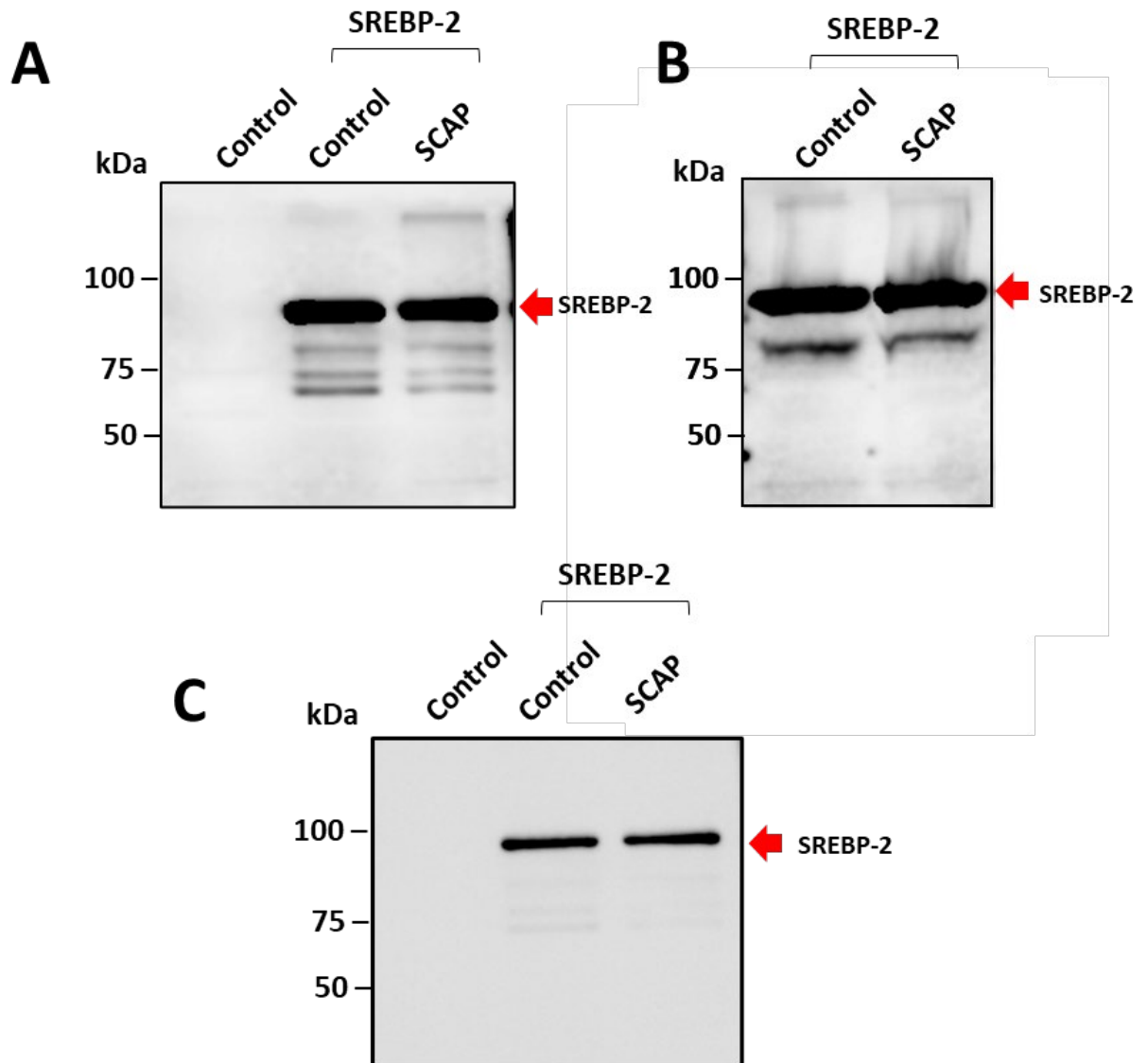


Figure 4.12: Cellular fractionation to assess SREBP processing

HEK-293T cells were co-transfected with Myc-SCAP and HA-SREBP-2 and cultured for 48 hours. Cell lysates were fractionated to collect cellular nuclei and membranes for immunoblotting and were then probed for SREBP-2 with anti-HA antibody. Three independent biological experiments are depicted (A, B and C). SREBP-2 precursor is indicated in each panel.

4.3.6 Development of a fluorescent SREBP processing assay

Due to the lack of success with the immunoblotting approach, an alternative fluorescence-based method was developed to confirm whether UGTs can increase SREBP processing. In this system, the mCherry fluorescent protein was fused to the N-terminus of the full length SREBP-2 precursor (Figure 4.13A-B). This assay is similar to that previously described by Bertolio et al. (2019). After transfection of this construct into cells, the mCherry-SREBP-2 precursor proteins could be visualized in the ER by fluorescence microscopy, and processing to the active form could be monitored by an increase in nuclear localisation. The SREBP-2 containing the S436A phosphodegron mutation was used to reduce turnover of nSREBP-2, allowing it to accumulate within the nucleus, thus increasing signal intensity.

Initially, validation of the mCherry-SREBP plasmid was performed by transfection in MDA-MB-231 cells (Figure 4.13C-E). MDA-MB-231 cells represent a triple negative luminal androgen receptor (TNBC-LAR) breast cancer subtype and were selected based on previous literature showing the effectiveness of this assay in this cell type (Bertolio et al., 2019). Furthermore, as identified in Chapter 3, a lack of ER expression and a high level of AR expression is consistent with tumour types where increased expression of these UGT isoforms is physiologically relevant. Furthermore, the glucuronate pathway (which includes UGTs) and fatty acid metabolism pathways are enriched in LAR patient tumours (Lehmann et al., 2011), providing additional evidence that this is a relevant model for these studies. Moreover, the *DHCR24* promoter construct was confirmed to be significantly induced by overexpression of SCAP in conventional lipid replete (but not in serum free) conditions in this cell line, which is indicative of increased SREBP processing (Figure 4.13C).

To optimise the fluorescence-based assay, MDA-MB-231 cells were transfected with mCherry-SREBP-2 and cultured under various media conditions. The extent of processing as indicated by nuclear accumulation of nSREBP-2 was estimated from the ratio of nuclear/cytoplasmic fluorescence. This ratio was similar when cells were cultured in conventional medium or serum (lipid) free conditions (nuclear/cytoplasmic fluorescence ~0.65) (Figure 4.13D). Modulating glucose levels is reported to alter SREBP processing, specifically, in high glucose conditions, SCAP is N-glycosylated, which reduces its association with INSIG and thus promotes an increase in SREBP processing (Cheng et al., 2015). Thus, to test the effects of glucose on the assay, MDA-MB-231 cells were transfected with the mCherry-SREBP-2 vector and cultured in low glucose medium (1 g/L) for 24 hours,

and then changed to high glucose medium (4.5 g/L) for 24 hours. Compared to cells that were maintained in low glucose conditions, the switch to high glucose induced a significant increase in the nuclear/cytoplasmic fluorescence ratio (Figure 4.13E). Because SREBP-2 activation was greater in high glucose culture media, the subsequent studies were performed under these conditions. MDA-MB-231 cells were co-transfected with mCherry-SREBP-2 and either SCAP, UGT2B11, or a control empty vector (Figure 4.13F). A statistically significant increase in the nuclear localisation of mCherry (mCherry-nSREBP-2) was observed under SCAP co-expression conditions. Under the same conditions, UGT2B11 also increased mCherry-nSREBP nuclear localisation. These data provided further support for the hypothesis that UGT2B11 has the capacity to increase the processing of inactive SREBP-2 precursors to their nuclear nSREBP-2 form.

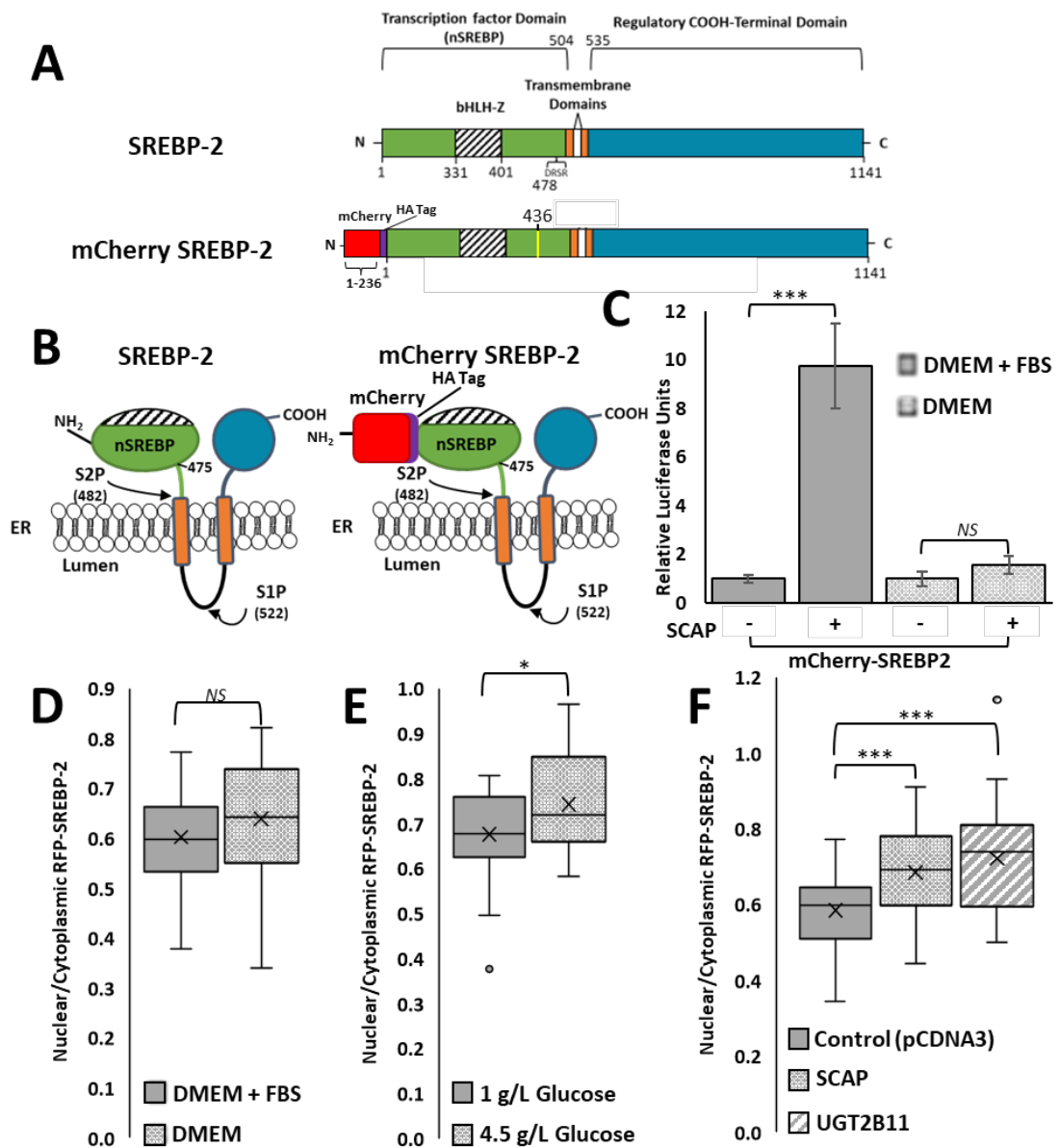


Figure 4.13: Development of a fluorescence based SREBP-2 processing assay

(A) Domain structure and **(B)** topology of mCherry SREBP-2 fusion construct. **(C)** MDA-MB-231 cells were transfected with 50 ng DHCR24 SRE containing luciferase reporter construct, 5 ng pRL-Null, 100 ng of mCherry-SREBP-2 with either 100 ng of SCAP or pcDNA3 and plated into DMEM with or without 10% FBS. Luciferase activity assayed 48 hours post transfection and normalised to Renilla luciferase and control condition. Representative data of at least two independent biological experiments depicted (Mean ± SEM for n=3). **(D, E)** MDA-MB-231 cells were transfected with 850 ng of mCherry-SREBP-2 and plated into high-glucose DMEM **(D)** with or without 10% FBS or plated into low glucose DMEM **(E)** with or without supplementation with glucose 24 hours post transfection. **(F)** MDA-MB-231 cells were transfected with 850 ng of mCherry-SREBP-2 and indicated plasmid. Cells were fixed and stained with DAPI 48 hours post transfection prior to imaging. All data were normalised to background fluorescence. Representative data of at least two independent biological experiments depicted (Mean ± SEM for n=20 imaged cells for panels **D, E**) or compiled data of two independent biological experiments depicted (Mean ± SEM for n=40 imaged cells for panel **F**). Statistical significance was assessed by Student's *t*-test or one-way-ANOVA and Dunnett's post hoc testing as appropriate and indicated as follows: NS - not significant * $p < 0.05$, *** $p < 0.001$.

4.3.7 Development of a reporter based SREBP processing assay

Data shown in sections 4.3.4 and 4.3.5 indicated that UGTs may modulate the processing of SREBP precursors. To further explore the molecular mechanisms by which UGTs may promote SREBP processing, a luciferase reporter-based processing assay was developed similar to that described by Takeuchi et al. (2010).

The SREBP processing assay was based on the GAL4-VP16 UAS-promoter transactivation system. In the first step of developing the assay, the DNA-binding domain from the GAL4 transcription factor was fused to the activation domain of VP16 to form a potent constitutive transactivating protein. This protein (GAL4-VP16) can bind and transactivate a reporter construct in which luciferase expression is controlled by a promoter bearing UAS elements (Figure 4.14A-B). Reporter activity was induced almost 300-fold by GAL4-VP16 after transfection of the vectors into HEK-293T cells as shown in Figure 4.14C.

The next step in developing the processing assay involved fusing the GAL4-VP16 protein upstream of the C-terminal regulatory domain of SREBP-2 (residues 477-1141) in place of the native N-terminal nSREBP domain. This new chimeric protein (GAL4-VP16 C-SREBP-2) contains the C-SREBP-SCAP interaction domains required for ER localisation, and the transmembrane cleavage sites required for proteolytic activation by S1P and S2P after transport to the Golgi (Figure 4.14A-B). Thus, the GAL4-VP16 C-SREBP 2 protein is essentially a synthetic transcription factor whose localisation is controlled by the C-terminal regulatory domain of SREBP. The protein will be retained in the ER unless appropriate signals (such as low sterols) trigger dissociation of the SCAP-C-SREBP complex from INSIG, resulting in translocation to the Golgi and proteolytic cleavage to release the GAL4-VP16 portion. The cleaved GAL4-VP16 domain translocates to the nucleus where its activity can be measured via the UAS reporter.

To confirm that the GAL4-VP16 C-SREBP 2 protein underwent processing and activation as expected, it was tested by transfection of the construct in HEK-293T, MDA-MB-453 and MDA-MB-231 cells (Figure 4.14D-F). When GAL4-VP16 SREBP-2 and the UAS-reporter were co-transfected with an empty vector control or with a GFP expression vector, no activation of the reporter was observed. GFP is frequently utilised as a control in reporter assays involving heterologous protein expression as it ensures that the extra demand on the translation system is comparable in all transfection conditions. Subsequent experiments

tested the ability of factors including SCAP and UGTs to modulate the activation of GAL4-VP16 C-SREBP 2, using GFP to normalise the amount of exogenous protein produced in each condition.

In all cell lines tested, co-expression of SCAP with GAL4-VP16 C-SREBP 2 caused a significant increase in reporter activity. This was expected as the excess SCAP is known to titrate endogenous INSIG, thus releasing complexes containing GAL4-VP16 C-SREBP 2 and native SCAP from ER retention. When SCAP and INSIG-1 were co-expressed, activation of the reporter was significantly reduced relative to transfection of SCAP alone. This was again expected as the additional INSIG is predicted to titrate the additional SCAP. These data suggested that the GAL4-VP16 C-SREBP-2 fusion protein indeed resides within the ER in association with SCAP and INSIG-1 and that its processing is appropriately controlled by the relative levels of these factors. The magnitude of processing induced by SCAP (as assessed by promoter activation) was greatest in MDA-MB-231 cells (~36.3-fold) and was several fold lower in HEK-293T (~8.2-fold) and MDA-MB-453 cells (~7-fold) (Figure 4.14 D-F). Thus, subsequent experiments were performed in the MDA-MB-231 cell line.

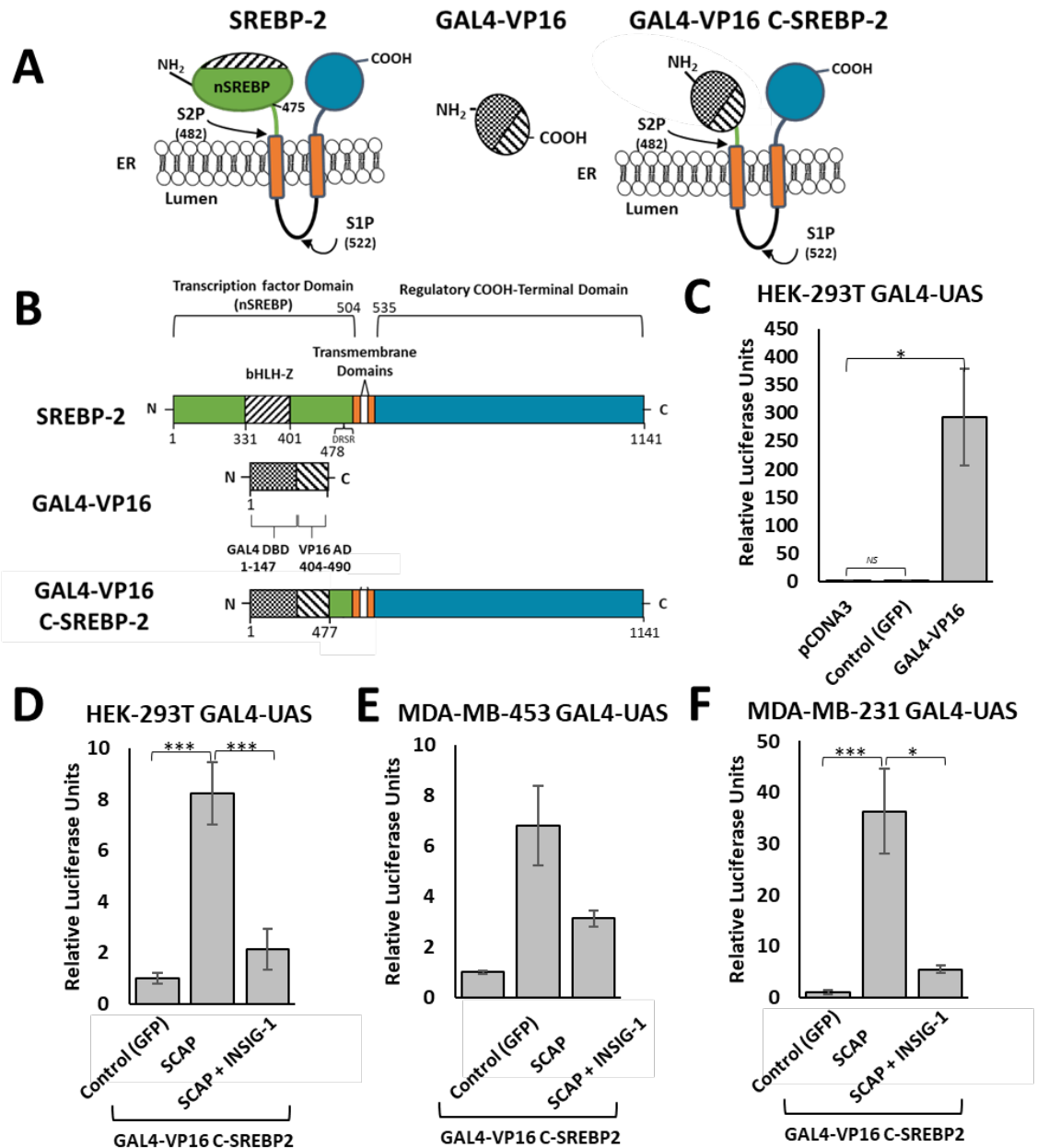


Figure 4.14: Development of GAL4-VP16 SREBP-2 Processing Assay

(A) Topology and (B) domain structure of GAL4-VP16 Fusion constructs. (C, D) HEK-293T cells were co-transfected with 50 ng pck-1 GAL4 UAS luciferase reporter, 5 ng pRL-Null and (C) 200 ng indicated plasmid DNA or (D) 10 ng of GAL4-VP16 C-SREBP-2 plasmid and 50 ng of indicated plasmid. (E) MDA-MB-453 or (F) MDA-MB-231 cells were co-transfected with 50 ng pck-1 GAL4 UAS luciferase reporter, 5 ng pRL-Null, 2 ng of GAL4-VP16 C-SREBP-2 plasmid and 50 ng of indicated plasmid. All transfections were equalized through addition of GFP plasmid where required. Luciferase activity was assayed 48 hours post transfection. All data were normalised to Renilla luciferase and control condition. Representative figure of at least three biological experiments depicted (Mean \pm SEM for $n=3$ technical replicates). Statistical significance was assessed by Student's *t*-test or one-way-ANOVA and Tukey post hoc testing as appropriate and indicated as follows: NS - not significant * $p < 0.05$, *** $p < 0.001$.

4.3.8 Overexpression of UGT2B11 and UGT2B28 variants induces processing of GAL4-VP16 C-SREBP-2

The ability of UGTs to alter processing of GAL4-VP16 C-SREBP-2 was tested by co-transfection of wildtype UGT2B11 or UGT2B28 with GAL4-VP16 C-SREBP-2 in MDA-MB-231 cells. Both UGTs moderately, but significantly, increased transactivation of the UAS-promoter by ~3-3.5-fold relative to the GFP control condition (Figure 4.15A). This enhancement is much less than that induced by SCAP, but it was consistent with the magnitude of UGT-mediated effects observed in previous assays (see Sections 4.3.4 and 4.3.5).

In addition to activation via the canonical SCAP-mediated sterol-sensing mechanism, a number of other cellular events are known to modulate SREBP activation, including ER stress (Colgan et al., 2007). ER stress is typically caused by excessive protein expression resulting in accumulation of misfolded proteins in the ER. In any assay system where heterologous protein production is high, there is a risk of generating ER stress. Thus, it was considered possible that overexpression of the UGTs increased SREBP processing indirectly by causing ER stress. GFP was used as a control in the assays to ensure that a comparable amount of total protein was produced in all conditions; however, GFP is primarily cytosolic (although it is observed in all cell compartments) and does not specifically accumulate in the ER. In contrast, UGTs are almost exclusively localised within the ER membrane. Thus, it is possible that overexpression of UGTs could cause more ER stress than expression of the GFP control. To accommodate this, an ER localized fluorescent protein (ER-RFP) was introduced as an additional control. ER-RFP contains a KDEL peptide fused to a red fluorescent protein (mCherry); the KDEL peptide binds to receptors that mediate retrieval of proteins that have escaped to the cis-Golgi, resulting in their net ER retention. Both ER-RFP and UGT proteins were predicted to accumulate in the ER to a similar degree and thus have similar potential to induce ER stress.

Co-expression of ER-RFP with GAL4-VP16 C-SREBP-2 did not increase promoter activity relative to GFP (Figure 4.15A), suggesting that its accumulation in the ER did not induce sufficient ER stress to trigger SREBP processing. Overall, the finding that UGTs, but not ER-RFP, enhanced processing suggested that it is not a non-specific effect of inducing ER stress, but instead involves a UGT-specific mechanism.

To begin to delineate the domains of the UGTs that are involved in enhancing SREBP processing, the aforementioned naturally occurring truncated variants of UGT2B11 and UGT2B28 were co-expressed with GAL4-VP16 C-SREBP-2 in the reporter assay. These variants lack the C-terminal transmembrane (UGT2B28 Tr) and sugar binding domains (UGT2B11 Tr). Loss of either of these domains has been shown to render UGTs catalytically inactive (Lévesque et al., 2001). Both UGT2B11 Tr and UGT2B28 Tr variants significantly enhanced processing relative to the control condition. The magnitude of the effect of each UGT Tr variant was not significantly different to that induced by any of the wildtype UGT proteins (Figure 4.15B). The finding that truncated UGT proteins enhanced SREBP processing was consistent with earlier studies (Section 4.3.4) in which they could also enhance the activity of the *DHCR24* promoter reporter.

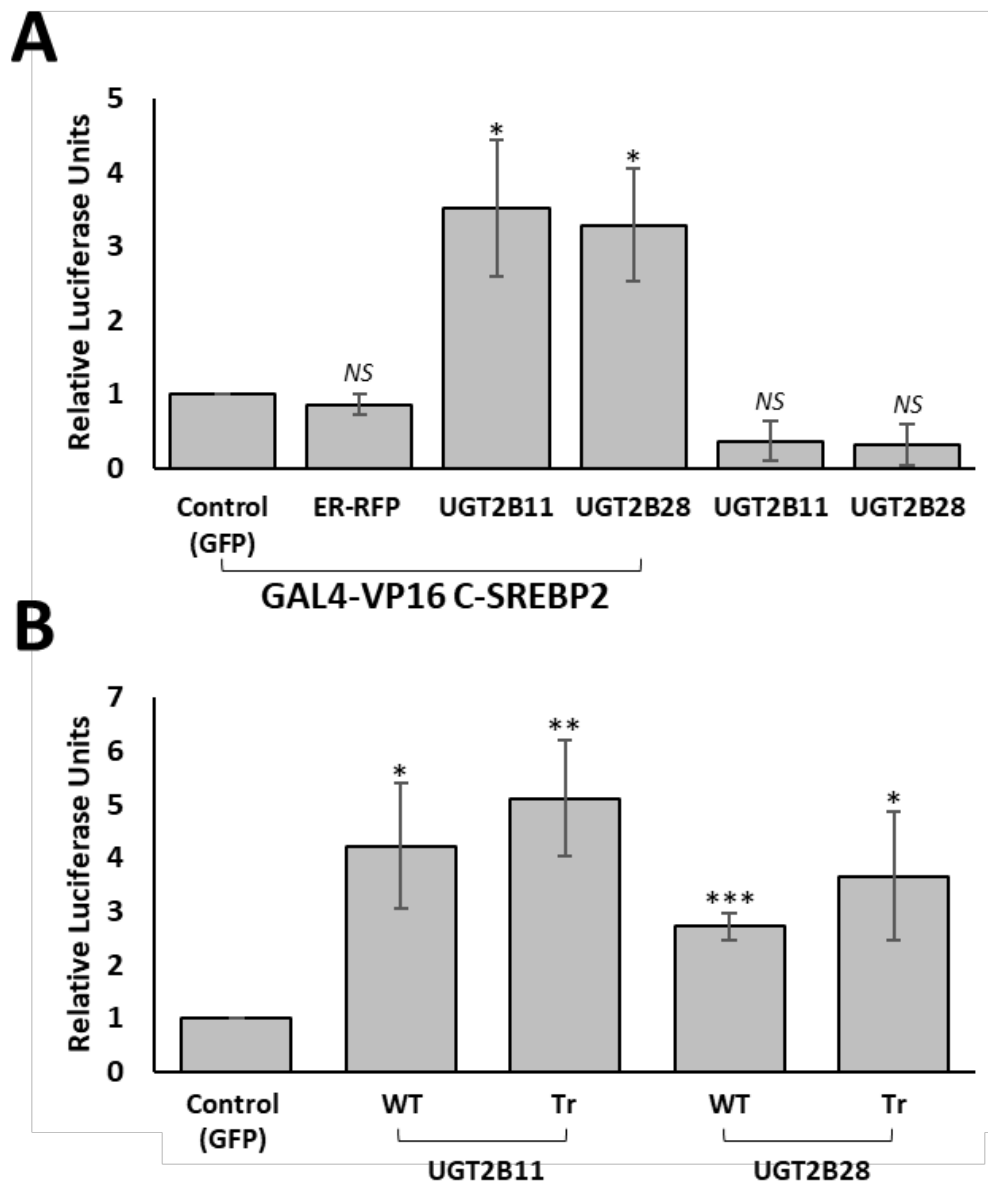


Figure 4.15: UGT2B11 and UGT2B28 promote activation of GAL4-VP16 C-SREBP-2

MDA-MB-231 cells were co-transfected with 50 ng pck-1 GAL4 UAS luciferase reporter, 5 ng pRL-Null, with or without 2 ng of GAL4-VP16 C-SREBP-2 plasmid and **(A)** 50 ng of indicated plasmid or **(B)** 100 ng of indicated UGT WT or truncated (Tr) UGT plasmid. Luciferase activity was assayed 48 hours post transfection. All data were normalised to Renilla luciferase and control condition. Mean data of at least three biological experiments depicted (Mean \pm SEM). Statistical significance was assessed by one-way-ANOVA and Dunnett's post hoc testing as appropriate and indicated as follow, relative to the control condition: *NS* - not significant * $p < 0.05$, ** $p < 0.01$, *** $p < 0.001$.

The mechanism(s) by which UGTs alter SREBP processing remains to be defined. Processing is canonically triggered by a reduction in sterol levels, which is sensed directly by SCAP. A different mechanism involving the liver X receptor (LXR) increases total SREBP levels upon reduction of saturated fatty acids, as described in Chapter 1 (Hegarty et al., 2005). In addition, it was reported that unsaturated fatty acids can stabilise INSIG (Lee et al., 2008). One hypothesis developed early in this study was that UGTs might modify certain lipids (sterols or fatty acids), which in turn could affect their ability to regulate the events leading to processing. However, the extent to which UGT2B11 and UGT2B28 can modify lipids remains to be fully understood. Previous work showed that UGT2B11, but not UGT2B28, can glucuronidate a range of hydroxy-fatty acid derivatives (Turgeon et al., 2003). To date, neither of these UGTs have been tested for activity with sterols. Moreover, when UGT2B28 was screened for activity with a large array of potential substrates from various chemical classes, no high activity substrates were identified (Lévesque et al., 2001).

The glucuronidation of sterols is an under-investigated area. Early studies identified cholesterol glucuronides in healthy liver (Hara & Taketomi, 1982), however, the UGT isoform(s) responsible for this have not been identified. Recent work in our laboratory examined whether UGT2B11 or UGT2B28 could glucuronidate cholesterol or its hydroxylated derivatives; 25-hydroxycholesterol and 24S-hydroxycholesterol. This was achieved via an assay that detects the conjugation of radiolabelled glucuronic acid. UGT2B11 and UGT2B28 failed to conjugate glucuronic acid to these substrates. In contrast, human liver microsomes (which contain multiple UGT isoforms in abundance) could glucuronidate cholesterol, 25-hydroxycholesterol and 24S-hydroxycholesterol (Figure 4.16).

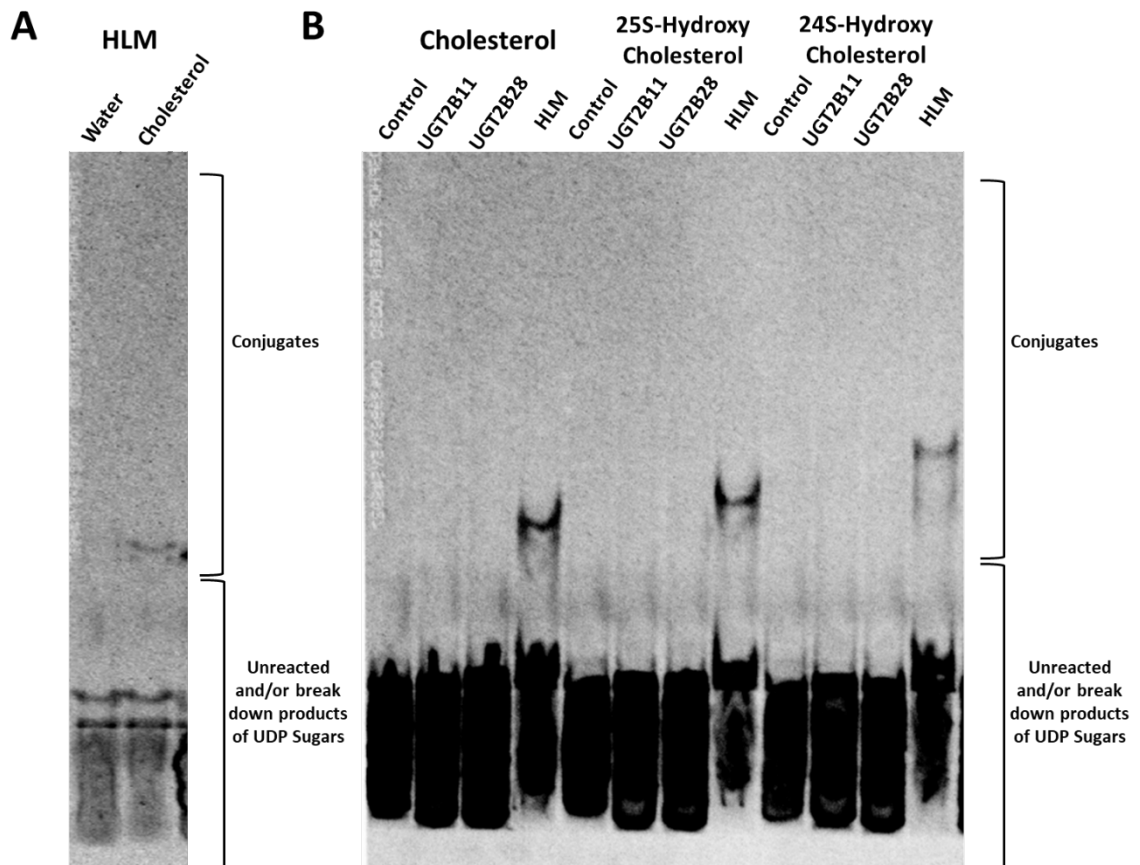


Figure 4.16: UGT2B11 and UGT2B28 do not conjugate cholesterol or its derivatives

Cholesterol and its derivatives were used as substrates for glycosylation by lysates of UGT overexpressing HEK-293T cells or Human liver microsomes (HLM). An autoradiograph of the TLC plate containing the conjugated products and unreacted UDP sugar and/or its breakdown products from assays without (**A**) or with 10 mM substrate (**B**) and 0.5 mM [14 C] UDP-glucuronic acid is shown. UGT containing lysates were prepared by transiently transfecting HEK-293T cells with either empty pIRES vector (control) or UGT2B11 and UGT2B28 encoding plasmids. A pool of HLM of unknown origin was utilised.

To summarise the data in this section: there are three lines of evidence to suggest that UGT2B11 and UGT2B28 do not exert their effects on SREBP processing via glucuronidation. First is the finding that UGT2B11 and UGT2B28 do not glucuronidate sterols, second is the previous report that UGT2B28 is inactive with fatty acids, and third is the finding that truncated forms of UGT2B11 and UGT2B28 can modulate SREBP processing.

UGTs are known to bind molecules that they do not glucuronidate. These molecules often serve as potent inhibitors of UGT activity by competing for binding with substrates (Grancharov et al., 2001). Thus, the possibility remains that UGT2B11 and UGT2B28 might

bind to sterol or fatty acid species without glucuronidating them, and that this interaction affects lipid sensing mechanism(s), resulting in activation of the SREBP processing cascade.

Experiments shown in Section 4.3.7 used sterol replete conditions. If UGT2B11 and UGT2B28 function by binding to sterols and reducing their capacity to be detected by SCAP, then this effect might be negated by increasing sterol levels to a superphysiological level that could not be reduced. Hence, the processing assay was repeated with the addition of cholesterol concentrations of 10 $\mu\text{g}/\text{mL}$ ($\sim 25 \mu\text{M}$) and 20 $\mu\text{g}/\text{mL}$ ($\sim 50 \mu\text{M}$), which were previously shown to inhibit SREBP processing (Figure 4.17) (Adams et al., 2004; Arito et al., 2008; DeBose-Boyd et al., 1999; Irisawa et al., 2009). The addition of cholesterol appeared to reduce the magnitude of the UGTs ability to enhance processing. However, the effect was not dose dependent. In fact, in the presence of 10 $\mu\text{g}/\text{mL}$ cholesterol the UGTs did not significantly induce processing; however, with 20 $\mu\text{g}/\text{mL}$ cholesterol, processing was again observed after UGT2B28 expression. However, the latter condition also showed high intra-experimental variability, which can be attributed to the negative response of cells to cholesterol treatment, which has been demonstrated by (Scully et al., 2023). Because the effect of increasing cholesterol levels was not dose dependent, the interpretation of these experiments remains equivocal.

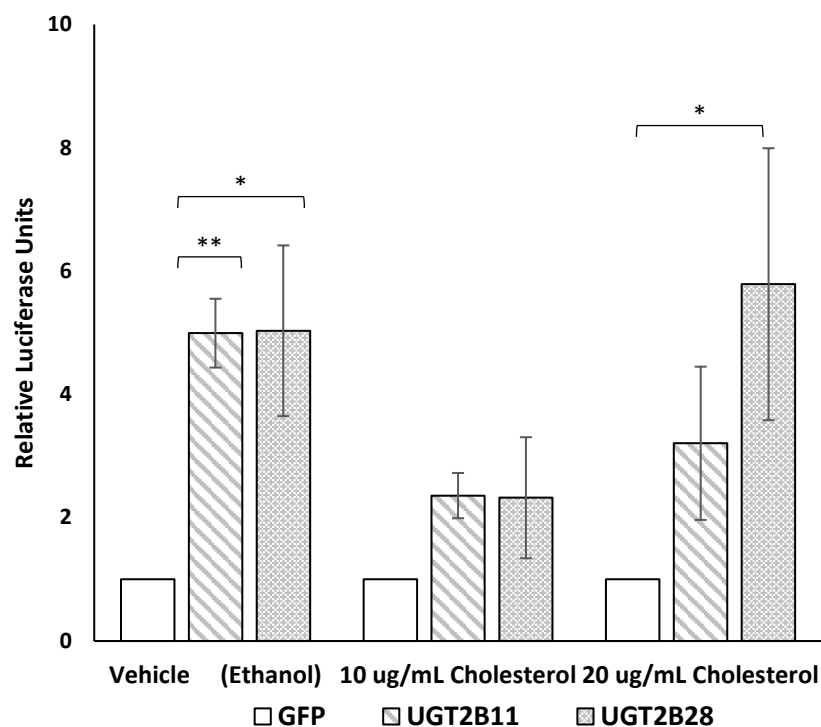


Figure 4.17: UGT mediated SREBP processing is inconsistently affected by sterols

MDA-MB-231 cells were co-transfected with 50 ng pck-1 GAL4 UAS luciferase reporter, 5 ng pRL-Null, 2 ng of GAL4-VP16 C-SREBP-2 plasmid and 100 ng of indicated UGT plasmid. Cells were treated with indicated concentration of cholesterol 24 hours post transfected and assayed for luciferase activity 48 hours post treatment. All data were normalised to Renilla luciferase and vehicle condition. Mean data of at least three independent biological experiments are depicted (Mean \pm SEM). Statistical significance was assessed by one-way-ANOVA and Dunnett's post hoc testing as appropriate and indicated as follow relative to the control condition: * $p < 0.05$, ** $p < 0.01$.

4.3.9 Specificity of UGT Domains

UGT2B15 shares a ~77% and ~76% amino acid sequence identity to UGT2B11 and UGT2B28, respectively. Therefore, due to this high degree of homology, it was predicted that immense transient overexpression of UGT2B15 may surpass the levels at which specificity between UGT2B isoforms is observed, and therefore UGT2B15 could be used in place of either UGT2B11 or UGT2B28 in SREBP processing assays. This prediction was validated as shown by the ~7-fold increase in transactivation of the UAS reporter when GAL4-VP16 C-SREBP-2 was transfected with wildtype UGT2B15 relative to the control condition (Figure 4.18). It should however be noted that UGT2B15 expression is not stimulated by androgens in the context of ER negative breast cancers (Hickey et al., 2012;

Hu et al., 2016), unlike UGT2B11 and UGT2B28, and hence it would not be the dominant isoform in the same cells in which these UGT isoforms would be rendering these effects.

Based on this validation, it was thus possible to utilise a series of pre-existing UGT2B15 fragment encoding plasmid constructs in an attempt to elucidate which UGT domains were responsible for the increase in SREBP processing (Figure 4.18A). Each of these recombinant peptides contain the signal peptide (25 aa) fused to its N-terminus, which allows for correct ER based localisation and folding, and is cleaved off during this process and is thus, unlikely to be involved in any UGT-mediated SREBP processing. ER localisation of each of these deletion constructs has previously been shown via confocal microscopy in currently unpublished works within our laboratory. This localisation is concordant with work by Miyauchi et al. (2019), which suggests there is no domain which UGT2B7 must contain to preserve its ER localisation due to its lack of any export signal.

As expected from the truncated UGT2B11 and UGT2B28 data (Figure 4.15B), the N-terminal first 300 amino acids were capable of significantly inducing SREBP processing (Figure 4.18B). Whilst the magnitude of response appears to vary slightly, UGT2B15 residues 100-200 aa and 100-300 aa were both able to increase SREBP processing. Unfortunately, attempts to clone UGT2B15 1-100 were met with failure. The C-terminal 230 residues of UGT2B15 were not able to significantly induce SREBP processing. Therefore, it is likely that the 100-200 aa region of UGT2B11 and UGT2B28 which contains a substrate recognition domain is responsible for the N-termini's capacity to induce processing. However, the possibility of multiple redundant domains within the N-terminus cannot be excluded (Figure 4.18B).

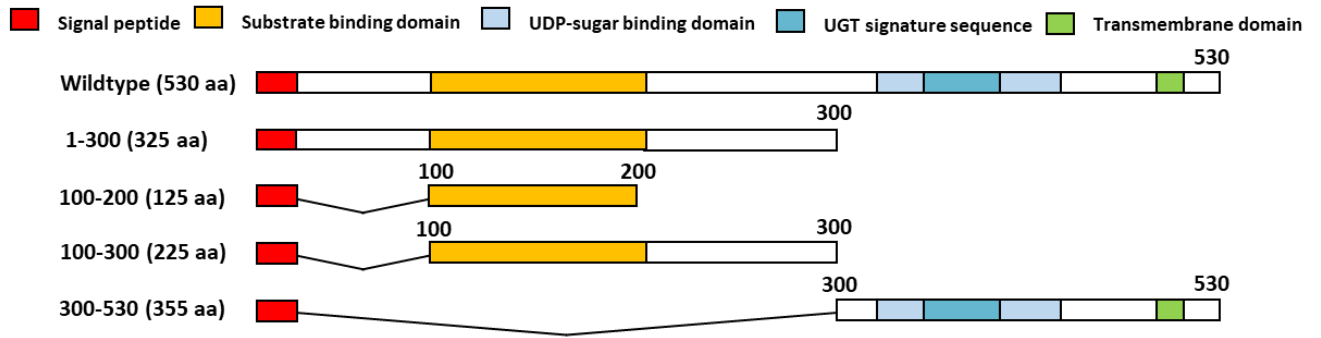
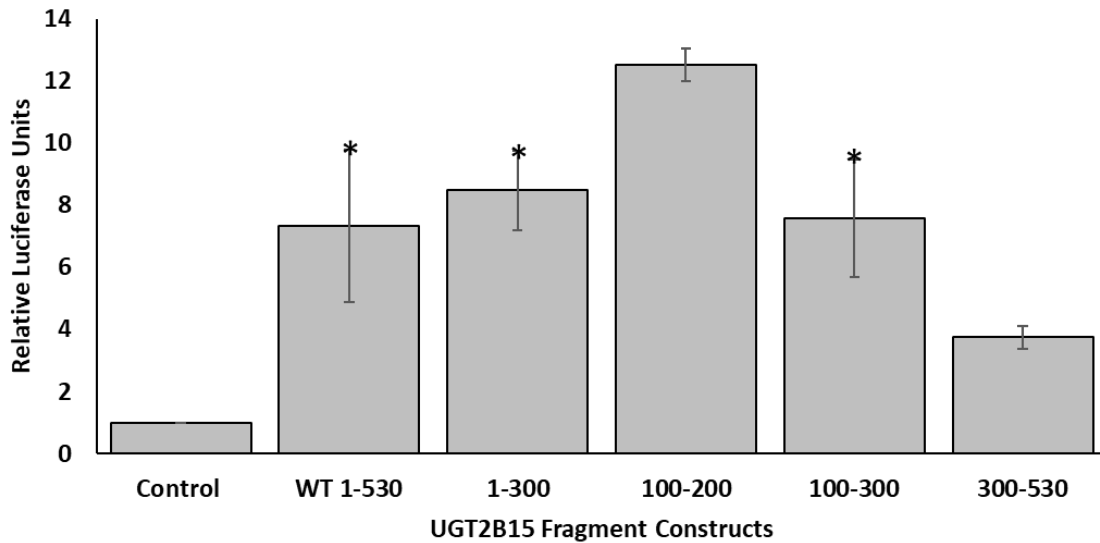
A**B**

Figure 4.18: UGT mediated SREBP processing by fragments of UGT2B15

(A) Domain structure of UGT2B15 constructs. **(B)** MDA-MB-231 cells were co-transfected with 50 ng pck-1 GAL4 UAS luciferase reporter, 5 ng pRL-Null, 2 ng of GAL4-VP16 C-SREBP-2 plasmid and 100 ng of indicated UGT2B15 plasmid. Cells were assayed for luciferase activity 72 hours post transfection. All data normalised to Renilla luciferase and control condition. Mean data of at least three independent biological experiments depicted (Mean ± SEM). Statistical significance was assessed by one-way-ANOVA and Dunnett's post hoc testing as appropriate and indicated as follow relative to the control condition: * $p < 0.05$.

4.3.10 UGT2B11 and UGT2B28 interact with components of the lipid sensing complex

An increase in the processing of inactive SREBP precursors to their active nuclear forms is mediated by members of the lipid sensing complex, INSIG and SCAP, which are endoplasmic reticulum bound (Yang et al., 2002). UGTs are primarily localised within this same intracellular compartment (Meech et al., 2019) and therefore it was assessed whether there was any physical interaction between UGTs and components of the lipid sensing complex that may mediate the observed increases in SREBP activation.

Interaction assays used UGT2B11 as a type isoform, due to the high homology between UGT2B11 and UGT2B28 and the capacity for both isoforms to induce SREBP processing in breast cancer cell models. Versions of UGT2B11, INSIG, SCAP, and SREBP 2 bearing different epitope tags were transiently co-expressed in HEK-293T cells, and their interactions were assessed via magnetic bead-based co-immunoprecipitation. Members of the lipid sensing complex are reported to be enriched in cholesterol rich microdomains which do not fully solubilise in the non-ionic detergent buffers typically used to maintain native conformation (Epan, 2006; Melkonian et al., 1999). Hence, after initial co-immunoprecipitation experiments (not shown), a high-speed centrifugation step was included to remove detergent insoluble material prior to capture of immunocomplexes. This helped to ensure that any associations were due to physical interactions of the proteins and not just co-localisation in these microdomains. As shown in Figure 4.19, HA-tagged INSIG could be immunoprecipitated with either SCAP or UGT2B11, but not with the unrelated ER-resident control protein oxidoreductase (Figure 4.19A). The INSIG-UGT interaction appeared equivalent in strength to that of the INSIG-SCAP interaction. Similarly, SCAP could be immunoprecipitated with UGT2B11 but not with oxidoreductase (Figure 4.19B). Lastly, SREBP-2 was co-immunoprecipitated with UGT2B11 but not with oxidoreductase (Figure 4.19C).

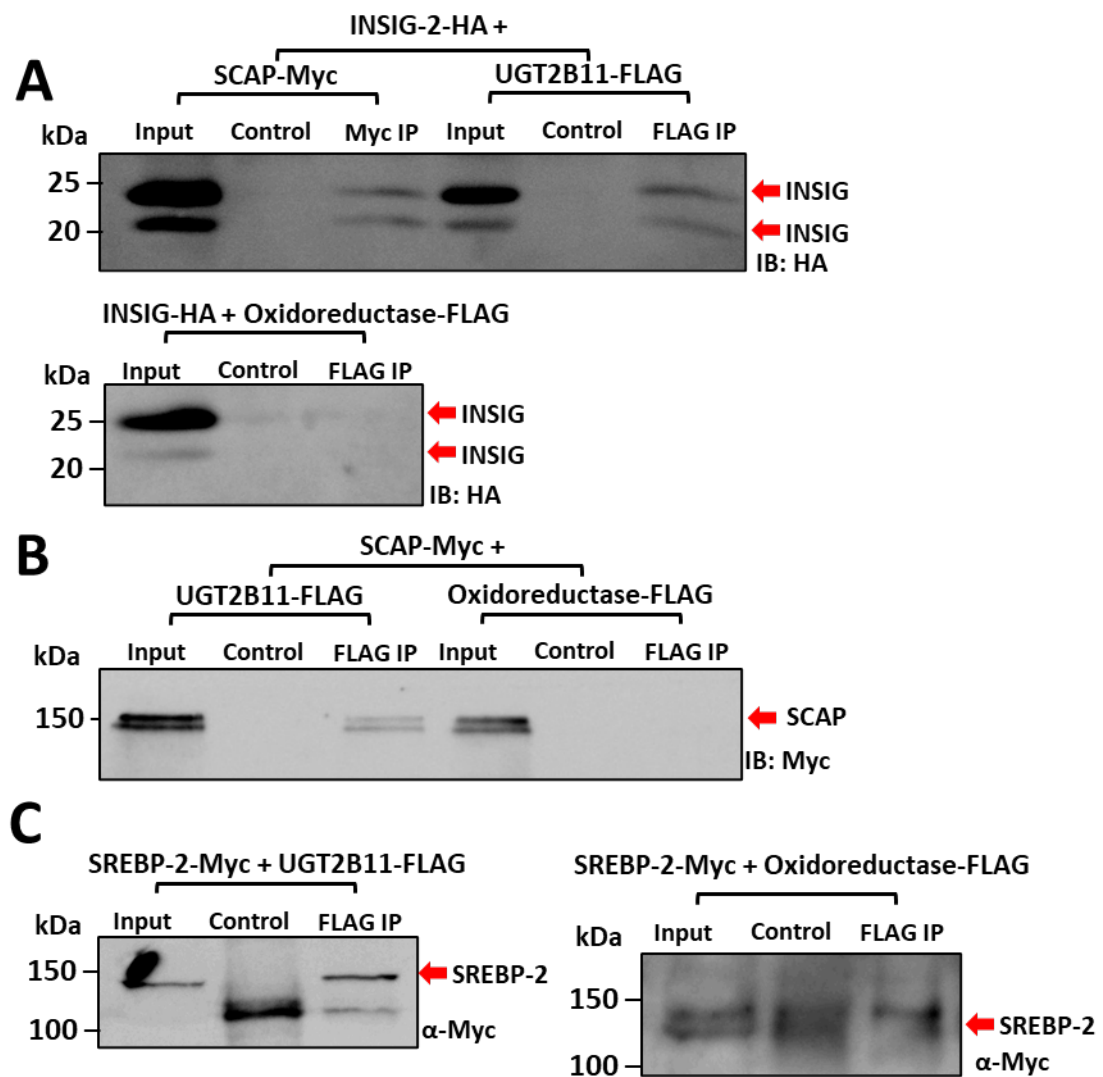


Figure 4.19: UGT2B11 physically interacts with members of the lipid sensing complex in HEK-293T cells

(A) HA-tagged INSIG-2 was co-immunoprecipitated with myc-tagged SCAP, FLAG-tagged UGT2B11 and FLAG-tagged oxidoreductase (negative control) using anti-myc or anti-FLAG antibody and probed with anti-HA antibody. **(B)** Myc-tagged SCAP was co-immunoprecipitated with FLAG-tagged UGT2B11 and FLAG-tagged oxidoreductase using anti-FLAG antibody and probed with anti-myc antibody. **(C)** Myc-tagged SREBP-2 was co-immunoprecipitated with FLAG-tagged UGT2B11 and FLAG-tagged oxidoreductase and probed with anti-myc antibody. Heavy chain IgG can be observed below the SREBP-2 band in control and FLAG IP lanes. Lysates for co-immunoprecipitation were prepared from HEK-293T cells transfected 48 hours prior to harvest with indicated plasmids. Each blot presented is representative of at least two independent biological experiments.

As INSIG is responsible for retaining SCAP in the ER, it was investigated whether UGT2B11 could disrupt the interaction between INSIG and SCAP (Figure 4.20). Such disruption would be expected to increase translocation of SCAP and associated SREBP precursors from the ER to the Golgi for processing. However, there was no clear reduction in interaction between INSIG and SCAP when UGT2B11 was expressed relative to a GFP control protein (Figure 4.20). This suggests that INSIG sequestration may not be the mechanism by which UGTs mediate SREBP processing.

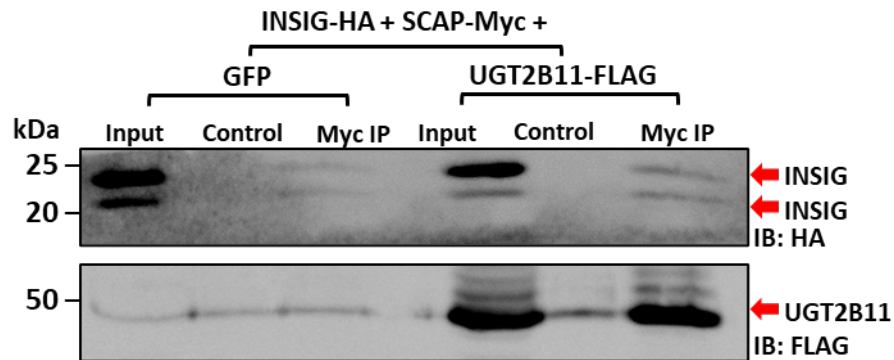


Figure 4.20: UGT2B11 Expression does not affect interaction between SCAP and INSIG

(A) HA-tagged INSIG-2 was co-immunoprecipitated with myc-tagged SCAP using anti-myc antibody and probed with anti-HA and anti-FLAG antibodies (IB indicates antibody used to probe for each blot). Lysates for co-immunoprecipitation were prepared from HEK-293T cells transfected 48 hours prior to harvest with indicated plasmids. Depicted blot presented is representative of at least two independent biological experiments.

4.4 DISCUSSION

4.4.1 Effect of UGT overexpression on MDA-MB-453 cells

To date, there is little understanding of the biological functions of UGT2B11 and UGT2B28, in part because they show very limited catalytic activities. The aim of this chapter was to characterise the role of UGT2B11 and UGT2B28 in SREBP-mediated lipid metabolism in a breast cancer context. This was prompted by bioinformatic studies in Chapter 3 that showed an expression correlation between these *UGTs* and SREBP target genes in normal or cancerous breast tissues, as well as literature reports correlating increased UGT expression with lipogenic gene signatures in breast cancer patients (Wang et al., 2013; Wang et al., 2017). It was also directed by findings from clinical datasets that increased expression of *UGT2B11* and *UGT2B28* in subsets of breast cancer patients correlated with worse survival outcomes. The guiding hypotheses in this chapter were that UGT2B11 and UGT2B28 may enhance SREBP activity and thus lipogenic signalling, potentially leading to more aggressive cancer phenotypes.

Studies in this Chapter primarily used overexpression systems to study the functions of UGT2B11 and UGT2B28. These studies included heterologous overexpression of the UGTs in MDA-MB-453 cells, which are considered a model of a molecular apocrine-like breast cancer (Holliday & Speirs, 2011; Moore et al., 2012). Previous work in our laboratory (unpublished data) showed that androgen treatment induces endogenous UGT2B11 and UGT2B28 over 100-fold in this cell line, indicating that these UGTs can reach high levels via naturally occurring steroid signalling pathways. It should be noted, however, that the overexpression models were not intended to precisely mimic the effects of androgens in terms of absolute UGT expression level.

MDA-MB-453 cells overexpressing UGT2B11, UGT2B28, or selected SNP or splice variants of these UGTs, showed increased proliferation relative to empty vector control lines (Figure 4.3 and Figure 4.5). This result was consistent in two independently derived sets of cell lines carrying the wildtype UGTs, and in a single set of lines carrying the truncated and SNP variants. Increased proliferative capacity of breast cancer cells is likely to lead to larger and more rapidly progressing tumours in the context of a breast cancer patient, potentially resulting in worse survival outcomes. These findings are hence broadly consistent with

observations of worse survival outcomes in subsets of breast cancer patients with higher UGT2B11 and UGT2B28 expression.

Expression levels of lipid metabolism genes, all of which are known direct targets of SREBP-1 or SREBP-2, were measured in the MDA-MB-453 stable overexpression lines. Cell lines carrying UGT2B11, UGT2B28, and their variants showed increased expression of a multiple genes that are targets of SREBP 1 or SREBP 2, relative to the control lines (Figure 4.4 and Figure 4.7). Interestingly, the set of genes that were differentially expressed in the UGT2B11 and UGT2B28 lines showed only partial overlap. These data suggest that the UGTs can in fact increase expression of SREBP targets, but their effects vary qualitatively and quantitatively and are not specific to one SREBP variant. These findings may explain the previously observed expression correlation between UGT2B11, UGT2B28 and SREBP target genes in breast tissues and tumours.

Increased lipogenesis could be a mechanism underlying the proliferation-enhancing effects of UGT2B11 and UGT2B28. However, there are other possible ways in which UGT expression could confer proliferative advantages to cancer cells. For example, recent research by Lacombe et al. (2023) in a prostate cancer cell context has shown that through interacting with huntingtin-interacting protein 1 (HIP1), UGT2B28 can lead to epidermal growth factor receptor (EGFR) activation and subsequent increased phosphorylation of extracellular signal-regulated kinase 1/2 (ERK1/2), which increased proliferation. Furthermore, other research in our laboratory has found that UGT2B11 and UGT2B28 can inhibit the activities of androgen metabolising UGTs, which could increase androgen levels and potentially androgen-mediated proliferation (Belledant et al., 2016; Meech et al., 2019) and unpublished data. MDA-MB-453 cells express AR, but whether their proliferation can be induced by androgens remains controversial in literature (Barton et al., 2015; Giovannelli et al., 2019).

As aforementioned, in addition to studying wildtype UGT2B11 and UGT2B28, SNP and splice variants were examined. Specifically, stable MDA-MB-453 cell lines were generated that over express a SNP variant of UGT2B28, and natural splice variants of both UGT2B11 and UGT2B28. The UGT2B28 SNP (rs4235127) results in a Leu365>His365 substitution in the sugar binding domain. The His365 residue is conserved in all of the other 21 human UGT enzymes and it was found to be important for the catalytic activity of UGT1A6 based on an alanine substitution experiment (Ouzzine et al., 2000). The Leu>His substitution may

therefore be functionally disruptive (Grantham, 1974). Although it is designated as the 'wildtype' or reference allele, *UGT2B28* Leu365 has only slightly higher population frequency (0.502) than that of *UGT2B28* His365 variant (0.498) (Sherry et al., 2001). To date, only the Leu365 form of the *UGT2B28* enzyme has been assessed for enzymatic activity and no significantly conjugated substrates have been found (Lévesque et al., 2001; Turgeon et al., 2003). Whether the *UGT2B28* His365 and Leu365 variants have different activity will need to be examined in future studies as it was beyond the scope of this project. However, it should be noted that the expression of both variants led to the same cellular effects in this study.

UGT2B11 and *UGT2B28* splice variants were also stably over expressed in MDA-MB-453 cells. These variants produce truncated proteins that are presumed to be inactive based on observations that deletion of the same regions from other UGTs abrogated activity (Meech et al., 2019). The effects of these truncated variants on cell proliferation were very similar to that of the full-length versions of the UGTs. This may indicate that the effects of *UGT2B11* and *UGT2B28* are non-catalytic in nature, as discussed further in Section 4.4.3. The information provided via TCGA-BRCA and METABRIC datasets did not distinguish between expression of wildtype, SNP and truncated variants of these UGTs. Whether such variants are associated with different survival outcomes could also be a subject for future work.

Due to time constraints, there was no lipidomic analysis of the stable UGT overexpression lines. This would be a valuable future direction to determine whether there was increased production of any particular lipid species. Enhanced cholesterol production could be assessed in future work using filipin staining or BIODIPY-cholesterol labelling (Hölttä-Vuori et al., 2008; Maxfield & Wüstner, 2012). If cholesterol biosynthesis were increased in these cells, it could allow for increased intratumoral *de novo* steroidogenesis, which has been shown to occur in prostate cancer cells (Mostaghel et al., 2012). Cholesterol-fuelled intratumoral androgen synthesis has been shown to accelerate the growth of prostate cancer tumours. Although as stated above, it remains unclear whether proliferation of the MDA-MB-453 cell line is actually enhanced by androgens. Work conducted prior to this project using Oil Red staining which detects neutral lipids, mainly triglycerides, suggested that there was no accumulation of these species in wildtype UGT-overexpressing stable lines (not shown). However, further examination of subtle changes in the distribution of

stored lipids could be assessed using lipophilic fluorochromes such as BODIPY 493/503, which is reported to have lower background and greater capacity to detect small lipid droplets (Harris et al., 2013; Strauss et al., 2020).

4.4.2 Attempts to knockdown UGT expression in MDA-MB-453 cells

To complement studies on UGT2B11 and UGT2B28 overexpression models, attempts were made to generate UGT2B11 and UGT2B28 knockdown MDA-MB-453 lines to determine whether reduction of UGT levels would have the opposite effect on growth. As aforementioned, the stably integrated CRISPRi constructs failed to reduce the expression of UGT2B11 and UGT2B28.

The CRISPRi constructs were built using the widely used px459 vector system (Gilbert et al., 2014; Ran et al., 2013). The parent vector (which carries an active Cas9 gene) was used in our laboratory to successfully knockout UGT2B7 in HepG2 cells and UGT2B15 and UGT2B17 in MCF7 cells (unpublished data). However, the modified version of the vector that carries the dCas9KRAB fusion protein (in place of Cas9) has been less successful, and did not reliably knockdown UGT2B7, UGT2B15 or UGT2B17 in a variety of breast cancer cell models in our laboratory (unpublished data). There are possible technical explanations for this. For example, the amount of the gRNA: dCas9KRAB complex that is expressed may be too low to effectively maintain repression of the target gene. Moreover, this may explain the result of Figure 4.8 where there may not be sufficient gRNA: dCas9KRAB to bind the large number of episomal copies of the UGT reporter vector that exist due to transient transfection. Accessibility of the *UGT* gene promoters may also be limited, hence the gRNA: dCas9KRAB complex may not get access to mediate repression. However, in the case of *UGT2B11* and *UGT2B28*, another possibility is that these genes might play an essential role in the MDA-MB-453 cell line. Given that increased expression of these UGTs enhanced growth, it is possible that reduced expression could impair it. To avoid integration artefacts, the CRISPRi lines are selected as stable mixed polyclonal populations rather than clonal lines. In a polyclonal population, cells expressing lower levels of these UGTs might be outcompeted by higher-expressing cells during selection. Analysis of the DepMap CRISPRi-based gene essentiality database indicates that UGT2B11 is essential for cell survival in a subset of the cell lines screened (DepMap, 2019; Meyers et al., 2017). No dependency was reported for UGT2B28, however, the CERES computational method utilised to estimate gene dependency might not adequately distinguish UGT2B28 from UGT2B11 due to their

homology. Alternative methods for UGT knockdown such as the use of siRNA were considered, however, due to the poor transfectability of MDA-MB-453 cells and close homology between these two UGT variants and that of other UGT2B family members, it was unlikely that it would be possible to knock down a single UGT isoform without non-specific effects caused by knocking down other UGT2B isoforms.

Further work should include conducting similar UGT2B11 and UGT2B28 perturbation studies in additional cell lines or a primary patient derived cell line, to further corroborate these results. Moreover, as these ER-negative subtypes of breast cancer have some molecular similarity to prostate cancers, it should be investigated whether these same cellular phenotypes (i.e. enhanced growth) arise in prostate cancer cell lines with increased *UGT2B11* or *UGT2B28* expression.

4.4.3 UGTs mediate increased SREBP activation

Having identified a possible role for UGT2B11 and UGT2B28 in controlling expression of SREBP target genes, a major goal of this Chapter was to determine whether these UGTs could increase SREBP activation. This was examined using four different experimental approaches.

1. Activation of an SREBP target promoter (*DHCR24*) was assessed after transfection with the SREBP-2 precursor, with or without SCAP, UGT2B11 or UGT2B28 (Figure 4.10). This assay revealed that, similar to SCAP, the UGTs enhanced activation of the target promoter. The simplest explanation for this result was that the UGTs increased processing of the SREBP-2 precursor into the nSREBP-2 transcription factor. However, it was conceptually possible that other effects mediated by the UGTs could have altered promoter transactivation indirectly (e.g. increased activity of coactivators). Hence further assays were designed to better separate increased processing from other effects that may increase reporter activity.

2. Immunoblotting was employed to detect SREBP-2 processing; however, the processed nSREBP-2 form was not identified in any cell line under any condition, even when its activity was clearly apparent in the reporter-based assays (Figure 4.11 and Figure 4.12). This may be simply due to the low sensitivity of immunoblotting, relative to the high sensitivity of the reporter assays.

3. A fluorescence-based assay was used to assess SREBP-2 localisation, with nuclear fluorescence indicating the processed nSREBP-2 form. Like SCAP, the UGTs enhanced nuclear accumulation of nSREBP-2 (Figure 4.13). This data provided strong support for the hypothesis that the UGTs increase processing of the SREBP-2 precursor.

4. A processing assay was developed using a chimeric ER-anchored protein that contained the potent transactivator GAL4-VP16 fused to the SREBP-2 regulatory (C-terminal) domain (Figure 4.14). Proteolytic processing to release GAL4-VP16 was assessed by reporter gene activation. The advantages of replacing the nSREBP-2 domain with GAL4-VP16 in this system were three-fold: first, GAL4-VP16 is a more potent activator than nSREBP; second, GAL4-VP16 does not bind to endogenous target sites throughout the genome; third, GAL4-VP16 does not undergo proteasomal turnover in the nucleus. Thus, the system provided a method for quantifying SREBP proteolytic activation that was much more sensitive than measuring nSREBP activity and was unlikely to trigger feedback processes associated with excessive activation of lipogenic genes. Processing in this system was strongly induced by SCAP, and modestly but significantly induced by both UGT2B11 and UGT2B28 (Figure 4.15).

Overall, data from the assays described above provided compelling evidence that UGT2B11 or UGT2B28 overexpression could enhance SREBP-2 processing, which is likely to explain the observed increase in SREBP target gene expression in the stable UGT-overexpressing MDA-MB-453 cell lines. Future work could use SREBP-1 constructs to determine whether both SREBP isoforms are equally sensitive to the effects of UGT2B11 or UGT2B28. However, given that SREBPs are much more different in their N-terminal than C-terminal domains, the finding that the UGTs could increase processing of GAL4-VP16 C-SREBP suggests that they act via the conserved C-terminal regulatory domain.

Tentative hypotheses were developed during this project about the mechanism(s) by which UGT2B11 and UGT2B28 might influence SREBP processing. One hypothesis was that the UGTs may interact with lipids in a way that impairs their ability to regulate SREBPs. Sterols and fatty acids regulate SREBP activities via different mechanisms as described in Chapter 1. Briefly, cholesterol is directly sensed by SCAP and controls its association with INSIG. Oxysterols bind to INSIG rather than SCAP but have a similar effect of stabilizing their interactions. Unsaturated fatty acids were found to increase the level of INSIG by increasing the interaction between INSIG and Ubx8 (Lee et al., 2008). Saturated fatty acids function indirectly by binding to LXR which regulates transcription of the *SREBP-1* gene. Apart from

regulation via LXR, these mechanisms are post-transcriptional and could therefore affect assays involving heterologous SREBP expression.

The classical function of UGTs is enzymatic conjugation of sugars to lipophilic chemicals (glycosidation or glucuronidation depending on the sugar used). If UGT2B11 or UGT2B28 were able to glucuronidate sterols or unsaturated fatty acids in the ER, this could affect ER-based lipid sensing mechanisms discussed above (i.e. recognition of sterols by SCAP, or stabilization of INSIG by fatty acids). However, various lines of evidence suggest that this is not their likely mechanism of action. Foremost is the finding that wildtype and truncated forms of UGT2B11 and UGT2B28 were similarly able to induce SREBP processing in the synthetic GAL4-VP16 C-SREBP based assay (Figure 4.15). Assuming that the truncated UGT proteins are catalytically inactive, this suggests that their modulation of SREBP processing is non-enzymatic. The effect of the truncated UGT2B11 and UGT2B28 isoforms in the processing assay were also consistent with the observation that MDA-MB-453 cell lines expressing these truncated forms showed similar phenotypic changes to those expressing the wildtype proteins.

Evidence for glucuronidation of relevant lipid species by UGT2B11 and UGT2B28 is also lacking. Some UGTs are reported to glucuronidate fatty acids and/or their metabolites. However, in a study that tested all UGT2B forms for activity with arachidonic acid and linoleic acid metabolites, UGT2B11 conjugated only 12-HETE, 15-HETE and 13-HODE, while UGT2B28 had no activity (Turgeon et al., 2003). Whilst unsaturated fatty acids can enhance INSIG stability (Lee et al., 2008), it is not clear that their metabolites have the same effect. Finally, in the present study it was confirmed that UGT2B11 and UGT2B28 do not glucuronidate cholesterol or its oxy metabolites.

While the data overall suggests that UGT2B11 and UGT2B28 do not modulate SREBP activity via glucuronidation of lipids, it remains possible that they could influence lipid sensing by interacting with lipids non-catalytically. It is well accepted that unsaturated fatty acids bind to most if not all UGTs and inhibit their catalytic activities with low micromolar inhibition constants (K_i) (Tsoutsikos et al., 2004). This is considered a largely nonspecific effect because the same unsaturated fatty acid species typically inhibit a broad range of UGTs. However, the K_i values are comparable to the K_m values for those UGTs that glucuronidate fatty acid metabolites (Jude et al., 2001). This suggests that UGTs might bind unsaturated fatty acids with similar strength regardless of whether they glucuronidate

them or not, and it is the presence/absence of a suitable acceptor moiety and its stereopositioning within the active site that determines whether glucuronidation occurs. Strong binding, as indicated by low inhibition constants, can also be seen with other classes of UGT inhibitors. For example, UGT2B7 can glucuronidate *trans* hydroxy-tamoxifen metabolites with a $K_m \sim 0.1 \mu\text{M}$ (Blevins-Primeau et al., 2009). It does not glucuronidate tamoxifen due to lack of a suitable acceptor group, yet tamoxifen is a strong inhibitor of UGT2B7 with a $K_i \sim 2 \mu\text{M}$ (unpublished data from our laboratory). It is possible that UGT2B11 and UGT2B28 bind to the unsaturated fatty acids without conjugating them, but this binding might still interfere with the ability of the fatty acids to stabilise the INSIG-Ubx8 association. The studies that showed that unsaturated fatty acids (e.g. oleic, linoleic, and arachidonic acids) stabilized INSIG, used concentrations of 50 - 100 μM (Lee et al., 2008). Interaction of oleic acid with Ubx8 has been studied quantitatively, revealing that its thermal stability was maximal at a concentration of 120 μM and that the dissociation constant (K_d) was 40 μM (Lee et al., 2010). UGTs may interact sufficiently strongly with unsaturated fatty acids to compete for their interaction with Ubx8, thus modulating the stabilization of INSIG. However, this hypothesis would need to be tested empirically using biochemical techniques.

The possibility that UGT2B11 and UGT2B28 interact non-catalytically with sterols also cannot be discounted. Compared to fatty acids, the binding of sterols to human UGTs is a relatively unexplored area. However, data in this Chapter showed that glucuronidation of cholesterol and its oxy metabolites occurs in HLM, indicating that some UGTs can indeed bind sterols. Thus, a formal hypothesis is that, like fatty acids and their derivatives, some UGTs can bind and glucuronidate sterols, while others may bind non-catalytically. If UGT2B11 and UGT2B28 do bind sterols, it could affect the ability of SCAP to sense their levels. It should also be noted that sterol glycosidation is a common function for UGTs found in some insects, plants, algae, and bacteria. Hence there might be conserved sterol-interaction domains in UGTs that have evolved either catalytic or non-catalytic functions (Warnecke et al., 1999). It would be valuable in future work to examine whether UGT2B11, UGT2B28 and other UGTs can bind directly to cholesterol and oxysterols and measure their binding affinities. SCAP is reported to undergo conformational change and dissociate from INSIG when the cholesterol concentration in the ER drops to $<5 \mu\text{M}$ (Yang et al., 2002). Binding of sterols by UGTs would likely need occur within this range of affinities to affect

sensing. It is also possible that local concentrations of sterols could be lowered by a high concentration of UGTs in close proximity to the SCAP sterol sensing domain. In this regard, it is notable that physical interactions between the UGTs and SCAP were detected in this study, as discussed further below.

The N-terminal region of UGTs is hydrophobic in nature, which facilitates its interaction with mainly hydrophobic substrates. A previous study identified a cluster of highly hydrophobic amino acid residues on the surface of UGT2B7 between amino acid residues 183–200 (Lewis et al., 2011). The region from amino acid residues 152-180 has also been proposed to contain a micro-anchoring site for interaction with the membrane (Rouleau et al., 2013). Thus, interactions of UGTs with lipids might involve these N-terminal regions. This would be consistent with observations that both full length and truncated forms of the UGTs were active in processing assays (Figure 4.18). Transient overexpression of specific UGT domains leads to the prediction that the 100-200 aa region containing the aglycone binding domain of these UGTs is most important in mediating increased SREBP processing, however, future work is required to confirm this via coimmunoprecipitation.

4.4.4 Novel interactions between UGTs and the lipid sensing complex

In this study, UGT2B11 was shown to robustly interact with all components of the lipid sensing complex (Figure 4.19). However, it is likely that some of these interactions are indirect, such that the UGT may interact directly with one component, and this interaction allows co-precipitation of all members of the complex. This joint precipitation of complex members might be facilitated by their co-localisation in cholesterol rich microdomains (Epanand, 2006; Melkonian et al., 1999). A tentative hypothesis is that the UGTs interact with SCAP or INSIG, rather than directly with SREBP. This is in part because of the very different membrane topologies of SREBP and UGTs. Both the N- and C-terminal domains of SREBPs reside on the cytosolic side of the ER membrane with just a ~ 30 aa loop in the lumen; in contrast, all of the UGT protein resides in the lumen apart from the ~ 50 aa transmembrane and cytoplasmic domains at the C-terminus. In addition, no extrinsic factors (i.e. those that are not members of the sensing complex) have been identified to date that interact directly with the SREBP precursor to aid processing. TRC8 (translocation in renal cancer from chromosome 8) interacts directly with SREBP but it decreases the activation of SREBPs (Irisawa et al., 2009).

Future work should use orthogonal approaches to confirm interactions between UGTs and members of the lipid sensing complex. These assays could include fluorescence complementation, membrane 2-hybrid assays, and potentially FRET or BRET-based methods. The focus of these studies would be to determine exactly which proteins interact, and what domains of the proteins are involved. This information would aid in developing hypotheses about the mechanism(s) by which the UGTs promote SREBP processing. Currently, some tentative hypotheses have been developed, which include both direct and indirect mechanisms, as discussed below.

Hypothesis 1: If UGT2B11 and UGT2B28 interact with INSIG, they might disrupt its associations with SCAP, thus releasing the latter to traffic to the Golgi. This suggestion is supported by a previous report that a distantly related UGT family member, the ceramide galactosyltransferase UGT8, can interact with INSIG (Hayashi et al., 2012). INSIG is a multifunctional protein that regulates lipid synthesis and protein quality control in the ER, by interacting with at least three different protein complexes in addition to the SCAP complex (Hayashi et al., 2012). One of these is the ER-associated protein degradation (ERAD) complex. It was reported that when UGT8 levels are high, it is degraded by a Sig-1R and INSIG containing ERAD complex. It was suggested that this increased demand for ERAD could lead to competition for INSIG between the ERAD complex and the SCAP complex. If the competition led to SCAP/SREBP complex becoming depleted of INSIG, it could promote trafficking to the Golgi (Hayashi et al., 2012). This would be considered an indirect mechanism for increased SREBP activation. However, it was reported that UGT8 was found only in the INSIG-ERAD complex and not in the INSIG-SCAP complex (Hayashi et al., 2012). In contrast, co-immunoprecipitation data shown in this chapter suggest that UGT2B11 and UGT2B28 interact with complexes that contain INSIG and SCAP. A hypothesis that harmonizes these findings is that while high levels of UGT8 might enhance SREBP processing indirectly by increasing demand for INSIG within ERAD complexes, UGT2B11 and UGT2B28 might function more directly by interacting with INSIG-SCAP complexes. This is also consistent with bioinformatic findings showing that only UGT2B11, UGT2B28, and few closely related UGT2Bs, correlate with SREBP target gene expression (see Table 3.1). There is currently insufficient information to speculate on exactly how UGTs might affect the interaction between INSIG and SCAP. Cryogenic electron microscopy (CryoEM) studies show that this interaction involves INSIG transmembrane (TM) domains TM3 and TM4, and

SCAP TM2, TM4, and TM5 (Kober et al., 2021). Hence future studies should investigate the domains of INSIG that bind to UGTs and whether this binding affects interaction with SCAP.

Related to the above hypothesis is the concern discussed previously that very high UGT expression levels in transient transfection experiments could lead to ER stress that might indirectly increase SREBP processing. When proteins are over-expressed at high levels, the capacity of chaperones to mediate correct folding can be overwhelmed. Accumulation of misfolded proteins causes ER stress, which is well characterised to increase SREBP activation (Colgan et al., 2007; Kim et al., 2019). The ERAD process discussed above has two main functions: removal of misfolded proteins to reduce ER stress, and regulated turnover of specific ER proteins to control responses to cellular signals (Chen et al., 2023). Sig-1Rs is known to be highly up-regulated under ER stress and contributes to targeting proteins to the INSIG-ERAD complex (Hayashi & Su, 2007). As discussed above, this could lead to depletion of INSIG from INSIG-SCAP complexes, leading to further SREBP activation (Kammoun et al., 2009). However, there are two reasons to think that overexpression of UGT2B11 and UGT2B28 did not induce SREBP processing indirectly due to ER stress in the studies in this Chapter. First, as noted previously, another ER-retained protein (ER-RFP) was included as a control in the processing assays. ER-RFP did not increase SREBP processing despite also being abundantly expressed in the transient HEK-293T cell transfection system. Second, phenotypes consistent with SREBP activation (e.g. increased expression of SREBP target genes) were observed in MDA-MB-453 cells with stable overexpression of UGT2B11 and UGT2B28. Unlike transient expression systems, there are few copies of plasmid per cell in stable lines and the overall level of expression is moderate. Overall, it is considered unlikely that these UGTs are acting indirectly by inducing ER stress. However, additional analyses of ER stress within each of the experimental models should be considered in a future study.

Hypothesis 2: If UGT2B11 and UGT2B28 interact with SCAP, they may influence its ability to sense sterols. SCAP has 8 transmembrane helices (TM) separated by 7 loops. The sterol sensing domain (SSD) encompasses the region from TM2-6, with cholesterol binding occurring in a region of the large luminal loop 1 that is described as 'dipping' into the membrane (Xu et al., 2024). When sterols are low, luminal loops 1 and 7 interact, producing the 'closed conformation'. This triggers conformational changes in cytoplasmic loop 6 that expose a hexapeptide motif (MELADL) that interacts with COPII coated vesicles, allowing

vesicular anterograde transport to the Golgi. In contrast, when levels of cholesterol are high, loops 1 and 7 do not associate, a state called the 'open conformation'. This conformation causes changes in loop 6 that mask the MELADL motif preventing interaction with COPII (Kober et al., 2021; Zhang et al., 2013). Both cholesterol binding in loop 1 and INSIG binding in the TM domain are required to fully curb ER to Golgi transport (Lee et al., 2005), which is likely because they cause similar conformational changes that affect loop 6 (Kober et al., 2021). UGT2B11 and UGT2B28 might modulate these events by interacting with the luminal loops, altering cholesterol binding, or the stability of the open/closed conformations. Recent work showed that loop 1 and loop 7 can be expressed from different plasmid constructs and retain their cholesterol sensing capacity as described by Kober et al. (2021). Therefore, a series of epitope or fluorescently tagged SCAP constructs containing these two main loops should be developed to allow for co-immunoprecipitation or biofluorescence complementation experiments with the UGT. This work has been initiated within our laboratory but was slowed by difficulties cloning the repetitive loops of SCAP. Due to time constraints, this project was deferred and will be the subject of future studies.

Relevant to the above mechanisms, the possibility that UGTs might modulate ER-Golgi transport was also considered as an indirect mechanism for modulating SCAP function. UGTs are retained in the ER by a combination of static retention and active retrieval from the Golgi by COPI-coated vesicle-mediated retrograde transport (Miyachi et al., 2019). Rat UGT2B1 was shown to interact with coatamer (COP) proteins as part of the latter mechanism (Meech & Mackenzie, 1998). After SCAP escorts SREBP to the Golgi via COPII-mediated anterograde transport, it is retrieved by COPI-mediated retrograde transport to the ER (Takashima et al., 2015). If overexpression of UGT2B11 and UGT2B28 caused sponging of COPI-coated vesicles, it might impair this retrieval leading to SCAP depletion. However, interaction of UGTs with COP proteins involves the conserved dilysine motif at the C-terminus and the truncated UGT2B11 and UGT2B28 variants that lack this region showed the same capacity as wildtype UGTs to promote SREBP processing. Thus, it is currently considered unlikely that the UGTs function indirectly via disrupting SCAP retrieval.

In addition to lacking a clear mechanism for how UGT2B11 and UGT2B28 may promote SREBP processing, another unresolved question is the extent to which these UGT isoforms are specific in their ability. Whether UGTs could alter processing was not examined in this study. If UGT2B11 and UGT2B28 function by binding non-catalytically to fatty acids, then

other UGTs might be expected to have similar effects as fatty acid binding is considered a general property of UGTs. UGT2B11 and UGT2B28 were selected as the subjects of this study because of their robust expression correlation with SREBP target genes in initial bioinformatic analyses. This analysis examined all UGTs, and significant Pearson correlation coefficients were seen for (in rank order of R value) UGT2B11, UGT2B28, UGT2B10 and UGT2B7 (see Table 3.1). These four UGTs form a phylogenetic cluster, being more closely related to each other than to any other UGTs. The notably higher R values for UGT2B11 and UGT2B28 prompted the focus on these two genes; however, it remains possible that UGT2B10 and UGT2B7 may have similar functions. Future studies could explore whether the ability to modulate SREBP processing and to interact with the lipid sensing complex, is confined to a subset of closely related UGTs, or is a more general phenomenon.

4.4.5 Conclusion

Evidence presented throughout this Chapter strongly supports the hypothesis that UGT2B11 and UGT2B28 overexpression enhances SREBP processing in breast cancer cell lines. This results in an increase in SREBP target gene expression, which could allow for an increased provision of lipids to cells, and potentially contribute to the observed increased proliferative capacity. Such a mechanism might explain the poorer survival outcomes observed in subsets of ER-negative breast cancer patients with high UGT2B11 and UGT2B28 expression. Moreover, the ability of androgens to dramatically increase the expression of these UGTs in ER-negative breast cancer cells provides a novel mechanism by which AR could promote progression in molecular apocrine or LAR-type tumours. The mechanism by which UGT2B11 and UGT2B28 enhance activation of SREBP is likely to involve the novel physical interactions identified between these UGTs and component of the ER-based lipid sensing complex. However, interactions of the UGTs with lipids remains a non-exclusive mechanism. These findings have been summarised in the below model (Figure 4.21).

Further work is required to fully elucidate the mechanism by which these UGTs are modulating SREBP activity, and this may lead to the identification of druggable targets within this complex molecular pathway which might provide new treatment avenues for these subtypes of breast cancers. Finally, due to the similarities between the breast cancers studied in this chapter and prostate cancers, UGTs might play a similar role in regulation of SREBP activation both cancer cell types, suggesting a valuable area for future research.

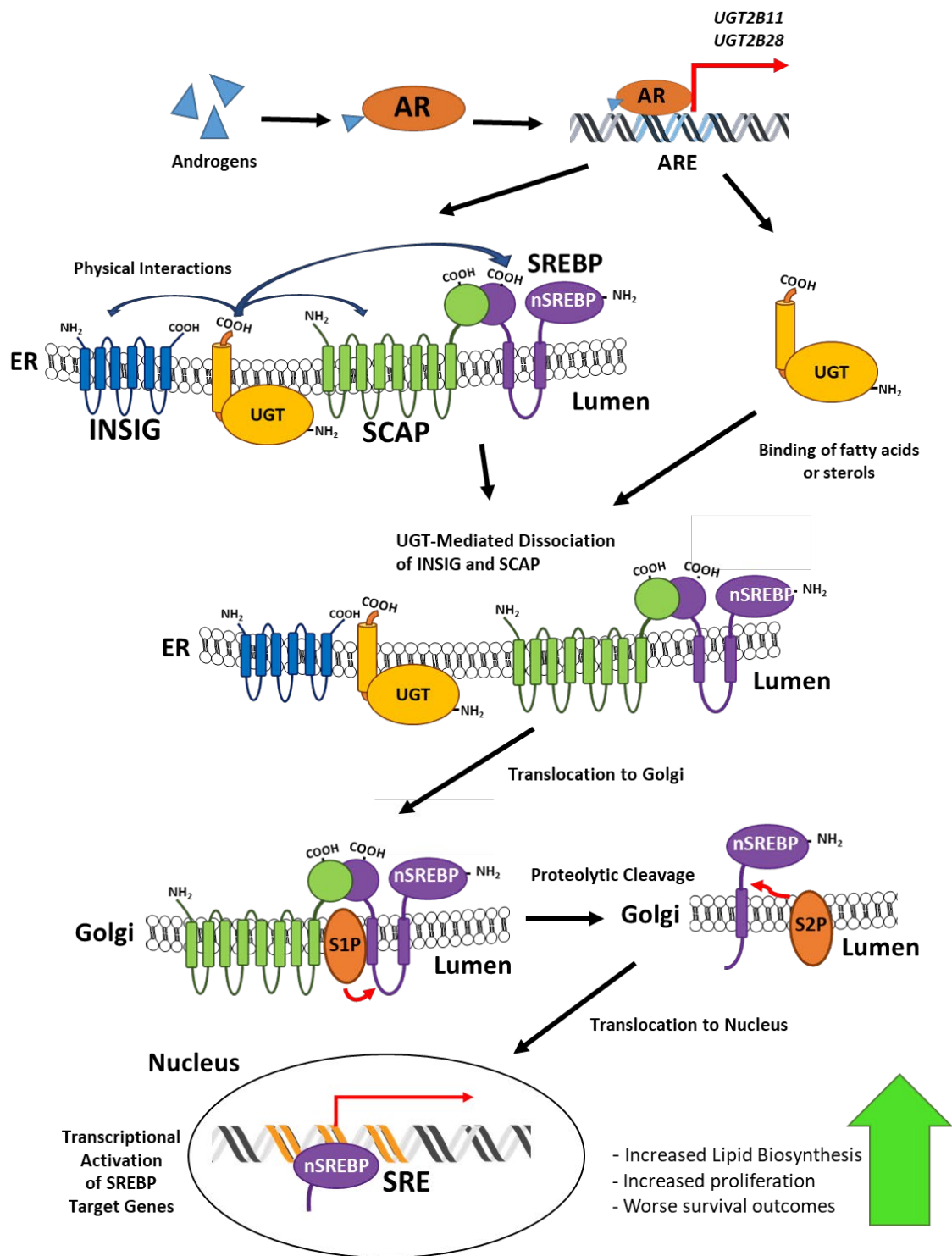


Figure 4.21: Proposed role of UGTs in SREBP activation

Upon binding to androgens, the androgen receptor translocates to the nucleus and promotes the expression of *UGT2B11* and *UGT2B28*. These UGTs promote trafficking of the SREBP: SCAP complex from the ER to the Golgi in COPII-coated vesicles through either physical interaction with components of the lipid sensing complex or binding to lipids. In the Golgi, proteolytic activation of the nuclear SREBP transcription factor domain occurs, allowing for translocation of nSREBP to the nucleus and thus the activation of SREBP target gene transcription.

5. CHAPTER 5 -
REGULATORY
MECHANISMS OF SREBP
ACTIVITY AND UGT
EXPRESSION

5.1 INTRODUCTION

5.1.1 Lipotoxicity

Whilst lipid metabolism is generally a tightly regulated process, the increased provision of lipids through increased lipid biosynthesis frequently occurs in cancerous cells. Although a degree of increased lipid provision is advantageous to cells, excessive accumulation of lipids can lead to lipotoxicity (Marí & Fernandez-Checa, 2014). Aberrant SREBP activity has been shown to contribute to a number of metabolic diseases which occur through the accumulation of lipids beyond normal levels, including but not limited to: hepatosteatosis, dyslipidemia and pancreatic β -cell dysfunction (Takahashi et al., 2005; Yahagi et al., 2002). Moreover, there is recent evidence that in liver cancers, induction of excessive accumulation of saturated free fatty acids leads to lethal lipotoxicity (Rudalska, Harbig, et al., 2021; Rudalska, Zender, et al., 2021; Setton et al., 2021). The SREBP signalling pathway contains tight feedback controls to avoid cellular toxicity, as discussed below. Studies in this chapter examined the mechanisms by which lipotoxicity is prevented, and investigated whether UGTs may play a role in this process.

5.1.2 Regulation of nuclear SREBP protein levels by UGTs

The active forms of many transcription factors are incredibly short lived, due to proteolytic turnover by the 26S proteasome. Transcriptionally active nuclear SREBPs (nSREBPs) possess a half-life of only \sim 3 hours as they are rapidly degraded by the nuclear ubiquitin-proteasome pathway (Hirano et al., 2001; Sundqvist et al., 2005; Sundqvist & Ericsson, 2003). This degradation of nSREBPs is modulated by a Cdc4 phosphodegron (CPD) motif located near the C-terminal end of the nSREBP protein. The phosphodegron is phosphorylated by glycogen synthase kinase-3 β (GSK-3 β) in a DNA-binding dependent manner, which then recruits F-box and WD repeat domain-containing 7 (FBW7) protein, a component of the SKP1-cullin 1-F-box protein (SCF) E3 ligase complex (Krycer et al., 2012). The SCF complex regulates the recruitment of ubiquitin ligases to target proteins and contains four core proteins: Cullin which forms a structural scaffold for the complex, RBX1 which is a RING E3 ubiquitin ligase, an F-box protein which confers substrate specificity, and Skp1 which is an adaptor between the F-box protein and Cullin. Consequently, nSREBPs then undergo polyubiquitination and proteasomal degradation (Sundqvist et al., 2005; Sundqvist & Ericsson, 2003). This degradation pathway is summarised below in Figure 5.1.

It should be noted that while FBW7 confers target specificity to the complex, nSREBP is not its only target, and it in fact induces degradation of multiple oncoproteins (Davis et al., 2014).

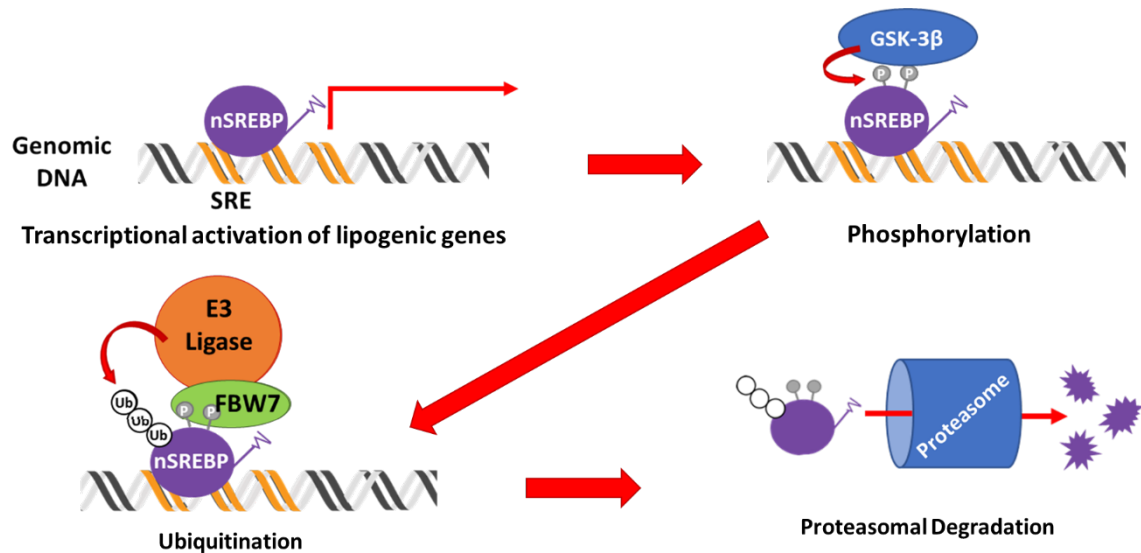


Figure 5.1: Schematic of nSREBP degradation

nSREBP signal termination is promoted by GSK-3 β -mediated phosphorylation of a phosphodegron motif. This leads to recruitment of the FBW7 component of the SCF E3 ubiquitin ligase complex, polyubiquitination and proteasomal degradation by the 26S proteasome.

The degradation of nSREBPs generally occurs in a tightly regulated manner which has been well defined experimentally. In addition, there is growing evidence for other mechanisms that control the level or activity of nSREBP in the nucleus. For example, while phosphorylation of the degron by GSK-3 β induces ubiquitination and degradation of nSREBP, phosphorylation at adjacent locations by some cell cycle dependent kinases can antagonise this process (Bengoechea-Alonso & Ericsson, 2016). Arginine methylation by PMRT5 and neddylation have also been reported to inhibit nSREBP degradation (Ju et al., 2020; Liu et al., 2016). In addition to mechanisms that control stability, other interactions can control nSREBP transcriptional activity. For example, sumoylation impairs the nSREBP transactivation function by inducing recruitment of a HDAC repressor complex (Arito et al., 2008). It has been shown that nSREBPs can interact with several other transcription factors that may either augment or inhibit their activity; these include the nuclear receptors hepatocyte nuclear receptor 4 (HNF4), liver receptor homolog-1 (LRH-1), peroxisome

proliferator-activated receptor gamma (PPARG), estrogen receptor (ER) and androgen receptor (AR) (Kanayama et al., 2007; Kim et al., 1998; Lopez et al., 2002; Misawa et al., 2003; Suh et al., 2008; Yamamoto et al., 2004). Finally, nSREBPs bind to the inner nuclear membrane protein lamin, which can influence intranuclear localisation and activity (Lloyd et al., 2002).

Novel work within our laboratory suggests that UGTs may be previously unrecognized factors that can control the levels of nSREBP-2 protein in the nucleus (Figure 5.2A). Whilst UGTs are resident ER membrane proteins, several studies have suggested that a fraction of UGT proteins are present within the nuclear envelope or the nucleus itself (Belledant et al., 2016; Lévesque et al., 2020; Radomska-Pandya et al., 2002). Moreover, unpublished work from our laboratory has suggested that some UGT2B enzymes can interact with the AR and alter its nuclear functions. In addition, fluorescently tagged versions of UGT2B proteins have been observed in the inner nuclear envelope where they colocalise with lamin.

The likely nuclear localisation of a fraction of UGTs raised the possibility that they could influence the activities of nuclear nSREBP. In experiments performed prior to the start of this project, a plasmid encoding the N-terminal (constitutively nuclear) nSREBP-2 domain was co-expressed in HEK-293T cells with a plasmid expressing UGT2B11, or with a control plasmid. The levels of both proteins were then examined by immunoblotting. There was markedly less nSREBP protein observed on the blot when it was co-expressed with the UGT2B11 plasmid, relative to the control plasmid (Figure 5.2A). As nSREBP-2 was expressed from a heterologous promoter, its reduction likely represents either decreased protein synthesis or increased degradation, rather than transcriptional regulation.

Whether the reduction in nSREBP-2 level in this assay represented a specific effect of UGT2B11, or a non-specific effect, was unclear. A non-specific decrease in protein synthesis may occur when the demand for heterologous protein production overwhelms the synthesis machinery. Similarly, ER stress due to excessive accumulation of ER resident protein may induce non-specific protein degradation. To further investigate these possibilities, follow-up experiments were performed with additional controls. First, in addition to the empty vector, other unrelated proteins (GFP and the ER-resident protein SLC35B4) were co-expressed as controls. Second, UGT2B11 was co-expressed with other proteins that are known to undergo nuclear degradation via the same GSK-3 β /FBW7-dependent pathway as nSREBPs. It was reasoned that if the UGT specifically targeted this

pathway, it may have a similar effect on the levels of these proteins. As shown in Figure 5.2B-C, the levels of exogenously produced Notch Intracellular Domain (NICD) and endogenously produced β -catenin, were reduced by co-expression of UGT2B11, while GFP and SLC35B4 had no effect. NICD and β -catenin are both regulated by GSK-3 β /FBW7-dependent nuclear turnover (Davis et al., 2014; Grimes & Jope, 2001; Gupta-Rossi et al., 2001; McCubrey et al., 2014). Interestingly, another potential target protein, CCAAT/enhancer-binding protein beta (C/EBP- β), was not affected by UGT2B11 (Figure 5.2C). C/EBP- β is regulated by SCF-mediated turnover, but GSK-3 β plays no role in this process (Bengoechea-Alonso & Ericsson, 2010). Overall, these data suggest the hypothesis that UGT2B11 may reduce levels of nSREBP and some other nuclear proteins by modulating GSK-3 β /FBW7-dependent degradation processes.

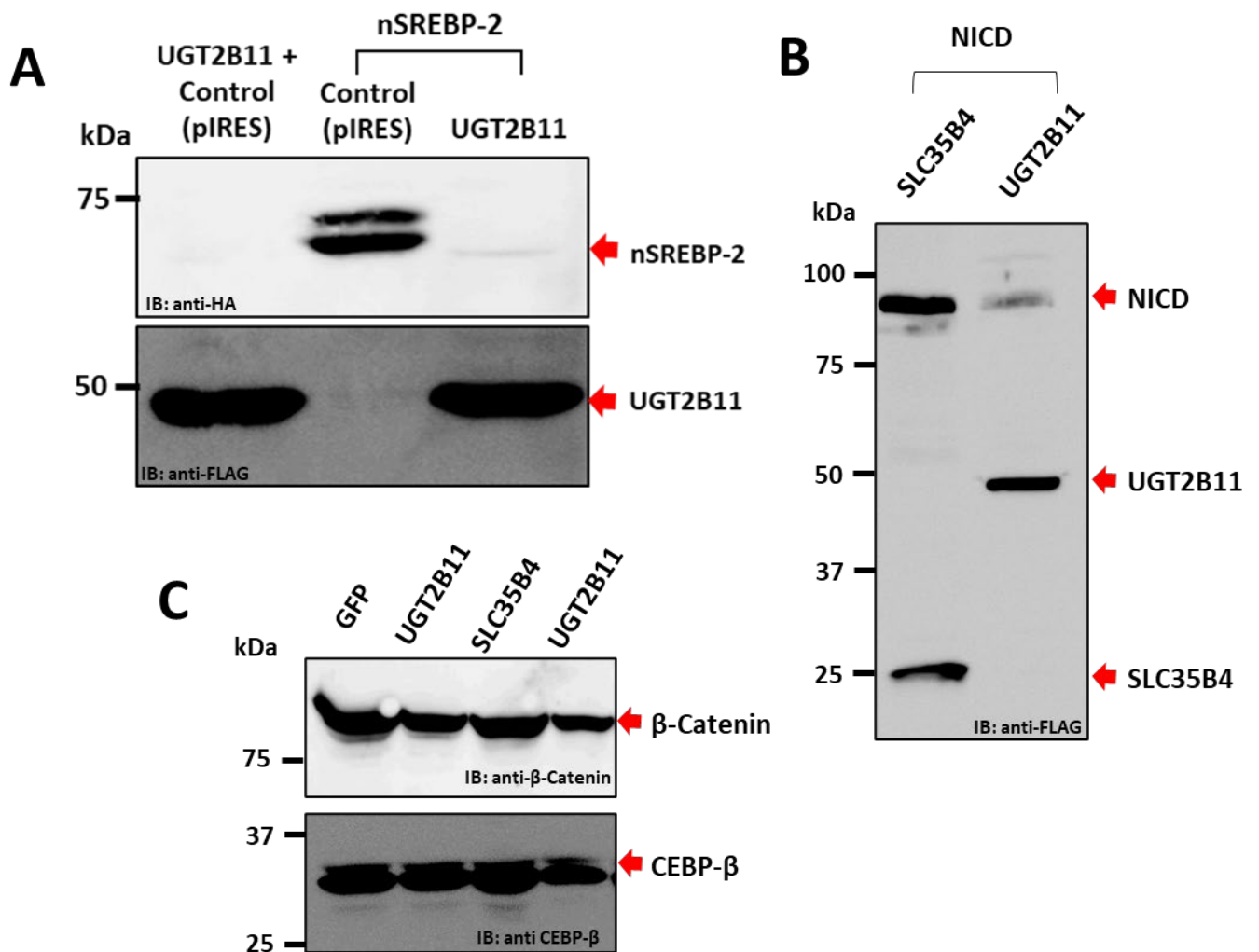


Figure 5.2: UGT2B11 destabilises GSK-3 β -target proteins

The overexpression of **(A)** HA-nSREBP-2 and **(B)** NICD was assessed via immunoblotting of lysates from HEK-293T cells transfected with 2.5 μ g of either FLAG-UGT2B11 or control plasmid (FLAG-SLC35B4 or empty vector) and 2.5 μ g of nSREBP or NICD expression plasmids. **(C)** The expression of endogenous transcription factors β -catenin and CEBP- β was assessed under FLAG-UGT2B11 or control plasmid (GFP or FLAG-SLC35B4) transfection. Two independent biological experiments are shown on this same blot.

Work presented in Chapter 4 provided compelling support for the hypothesis that UGT2B11 and UGT2B28 can induce SREBP activation and lipogenic gene expression, which may be at least partly responsible for the proliferative advantage that these UGTs confer to breast cancer cells. However, excessive SREBP activation could negate this advantage by inducing lipotoxicity. Given the preliminary evidence presented in Figure 5.2 that UGT2B11 may be able to modulate nSREBP turnover, it was speculated that UGTs may in fact play a role in

both SREBP signal *activation* and *termination*, which may allow breast cancers to maintain an optimal level of lipogenesis without crossing the threshold of lipotoxicity.

5.1.3 Crosstalk between SREBPs, UGTs, and Androgen Receptor signalling

The AR is ligand-dependent nuclear transcription factor which has been shown to be a large driver of growth in prostate cancer as well as subtypes of breast cancer with high AR expression and no expression of the estrogen receptor (ER-negative). The classical understanding of AR function in most cell types is that through binding androgens in the cytoplasm, it homodimerises, translocates to the nucleus, and then binds to androgen responsive elements within the promoter and enhancer regions of androgen driven genes to modulate gene expression (Lonergan & Tindall, 2011). Through androgen-binding induced conformational changes in AR, it is able to interact with a range of co-activators that facilitate histone and DNA modification, DNA occupancy and transcriptional coordination, ultimately enhancing AR transactivation (Heemers & Tindall, 2007). Furthermore, a range of co-repressors exist, which suppress AR transactivation through a multitude of mechanisms: inhibition of DNA binding, recruitment of histone deacetylases, interruption of interactions with AR co-activators, interruption of AR homodimerisation and repression of transcription (Wang et al., 2005).

There is extensive crosstalk between AR and SREBP signalling. First, AR upregulates expression of the *SCAP* gene, which can increase SREBP processing and lead to increased expression of lipogenic genes (Heemers et al., 2004). This is considered an important mechanism by which elevated AR expression and activity in prostate cancers fuels cellular growth. Second, nSREBP has been reported to bind upstream of the *AR* gene and directly regulate its expression, thus creating a feed forward loop (Huang et al., 2010). Third, AR and nSREBP are known to physically interact and to bind common target genes (Suh et al., 2008). These interactions may be cooperative or antagonistic. In prostate cancers, it has been shown that nSREBPs can interact with AR and repress its transcriptional activity on AR-responsive targets (Suh et al., 2008). This was reported to occur through competition for AR-coactivators: steroid receptor coactivator 1 (SRC-1) and Androgen receptor trapped clone-27 (ART-27), and potential recruitment of histone deacetylases.

UGT2B11 and *UGT2B28* are two of the most androgen responsive genes in the human genome (Chouinard et al., 2006; Lacombe et al., 2023; Moore et al., 2012; Moore et al., 2020). Previous work showed that *UGT2B11* and *UGT2B28* can be induced by androgens in prostate cancer cells (Chouinard et al., 2006; Lacombe et al., 2023), while *UGT2B28* was also shown to be induced by androgens in breast cancer cells that express high levels of AR (Moore et al., 2012). The transcriptional regulation of these genes by AR in breast cancer cells has been the subject of extensive study by our laboratory, with induction of both genes by up to 200-fold observed in MDA-MB-453 cells after treatment with DHT (manuscript in preparation). The *UGT2B11* and *UGT2B28* proximal promoters, which share 96% identity, as well as distal intergenic and intronic regions, contain several ARE-like elements in addition to FOXA1 binding sites which are essential for AR-mediated transactivation. Whilst the functions of these elements in AR-mediated regulation have been well defined, the potential for interacting partners of AR to modulate the induction of *UGT2B11* and *UGT2B28* has not been explored.

The information discussed here suggests that UGT expression may be linked to the SREBP-AR nexus in two ways. 1) Induction of *UGT2B11* and *UGT2B28* by AR could provide another mechanism for AR to control SREBP activity. 2) nSREBPs may be able to modulate the ability of AR to induce expression of *UGT2B11* and *UGT2B28*. The latter could provide a form of feedback to help maintain homeostasis of lipid and androgen signalling.

5.1.4 Tet-On Inducible System

Studies described in Chapter 4 used overexpression of UGTs in MDA-MB-453 cells by stable transfection to understand how they might affect lipid signalling. In this Chapter, the effects of overexpressing nSREBP were examined in the same cell line model. Because overexpression of nSREBP can induce toxicity, these studies required an inducible expression system. Hence a tetracycline (Tet) inducible system was used.

The Tet inducible system is based on regulatory elements that control the activity of the tetracycline-resistance operon in *E. coli*. In these bacteria, the genes of this operon are negatively regulated by the Tet repressor protein (TetR) by blocking transcription of the tet operator motifs (TetO). The original Tet-Off system was developed through fusing the transcription activation domain (AD) of the herpes simplex virus VP16 protein to TetR, to form the tetracycline-controlled transcriptional activator (tTA). The promoter that

responds to this is a fusion tetO and minimal CMV promoter, which allows expression of a gene of interest in the absence of tetracycline, but in its presence, tTA binds the promoter and prevents transcription (Gossen & Bujard, 1992). To create the Tet-On system, a reverse tetracycline-controlled transcriptional coactivator tTA (rtTA) was generated through the mutation of four amino acids. This rtTA binds the promoter in the absence of tetracycline, but does not induce expression until tetracycline or its derivative, doxycycline is added (Gossen et al., 1995). There are numerous benefits of using this system, including tight on/off signalling with minimal leaky expression in the absence of doxycycline, and high levels of inducibility with a quick response (Das et al., 2016).

This Tet-On system was used to allow transient high expression of nSREBP, avoiding the adverse effects of continuous expression and the need to perform repeated transient transfections in a difficult to transfect cell line.

5.1.5 Aims

The preliminary studies presented here indicate that UGT2B11 might be able to induce termination of SREBP signalling by inducing degradation of nuclear nSREBP transcription factors. In addition, the relationships described between UGTs, AR, and SREBPs suggest the possibility that nSREBPs may be able to regulate the expression of *UGT2B11* and *UGT2B28* through modulating AR activity. These molecular mechanisms would allow for highly controlled regulation of intracellular lipid levels, preventing lipotoxicity whilst simultaneously ensuring there are sufficient lipids and sterols to maintain cellular growth. This chapter investigated these two predicted regulatory pathways and attempted to identify molecular mechanisms of this regulation.

The specific aims of this chapter were as follows:

1. Validate preliminary findings that indicate a role for UGTs in regulating the degradation of nSREBPs.
2. Identify mechanisms by which UGTs may regulate nSREBP degradation.
3. Identify the role, if any, of nSREBPs in transcriptional regulation of UGTs.

5.2 METHODS

5.2.1 Plasmids

For all plasmids constructed in this chapter, sequences and plasmid maps are listed in Appendix 2. All other plasmids have been previously described in Chapter 2 (Section 2.1.4).

The dual epitope tagged (N-terminal myc and C-terminal HA) GSK-3 β ([GSK-3 \$\beta\$ -myc\(N\)-HA\(C\)-pcDNA3](#)) plasmid construct was generated by amplification of cDNA isolated from MDA-MB-453 cells using a HA-containing primer with Phusion (Thermo Fisher), and cloning of the resultant PCR product EcoRI-XbaI into pcDNA3 already containing an N-terminal myc-tag.

To generate the S436A CPD phosphodegron mutant of nSREBP-2 (nSREBP-2 (Mut)-HA(N)-pcDNA4), serine 346 was mutated to alanine in nSREBP-2-HA(N)-pCDNA4 through site directed mutagenesis as per Chapter 2, Section 2.2.8.6 ([Site-Directed Mutagenesis](#)). No map is provided for nSREBP-2 (Mut)-HA(N)-pcDNA4 due to lack of details regarding the parent vector construction, however, the mutated nucleotides and flanking regions were confirmed via sequencing.

To assess UGT mediated degradation of mature SREBPs via luciferase assay, full length nSREBP-1a ([GAL4-VP16-GFP-nSREBP-1a-pM](#)) and amino acids 1-336 of nSREBP-1a ([GAL4-VP16-GFP-nSREBP-1a\[1-336\]-pM](#)) were fused to the GAL4 DNA binding domain and VP16 activation domain fusion transcription factor, via amplification from nSREBP-1a-pEPI (Hübner et al., 2006) using Phusion. This was cloned SalI/XbaI and SalI/blunted XbaI, respectively, into in the previously described GAL4-VP16-pM (see Chapter 4, Section 4.2.1).

The CRISPRi-FBW7 construct targeting FBW7 was generated by cloning guide RNAs (gRNAs), designed using CRISPR-ERA (Liu et al., 2015) that target the *FBW7* proximal promoter regions, into the BpI cloning site of the previously described KRAB-dCas9-PX459 (see Chapter 4, Section 4.2.1).

To generate the TET-on inducible constructs, GFP-nSREBP-1a and GAL4-VP16-GFP-nSREBP-1a were amplified via amplification with Phusion from GAL4-VP16-GFP-nSREBP-1a-pM and cloned into pINDUCER by Professor Robyn Meech (Flinders University, South Australia). pINDUCER was obtained from Addgene (Plasmid #44012) and has been described previously (Meerbrey et al., 2011).

5.2.2 Oligonucleotides

Table 4.1: Sequence of primers used during this chapter.

For cloning primers, restriction sites are shown in bold and epitope tags are underlined.

For site-directed mutagenesis primers target bases for mutation are shown in bold.

Primer Name	Sequence (5'→3')
Cloning	
GSK-3β EcoRI F	GCG GAATTC ATGTCAGGGCGGCCAGAAC
GSK-3β HA XbaI R	TAAT CTAGAT <u>CAAGCGTAATCTGGAACATCGTATGGGTAGGTGGAGTTGGAAGCTGATG</u>
GFP Sall F	CGC GTCGAC ATGGTGAGCAAGGGCGAGGA
nSREBP-1a XbaI R	TGAT CTAGAT CA GTCAGGCTCCGAGTCACTGCCA
CRISPRi FBW7 F	CACCGGCGGGCGCCGAGAAAGTGGGT
CRISPRi FBW7 R	AAACACCCACTTTCTCGGCGCCGC
Site-Directed Mutagenesis	
nSREBP-2 S436A F	CCAGCC G CTGACTCAGGG
nSREBP-2 S436A R	CCCTGAGTCAG C GGCTGG
nSREBP-2 S436A Screening R	CCTGGGACCCTGAGTCAG C
qRT-PCR	
GAPDH F	GAAGGTGAAGGTCGGAGTC
GAPDH R	GAAGATGGTGATGGCATTTC
18s rRNA F	CGATGCTCTTAGCTGAGTGT
18s rRNA R	GGTCCAAGAATTTACCTCT
UGT2B11 F	CTCCATTCTTTTTGATCCCAAT
UGT2B11 R	TAAGCGGAGACTGTACACAAC
UGT2B28 F	TAAGCGGAGACTGTACACAAC
UGT2B28 R	AATGTCTGACCATCTCTTAA

5.2.3 Luciferase Assays

Luciferase assays were performed in HEK-293T cells and MDA-MB-453 cells. For HEK-293T cells, triplicate wells of a 48-well plate were transfected as described previously with lipofectamine 2000 (Chapter 2, Section 2.2.1.3 [Transfection](#)) at a density of 3.6×10^4 cells per well with 200 ng of indicated plasmid, 50 ng of luciferase reporter construct and 5 ng

of pRL-null. Cells were harvested 48-hours post transfection. For MDA-MB-453 cells, triplicate wells of a 48-well plate were transfected as described previously with lipofectamine LTX (Chapter 2, Section 2.2.1.3 [Transfection](#)) at a density of 5×10^4 cells per well with 100 ng of indicated nSREBP expression or control plasmid, 50 ng of luciferase promoter construct and 5 ng of pRL-null. Cells were grown for time period indicated before cell lysates were harvested, and Firefly and *Renilla* luciferase activity were measured as per Chapter 2, Section 2.2.6 [Luciferase assays](#). Variations to these conditions have been listed in the relevant figure caption. To facilitate the measurement of androgen responses in some experiments, cells were grown in steroid deplete media, comprised of phenol free RPMI 1640 with 5% charcoal stripped serum. Cells were treated with 10 nM DHT 24 hours post transfection, with assays harvested 48 hours post DHT treatment. In a subset of studies, Firefly luciferase values were normalised to total protein in each sample, rather than to *Renilla* luciferase activity. This approach was used when the *Renilla* luciferase activity appeared to respond to the experimental treatment, rather than remaining consistent between treatments and controls. For example, in MDA-MB-453 cells, the *Renilla* luciferase pRL-null vector was moderately induced by DHT treatment in steroid-replete media, although it was less affected in steroid-deplete media. This induction of luciferase from various *Renilla* luciferase vectors in some cell lines has been previously characterised by Shifera and Hardin (2010).

5.2.4 Protein Co-expression

To assess nSREBP-2 degradation and protein expression of new plasmid constructs via immunoblotting, HEK-293T cells were reverse-transfected in T25 flasks as previously described (see Chapter 2, Section 2.2.1.3 [Transfection](#)) with a total of 3-4 μg of plasmid DNA and cultured for 48 hours. Lysates were prepared either in hypotonic lysis buffer (Chapter 2, Section 2.2.4.1 [Lysate Preparation](#)) or in RIPA buffer (Chapter 2, Section 2.2.5.1 [Lysate Preparation](#)) and subjected to immunoblotting for analysis as per Section 2.2.5 [Western Blotting](#).

5.2.5 Co-immunoprecipitation

For co-immunoprecipitation of UGT2B11 with GSK-3 β , HEK-293T cells were reverse-transfected in two T25 flasks as described (see Chapter 2, Section 2.2.1.3 [Transfection](#)) with 1.5 μg of plasmid DNA of each UGT2B11-Flag(C)-pIRES and GSK-3 β -myc(N)-HA(C)-pcDNA3

constructs per flask. Cells were cultured for 48 hours and lysates were prepared and co-immunoprecipitation was performed as per Section 2.2.4 [Protein Co-expression and Co-immunoprecipitation analysis](#), and subjected to immunoblotting analysis as per Section 2.2.5 [Western Blotting](#).

5.2.6 Fluorescence Microscopy

For analysis of nSREBP degradation, HEK-293T cells were reverse-transfected in 48 well plate wells as previously described (see Chapter 2, Section 2.2.1.3 [Transfection](#)) at a density of 3.6×10^4 cells/well with 100 ng of nSREBP and UGT or control expression plasmid. Live cells were imaged 48-hours post transfection as detailed in Sections 4.2.4 and 2.2.7 [Fluorescence Microscopy](#).

5.2.7 Generation of Tet-On Cell lines

Tet-On vectors (GFP, GFP-nSREBP-1a and GAL4-VP16 GFP-nSREBP-1a) were transfected into MDA-MB-453 cells using Lipofectamine LTX (Invitrogen) as per the manufacturer's protocol. Approximately 5×10^6 cells were transfected in T25 flasks using 5 μ g plasmid DNA with a 1:1 DNA: Plus reagent ratio and 1:4 DNA: lipofectamine ratio. To select for a heterologous pool of cells with vector integration, puromycin selection was undertaken 48 hours post transfection, with transfected cells treated with increasing puromycin up to a final 0.55 μ g/mL. This was based on a previously established killing curve for MDA-MB-453 cells (data not shown). Once established, cells were maintained under regular growth conditions with consistent puromycin exposure. These cell lines were validated for lack of leaky expression using an EVOS microscope where no fluorescence was observed without induction by doxycycline.

5.2.8 Quantitative PCR

To analyse the level of mRNA transcripts for target genes, HEK-293T or MDA-MB-453 cells were plated into wells of a 6-well plate such that they would be 80-90% confluent prior to harvest. Exact conditions are listed in relevant figure captions. RNA extraction, reverse transcription and qPCR was conducted as detailed in Section 2.2.2 [Gene Expression Analysis](#).

5.3 Results

5.3.1 UGT2B11 and UGT2B28 reduce the levels of nSREBP-2 protein

As aforementioned, previous work from our laboratory suggested that UGT2B11 could regulate the level of nSREBP protein, potentially via promoting its degradation. The first aim of this Chapter was to confirm the previous findings for UGT2B11, to extend the analysis to UGT2B28, and to determine whether the effects of the UGTs on nSREBP required their catalytic functions. To achieve this, an epitope-tagged nSREBP-2 construct was co-transfected with epitope-tagged wildtype and truncated forms of UGT2B11 and UGT2B28 in HEK-293T cells. As a control, the nSREBP-2 construct was co-transfected with the empty pIRES vector. After 48 hours, expression levels of the proteins were assessed via immunoblotting (Figure 5.3A). The UGTs were detected at positions consistent with their predicted molecular weights: ~50 kDa for full-length UGT2B11 and UGT2B28, ~42 kDa for truncated UGT2B11, and ~28k Da for truncated UGT2B28. Truncated UGT2B28 forms two bands that are thought to be due to variable glycosylation. Each of the UGT proteins were produced at similar levels. However, there was a reduction in the level of nSREBP-2 protein when co-expressed with any of the UGT2B11 or UGT2B28 isoforms, as compared to the control vector condition. These data suggested that reduction in nSREBP protein can be mediated by both UGT2B11 and UGT2B28 and that it involves non-catalytic activities given that the truncated variants are inactive.

The mechanism(s) by which UGTs reduce nSREBP-2 protein in this co-expression system remains unclear. Non-specific effects that could lower nSREBP protein levels include reaching a 'ceiling' for total protein production, general transfection stress, or ER-stress caused by excessive levels of ER-localised UGT protein. As such these concerns were addressed by including conditions in which non-UGT control proteins were expressed, rather than empty vector. These controls included cytosolically localised GFP, and ER-localised SLC35B4. Co-expression of these proteins did not reduce nSREBP-2 protein levels (Figure 5.3B-C). This suggests that the reduction in nSREBP protein is due to a specific function of the UGTs, rather than non-specific effects of excessive protein production.

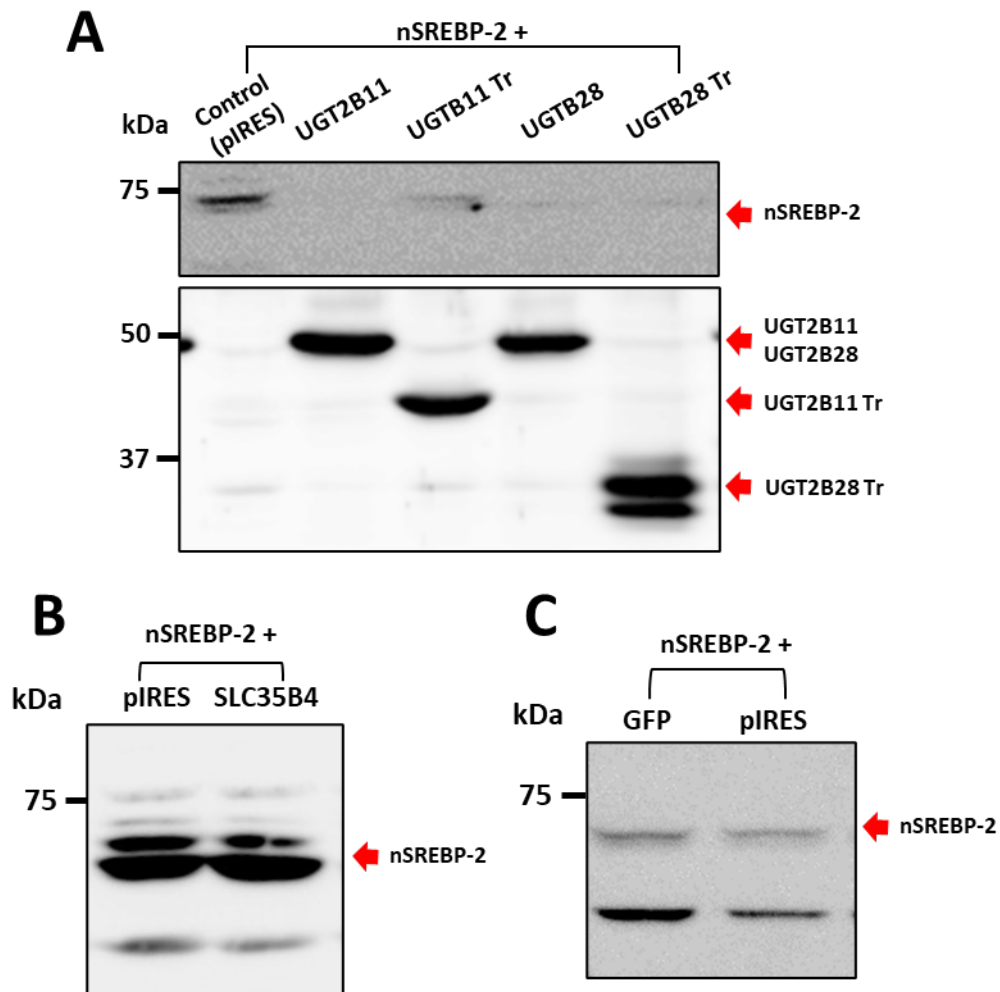


Figure 5.3: UGT2B11 and UGT2B28 isoforms reduce protein levels of nSREBP-2

HA-epitope tagged nSREBP-2 was co-expressed with **(A)** UGT2B11 and UGT2B28 wildtype and truncated isoforms or with control proteins: **(B)** SLC35B4 or **(C)** GFP. The amount of each of the proteins expressed was examined by immunoblotting of cell lysates. Representative immunoblots from at least 3 independent experiments shown. Immunoblots for nSREBP-2 were probed with anti-HA antibody. Immunoblots for UGTs were probed with an antibody raised to UGT2B7 that recognizes UGT2B7, UGT2B10, UGT2B11 and UGT2B28.

The data shown in Figure 5.3 appear to support the preliminary findings that these UGTs can modulate the levels of nSREBP protein within the cell. The reduction in SREBP levels may be expected to reduce the activation of nSREBP targets. To confirm this functional outcome, a reporter assay was developed to assess nSREBP-2 activity in HEK-293T cells. This assay used the SREBP responsive *DHCR24-300-pGL3-Basic* luciferase reporter construct. When co-transfected with a GFP control, nSREBP-2 activated the reporter ~ 2-fold. When UGT2B11 was co-expressed with nSREBP, this activation was significantly reduced on average by 28.5% (n=6) (Figure 5.4). This suggests that the decrease in nSREBP-2 levels observed upon co-expression of UGTs does result in a decrease in nSREBP-2 transactivation.

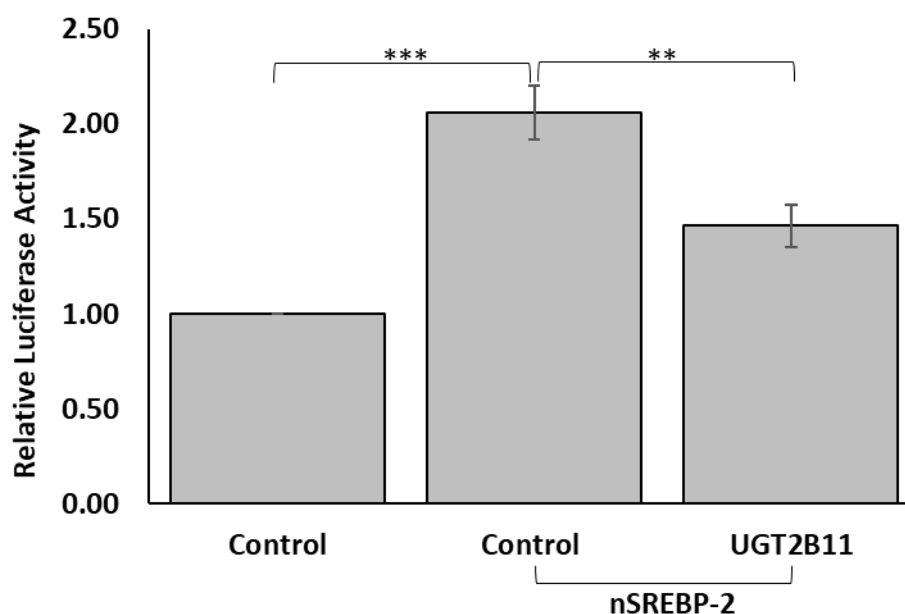


Figure 5.4: UGT2B11 reduces the transactivation activity of nSREBP-2

HEK-293T cells were co-transfected with 50 ng *DHCR24-300-pGL3* Luciferase reporter construct, 5 ng pRL-Null, 100 ng each of indicated control (GFP) or UGT2B11, and 100 ng of nSREBP-2 plasmid DNA. Luciferase activity assayed 48 hours post transfection. All data were normalised to *Renilla* Luciferase and control condition. Mean ± SEM for six independent biological experiments is depicted. Statistical significance was assessed by one-way-ANOVA and Tukey post hoc testing and indicated as follows: ** $p < 0.01$, *** $p < 0.001$.

5.3.2 UGT2B11 and UGT2B28 also modulate levels of nSREBP-1a protein

To corroborate the above findings with an orthogonal approach, a fluorescence-based assay using a GFP-fusion protein was developed. A plasmid expressing the nSREBP-1a-GFP fusion protein was co-expressed with UGT2B11 and UGT2B28 in HEK-293T cells, and nuclear fluorescence was assessed via microscopy (Figure 5.5). There was a statistically significant reduction in GFP fluorescence in both the UGT2B11 and UGT2B28 co-expression conditions, relative to the control condition. These data suggest that these UGTs reduce levels of nSREBP-1a similar to their effects on nSREBP-2.

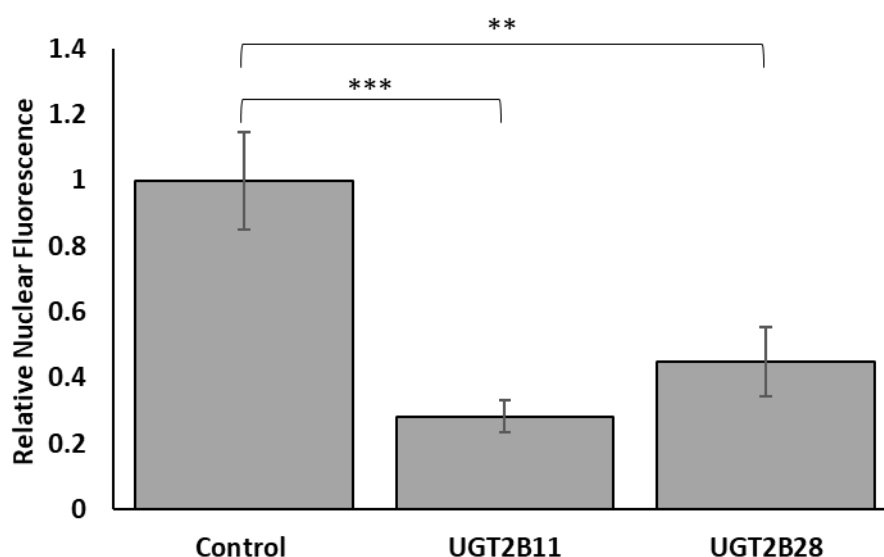


Figure 5.5: UGT2B11 and UGT2B28 reduces the nuclear abundance of nSREBP-1

HEK-293T cells were co-transfected with 100 ng each of indicated control or UGT plasmid, and 100 ng of nSREBP-1a-GFP plasmid DNA. Cells were imaged 48 hours post transfection. Nuclear fluorescence of nSREBP-1a GFP in individual cells was quantified using ImageJ. Data normalised to control condition. Mean \pm SEM for a minimum of 10 individual cells shown per condition. Statistical significance was assessed by one-way-ANOVA and Dunnett's post hoc testing and indicated as follows: ** $p < 0.01$, *** $p < 0.001$.

5.3.3 UGT2B11 and UGT2B28 variants affect the level of nSREBP proteins in MDA-MB-453 cells

The data shown in Sections 5.3.1 and 5.3.2 indicates that UGT2B11 and UGT2B28 can reduce the levels of nSREBP proteins, most likely by modulating their nuclear turnover. However, these data were generated in HEK-293T cells which do not naturally express these UGTs. Thus, it was important to determine whether the UGTs had similar effects in a relevant breast cancer model, such as MDA-MB-453 cells. This cell line shows comparatively poor transfectability and lower levels of heterologous protein expression, so a more sensitive luciferase reporter assay was needed to use in this model. This was created using the highly active GAL4-VP16 fusion protein previously described in Chapter 4. The GAL4-VP16 protein was fused to GFP-nSREBP-1a to create a 'hyperactive' nSREBP variant (GAL4-VP16-GFP-nSREBP-1a, Figure 5.6A) which had the capacity to strongly transactivate a luciferase reporter construct driven by the UAS promoter. To test this system, the GAL4-VP16-GFP-nSREBP-1a vector was transfected with the UAS promoter construct in HEK-293T and MDA-MB-453 cells. As shown in Figure 5.6C-D, in both cell lines the fusion protein activated the GAL4-UAS promoter construct by 300-400-fold. Next, the GAL4-VP16-GFP-nSREBP-1a and reporter vectors were co-transfected with plasmids expressing UGT2B11, UGT2B28, or truncated UGT variants, or one of several unrelated control proteins. The control proteins included ER localised SLC35B4, calnexin and NADH oxidoreductase, and cytosolic GFP. As previously described, these unrelated proteins act as controls for non-specific effects that may be caused by overwhelming the protein synthesis machinery or by accumulation of excessive ER protein which may lead to ER stress (Sano & Reed, 2013)

In HEK-293T cells, co-transfection of GAL4-VP16-GFP-nSREBP-1a with UGT2B11 or UGT2B28 significantly reduced activation of the reporter by ~50-60%. Only one of the control proteins (calnexin) had a significant effect on transactivation, but this was not consistent between HEK-293T cells and MDA-MB-453 cells. In MDA-MB-453 cells, co-transfection of GAL4-VP16-GFP-nSREBP-1a with UGT2B11, UGT2B28, or their truncated variants caused a significant reduction in the activation of the reporter by ~60-90%. None of the control proteins reduced transactivation (Figure 5.6E-F). To ensure that the effects of the UGTs were specific to the nSREBP1a domain, they were also transfected with the GAL4-VP16 protein (Figure 5.6B). The UGTs had no effect on the ability of GAL4-VP16 to activate the reporter, suggesting that the effect requires the presence of the nSREBP1a

domain. Overall, these data show that UGTs can robustly reduce the activity of a GAL4-VP16-GFP-nSREBP-1a in MDA-MB-453 cells.

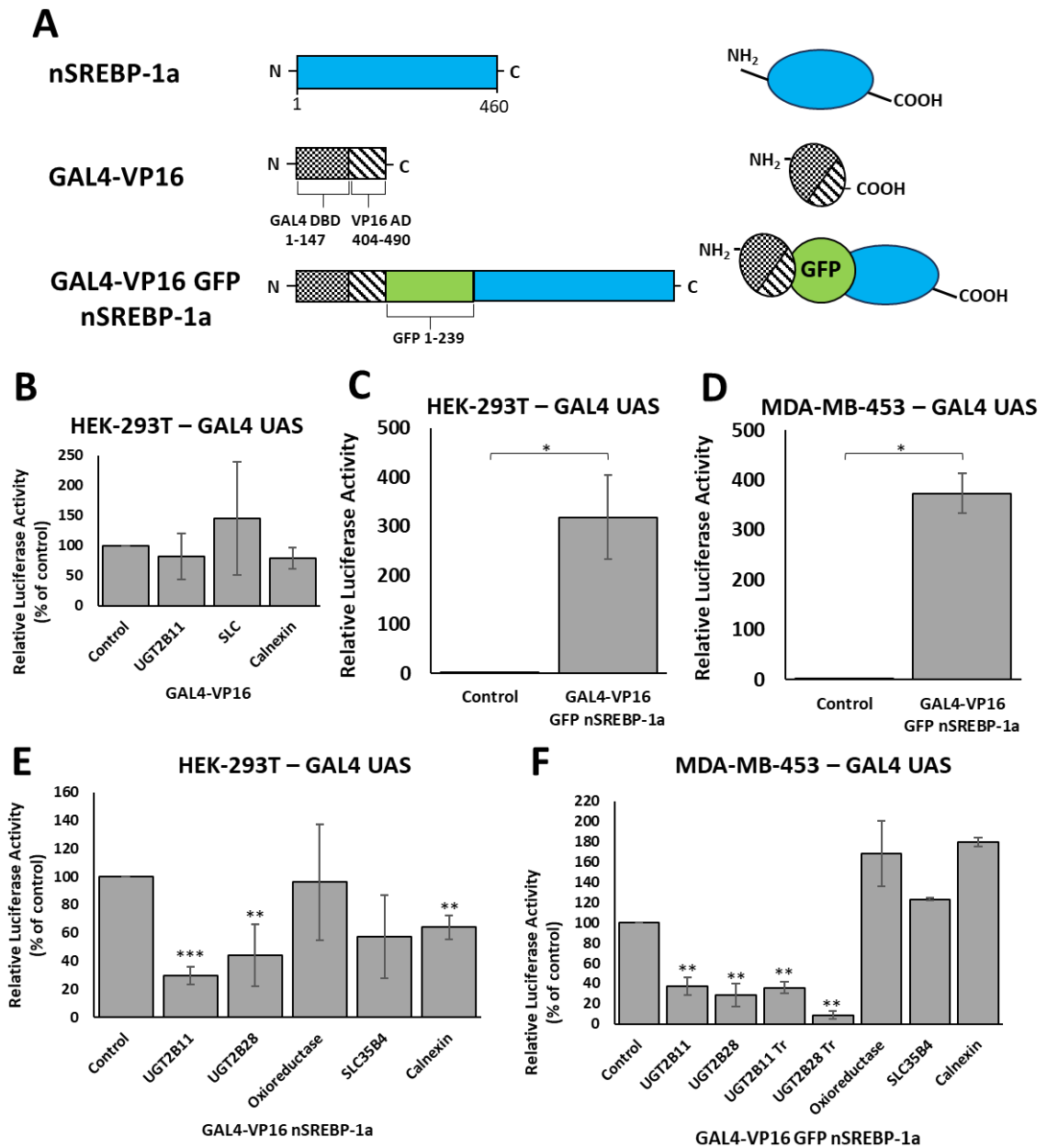


Figure 5.6: UGT2B11 and UGT2B28 reduce the transactivation of a GAL4-VP16 nSREBP-1a fusion protein

(A) Topology and domain structure of GAL4-VP16 Fusion constructs. HEK-293T or MDA-MB-453 cells were co-transfected with 50 ng pck-1 GAL4 UAS luciferase reporter, 5 ng pRL-Null and 100 ng indicated plasmid DNA (**B-F**). Luciferase activity was assayed 48 hours post transfection. All data were normalised to *Renilla* luciferase and control condition. Data from 2-6 biological experiments depicted (Mean \pm SEM) for each condition. Statistical significance was assessed by *Student's t-test* or one-way-ANOVA and Dunnett's post hoc testing as appropriate and indicated as follows: * $p < 0.05$, ** $p < 0.01$, *** $p < 0.001$.

5.3.4 Attempted knock down of FBW7 in HEK-293T cells

Data in Sections 5.3.1 to 5.3.3 show that UGT2B11 and UGT2B28 reduce levels of nSREBP proteins. Although the possibility that this is due to reduced protein synthesis cannot be fully ruled out, it was considered most likely that it involves increased protein turnover. This is in large part because there is no known mechanism for selectively regulating translation of the synthetically encoded nSREBP protein, whilst in contrast, the mechanism for nSREBP turnover is well defined, very robust, and essentially ubiquitous. As described previously, the canonical pathway by which nSREBPs are degraded involves their polyubiquitination by a SCF complex, in which FBW7 serves as the target specificity factor (Sundqvist et al., 2005). It was reasoned that if UGTs modulate FBW7-dependent turnover, then knockdown of FBW7 could ablate this effect. To examine the role of FBW7 in UGT-mediated nSREBP turnover, previous work in our laboratory had generated a CRISPR inhibition (CRISPRi) construct targeted to FBW7 (designated FBW7i). This vector was shown to express the KRAB-dCas9 domain when transiently transfected into HEK-293T cells (data not shown); however, its ability to knockdown FBW7 had not been fully validated. In the current project, transient transfection of the FBW7i vector into HEK-293T cells was shown to reduce FBW7 mRNA levels by 57% (Figure 5.7A).

The capacity of the FBW7i construct to inhibit FBW7-mediated turnover of nSREBP-2 was subsequently assessed. In a pilot experiment, expression of the FBW7i vector increased the amount of nSREBP-2 protein relative to the empty CRISPRi vector control as assessed via immunoblotting, whilst having no effect on the stability of a control protein (SLC35B4) (Figure 5.7B). However, subsequent repeat experiments showed inconsistent effects on the nSREBP-2 protein level (not shown). It was speculated the effect of FBW7i may depend on the level of its expression and the timing of the analysis. To optimise these variables, a rapid reporter-based assay system was established using the *DHCR24-300* SRE-containing luciferase reporter construct (see Chapter 4). These experiments were prompted by the study of Garvin et al. (2019) and Iwase et al. (2019), in which they used reporter assays to measure the activity of FBW7-dependent targets as a proxy for their turnover. However, in the present studies, transient co-expression of the FBW7i construct with nSREBP failed to increase transactivation of the *DHCR24-300* luciferase reporter construct (Figure 5.7C-D). It was hypothesised that this failure to affect transactivation may be due to the timing of the expression of each component in the reporter system. Specifically, because CRISPRi

reduces expression of FBW7, its depletion in the cell is dependent on its protein half-life. FBW7 may not turn over rapidly enough after transfection of the FBW7i construct, to affect the level of reporter activation by nSREBP. Studies in H1299 and PANC-1 cells suggested that FBW7 half-life may be ~4-6 hours, although this may be cell line dependent (Ji et al., 2015; Lan et al., 2019). To ensure that FBW7 was fully depleted for analysis of nSREBP activity in the reporter assay, a double transfection method was trialled in which the CRISPRi constructs were transfected one day prior to transfecting the reporter and nSREBP. However, this also failed to enhance transactivation (Figure 5.7D). This double transfection method was also trialled for another FBW7 target, NICD; however, it did not increase the transactivation of a NICD target promoter (CBFRE) construct by NICD (Figure 5.7E).

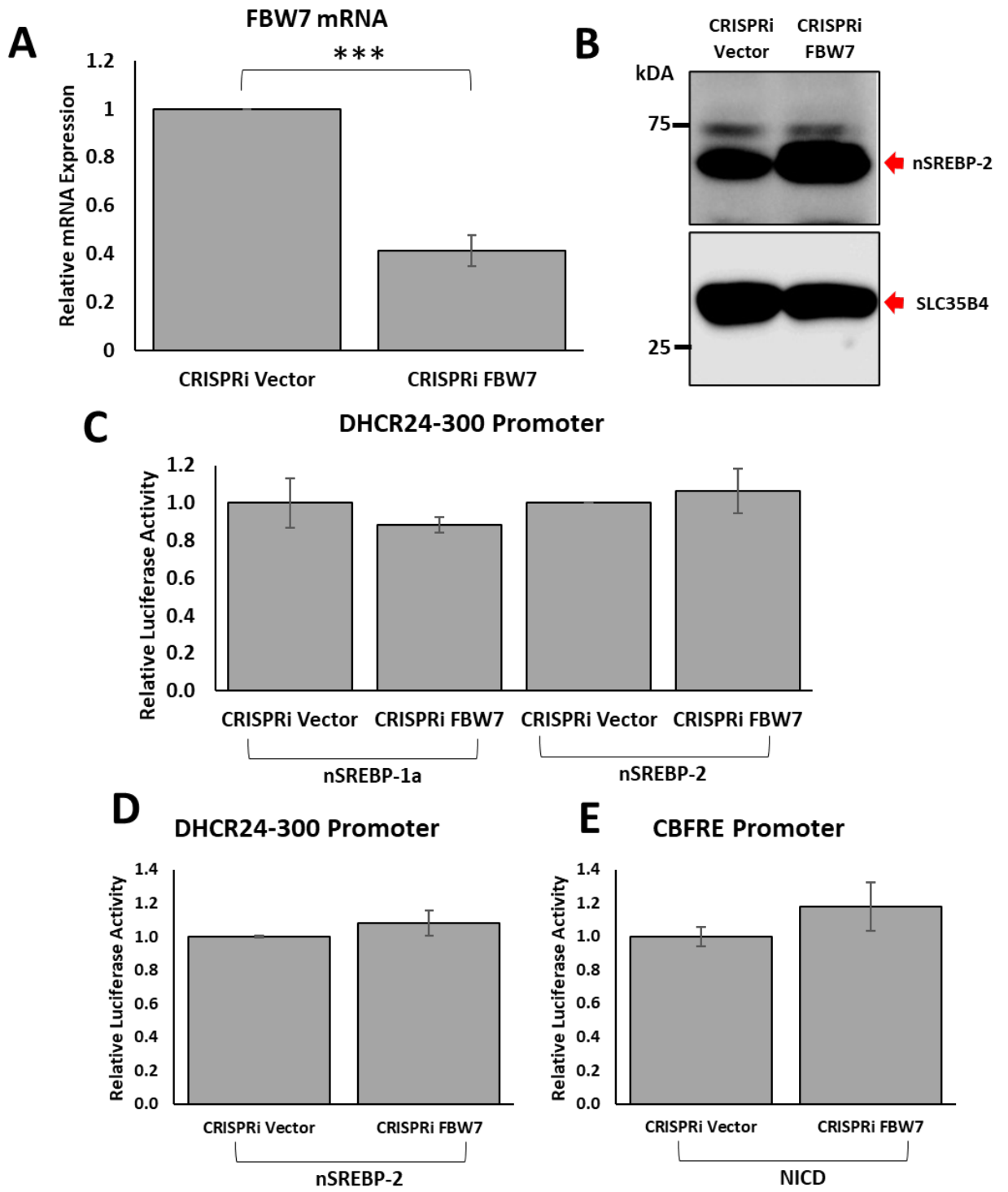


Figure 5.7: Transient *FBW7* CRISPRi vector validation in HEK-293T cells

(A) *FBW7* mRNA was quantified via qRT-PCR as described in methods from HEK-293T cells transiently transfected 2 µg of empty px459 CRISPRi vector or *FBW7*-targeted CRISPRi vector and cultured for 48 hours. Data from two biological experiments depicted (Mean ± SEM for n=7 technical replicates), normalised to 18s rRNA. Significance was assessed via t-test and indicated as follows; p<0.001 ***. **(B)** HA-tagged nSREBP-2 was co-transfected with FLAG-tagged SLC35B4 and with the px459 CRISPRi vector containing either no gRNA or an *FBW7* targeting gRNA. Immunoblots were probed with anti-HA antibody for nSREBP-2 and anti-FLAG for SLC35B4. **(C)** HEK-293T cells were co-transfected with 50 ng *DHCR24-300*-pGL3 Luciferase reporter construct, 5 ng pRL-Null, 100 ng each of nSREBP expression plasmid, and 100 ng of indicated CRISPRi plasmid DNA. **(D, E)** HEK-293T cells were transfected with 100 ng of indicated CRISPRi plasmid DNA, 24 hours later they were re-transfected with 50 ng indicated reporter, 5 ng pRL-Null, 100 ng each of nSREBP or NICD expression plasmid and 100 ng of indicated CRISPRi plasmid DNA. Luciferase activity was assayed 48 hours post final transfection. All data were normalised to *Renilla* Luciferase and control condition. Mean ± SEM for one (nSREBP-1a, n=3 technical replicates) or four (nSREBP-2) independent biological experiments depicted **(C)**. Representative figure of two independent biological experiments shown (Mean ± SEM for n=3 technical replicates) **(D, E)**.

Overall, the data showed that the *FBW7i* construct did not increase nSREBP or NICD-mediated transactivation of their target promoters, suggesting that it was ineffective in stabilizing these proteins. Moreover, titration of the amount of nSREBP expressed in the system did not change the reporter response (data not shown), suggesting that a ceiling for *DHCR24-300* promoter activation was reached at quite a low concentration of nSREBP. This assay was then repeated with UGT co-transfection, which was previously shown to reduce the amount of nSREBP available. As shown in Figure 5.8, when the *FBW7* CRISPRi vector was co-transfected with the UGT and nSREBP-2, there was no rescue of the UGT-mediated decrease in nSREBP activity. However, given the uncertainty about whether *FBW7* knockdown was effective (see Figure 5.7 and Figure 5.11), it cannot be determined from these results whether *FBW7* is in fact required for the UGT to modulate nSREBP activity.

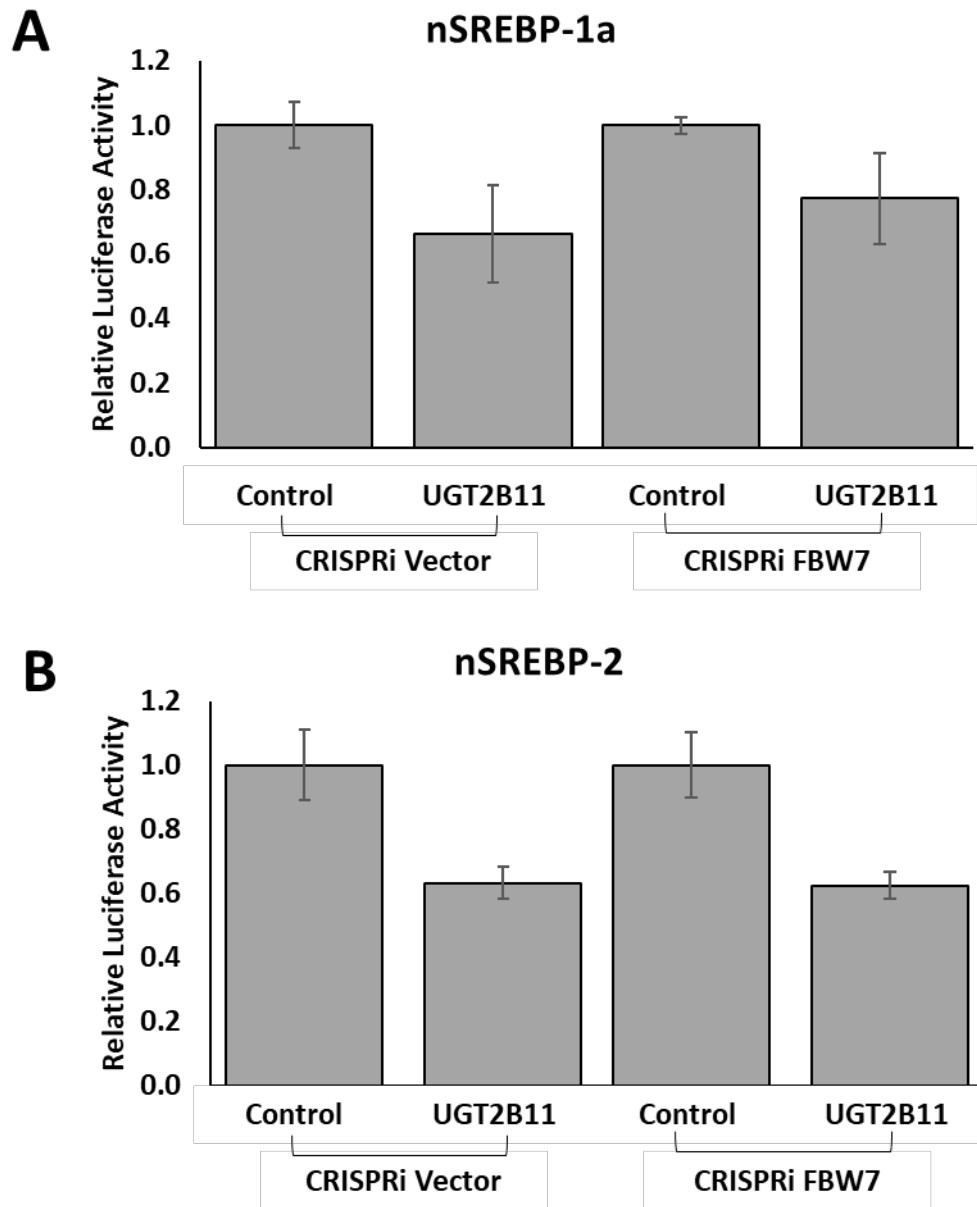


Figure 5.8: Decrease in nSREBP transactivation not altered by FBW7 CRISPRi

HEK-293T cells were co-transfected with 50 ng *DHCR24-300*-pGL3 Luciferase reporter construct, 5 ng pRL-Null, 75 ng of either UGT2B11 or GFP (Control) expression plasmids, 100 ng indicated CRISPRi plasmid DNA and 75 ng of nSREBP-1a (**A**) or nSREBP-2 (**B**) expression plasmids. Luciferase activity assayed 48 hours post transfection. All data normalised to *Renilla* Luciferase and control condition. Representative example of 2-4 biological experiments is depicted (Mean \pm SEM for n=3 technical replicates).

Since the FBW7i vector had not produced consistent knockdown effects in transient transfections, it was reasoned stable expression of the construct may lead to a more reproducible effect. Hence two independent HEK-293T lines (example data from one set of lines is presented in Figure 5.9) with stable integration of the FBW7i construct or the empty CRISPRi vector, were generated. To validate the cell lines after selection, the mRNA for the components of the CRISPRi system, KRAB (Kruppel Association Box) and Cas9 were measured. These mRNAs were absent in the parental cells and were detected at approximately equivalent levels in the FBW7i and CRISPRi stable cell lines (Figure 5.9A-B), suggestive of successful vector integration. However, *FBW7* mRNA levels were not reduced in the FBW7i stable lines relative to the empty CRISPRi vector control cell line (Figure 5.9C). Follow up analyses examined whether the FBW7 gRNA was expressed in the FBW7i line. This was assessed with one primer in the tracrRNA region, and another in the FBW7 gRNA region, which if present, allows for the detection of the one contiguous RNA strand. The gRNA was not detected (not shown).

It should be noted that there was considerably less Cas9 and KRAB mRNA expressed in these stable lines relative to the experiments conducted via transient transfection. There was 50-300-fold more Cas9 and KRAB mRNA in the transiently transfected HEK-293T cell lines at 96 hours post-transfection compared to the stably selected lines. Therefore, a higher level of expression may be required to achieve target inhibition. Although this is a different model, it is consistent with the previous inability to generate stable UGT knock-down models in breast cancer cell lines using the px459 CRISPRi vector system. Due to the lack of success with the CRISPRi vectors, attempts to investigate the role of FBW7 in UGT-mediated modulation of nSREBP stability were ceased; these remain an area for future investigation.

5.3.5 The UGT-mediated degradation of nSREBP isoforms is independent of GSK-3 β

As previously mentioned, nSREBPs are regulated by a suite of post transcriptional modifications and mechanisms. The key mechanism that controls their stability is their phosphorylation of the phosphodegron (T426, S430 and S434) in nSREBP-1a (or equivalent residues present within nSREBP-1c and nSREBP-2) by GSK-3 β . Phosphorylation results in recruitment of FBW7 and hence polyubiquitination and proteasomal degradation (Bengoechea-Alonso & Ericsson, 2009; Sundqvist et al., 2005). The question of whether UGTs reduce nSREBP protein levels by a mechanism(s) that involves the nSREBP phosphodegron motif was tackled using various approaches in parallel studies. These approaches, as described in this section, included determining whether degradation of nSREBP occurred when the phosphodegron was deleted or mutated, and assessing whether UGTs could interact with GSK-3 β .

To assess whether these UGTs interact with GSK-3 β , a dual epitope tagged (Myc and HA) GSK-3 β expression construct was generated, and its heterologous expression was validated via immunoblotting (Figure 5.10A). Tagged GSK-3 β was then co-transfected alongside FLAG tagged UGT2B11 in HEK-293T cells and extracts were subjected to magnetic bead-based co-immunoprecipitation. UGT2B11 was not found to interact with GSK-3 β (Figure 5.10B). This does not discount the possibility that the UGT may modulate its activity indirectly but suggests there is no direct physical interaction of GSK-3 β and UGT2B11.

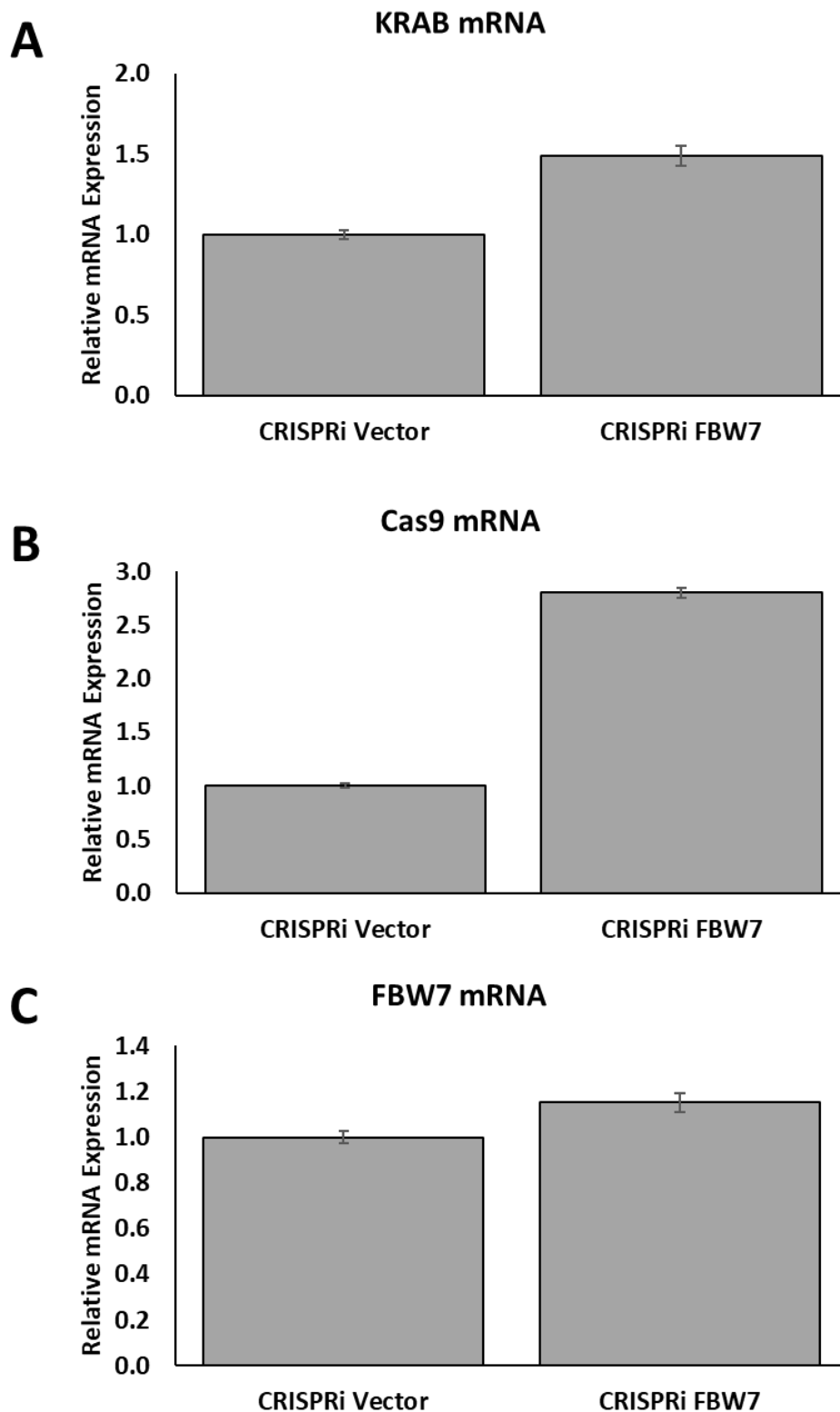


Figure 5.9: KRAB, Cas9 and FBW7 mRNA levels in stable CRISPRi HEK-293T cell lines

KRAB (A), *Cas9* (B) and *FBW7* (C) mRNA was quantified via qRT-PCR as described in methods for HEK-293T cells stably expressing either empty px459 CRISPRi vector or FBW7-targeted CRISPRi vector. A representative figure of at least two biological experiments is depicted (Mean for n=3 technical replicates), normalised to GAPDH and empty px459 vector stable line.

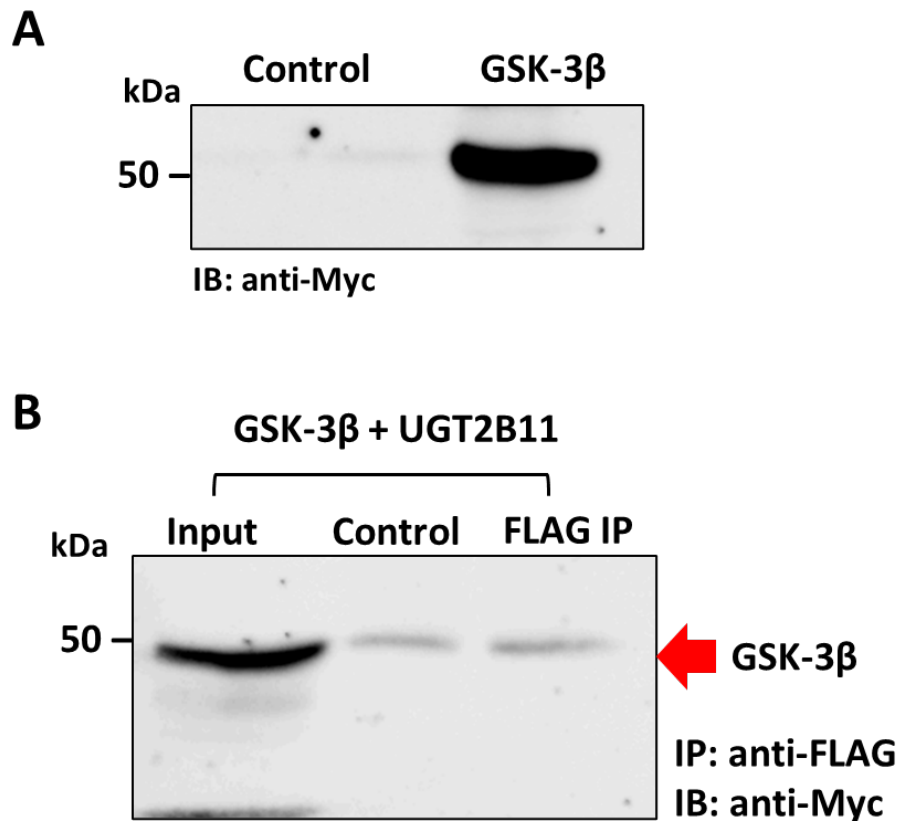


Figure 5.10: UGT2B11 does not co-immunoprecipitate GSK-3β

(A) The expression of GSK-3β was initially confirmed via immunoblotting lysates from HEK-293T cells were transfected with either control (GFP) or Myc tagged GSK-3β expression plasmid. **(B)** Myc-tagged GSK-3β and FLAG-tagged UGT2B11 were co-immunoprecipitated using anti-FLAG antibody. Immunoblots probed with anti-Myc antibody for GSK-3β.

To determine whether UGT-mediated reduction in nSREBP level requires the presence of the phosphodegron, a new plasmid construct was made in which a C-terminally truncated version of nSREBP-1a (comprised of only residues 1-336) was fused downstream of the previously described GAL4-VP16 protein (Figure 5.11A). The truncated form of nSREBP-1a lacks the C-terminal phosphodegron motif and is therefore constitutively nuclear and does not undergo GSK-3β-mediated proteasomal degradation.

The capacity of the GAL4-VP16 nSREBP-1a (1-336aa) construct to transactivate the UAS luciferase promoter construct was tested in both HEK-293T and MDA-MB-453 cells (Figure 5.11B-C). In HEK-293T cells, GAL4-VP16 nSREBP-1a (1-336aa) activated the promoter by ~800-fold, which is about twice the level of activation induced by the 'wildtype' GAL4-VP16 nSREBP-1a construct that has an intact C-terminal domain (Figure 5.6). In MDA-MB-453 cells, GAL4-VP16 nSREBP-1a (1-336aa) activated the promoter by ~200-fold, which is

comparable to the level of activation induced by the wildtype GAL4-VP16 nSREBP-1a construct (Figure 5.6). As shown in both cell models (Figure 5.11), when GAL4-VP16 nSREBP-1a (1-336aa) was co-transfected with UGT2B11 or UGT2B28, its ability to activate the promoter was significantly reduced by approximately 50 – 90%. This was similar to the effects of these UGTs on the activity of the wildtype GAL4-VP16 nSREBP-1a construct (Figure 5.6). This suggested that UGT mediated reduction in nSREBP levels does not involve the C-terminal region of nSREBP that contains the phosphodegron.

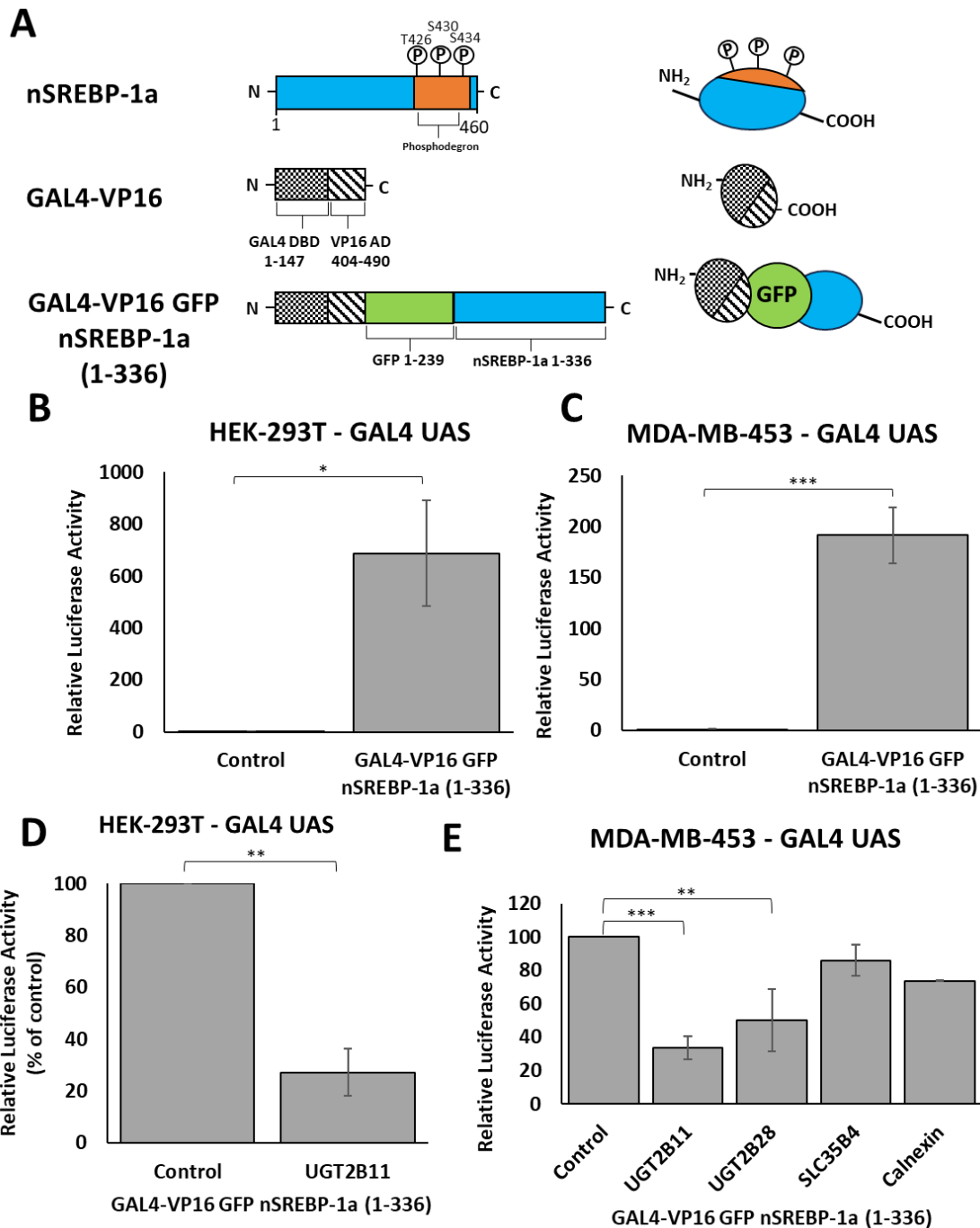


Figure 5.11: UGT-mediated reduction in the activity of truncated nSREBP-1a (1-136)

(A) Topology and Domain structure of GAL4-VP16 Fusion constructs. HEK-293T or MDA-MB-453 cells were co-transfected with 50 ng pck-1 GAL4 UAS luciferase reporter, 5 ng pRL-Null and 100 ng indicated plasmid DNA (B-E). Luciferase activity assayed 48 hours post transfection. All data normalised to *Renilla* luciferase and control condition. Data from 3 biological experiments depicted (Mean \pm SEM) for each condition in HEK-293T cells and from one representative biological experiment in MDA-MB-453 cells (Mean \pm SEM, n=3 technical replicates). Statistical significance was assessed by Student's *T*-test or one-way-ANOVA and Dunnett's post hoc testing as appropriate and indicated as follows: * $p < 0.05$, ** $p < 0.01$, *** $p < 0.001$.

To further define whether the nSREBP C-terminal phosphodegron was required for the ability of UGTs to reduce nSREBP levels, serine 436 was mutated to alanine in an nSREBP-2 construct (nSREBP-2 S436A). Sundqvist et al. (2005) showed that this mutation prevents GSK-3 β -mediated degradation and has the equivalent stabilizing effect as mutating all serine residues within the phosphodegron. The nSREBP-2 S436A construct activated the *DHCR24-300* luciferase promoter by an average of 2.4-fold, which is equivalent to wildtype nSREBP-2 (Figure 5.12A). Co-transfection of UGT2B11 with nSREBP-2 S436A led to a statistically significantly ~20% reduction in transactivation of the reporter (Figure 5.12B), which was similar to its effect on wildtype nSREBP-2 (as previously shown in Figure 5.4). To examine that the effect on promoter activity was due to reduced nSREBP protein levels, the amount of nSREBP-2 S436A protein was tested by immunoblotting in two independent biological experiments, where the protein levels were clearly reduced as with the WT nSREBP variant (Figure 5.12C).

Overall, taking together the results shown in Figure 5.11 and Figure 5.12, it appears that the mechanism by which UGT2B11 reduces the level or activity of nSREBPs does not involve the phosphodegron.

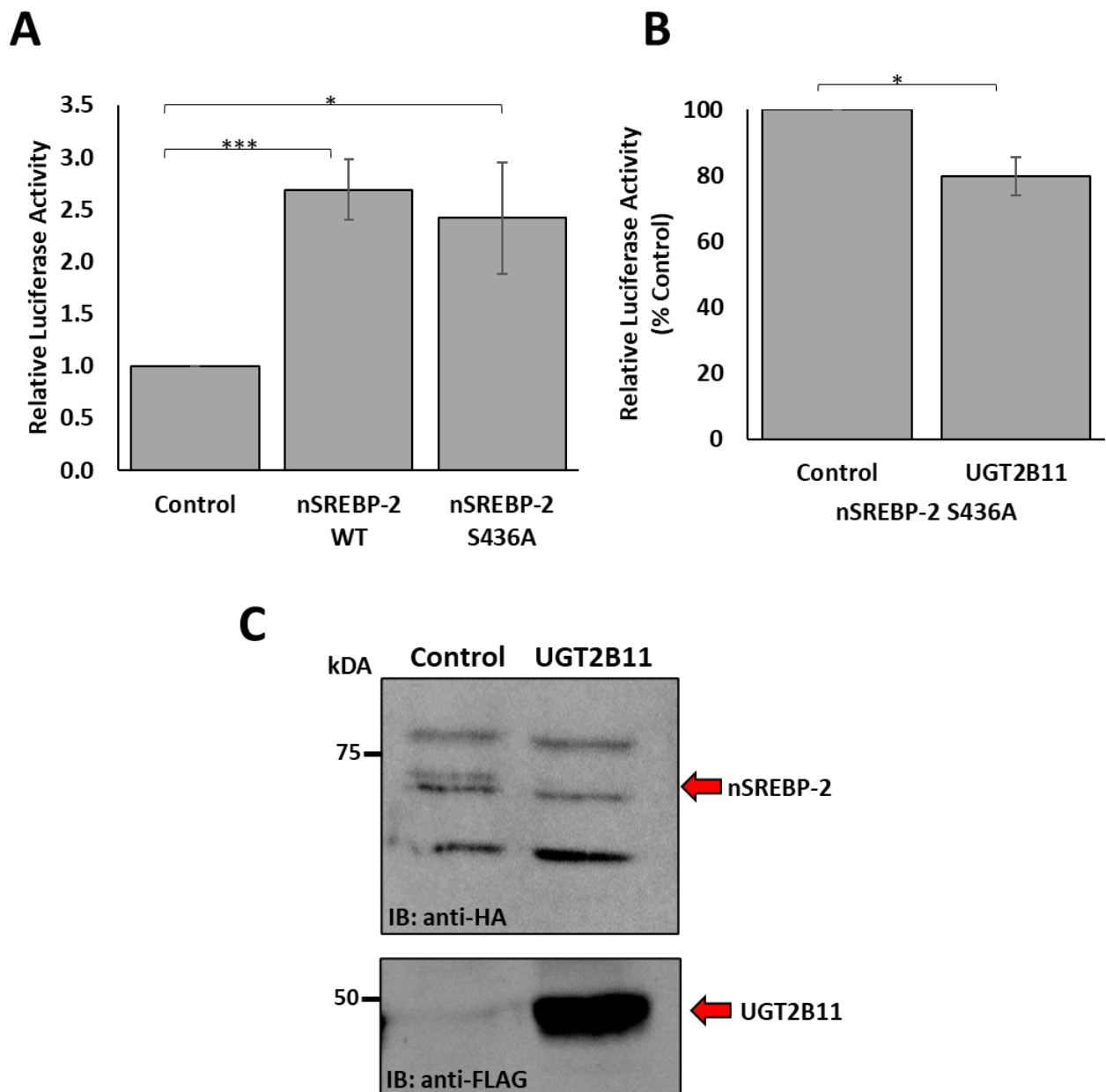


Figure 5.12: UGT-mediated reduction in the activity of mutated nSREBP-2 S436A

(A) HEK-293T cells were transfected with 50 ng pck-1 GAL4 UAS luciferase reporter, 5 ng pRL-Null and 100 ng indicated nSREBP2 plasmid. **(B)** HEK-293T cells were transfected with 50 ng pck-1 GAL4 UAS luciferase reporter, 5 ng pRL-Null, 100 ng of nSREBP2 S436A expression plasmid and 100 ng of either GFP (control) or UGT2B11 expression plasmid. Luciferase activity was assayed 48 hours post transfection. All data normalised to *Renilla* luciferase and control condition. Data from 3 biological experiments are depicted (Mean \pm SEM). Statistical significance was assessed by *T*-test or one-way-ANOVA and Tukey post hoc testing as appropriate and indicated as follows: * $p < 0.05$, *** $p < 0.001$. **(C)** HA-tagged nSREBP-2 S436A was co-expressed with FLAG-UGT2B11 or control (GFP). The amount of each of the proteins expressed was examined by immunoblotting of cell lysates. Representative immunoblots from at least 2 independent experiments shown. Immunoblots for nSREBP-2 and UGT2B11 were probed with anti-HA and anti-Flag antibodies respectively.

5.3.6 nSREBPs repress the transactivation of UGT2B11 and UGT2B28 promoters

It has been shown by Suh et al. (2008) that nSREBPs can modulate the transcriptional activity of the AR in prostatic cells. As aforementioned, the *UGT2B11* and *UGT2B28* genes are induced by AR in an androgen dependent manner in both prostate and breast cancer contexts. Thus, it was considered possible that nSREBPs could modulate the regulation of these UGTs by AR. By regulating the amount of UGT present in cells, nSREBPs could control the extent of UGT-mediated regulation of SREBP precursor processing (see Chapter 4) and nSREBP stability. This would represent a novel feedback mechanism.

The finding by Suh et al. (2008) that nSREBPs inhibit AR activity was initially confirmed in MDA-MB-453 cells using a promoter-luciferase reporter plasmid carrying the androgen-responsive probasin promoter (ARR3-tk-Luciferase). This promoter construct consists of three tandem copies of the minimal probasin promoter sequence; each of which contain two strong and two weak AR binding sites (Farla et al., 2005; Rennie et al., 1993), and a thymidine kinase enhancer element upstream of the luciferase reporter gene (Snoek et al., 1996). MDA-MB-453 cells were transfected with ARR3-tk-Luciferase and then treated with 10 nM DHT. The promoter was induced ~8-fold in response to DHT, an effect mediated by endogenously expressed AR. Expression of either nSREBP-1a or nSREBP-2 reduced the ability of DHT to induce the promoter when compared to a GFP control (Figure 5.13). These data confirmed the previous report by Suh et al. (2008) that nSREBPs can inhibit AR-mediated transactivation, and extends those findings to MDA-MB-453 breast cancer cells.

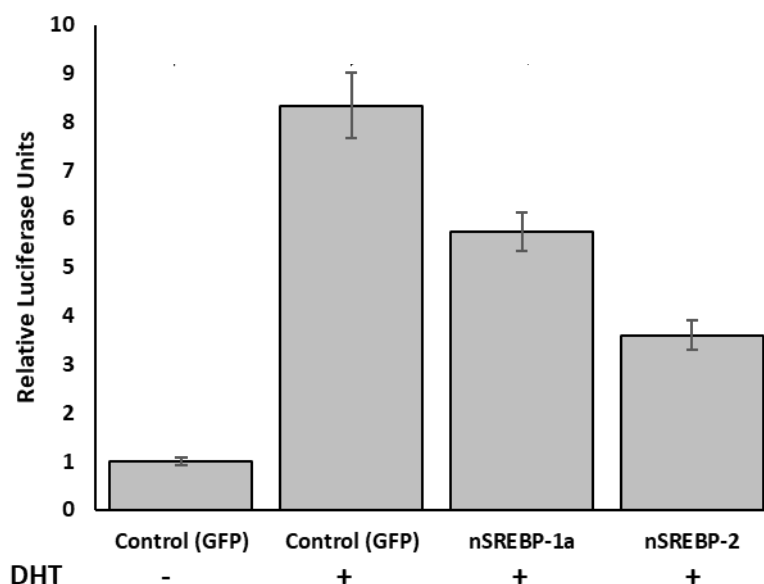


Figure 5.13: nSREBPs repress transactivation of the ARR3 promoter by AR.

MDA-MB-453 cells were co-transfected with 50 ng ARR3-TK-Luciferase reporter construct, 5 ng pRL-Null and 100 ng of indicated control or nSREBP plasmid DNA. Cells were treated with 10 nM DHT 24 hours post transfection, for 48 hours. Luciferase activity was assayed 72 hours post transfection. All data were normalised to protein concentration and the control condition. A representative figure of at least three biological experiments is depicted (Mean \pm SEM for n=3 technical replicates). Statistical significance was assessed by one-way-ANOVA and Tukey post hoc testing and indicated as follows: ** p < 0.01, *** p < 0.001.

Subsequent to the validation of the effect of nSREBPs on the ARR3-tk-Luciferase promoter, the ability of nSREBPs to reduce AR-mediated induction of the *UGT2B11* and *UGT2B28* promoters was assessed. Two different luciferase promoter constructs were used that had been previously prepared in the laboratory: *UGT2B11* 2kb pGL3 and *UGT2B28* 1kb pGL3 (Figure 5.14). Both constructs contain androgen responsive elements (ARE) that had been previously shown to mediate activation by androgen-liganded AR (See Chapter 1, Section 1.5.5, Figure 1.6). Both *UGT2B11* and *UGT2B28* promoters were induced by up to 2-fold by DHT. Co-expression of either nSREBP-1a or nSREBP-2 significantly reduced the ability of DHT to induce the promoters by around 40 – 70% when compared to a GFP control (Figure 5.14A-B).

To confirm that this reduction in transactivation was caused by modulating the activity of the AR, nSREBP-2 was co-transfected with a constitutively active AR splice variant (AR-v7) which activates AR target genes in the absence of any ligand. nSREBP significantly reduced the ability of Ar-v7 to induce the *UGT2B28* promoter by ~60% (Figure 5.14C).

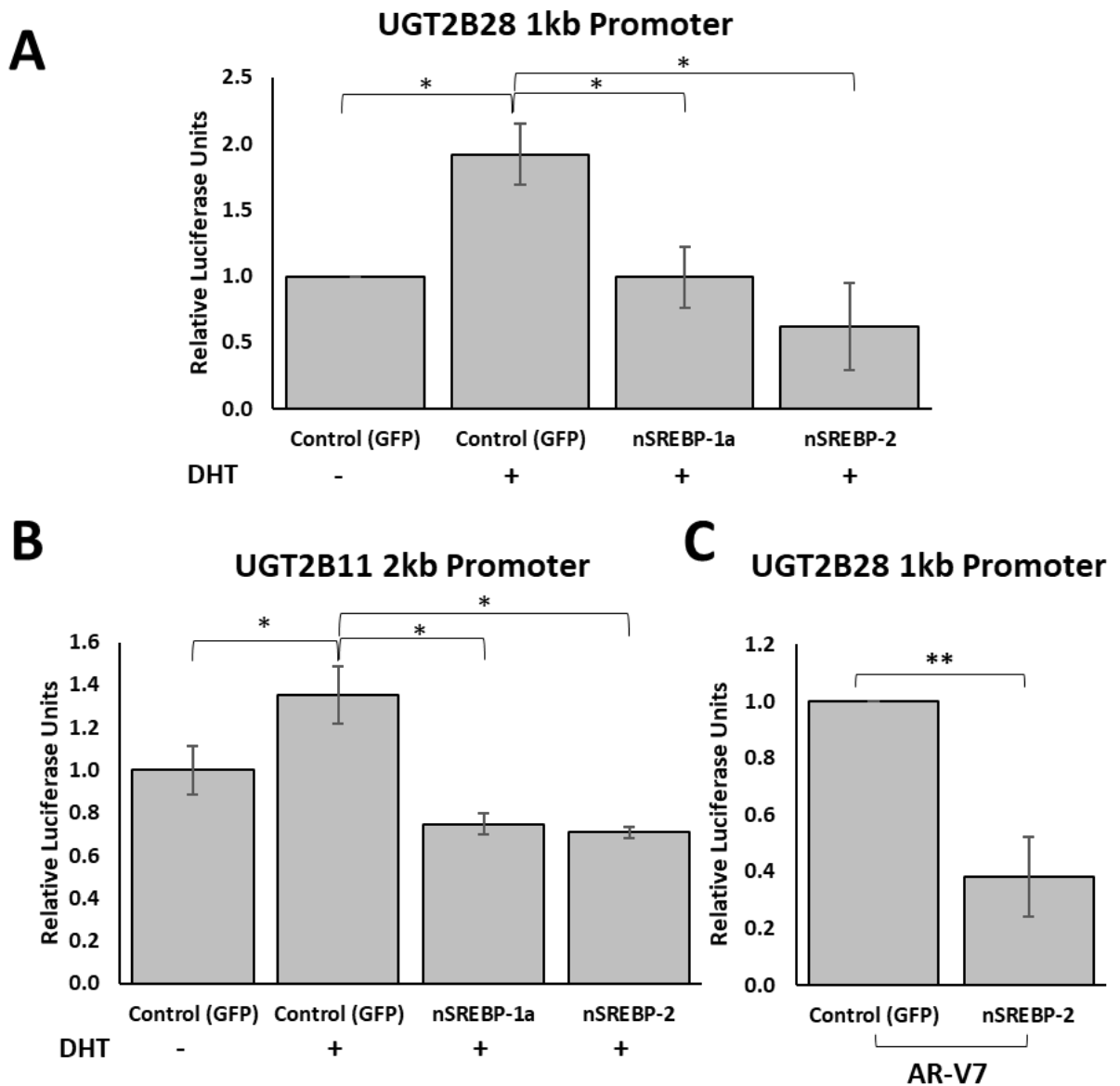


Figure 5.14: nSREBPs repress transactivation of the UGT2B28 promoter by AR and AR-v7

MDA-MB-453 cells were seeded under stripped conditions (phenol free RPMI 1640 media with 5% charcoal stripped serum) for 5-8 days prior to being co-transfected with 50 ng of indicated control or nSREBP plasmid DNA and (C) 100 ng of AR-v7. For (A, B) cells were treated with 10 nM DHT 24 hours post transfection. Luciferase activity assayed 72 hours post transfection. All data normalised to Renilla luciferase and control condition. Mean \pm SEM is depicted of either at least three independent biological experiments (A, C) or representative figure of at least three biological experiments depicted (Mean \pm SEM for n=3 technical replicates) (B). Statistical significance was assessed by Student's T-test or one-way-ANOVA and Dunnett's post hoc testing as appropriate and indicated as follows: * $p < 0.05$, ** $p < 0.01$.

5.3.7 nSREBPs induce toxicity when stably overexpressed

To determine whether nSREBPs can alter expression of the endogenous *UGT2B11* and *UGT2B28* genes, nSREBPs were over-expressed in MDA-MD-453 cells. Due to the relatively poor transfectability of MDA-MB-453 cells, efforts were made to generate stably expressing cell pools by puromycin selection. While a fraction of cells was transiently transfected with the nSREBP constructs, they did not survive under puromycin selection. After one week of puromycin treatment, all cells transfected with nSREBP constructs died, while approximately 50% of the cells transfected with the empty vector survived. It was hypothesised that excessive nSREBP expression could lead to excessive lipogenesis and hence lipotoxic cell death.

5.3.8 Validation of Doxycycline Inducible nSREBP stable lines

Due to the difficulties associated with generating MDA-MB-453 cells stably overexpressing nSREBP, a series of doxycycline inducible nSREBP-1a vectors were generated. This allows cells to be selected for plasmid integration in the absence of nSREBP expression from the plasmid. GFP-nSREBP-1a and GAL4-VP16 GFP-nSREBP-1a constructs were cloned in a Tet-On inducible vector backbone. The former produces wildtype nSREBP-1 conjugated to GFP, which is functionally equivalent to nSREBP-1 (Hübner et al., 2006), whereas the latter contains the GAL4-VP16 fusion transcription factor, which greatly increases the transactivation capacity of nSREBP (see Chapter 4). These Tet-On vectors were transfected into MDA-MB-453 cells, and a heterologous pool of cells with vector integration were generated using puromycin selection. To confirm that these Tet-On cell lines were capable of inducing the nSREBP proteins, luciferase assays were performed by transiently transfecting them with the SREBP responsive *DHCR24*-300 proximal promoter and the GAL4 UAS responsive *pck-1* promoter (Figure 5.15). After induction with doxycycline, both GFP-nSREBP-1a and GAL4-VP16 GFP-nSREBP-1a expressing Tet-On lines were able to activate the *DHCR24* promoter by ~ 3.5-fold, whilst only the latter was able to activate the *pck-1* promoter (by ~ 400-fold). There was no significant difference between the baseline promoter activity of each Tet-On stable line without doxycycline induction as assessed via one-way ANOVA (Figure 5.15A), suggesting that there was minimal 'leaky' expression.

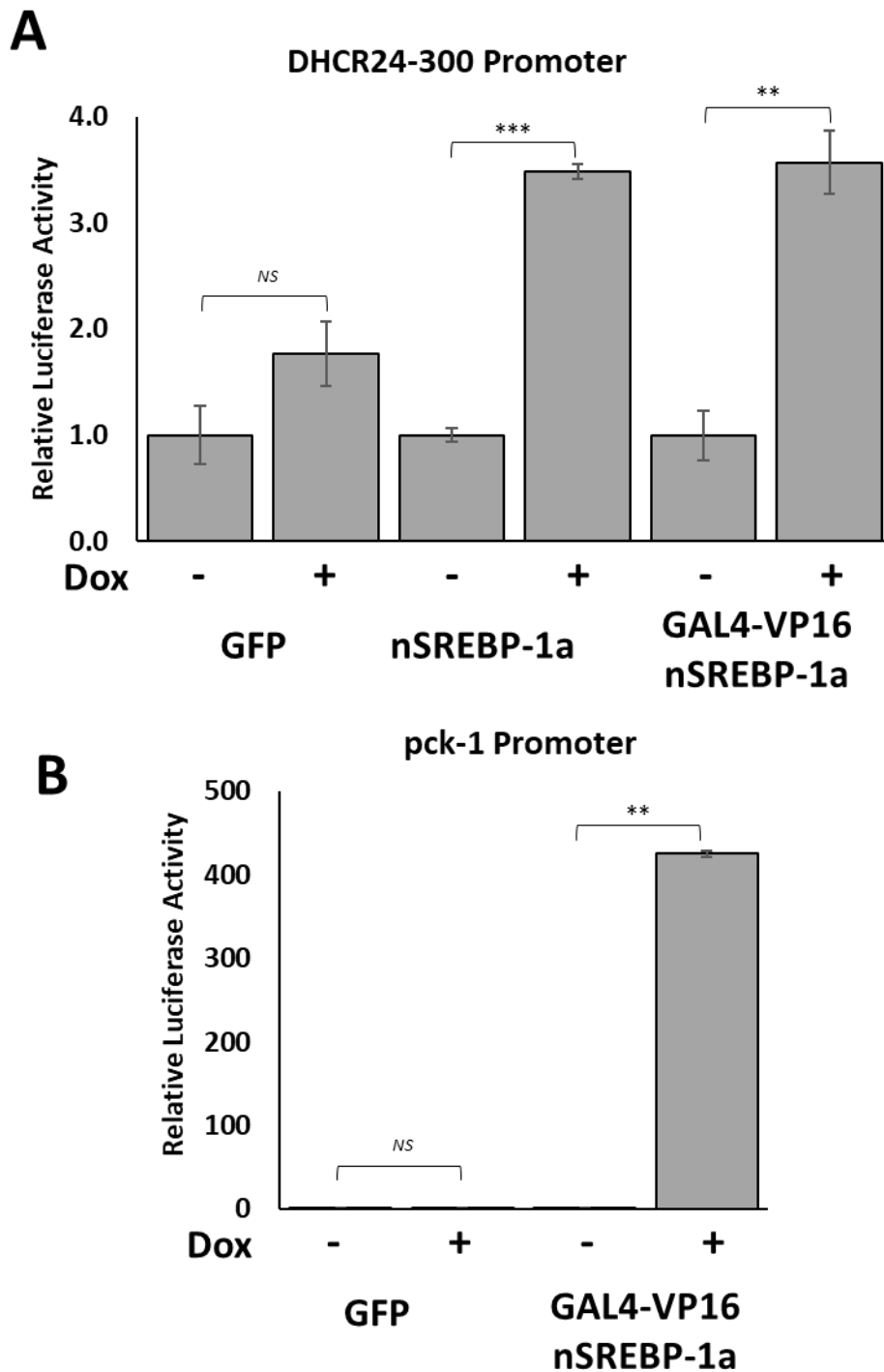


Figure 5.15: Validation of doxycycline inducible nSREBP-1a stable MDA-453 cells

MDA-MB-453 Tet-On cell lines stably expressing doxycycline inducible control proteins (GFP) or nSREBP-1a variants were transfected with 100 ng of either SREBP responsive *DHCR24-300* (A) or GAL4 UAS responsive *pck-1* luciferase promoter constructs (B) and 5 ng pRL-Null. Tet-On cell lines were treated with 2.5 $\mu\text{g}/\text{mL}$ doxycycline and Luciferase activity was assayed 48 hours post transfection. All data were normalised to Renilla luciferase and control condition. Representative figure of at least two biological experiments depicted (Mean \pm SEM for $n=3$ technical replicates). Statistical significance was assessed by T-test and indicated as follows: NS - not significant, ** $p < 0.01$, *** $p < 0.001$.

5.3.9 Inducible nSREBP-1a stable lines show reduction of UGT2B28 promoter transactivation

To determine the effect of nSREBP activity on UGT promoter transactivation, the nSREBP-1a and control GFP expressing Tet-On cell lines were transfected with the UGT2B28 1kb proximal promoter construct. In the absence of doxycycline, 10 nM DHT induced the promoter ~4-fold in the GFP control line. Moreover, the magnitude of induction was the same in the nSREBP-1a and GAL4-VP16 nSREBP-1a lines (Figure 5.16A). When the cells were treated with doxycycline the promoter was still induced ~ 4-fold by DHT in the GFP control line (Figure 5.16B). However, in the nSREBP-1a and GAL4-VP16 nSREBP-1a cell lines, the magnitude of transactivation was significantly reduced. Interestingly, the basal level of promoter expression (in the vehicle condition) was also slightly reduced in the GAL4-VP16 nSREBP-1a cell line relative to the GFP line. This is likely because the basal activity level is influenced by residual endogenous androgens within the cells. Similar results were observed when cells were deprived of androgens (stripped) for either one or four days (data not shown) prior to transfection.

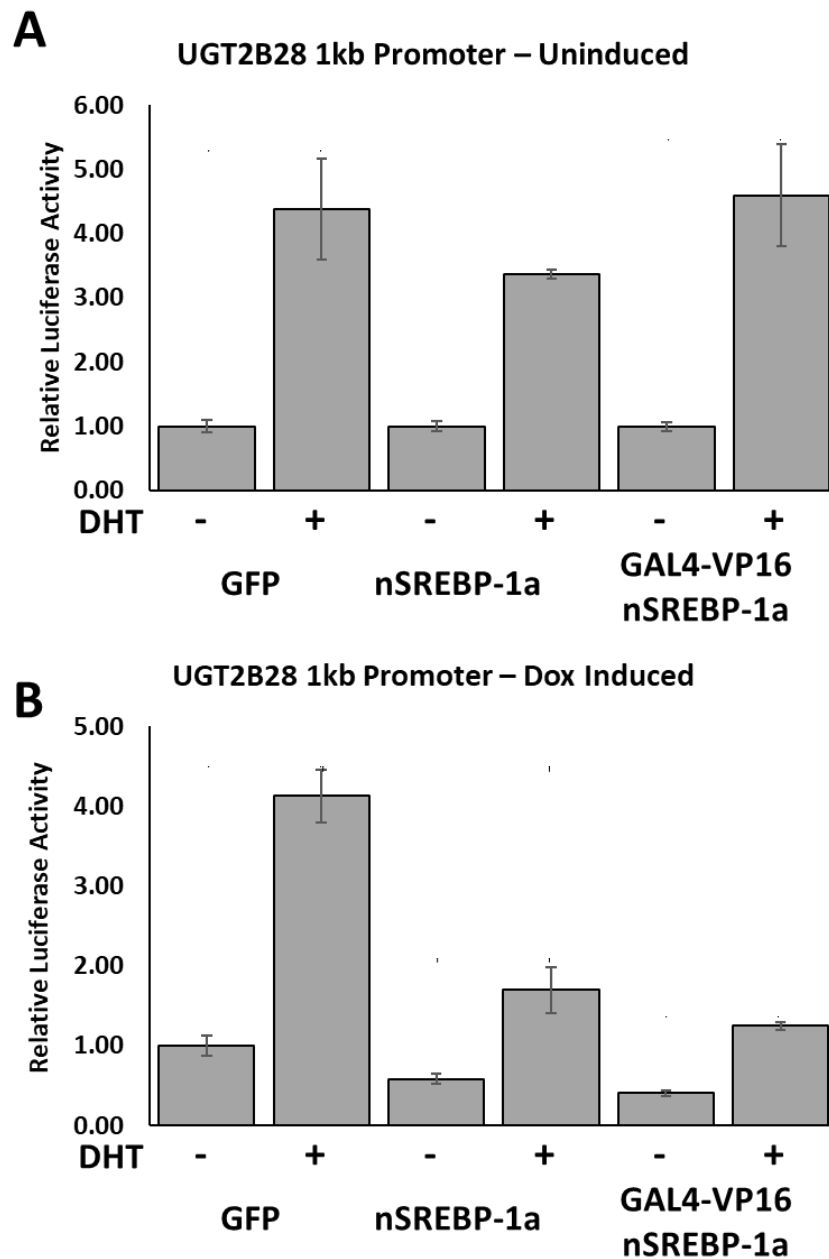


Figure 5.16: UGT2B28 1kb Proximal promoter response in nSREBP-1a inducible MDA-MB-453 Cells

MDA-MB-453 stable cell lines were transfected with 100 ng of UGT2B28 1kb proximal promoter and 5 ng pRL-Null in regular RPMI 1640 with 10% FBS without **(A)** or with 2.5 $\mu\text{g}/\text{mL}$ doxycycline **(B)**. Media was replaced with phenol-free RPMI 1640 with 10% CSS and either ethanol or 10 nM DHT and 2.5 $\mu\text{g}/\text{mL}$ doxycycline 24 hours post transfection. All data were normalised to Renilla luciferase and control condition. A single experiment is depicted with mean \pm SEM for n=3 technical replicates.

To confirm that basal promoter activity was dependent on endogenous androgens, this experiment was repeated using the antiandrogen bicalutamide (Figure 5.17). Bicalutamide competes with androgens for binding of AR, blocking their action (Kolvenbag et al., 1998). Cell lines were grown in either replete or steroid depleted medium conditions, transfected with the UGT2B28 1kb proximal promoter construct, and then treated with 2.5 µg/mL doxycycline for 24 hours. Promoter activity was lower in the nSREBP cell lines than the GFP line in both media conditions. However, when bicalutamide was added to the cells, there was no significant difference in the basal promoter activity in any cell lines under either media condition. This indicates that the basal promoter is sensitive to the low level of residual androgen present in steroid stripped media. Moreover, it suggests that nSREBP-1a represses basal UGT2B28 promoter activity by inhibiting this endogenous androgen-mediated AR activity.

UGT2B28 1kb Promoter

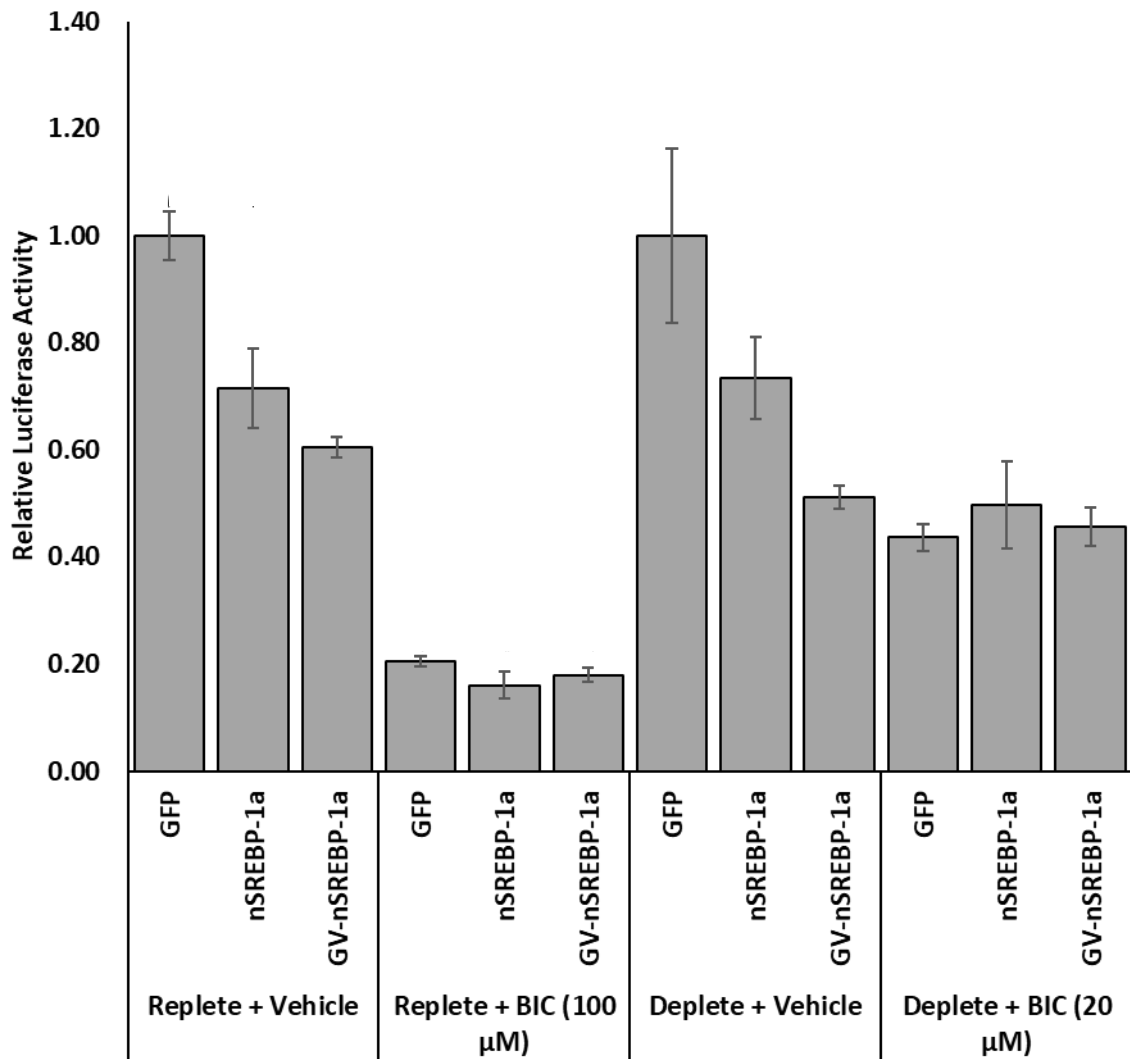


Figure 5.17: UGT2B28 1kb Proximal promoter response to bicalutamide in nSREBP-1a stable MDA-MB-453 cells

MDA-MB-453 stable cell lines were cultured in regular RPMI 1640 with 10% FBS or phenol-free RPMI 1640 with 10% CSS for 48 hours prior to transfection with 2.5 µg/mL doxycycline. Cells were then transfected with 100 ng of UGT2B28 1kb proximal promoter and 5 ng pRL-Null and treated with indicated amount of bicalutamide (BIC) or vehicle (Ethanol). Luciferase activity was assayed 48 hours post transfection. All data were normalised to Renilla luciferase and control condition. A representative figure of two biological experiments is depicted (Mean ± SEM for n=3 technical replicates). Statistical significance was assessed by ANOVA with Tukeys post hoc testing and indicated as follows: * p < 0.05, ** p < 0.01, *** p < 0.001.

5.3.10 *nSREBP-1a* overexpression does not reduce *UGT2B28* mRNA Levels

Utilising these validated inducible *nSREBP-1a* stable MDA-MB-453 cell lines, the capacity for *nSREBPs* to reduce *UGT2B28* mRNA was examined. This was conducted using cells grown in replete media and assessed via qPCR. *UGT2B28* was used as a type-isoform for both *UGT2B11* and *UGT2B28* due to their almost identical promoter sequences and capacity for regulation by androgens.

Initially, *UGT2B28* mRNA levels were measured in the control GFP cell line (Figure 5.18). As previously shown in our laboratory, *UGT2B28* mRNA levels are much more sensitive to DHT than the luciferase reporter constructs: 0.5 nM and 5.0 nM DHT induced mRNA expression by 200-fold and 400-fold, respectively, relative to the vehicle condition. Induction of GFP with doxycycline did not alter the capacity of DHT to induce *UGT2B28* expression in this line.

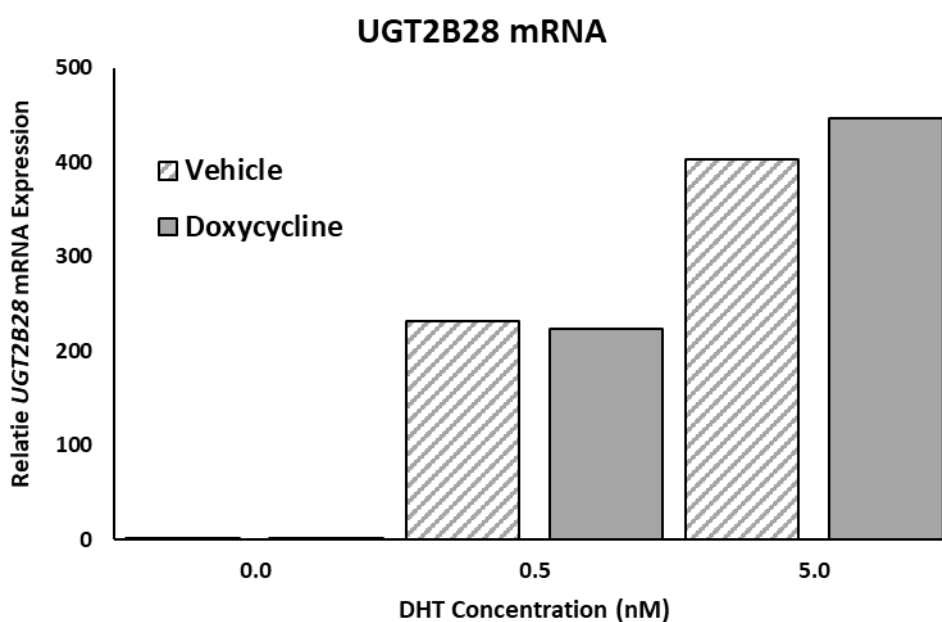


Figure 5.18: UGT2B28 mRNA induction by DHT in control GFP-expressing MDA-MB-453 stable cells

Control GFP MDA-MB-453 stable cell line was cultured in complete RPMI 1640 with ethanol or 2.5 $\mu\text{g}/\text{mL}$ doxycycline for 24 hours. Cells were then treated with indicated concentration of DHT for 48 hours prior to harvest. *UGT2B28* mRNA was quantified via qRT-PCR as described in methods and presented as mean (n=3 technical replicates) normalised to GAPDH.

Subsequently, the mRNA levels of *UGT2B28* were examined in all three Tet-on lines under varying doses of DHT (0 nM, 0.5 nM and 5 nM) (Figure 5.19). The data shown is normalized to the mRNA level in the control GFP cell line without doxycycline. The addition of doxycycline (which induces GFP, nSREBP-1a, or GAL4-VP16-nSREBP-1a in the respective cell lines) did not alter *UGT2B28* mRNA level under any DHT treatment condition. These data suggest that nSREBP-1 may not repress the endogenous *UGT2B28* gene in MDA-MB-453 cells.

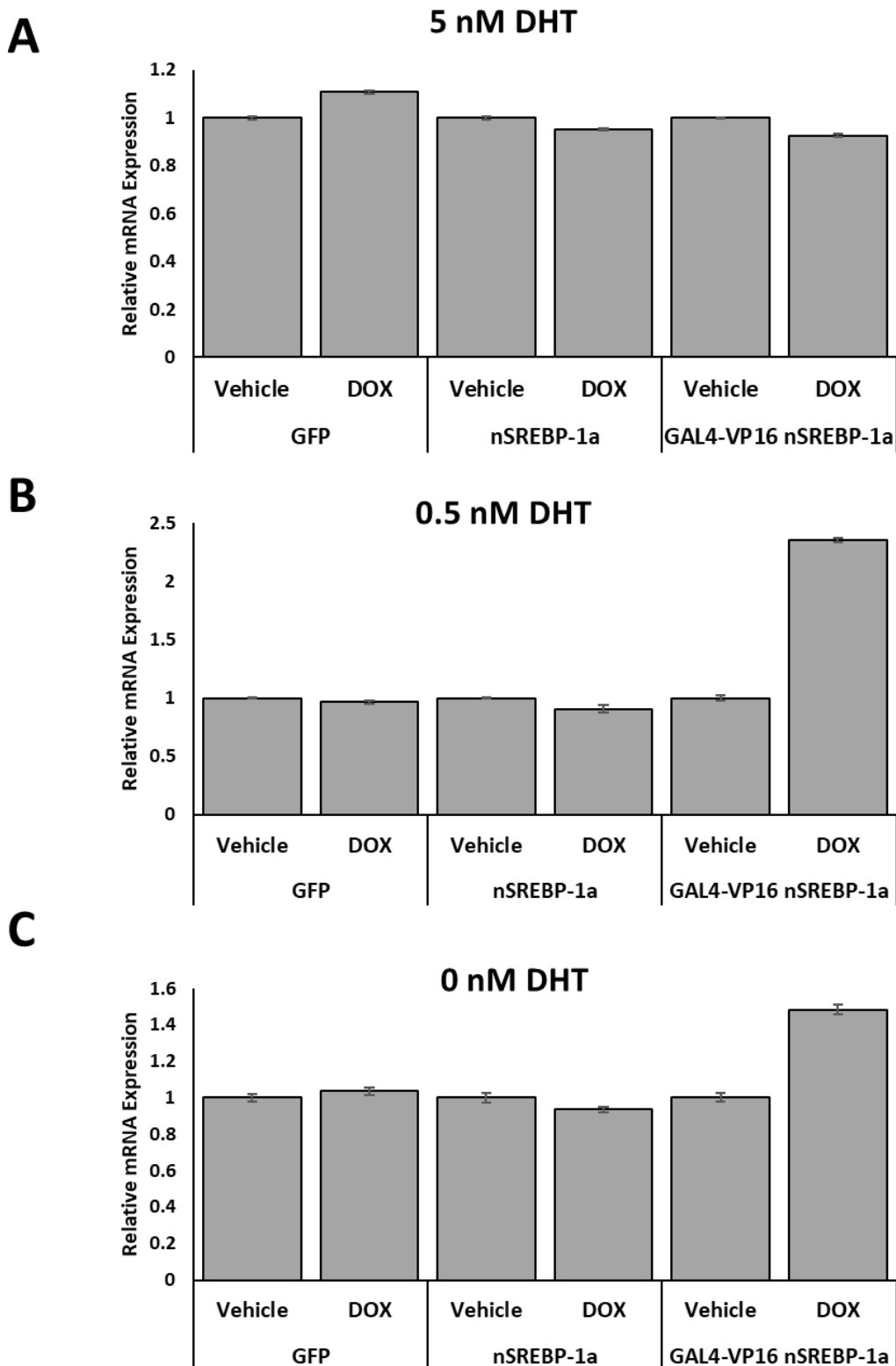


Figure 5.19: UGT2B28 mRNA induction by DHT in nSREBP-1a MDA-MB-453 stable cell lines

Control and nSREBP-1a MDA-MB-453 stable cell lines were cultured in complete RPMI 1640 with ethanol (vehicle) or 2.5 $\mu\text{g}/\text{mL}$ doxycycline for 24 hours. Cells were then treated with 5 nM **(A)** 0.5 nM **(B)** or 0 nM **(C)** DHT for 48 hours prior to harvest. UGT2B28 mRNA was quantified via qRT-PCR as described in methods and presented as Mean \pm SEM ($n=3$ technical replicates) normalised to GAPDH and vehicle condition for each cell line.

5.4 Discussion

5.4.1 nSREBP signal termination by UGTs

Studies presented in this chapter examined the possibility that UGTs may contribute to the termination of nSREBP signalling. Initially, the capacity for UGT2B11 and UGT2B28 to modulate the level of transcriptionally active nSREBP proteins was assessed (Figure 5.3). Both wildtype and truncated variants of UGT2B11 and UGT2B28 were shown to reduce the level of both nSREBP-1a and nSREBP-2 protein in co-expression systems (Figure 5.4 and Figure 5.5). Reporter-based assays showed a reduction in the transactivation of the SREBP target DHCR24 promoter when nSREBP variants were co-transfected with UGTs, demonstrating that this reduction in protein led to reduced lipogenic gene activation. The reduction in nSREBP protein levels could be due to decreased production or increased degradation. While it was not shown unequivocally which of these processes were altered by the UGTs, increased degradation is considered the most likely. This conclusion is based on four lines of evidence. First, control proteins that were co-expressed with the nSREBPs had no effect on the protein levels of the latter. Hence it is unlikely that cells were reaching a 'ceiling' for production of total protein, or for ER-resident proteins specifically. Second, the effect occurs not only in HEK293T cells, but also in a breast cancer cell line that did not show very high levels of protein overexpression after transfection (Figure 5.6). Third, there is no known mechanism for selectively regulating the translation of a heterologous-expressed protein of this type. More specifically, nSREBP was expressed from a plasmid containing non-native promoter (CMV), 5'UTR, and 3'UTR sequences, whereas all mechanisms for selective translational control of specific mRNAs work by recognition of the native versions of these sequences. Fourth, in contrast to the lack of obvious mechanisms available to suppress translation of heterologous expression of nSREBP, there is a well-defined, robust, and essentially ubiquitous mechanism for nuclear turnover that requires only appropriate regions of the nSREBP protein be present, and not any regulatory sequences. Thus, our working model to explain the reduction in nSREBP protein after UGT co-expression is that the UGTs enhance nSREBP turnover.

The mechanism(s) by which the UGTs may promote nSREBP turnover was not defined in these studies. As truncated UGT variants are catalytically inactive, the mechanism is presumed to involve their non-catalytic functions. Previous work has suggested that UGTs

may have a range of non-enzymatic functions in association with other partner proteins in different organelles; this is termed moonlighting (Hu, Hulin, et al., 2019).

The potential for the UGTs to function via the canonical phosphodegron-mediated turnover mechanism was explored. These studies included 1) FBW7 knockdown, 2) analysis of interactions with GSK3 β , and 3) truncation and mutations of the phosphodegron, as discussed below:

1) If the UGTs functioned by increasing recruitment of FBW7, then knockdown of this protein might have been expected to negate their effects. While transient knockdown of FBW7 was achieved via CRISPRi in HEK293T cells, its effects on nSREBP were inconsistent (Figure 5.7 and Figure 5.8). Moreover, stable knock down of FBW7 in MDA-MB-453 cells was unsuccessful. The latter may have been due to the relatively small number of plasmid copies integrated into the genome, as supported by the lack of detectable gRNA in the stable lines. These same issues had been experienced within our laboratory when attempting to knock down UGT isoforms and suggests an overall problem with generating stable knock down lines with the px459 CRISPRi vector system. Future studies could employ siRNA or other knockdown approaches.

2) Previous work from our laboratory suggested that UGT2B11 may destabilise not only nSREBPs but also other GSK-3 β target proteins: NICD and β -catenin (Figure 5.2). Interestingly, UGT2B17, which shares considerable homology with UGT2B11 (75.5% amino acid identity), has been shown to interact with c-Src kinase to promote the phosphorylation of AR, leading to ligand-independent activation (Li et al., 2016). Notably, GSK-3 β shares homology with the kinase domain of c-SRC (Harwood, 2001). Overall, this prompted a hypothesis that some UGTs may affect the activities of some transcription factors by interacting with kinases that modify them. However, co-immunoprecipitation studies showed that UGT2B11 does not interact with GSK-3 β (Figure 5.10).

3) The phosphodegron motif is the nexus for regulated turnover of nSREBP by the SCF complex after phosphorylation by GSK-3 β . To determine whether this motif was required for the UGTs to mediate increased protein turnover, variants of nSREBP-1a and nSREBP-2 lacking this motif were generated (via truncation or site-directed mutagenesis) and the ability of the UGTs to reduce their levels was assessed via a reporter assay in which

transactivation capacity served as the proxy for protein abundance (Figure 5.11). The UGTs reduced the activity of the truncated and mutated nSREBP proteins similarly to that of full length nSREBP proteins. This strongly suggested that the UGTs did not function via the phosphodegron motif. This result was unexpected as previous data from our laboratory indicated that UGT2B11 also destabilised other proteins that are targets of both GSK-3 β and FBW7.

Based on the above-discussed findings, the mechanisms by which the UGTs might control nuclear nSREBP levels remains unclear and mechanisms that do not involve the phosphodegron must be investigated. It was shown by Dong et al. (2015) that rat SREBP-1c can be phosphorylated upstream of the canonical phosphodegron at serine 73 by GSK-3 β and that this contributes to the formation of a putative docking site for the SCF-FBW7 ubiquitin ligase and ultimately leads to degradation by the proteasomal pathway. This serine residue is conserved in its local sequence context in rat and human nSREBP-1a, -1c and -2. However, the study by Dong et al. (2015) was unable to confirm phosphorylation of the corresponding serine residue in rat SREBP-1a via mass spectrometry after incubation with purified GSK-3 β . They also did not examine phosphorylation of rat SREBP-2 or of any human SREBP isoforms. However, if this phosphorylation event does occur in human SREBP isoforms, this may be a target for modulation by UGTs and may explain why deletion and mutation of the canonical phosphodegron near the C-terminus of nSREBP did not affect UGT mediated degradation. Moreover, this site may become more important for FBW7 docking when the canonical phosphodegron is impaired. Therefore, future work should first confirm whether the equivalent amino acids in human SREBP isoforms are phosphorylated by GSK-3 β and subsequently whether mutation of this site affects UGT mediated nSREBP degradation. These assays could also be repeated in the context of GSK-3 β inhibition or knockdown via CRISPR or siRNA to determine whether the effects of the UGTs are modulated by GSK-3 β activities.

Although UGTs are typically ER resident proteins, it has been reported that a fraction of the UGT protein in cells is nuclear localised. This was described by Belledant et al. (2016) and Ravindran et al. (2022) for UGT2B28 in prostate cancer tissues. UGT2B7 and UGT1A6 were previously shown to be present within both the inner and outer nuclear membranes in human hepatocytes (Radomska-Pandya et al., 2002) and our laboratory has shown expression of GFP-fused UGT2B15 in the inner nuclear membrane where it colocalises with

lamin (unpublished data). To date nuclear localisation of UGT2B11 has not been studied. Lacombe et al. (2023) also showed nuclear localisation for UGT2B28 in LNCaP and LAPC4 prostate cancer cell lines via immunofluorescence imaging. Subsequently, they identified a number of interaction partners via co-immunoprecipitation and LC-MS/MS. Interestingly, a number of these partners are expressed in both the cytosol and nucleoplasm (HIP1, KDM4B, BCL6, R3HCC1L, BCLAF1 and HNRNPL), with the localisation of these interactions remaining unknown, but potentially occurring within the nucleus. This potential nuclear localisation and capacity to interact with nuclear proteins may be particularly relevant for truncated variants of these UGTs that do not possess the transmembrane domains that would anchor them in the ER membrane. Due to this reported nuclear localisation of UGT2B28 and other UGT isoforms, attempts were made to assess whether it could interact directly with nSREBPs via co-immunoprecipitation of lysates from co-transfected HEK-293T cells that had been treated with the proteasomal inhibitor MG132 (data not shown). However, at doses recommended by literature (Punga et al., 2006) nSREBP protein levels were not stabilized sufficiently to identify on immunoblots, while at higher doses, cells either died or did not express enough protein to conduct co-immunoprecipitation. This was likely due to caspase-8 mediated MG132-induced apoptosis which occurs due to accumulation of damaged and misfolded proteins (Pan et al., 2011). Therefore, the possible direct interaction of UGTs with nSREBP remains a future direction which could be examined to ascertain the molecular mechanism by which UGT induces nSREBP degradation.

5.4.2 nSREBP regulation of UGT2B11 and UGT2B28

Much of the work presented in this Chapter examined how UGT2B11 and UGT2B28 could control the level or activity of nSREBP transcription factors. However, studies shown in Sections 5.3.6 to 5.3.10 examined whether the converse was true: whether nSREBP could control the levels of UGT2B11 and UGT2B28. These studies were prompted in part by preliminary data showing that transient transfection of UGT2B11 and UGT2B28 constructs into HEK-293T cells reduced their proliferation (data not shown). This is in stark contrast to the findings in Chapter 4 that stable *UGT2B11* and *UGT2B28* overexpression in MDA-MB-453 cells conferred a proliferative advantage. Because the level of UGT mRNA and protein expression was much higher in HEK293T cells than in the MDA-MB-453 stable lines, these observations prompted the hypothesis that there may be a range within which increased *UGT2B11* and *UGT2B28* expression enhances growth, but that excessive levels may

become detrimental. This somewhat mirrors what is observed with SREBPs, where modest increases in expression enhance cancer cell growth, but excessive levels lead to toxicity.

A previous study in prostate cancer models demonstrated the ability of nSREBP variants to repress the ligand-dependent activity of endogenous AR on the androgen responsive promoter construct pARE2-TATA-Luc, and decrease mRNA levels of the androgen responsive gene *PSA* (Suh et al., 2008). Another study reported that nSREBP could inhibit activation of pARE2-TATA-Luc by exogenously-expressed AR in HEK-293T cells (Jeong et al., 2004). Studies in this Chapter (section 5.3.6) provided the first evidence that nSREBPs have the capacity to regulate the transactivation of UGT promoters by endogenous AR in a breast cancer MDA-MB-453 cell model (Figure 5.15). Suh et al. (2008) proposed that nSREBPs reduce the activity of AR by physically interacting with AR, and/or by sequestering AR co-activators. The study found that overexpression of two AR coactivators, Androgen receptor trapped clone-27 (ART-27) and steroid receptor coactivator-1(SRC-1), could negate the effect of SREBP-1c and that SREBP-1c interfered with interaction of AR and ART-27. Expression of ART-27 is negligible in prostate cancer and hence its sequestration from AR may not be the main mechanism by which nSREBPs can reduce AR-transcriptional activity in that context (Taneja et al., 2004). ART-27 has been shown to be expressed in epithelial breast tissues (Taneja et al., 2004) but there is no reported analysis of its expression in breast cancers and as it is considered a tumour suppressor, it is likely that the levels in breast cancers are low. SRC-1 is known to be expressed in breast cancers and is associated with HER2 positivity (Walsh et al., 2012); however, it was reported that the protein level in MDA-MB-453 cells was considerably lower than that of many other breast cancer cell lines (Stanley et al., 2017). Overall, nSREBPs may interfere with AR activity by interactions with AR and/or its co-activators and that the latter may be cell-type specific.

There are also factors in addition to AR that regulate the activity of the *UGT2B11* and *UGT2B28* promoters in breast cancer cells. Of those, FOXA1 could be the most critical. In HEK-293T cells that do not express AR or FOXA1, overexpression of AR alone is insufficient to allow DHT-mediated transactivation of the *UGT2B11* and *UGT2B28* promoters. In contrast, expression of FOXA1 alone is sufficient to activate the promoter. Moreover, co-expression of FOXA1 and AR in combination with DHT treatment does not increase activation relative to that induced by FOXA1 alone (data not shown).

In contrast to the results observed in *UGT*-promoter assays, nSREBPs did not suppress the induction of the endogenous *UGT2B28* gene by DHT in MDA-MB-453 cells (Figure 5.19). There may be multiple reasons for this incongruity. Foremost is the fact that the native *UGT* genes are induced ~200-fold by androgen in MDA-MB-453 cells, while their proximal promoters are only induced ~2-3-fold. Our research group has proposed that the much greater induction of the native genes is due to the cooperative effect of multiple AREs and FOXA1 sites. These sites located in the proximal promoter, and distally in introns and intergenic regions, may cooperate through long range interactions. This may lead to a very high level of AR and co-activator binding that cannot be overcome by nSREBPs. FOXA1 may play an important role in this, as it has been reported to mediate epigenetic changes to chromatin that facilitate accessibility of nuclear receptors and their co-activators. Notably, the magnitude of androgen-mediated *UGT2B28* mRNA induction is lower in some other AR-positive breast cancer cell lines (unpublished data from our laboratory). This may be due to differing levels of AR or FOXA1 expression, or different chromatin architecture around the extended *UGT2B11-UGT2B28* locus. Due to time constraints, it was not possible to make Tet-On models in these other lines, however, this could be a valuable future direction to clarify whether this mechanism of *UGT* gene regulation can occur in a breast cancer cell context.

Another possible reason that nSREBP did not reduce expression of native *UGT2B11* and *UGT2B28* genes may be that the *UGT* mRNAs have a very long half-life. Turnover of the RNAs may not have been measurable during the period of treatment. Prolonging the assays was not possible due to reduction in cellular health associated with an extended period of transcriptionally active nSREBP expression. In future experiments the amount of nSREBP expressed could be titrated so that the period of expression could be extended without cell death. Finally, *UGT* protein levels were not measured because a suitably specific antibody for either *UGT2B11* and *UGT2B28* was not available, and the lack of high activity substrates precluded establishment of a sensitive activity assay.

Interestingly, a recent study suggested that regulation of *UGTs* by nSREBP could occur in cancers other than breast and prostate. This study found that the protein haematological and neurological expressed 1 (HN1) regulates lipogenesis in hepatocellular carcinoma cells through the SREBP pathway. Knockdown of HN1 downregulated SREBP-1 and -2 expression and decreased nuclear translocation of nSREBPs (Jin et al., 2024). This was found to result

in a significant upregulation of *UGT2B11* and *UGT2B28* mRNA (Jin et al., 2024). However, whether this effect was a direct consequence of nSREBP activity at the *UGT2B11* and *UGT2B28* promoters remains to be determined.

SCAP is also an AR target gene, and its induction by androgens in prostate cancer cell lines has been demonstrated to involve AREs located in intron 8 (Heemers et al., 2001; Heemers et al., 2004). As aforementioned, increased expression of SCAP reduces the ER-retention capacity of INSIG, leading to nuclear accumulation of nSREBPs and hence increased lipid biosynthesis. Although there are no current reports in literature, it is quite possible that the ability of nSREBPs to reduce the expression of androgen responsive genes may extend to SCAP. In prostate cancers, and subtypes of breast cancer with high levels of AR, nSREBP mediated reduction of SCAP levels could be another mechanism by which lipotoxicity could be prevented. Confirmation of this hypothesis would require further work, as it remains unknown whether nSREBPs can inhibit expression of endogenous androgen regulated genes in breast cancer.

5.4.3 Conclusion

Throughout this chapter, two distinct mechanisms of cellular regulation were examined. Signal termination of mature transcriptionally active nSREBPs by both *UGT2B11* and *UGT2B28* was shown in breast cancer cells. This was presumed to involve increased nSREBP degradation (rather than decreased translation) but appeared to be independent of the canonical degradation pathway involving phosphorylation of the phosphodegron motif by GSK-3 β . This mechanism of regulation may reduce the potential for excessive lipogenesis induced by increased AR activity in relevant subtypes of breast cancer. The capacity for nSREBPs to reduce activation of *UGT2B11* and *UGT2B28* promoters by AR was also demonstrated, although it remains to be determined whether the native genes are similarly regulated. If nSREBPs do in fact reduce UGT levels, this could attenuate UGT-mediated processing of SREBP precursors (as shown in Chapter 4) and thus reduce excessive lipogenesis. However, it could also attenuate UGT-mediated reduction of mature nSREBP, which would have a converse effect. A harmonizing model is that UGTs play a role in maintaining homeostatic levels of SREBP activity by modulating both signal activation and termination. They may also be novel players in the AR-SREBP regulatory nexus, being

induced by AR and potentially repressed by nSREBPs. Due to the similarities between the ER-/High AR expressing breast cancers studied and prostate cancer, many of the molecular mechanisms studied here may function in both cell types and it would be prudent to investigate them in the context of prostate cancer in future research.

The novel roles of UGTs demonstrated in this chapter, and the tentative identification of an AR-UGT-SREBP signalling network, suggests new models for lipogenic regulation in AR-positive breast cancer tumours that may enhance lipid-fuelled proliferation whilst avoiding lipotoxicity. Further elucidation of these novel regulatory mechanisms may lead to the identification of druggable pathways or targets that could be used in treatment for breast or prostate cancers.

6. CHAPTER 6 - GENERAL DISCUSSION AND OVERALL SIGNIFICANCE OF FINDINGS

UGTs are critical for the biotransformation of exogenous compounds and endogenous signalling molecules (Meech et al., 2019; Rowland et al., 2013). Whilst the functional role of many UGTs is well characterised, the biological functions of the UGT2B family enzymes UGT2B11 and UGT2B28 remain poorly understood. Due to a lack of well-defined high activity substrates and associated biological functions, these enzymes have been referred to as orphan or near-orphan enzymes (Kaivosaaari et al., 2007; Meech et al., 2019).

UGT2B11 and UGT2B28 are frequently overexpressed in cancers, particularly those arising in steroid-dependent tissues such as the breast and prostate (Beaulieu et al., 1998; Belledant et al., 2016; Dozmorov et al., 2009; Lévesque et al., 2001; Wang et al., 2013; Zhu et al., 2019). Across a number of studies, UGT2B11 and/or UGT2B28 have been associated with altered lipid production in prostate cancers, both *in vitro* (Bidgood et al., 2024; Neuwirt et al., 2020) and *in vivo* (Rouleau et al., 2022). In addition, differential expression of these genes was associated with the accumulation of fat deposits in hepatic diseases (Mathur et al., 2020; Yan-qin et al., 2022).

Wang et al. (2017) identified UGT2B11 and UGT2B28 as part of lipogenic expression signature in ER-negative breast cancers; to date this is one of very few published studies to address their possible roles in breast cancer. Data generated in this laboratory before the onset of this thesis project further examined the possible role of these UGTs in breast cancer context. Overexpression of these UGTs in ER-negative breast cancer cells was associated with increased lipogenic gene expression. Consistent with this finding, bioinformatic analyses performed using RNA-seq gene expression data from The Cancer Genome Atlas breast cancer (TCGA-BRCA) dataset showed that expression of UGT2B11 and UGT2B28 was closely correlated with the expression of genes within lipid metabolism pathways, and specifically, genes that are known targets of the SREBP transcription factors.

The SREBP transcription factor family is considered to be the master regulator of lipid biosynthesis that tightly controls the expression of essentially all lipogenic genes involved in the synthesis of fatty acids and sterols. Guided by the preliminary studies, it was hypothesised that UGT2B11 and UGT2B28 may be involved in regulating lipogenesis through modulating the activities of SREBPs. It was further hypothesized that these UGTs may alter breast cancer outcomes by modulating lipogenesis. To address these hypotheses, several specific aims were developed. The first aim was to characterise associations of

UGT2B11 and *UGT2B28* expression with breast cancer subtypes and clinical outcomes (**Chapter 3**). The second aim examined how *UGT2B11* and *UGT2B28* affected SREBP activity, lipogenic gene expression, and cell behaviour (**Chapter 4**). The third aim identified a possible regulatory axis between AR, *UGT2B11* and *UGT2B28*, and nSREBP (**Chapter 5**).

Chapter 3 examined associations of *UGT2B11* and *UGT2B28* expression levels with clinical and biochemical parameters in breast cancer patient cohorts. Previous analysis of the TCGA-BRCA dataset indicated an association between increased *UGT2B11* and *UGT2B28* expression and poorer survival outcomes in particular subsets of breast cancer. In the first part of this thesis, the METABRIC (Molecular Taxonomy of Breast Cancer International Consortium) and TCGA-BRCA datasets were interrogated to confirm and extend these findings.

Breast cancer cohorts were stratified by *UGT2B11* and *UGT2B28* mRNA levels. The subset of tumours showing high levels of these UGTs was significantly enriched in tumours that did not express estrogen receptor alpha (ER-) and expressed high levels of both human epidermal growth factor 2 (HER2) and androgen receptor (AR). There is no conventional molecular subtype associated with an ER-, HER2+ and AR-enriched transcriptional profile, however, it is broadly consistent with molecular apocrine (MA) tumours. The observation that *UGT2B11* and *UGT2B28* expression is associated with high AR expression is consistent with previous findings that these UGTs are positively regulated by androgens in breast cancer cells (Moore et al. (2012) and unpublished data from this laboratory). This association of *UGT2B11* and *UGT2B28* expression with HER2 levels was a new finding and is consistent with recent RNAseq studies (Atallah et al., 2023; Yam et al., 2023), however, no molecular mechanism for this has been investigated to date.

In the cohort of patients with ER- breast tumours, high *UGT2B11* or *UGT2B28* expression was associated with poorer survival outcomes. Further stratification into ER-/HER2+ and ER-/HER2- subtypes indicated that the presence or absence of HER2 did not influence the prognostic value of UGT expression in ER- patients. However, this was likely confounded by the small size of the ER-/HER2+ subgroup. Previous work showed that high *UGT2B28* expression is associated with cancer progression and poorer outcomes in prostate cancers (Belledant et al., 2016). As molecular apocrine breast cancers have similar molecular features to prostate cancers (including high AR expression), it may be that the association

between these UGTs and outcomes are based on similar cellular functions for the enzymes. Overall, our new findings in breast cancer expand the scope for using these UGTs as potential prognostic markers in AR-positive cancers.

Pathway enrichment analyses were performed using the TCGA-BRCA RNA-seq datasets, revealing that ER negative breast tumours with high levels of *UGT2B11* and *UGT2B28* expression showed enriched expression of numerous lipid biosynthetic genes that are direct targets of SREBP signalling. This finding lent further support to the hypothesis that *UGT2B11* and *UGT2B28* may regulate lipid biosynthesis via modulating SREBP signals. Increasing the provision of lipids to cancer cells can enhance their proliferation and is also associated with other cellular processes that make cancers more aggressive. This chapter therefore aided in the development of the main hypothesis for the *in vitro* experiments conducted in Chapter 4, that these UGTs may modulate the SREBP activation pathway. Moreover, data from this chapter suggested that ER negative breast cancer models would be a relevant context for subsequent studies that examined how UGTs may regulate lipogenesis.

Chapter 4 focused upon defining the role of *UGT2B11* and *UGT2B28* in modulating SREBP activation. Wildtype and variant forms of these UGTs were stably over-expressed in MDA-MB-453 cells. These cells were selected because they represent a molecular apocrine-like ER-negative breast cancer model, which is broadly reflective of the cancer types in which *UGT2B11* and *UGT2B28* expression was associated with lipid signalling in Chapter 3. The UGT over-expressing cell lines showed an increase in the expression of SREBP target genes and increased proliferation, supporting the hypothesis developed in Chapter 3 that these UGTs may be affecting SREBP activity. These findings prompted a major area of study in this project: elucidating the molecular pathway(s) by which UGTs may alter SREBP activities and whether these activities are caused by the catalytic activities of these UGTs or novel moonlighting functions.

Data generated using three independent experimental approaches provided compelling evidence that *UGT2B11* or *UGT2B28* overexpression could enhance SREBP-2 processing. Firstly, activation of an SREBP target promoter (*DHCR24*) was found to be enhanced when the SREBP-2 precursor was co-expressed with *UGT2B11* or *UGT2B28*. Secondly, co-expression of *UGT2B11* or *UGT2B28* with a fluorescently tagged SREBP-2 protein increased

the amount of the fluorescent protein that localized within the nucleus. Both of these findings strongly suggested that UGT2B11 and UGT2B28 increased processing of the SREBP-2 precursor into its mature nuclear form (nSREBP). The third approach utilised a synthetic processing assay that was based on an ER-localized chimeric transcription factor that contained the potent transactivator GAL4-VP16 fused to the SREBP-2 regulatory (C-terminal) domain. Proteolytic processing of this chimeric protein released GAL4-VP16 which could translocate to the nucleus and activate a reporter gene. Because no nSREBP domain was expressed in this system, it provided a sensitive method for quantifying SREBP proteolytic activation that did not trigger feedback processes associated with activation of lipogenic genes. Co-expression of UGT2B11 and UGT2B28 with the chimeric transcription factor caused an increase in reporter activity, consistent with increased processing.

The consistent effect of UGT2B11 or UGT2B28 in each of these assays supported the hypothesis that the UGTs function to increase SREBP precursor processing, resulting in increased nuclear nSREBP activity. This function is likely to explain the increase in SREBP target gene expression observed in stable UGT-overexpressing MDA-MB-453 cell lines. The mechanism(s) by which the UGTs could alter SREBP precursor processing was examined in subsequent studies described in Chapter 4. Two hypothesised pathways were considered: 1) modulation of the levels of lipids that are sensed by the SREBP-SCAP-INSIG complex, and 2) modulation of the SREBP-SCAP-INSIG complex through physical interactions with one or more of these proteins. It is important to note that these hypotheses were not considered mutually exclusive.

SCAP is responsible for sensing levels of sterols in the ER lumen to control SREBP precursor localisation. As described in Chapter 5, binding of sterols to SCAP alters its association with INSIG and COP proteins, while fatty acids control INSIG stability and hence its availability to anchor SCAP in the ER. Through these two mechanisms, levels of sterols, and to a lesser degree fatty acids, control translocation of the SCAP-SREBP complex to the Golgi. Many UGTs have been reported to bind to fatty acids, with this binding often inhibiting their enzymatic activities. Moreover, a subset of UGTs (including UGT2B11) can conjugate hydroxylated fatty acids with glucuronic acid (Turgeon et al., 2003). There is also some evidence (including unpublished data from our laboratory) that sterols can be glucuronidated, however, the UGT family members involved remain undefined. It was therefore considered possible that glucuronidation of lipid species (fatty acids or sterols)

by UGTs could be a pathway for altering lipid sensing and hence SCAP-mediated SREBP processing. To interrogate this possibility, experiments were performed using naturally occurring truncated variants of UGT2B11 and UGT2B28 that lack domains that are critical for catalytic activity. In all experiments, the truncated variants showed the same capacity as full-length UGTs to promote SREBP processing. This suggested that the UGTs do not modulate SREBP processing by converting lipids into glucuronides that are not recognised by the SCAP-INSIG lipid sensing complex. It remains possible that UGT2B11 and UGT2B28 interact non-catalytically with lipids in a way that alters their recognition by the SCAP-INSIG lipid sensing complex; however, due to the technical challenges of measuring such interactions, they were not pursued in this project.

Possible physical interactions between the UGTs and the lipid sensing complex were explored using co-immunoprecipitation methods. UGT2B11 robustly co-immunoprecipitated with all components of the lipid sensing complex: INSIG, SCAP and the SREBP precursor. It was not possible within the time constraints of the project to identify whether these UGTs interacted directly with each of these proteins. The current working hypothesis is that UGT2B11 and UGT2B28 may interact directly with one member of the complex and that this interaction allows co-precipitation of all members of the lipid sensing complex. This may be further facilitated by their co-localisation in cholesterol rich microdomains (Epanand, 2006; Melkonian et al., 1999). Of the three proteins within the INSIG-SCAP-SREBP complex, only SCAP has a large portion of its polypeptide chain residing in the ER lumen (specifically luminal loops 1 and 7). Given that more than 90% of the UGT polypeptide chain is located within the ER lumen, it is speculated that UGTs may directly interact with SCAP. Such an interaction with the luminal loops may influence its ability to sense sterols, ultimately increasing translocation of SREBP precursors to the Golgi. However, it is also a possibility that UGT2B11 and UGT2B28 interact with INSIG, which might disrupt its associations with SCAP, thus releasing the latter to traffic to the Golgi.

Whilst the mechanisms by which the UGTs increased SREBP processing were not fully defined within this chapter, the novel findings provide opportunities for future study. These include further characterization of the interactions between UGTs and the lipid sensing complex and the potential for this to modulate the lipid sensing process. It also remains to be determined whether increased SREBP target gene expression in UGT2B11 and UGT2B28

over-expressing breast cancer cell lines leads to increased lipid production. Increased lipogenesis could underlie the pro-proliferative effects of UGT2B11 and UGT2B28 overexpression, either through their structural role in new cell membrane synthesis; or through signalling functions (synthesis of bioactive lipids) in oncogenic signal cascades. The exact nature of the lipogenic changes that may promote cancer cell proliferation could be examined in future work using lipidomic methods.

In **Chapter 5**, two distinct mechanisms of cellular regulation were examined that led to the tentative identification of a novel AR-UGT-SREBP signalling network. The tight regulation of SREBP signalling is of fundamental importance to normal cellular functioning. The mature nuclear nSREBP transcription factor has a very short half-life and is rapidly degraded by the nuclear proteasome, which is essential in preventing excessive lipogenesis and hence lipotoxicity. Preliminary data from our laboratory had suggested that UGT2B11 and UGT2B28 could reduce the levels of nuclear nSREBP proteins, likely by increasing their degradation. This would provide a mechanism for enhancing termination of SREBP signalling, which could be important for preventing lipotoxic stress. The preliminary findings were confirmed by studies in Chapter 5 that showed that wildtype and truncated variants of UGT2B11 and UGT2B28 could reduce the level of both nSREBP-1a and nSREBP-2 proteins in co-expression systems. Data from multiple experimental systems supported this finding, including direct protein detection (immunoblotting assays), and indirect reporter gene-based assays. Moreover, the UGT-induced reduction in nSREBP proteins led to reduced lipogenic gene reporter activation.

The mechanism by which UGT2B11 and UGT2B28 reduced nSREBP protein levels was not definitively determined in these studies. It was initially hypothesised that the UGTs may enhance nSREBP degradation via the canonical turnover mechanism that involves phosphorylation of a phosphodegron motif by GSK-3 β . However, co-immunoprecipitation studies showed that UGT2B11 does not interact with GSK-3 β . Furthermore, the use of reporter assays with truncated and mutated variants of nSREBP proteins suggested that the UGTs did not function via the canonical phosphodegron motif. Therefore, mechanisms that do not involve the canonical degradation pathway should be investigated in the future. While UGTs reside predominantly in the ER, previous studies have reported that a fraction of the UGT protein localises to the nuclear envelope or nuclear interior in a variety of cell types (Belledant et al., 2016; Lévesque et al., 2020; Radominska-Pandya et al., 2002). Thus,

it is possible that UGTs could modulate nSREBP stability by direct effects in the nucleus; alternatively, they may function indirectly via as yet unidentified protein intermediates.

An intriguing area for future study is the role of cellular stress in UGT localisation and activities. Several proteins that commonly reside in the ER have been shown to relocate to the nucleus under conditions of cell stress. These include various transcription factors that, like SREBPs, are subject to regulated intramembrane proteolysis (RIP). An example is Activating transcription factor 6 (ATF6) which undergoes RIP in response to accumulation of unfolded proteins in the ER, allowing it to enter the nucleus and activate genes that facilitate protein folding (Ye, 2020). To date there is no indication that UGTs undergo RIP. However, there may be other pathways that promote translocation of UGTs to the nucleus under cell stress. For example, the ER resident folding chaperon glucose-regulated protein (GRP78) (also referred to as binding immunoglobulin protein (BiP)) was found to locate partly to the nucleus when its expression was increased in response to cell stress (Liu et al., 2023). A working model for the effects of expression level and cell stress on UGT function was developed as follows: When levels of UGT2B11 and UGT2B28 are relatively low, they reside in the ER where they can interact with the INSIG-SCAP-SREBP complex; in this context, modest increases in expression may result in modest increases in SREBP activation and thus lipogenesis. This idea is consistent with the fact that lipogenic gene expression was increased in stably transfected breast cancer cell lines that showed moderate levels of UGT overexpression (Chapter 4). In contexts where UGT2B11 and UGT2B28 levels are highly elevated, potentially causing excessive lipogenesis and lipotoxic stress, an increased fraction of protein may enter the nucleus to promote nSREBP turnover. This idea is consistent with findings in this project (Chapter 5) that co-expression of nSREBP and UGTs led to reduction in nSREBP protein only when the level of UGT expression was very high.

UGT2B11 and *UGT2B28* are direct AR target genes and are induced by AR in an androgen dependent manner in both prostate and breast cancer contexts. Notably, they have been identified as two the most highly androgen-induced genes in AR-positive breast cancer models. Given that the enzymatic functions of UGT2B11 and UGT2B28 are largely undefined, the reason for their potent induction by androgen/AR signalling has been opaque. An intriguing proposal based on the current studies is that these genes are induced by AR in order to modulate lipogenesis. Moreover, induction of the *UGT* genes to varying

levels, as discussed above, may provide a mechanism for androgens to enhance lipogenic gene expression, while also preventing excessive nSREBP activity that could lead to toxicity.

In addition to the regulatory circuit described above, in which AR regulates SREBP activity (with UGTs serving as intermediates), there is also evidence that SREBPs can regulate AR activity. Suh et al. (2008) demonstrated that nSREBPs can suppress the transcriptional activity of the AR in prostatic cells by interfering with co-activator recruitment. Given that *UGT2B11* and *UGT2B28* genes are directly regulated by AR, it was considered possible that nSREBPs could suppress their induction by AR. Supporting this hypothesis, nSREBPs were found to reduce activation of the *UGT2B11* and *UGT2B28* promoters by AR in MDA-MB-453 cells. However, it remains to be determined whether the native *UGT* genes are regulated in the same manner. A recent study suggested that regulation of UGTs by nSREBP could occur in hepatocellular carcinoma cells (Jin et al., 2024), however, whether this was a direct consequence of nSREBP activity at the *UGT* promoters was not identified. If nSREBPs do in fact reduce UGT levels, this could represent an additional feedback mechanism by which nSREBPs could control the extent of UGT-mediated regulation of SREBP activities.

Overall, the work presented in this thesis has demonstrated a novel role for *UGT2B11* and *UGT2B28* as modulators of lipid biosynthesis in breast cancer. The overall findings of this thesis have been summarised in the below model (Figure 6.1). In brief, in androgen responsive breast cancers, exposure to androgens enhances *UGT2B11* and *UGT2B28* expression. Through a yet to be defined mechanism, these UGTs promote SREBP processing and increase nuclear accumulation of the nSREBP transcription factor. This would lead to increased lipogenesis, which provides a plausible explanation for the observed association of high *UGT2B11* and *UGT2B28* expression with elevated lipogenic gene expression and poorer survival outcomes in breast cancer patients. Evidence was also provided for two UGT-mediated feedback mechanisms that could prevent an excessive activation of nSREBP. First, when *UGT2B11* and *UGT2B28* levels become very high, particularly in association with cell stress, they may promote nuclear nSREBP degradation. Second, when nSREBPs levels become high, they may inhibit transcriptional induction of the *UGT2B11* and *UGT2B28* genes by AR, which in turn could reduce the amount of UGT available to promote of SREBP processing in the ER.

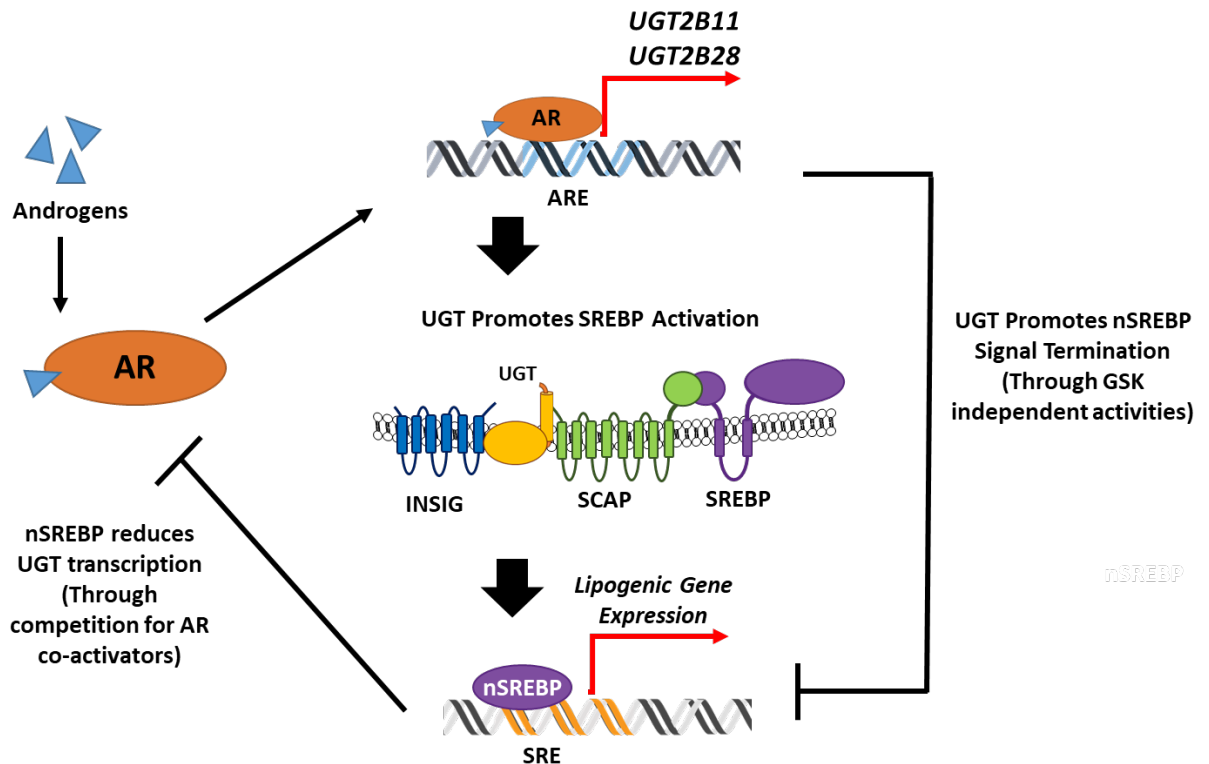


Figure 6.1: Overall working model of UGT modulation of lipid metabolism

While the mechanistic details of some of the events discussed above are yet to be fully defined, the findings of this project strongly support a model in which UGTs serve as intermediates in both positive and negative regulation of SREBP activities by AR/androgen signalling. While other regulatory connections between AR and SREBPs have been described in literature, this novel paradigm adds significantly to our overall understanding of this regulatory nexus, and also provides a likely explanation for the exceptional capacity of AR to induce *UGT2B11* and *UGT2B28* expression.

Further elucidation of UGT-based mechanisms for controlling lipogenesis could lead to the identification of druggable pathways in cancer. Pharmacological inhibitors have been developed to target many lipogenic genes and have been shown to produce synergistic effects when provided alongside conventional chemotherapeutics and a capacity to treat drug-resistant cancers (Liang & Dai, 2022; Wang et al., 2023). Moreover, as identified in a subset of breast cancer patients, these UGTs have prognostic value and could be used as biomarkers to indicate the predicted severity of disease state. The identification of these UGTs as biomarkers or as members of druggable pathways could be particularly valuable

in AR-driven tumours such as prostate cancer and luminal AR (LAR) or molecular apocrine-type breast cancers, which are characterized by highly lipogenic molecular phenotypes. Moreover, whilst these studies have all been conducted in a breast cancer cell context, the capacity to modulate this pathway may also be relevant to AR driven prostate cancer, and potentially other cancers with lipogenic phenotypes such as liver cancer. Thus future work should also examine roles for these UGTs in modulating SREBP activities in a broader range of cancer contexts.

7. APPENDICES

6.1 Appendix 1: Materials and Buffer Compositions

Table S1. Chemical Reagents and Suppliers

Reagent	Supplier
General Chemicals	
Acetic Acid	Ajax Finechem, New South Wales, Australia
Bromophenol blue	Sigma-Aldrich, New South Wales, Australia
Calcium Chloride Dihydrate (CaCl ₂ .2H ₂ O)	Univar Solutions, Illinois, USA.
Chloroform	VWR, Pennsylvania, USA
Dimethyl sulfoxide (DMSO)	Merck, New Jersey, USA
Disodium phosphate (Na ₂ HPO ₄)	Ajax Finechem
Ethanol	Chem-Supply, South Australia, Australia
Ethylenediaminetetra-acetic acid (EDTA)	Astral Scientific, New South Wales, Australia
Formaldehyde	Sigma-Aldrich
Glycerol	Amresco, Ohio, USA
Glycine	Amresco
Hydrochloric Acid (HCl)	VWR
Isopropanol	Chem-Supply
Lithium Chloride	Sigma-Aldrich
Magnesium Chloride (MgCl ₂)	Amresco
Methanol	Chem-Supply
Magnesium Chloride Hexahydrate (MgCl ₂ .6H ₂ O)	Sigma-Aldrich
Manganese Chloride Tetrahydrate (MnCl ₂ .4H ₂ O)	Sigma-Aldrich
Nondiet P-40 Sigma-Aldrich	Sigma-Aldrich
Potassium Acetate	Amresco
Potassium Chloride (KCl)	Amresco
Potassium Dihydrogen Phosphate (KH ₂ HPO ₄)	Amresco
Sodium Acetate (C ₂ H ₃ NaO ₂)	Amresco
Sodium Chloride (NaCl)	Astral Scientific
Sodium deoxycholate	Amresco
Sodium Dodecyl Sulphate (SDS)	AG Scientific, California, USA
Tris[hydroxymethyl]aminomethane (Tris)	Astral Scientific
Molecular Cloning	
1 kb plus and 100 bp DNA Ladders	New England Biolabs (NEB), Massachusetts, USA
Agarose	Astral Scientific
Antarctic Phosphatase	NEB
Phire HotStart DNA Polymerase	Thermo Fisher Scientific, California, USA
Phusion High Fidelity DNA Polymerase	Thermo Fisher Scientific
Purple Gel Loading Dye	NEB
QIAquick PCR Purification Kit	Qiagen, Victoria, Australia
Quick Ligation Kit	NEB
Restriction Enzymes	NEB
SYBR Safe DNA Gel Stain	Invitrogen (Thermo Fisher Scientific)
Zero Blunt PCR Cloning Kit	Invitrogen

Mammalian Tissue Culture and Transfection	
Collagen	Gibco (Thermo Fisher Scientific)
Dulbecco's modified Eagle's medium (DMEM)	Invitrogen
Foetal Bovine Serum (FBS)	Bovogen Biologicals, Victoria, Australia
Lipofectamine 2000	Invitrogen
Lipofectamine LTX with Plus Reagent	Invitrogen
MG132	Sigma-Aldrich
Puromycin	Astral Scientific
Roswell Park Memorial Institute medium (RPMI 1640-)	Invitrogen
Trypsin-EDTA	Invitrogen
Minimum Essential Media (MEM)	Invitrogen
Bacterial Culture and Plasmid Purification	
Agar	Amresco
Ampicillin	Aspen Pharmacare, New South Wales, Australia
Kanamycin	Aspen Pharmacare
Luria Broth (LB) EZMix	Amresco
QIAGEN Plasmid Midi/Miniprep kits	Qiagen
PCR and Gene Expression Analysis	
Amplification grade DNase 1	Life Technologies (Thermo Fisher)
Chloroform	VWR
Deoxynucleotide-triphosphate mix (dNTPs)	NEB
GoTaq qPCR master mix	Promega, Wisconsin, USA
NxGen M-MuLV Reverse Transcriptase	Lucigen, Wisconsin, USA
NxGen RNase Inhibitor	Lucigen
TRIzol	Life Technologies (Thermo Fisher Scientific)
Western Blotting	
Acrylamide/Bis-acrylamide 30% solution (29:1)	Bio-Rad, New South Wales, Australia
Ammonium persulphate (APS)	Amresco
Bio-Rad Protein Assay Reagent	Bio-Rad
Bovine serum albumin (BSA) solution	NEB
Complete Proteinase Inhibitor tablets	Roche Diagnostics, South Australia, Australia
N, N, N', N'-Tetramethyl-1,2-diaminomethane (Temed)	Sigma-Aldrich
Skim milk powder	Fonterra Brands, New Zealand
SuperSignal West Pico chemiluminescent (ECL) HRP substrate	Thermo Fisher Scientific
Trans-blot nitrocellulose membrane	Bio-Rad
Tween-20	Astral Scientific
HA, Myc and FLAG primary antibodies	Sigma-Aldrich
β -mercaptoethanol	BDH Laboratory Supplies, Poole, England.
Co-Immunoprecipitation	
ChIP grade Protein G magnetic beads	Cell Signaling Technology, Massachusetts, USA

Dithiothreitol (DTT)	Sigma-Aldrich
Glycerol-2-Phosphate	Sigma-Aldrich
PhosSTOP Phosphatase Inhibitor Tablets	Roche Diagnostics
Triton X-100	Sigma-Aldrich
Cellular Biology Assays	
Crystal Violet Staining Powder	Sigma-Aldrich
Oil Red O	Sigma-Aldrich
Other	
Dual-Luciferase Assay System	Promega

Table S2. Buffer Compositions

<p>General 1X Buffers</p> <p>Phosphate Buffered Saline (PBS) 137 mM NaCl 2.7 mM KCl 10 mM Na₂HPO₄ 1.8 mM KH₂PO₄ pH 7.4</p> <p>TE Buffer 1 mM EDTA 10 mM Tris pH 8.0</p> <p>Tris-acetate EDTA Electrophoresis Buffer (TAE) 40 mM Tris (pH 7.6) 20 mM Acetic acid 1 mM EDTA</p> <p>CCMB80 Buffer Hanahan <i>et al.</i>[98] 10 mM Potassium Acetate 80 mM CaCl₂.2H₂O 20 mM MnCl₂.4H₂O 10 mM MgCl₂.6H₂O 10% Glycerol pH 6.4</p> <p>Co-Immunoprecipitation Hypotonic Lysis Buffer Klenova <i>et al.</i>[95] 20 mM Tris pH 7.4 10 mM MgCl₂ 10 mM KCl 2 mM EDTA 10% Glycerol 1% Triton X-100 1 mM DTT</p>	<p>Western Blotting</p> <p>SDS Sample Dye 50 mM Tris-HCl, pH 6.8 10% SDS 30% Glycerol 5% β-mercaptoethanol 0.02% Bromophenol blue</p> <p>SDS-PAGE Running buffer 25 mM Tris 192 mM Glycine 0.1% SDS pH 8.3</p> <p>SDS-PAGE Transfer buffer 25 mM Tris 192 mM Glycine 20% Methanol pH 8.3</p> <p>Tris-buffered Saline (TBS) 10 mM Tris 150 mM NaCl pH 8</p> <p>Radioimmunoprecipitation assay (RIPA) Buffer 50 mM Tris-HCl, pH 8.0 150 mM NaCl 1% NP-40 0.5% Sodium deoxycholate 0.1% SDS</p>
---	---

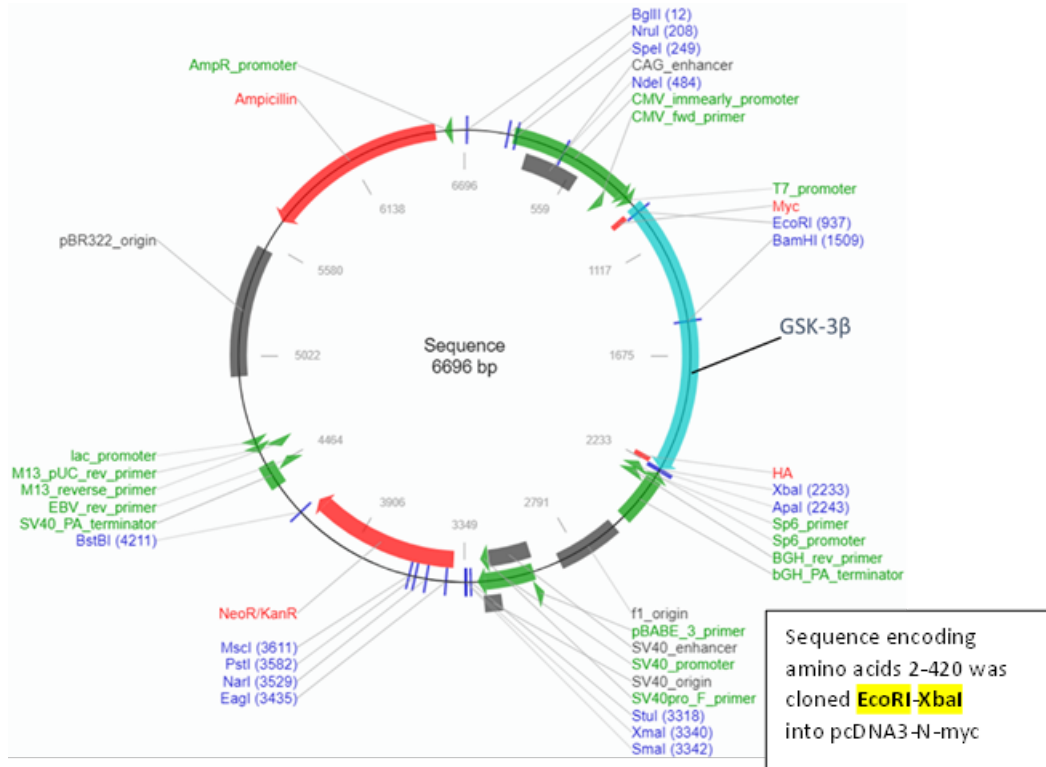
6.2 Appendix 2: Plasmid Maps and Sequences

The plasmids presented within this appendix were constructed during this project. For each plasmid, a schematic, full nucleotide sequence and translation of the protein expression product (where appropriate) have been provided. Plasmid maps were generated using the Addgene sequence analysis tool (<https://www.addgene.org/analyze-sequence/>).

Plasmid Map and Sequence Legend:

- 1) All features of importance are shown in **bold and are underlined**
- 2) Open Reading Frames for genes of interest are shown in **blue**
- 3) Recombinant or fluorescent protein tags are shown in **green**
- 4) Epitope tag sequences are shown in **red**
- 5) Restriction enzyme sites utilised for cloning are highlighted in **yellow**
- 6) For mutant/wildtype variants generated by SDM, SDM site is highlighted in **blue**

GSK-3β-myc(N)-HA(C)-pcDNA3



>GSK-3β-myc(N)-HA(C)-pcDNA3 Amino Acid Coding Sequence

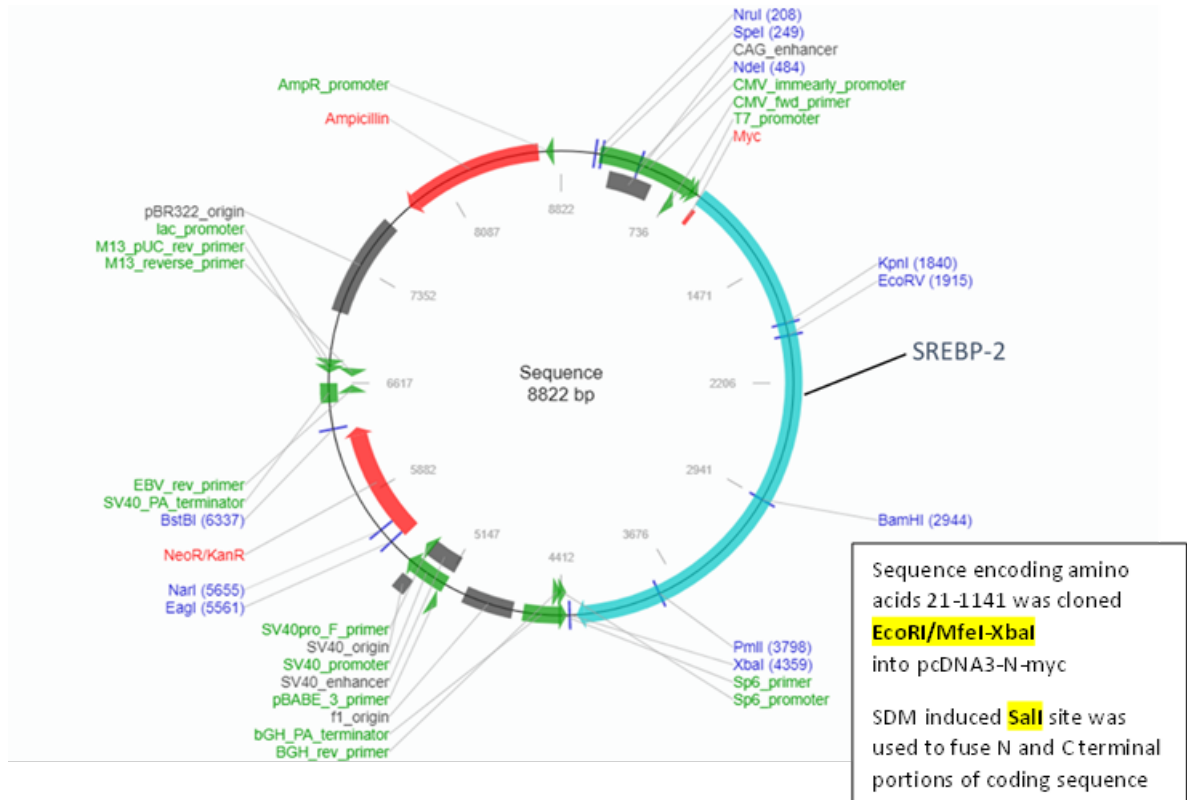
MEQKLISEEDLNEFMSSGRPRRTSFAESCKPVQQPSAFSGSMKVSARDKDGSKVTTVVATPGQGPDRPQEVSYTDTKVIWNGSGFVYVYQAKLDCDSGELVAIKV LQDKRFKNRELQIMRKLDCNIVRLRYFFYSSEGEKKDEVYLNVLVDYVPETVYRVARHYSRAKQTLPIVYVKLYMYQLFRSLAYIHSFGICHRDIKPNLLDLPD TAVLKLCDFGSAKQLVVRGEPNVSYYICRSYYRAPELIFGATDYTSSIDVWSAGCVLAELLGQPIFPDGSVDQLVEIKVLGTPTRREQIREMNPNYTEFKFPQIKA HPWTKVFRPRTPPEAIALCSRLLLEYPTRARLTPLLEACAHSFDELDPNVKLPNGRDTPALFNFTTQELSSNPPLATILIPPHARIQAAASTPTNATAASDANTG DRGQTNNAASASASNST**YPYDVVPDYA**

>GSK-3β-myc(N)-HA(C)-pcDNA3 Plasmid Sequence

GACGGATCGGGAGATCTCCCGATCCCTATGGTGCAGTCTCAGTACAATCTGCTCTGATGCCGCATAGTTAAGCCAGTATCTGCTCCCTGCTTGTGTGT TGGAGGTGCTGAGTAGTGCAGGAGCAAAAATTAAGCTACAACAAGGCAAGGCTTGACCGACAATTGCATGAAGAATCTGCTTAGGGTTAGGCGTTT TGCGTCTTCGCGATGACGGGCCAGATATACGCGTTGACATTGATTATGACTAGTTAATAGTAATCAATTACGGGGTCATTAGTTCATAGCCC ATATATGGAGTTCGCGTTACATAACTTACGGTAAATGGCCCGCTGGCTGACCGCCCAACGACCCCGCCATTGACGTCATAATGACGTATGTTCC CATAGTAACGCAATAGGGACTTTCCATTGACGTCATGGGTGACTATTTACGGTAACTGCCACTTGCCAGTACATCAAGTGTATCATATGCCAA GTACGCCCTATTGACGTCATGACGGTAAATGGCCCGCTGGCATTATGCCAGTACATGACCTTATGGGACTTTCCTACTTGGCAGTACATCTACG TATTAGTCATCGCTATTACCATGGTGTATGCGGTTTTGGCAGTACATCAATGGGCGTGGATAGCGGTTGACTCACGGGGATTCCAAGTCTCCACCCC ATTGACGTCATGGGAGTTTGTTTGGCACCAAAATCAACGGGACTTTCCAAAATGTGTAACAACTCCGCCATTGACGCAATGGGCGGTAGGCG TGACGGTGGGAGGTCTATATAAGCAGAGCTCTCTGGCTAACTAGAGAACCCTGCTTACTGGCTATCGAAATTAATACGACTCACTATAGGGAGA CCAAAGCTTGCCACC**ATGAGGAGCAGAAGCTGATCTCTGAGGAGGACCTG**AAC**GAATTC**ATGTCAGGGCGGCCAGAACCCCTCTTTCGCGAGAGC TGCAAGCCGTGACGAGCCTTCAGCTTTTGGCAGCATGAAAGTTAGCAGAGACAAGGAGGCGAGCAAGTGACAACAGTGGTGGCAACTCCTGGG CAGGGTCCAGACAGGCCACAAGAAGTACGATATACAGACACTAAAGTATTGAAATGGATCATTGGTGTGGTATATCAAGCCAACTTTGTGATT CAGGAGAAGTGGTGCCTATCAAGAAAGTATTGCAGGACAAGAGATTTAAGAATCGAGAGCTCCAGATCATGAGAAAGCTAGATCACTGTAACATAGT CCGATTGCGTTATTTCTTACTCCAGTGGTGAGAAGAAAGATGAGGCTATCTTAATCTGGTCTGGACTATGTTCCGGAAAACAGTATACAGAGTTG CCAGACACTATAGTCGAGCCAAACAGACGCTCCCTGTGATTTATGTCAAGTTGATATGTATCAGCTGTTCCGAAGTTAGCTATATCCATTCCTTTGG AATCTGCCATCGGGATATTAACCGCAGAACCTCTTGTGGATCTGATACTGCTGTATTAACCTCTGTGACTTTGGAAGTGCAAGCAGCTGTGCC GAGGAGAACCAATGTTTCGTATATCTGTTCTCGGTAATAAGGACACAGAGTTGATCTTTGGAGCCACTGATTACCTCTAGTATAGATGATAGGT CTGCTGGCTGTGTTGGTGGTACTAGGACAACCAATATTTCCAGGGGATAGTGGTGGATCAGTTGGTAGAAAATCAAGGCTCTGGG AACCCAAAGGAGCAAAATCAGAGAAATGAACCCAACTACACAGAAATTTAAATCCCTCAAATTAAGGCACATCTGGACTAAGGCTCTCCGAC CCCGAACTCCACCGGAGGCAATTGCACTGTGTAGCCGTCTGCTGGAGTATACACCAACTGCCGACTAACCACTGGAAGCTTGTGCACATTCATTTT TTGATGAATTACGGGACCAAAATGTCAAACCTACCAATGGGCGAGACACACTGCCTTCAACTTCAACTCAAGAACTGTCAAGTAATCCACCTC TGGCTACCATCCTTATTCCTCCTCATGCTCGGATTCAAGCAGCTGCTCAACCCCAAAATGCCACAGCAGCGTCAGATGCTAATACTGGAGACCGTG GACAGACCAATAATGCTGCTCTGCATCAGCTTCCAATCCAC**TACCATACGATGTTCCAGATTACGCTTGA****TCTAGA**GGGCGCTATTCTATAGTGT CACCTAAATGCTAGAGCTGCTGATCAGCCTGACTGTGCTTCTAGTGGCAGCATCTGTTGTTTCCCTCCCGTGCCTTCCCTGACCTGGAAG GTGCCACTCCACTGCTCTTCTTAATAAAATGAGGAAATTCATCGCATTGCTGAGTAGGTTGTCATTCTATTCTGGGGGGTGGGGTGGGGCAGGAC AGCAAGGGGGAGGATTGGGAAGACAATAGCAGGCATGCTGGGGATGCGGTGGGCTCTATGGCTTCTGAGGCGGAAAGAACAGCTGGGGCTCTAG GGGGTATCCACGCGCCTGTAGCGCGCATTAAAGCGCGCGGGTGTGGTGTAGCGCGAGCGTGACCGCTACACTTGCAGCGCCCTAGCGCCC GCTCCTTTCGCTTCTTCCCTTCTTCTCGCCACGTTCCGCCGCTTCCCGTCAAGCTCAAAATCGGGGCATCCCTTAGGGTTCCGATTAAGTCTT ACGGCACCTGACCCCAAAAATGATTAGGGTGTGTTACAGTAGTGGCCATCGCCCTGATAGACGGTTTTTCGCCCTTGGACGTTGGAGTCCA CGTTCTTAATAGTGGACTCTGTTCCAACTGGAACAACACTCAACCTATCTCGTCTATTCTTTGATTATAAGGGATTTGGGGATTTCCGCTCA

TTGGTTAAAAATGAGCTGATTTAACAAAAATTTAACCGGAATTAATCTGTGGAATGTGTGTCAGTTAGGGTGTGGAAAGTCCCCAGGCTCCCCAGG
CAGGCAGAAGTATGCAAAGCATGCATCTCAATTAGTCAGCAACCAGGTGTGGAAAGTCCCCAGGCTCCCCAGCAGGCAGAAGTATGCAAAGCATGC
ATCTCAATTAGTCAGCAACCATAGTCCCGCCCTAACTCCGCCATCCCGCCCTAACTCCGCCAGTTCCGCCATTCTCCGCCCATGGCTGACTAAT
TTTTTTATTTATGACAGAGGCCGAGGCCCTCTGCCTCTGAGCTATCCAGAAGTAGTGAGGAGGCTTTTTGGAGGCCTAGGCTTTTGCAAAAAGCT
CCCGGAGACTTGTATATCCATTTTCGGATCTGATCAAGAGACAGGATGAGGATCGTTTCGCATGATTGAACAAGATGGATTGCACGCAGGTTCTCCGG
CCGCTTGGGTGGAGAGGCTATTCGGCTATGACTGGGCACAACAGACAATCGGCTGCTGATGCCCGCTGTTCCGGCTGTCAGCGCAGGGGCGCC
GGTCTTTTTGTCAAGACCGACCTGTCGGGTGCCCTGAATGAAGTGCAGGACGAGGCGCGGCTATCGTGGCTGGCCACGACGGGCGTTCCTTGC
GCAGCTGTGCTCGACGTTGTCACTGAAGCGGGAAGGGACTGGCTGCTATTGGCGAAGTCCGGGGCAGGATCTCTGTCACTCACCTTGCTCCTG
CCGAGAAAGTATCCATCATGGCTGATGCAATGCGGCGGCTGCATACGCTTATCCGGTACCTGCCATTCCGACCACCAAGCAAACATCGCATCGAG
CGAGCACGTACTCGGATGGAAGCCGGTCTTGTGATCAGGATGATCTGGACGAAGAGCATCAGGGGCTCGCCGACCCGAACTGTTCCGACGGCTC
AAGGCGCGCATGCCGACGCGAGGATCTGCTGTCGACCATGGCGATGCTGCTTCCGAATATCATGGTGGAAATGGCCGCTTTCTGGATTCA
TCGACTGTGGCCGGTGGGTGTGGCGGACCGCTATCAGGACATAGCGTTGGCTACCCGTGATATTGCTGAAGAGCTTGGCGGCAATGGGCTGACC
GCTTCTCGTGTTCACGGTATCGCCGCTCCGATTCCGAGCGCATCGCTTCTATCGCTTCTTACGAGTTCCTTACGCGGACTCTGGGGTTCGA
AATGACCGACCAAGCGACGCCAACCTGCCATCACGAGATTTGATTCCACCGCCGCTTCTATGAAAGGTTGGGCTTCGGAATCGTTTTCCGGGACG
CCGGTGGATGATCTCCAGCGCGGGATCTCATGCTGGAGTTCCTCCGCCACCCCACTTGTATTGCAGCTTATAATGTTACAAATAAAGCAATA
GCATCACAATTTACAAATAAAGCATTTTTTCTACTGACTTCTAGTTGTGGTTTCCAAAACATCAATGTATCTTATCATGTCTGTATACCGTCGACC
TCTAGCTAGAGCTTGGCGTAATCATGGTCATAGCTGTTTCTGTGTGAAATGTTATCCGCTCACAATCCACACAACATACGAGCCGGAAGCATAAAG
TGAAAGCCTGGGGTGCCTAATGAGTGAGCTAACTACATTAATGCGTTGCGCTCACTGCCGCTTCCAGTCGGGAAACCTGTCGTGCCAGCTGCA
TTAATGAATCGGCCAACGCGCGGGGAGAGGCGGTTGCGTATTGGGCGCTCTCCGCTTCTCGCTCACTGACTCGCTCGCTCGGCTCGTTCGGCTC
GGCGAGCGGTATCAGCTCACTCAAAGCGGTAATACGGTATCCACAGAATCAGGGGATAACGCGAGGAAAGAACATGTGAGCAAAAAGGCCAGCAA
AGGCCAGGAACCGTAAAAAGGCCGCTTGTGGCGTTTTCCATAGGCTCCGCCCTGACGAGCATCACAATAACGACGCTCAAGTCAGAGGTG
GCGAAACCCGACAGGACTATAAGATACAGGCGTTTTCCCTGGAAGCTCCCTCGTGCCTCTCTGTTCCGACCTGCCGCTTACCGGATACCTGTC
CGCTTTCTCCCTCGGAAAGCGTGGCGCTTCTCAATGCTCACGCTGTAGGTATCTCAGTTCGGTGTAGGTGTTCCGCTCAAGCTGGGCTGTGTGCA
CGAACCCCGTTTCAGCCGACCGCTGCGCTTATCCGGTAAGTATGCTTGTAGTCCAACCCGTAAGACAGACTTATCGCCACTGGCAGCAGCCA
CTGGTAACAGGATTAGCAGAGCGAGGTATGTAGGCGGTGTACAGAGTCTTGAAGTGGTGGCCTAACTACGGCTACACTAGAAGGACAGTATTTG
GTATCTGCGCTGCTGAAGCCAGTACCTTCGAAAAAGAGTTGGTAGCTCTGATCCGGCAAACAACCCGCTGGTAGCGGTGGTTTTTTGTTT
GCAAGCAGCAGATTACGCGCAGAAAAAGGATCTCAAGAAGATCCTTTGATCTTTTACGGGGTCTGACGCTCAGTGGAAACGAAAACCTCACGTTA
AGGGATTTGGTCATGAGATTACAAAAAGGATCTCACCTAGATCCTTTAAATTAATAAATGAAGTTTTAAATCAATCTAAAGTATATATGAGTAAAC
TTGGTCTGACAGTTACCAATGCTTAATCAGTGAGGCACCTATCTCAGCGATCTGCTATTTTCGTTTATCCATAGTTGCCTGACTCCCGTCTGTAGATA
ACTACGATACGGGAGGGCTTACCATCTGGCCCAAGTGTGCAATGATACCGCGAGACCCAGCTCACCGGCTCCAGATTTATCAGCAATAAACAGCC
AGCCGGAAGGGCCGAGCGCAGAAGTGGTCTGCACTTTATCCGCTCCATCCAGTCTAATTAATTGTTCCGGGAAGCTAGAGTAAGTAGTTCGCCA
GTTAATAGTTTGCACAACGTTGTTGCCATTGTACAGGCATCGTGGTGTACGCTCGTCTGTTGGTATGGCTTATTAGCTCCGTTCCCAACGATCA
AGGCGAGTTACATGATCCCCATGTTGTGCAAAAAAGCGGTTAGCTCCTTCCGCTCCGATCGTTGTGAGAAGTAAAGTTGGCCGAGTGTATCACT
CATGTTATGGCAGCACTGCATAATCTTACTGTGATGCCATCCGTAAGATGCTTTTCTGTGACTGGTGAAGTACTCAACCAAGTCACTTCTGAGAATA
GTGATGCGGCGACCGAGTTGCTTTCGCCGGCGTCAATACGGGATAAATCCGCGCACATAGCAGAACTTTAAAAGTGTCTCATCTTGGAAAAAGCTT
CTTCGGGGGCAAACTCTCAAGGATCTTACCCTGTTGAGATCCAGTTCGATGTAACCCACTCGTGCACCCAACTGATCTTCAGCATCTTTTACTTTTAC
CAGCGTTTCTGGGTGAGCAAAAACAGGAAGGCAAAATGCCGCAAAAAGGGAATAAGGGCGACACGGAAATGTTGAATCTCATACTCTTCTTTTT
CAATATTATTGAAGCATTTATCAGGGTATTGTCTCATGAGCGGATACATATTTGAATGATTTTAGAAAAATAAACAAATAGGGGTTCCGCGCACATTT
CCCCAAAAGTGCCACCTGACGTC

SREBP-2-myc(N)-pcDNA3



>SREBP-2-myc(N)-pcDNA3 Amino Acid Coding Sequence

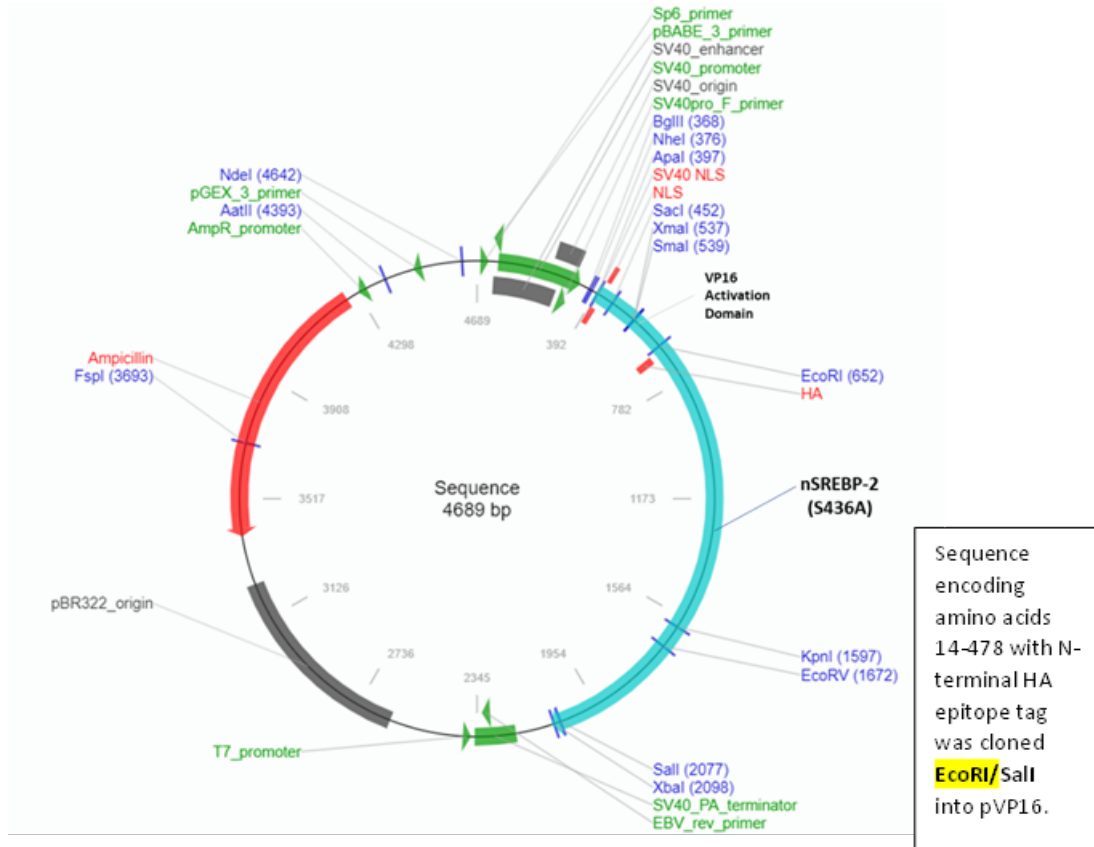
MEQKLISEEDLNEFDSDGELTGDIDEMQLQVFNQVGFEPDLFSEQLCCSFPGSGGSGSSGSSSSSSSSNNGRSGSSGAVDPSVQRSTQVTLPSFSPSAASP QAPTLQVKVSPTSVPTTTPRATPILQPRPQPQPTQLQQQVMTPTFSTTPQTRIIQQPLIYQNAATSFQVLQPVQVSLVSSQVQPVTIQQVQVTVQA QRVLTQTANGTLQTLAPATVQTVAAPQVQVPLVQVQPIKTDLSLVTLTKDGSPPVMAAVQNPALTAITPIQTAALQVPTLVGSSGILTTPMVMGMGQ EKVPKIQVPGGVKLEPPKEGERRTTHNIEKRYRSSINDKIELKDLVMTDAKMHKSGVLRKAIDYIKYKLVQVNHKLRQENMVLKLANQKNLLKGIDLGLS VDNEVDLKIEDFNQNVLLMSPASDSGSQAGFSYPSIDSEPSPLDDAKVKDEPDPSPVALGMVDRSRILLCVLFLCLFSNPLTSLQWGGAHSDQHPH SGSGRSVLSFESGGWVMMPTLLLWLNVGVIVLVSFVKLLVHGEPVIRHSRSTVTFWRHRKQADLDLARGDFAAAGNLQTCCLAVLGRALPSTRLD LACLSWNVIRYSKQLRLVRWLLKKVFQRRATPATEAGFEDEAKTSARDAALAYHRLHLHITGKLPAGSACSDVHMALCAVNLAECAEIKPSTLVEIHL TAAMGLKTRCGGKGLFSLASFLSRAQSLCGPEHSVAVPDSLRWLCHPLGQKFFMERSWSVKSAAKESLYCAQRNPADPIAQVHQAFCKNLLERIAESLVKPKQ AKKKAGDQEESECFSSALEYLKLLHSFVDSVGMSPPLSRSSVLKALGPDIIICRWVWTSAITVAISWLQGDAAVRSHTFKVERIPKALEVTESPLVKAIFHAC RAMHASLPGKADGQSQSFCHCERASGHLWSSLNVSGATSDPALNHVVQLLTCDLLSLRALTALWQKQASASQAVGETYHSGAELAGFQRDLGSLRRLAHS FRPAYRKVFLHEATVRLMAGASPTRTHQLLEHSRRLRTQSTKHGEVDAWPGQREERATAILLACRHLPLSLSSPGQRAVLLAEARTLEKVGDRRCNDCQ QMIVKLGGGTAIAAS

>SREBP-2-myc(N)-pcDNA3 Plasmid Sequence

GACGGATCGGGAGATCTCCCGATCCCCTATGGTCGACTCTAGTACAATCTGCTCTGATGCCGCATAGTTAAGCCAGTATCTGCTCCCTGCTTGTGTGT TGGAGGTCGCTGAGTAGTGCAGCAGCAAAATTAAGCTACAACAAGGCAAGGCTGACCGACAATTGCATGAAGAATCTGCTTAGGGTTAGGCGTTT TGGCGTCTTCGCGATGTACGGGCCAGATATACGCGTTGACATTGATTATTGACTAGTTATTAATAGTAATCAATTACGGGGTTCATTAGTTCATAGCCC ATATATGGAGTTCGCGTTACATAAATCGGTAATGGCCCGCTGGCTGACCGCCCAACGACCCCGCCATTAGCTCAATAATGACGTATGTTCC CATAGTAACGCCAATAGGGACTTTCATTGACGTCAATGGGTGGACTATTTACGGTAAACTGCCACTTGGCAGTACATCAAGTGATCATATGCCAA GTACGCCCTTATTGACGTCAATGACGGTAAATGGCCCGCTGGCATTATGCCAGTACATGACCTTATGGGACTTTCCTACTTGGCAGTACATCTACG TATTAGTCATGCTATTACCATGGTGTATGCGTTTTGGCAGTACATCAATGGGCGTGGATAGCGGTTTACTCACGGGGATTTCCAAGTCTCCACCCC ATTGACGTCAATGGGAGTTTGTTTGGCACCAAAATCAACGGGACTTTCAAAATGTCTGAACAACCTCCGCCCATTTGACGCAAAATGGGCGGTAGGCG TGTACGGTGGGAGTATATAAGCAGAGCTCTCTGGTAAGTACAGAACCCACTGCTTACTGGCTTATCGAAATTAACGACTCACTATAGGGAGA CCCAAGCTTGCCACC**ATGGAGCAGAAGCTGATCTCTGAGGAGGACCTG**AAC**GAATTG**GACGACAGCGGCGAGCTGACCTGGGAGACATCGACGA GATGCTGCAATTTGTCAAGTAACTCAAGTGGGAGAGTTCCTGACTTGTTCAGAACAGCTGTGTAGCTCCTTCTGGCAGTGGTGGTAGTGGTAGCA GCAGCGGCAGCAGTGGCAGCAGCAGCAGCAGCAATGGCAGGGGAGCAGCAGCGGAGCTGTGGACCTTCAAGTGAACGGTTCATTACCCAG GTCACATTACCTTCTCTCTCCCTCGGCGGCCTCCCAACAGGCTCCAATCTGCAAGTCAAGGTTTCTCCACCTCAGTTCACCCACACCCAGGGCAA CTCTCTATTTACGCCCCGCCCCAGCCCCAGCCTCAACTCAACTCAGCTGCAACAACAGACGGTAATGATCAGCCCAACTCAGCACCCTCCCG AGACGAGGATCACCAGCAGCCTTTGATATACCAAGAATGCAGCTACTAGCTTTCAAGTCTTCAAGCTCCTCAGCCTCAAGTCCAAGCTGGTGAACCTCCAG GTACAGCGGTCAACATTACGACGAGGTGACAGACAGTACAGGCCAGCGGGTGTGACACAAACGGCAATGGCAGCTGACAGCCCTTGGCCG GCTACGGTGCAGACAGTGTCTGCGCCACAGGTGACAGAGTCCCGTCTGGTCCAGCCTCAGATCATCAAGACAGATTCCCTTGTGTTGACCACT GAAGACAGATTGGCAGCCCTGTTATGGCTGCGGTCCAGAACCAGCCCTCACCAGCCTCACCACCTATCCAGACGGCTGCCCTCAAGTACCAACCC TGGTGGGACAGCAGTGGGACATTCTGACCACAATGCCTGTAATGATGGGGCAAGAGAAAGTGGCCATTAAGCAGGTACCTGGGGGAGTCAAGCAGC TTGAGCCCCCAAGAAGGAGAAAGGGGACAAACCAATATCATTTGAGAAACGATATCGCTCCTCCATCAATGACAAAATCATGAAATTTGAAAGA CCTGGTATGGGGACAGACGCCAAGATGCACAAGTCTGGCGTCTGAGGAAGGCCATTGATTACATCAAATACTGACGAGGTCAATCATAAACTG GCCAGGAGAACATGGTGTGAACTGGCAATCAAAGAACAGCTTCAAAGGGCATCGACCTAGGCAGTCTGGTGGACAAATGAGGTGGACCTG

AAGATCGAGGACTTTAATCAGAATGTCTTCTGATGTCCCCCAGCCTCTGACTCAGGGTCCCAGGCTGGCTTCTCTCCCTACTCATTGACTCTGAGC
CAGGAAGCCCTCTATTGGATGATGCAAAGTCAAAGATGAGCCAGACTCTCTCTGTGGCGTGGGCATG**GTCTGAC**CGCTCACGGATTCTTCTGTGT
GTCTCACCTTCTGTGCCTCTCTTTAACCCCTGACTTCCCTGCTGAGTGGGGAGGGGCCACGACTCTGACCGACCCACACTCAGGCTCTGGC
CGCAGTGTCTGTCAATCGAGTCAAGTCTGGGGGCTGGTTGACTGGATGATGCCTACTTCTCTTATGGCTGGTAAATGGTGTATTGTCTGAGC
GTCTTTGTGAAGTGTCTGGTTCATGGGGAGCCAGTATCCGGCCACACTCGCGCTCTCCGGTCACTTCTGGAGGCACCGAAACAGGCAGATCTGG
ATCTCGCCAGAGGAGATTTTGCAGCTGTGCCGGCAACCTACAACTGCCTGGCAGTTTTGGCCGGGCACTGCCACCTCCCGCTGGACCTGGCC
TGCAGCTCTCTGGAACGTATCCGTACAGCTGCAGAAGTACGCTGTGGCTGGCTGCTCAAGAAAGTCTTCCAGTCCCGGGGGCCACGC
CAGCCACTGAGGCAGGCTTTGAAGACGAAGCTAAGACCAGCCGCGGGATGCGAGCTGGCCATACACAGCTTCCAGTCCAGCAAGGTGCACATCACAGGGA
AGCTTCTGCAGGATCCGCTGTTCCGATGTACACATGGCGTGTGTGCCGTGAACCTGGCTGAATGTGCAGAGGAGAAGATCCACCGAGCACACT
GGTTGAGATCCATCTGACTGTGCCATGGGGCTCAAGACCCGGTGTGGAGGCAAGCTGGGCTTCTGGCCAGTACTTCTCAGCCGAGCCAGAGC
CTGTGTGGCCCCGAGCACAGTGTCTTCTGACTCCTCGCTGGCTCTGCCACCCCTGGGCCAGAAGTTTTTCATGGAGCGGAGCTGGTCTGTGAA
GTCAGCTGCCAAGGAGAGTCTACTGTGCCAGAGGAACCCAGTACCCTTGTCCGAGGTCACCAGGCTTCTGCAAGAACCTGTGGAGCGA
GCTATAGAGTCTTTGGTGAACCTCAGGCCAAGAAGAGGCTGAGACCAGGAAAGAGAGCTGTGAATCTCCAGTCTGTGGATGTGAA
TTACTTACTTCTTTGTGGACTCTGTGGGGTTATGAGCCCCACTCTCCAGGAGCTCCGTGCTCAAGTCCGCCCTGGGTCCAGACATCATCTGTCCG
TGGTGGAGCTGTCAATCACTGTGGCCATCAGCTGGTCCAGGGAGACGATGAGCTGTGGCTCTCATTTTACAAAGTGGAACGCATCCCCAAG
CCCTGGAAGTGACAGAGAGCCCCCTGGTGAAGGCCATCTCCATGCTGCAGAGCCATGCATGCCTCACTCCCTGGGAAAGCAGATGGGCAGCAGAG
TTCCTTCTGCCATTGCGAGAGGGCCAGTGGCCACCTATGGAGCAGCTCAACGTCACTGGGGCCACTCTGACCCTGCCCTCAACCACGTGGTCCAGC
TGCTCACTGTGACTGTACTGTCTGCTACGGACAGCGCTCTGGCAAAAACAGGCCAGTCCAGCCAGGCTGTGGGGGAGACCTACCACGCGTCAAG
GGCAGTGTCTGGCCGAAGTCCCGCACCTGGGAGAAGTGGGGCAGCCGGCCTCTGCAACGACTGCCAGCAGATGATTGTTAAGTGGGTGG
TGGCACTGCCATTGCCCTCT**GTG**ACCACAGGCTCAGCCACCCCTCACCTCTCTCGATTT**CTAGA**GGGCCCTATTCTATAGTGTACCTAAAT
GCTAGAGCTCGTGCAGCCTCGACTGTGCCTTCTAGTTGGCCAGCCATCTGTTTTGGCCCTCCCGTGCCTTCTTACCCCTGGAAAGTGGCCACT
CCACTGTCTTTCTAATAAAATGAGGAAATGCATCGCATTGTCTGAGTAGGTGTCTATTCTATTCTGGGGGTGGGGTGGGGCAGGACAGCAAGGG
GGAGGATGGGAAGACAATAGCAGGCATGCTGGGGATCGGGTGGGCTATGGCTTCTGAGGCGAAAGAACCAGCTGGGGCTAGGGGGTATC
CCCACGCGCCCTGTAGCGCGCATTAAAGCGCGCGGGTGTGGTGTACGCGCAGCGTACCGCTACACTTCCAGCGCCCTAGCGCCGCTCTTT
CGTTTTCTCCCTCTTTCTGCCACGTTCCGGGCTTTCCCGTCAAGCTCTAAATCGGGGCATCCCTTAGGGTCCGATTTAGTGTCTTACGGCACC
TCGACCCCAAAAACTTGAATAGGGTGTGGTTCACGTAGTGGGCCATCGCCCTGATAGACGGTTTTTCGCCCTTGGACGTTGGAGTCCACGTTCTTTA
ATAGTGGACTCTTGTCCAAACTGGAACAACACTCAACCTATCTCGGTCTATTCTTTGATTATAAGGGATTTTGGGATTTCCGGCTATTGGTTAAA
AAATGAGCTGATTTAACAAAAATTAACGCGAATTAATTCTGTGAATGTGTGCAGTTAGGGTGTGGAAAGTCCCAAGGCTCCCAAGCAGGCAGA
AGTATGCAAAGCATGCATCTCAATAGTACAGCAACAGGTGTGGAAAGTCCCAAGGCTCCCAAGCAGGCAGAAATGCAAAGCATGCATCTCAAT
AGTCAGAACCATAGTCCCGCCCTAACTCCGCCATCCCGCCCTAACTCCGCCCAGTCCCGCCATTTCCCGCCCATGGCTGACTAATTTTTTTTAT
TATGCAGAGCCGCGCCGCTCTGCCTGAGCTATTCCAGAAGTAGTGGAGGCTTTTTGGAGGCTAGGCTTTTTGCAAAAAGCTCCCGGGAG
CTTGATATCCAGTTCCGATCTGATCAAGAGACAGGATGAGGATCTGTTCCGATGATTGAACAAGATGGATTTGACGCGAGGTTCTCCGGCCGCTTGG
GTGGAGAGGCTATTCGGCTATGACTGGGCACAACAGACAATCGGCTGCTGATGCCCGCTGTTCCGGCTGTGAGCGCAGGGGCGCCCGGTTCTTT
TTGTCAAGACCGACTGTCCGGTGCCTGAATGAAGTGCAGGACGAGGCAGCGCGCTATCGTGGCTGGCCAGACGGGCGTCTTTCGCGCAGCTGT
GCTCGACGTTGTCACTGAAGCGGGAAGGGACTGGTGTCTATTGGGCGAAGTGGCCGGCAGGATCTCTGTCACTCTCACCTTGCTCTGCCGAGAAA
GTATCCATCATGGTGTGATGAATGCGGCGGCTGCATACGCTTGTCCGGTACCTGCCATTCGACCACCAAGCGAAACATCGCATCGAGCGAGCAGC
TACTCGGATGGAAGCGGCTTGTGATCAGGATGATGGACGAAGAGCATGAGGGGCTCGCGCCAGCCGAAGTCTGACGAGGCTCAAGGCAGCTCAAGGC
CATGCCGACGGCGAGGATCTCGTGTGACCCATGGCGATGCTGTTGCCGAATATCATGGTGGAAATGGCCGCTTTTCTGGATTCACTGACTGTG
GCCGGTGGGTGTGGCGGACCGCTATCAGGACATAGCGTGGCTACCCGTGATATTGCTGAAGAGCTTGGCGGCAATGGGCTGACCGCTTCTCGT
GCTTACGGTATCGCGCTCCCGATTGCGAGCGCATCGCTTCTATCGCTTCTTACGAGTCTTCTGAGCGGGACTCTGGGGTTCGAAATGACCGAC
CAAGCGACGCCAACCTGCCATCACGAGATTTGATTTCCACCCCGCCCTTCTATGAAAGTGGGCTTCCGAAATCGTTTTCCGGGACGCGCGCTGGAT
GATCTCCAGCGCGGGGATCTCATGCTGGAGTCTTCGCCACCCCACTGTTTTATTGACGCTTATAATGGTTACAATAAAGCAATAGCATCAACA
TTTCAAAATAAAGCATTTTTTTTCACTGCATTCTAGTTGTGGTTGTCCAAACTCATCAATGTATCTTATCATGTCTGTATACCGTCGACCTCTAGCTAGA
GCTTGGCGTAATCATGGTATAGCTTTTCTGTGAAATGTTATCCGCTCACAATCCACACAACATACGAGCCGGAAGCATAAAGTGAAGGCT
GGGGTGCTAATGAGTGAAGTCAACTCACATTAATTGCGTTCGCTCACTGCCCGCTTCCAGTCCGGAAACCTGCTGTCGAGCTGCATTAATGAATC
GGCAACGCGCGGGGAGAGGCGGTTTTCGATTTGGGCGCTTCCGCTTCTCGTCACTGACTCGCTGCCTCGGCTCGGCTCGGCTCGGCGAGCGG
TATCAGCTCACTCAAAGCGGTAATACGTTATCCACAGAATCAGGGGATAACGAGGAAAGAACATGTGAGCAAAAGGCCAGCAAAAGGCCAGGA
ACCGTAAAAAGCCGCGTGTGCGGTTTTCCATAGGCTCCGCCCTGACGAGCATCAAAAAATCGAGCTCAAGTCAGAGGTTGGCGAAACCC
GACAGGACTATAAGATACAGGCGTTTTCCCTGGAAGCTCCCTGTCGCTCTCTGTTCCGACCTGCCGCTTACCGGATACCTGTCCGCTTTCT
CCCTTCCGGAAAGCGTGGCGCTTCTCAATGCTCACGCTGTAGGTATCTCAGTTCGGTGTAGGTGTTCCGCTCAAGCTGGGCTGTGTGCACGAACCC
CCGTTACGCCGACCGCTGCGCTTATCCGGTAACTATCGTCTTGTAGTCCAACCCGGTAAGACACGACTTATCGCACTGGCAGCAGCCACTGGTAA
AGGATTAGCAGAGCGAGGTATGTAGCGGTGTACAGAGTCTTGAAGTGGTGGCCTAACTACGGCTACACTAGAAGGACAGTATTTGGTATCTCGC
CTCTGCTGAAGCGATTAACCTCGGAAAAGAGTTGGTAGCTTGTATCCGGCAAAACAAACCAGCTGGTAGCGGTGTTTTTTTTGTTTGAAGCAG
CAGATTACGCGCAGAAAAAAGGATCTCAAGAAGATCTTTGATCTTTTACGGGGTCTGACGCTCAGTGGAAACGAAAACCTCACGTTAAGGATTTT
GGTCATGAGATTATAAAAGGATCTTCACTAGATCTTTAAATTAATAAATGAAGTTTTAAATCAATCTAAAGTATATAGTAAACTTGGTCTGA
CAGTTACCAATGCTAATCAGTGAAGCCTATCTCAGGATCTGTCTATTTCTCATCCTAGTTGCTGACTCCCGCTGTGTAGATAACTACGATA
CGGGAGGGCTTACCATCTGGCCAGTGTGCAATGATACCGGAGACCCAGCTCACCGGCTCCAGATTTATCAGCAATAAACCAGCCAGCCGGAA
GGGCCGAGCGCAGAAGTGGTCCGCAACTTTATCCGCTCCATCCAAGTCTAATAATTGTTCCGGGAAAGTGAAGTAACTACTCATCTTCTTTTCAATATT
TTGCGCAACGTTGTTGCCATTGTACAGGCATCGTGGTGTACGCTGCTGTTGGTATGGCTTATTAGCTCCGGTCCCAACGATCAAGGCGAGTT
ACATGATCCCATGTTGTGCAAAAAGCGGTTAGCTCCTCGGCTCCGATCGTTGTGAGAAGTAAAGTGGCCGAGTGTATCACTCATGTTTATG
GCAGCACTGCATAATTCTTACTGTATGCCATCCGTAAGATGCTTTTCTGTGACTGGTGAAGTACTCAACCAAGTACTTCTGAGAATAGTGTATGCGG
CGACCGAGTTGCTTTCGCCGGCTCAATACGGGATAATACCGCGCCACATAGCAGAATTTAAAGTGTCTATCTTGGAAAACGTTTCTCGGCGG
AAAATCTCAAGGATCTTACCGCTGTTGAGATCCAGTTCAGTAAACCACTGTGACCCCACTGATCTTCAAGTCTTTTACTTTTACCAGCGTTTTCT
GGGTGAGCAAAAACAGGAAGGCAAAATGCCGCAAAAAGGGAATAAGGGCGACACGGAAATGTTGAATACTCATACTCATCTTCTTTTCAATATT
GAAGCATTTATCAGGTTATTGTCTCATGAGCGGATACATATTGAATGATTTAGAAAAATAAACAATAGGGGTTCCGCGCACATTTCCCGAAAA
GTGCCACTGACGTC

nSREBP-2 (Mut)-HA(N)-pVP16



>SREBP-2-S436A-HA(N)-pvp16 Amino Acid Coding Sequence

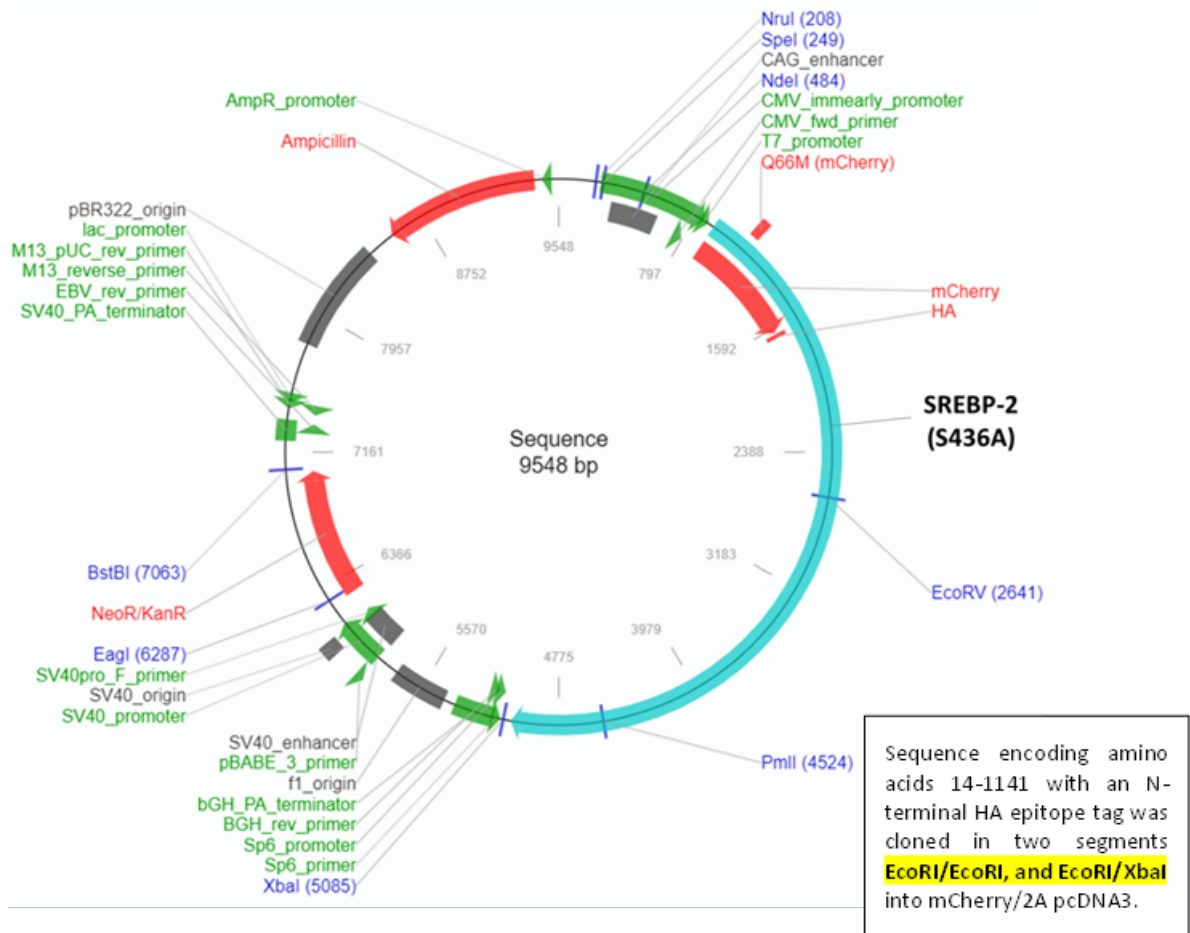
MGPKKKRKVAPPTDVSLGDELHLDGEDVAMAHADALDDFDLMDLGDGSDPGPFTPHDSAPYGALDMADFEFEQMFDTALGIDIEYGGGEF**MYPYDVPD**
YAETLTELDELTLGDIDELMQFVSNQVGEFDFLSEQLCSSFPGSSGSSGSSSSSSSSNGRGSSSGAVDPSVQRSFTQVTLPSFSPAASPOAPTLQVK
 VSPTSVPPTPRATPILQPRPQPQPQQTQLQQQVMITPFTSTTPQTRIIQQPLIQNAATSFQVLQPVQVLSVSSQVQPVTIQQVQVTVQAQRVLTQTA
 NGTLQLTAPATVQVAAPQVQVQVPLVQVQIHKTDSLVLTLKTDGSPVMAAVQNPAALTALTPIQTAALQVPTLVGSSGILTTPMVMGMQEKVPIKQVP
 GGVKQLEPPKEGERRTTHNIEKRYRSINDKIIELKDLVMGTDAMHKSGVLRKAIDYIKYLQVNHKLRQENMVLKLANQKNKLLKIDGLSLVDNEVDLKI
 EDFNQVLLMSPPAADSGSQAGFSPYSIDSEPGSPLDDAKVKDEPDSPVALGMVDASAEASR

>SREBP-2-S436A-HA(N)-pvp16 Plasmid Sequence

TATGTATCATACATACGATTTAGGTGACACTATAGAATCGACTGTGGAATGTGTGTCAGTTAGGGTGTGAAAAGTCCCAGGCTCCCAGCAGGC
 AGAAGTATGCAAAGCATGCATCTCAATTAGTCAGCAACAGGTGTGAAAAGTCCCAGGCTCCCAGCAGGCAGAAAGTATGCAAAGCATGCATCTCA
 ATTAGTCAGCAACCATAGTCCGCCCCTAACTCCGCCATCCGCCCCTAACTCCGCCAGTTCGCCCCATTCGCCCCATGCTGACTAATTTTTTTT
 ATTTATGCAGAGGCCGAGGCCCTCGGCCCTGAGCTATTCAGAAAGTGTGAAGAGGCTTTTTGGAGGAGATCTAAGCTAGCGCCGCCACCATG
 GGCCCTAAAAAGAAGCGTAAAGTCGCCCCCGACCGATGTCAGCCTGGGGGACGAGCTCCACTTAGACGGCAGGACGTTGGCGATGGCGCATGCC
 GACGCGCTAGACGATTCGATCTGGACATGTTGGGGGACGGGGATTCCCGGGGGGATTACCCCGGACTCCGCCCCCTACGGCCCTGCTGG
 ATATGGCCGACTTCGAGTTTGAGCAGATGTTTACCGATGCCCTTGGAATTGACGAGTACGGTGGG**GAATTCATGTACCCATACGATGTTCCAGATTA**
CGCGGAGACCCTCAGGAGCTGGGCGACGAGCTGACCCTGGGAGACATCGACGAGATGCTGCAATTTGTCAGTAATCAAGTGGGAGAGTCCCTGA
 CTTGTTTTCAGAACAGCTGTGTAGCTCCTTCTGGCAGTGGTGTAGTGGTAGCAGCAGCGGCAGCAGTGGCAGCAGCAGCAGCAGCAATGGC
 AGGGGACAGCAGCAGCGGAGCTGTGGACCCTCAGTGAACGGTCAATCACCCAGGTCACATTACCTTCTCTCCCTCGGCGGCTCCCACAGGC
 TCCAACTGCAAGTCAAGTTTTCTCCACCTCAGTCCACCACACCCAGGGCACTCTATTCTCAGCCCCGCCCCAGCCCCAGCCTCAACCTCAA
 ACTCAGCTGCAACAACAGACGGTAATGATCAGCACAACATTCAGCACCACTCGCAGACGAGGATCATCCAGCAGCCTTTGATATACCAAGATGCAGC
 TACTAGCTTCAAGTCTTACGCTCAAGTCCAAGCCTGGTACATCCTCCAGGTACAGCCGTCACCATTCAGCAGCAGGTGCAGACGATACAGG
 CCCAGCGGTGCTGACACAAACGGCAATGGCAGCTGCAGACCCTGCCCCGGTACGGTGCAGACAGTTGCTGCGCCACAGGTGCAGCAGTCCC
 GGCTCTGGTCCAGCCTCAGATCATCAAGCAGATTCCCTGTTTTGACCACACTGAAGCAGATGGCAGCCCTGTTATGGCTCGGTCAGAACCCGG
 CCCTACCCGCCCTCACCACCCCTATCCAGACGGCTGCCCTTCAAGTACCAACCTGGTGGGCAGCAGTGGGACCATTCTGACCACAATGCCTGTAATGA
 TGGGGCAAGAGAAAGTGCCATTAAGCAGTACCTGGGGGAGTCAAGCAGCTTGAGCCCCAAAGAAGGAGAAAGCGGCAACCCATAATATC
 ATTGAGAAACGATATCGCTCCTCCATCAATGACAAAATCATGAAATTGAAAGACTGGTATGGGGACAGACGCAAGATGCACAAGTCTGGCGTTCT
 GAGGAAGGCCATTGATTACATCAAACTTGCAGCAGGTCAATCATAAATGCGCCAGGAGAACATGGTGTGAAGCTGGCAAATCAAAGAACA
 GCTTCTAAAGGGCATGCACCTAGGAGTCTGGTGGACAATGAGTGGACCTGAAGATCGAGGACTTAAATCAGAATGTCCTTCTGATGTCACCCCA
 GCCCTGACTCAGGGTCCAGGCTGGCTTCTCCCTACTCCATTGACTCTGAGCCAGGAAGCCCTTATTGGATGATGCAAAGGTCAAAGATGAGCC
 AGACTCTCCTCTGTGGCGCTGGCATG**GTCGAC**GCGTCTGCAGAAGCTTCTAGATAAGTAATGATCATAATCAGCCATACCACATTTGTAGAGGTTT
 TACTTGCTTTAAAAAACCTCCACACCTCCCTGAACCTGAAACATAAAATGAATGCAATTTGTTGTTGTTAACTGTTTATTGACGCTTAAATGGTTA
 CAAATAAAGCAATAGCATCACAATTTCAAATAAAGCATTTTTTCACTGCATTCTAGTTGTGGTTTGTCCAACTCATCAATGTATCTTATCATGTCT
 GGATCTGCCGGTCTCCCTATAGTAGTGTATTAATTTGATAAGCCAGGTTAACCTGCATTAATGAATCGGCCAACCGCGGGGAGAGGCGGTTTG
 CGTATTGGGCGCTTCCGCTTCTCGCTCACTGACTCGCTCGGCTCGGCTCGGCTCGGCGAGCGGTATCAGCTCACTCAAAGCGGTAATACG
 GTTATCCACAGAATCAGGGGATAACGCAGGAAAGAACATGTGAGCAAAAGCCAGCAAAAGGCCAGAACCGTAAAAAGCCGCTTGTGCTGCGCT

TTTTCCATAGGCTCCGCCCCCTGACGAGCATCACAAAAATCGACGCTCAAGTCAGAGGTGGCGAAACCCGACAGGACTATAAGATACCAGGCGTTT
CCCCTGGAAGCTCCCTCGTGCCTCTCTGTTCCGACCCTGCCGTTACCGGATACCTGTCCGCTTTCTCCCTTCGGGAAGCGTGGCGCTTTCTCAAT
GCTCACGCTGTAGGTATCTCAGTTCGGTGTAGGTCGTTCCGCTCCAAGCTGGGCTGTGTGCACGAACCCCGTTTCAGCCCGACCGCTGCGCCTTATCC
GGTAACTATCGTCTTGAGTCCAACCCGGTAAGACACGACTTATCGCCACTGGCAGCAGCCACTGGTAACAGGATTAGCAGAGCGAGGTATGTAGGCG
GTGCTACAGAGTCTTGAAGTGGTGGCTAACTACGGCTACACTAGAAGGACAGTATTTGGTATCTGCGCTCTGCTGAAGCCAGTTACCTTCGGAAAA
AGAGTTGGTAGCTCTTGATCCGGCAAACAACCCCGCTGGTAGCGGTGTTTTTTTTGTTTGAAGCAGCAGATTACGCGCAGAAAAAAGGATCTC
AAGAAGATCCTTTGATCTTTCTACGGGGTCTGACGCTCAGTGGAAACGAAAACCTCACGTTAAGGGATTTTGGTCATGAGATTATCAAAAAGGATCTTC
ACCTAGATCCTTTAAATTAATAAATGAAGTTTTAAATCAATCTAAAGTATATAGTAAACTTGGTCTGACAGTTACCAATGCTTAATCAGTGAGGCA
CCTATCTCAGCGATCTGTCTATTTTCGTTCCATAGTTGCCTGACTCCCGCTCGTGTAGATAACTACGATACGGGAGGGCTTACCATCTGGCCCCAGT
GCTGCAATGATACCGCGAGACCACGCTCACC GGCTCCAGATTTATCAGCAATAAACCCAGCCAGCCGGAAGGGCCGAGCGCAGAAAGTGGTCCTGCAA
CTTTATCCGCTCCATCCAGTCTATTAATTGTTGCCGGGAAGCTAGAGTAAGTAGTTCCGCCAGTTAATAGTTTGCAGAACGTTGTTGCCATTGCTACAG
GCATCGTGGTGTGACGCTCGTCGTTTGGTATGGCTTCATTGAGCTCCGGTTCACCAAGTCAAGGCGAGTTACATGATCCCCATGTTGTGCAAAAA
GCGGTTAGCTCCTTCGGTCTCCGATCGTTGTCAGAAGTAAGTTGGCCGAGTGTATCACTCATGGTTATGGCAGCACTGCATAATTCTTACTGTCT
ATGCCATCCGTAAGATGCTTTTCTGTGACTGGTGAGTACTCAACCAAGTCACTTCTGAGAATAGTGTATGCGGCGACCGAGTTGCTTTCGCCGGCGTC
AATACGGGATAATACCGGCCACATAGCAGAACTTTAAAAGTGTCTCATCATTGAAAAACGTTCTTCGGGGCGAAAACTCAAGGATCTTACCCTGT
TGAGATCCAGTTCGATGTAACCCACTCGTGACCCAACTGATCTTACGATCTTTACTTTTACCAGCGTTTCTGGGTGAGCAAAAAACGGAAGGCAAA
ATGCCGAAAAAAGGGAATAAGGGCGACACGGAAATGTTGAATACTCATACTCTTCTTTTCAATATTATTGAAGCATTATCAGGGTTATTGTCTCA
TGAGCGGATACATATTTGAATGATTTAGAAAAATAACAATAGGGGTTCCGCGCACATTTCCCGAAAAGTGCCACCTGACGTCTAAGAAACCAT
ATTATCATGACATTAACCTATAAAAAATAGGCGTATCACGAGGCCCTTTTCGCTCGCGCTTTTCGGTGATGACGGTAAAAACCTTGACACATGCAGCTC
CCGGAGACGGTCACAGCTTGTCTGTAAGCGGATGCCGGGAGCAGACAAGCCCGTCAGGGCGCTCAGCGGGTGTGGCGGGTGTGGGGCTGGCT
TAACTATGCGGCATCAGAGCAGATTGACTGAGAGTGCACCATATGGACATATTGCTGTTAGAACGCGGCTACAATTAATACATAACCT

mCherry SREBP-2(Mut)-HA(N)-pcDNA3



>mCherry-SREBP-2-S436A-HA(N)-pcDNA3 Amino Acid Coding Sequence

MVSKGEEDNMAIIEKFMRFKVMHEGVSNGHEFEIEGEGEGRPYEGTQTAKLKVTKGGPLPFAWDILSPQFMYGSKAYVKHPADIPDYLKLSFPEGFKWERY
 MNFEDGGVVTVTQDSSLQDGEFIYKVKLRGTNFPSDGPMQKKTMGWEASSERMYPEDGALKGEIKRRLKLDGGHYDAEVKTTYKAKKPVQLPGAYNV
 NIKLDITSHNEDYIVEQYERAEGRHSTGGMDELYKEF**MYPYDVPDYA**ETLTELGDLETLGDIDEMLQFVSNQVGFPPDLFSEQLCSSFPGSGGSSSSSSSSG
 SSSSSSNGRSGSSGAVDPSPVQSRFTQVTLPSFSPSAASPQAPTLQVKVSPVTPTRATPILQPRPQPQPQPTLQQLQQTVMITPTSTTPQTRIIQQLPIYQ
 NAATSFQVLQPQVQLVTSQQVPTIQQQVQVQAQRVLTQTANGTLQLTAPATVQTVAAAPVQVQVPLVLPQPIKHTDSLVLTLTKDGSPPVMAAVQN
 PALTALTPICQTAALQVPTLVGSSGTLTTPMVMMGQEKVPIKQVPGVQKLEPPKEGERRTTHNIEKRYRSSINDKIELKDLVMGTDAMHKSGVLRKAID
 YIKYLQVNHKLRQENMVLKANQNKLLKIDGLSLVDNEVDLKIENFNQVLLMSPPAADSGSQAGFSPYSIDSEPGSPLLDDAKVDEPDSPVALGMV
 DRSRILLCVLTLFCLSNPLTSLQWGGAHDSQHPHSGSGRSVLSFESGSGGWFDMMPPTLLLWLNVGVIVLVSFVKLLVHGEPVIRPHSRSSVTFWRHR
 KQADLDLARGDFAAAAGNLQTLAVLGRALPTSRDLACLSLWNVIRYSLQKRLRVRLLKKVFCRRATPATEAGFEDEAKTSARDAALAYHRLHLQHLITG
 KLPAGSACSDVHMALCAVNLAECAEEKIPPSTLVEIHLTAAMGLKTRCGGKLGFLASYFLSRAQSLCGPEHSVAPDLSRLWLCHPLGQKFFMERSWSVSKAAK
 ESLYCAQRNPADPIAQVHQAFCKNLLERAIESLVKPAKAKKAGDQEEESCFSSALEYKLLHSFVDSVGVMSPPLSRSSVLKLSALGPDICRWWTSAITVAIS
 WLQGDAAVRSHTKVERIPKALEVTEPLVKAIFHACRAMHASLPGKADGQSSFCHERASGHLWSSLNVSGATSDPALNHVQLLTDLLSLRALTALW
 QKQASASQAVGETYHASGAELAGFQRDLGSLRRLAHSFRPAYRKVFLHEATVRLMAGASPTRTHQLLEHSLRRRTTQSTKHGEVDAWPGQRERATAILLAC
 RHLPLSFLSSPQRAVLLAEARTLEKVGDRRSCNDCQMQMIVKLGGGTAIAAS

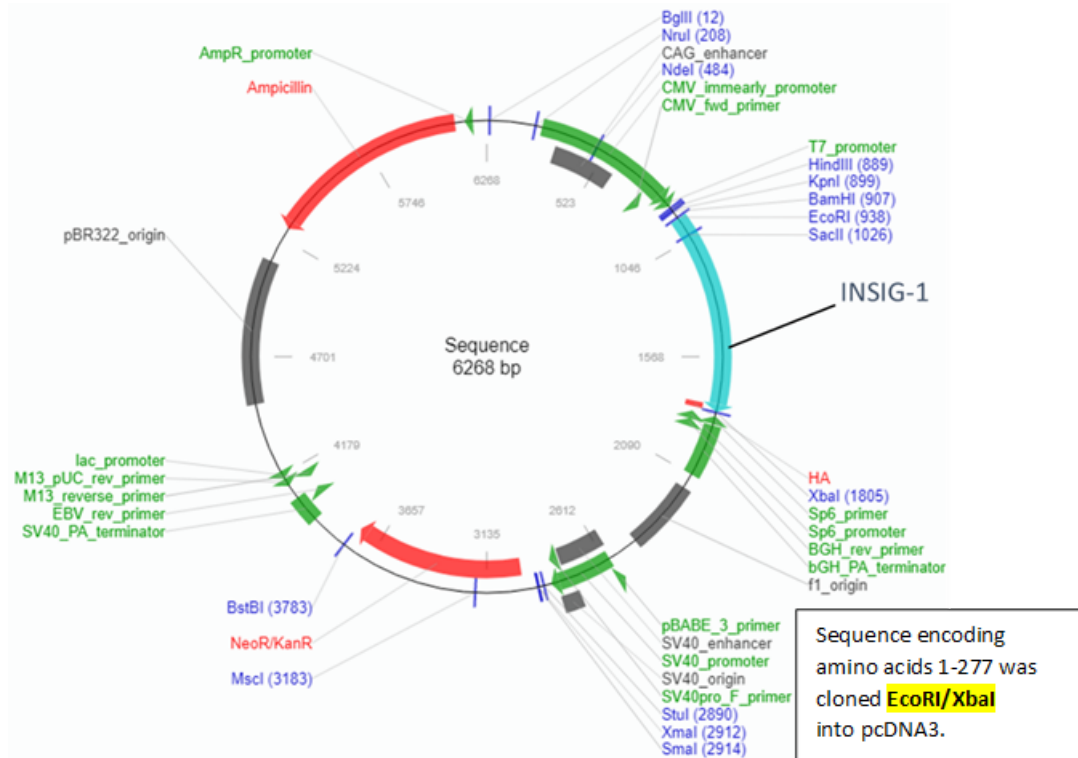
>mCherry-SREBP-2-S436A-HA(N)-pcDNA3 Plasmid Sequence

GACGGATCGGGAGATCTCCCGATCCCTATGGTGCAGTCTCAGTACAATCTGCTCTGATGCCGCATAGTTAAGCCAGTATCTGCTCCCTGCTGTGTGT
 TGGAGTGCCTGAGTAGTGCCGAGCAAAATTAAGCTACAACAAGGCAAGGCTTGACCGACAATTGCATGAAGAATCTGCTTAGGGTTAGCGCTTT
 TGCGCTGCTTCGCGATGACGCGCCAGATATACGCGTTGACATTGATTATTGACTAGTTAATAGTAATCAATTAATAGTAACTATTAGTTCATAGCCC
 ATATATGGAGTTCGCGTTACATAACTACGGTAAATGGCCCGCTGGCTGACCGCCCAACGACCCCGCCATTGACGTCAATAATGACGTATGTTCC
 CATAGTAACGCCAATAGGGACTTCCATTGACGTCAATGGGTGGACTATTTACGGTAAACTGCCCACTGGCAGTACATCAAGTGATCATATGCCAA
 GTACGCCCTATTGACGTCAATGACGGTAAATGGCCCGCTGGCATTATGCCAGTACATGACCTTATGGGACTTCTACTTGGCAGTACATCTACG
 TATTAGTCATCGCTATTACCATGGTATGCGGTTTTGGCAGTACATCAATGGGCGTGGATAGCGGTTGACTCACGGGGATTCCAAGTCTCCACCCC
 ATTGACGTCAATGGGAGTTTTGTTTGGCACAAATCAACGGGACTTCCAAAATGTCGTAACAACCTCCGCCATTGACGCAATGGCGGTAGGCCG
 TGTACGGTGGGAGGTCTATATAAGCAGAGCTCTCGGCTAAGTACAGAGAACCCACTGCTTACTGGCTTATCGAAATTAATACGACTCACTATAGGGAGA
 CCAAAGCTTGGTACCGAGCTCGGATCCATGGTGAGCAAGGGCGAGGAGGATAACATGGCCATCATCAAGGAGTTCATGCGCTTCAAGGTGCACATG
 GAGGGCTCCGTGAACGCCACGAGTTTCGAGATCGAGGGCGAGGGCGAGGGCCGCCCTACGAGGGCACCAGACCGCAAGCTGAAGGTGACCAA
 GGGTGGCCCTCGCTTGCCTGGGACATCCTGCTCCCTCAGTTCATGTACGGCTCCAAGGCTACGTGAAGCACCAGCCGACATCCCGACTACTT
 GAAGCTGCTTCCCGAGGGCTTCAAGTGGGAGCGCGTGTGAACTGTACGAGGCGGGCGTGGTACCGTACCCAGACTCCCTCCCTGCAGGA
 CGCGAGTTCATCTACAAGGTGAAGTGCAGCGCACCAACTTCCCTCCGACGGCCCGTAATGCAGAAGAAGACCATGGGCTGGGAGGCTCCTCC

GAGCGGATGATCCCGGAGGACGGCCCTGAAGGGCGAGATCAAGCAGAGGCTGAAGTGAAGGACGGCGGCCACTACGACGCTGAGGTCAAGAC
CACCTACAAGGCCAAGAAGCCGTGCAGTGCCTCCGCGCCTACAACGTCAACATCAAGTTGGACATCACCTCCCAACAGGACTACACCTCGTG
GAACAGTACGAACCGCGGAGGGCCGCACTCCACGGCGCATGGACGAGTGTACAAGGAATTCATGTACCCATACAGATGTTCCAGATTACCGG
GAGACCCACGAGGCTGGGCGACGAGTACCCTGGGAGACATCGACGAGATGCTGCAATTTGTCAGTAATCAAGTGGGAGAGTTCCTGACTTGT
TTTCAGAAGCAGCTGTGTAGCTCTTTCTGGCAGTGGTGTAGTGGTAGCAGCAGCGGAGCAGTGGCAGCAGCAGCAGCAGCAATGGCAGGG
GCAGCAGCAGCGGAGCTGTGGACCTTCAGTGCAACGGTCAATCACCCAGGTACATTACCTTCTCTCTCCCTGGCGGCCTCCCAACAGGCTCAA
CTCTGCAAGTCAAGGTTTCTCCACCTCAGTTCACCCACACCCAGGGCACTCTATTCTTCCAGCCCCCCCCAGCCCCAGCCTCAACCTCAAATCA
GCTGCAACAACAGACGTAATGATCACGCCAACATTACAGCACCCTCCGAGACGAGGATCATCCAGCAGCTTTGATATACCAGAATGCAGTACTA
GCTTTCAAGTCTTTCAGCCTCAAGTCCAAAGCCTGGTGACATCTCCAGGTACAGCGGTACCATTACGACAGCAGGTGCAGACAGTACAGGCCAG
CGGGTGTGACACAAACGGCCAAATGGCAGCTGCAGACCTTCCCGGCTACGGTGCAGACAGTTGCTGCCACAGGTGCAGCAGTCCCGTGC
CTGGTCCAGCCTCAGATCATCAAGACAGATTCCCTTGTGTTGACCCACTGAAGACAGATGGCAGCCCTGTTATGGCTGCGGTCCAGAACCCGGCCCT
CACCGCCCTCACCACCCCTATCCAGACGGTGCCTTCAAGTACCAACCTGGTGGGACGAGTGGGACCATTCTGACCAATGCCTGTAATGATGG
GGCAAGGATAAGTGGTCCATTAAAGCAGGTACCTGGGGAGTCAACAGCAGCTTCCAGCCCCAAAGAAGGAGAAACCAACCTAATATCATTTG
AGAAACGATATCGCTCTCCATCAATGACAAAATCATCGAATTGAAAGACCTGGTGCATGGGGACAGACGCCAAGATGCACAAGTCTGGCTTCTGAG
GAAGGCCATTGATTACATAAATACTTGACGAGGTCAATCATAAAGTGCAGGAGAACATGGTGTGAAGTGGCAATCAAAGAACAAGCTT
CTAAAGGGATCGACCTAGGCAGTCTGGTGGACAATGAGGTGGACTGAAGATCGAGGACTTAAATCAGAATGCCTTCTGATGTCCCCCAGCCG
CTGACTCAGGGTCCCAGGCTGGCTTCTCTCTACTCCATTGACTCTGAGCCAGGAAGCCCTTATTGGATGATGAAAGGTCAAAGATGAGCCAGAC
TCTCTCTGTGGCGCTGGCATGGTGCAGCCCTCAGGATTTCTGTGTCTCCTCCTCTCTGTCTTAAACCCCTGACTTCCCTGACTGCTGCA
GTGGGAGGGGCCACGACTGACCCAGCACCACACTCAGGCTCTGGCCGACAGTCTCTGTATTCCAGTTCAGTTCTGGGGCTGGTTTGTACTGG
ATGATGCCTACTTCTCTTATGGCTGTAATGGTGTGATTGCTGAGCGTCTTTGTGAAGTGTGGTTCATGGGGAGCCAGTATCCGGCCACA
CTCGCGCTCTCGGTACCTTCTGGAGGCACCGAAACAGGCAGATCTGGATCTCGCCAGAGGAGATTTTGCAGCTGCTGCCGGCAACCTACAACT
GCCTGGCAGTTTTGGCCGGGCACTGCCACCTCCCGCTGGACCTGGCTGCAGCTCTCTGGAACTGTATCCGTACAGCTGCAGAAGTACGC
CTGGTGGCTGGTGTCAAGAAAGTCTCCAGTCCCGGGGGCCACGCCAGCCTGAGGCAGGCTTTGAAGCAGAACTAAGACCAGCCGCGCG
GATCGGGCTGTGGCTTACCAGCTGCACAGCTGCACATCAACAGGAAAGCTTCCAGAGATCCGCTGTGGGAGTACACATGGCTTGTGTGC
CGTGAACCTGGTGAATGTGCAGAGGAGAAGATCCACCCAGCAGACTGGTGTGATCCATCTGACTGCTGCCATGGGGCTCAAGACCCGGTGTGG
AGGCAAGCTGGGCTTCTGGCCAGTACTTCTCAGCCGAGCCAGAGCTGTGTGGCCCGAGCAGTGTCTGCTGACTCCCTGCGTGGCTCT
GCCACCCCTGGCCAGAAAGTTTTATGAGGCGGAGCTGGTCTGGAAGTCACTGCAAGGAGAGTCTATACTGTGCCAGAGAAACCCAGCTGA
CCCCATTGCGCAGGTCACCAAGGCTTCTGCAAGAAGCTGCTGGAGCGAGCTATAGAGTCTTGGTGAACCTCAGGCCAAGAAGAGGCTGGAGAC
CAGGAAGAAGAGAGCTGTGAATTCAGTTCACAGTCTGGAGTACTTAAATTAATTCATCTTTTGTGGACTCTGTGGGGGTTATGACCCCCACTCTC
AGGAGTCCGTGCTCAAGTCCGCTGGGTCCAGACATCATCTGTGGTGGTGGACGCTGCAATCACTGTGGCCATCAGTGGTCCAGGGAGACG
ATGCAGTGTGCGCTCATTTTTACAAAGTGAACGCATCCCAAGGCCCTGGAAGTGCAGAGAGCCCTGGTGAAGGCCATCTTCCATGCCTGC
AGAGCATTGATGCTCACTCCCTGGGAAAGCAGATGGCAGCAGAGTTCCTTCTGCCATTGCGAGAGGGCAGTGGCCACCTATGGAGCAGCTCA
ACGTGAGTGGGGCCACTGACCCCTGCCCTCAACCAGTGGTCCAGTGTCTCACCTGTGACTGTACTGTGCTACGGACAGCGCTGTGGCAAAA
CAGGCCAGTCCAGCAGCTGTGGGGAGACCTACCACGCTCAGCCGCTGAACTGGCGGGTTCAACGGAGCTGGGCAGCTCCGAGCT
GGCACACAGTCTCGCCAGCATAACCGAAGTGTCTGATGAAGCCAGTGGCTGCGCTGATGGCAGGAGCCACCCAGCCACCCAGCAGCTG
CTGGAACACAGCTGCGGCGGCGCACCCAGCAGACCAAGCAGGAGAGTGGATGCTGGCCGGCCAGCAGAGCGGGCCACCCGATCCT
GCTGGCTGCGCCACCTGCCCTCTCTCTCTCCCGGGCCAGCGGGCAGTGTGCTGGCCGAAGTGCAGCCGACCTGGAGAAAGTGGG
GACCGGGCTCTGCAACGACTGCCAGCAGATGATTGTAAGCTGGTGGTGGCACTGCCATTGCCCTCTGACACCAGGCTCAGCCACCCCTC
CACTCTCTCCGATTTCTAGAGGGCCCTATTTATAGTGTCACTAAATGTAGAGCTCGTGTATCAGCTCGACTGTGCTTCTAGTGTCCAGCCA
TGTGTTGTTTCCGCTCCCGTCCCTTCTTCCAGTGGAAAGTGCACCTCCACTGCTCTTCTTCTTAAATAAATAAGGAAATGATCGCTGATCTGA
GTAGGTGTCATTCTTCTGGGGGTGGGGTGGGGCAGGACAGCAAGGGGGAGGATTGGGAAGACAATAGCAGGCATGCTGGGGATGCGGTGGG
CTCTATGGCTTCTGAGCGGAAAGAACAGCTGGGGCTTAGGGGTATCCACGCGCCCTGTAGCGGCGCATTAGCGCGCGGGTGTGGTGGT
TACCGCAGCGTACCGCTCACTTGGCAGCGCCTAGCGCCGCTCTTTCGCTTCTTCCCTCTTCTGCCACGTTGCGCGGCTTCCCGCTCAA
GCTCTAAATCGGGGATCCCTTTAGGGTTCGATTTAGTGTCTTACGGCACCTCGACCCAAAAAATTGATTAGGGTGTGTTACAGTGTGGCC
ATCGCCCTGATAGACGGTTTTTGCCCCCTTGGAGTGGAGTCCAGCTTCTTAAATAGTGGACTTGTGTTCAAACCTGAAACAACACTAACCTGTG
GTCTATTCTTTGATTATAAGGGATTTTGGGATTTGCGCTATTGTTAAAAAATGAGCTGATTAAACAAAAATTAACCGCAATTAATCTGTGGA
ATGTGTGTCAGTTAGGGTGTGAAAGTCCCAGGCTCCCAGGCAGGAGAAGTATGCAAGCATGCATCTCAATAGTACAGCAACAGGTGTGGAA
AGTCCCCAGGCTCCCCAGCAGGAGAGATGCAAGCATGCATCTCAATAGTACAGCAACCATAGTCCCGCCCTAACTCCGCCATCCCGCCCTAA
CTCCGCCAGTTCGCCCCATTCTCGCCCCATGGTACTAATTTTTTATTATGCAGAGGCGGAGGCCGCTCTGCTGTGAGTATCCAGAAGTA
TGGAGGAGCTTTTTGAGGCGCTAGGCTTTTGAAGAAAGTCCCGGGAGCTGTATATCCATTTTCGATCTGATCAAGAGACAGGATGAGGATG
TTTCGATGATTGAACAAAGTGGATTGCACGAGGTTCTCGCGGCTTGGTGGAGAGGCTATTGCGCTATGACTGGCACAAGACATGCGCT
GCTGATGCGCGGTTCCGGCTGTACGCGCAGGGGCGCCGCTTCTTTTGTCAAGACCGACTGTCGGTGCCTGAATGAAGTGCAGGACGA
GGCAGCGCGGCTATCGTGTGCTGCCAGCGGCGTTCCTTGCAGCTGTGCTGACGTTGTCAAGCGGAAAGGACTGGCTGCTATTGGG
CGAAGTCCGGGGCAGGATCTCTGTATCTACCTTGTCTGCGGAGAAAGTATCCATCATGGCTGATGCAATGCGGGGCTGCATACGCTTGTG
CGGCTACCTGCCATTCGACCACAAGCGAAACATCGCATCGAGCGAGCAGTACTCGGATGGAAGCCGGTCTTGTGATCAGGATGATGAGCA
AGAGCATCAGGGGCTCGCGCCAGCCGAAGTTCGCCAGGCTCAAGGGCGCATGCCCGACGCGAGGATCTGCTGTTGACCCATGGCGATGCTG
CTTGGCAATATCATGGTGGAAAATGGCCGCTTTTCTGGATTATCGACTGTGGCCGGTGGTGTGGCGGACCGCTATCAGGACATAGCGTTGGCT
ACCCGTGATATTGCTGAAGAGCTTGGCGGGAATGGGCTGACCGCTTCTCGTGTACGGTATCGCGCTCCGATTGCGAGCGCATCGCTTCTAT
CGCTTCTTACGAGTTCCTTGTAGCGGGACTCTGGGGTTCGAAATGACCGACCAAGCGACGCCAACCTGCCATCAGGATTTGATTCCACCGCC
GCCTTCTATGAAGGTTGGGCTCGGAATCGTTTTCCGGGACCGGGCTGGATGATCTCCAGCGCGGGATCTCATGCTGGAGTCTTCCGCCACCC
CAACTGTTTTATTGACGCTTATAATGTTTACAAAATAAAGCAATAGCATCAAAATTTTCAAAATAAAGCAATTTTTTCACTGATTGATGTTGGTTTTG
TCAAACCTCATCAATGTATCTTATCATGTCTGTATACCGTGCACCTCTAGTACAGCTTGGCGTAATCATGGTTCATAGCTTTCTGTGTGAAATGTT
ATCCGCTCACAATCCACACAACATACGAGCCGGAAGCATAAAGTGTAAAGCCTGGGGTGCCTAATGAGTGTGACTAATCACATTAATGCGTTGCGC
TACTGCCCGCTTCCAGTCCGGAAACCTGTGCTGCCAGTGCATTAATGAATCGCCAAACGCGCGGGAGAGGGGTTTTGCGTATTGGGCGCTCT
CCGCTTCTCGCTACTGACTCGCTGCGCTCGGTCTGGCTGCGGCGAGCGGATCAGCTCACTCAAAGCGGTAATACGGTTATCCACAGAATCA
GGGATAACGAGAAAGAAACATGTGAGCAAAAGGCCAGCAAAAGGCCAGAAACCTGAAAGAGCCGCTTGTGGCTTTTTCCATAGGCTCCGC
CCCCGACGAGCATCAAAAATCGACGCTCAAGTCAGAGTGGCGGAAACCCGACAGGACTATAAAGATAACCAAGGCTTTTTCCCTGGAAGTCCC
TCGTGCGCTCTCTGTTCCGACCTGCGCTTACCGGATACCTGTCGCTTCTCCCTTCCGGAAGCGTGGCGCTTCTCAATGCTCACGCTGTAGGTA
TCTCAGTTCGGTGTAGTGTCTTCCCTCAAGCTGGGCTGTGTGACGAACCCCGCTTACGCCGACCGCTGCGCTTATCCGGTAACATATCGTCTTGA
GTCCAACCCGGTAAGACAGGACTTATCGCACTGGCAGCAGCAGTGTAAACAGGATAGCAGAGCGAGGATGTAGGGCGTGTACAGAGTCTTG
AAGTGGTGGCTAAGTACGCTACTAGAAAGCAGTATTTGGTATCTGCGCTGCTGAAAGCAGTACCTTCCGAAAAGAGTTGGTAGCTCTTG
ATCCGGCAAAACAAACCCGCTGGTAGCGGTGTTTTTTTTGTAAGCAGCAGGATTAACGCGCAGAAAAAGGATCTCAAGAAAGATCTTCTGATCT
TTTCTACGGGCTGACGCTCAGTGAACGAAAACCTCACGTTAAGGGATTTTGGTGCATGAGATTCAAAAAGGATCTTACCTAGATCTTTAAAT

AAAAATGAAGTTTTAAATCAATCTAAAGTATATATGAGTAAACTTGGTCTGACAGTTACCAATGCTTAATCAGTGAGGCACCTATCTCAGCGATCTGTC
TATTTTCGTTCCATAGTTGCCTGACTCCCCGTCGTGTAGATAACTACGATACGGGAGGGCTTACCATCTGGCCCCAGTGCTGCAATGATACCGCGAG
ACCCACGCTCACCGGCTCCAGATTTATCAGCAATAAACCCAGCCAGCCGGAAGGGCCGAGCGCAGAAAGTGGTCTGCAACTTTATCCGCCTCCATCCAG
TCTATTAATTGTTGCCGGGAAGCTAGAGTAAGTAGTTCGCCAGTTAATAGTTTGCAGCACTGTTGTTGCCATTGCTACAGGCATCGTGGTGTACCGCTC
GTCGTTTGGTATGGCTTCATTAGCTCCGGTTCCAACGATCAAGGGCAGTTACATGATCCCCATGTTGTGCAAAAAAGCGGTTAGCTCCTTCGGTCC
TCCGATCGTTGTCAGAAGTAAGTTGGCCGAGTGTATCACTCATGGTTATGGCAGCACTGCATAATTCTTACTGTATGCCATCCGTAAGATGCTT
TTCTGTGACTGGTGAGTACTCAACCAAGTCATTCTGAGAATAGTGTATGCGGGCAGCCGAGTTGCTCTTGCCCGGCGTCAATACGGGATAATACCGCGC
CACATAGCAGAACTTTAAAAAGTCTCATCATTGGAAAACGTTCTTCGGGGCGAAAACCTCAAGGATCTTACCCTGTTGAGATCCAGTTCGATGTAA
CCCACTCGTGCACCCAACTGATCTTCAGCATCTTTTACTTTACCAGCGTTTCTGGGTGAGCAAAAACAGGAAGGCAAAATGCCGAAAAAAGGGAAT
AAGGGCGACACGGAAATGTTGAATACTCATACTTCTTTTTCAATATTATTGAAGCATTTATCAGGGTATTGTCTCATGAGCGGATACATTTGA
ATGTATTTAGAAAAATAAACAAATAGGGGTTCCGCGCACATTTCCCGAAAAAGTGCCACCTGACGTC

INSIG-1-HA(C)-pcDNA3



>INSIG-1-HA(C)-pcDNA3 Amino Acid Coding Sequence

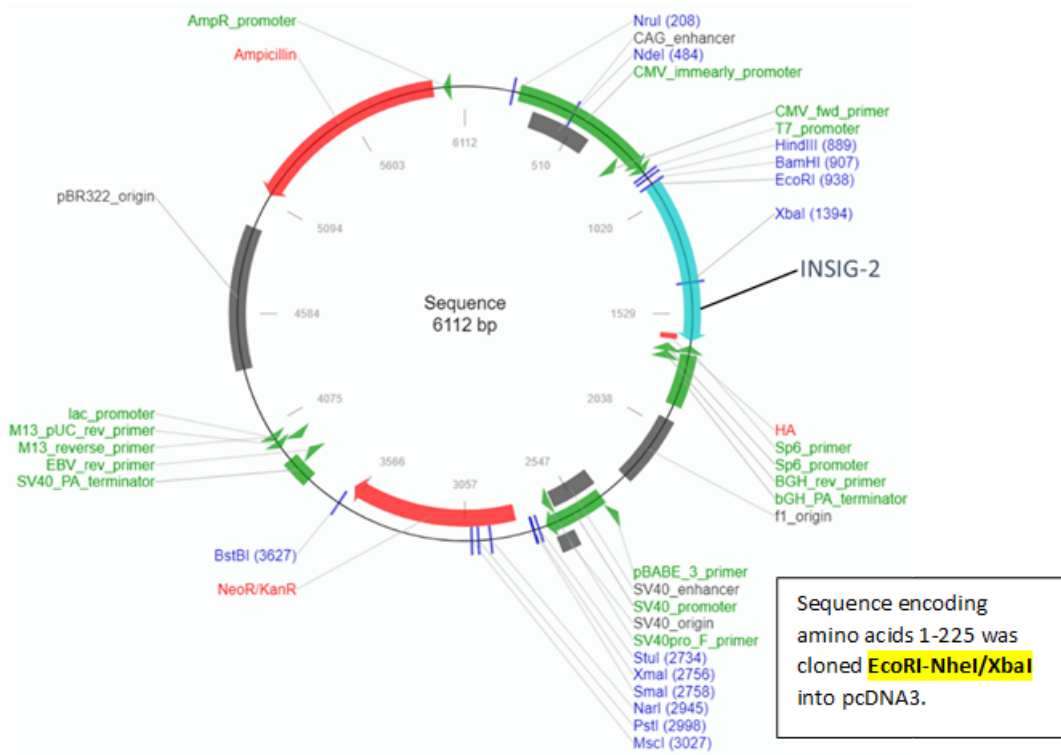
MPRLHDHFWSCSAHSARRRPPRASAAGLAALKVGEINVSVSGPSLLAAHGAPDADPAPRGRSAAMSGPEPGSPYPNTWVHRRLLQSRSLVLSVGVVLA
 LVLNLLQIQNRVTLFPEEVIATIFSSAWVVPCCGTAADVLLYPCIDSHLGEPHKFKREWASVMRCIAVFGVINHASAKLDFANNVQLSLTLAALSGLLW
 WTFDRSRSLGLGITIAFLATLITQFLVYNGVYQYTPDFLYIRSWLPCIFFSGGVTVGNIGRQLAMGVPEKPHSD**YPYDVPDYA**

>INSIG-1-HA(C)-pcDNA3 Plasmid Sequence

GACGGATCGGAGAGTCTCCCGATCCCTATGGTGCAGTCTCAGTACAATCTGCTCTGATGCCGCATAGTTAAGCCAGTATCTGCTCCCTGTTGTGTG
 TGGAGGTCGCTGAGTAGTGCGCGAGCAAAATTAAGCTACAACAAGGCAAGGCTTACCAGACAATTGCATGAAGAATCTGCTTAGGGTTAGGCGTTT
 TGGCGTCTTCGCGATGTACGGGCCAGATATACGCGTTGACATTGATTATTGACTAGTTATTAATAGTAATCAATTACGGGGTATTGTTTCATAGCCC
 ATATATGGAGTCCCGCTTACATAACTTACGGTAAATGGCCCGCTGGCTGACCGCCCAACGACCCCGCCATTGACGTCATAAATGACGTATGTTCC
 CATAGTAACGCCAATAGGGACTTTCATTGACGTCAATGGGTGGACTATTTACGGTAAACTGCCACTTGGCAGTACATCAAGTGTATCATATGCCAA
 GTACGCCCTATTGACGTCATGACGGTAAATGGCCCGCTGGCATTATGCCAGTACATGACCTTATGGGACTTTCCTACTTGGCAGTACATCTACG
 TATTAGTCATCGCTATTACCATGGTGTGCGGTTTTGGCAGTACATCAATGGCGTGGATAGCGGTTTGAATCAGCGGGATTTCCAAGTCTCCACCCC
 ATTGACGTCATGGGAGTTTGTGGCACAAAATCAACGGGACTTTCAAAATGTCGTAACAACCTCCGCCATTGACGCAATGGGCGGTAGGCG
 TGTACGGTGGGAGGTCTATATAAGCAGAGCTCTCTGGCTAATAGAGAACCCTACTGTTACTGGCTTATCGAAATTAATACGACTCACTATAGGGAGA
 CCAAAGTGGTACCGAGCTCGGATCCACTAGTAACGGCCGCAAGTGTGCTG**GAATTC**ATGCCAGATTGCACGACCACTTCTGGAGCTGCTCCTGTG
 CGCACAGCGGAGGGCGCCGAGGCCCGCGAGCCAGCCGCGGGGCTGGCGGCAAGGTTGGGAGATGATCAACGTTCCGTTCCCGGGCC
 TCCCTGCTGGCGCCACGGTGCCTCGGACGCTGACCCCGCCAGGGGCGCAGTGTGCGATGAGCGCCCGCCAGCCCGGACGCCCTACCCC
 AACACCTGGCATCATCGCTGTTGCAGAGGAGCCTCGTCTCTTCTCGGTTGGGTTGGTCTAGCCCTGGTCTCAACTGCTGCAGATCCAGAGGAA
 TGCTACTCTTCCCGAGGAGGTGATCGCCACCCTTTTCTCGCCTGGTGGTCCCTCCCTGCTGCGGGACAGCAGCTGCTGTTGTTGGCTACT
 GTACCCCTGTATCGACAGTCACTCGGAGAACCCACAAATTAAGAGAGAATGGGCCAGTGTATGCGCTGCATAGCAGTTTTTGTGGCATTAAAC
 ACGCCAGTCTAAATGGATTTGCCAATAATGTCAGCTGTCCTTACTTATAGCAGCCTATCTTGGGCTTTGGTGGACATTTGATCGTTCCAGAA
 GTGGCCTTGGGCTGGGATCACCATAGCTTTTCTAGCTACGCTGATCAGCAGTTTTCTCGTGTATAATGGTGTCTACAGTATACATCCCCAGATTTCT
 CTATATTCGTTCTGGCTCCCTTGTATATTTTCTCAGGAGGCGTACGGTGGGGAACATAGGACGACAGTTAGCTATGGGTGTTCTGAAAAGCCCCA
TAGTGATTACCCATACGATGTTCCAGATTACGCTTGA**CTAGA**AGGCCCTATTCTATAGTGTACCTAAATGCTAGAGCTCGCTGATCAGCTCGACT
 GTGCCTTCTAGTTGCCAGCATCTGTTGTTGGCCCTCCCGTGCCTTCTTACCTGGAAGGTGCCACTCCCACTGCTCTTCTAATAAAATGAGG
 AAATTGCATCGCATTGTCTGAGTAGGTGTCATTCTATTCTGGGGGTGGGGTGGGGCAGGACAGCAAGGGGAGGATTGGGAAGACAATAGCAGG
 CATGCTGGGATGGGCTATGGCTTCTAGGGCGAAAGAACACAGTGGGGCTTACGGGGTATCCCCACGCTTCCAGCCCTGTAGCGGCGCATT
 AGCGCGGCGGTTGGTGGTTACGCGCAGCGTACCCTACACTTGCACGCGCCTAGCGCCGCTCTTTCGTTTCTTCTTCTTCTCGCCACG
 TTCGCGGCTTCCCGTCAAGCTCTAAATCGGGCATCCCTTAGGGTCCGATTTAGTGTCTTACGGCACCTGACCCCAAAAAACTTGATTAGGGT
 GATGGTTACAGTGTGGCCATCGCCTGATAGACGTTTTTTCGCTTGTGAGCTTGGAGTCCACGTTCTTAATAGTGGACTCTGTTCCAAACTGGA
 ACAACTCAACCTATCTCGTCTATTCTTTGATTTATAAGGGATTTGGGGATTTGGCCTATTGGTTAAAAAATGAGCTGATTTAACAATAAATTA
 ACGCAATTAATCTGTGAATGTGTGTCAGTTAGGGTGTGAAAGTCCCAAGTCCCAAGCAGGACAGGATGCAAAAGCATGCATCTCAATTA
 GTCAGCAACCAAGTGTGAAAGTCCCAAGTCCCAAGCAGGACAGGATGCAAAAGCATGCATCTCAATTAAGTCAAGCAACCATAGTCCCGCCCTA
 ACTCCGCCATCCCGCCCTAACTCCGCCAGTCCGCCATTCTCCGCCCATGGCTGACTAATTTTTTTTATTTATGCAAGAGCCGAGCCGCTCTG
 CCTCTGAGCTATCCAGAAGTAGTGAGGAGGCTTTTTGGAGGCTAGGCTTTGCAAAAAGCTCCCGGAGCTGTATATCCATTTTCGGATCTGAT
 AAGAGACAGGATGAGGATCGTTTCGCATGATTGAACAAGATGGATTGCACGAGGTTCTCCGGCGCTTGGGTGGAGAGGCTATTCGGCTATGACT
 GGGCACAACAGACAATCGGCTGCTCTGATGCCCGGTTCGGCTGTGACGCGAGGGCGCCGCTTCTTTTGTCAAGACCGACTGTCCGGTGC
 CCTGAATGAATGCAGGACGAGCGCGGCTATCGTGGTGGCCACGACGGCGGCTTCTTGCAGCTGTGCTCGACGTTGTCACTGAAGCGG

AAGGGACTGGCTGCTATTGGGCGAAGTGCCGGGGCAGGATCTCCTGTCTACCTTGTCTGCCGAGAAAGTATCCATCATGGCTGATGCAATG
CGGCGGCTGCATACGCTTGTATCCGGCTACCTGCCATTCCGACCACCAAGCGAAACATCGCATCGAGCGAGCAGTACTCGGATGGAAGCCGGTCTTG
TCGATCAGGATGATCTGGACGAAGAGCATCAGGGGCTCGCGCCAGCCGAACTGTTCCGCAAGGCTCAAGGCGCGCATGCCGACGGCGAGGATCTCG
TCGTGACCCATGGCGATGCTGCTTCCGCAATATCATGGTGGAAATGGCCGCTTTTCTGGATTATCGACTGTGGCCGGCTGGGTGGCGGACCG
CTATCAGGACATAGCGTTGGCTACCCGTGATATTGCTGAAGAGCTTGGCGGCGAATGGGCTGACCCGCTTCTCTGTGCTTTACGGTATCGCCGCTCCCG
ATTCGCAGCGCATCGCCTTATCGCCTTCTTGACGAGTCTTCTGAGCGGGACTCTGGGGTTCGAAATGACCGACCAAGCGACGCCAACCTGCCAT
CACGAGATTTGATTCCACCGCCGCTTCTATGAAAGGTTGGGCTTCCGAAATCGTTTTCCGGACGCGCGGCTGGATGATCTCCAGCGCGGGGATCTC
ATGCTGGAGTCTTCGCCACCCCAACTGTTTTATTGCAGCTTATAATGGTTACAAATAAAGCAATAGCATCACAAATTTACAAATAAAGCATTTTTTT
CACTGCATTCTAGTTGGTTTGTCCAAACTCATCAATGTATCTTATCATGTCTGTATACCCGTCGACCTCTAGCTAGAGCTTGGCGTAATCATGGTCATA
GCTGTTTCTGTGAAAATTGTTATCCGCTCACAATCCACACAACATACGAGCCGGAAGCATAAAGTGAAAGCCTGGGGTGCCTAATGAGTGAGCT
AACTCACATTAATTGCGTTGCGCTCACTGCCCGCTTCCAGTCGGGAAACCTGTCGTGCCAGCTGCATTAAATGAATCGCCAAACGCGCGGGGAGAGGC
GGTTTGCATATTGGGCGCTTCTCCGCTTCTCGCTCACTGACTCGCTGCGCTCGGTGTTCCGGTGCAGGAGCGGATACAGTCACTCAAAGGCGGT
AATACGGTTATCCACAGAATCAGGGGATAACGCAGGAAAGAACATGTGAGCAAAGGCCAGCAAAGGCCAGGAACCGTAAAAAGGCCGCTTGC
TGGCGTTTTTCCATAGGCTCCGCCCTGACGAGCATCAAAAAATCGACGCTCAAGTCAGAGGTGGCGAAACCCGACAGGACTATAAAGATACCA
GGCGTTTCCCGTGAAGCTCCCTCGTGCCTCTCTGTTCCGACCCTGCCGTTACCGGATACTGTCCGCTTCTCCCTTCCGGAAAGCGTGGCGCTT
TCTCAATGCTCAGCTGTAGGTATCTCAGTTCGGTGTAGGTGCTTCCGCTCAAGCTGGGCTGTGTGCACGAACCCCGTTACGCCGACCGCTGCGC
CTTATCCGGTAACTATCGTCTTGTAGTCAACCCGGTAAGACACGACTTATCGCCACTGGCAGCAGCCACTGGTAACAGGATTAGCAGAGCGAGGTATG
TAGGCGGTGCTACAGAGTCTTGAAGTGGTGGCCTAACTACGGCTACACTAGAAGGACAGTATTTGGTATCTGCGCTCTGCTGAAGCCAGTTACCTTC
GGAAAAAGAGTTGGTAGCTCTTGATCCGGCAAACAACCACCGCTGGTAGCGGTGGTTTTTTTTGTTTGAAGCAGCAGATTACGCGCAGAAAAAAG
GATCTCAAGAAGATCCTTTGATCTTTTCTACGGGGTCTGACGCTCAGTGGAACGAAACTCACGTTAAGGGATTTTGGTCATGAGATTATCAAAAAGG
ATCTTCACTAGATCCTTTAAATTAATAATGAAGTTTTAAATCAATCTAAAGTATATATGAGTAAACTGGTCTGACAGTTACCAATGCTTAATCAGTG
AGGCACCTATCTCAGCGATCTGTCTATTTCTGTTATCCATAGTTGCTGACTCCCGCTGTGTAGATAACTACGATACGGGAGGGCTTACCATCTGGCC
CCAGTGTGCAATGATACCCGCGAGACCCACGCTCACCAGGCTCCAGATTTATCAGCAATAAACCAGCCAGCCGGAAGGGCCGAGCGCAGAAGTGGTCC
TGCAACTTTATCCGCTCCATCCAGTCTATTAATTGTTGCCGGAAAGTAGAGTAAGTAGTTCCGCAAGTTAATAGTTTGCAGCAACGTTGTTGCCATTGC
TACAGGCATCGTGGTGTACGCTCGTCTGTTGGTATGGCTTCACTCAGCTCCGCTTCCCAACGATCAAGGCGAGTTACATGATCCCCATGTTGTGCAA
AAAAGCGTTAGCTCCTTCCGCTCCTCCGATCGTTGTGAGAAGTAAGTTGGCCGAGTGTATCACTCATGGTTATGGCAGCACTGCATAATTTCTTAC
TGTCATGCCATCCGTAAGATGCTTTTCTGTGACTGGTGTACTCAACCAAGTCACTTCTGAGAATAGTGTATGCCGCGACCGAGTTGCTTGGCCGGC
GTCAATACGGGATAATACCCGCGCCACATAGCAGAACTTTAAAAGTGTCTATCATTGGAAAACGTTCTTCCGGGGCGAAAACCTCAAGGATCTTACCGC
TGTTGAGATCCAGTTCGATGTAACCCACTCGTGCACCAACTGATCTTACGATCTTTTACTTTACCCAGCGTTTTCTGGGTGAGCAAAAACAGGAAGGC
AAAATGCCGCAAAAAGGGAATAAGGGCGACACGGAATGTTGAATACTCATACTCTTCTTTTCAATATTATTGAAGCATTATCAGGGTTATTGTC
TCATGAGCGGATACATATTTGAATGATTTAGAAAAATAAACAATAGGGTTCGCGCACATTTCCCGAAAAGTGCCACCTGACGTC

INSIG-2-HA(C)-pcDNA3



>INSIG-2-HA(C)-pcDNA3 Amino Acid Coding Sequence

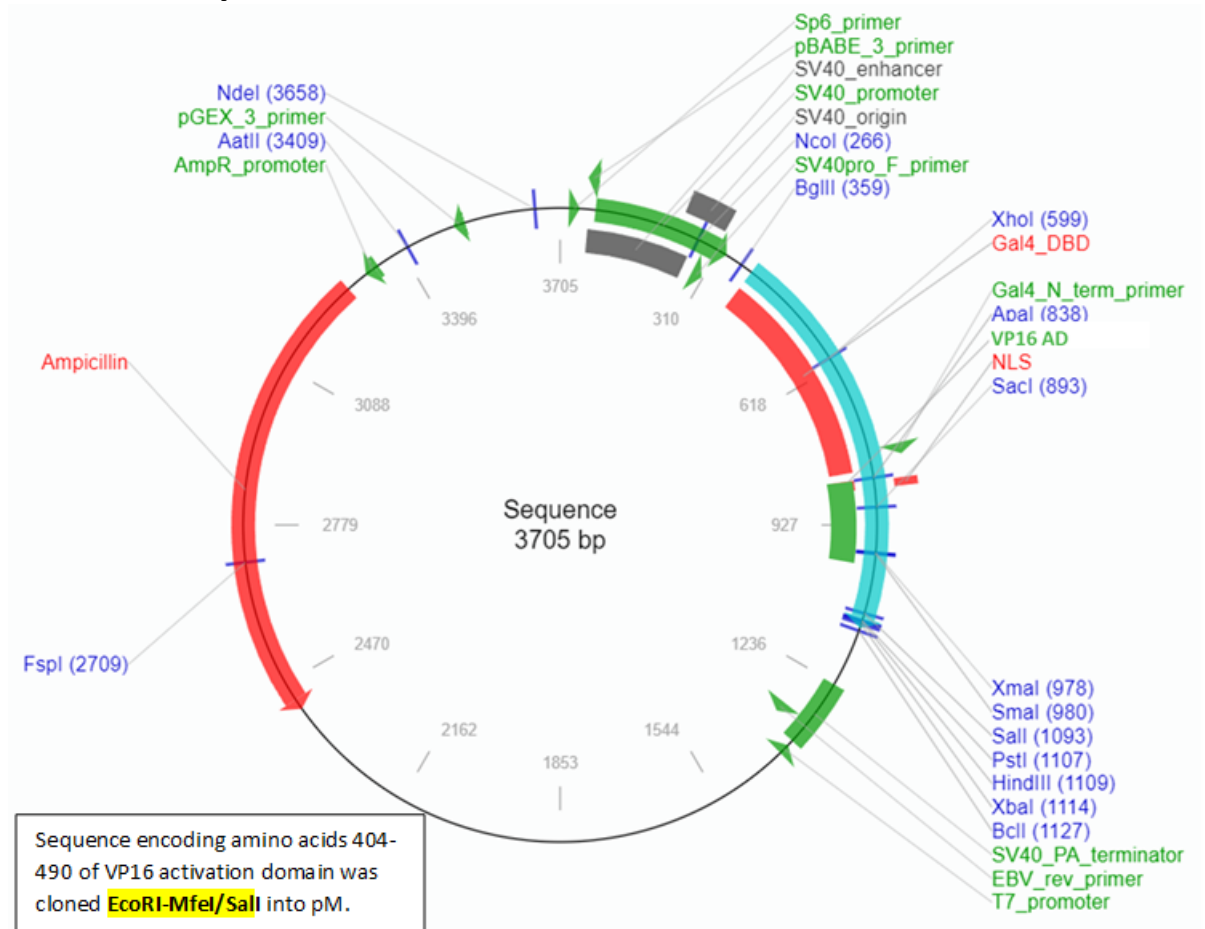
MAEGETESPGKKCGPIYSSVTSQSVNLMIRGVVLFVIFVFLALVLLNLLQIQRNVTLPFPDVIASIFSSAWVWVPPCCGTASAVIGLLYPCIDRHLGEPHKFKRE
 WSSVMRCVAVFVGINHASAKVDFDNNIQLSLTLAALSIGLWVWTFDRSRSGFGLGVGIAFLATVVTQLLVYNGVYQYTSDFLYVRSWLPCIFFAGGITMGNL
 GRQLAMYECKVIAEKSHQEYPYDVDPDYA

>INSIG-2-HA(C)-pcDNA3 Plasmid Sequence

GACGGATCGGGAGATCTCCGATCCCTATGGTCGACTCTCAGTACAATCTGCTCTGATGCCGCATAGTTAAGCCAGTATCTGCTCCCTGTTGTGTGT
 TGGAGGTCGCTGAGTAGTGCGCGAGCAAAATTAAGCTACAACAAGGCAAGGCTTACCACGACAATTGCATGAAGAATCTGCTTAGGGTTAGGCGTTT
 TGGCGTCTTCGCGATGTACGGGCCAGATATACGCGTTGACATTGATTACTAGTATTATAAGTAATCAATTACGGGGTATTGTTTATAGCCCC
 ATATATGGAGTCCCGCTTACATAACTACGTTAAATGGCCCGCTGCTGACCGCCCAACGACCCCGCCATTGACGTCATAATGACGTATGTTCC
 CATAGTAACGCCAATAGGGACTTTCATTGACGTCAATGGGTGGACTATTTACGGTAACTGCCACTTGGCAGTACATCAAGTGTATCATATGCCAA
 GTACGCCCTATTGACGTCATGACGTAATGGCCCGCTGGCATTATGCCAGTACATGACCTTATGGGACTTTCCTACTTGGCAGTACATCTACG
 TATTAGTATCGCTATTACCATGGTGATGCGGTTTTGGCAGTACATCAATGGGCGTGGATAGCGGTTTACTCACGGGATTTCCAAGTCTCCACCCC
 ATTGACGTCATGGGAGTTGTTTTGGCACAAAATCAACGGGACTTTCAAAATGTCGTAACAACCTCCGCCATTGACGCAATGGGCGGTAGGGC
 TGTACGGTGGGAGGTCTATATAAGCAGAGCTCTCGGCTAAGTAGAGAACCCTGCTTACTGCTTATCGAAATTAATACGACTCACTATAGGGAGA
 CCCAAGCTTGGTACCGAGCTCGGATCCACTAGTAACGGCCGCAAGTGTGCTGGAATTCATGGCAGAAAGGAGAGACAGAGTCACTGGGCCAAAAA
 GTGTGGCCATATATTTCTATCTGACTAGCCAGAGTGAACCTGATGATTGAGGAGTAGTGCTATTTTTATTGGAGTATTTCTTGCAATTAGTGTTA
 AATTTACTCAGATTCAGAGAAATGTGACGCTCTTCCACCTGATGTGATTGCAAGCATCTTTTCTCTGCATGGTGGGTACCCCATGCTGTGGCACG
 GCTTCAGCTGTGATTGGGTTATTATACCCCTGCATTGACAGACATCTAGGAGAACCACATAAAATTTAAAAGAGAGTGGTCCAGTGAATGCGGTGTGT
 AGCAGTCTTTGTTGATAAATCATGCCAGTCTAAAGTGGATTCGATAACAACATACAGTTGCTCTCACACTGGTGCACATCCATTGGACTGTG
 GTGGACTTTTGATAGTCTAGAAGTGGTTTTGGCCTTGGAGTAGGAATGCTTCTTGGCAACTGTGGTCACTCAACTGCTAGTATATAATGGTGTGTTA
 CCAATATACATCTCCAGATTTCTCTATGTTGTTCTGGTACCATGATATTTTTGCTGGAGGCATAACAATGGGAAACATTGGTCGACAACCTGGCA
 ATGTACGAATGTAAAGTTATCGCAGAAAAATCTATCAGGAAATACCCATACGATGTTCCAGATTACGCTTGGAGCTAGCGGGCCCTATTCTATGCTC
 ACCTAAATGCTAGAGCTCGTGTACGCTCGACTGTGCCTTCTAGTTGCCAGCCTCTGTTGTTTGGCCCTCCCGTGCCTTCTTGACCCTGGAAGG
 TGCCACTCCACTGCTCTTCTAATAAAATGAGGAAATGCATCGCATTGCTGAGTAGGTGTCATTCTATTCTGGGGGTGGGGTGGGGCAGGACA
 GCAAGGGGGAGGATTGGGAAGACAATAGCAGGCATGCTGGGGATGCGGTGGGCTCTATGGCTTCTGAGCGGAAAGAACAGCTGGGGCTCTAG
 GGGGTATCCACGCGCCTGTAGCGGCGCATTAAAGCGCGCGGGTGTGGTGTACGCGCAGCGTGACCCTACACTGCCAGCGCCCTAGCGCCC
 GCTCCTTTCCGCTTCTCCCTTCTTCTCGCCAGTTCGCGGCTTCCCGCTTAAAGCTAAATCGGGGCACTCCCTTAAAGGTTCCGATTTAGTGTCTT
 ACGGCACCTCGACCCAAAAAATCTGATTAGGGTGTGTTACGTAAGTGGCCATCGCCCTGATAGACGGTTTTTTCGCTTTGACGTTGGAGTCCA
 CGTCTTTAATAGTGGACTCTGTTCCAACTGGAACAACACTCAACCCTATCTCGTCTATTCTTTGATTTATAAGGGATTTTGGGGATTTCCGCCTA
 TTGGTTAAAAAATGAGCTGATTTAACAATAAATTAACCGCAATTAATCTGTGGAATGTGTGTCAGTTAGGGTGTGGAAGTCCCGAGCTCCCGAGG
 CAGGCAAGAATGCAAAGCATGCATCTCAATTAGTCAGCAACCGAGTGTGGAAGTCCCGAGCTCCCGAGCAGGAGAGTATGCAAAGCATGC
 ATCTCAATTAGTCAGCAACCATAGTCCCGCCCTAACTCCGCCATCCCGCCCTAACTCCGCCAGTTCGGCCATTCTCCGCCCATGGCTGACTAAT
 TTTTTTATTATGCAGAGCCGAGGCCCTCTGCCTCTGACTATCCAGAAGTAGTGAGGAGGCTTTTTGGAGGCTAGGCTTTTGCAAAAAGCT
 CCCGGAGGCTTGTATATCATTTTTCGGATCTGATCAAGAGACAGGATGAGGATCGTTTGCATGATTGAACAAGATGGATTGCACGAGGTTCTCCGG
 CCGCTTGGGTGGAGAGGCTATTCGGCTATGACTGGGCACAACAGACAATCGGCTGCTGATGCCCGCTGTTCCGGCTGTACGCGCAGGGGCGCC
 GGTCTTTTTGTCAAGACCGACTGTCCGGTGCCTGAATGAAGTGCAGGACGAGGCGAGCGGCTATCGTGGTGGCCACGAGGGCGTCTCTTCG
 GCAGCTGTGCTGACGTTGTCACTGAAGCGGGAAGGACTGGCTGCTATTGGGCGAAGTCCCGGGCAGGATCTCTGTCACTCACTTGTCTCTG
 CCGAGAAAGTATCCATCATGCTGATGCAATGCCGCGCTGCATACGCTTGTACCGGCTACCTGCCATTCCAGCCAAAGCAGCAAAATCGCATCGAG
 CGAGCACGTAAGTGGATGGAAGCGGCTTGTGCTGATCAGGATGATCTGGACGAAGAGCATCAGGGGCTCGCGCCAGCCGAAGTGTTCGCCAGGCTC

AAGGCGCGCATGCCCGACGGCGAGGATCTCGTCTGACCCATGGCGATGCCTGCTTGCCGAATATCATGGTGGAAAATGGCCGCTTTTCTGGATTCA
TCGACTGTGGCCGGTGGGTGTGGCGGACCGCTATCAGGACATAGCGTTGGCTACCCGTGATATTGCTGAAGAGCTTGGCGGCGAATGGGCTGACC
GCTTCCTCGTGCTTTACGGTATCGCCGCTCCCGATTTCGACGCGCATCGCCTTCTATCGCCTTCTTGACGAGTTCTTCTGAGCGGGACTCGGGGTTCGA
AATGACCGACCAAGCGACGCCAACCTGCCATCAGAGATTTTCGATTCCACCGCCGCTTCTATGAAAGGTTGGGCTTCGGAATCGTTTTCCGGGACG
CCGGTGGATGATCTCCAGCGCGGGATCTCATGCTGGAGTTCTTCGCCACCCCACTTGTATTGACGCTTATAATGGTTACAAATAAAGCAATA
GCATCACAATTTCAAAATAAAGCATTTTTTTCACTGCATTCTAGTTGGTTTTGTCCAAACTCATCAATGTATCTTATCATGTCTGTATAACCGTCGACC
TCTAGCTAGAGCTTGGCGTAATCATGGTCATAGCTTTTTCTGTGTGAAATTTGATCCGCTCACAATCCACACAACATACGAGCCGGAAGCATAAAG
TGTAAGCCTGGGGTGCCTAATGAGTGAGCTAACTCACATTAATTGCGTTGCGCTCACTGCCCGCTTCCAGTCGGGAAACCTGTCGTGCCAGCTGCA
TTAATGAATCGGCCAACGCGCGGGGAGAGGCGGTTTGCCTATTGGGCGCTTCCGCTTCTCGCTCACTGACTCGCTCGGCTCGGTCGTTCCGGCTGC
GGCGAGCGGTATCAGCTCAAAAGCGGTAATACGGTTATCCACAGAATCAGGGGATAACGCAGGAAAGAATGTGAGCAAAAGGCCAGCAAA
AGGCCAGGAACCGTAAAAAGCCGCTTGTGGCGTTTTTCCATAGGCTCCGCCCTGACGAGCATCACAATAATCGACGCTCAAGTCAGAGGTG
GCGAAACCCGACAGGACTATAAAGATACCAGGCGTTTTCCCTGGAAGCTCCCTCGTGCCTCTCTGTTCCGACCTGCCGCTTACCGGATACCTGTC
CGCCTTCTCCCTTCGGGAAGCGTGGCGTTTTCTCAATGCTCACGCTGTAGGTATCTCAGTTCGGTGTAGTTCGTTCCGTTCCAAAGTGGGCTGTGTGCA
CGAACCCCGTTTCAGCCGACCGCTGCGCCTTATCCGTAATCATGCTTGTAGTCCAACCCGGTAAGACACGACTTATCGCCACTGGCAGCAGCCA
CTGGTAACAGGATTAGCAGAGCGAGGTATGTAGGCGGTGCTACAGAGTTCTTGAAGTGGTGGCCTAACTACGGCTACACTAGAAGGACAGTATTTG
GTATCTGCCTCTGCTGAAGCCAGTTACCTTCGAAAAAGAGTTGGTAGCTCTTGATCCGCAAAACAAACCACCGTGGTAGCGGTGGTTTTTTGTTT
GCAAGCAGCAGATTACGCGCAGAAAAAAGGATCTCAAGAAGATCCTTTGATCTTTTACGGGGTCTGACGCTCAGTGAACGAAAACCTCACGTTA
AGGGATTTTGGTCATGAGATTATCAAAAAGGATCTCACCTAGATCCTTTTAAATTAATAAATGAAGTTTTAAATCAATCTAAAGTATATAGATAAAC
TTGGTCTGACAGTTACCAATGCTTAATCAAGTGAAGCACCTATCTCAGCGATCTGTCTATTTGTTTCATCCATAGTTGCCTGACTCCCGCTGTGTAGATA
ACTACGATACGGGAGGGCTTACCATCTGGCCCCAGTGTGCAATGATACCGCGAGACCCACGCTCACCGGCTCCAGATTTATCAGCAATAAACAGCC
AGCCGGAAGGGCCGAGCGCAGAAGTGGTCTGCAACTTTATCCGCTCCATCCAGTCTATTAATTGTTGCCGGGAAGCTAGAGTAAGTAGTTCGCCA
GTTAATAGTTTGCACAACGTTGTTGCCATTGTACAGGCATCGTGGTGTACGCTCGTCTGGTATGGCTTCAATCAGCTCCGTTCCCAACGATCA
AGGCGAGTTACATGATCCCCATGTTGTGCAAAAAAGCGTTAGCTCCTTCGGTCTCCGATCGTTGTCAGAAGTAAGTTGGCCGAGTGTATCACT
CATGTTATGGCAGCACTGCATAATTCTTACTGTATGCCATCCGTAAGATGCTTTTCTGTGACTGTTGAGTACTCAACCAAGTCATTCTGAGAATA
GTGTATGCGGCGACCGAGTTGCTCTTCCCGGCGTCAATACGGGATAAATACCGCGCCACATAGCAGAACTTTAAAGTGCTCATTTGGAAAACGTT
CTTCGGGGCGAAAACCTCAAGGATCTTACCGCTGTTGAGATCCAGTTCGATGTAACCCACTCGTGCACCCAACTGATCTTCAGCATCTTTACTTTTAC
CAGCGTTTCTGGGTGAGCAAAAACAGGAAGGCAAAATGCCGCAAAAAGGGAATAAGGGCGACACGGAATGTTGAATACTCATACTCTTCTTTT
CAATATTATTGAAGCATTTATCAGGGTTATTGTCTCATGAGCGGATACATATTTGAATGTATTTAGAAAAATAACAAATAGGGGTTCCGCGCACATTT
CCCCGAAAAGTGCCACCTGACGTC

GAL4-VP16-pM



>GAL4-VP16-pM Amino Acid Coding Sequence

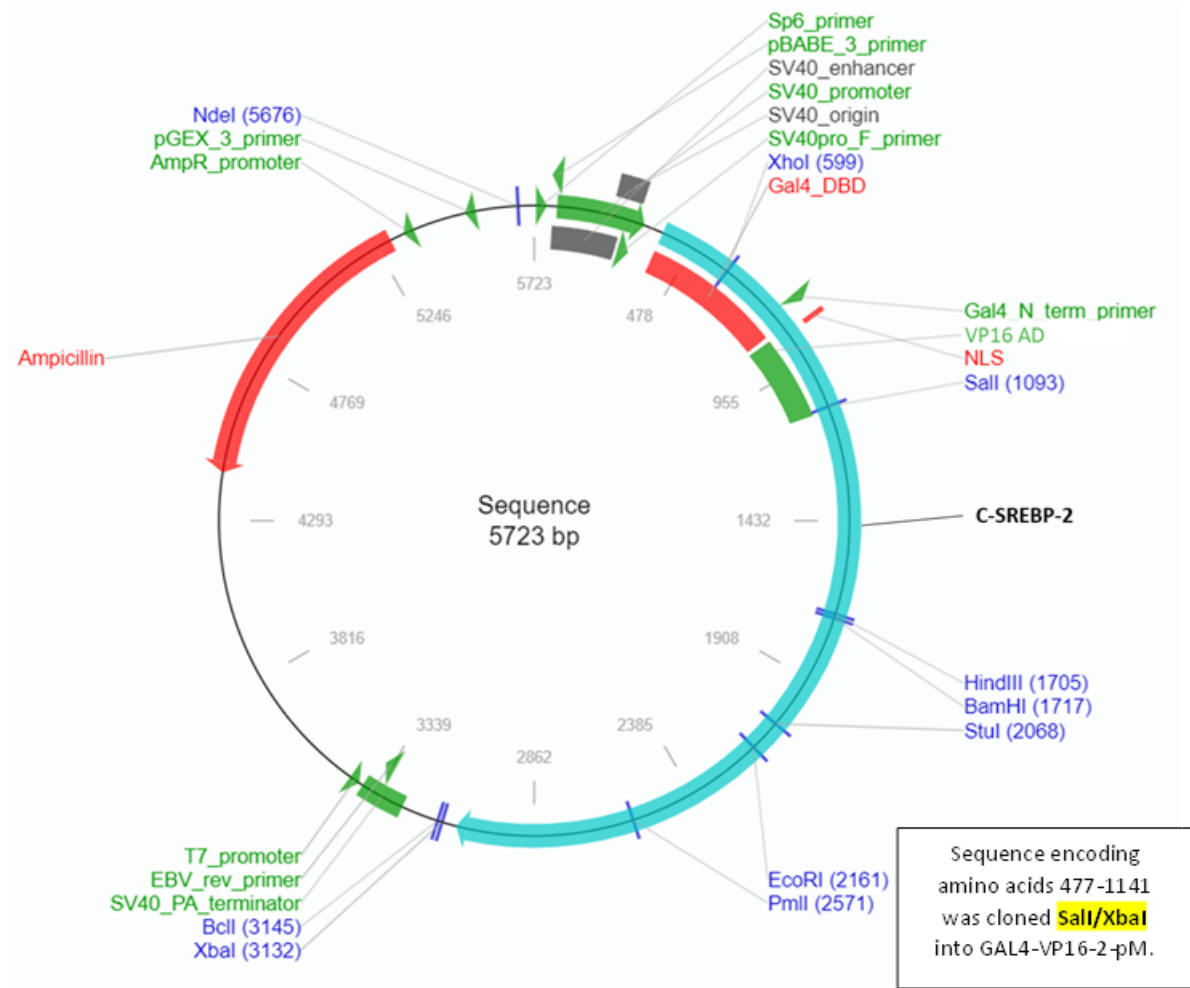
MKLLSSIEQACDICRLKLLKCSKEPKCAKCLKNNWECRYSPKTKRSLPTRAHLTEVESRLERLEQLFLIFPREDLDMILKMDLSQDIKALLTGLFVQDNVNDK
 AVTDRLASVETDMLPLLRQHRISATSSSESSNKGQRQLTVSPELMGPKKRRKVPAPPTDVSLGDELHLDGEDVAMAHADALDDFDLMDLGDGDSPPGPT
 PHDSAPYGALDMADFEFEQMFTDALGIDEYGGVDASAEASR

>GAL4-VP16-pM Plasmid Sequence

TATGTATCATACATACGATTTAGGTGACACTATAGAATCGATGTGGAATGTGTGTCAGTTAGGGTGTGGAAGTCCCCAGGCTCCCAGCAGGCA
 GAAGTATGCAAAGCATGCATCTCAATTAGTCAGCAAGGAAAGTCCCAGGCTCCCAGCAGGCAAGATGCAAAGCATGCATCTCAATTAGTCAG
 CAACCATAGTCCCGCCCTAACTCCGCCATCCCGCCCTAACTCCGCCAGTCCCGCCATTCTCCGCCCATGGCTGACTAATTTTTTTTATTTATGCA
 GAGGCCGAGGCCGCTCGGCTCTGAGCTATTCCAGAAGTAGTGAAGAGGCTTTTTGGAGGAGATCTAAGCTGCCTCTGAAAGATGAAGCTACTG
 TCTTCTATCGAACAAGCATGCGATATTTGCCGACTTAAAAGCTCAAGTGTCTCAAAGAAAAACCGAAGTGCGCCAAGTGTCTGAAGAACAAGTGGG
 AGTGTGCTACTCTCCAAAACAAAAGGTCTCCGCTGACTAGGGCAGCATCTGACGAGAAGTGAATCAAGGCTAGAAAAGTGGAAACAGCTATTTCT
 ACTGATTTTTCTCGAGAAGACCTTGACATGATTTGAAAATGGATCTTTTACAGGATATAAAAAGCATTGTTAACAGGATTATTTGACAAGATAATGT
 GAATAAAGATGCCGTACAGATAGATTGGCTTCAAGTGGAGACTGATGCTCTAACCATTGAGACAGCATAGAAATAGTGCAGCATCATCATCGGAA
 GAGAGTAGTAAACAAGTCAAAGACAGTTGACTGTATCGCCGGAATTGATGGCCCTAAAAGAAAGCGTAAAGTCCGCCCCGACCGATGTCAGC
 CTGGGGGACGAGCTCCACTAGACGGCGAGGACGTGGCGATGGCGCATGCCGACGCGCTAGACGATTTGATCTGGACATGTTGGGGGACGGGGA
 TTCCCGGGGGCGGATTACCCCGGACTCCGCCCTACGGCGCTCTGGATATGGCCGACTTCGAGTTGAGCAGATGTTTACCGATGCCCTTG
 GAATTGACGAGTACGGTGGGCTCGCAGAGCTTCTAGA7AAGTAATGATCATAATCAGCCATATCACATCTGTAGAGGTTTTACTTGCT
 TTAATAAACTCCACACCTCCCTGAACCTGAAACATAAAATGAATGCAATTTGTTGTTAATTGTTTATTGCGACTTATAATGGTTACAATAAA
 GCAATAGCATCAAAATTTACAATAAAGCATTTTTTCACTGCAATCTAGTTGTGGTTTTGTCAAAACATCAATGATCTTATCATGTCTGGATCTGC
 CGGTCTCCTATAGTGAGTGTATTAATTTGATAAGCCAGGTTAAGTGCATTAATGAATCGGCCAACCGCGGGGAGAGGCGGTTTGCATTGTTG
 GCGCTCTCCGCTTCTCGCTACTGACTCGTCTCGCTCGGTCTGCGCTGCGGCGAGCGGTATCAGTCACTCAAAGCGGTAATACGGTTATCCA
 CAGAATCAGGGGATAACCGAGGAAAGAACATGTGAGCAAAAGGCCAGCAAAGGCCAGGAACCGTAAAAGGCCGCTGTTGCTGGCGTTTTCCATA
 GGCTCCGCCCTGACGAGCATCAAAAATCGACGCTCAAGTCAAGGTTGGCGAAACCCGACAGGACTATAAAGATACCAGGCGTTTTCCCTGG
 AAGCTCCCTCGTGGCTCTCCTGTTCCGACCTGCGCTTACCGGATACCTGTCCGCTTTTCCCTTCGGGAAGCGTGGCGCTTTCTCATAGTCAACGC
 TGAGGTATCTCAGTTCGGTGTAGGTCGTTGCTCCAAGTGGGCTGTGTGCACGAACCCCGTTCAGCCCGACCGCTGCGCTTATCCGGTAATCAT
 CGTCTTGTAGTCAACCCGTAAGACACGACTTATCGCACTGGCAGCAGCCTGTTAACAGGATTAGCAGAGCGAGGTATGTAGGCGGTGCTACAG
 AGTCTTGAAGTGGTGGCTAACTACGGCTACTAGAAAGACAGTATTTGGTATCTGCGCTCTGCTGAAGCCAGTTACCTTCGAAAAGAGTTGGT
 AGCTCTTGTACCGGCAAAACACCGCTGTTAGCGGTGGTTTTTTGTTTGAAGCAGCAGATTACGCGCAGAAAAAAGGATCTCAAGAAGATC
 CTTTGTATTTTTTACGGGGTCTGACGCTCAGTGGAAACGAAACTCAGTTAAGGATTTTGGTTCATGAGATTACAAAAGGATCTTACCTAGATCC
 TTTTAAATAAAAATGAAGTTTTAAATCAATCTAAAGTATATAGTAAACTTGGTCTGACAGTTACCAATGCTTAATCAGTAGGACCACTATCTCAG
 CGATCTGTCTATTTGTTTATCCATAGTTGCTGACTCCCGCTGTGATAGTAACTACGATACGGGAGGGCTTACCATCTGGCCCCAGTGTCAATGA
 TACCGGAGACCCAGCTACCGGCTCAGATTTATCAGCAATAAACCAGCCAGCCGGAAGGCCGAGCGCAGAAGTGGTCTGCAACTTTATCCGC
 CTCCATCCAGTCTAATTTGTTGCCGGAAGCTAGAGTAAGTAGTTCGCCAGTTAATAGTTTGCGCAACGTTGTTGCCATTGCTACAGGCATCGTGGT

GTCACGCTCGTCGTTTGGTATGGCTTCATTCAGCTCCGGTCCCAACGATCAAGGCGAGTTACATGATCCCCATGTTGTGCAAAAAAGCGGTTAGCTC
CTTCGGTCCCGATCGTTGTCAGAAGTAAGTTGGCCGAGTGTTATCACTCATGGTTATGGCAGCACTGCATAATTCTTACTGTCATGCCATCCGTA
AGATGCTTTTCTGTGACTGGTGAGTACTCAACCAAGTCATTCTGAGAATAGTGATGCGGCGACCGAGTTGCTCTTGCCCGGCGTCAATACGGGATAA
TACCGGCCACATAGCAGAACTTTAAAAGTGCTCATCATTGGAAAACGTTCTTCGGGGCGAAAACCTCTCAAGGATCTTACCGCTGTTGAGATCCAGTT
CGATGTAACCCACTCGTGCACCCAACTGATCTTCAGCATCTTTACTTTACCAGCGTTTCTGGGTGAGCAAAAACAGGAAGGCAAAATGCCGAAAA
AAGGGAATAAGGGCGACACGGAAATGTTGAATACTCATACTCTTCCTTTTCAATATTATTGAAGCATTATCAGGGTTATTGTCTCATGAGCGGATAC
ATATTTGAATGATTTAGAAAAATAAACAAATAGGGGTTCCGCGCACATTTCCCGAAAAGTGCCACCTGACGTCTAAGAAACCATTATTATCATGACA
TTAACCTATAAAATAGGCGTATCACGAGGCCCTTTCGTCTCGCGCGTTTCGGTGATGACGGTGAAAACCTTGACACATGCAGCTCCCGGAGACGGT
CACAGCTTGTCTGTAAGCGGATGCCGGGAGCAGACAAGCCCGTCAGGGCGCGTCAGCGGGTGTGGCGGGTGTGGGGGCTGGCTTAACATATGCGGC
ATCAGAGCAGATTGTAAGTGCACCATATGGACATATTGTCGTTAGAACCGGCTACAATTAATACATAACT

GAL4-VP16-C-SREBP-2-pM



>GAL4-VP16-C-SREBP-2-pM Amino Acid Coding Sequence

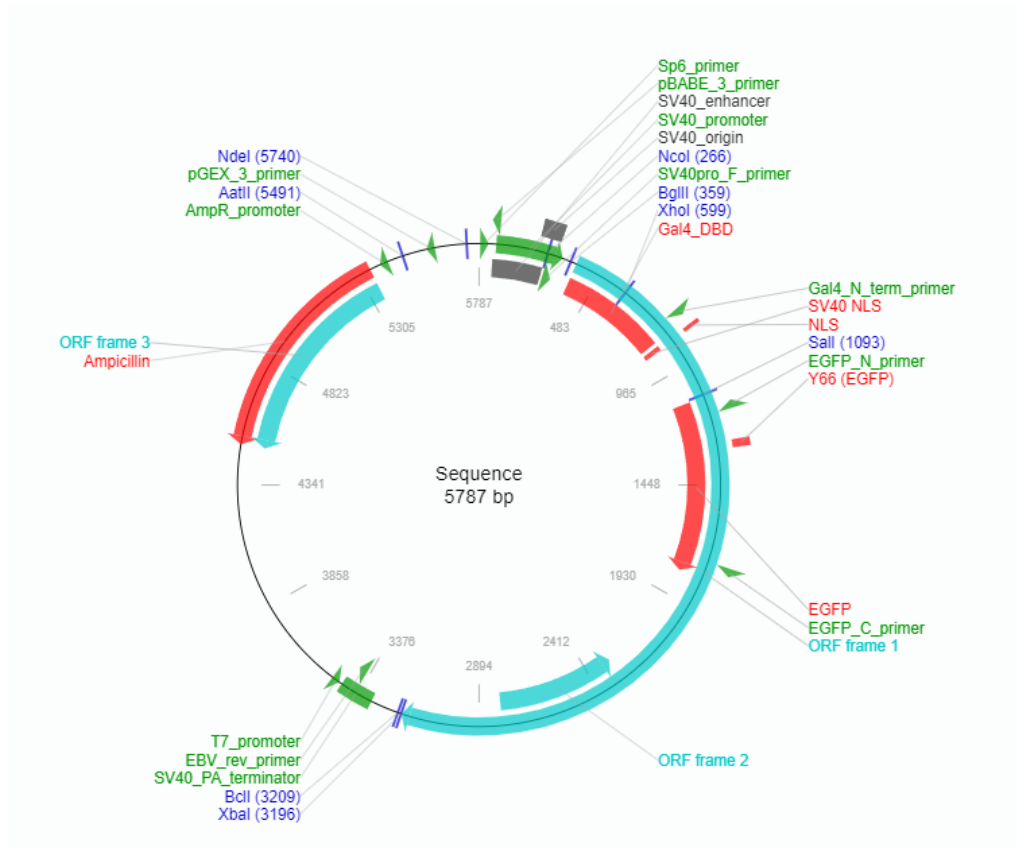
MKLLSSIEQACDICRLKLLKKSKEKPKCAKCLKNNWECRYSPTKRSPLTRAHLTEVESRLERLEQLFLLIFPREDLDMILKMDLSLQDIKALLTGLFVQDNVSKD
 AVTDRLASVETDMPLTLRQHRISATSSSESSNKGQRQLTVSPELMGPKKKRVAAPPTDVSLGDELHLDGEDVAMAHADALDDFDLMDLGDGDSPPGPGFT
 PHDSAPYGALDMADFEFEQMFMDALGIDEYGGVDRSRILLCVLTFCLCSFNPLTSLQWGGAHDSQHPHSGSRSVLSFESGSGWFDWMMPTLLWL
 VNGVIVLSVFKLLVHGEPVIRPHSRSSVTFWRHRKQADLDLARGDFAAAAGNLQTCCLAVLGRALPTSRDLACLSLWNVIRYSLQKRLRVRLLKVKVQCR
 ATPATEAGFEDEAKTSARDAALAYHRLHQLHITGKLPAGSACSDVHMALCAVNLAECAEEKIPPSTLVEIHLTAAMGLKTRCGGKLGFLASVFLSRAQSLCGP
 EHSVAVPSLRWLCPLGQKFFMERSWSVKSAAKESLYCAQRNPADPIAQVHQAFCKNLLERAIESLVKPKQAKKAGDQEESECFSSALEYKLLHFSVDSV
 GVMSPPLSRSSVLKALGPDICRWWTSAITVAISWLQGDAAVRSHTKVERIPKALEVTESPLVKAIFHACRAMHASLPGKADGQSSSFCHCERASGHLW
 SSLNVSGATSDPALNHVVQLTCDLLLSLRTALWQKQASASQAVGETYHASGAELAGFQRDLGSLRRLAHSFRPAYRKVFLHEATVRLMAGASPTRTHQLLE
 HSLRRRTTQSTKHGEVDAWPGQREERATAILLACRHLPLSLFSSPGQRAVLLAEARTLEKVGDRRSCNDCQQMIVKLGGGTAIAAS

>GAL4-VP16-C-SREBP-2-pM Plasmid Sequence

TATGTATCATACATACGATTTAGGTGACACTATAGAAGTCTGATGTGGAATGTGTGTCAGTTAGGGTGTGGAAAGTCCCCAGGCTCCCCAGCAGGCCA
 GAAGTATGCAAAGCATGCATCTCAATTAGTCAGCAAGGAAAGTCCCCAGGCTCCCCAGCAGGCAGAAAGTATGCAAAGCATGCATCTCAATTAGTCAG
 CAACCATAGTCCCCGCCCTAACTCCGCCATCCCGCCCTAACTCCGCCAGTTCGCCCATCTCCGCCCATGGCTGACTAATTTTTTTTATTTATGCA
 GAGGCCGAGGCCCGCCTCGGCCTCTGAGCTATTCCAGAAGTAGTGAAGAGGCTTTTTTGGAGGAGATCTAAGCTGCCTCCTGAAAGATGAAGXACTG
 TCTTCTATCGAACAAGCATGCGATATTTGCCGACTTAAAAAGCTCAAGTGTCCAAAGAAAAACCGAAGTGCGCCAAGTGTCTGAAGAACAAGTGGG
 AGTGTGCTACTCTCCAAAACAAAAGTCTCCGCTGACTAGGGCACATCTGACAGAAGTGGAAATCAAGGCTAGAAAGACTGGAACAGCTATTTCT
 ACTGATTTTTCTCGAAGAAGCCTTGACATGATTTGAAAATGGATCTTTACAGGATATAAAAGCATTGTTAACAGGATTATTTGTACAAGATAATGT
 GAATAAAGATGCCGTCACAGATAGATTGGCTCAGTGGAGACTGATATGCCTTAACATTGAGACAGCATAGAATAAGTGCACATCATATCGGAA
 GAGAGTAGTAACAAGGTCAAAGACAGTTGACTGTATCGCCGGAAATTGATGGGCCCTAAAAAGAAAGCGCTAAAGTGCCTCCGCCAGCATTGTCAGC
 CTGGGGGACGAGCTCCAATTAGACGGCGAGGACGTGGCGATGGCGCATGCCGACGCGCTAGACGATTTCCGATCTGGACATGTTGGGGGACGGGGA
 TTCCCGGGGCGGGGATTTACCCCCAGACTCCGCCCTACGGCGCTCTGGATATGGCCGACTTCGAGTTTGAGCAGATGTTTACCGATGCCCTTG
 GAATTGACGAGTACGGTGGGGGCTCGACTCACGGATCTTCTGTGTGTCTCACCTTCTGTGCTCTCCTTAAACCCCTGACTTCCTGCTGCAGTG
 GGGAGGCCCCAGACTCTGACCAGCACCCACTCAGGCTCTGGCCGAGTGTCTGTCTTTCGAGCTGCTGGTTATGGGGGCTGGTTTGCATGGATG
 ATGCCTCTTCTTCTTGGCTGTAATGGTGTGATTGTCTGAGCTCTTTGTGAAGCTGCTGGTTATGGGGGAGCCAGTATCCGGCCACTC
 GCGCTCTCGGTCACTTCTGGAGGCACCGGAAACAGGCAGATCTGGATCTCGCCAGAGGAGATTTTGCAGCTGCTGCGGCAACTACAACCTGC
 CTGGCAGTTTTGGGCCGGGACTGCCACCTCCCGCTGGACCTGGCCTGCGACCTCTCTGGAACGTGATCCGCTACAGCTGCAGAAGCTACGCT
 GGTGCGCTGCTGCTCAAGAAAGTCTTCCAGTCCGGCGGGCCACGCCAGCCACTGAGGCAGGCTTTGAAGACGAAGTAAGACAGCGCCGGGA
 TGCGGCTCTGGCCTATACCGGCTGCACAGCTGCACATCACAGGAAAGTCTCTGCAAGTCCGCTGTTCCGATGACACATGGCGTTGTGTGCCG
 TGAACCTGGCTGAATGTGCAGAGGAGAAGATCCCACCGACACTGTTGAGATCCATCTGACTGCTGCCATGGGGCTCAAGACCCGGTGTGGAG
 GCAAGCTGGGCTTCTGGCCAGCTACTTCTCAGCCGAGCCAGAGCCTGTGTGGCCCCGAGCACAGTGTCTTCTGACTCCCTGCGCTGGCTCTGC

CACCCCTGGGCCAGAAGTTTTTCATGGAGCGGAGCTGGTCTGTGAAGTCAGCTGCCAAGGAGAGTCTATACTGTGCCAGAGGAACCCAGCTGACC
CCATTGCGCAGGTCCACCAGGCTTCTGCAAGAACCTGCTGGAGCGAGCTATAGAGTCTTGGTGAACCTCAGGCCAAGAAGAAGGCTGGAGACCA
GGAAGAAGAGAGCTGTGAATTCCTCCAGTGTCTGGAGTACTTGAAATTACTTCACTCTTTTGTGGACTCTGTGGGGTTATGAGCCCCCACTCTCCA
GGAGCTCCGTGCTCAAGTCCGCCCTGGGTCCAGACATCATCTGTCGGTGGTGGACGTCTGCAATCACTGTGGCCATCAGCTGGTCCAGGGAGACGA
TGCAGCTGTGCGCTCTCATTTTACCAAGTGAACGCATCCCCAAGGCCTGGAAGTGACAGAGAGCCCCCTGGTGAAGGCCATCTTCCATGCCTGCA
GAGCCATGCATGCCTCACTCCCTGGGAAAAGCAGATGGGCAGCAGAGTTCCTTCTGCCATTGCGAGAGGGCCAGTGGCCACCTATGGAGCAGCTCAA
CGTCAGTGGGGCCACCTCTGACCCTGCCCTCAACCACGTGGTCCAGCTGCTCACCTGTGACCTGCTACTGTGCTACGGACAGCGCTCTGGCAAAAAC
AGGCCAGTGCACGCCAGGCTGTGGGGGAGACTACCACGCGTCAGGCGCTGAACTGGCGGGCTTCCAACGGGACCTGGGCAGCCTGCCAGGCTG
GCACACAGCTTCCGCCAGCATACCGCCAAGGTGTTCTGCATGAAGCCACCGTGCCTGATGGCAGGAGCCAGCCCCACCCGACCCACCAGCTGT
GGAACACAGCTGCGGCGGCGCACCACGAGACCAAGCAGGAGAGGTGGATGCCTGGCCCGCCAGCAGAGCGGGCCACCGCCATCTGC
TGGCCTGCCGCCACTGCCCTCTCTCTCTCTCCCGGGCCAGCGGGCAGTGTGCTGGCCGAAGCTGCCCGCACCTGGAGAAGGTGGGCGAC
CGGCGCTCTGCAACGACTGCCAGCAGATGATTGTTAAGCTGGTGGTGGCCTGCCATTGCCGCCTCTGACCACCAGGCTCAGCCACCCCTCCAC
CTCTCTCGATTTCTAGATAAGTAAATGATCATAATCAGCCATATCACATCTGTAGAGGTTTACTTGCTTTAAAAAACCTCCACACCTCCCCCTGAA
CCTGAAACATAAAATGAATGCAATTGTTGTTGTTAACTGTTTATTGACGCTTATAATGTTTACAAATAAAGCAATAGCATCACAAATTTACAAATAA
AGCATTTTTTCACTGCATTCTAGTTGGTGTTCCAAACCTCATCAATGTATCTTATCATGTCTGGATCTGCCGCTCCCTATAGTGAGTCGATTAAT
TTCGATAAGCCAGGTTAACTGCATTAATGAATCGGCCAACGCGCGGGGAGAGGCGGTTTGCCTATTGGGCGCTCTCCGCTTCTCGCTCACTGACT
CGTGCCTCGGTCGTTCCGGTGGCGGAGCGGTATCAGCTCAAAAGCGGTAATACGGTATCCACAGAATCAGGGGATAACGCGAGGAAAGA
ACATGTGAGCAAAAAGGCCAGCAAAAAGGCCAGGAACCGTAAAAAGCCGCTGTGCTGGCTTTTCCATAGGCTCCGCCCCCTGACGAGCATCACAA
AAATCGACGCTCAAGTCAGAGGTGGCGAAAACCCGACAGGACTATAAAGATACCAGGCGTTTCCCTGGAAAGCTCCCTCGTGCCTCTCTGTTCCGA
CCCTGCCGTTACCGGATACCTGTCCGCTTTCTCCCTCGGGAAGCGTGGCGCTTCTCATAGCTCACGCTGTAGGTATCTCAGTTCGGTGTAGGTCG
TTCGTTCAAGCTGGGCTGTGTGCACGAACCCCGTTACGCCGACCCTGCGCCTTACCGGTAATATCGTCTTGAAGTGGTGGCCTAACTACG
GACTTATCGCCACTGGCAGCAGCCACTGGTAACAGGATTAGCAGAGCGAGGTATGTAGGCGGTGCTACAGAGTCTTGAAGTGGTGGCCTAACTACG
GCTACACTAGAAGAACAGTATTTGGTATCTGCGCTGTGTAAGCCAGTTACCTTCGAAAAAGAGTTGGTAGCTCTTATCCGGCAAAACAAACCACC
GCTGGTAGCGGTGGTTTTTTTTGTTTGAAGCAGCAGATTACGCGCAGAAAAAAGGATCTCAAGAAGATCCTTTGATCTTTTCTACGGGGTCTGACGC
TCAGTGGAACGAAAACCTCACGTTAAGGGATTTTGGTCATGAGATTACAAAAAGGATCTTACCTAGATCCTTTTAAATTAATAAATGAAGTTTTAAATC
AATCTAAAGTATATATGAGTAACTTGGTCTGACAGTTACCAATGCTTAATCAGTGAGGCACCTATCTCAGCGATCTGTCTATTTCTGTTCCATCAGT
GCCTGACTCCCGTCTGTAGATAACTACGATACGGGAGGGCTTACCATCTGGCCCAAGTGTCAATGATACCGCGAGACCACGCTCACCGGCTCC
AGATTTATCAGCAATAAACAGCCAGCCGGAAGGGCCGAGCGCAGAAGTGGTCTGCAACTTTATCCGCTCCATCCAGTCTATTAATTTGTTGCCGGG
AAGCTAGAGTAAAGTAGTTCGCCAGTTAATAGTTTGGCAAGCTTGTGGCATTGCTACAGGCATCGTGGTGTACCGCTCGTCTTTGGTATGGCTTCAT
TCAGTCCGGTCCCAACGATCAAGGCGAGTTACATGATCCCCATGTTGTGCAAAAAAGCGGTTAGCTCCTCGGCTCCGATCGTTGTGCAAGT
AAGTTGGCCGAGTGTATCACTCATGGTTATGGCAGCACTGCATAATTTCTTACTGTATGCCATCCGTAAGATGCTTTTCTGTGACTGGTGGTAC
TCAACCAAGTCACTCTGAGAAATAGTATGCGGCGACCGAGTTGCTTGGCCGCGTCAATACGGGATAATACCGGCCACATAGCAGAACTTTAAA
AGTGTCTATCATTGAAAAAGTCTTCCGGGGCGAAAACCTCAAGGATCTTACCGCTGTTGAGATCCAGTTCGATGTAACCCACTCGTGACCCAACT
GATCTTCAAGTCTTTTACTTTACCAGCTTTCTGGGTGAGCAAAAACAGGAAGGCAAAATGCCCAAAAAAGGGAATAAGGGCGACACGGAAATG
TTGAATACTCATACTCTCTTTTCAATATTATTGAAGCATTATCAGGGTATTGTCTCATGAGCGGATACATATTTGAATGATTTTAGAAAAATAAAC
AAATAGGGGTTCCGCGCACATTTCCCGAAAAGTGCCACCTGACGTCTAAGAAACCATTATTATCATGACATTAACCTATAAAAAATAGGCGTATCAG
AGGCCCTTCTGCTCGCGCTTTCGGTGTGACGGTGAACCTCTGACACATGCAGCTCCCGGAGACGCTCACAGCTTGTGTAAGCGGATGCCG
GGAGCAGACAAGCCGTCAGGGCGCTCAGCGGTGTTGGCGGTGTGCGGGCTGGCTAACTATGCGGCATCAGAGCAGATTGACTGAGAGTG
CCCATATGGACATATTGCTGTTAGAACGCGGCTACAATTAATACATAACCT

GAL4-VP16-GFP-nSREBP-1a-pM



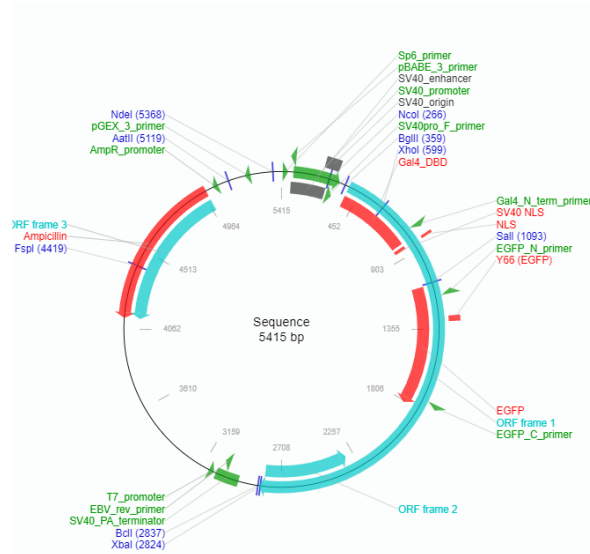
>GAL4-VP16- GFP-nSREBP-1a-pM Amino Acid Coding Sequence

MKLLSSIEQACDICRLKLLKCSKEPKCAKCLKNNWECRYSPTKRSPLTRAHLTEVESRLERLEQLFLLIIPREDLDMILKMDSLQDIKALLTGLFVQDNVKNK
 AVTDRLASVETDMLPLLRQHRISATSSSESSNKQQRQLTVSPELMGPKKRRKVAPPTDVSLGDELHLDGEDVAMAHADALDDFDLMDLGDGDSPPGPT
 PHDSAPYGALDMADFEFEQMFDTDALGIDEYGGVDMVSKGEELFTGVVPIVLVDGDVNGHKFVSVGEGEDATYGKLTGKLPVVPWPTLVTTLYG
 VQCFSRYPDHMKQHDFKFSAMPEGYVQERTIFFKDDGNYKTRAEVKFEGDGLVNRLEKIDFKEDGNILGHKLEYNHYNHNVIMADKQKNGIKVNFKIRH
 NIEDGSVQLADHYQNTPIGDGPVLLPDNHYLSTQSALSQKDPNEKRDMVLEFVTAAGITLGMDELYKDEPPFSEAALEQALGEPDLDAAALLDIEDMLQ
 LINNQDSDPFLDFPPYAGSGAGGTDSPASPTSSPGLSPPPATLSSLEAFLSGPQAAPSPSPQAPPTPLKMYPSMPAFSPGPGIKEESVPLSILQTPTPQP
 LPGALLPQSFAPAPPQFSSSTPVLGYSPGGFSTGSPGNTQQPLPLASPPGVPVSLHTQVQSVVPQQLLTVTAAPTAAPVTTVTSTQIQVVPVLLQP
 HFIKADSLLTAMKTDGATVKAAGLSPLVSGTTVTQGLPTLVSGGITLATVPLVVDKELPINRLAAGSKAPASQAQRGEKRTAHNAIEKRYRSSINDKIELKD
 LVVGTAKLNKSAVLRKAIDYIRFLQHSNQKQKQENLSLRTAVHKSXLKDLVSAACGSGGNTDVLMEGVKTEVEDTLTPPPSDAGSPFQSSPLSLGSRGSGS
 GSGDSEPD

>GAL4-VP16- GFP-nSREBP-1a-pM Plasmid Sequence

TATGTATCATACATACGATTTAGGTGACACTATAGAATCGATGTGGAATGTGTGTCAGTTAGGGTGTGGAAAGTCCCCAGGCTCCCCAGCAGGCA
 GAAGTATGCAAAGCATGCATCTCAATTAGTCAGCAAGGAAAGTCCCCAGGCTCCCCAGCAGGCAAGTATGCAAAGCATGCATCTCAATTAGTCAG
 CAACCATAGTCCC GCCCTAACTCCGCCATCCCGCCCTAACTCCGCCAGTTCCGCCATTCTCCGCCCATGGCTGACTAATTTTTTTTATTTATGCA
 GAGGCCGAGGCCGCTCGGCCCTGAGCTATTCCAGAAGTAGTGAAGAGGCTTTTTGGAGGAGATCTAAGCTGCCTCCTGAAAGTAAAGCTACTG
 TCTTCTATCGAACAAGCATGCGATATTTGCCGACTTAAAAGCTCAAGTGCCTCAAAGAAAAACCGAAGTGCGCCAAGTGTGAAGAACAACCTGGG
 AGTGTGCTACTCTCCAAAACAAAAGGTCTCCGCTGACTAGGGCAGCATCTGACAGAAAGTGAATCAAGGCTAGAAAAGACTGGAACAGCTATTTCT
 ACTGATTTTCTCGAGAAGACCTTGACATGATTTGAAAATGGATCTTTACAGGATATAAAAAGCATTGTTAACAGGATTATTTGTACAAGATAATGT
 GAATAAAGATGCCGTACAGATAGATTGGCTTACAGTGGAGACTGATATGCCTTAACATTGAGACAGCATAGAATAAGTGCACATCAATCATCGGAA
 GAGAGTAGTAACAAGGCTCAAAGACAGTTGACTGTATCGCCGGAATTGACCATGGGCCCTAAAAGAAGCGTAAAGTGCACCCCGGACCGATGTC
 GCCTGGGGGACGAGCTCCACTTAGACGGCGAGGACGTGGCGATGGCGCATGCCGACGCTAGACGATTTTCGATCTGGACATGTTGGGGGACGGG
 GATCCCCGGGGCGGGATTTACCCCCACGACTCCGCCCTACGGCCCTGGATATGGCCGACTTCGAGTTTGAGCAGATGTTTACCGATGCCCT
 TGGAATTGACGAGTACGGTGGGGTGTGACGCAAGGGCGAGGAGCTGTTACCGGGGTGGTGCCTCCTGGTGCAGCTGGACGGCGACG
 TAAACGGCCACAAGTTACAGCTGTCCGGCGAGGGCGAGGGCGATGCCCTACGGCAAGCTGACCCTGAAGTTCATCTGCCACCACCGGCAAGCTGCC
 CGTGCCTGGCCACCCTCGTACCCCTGACCTACGGCGTGCAGTGCCTCAGCCGCTACCCGACCACATGAAGCAGCAGCAGCTTCTCAAGTCCG
 CCATGCCGAAGGCTACGTCCAGGAGCGCACCATCTTCTCAAGGACGACGGCAACTACAAGACCCGCGCGAGGTGAAGTTCGAGGGCGACACCCT
 GGTGAACCGCATCGAGCTGAAGGCATCGACTTCAAGGAGGACGGCAACATCTGGGGCACAAGCTGGAGTACAACACACGCAACGCTCTA
 TATCATGGCCGACAAGCAGAAGAAGCGCATCAAGGTGAACCTCAAGATCCGCCACAACATCGAGGACGGCAGCGTGCAGCTCGCCGACCACTACCA
 GCAGAACACCCCATCGCGACGCCCCGTGCTGCTGCCGACAACCACTACCTGAGCACCAGTCCGCCCTGAGCAAAGACCCCAACGAGAAGCGC
 GATCATAGTCTGCTGGAGTTCGTGACCGCCGCGGGATCACTCTGGCATGGACGAGCTGTAACAAGCAGGACCCCTTACGCGAGGGCGGCTT
 TGGAGCAGGGCTGGGGCAGCCGTGCGATCTGGACGCGGGCTGCTGACCCAGCATCGAAGACATGCTTACGTTTACAACAACCAAGCAGTGA
 CCTGGCCTATTTGACCCCTATGCTGGAGTGGGGCAGGGGACGAGCCAGCCCTCCAGCCCGATACCCAGGCTTGTCTTCCACCTC
 CTGCCACATTGAGCTCCTCTTGAAGCCTTCTGAGCGGGCGCAGGACGCGCCCTACCCCTGTCCCTCCCGCCTGACCCACTCCATTGAAGA

GAL4-VP16-GFP-nSREBP-1a [1-336]-pM



>GAL4-VP16- GFP-nSREBP-1a [1-336]-pM Amino Acid Coding Sequence

MKLLSSIEQACDICRLKCLKSKEPKCAKCLKNNWECRYSPKTKRSLTRAHLTEVESRLERLQLFLIFPREDLDMILKMSDLQDIKALLTGLFVQDNVNDK
 AVTDRLASVETDMPLTLRQHRISATSSSESSNKGQRQLTVSPELMGPKKRRKRVAPPTDVLGDELHLDGEDVAMAHADALDDFDLMDLGDGDSPPGGFT
 PHDSAPYGALDMADFEFEQMFTDALGIDEYGGVDMVSKGEELFTGVVPILVELDGDVNGHKFSVSGEGEGDATYGLTLKFICTTGKLPVPWPVPTLVTLTYG
 VQCFSRYPDHMKQHDFFKSSAMPEGYVQERTIFFKDDGNYKTRAEVKFEGDTLVNRIELKGIQDFKEDGNILGHKLEYNYNHNVIMADKQKNGIKVNFKIRH
 NIEDGSVLADHYQNTPIGDGPVLLPDNHYLSTQSALS KDPNEKRDMVLLFVTAAGITLGMDELKDEPFSEAALEQALGEPCLDLAALLTDIEDMLQ
 LINNQDSDFPGLDFPPYAGSGAGGTDPAASDTSSPGLSPPPATLSSLEAFLSGPAAPSPLSPQPAPTPLKMYPSMPAFSPGPGIKEESVPLSILQPTPTQP
 LPGALLPQSFAPAPPQFSSTPVLGYPSPGGFSTGSPPGNTQPLPLPLASPGVPPVSLHTQVQSVVPOQLLTVTAAPTAAPVTTTPTSQIQQVVPVLLQP
 HFIAKDSLTLTAMKTDGATVKAAGLSPLVSGTTVQTGPLPTLVSGGITLAVPLVVDKELPINRLAAGSKAPASASQSRGEKRTAHNAIEKRYRSSR

>GAL4-VP16- GFP-nSREBP-1a [1-336]-pM Plasmid Sequence

TATGTATCATACATACGATTTAGGTGACACTATAGAATCGATGTGGAATGTGTGTCAGTTAGGGTGTGGAAAGTCCCAGGCTCCCAGCAGGCA
 GAAGTATGCAAAGCATGCATCTCAATTAGTCAGCAAGGAAAGTCCCAGGCTCCCAGCAGGCAGAAGTATGCAAAGCATGCATCTCAATTAGTCAG
 CAACCATAGTCCCGCCCTAACTCCGCCATCCCGCCCTAACTCCGCCAGTCCGCCCATCTCCGCCATGGCTGACTAATTTTTTTTATTTATGCA
 GAGCCGAGGCCCGCTCGGCCCTGAGCTATTCCAGAAGTGAAGAGGCTTTTTTGGAGGAGATCTAAGCTGCCTCCTGAAAG AAGCTACTGT
 CTTCTATCGAACAAAGCATGCGATATTTGCCGACTTAAAAAGCTCAAGTGCTCCTCAAGAAAACCGAAGTGCGCCAAGTGTCTGAAGAACTACTGGGA
 GTGTGCTACTCTCCAAAACCAAAGGTCTCGCTGACTAGGGCACATCTGACAGAAAGTGAATCAAGGCTAGAAAGACTGGAACAGCTATTTCTAC
 TGATTTTTCTCGAAGACCTTGACATGATTTTGAATGGATTCTTTACAGGATATAAAAGCATTGTTAACAGGATTATTTGTACAAGATAATGTGA
 ATAAAGTCCCGTACAGATAGATTGGCTTCAGTGGAGACTGATATGCCTCAACATTTAGACAGCATAGAATAAGTGCAGCATCATCATCGGAAGA
 GAGTAGTAACAAAGGTCAAAGACAGTTGACTGTATCGCCG GAATTGATGGGCCCTAAAAAGAAGCGTAAAGTCGCCCCCGCCAGCGATGTCAAGCCTT
 GGGGACGAGCTCCACTTAGACGCGGAGGACGTGGCGATGGCGCATGCCGACGCGCTAGACGATTTGATGTCGACATGTTGGGGGACGGGGATT
 CCCGGGGCCGGGATTACCCCCAGGACTCCGCCCTACGGCGCTCTGGATATGGCCGACTTCGAGTTGAGCAGATGTTACCGATGCCCTTGAA
 TTGACGAGTACGGTGGG GTCGAC GTGAGCAAGGGCGAGGAGCTGTTACCGGGGTGGTGCCATCCTGGTCGAGCTGGACGGCGACGTAAC
 GGCCACAAGTTCAGCGTGTCCGGCGAGGGCGAGGGCGATGCCACTACGGCAAGCTGACCCTGAAGTTCATCTGCACCACCGGCAAGTGCCTG
 CCCTGGCCACCTCGTGACCACCTGACCTACGGCGTGCAGTCTTACGCCCTACCCGACCACATGAAGCAGCAGCTTCAAGTCCGCAT
 GCCCAGAGGCTACGTCAGGAGCGCACCATCTTCTCAAGGACGACGCACTACAAGACCCGCGCCGAGGTGAAGTTCGAGGGCGACACCCTGGT
 GAACCGCATCGAGCTGAAGGGCATCGACTTCAAGGAGGACGGCAACATCTGGGACACAAGCTGGAGTACAATAACAACGCCACAACGTCTATAT
 CATGGCCGACAAGCAGAAGACGGCATCAAGGTGAACCTCAAGATCCGCCACAACATCGAGGACGGCAGCGTGCAGCTCGCCGACCACTACCAGCA
 GAACACCCCATCGGCGACGGCCCGTGTGTGCTGCCGACAACCACTACTGAGCACCAGTCCGCCCTGAGCAAAGACCCCAACGAGAAGCGCGAT
 CACATGGTCTGCTGGAGTTCGTGACCGCCCGGGATCACTCTCGCATGGACGAGCTGTACAAGGACGACCCTTACGCGAGGCGGCTTTGG
 AGCAGGCGCTGGGGGAGCCGTGCGATCTGACGCGGGCGCTGCTGACCGACATCGAAGACATGCTCAGCTTATCAACAACCAAGACAGTGACTTCC
 TGGCCTATTTGACCCACCTATGCTGGGAGTGGGGCAGGGGGCACAGACCCTGCCAGCCCGATACCAGCTCCCAGGCAGCTTGTCTCCACCTCCTG
 CCACATTGAGCTCCTCTTGAAGCCTTCTGAGCGGGCGCAGGCGCCCTCACCCCTGTCCCCTCCCAGCCTGCACCCACTCCATTGAAGATGT
 ACCGTCTTACCCGCTTCTCCCCTGGGCTGGTATCAAGGAAGAGTCAAGTCCACTGAGCATCCTGCAGACCCCCACCCACAGCCCTGCCAGGG
 GCCCTCTGCCACAGACTCCCAGCCCCAGCCCCACCGCAGTTCACTGCTACCCCTGTGTTAGGCTACCCAGCCCTCCGGGAGGCTTCTCTACAGGA
 AGCCCTCCGGGAACACCCAGCAGCCGCTGCTGGCTGCCACTGCTTCCCGCAGGGGTCCCGCCGCTCTCTTGCACACCCAGGCTCCAGAGTGT
 GGTCCCCAGCAGCTACTGACAGTACAGCTGCCCCACGGCAGCCCTGTAACGACCACTGTGACCTCGCAGATCCAGCAGGTCGGGCTCTGCTGC
 AGCCCATCTCATCAAGGCACTCGTCTTCTGACAGCATGAAGACAGAGGAGCCACTGTGAAGGGCGCAGGTCAGTCCCCTGGTCTCTGG
 CACCATTGTGACAGAGGGCTTTCGCCGACCCTGGTGAAGTGGCGAACCATCTTGGCAACAGTCCCACTGGTCTGATGCGGAGAAGCTGCCTATC
 AACCCTCGCAGCTGGCAGCAAGGCCCGGCTCTGCCAGAGCCGTGGAGAGAAGCGCACAGCCCAACGCCATTGAGAAGCGCTACCGCTCC
 TCTAGATAA GTAATGATCATAATCAGCCATACATCTGTAGAGGTTTACTGTCTTAAAAAACCCTCCACACTCCCTGAACTGAAACATAAAA
 TGAATGCAATTTGTTGTTAATCTGTTTATTGACGCTTATAATGGTTACAATAAAGCAATAGCATCACAATTTTACAATAAAGCATTTTTTCACT
 GCATTCTAGTTGTTGTTTGTCCAACTCATCAATGTATCTTATCATGTCTGGATCTGCCGCTCCCTATAGTGAAGTCTATTAATTTGATAAGCCAGG
 TTAACCTGCATTAATGAATCGGCCAACGCGGGGAGAGGCGGTTTGCATTTGGGCGCTTCCGCTTCTCGCTCACTGACTCGCTCGCTCGGT
 GTTCGGCTGCGGGCAGCGGTATCAGTCACTCAAAGGCGGTAATACGGTTATCCACAGAATCAGGGGATAACGCGAGAAAGCAATGTGAGCAAAA
 GGCCAGCAAAAAGCCAGGAACCGTAAAAAGCCGCGTGTGCGGTTTTCCATAGGCTCCGCCCTGACGAGCATCAAAAATCGACGCTCAA
 GTCAGAGTGGCGAAACCCGACAGGACTATAAAGTACCAGGCGTTTTCCCTGGAAGCTCCCTCGTGCCTCTCTGTCCGACCTGCGCCTTACC

GGATACCTGTCCGCTTTCTCCCTTCGGGAAGCGTGGCGCTTTCTCATAGCTCACGCTGTAGGTATCTCAGTTCGGTGTAGGTCGTTCCGCTCCAAGCTG
GGCTGTGTGCACGAACCCCGTTACGCCGACCGCTGCGCCTTATCCGGTAACTATCGTCTTGAGTCCAACCCGGTAAGACACGACTTATCGCCACT
GGCAGCAGCCACTGGTAAACAGGATTAGCAGAGCGAGGTATGTAGGCGGTGTACAGAGTCTTGAAGTGGTGGCCTAACTACGGGTACACTAGAAG
AACAGTATTTGGTATCTGCGCTCTGCTGAAGCCAGTTACCTTCGGAAAAAGAGTTGGTAGCTCTTGATCCGGCAAACAAACCACCGCTGGTAGCGGTG
GTTTTTTGTTTGAAGCAGCAGATTACGCGCAGAAAAAAGGATCTCAAGAAGATCCTTTGATCTTTCTACGGGGTCTGACGCTCAGTGAACGAA
AACTCACGTTAAGGGATTTTGGTCATGAGATTATCAAAAAGGATCTTACCTAGATCCTTTAAATTAATAAATGAAGTTTTAAATCAATCTAAAGTATAT
ATGAGTAACTTGGTCTGACAGTTACCAATGCTTAATCAGTGAGGCACCTATCTCAGCGATCTGTCTATTTCTGTTTCCATAGTTGCCTGACTCCCCGT
CGTGTAGATAAATAAGTACGATACGGGAGGGCTTACCATCTGGCCCCAGTGTGCAATGATACCCGCGAGACCCACGCTCACCGGCTCCAGATTTATCAGCAA
TAAACCAGCCAGCCGGAAGGGCCGAGCGCAGAAAGTGGTCTGCAACTTTATCCGCTCCATCCAGTCTATTAATTGTTGCCGGAAGCTAGAGTAAG
TAGTTCGCCAGTTAATAGTTTGCACAACGTTGTTGCCATTGCTACAGGCATCGTGGTGTACGCTCGTCTTTGGTATGGCTTCATTGAGTCCGGTTC
CCAACGATCAAGGCGAGTTACATGATCCCCATGTTGTGCAAAAAAGCGTTAGCTCCTTCGGTCTCCGATCGTTGTGAGAAGTAAGTTGGCCGAG
TGTTATCACTCATGGTTATGGCAGCACTGCATAATTCTTACTGTGTCATGCCATCCGTAAGATGCTTTTCTGTGACTGGTGAGTACTCAACCAAGTCATT
CTGAGAATAGTGTATGCGGCGACCGAGTTGCTTGGCCGGCGTCAATACGGGATAATACCCGCGCCACATAGCAGAACTTAAAAAGTGTCTCATATTG
GAAAACGTTCTTCGGGGCGAAAACCTCAAGGATCTTACCGTGTGAGATCCAGTTCGATGTAACCCACTCGTGACCCAACTGATCTTCAGCATCTT
TTACTTTCACCAGCGTTTCTGGGTGAGCAAAAACAGGAAGGCAAAATGCCGCAAAAAAGGGAATAAGGGCGACACGGAATGTTGAATACTCATACT
CTTCTTTTTCAATATTATTGAAGCATTATCAGGGTATTGTCTCATGAGCGGATACATATTTGAATGATTTAGAAAAATAAACAAATAGGGGTTCCG
CGCACATTTCCCGAAAAGTGCCACCTGACGTCTAAGAAACATTATTATCATGACATTAACCTATAAAAAATAGGCGTATCACGAGGCCCTTTCGTCTC
GCGGTTTCGGTGTGACGGTGAACCTCTGACACATGCAGCTCCCGGAGACGGTACAGCTTGTCTGTAAGCGGATGCCGGGAGCAGACAAGCC
CGTCAGGGCGCGTCAGCGGTGTTGGCGGGTGTGCGGGCTGGCTTAACTATGCGGCATCAGAGCAGATTGACTGAGAGTGACCATATGGACATA
TTGCTGTAGAACGCGGTACAATTAATACATAACCT

8. References

- Adams, C. M., Reitz, J., De Brabander, J. K., Feramisco, J. D., Li, L., Brown, M. S., & Goldstein, J. L. (2004). Cholesterol and 25-Hydroxycholesterol Inhibit Activation of SREBPs by Different Mechanisms, Both Involving SCAP and Insigs*. *Journal of Biological Chemistry*, 279(50), 52772-52780. <https://doi.org/https://doi.org/10.1074/jbc.M410302200>
- Agnese, S. T., Spierto, F. W., & Hannon, W. H. (1983). Evaluation of four reagents for delipidation of serum. *Clinical Biochemistry*, 16(2), 98-100. [https://doi.org/https://doi.org/10.1016/S0009-9120\(83\)90676-8](https://doi.org/https://doi.org/10.1016/S0009-9120(83)90676-8)
- Alexandrov, L. B., Nik-Zainal, S., Wedge, D. C., Aparicio, S. A., Behjati, S., Biankin, A. V., Bignell, G. R., Bolli, N., Borg, A., & Børresen-Dale, A.-L. (2013). Signatures of mutational processes in human cancer. *Nature*, 500(7463), 415-421.
- Allain, E. P., Rouleau, M., Lévesque, E., & Guillemette, C. (2020). Emerging roles for UDP-glucuronosyltransferases in drug resistance and cancer progression. *British Journal of Cancer*, 122(9), 1277-1287. <https://doi.org/10.1038/s41416-019-0722-0>
- Amemiya-Kudo, M., Shimano, H., Hasty, A. H., Yahagi, N., Yoshikawa, T., Matsuzaka, T., Okazaki, H., Tamura, Y., Iizuka, Y., & Ohashi, K. (2002). Transcriptional activities of nuclear SREBP-1a, -1c, and -2 to different target promoters of lipogenic and cholesterologenic genes. *Journal of lipid research*, 43(8), 1220-1235.
- Angstadt, A. Y., Berg, A., Zhu, J., Miller, P., Hartman, T. J., Lesko, S. M., Muscat, J. E., Lazarus, P., & Gallagher, C. J. (2013). The effect of copy number variation in the phase II detoxification genes UGT2B17 and UGT2B28 on colorectal cancer risk. *Cancer*, 119(13), 2477-2485. <https://doi.org/10.1002/cncr.28009>
- Aqil, A., Speidel, L., Pavlidis, P., & Gokcumen, O. (2023). Balancing selection on genomic deletion polymorphisms in humans. *eLife*, 12, e79111. <https://doi.org/10.7554/eLife.79111>
- Arendt, L. M., & Kuperwasser, C. (2015). Form and function: how estrogen and progesterone regulate the mammary epithelial hierarchy. *J Mammary Gland Biol Neoplasia*, 20(1-2), 9-25. <https://doi.org/10.1007/s10911-015-9337-0>
- Arito, M., Horiba, T., Hachimura, S., Inoue, J., & Sato, R. (2008). Growth factor-induced phosphorylation of sterol regulatory element-binding proteins inhibits sumoylation, thereby stimulating the expression of their target genes, low density lipoprotein uptake, and lipid synthesis. *J Biol Chem*, 283(22), 15224-15231. <https://doi.org/10.1074/jbc.M800910200>
- Atallah, N. M., Haque, M., Quinn, C., Toss, M. S., Makhoulouf, S., Ibrahim, A., Green, A. R., Alsalem, M., Rutland, C. S., Allegrucci, C., Mongan, N. P., & Rakha, E. (2023). Characterisation of luminal and triple-negative breast cancer with HER2 Low protein expression. *European Journal of Cancer*, 195, 113371. <https://doi.org/https://doi.org/10.1016/j.ejca.2023.113371>
- Baenke, F., Peck, B., Miess, H., & Schulze, A. (2013). Hooked on fat: the role of lipid synthesis in cancer metabolism and tumour development. *Disease Models & Mechanisms*, 6(6), 1353-1363. <https://doi.org/10.1242/dmm.011338>
- Bailey, M. H., Tokheim, C., Porta-Pardo, E., Sengupta, S., Bertrand, D., Weerasinghe, A., Colaprico, A., Wendl, M. C., Kim, J., & Reardon, B. (2018). Comprehensive characterization of cancer driver genes and mutations. *Cell*, 173(2), 371-385. e318.
- Barton, V. N., D'Amato, N. C., Gordon, M. A., Christenson, J. L., Elias, A., & Richer, J. K. (2015). Androgen Receptor Biology in Triple Negative Breast Cancer: a Case for Classification as AR+ or Quadruple Negative Disease. *Horm Cancer*, 6(5-6), 206-213. <https://doi.org/10.1007/s12672-015-0232-3>

- Beaulieu, M., Lévesque, E., Hum, D. W., & Bélanger, A. (1996). Isolation and characterization of a novel cDNA encoding a human UDP-glucuronosyltransferase active on C19 steroids. *J Biol Chem*, 271(37), 22855-22862. <https://doi.org/10.1074/jbc.271.37.22855>
- Beaulieu, M., Lévesque, É., Hum, D. W., & Bélanger, A. (1998). Isolation and Characterization of a Human Orphan UDP-Glucuronosyltransferase, UGT2B11. *Biochemical and Biophysical Research Communications*, 248(1), 44-50. <https://doi.org/https://doi.org/10.1006/bbrc.1998.8908>
- Belledant, A., Hovington, H., Garcia, L., Caron, P., Brisson, H., Villeneuve, L., Simonyan, D., Têtu, B., Fradet, Y., Lacombe, L., Guillemette, C., & Lévesque, E. (2016). The UGT2B28 Sex-steroid Inactivation Pathway Is a Regulator of Steroidogenesis and Modifies the Risk of Prostate Cancer Progression. *European Urology*, 69(4), 601-609. <https://doi.org/https://doi.org/10.1016/j.eururo.2015.06.054>
- Bengoechea-Alonso, M. T., & Ericsson, J. (2009). A Phosphorylation Cascade Controls the Degradation of Active SREBP1. *Journal of Biological Chemistry*, 284(9), 5885-5895. <https://doi.org/10.1074/jbc.M807906200>
- Bengoechea-Alonso, M. T., & Ericsson, J. (2010). The ubiquitin ligase Fbxw7 controls adipocyte differentiation by targeting C/EBPalpha for degradation. *Proceedings of the National Academy of Sciences of the USA*, 107(26), 11817-11822. <https://doi.org/10.1073/pnas.0913367107>
- Bengoechea-Alonso, M. T., & Ericsson, J. (2016). The phosphorylation-dependent regulation of nuclear SREBP1 during mitosis links lipid metabolism and cell growth. *Cell Cycle*, 15(20), 2753-2765. <https://doi.org/10.1080/15384101.2016.1220456>
- Bertolio, R., Napoletano, F., Mano, M., Maurer-Stroh, S., Fantuz, M., Zannini, A., Bicciato, S., Sorrentino, G., & Del Sal, G. (2019). Sterol regulatory element binding protein 1 couples mechanical cues and lipid metabolism. *Nature Communications*, 10(1), 1326. <https://doi.org/10.1038/s41467-019-09152-7>
- Bidgood, C. L., Philp, L. K., Rockstroh, A., Lehman, M., Nelson, C. C., Sadowski, M. C., & Gunter, J. H. (2024). Valine Catabolism Drives Bioenergetic and Lipogenic Fuel Plasticity in Prostate Cancer. *bioRxiv*, 2024.2001.2001.573829. <https://doi.org/10.1101/2024.01.01.573829>
- Blevins-Primeau, A. S., Sun, D., Chen, G., Sharma, A. K., Gallagher, C. J., Amin, S., & Lazarus, P. (2009). Functional Significance of UDP-Glucuronosyltransferase Variants in the Metabolism of Active Tamoxifen Metabolites. *Cancer Research*, 69(5), 1892-1900. <https://doi.org/10.1158/0008-5472.Can-08-3708>
- Bonnefoi, H., MacGrogan, G., Poncet, C., Iggo, R., Pommeret, F., Grellety, T., Larsimont, D., Bécette, V., Kerdraon, O., Bibeau, F., Ghnassia, J. P., Picquetot, J. M., Thomas, J., Tille, J. C., Slaets, L., Bodmer, A., Bergh, J., & Cameron, D. (2019). Molecular apocrine tumours in EORTC 10994/BIG 1-00 phase III study: pathological response after neoadjuvant chemotherapy and clinical outcomes. *Br J Cancer*, 120(9), 913-921. <https://doi.org/10.1038/s41416-019-0420-y>
- Brønstad, I., Wolff, A. S. B., Løvås, K., Knappskog, P. M., & Husebye, E. S. (2011). Genome-wide copy number variation (CNV) in patients with autoimmune Addison's disease. *BMC Medical Genetics*, 12(1), 111. <https://doi.org/10.1186/1471-2350-12-111>
- Brovkovich, V., Aldrich, A., Li, N., Atilla-Gokcumen, G. E., & Frasor, J. (2019). Removal of Serum Lipids and Lipid-Derived Metabolites to Investigate Breast Cancer Cell Biology. *Proteomics*, 19(18), 1800370. <https://doi.org/https://doi.org/10.1002/pmic.201800370>
- Butler, L. M., Centenera, M. M., & Swinnen, J. V. (2016). Androgen control of lipid metabolism in prostate cancer: novel insights and future applications. *Endocrine-Related Cancer*, 23(5), 219-227. <https://doi.org/10.1530/ERC-15-0556>
- Cayrol, R., Wosik, K., Berard, J. L., Dodelet-Devillers, A., Ifergan, I., Kebir, H., Haqqani, A. S., Kreymborg, K., Krug, S., Moumdjian, R., Bouthillier, A., Becher, B., Arbour, N., David, S., Stanimirovic, D., & Prat, A. (2008). Activated leukocyte cell adhesion molecule promotes leukocyte trafficking into the central nervous system. *Nature Immunology*, 9(2), 137-145. <https://doi.org/10.1038/ni1551>

- Cerami, E., Gao, J., Dogrusoz, U., Gross, B. E., Sumer, S. O., Aksoy, B. A., Jacobsen, A., Byrne, C. J., Heuer, M. L., Larsson, E., Antipin, Y., Reva, B., Goldberg, A. P., Sander, C., & Schultz, N. (2012). The cBio cancer genomics portal: an open platform for exploring multidimensional cancer genomics data. *Cancer Discov*, 2(5), 401-404. <https://doi.org/10.1158/2159-8290.Cd-12-0095>
- Chen, X., Shi, C., He, M., Xiong, S., & Xia, X. (2023). Endoplasmic reticulum stress: molecular mechanism and therapeutic targets. *Signal Transduction and Targeted Therapy*, 8(1), 352. <https://doi.org/10.1038/s41392-023-01570-w>
- Cheng, C., Ru, P., Geng, F., Liu, J., Yoo, J. Y., Wu, X., Cheng, X., Euthine, V., Hu, P., Guo, J. Y., Lefai, E., Kaur, B., Nohturfft, A., Ma, J., Chakravarti, A., & Guo, D. (2015). Glucose-Mediated N-glycosylation of SCAP Is Essential for SREBP-1 Activation and Tumor Growth. *Cancer cell*, 28(5), 569-581. <https://doi.org/10.1016/j.ccell.2015.09.021>
- Chouinard, S., Pelletier, G., Bélanger, A., & Barbier, O. (2006). Isoform-Specific Regulation of Uridine Diphosphate-Glucuronosyltransferase 2B Enzymes in the Human Prostate: Differential Consequences for Androgen and Bioactive Lipid Inactivation. *Endocrinology*, 147(11), 5431-5442. <https://doi.org/10.1210/en.2006-0229>
- Colgan, S. M., Tang, D., Werstuck, G. H., & Austin, R. C. (2007). Endoplasmic reticulum stress causes the activation of sterol regulatory element binding protein-2. *Int J Biochem Cell Biol*, 39(10), 1843-1851. <https://doi.org/10.1016/j.biocel.2007.05.002>
- Consortium, I. T. P.-C. A. o. W. G. (2020). Pan-cancer analysis of whole genomes. *Nature*, 578(7793), 82-93.
- Court, M. H., Zhang, X., Ding, X., Yee, K. K., Hesse, L. M., & Finel, M. (2012). Quantitative distribution of mRNAs encoding the 19 human UDP-glucuronosyltransferase enzymes in 26 adult and 3 fetal tissues. *Xenobiotica*, 42(3), 266-277.
- Curtis, C., Shah, S. P., Chin, S.-F., Turashvili, G., Rueda, O. M., Dunning, M. J., Speed, D., Lynch, A. G., Samarajiwa, S., Yuan, Y., Gräf, S., Ha, G., Haffari, G., Bashashati, A., Russell, R., McKinney, S., Caldas, C., Aparicio, S., Curtis†, C.,...Data analysis, s. (2012). The genomic and transcriptomic architecture of 2,000 breast tumours reveals novel subgroups. *Nature*, 486(7403), 346-352. <https://doi.org/10.1038/nature10983>
- Daemen, A., & Manning, G. (2018). HER2 is not a cancer subtype but rather a pan-cancer event and is highly enriched in AR-driven breast tumors. *Breast Cancer Research*, 20(1), 8. <https://doi.org/10.1186/s13058-018-0933-y>
- Dai, X., Xiang, L., Li, T., & Bai, Z. (2016). Cancer Hallmarks, Biomarkers and Breast Cancer Molecular Subtypes. *Journal of Cancer*, 7(10), 1281-1294. <https://doi.org/10.7150/jca.13141>
- Dang, L., Yoon, K., Wang, M., & Gaiano, N. (2006). Notch3 Signaling Promotes Radial Glial/Progenitor Character in the Mammalian Telencephalon. *Developmental Neuroscience*, 28(1-2), 58-69. <https://doi.org/10.1159/000090753>
- Das, A. T., Tenenbaum, L., & Berkhout, B. (2016). Tet-On Systems For Doxycycline-inducible Gene Expression. *Curr Gene Ther*, 16(3), 156-167. <https://doi.org/10.2174/1566523216666160524144041>
- Dates, C. R., Fahmi, T., Pyrek, S. J., Yao-Borengasser, A., Borowa-Mazgaj, B., Bratton, S. M., Kadlubar, S. A., Mackenzie, P. I., Haun, R. S., & Radominska-Pandya, A. (2015). Human UDP-Glucuronosyltransferases: Effects of altered expression in breast and pancreatic cancer cell lines. *Cancer biology & therapy*, 16(5), 714-723. <https://doi.org/10.1080/15384047.2015.1026480>
- Davey, R. A., & Grossmann, M. (2016). Androgen Receptor Structure, Function and Biology: From Bench to Bedside. *The Clinical biochemist. Reviews*, 37(1), 3-15. <https://www.ncbi.nlm.nih.gov/pubmed/27057074>
- <https://www.ncbi.nlm.nih.gov/pmc/PMC4810760/>
- Davis, R. J., Welcker, M., & Clurman, B. E. (2014). Tumor suppression by the Fbw7 ubiquitin ligase: mechanisms and opportunities. *Cancer cell*, 26(4), 455-464. <https://doi.org/10.1016/j.ccell.2014.09.013>

- De Piano, M., Manuelli, V., Zadra, G., Otte, J., Edqvist, P.-H. D., Pontén, F., Nowinski, S., Niaouris, A., Grigoriadis, A., Loda, M., Van Hemelrijck, M., & Wells, C. M. (2020). Lipogenic signalling modulates prostate cancer cell adhesion and migration via modification of Rho GTPases. *Oncogene*, 39(18), 3666-3679. <https://doi.org/10.1038/s41388-020-1243-2>
- DeBose-Boyd, R. A., Brown, M. S., Li, W.-P., Nohturfft, A., Goldstein, J. L., & Espenshade, P. J. (1999). Transport-Dependent Proteolysis of SREBP: Relocation of Site-1 Protease from Golgi to ER Obviates the Need for SREBP Transport to Golgi. *Cell*, 99(7), 703-712. [https://doi.org/https://doi.org/10.1016/S0092-8674\(00\)81668-2](https://doi.org/https://doi.org/10.1016/S0092-8674(00)81668-2)
- DepMap. (2019). *DepMap 19Q3 Public* (<https://doi.org/DOI:10.6084/m9.figshare.9201770.v1>).
- Dluzen, D. F., Sutliff, A. K., Chen, G., Watson, C. J., Ishmael, F. T., & Lazarus, P. (2016). Regulation of UGT2B Expression and Activity by miR-216b-5p in Liver Cancer Cell Lines. *J Pharmacol Exp Ther*, 359(1), 182-193. <https://doi.org/10.1124/jpet.116.235044>
- Doane, A., Danso, M., Lal, P., Donaton, M., Zhang, L., Hudis, C., & Gerald, W. (2006). An estrogen receptor-negative breast cancer subset characterized by a hormonally regulated transcriptional program and response to androgen. *Oncogene*, 25(28), 3994-4008.
- Dolatabadi, S., Candia, J., Akrap, N., Vannas, C., Tesan Tomic, T., Losert, W., Landberg, G., Åman, P., & Ståhlberg, A. (2017). Cell Cycle and Cell Size Dependent Gene Expression Reveals Distinct Subpopulations at Single-Cell Level [Original Research]. *Frontiers in Genetics*, 8(1). <https://doi.org/10.3389/fgene.2017.00001>
- Dong, Q., Giorgianni, F., Beranova-Giorgianni, S., Deng, X., O'Meally, R. N., Bridges, D., Park, E. A., Cole, R. N., Elam, M. B., & Raghov, R. (2015). Glycogen synthase kinase-3-mediated phosphorylation of serine 73 targets sterol response element binding protein-1c (SREBP-1c) for proteasomal degradation. *Biosci Rep*, 36(1), e00284. <https://doi.org/10.1042/bsr20150234>
- Dozmorov, M. G., Hurst, R. E., Culkin, D. J., Kropp, B. P., Frank, M. B., Osban, J., Penning, T. M., & Lin, H.-K. (2009). Unique patterns of molecular profiling between human prostate cancer LNCaP and PC-3 cells. *The Prostate*, 69(10), 1077-1090. <https://doi.org/10.1002/pros.20960>
- Eberlé, D., Hegarty, B., Bossard, P., Ferré, P., & Foulle, F. (2004). SREBP transcription factors: master regulators of lipid homeostasis. *Biochimie*, 86(11), 839-848. <https://doi.org/https://doi.org/10.1016/j.biochi.2004.09.018>
- Epand, R. M. (2006). Cholesterol and the interaction of proteins with membrane domains. *Progress in Lipid Research*, 45(4), 279-294. <https://doi.org/https://doi.org/10.1016/j.plipres.2006.02.001>
- Espenshade, P. J., Li, W.-P., & Yabe, D. (2002). Sterols block binding of COPII proteins to SCAP, thereby controlling SCAP sorting in ER. *Proceedings of the National Academy of Sciences of the USA*, 99(18), 11694-11699. <https://doi.org/10.1073/pnas.182412799>
- Fabregat, A., Korninger, F., Hausmann, K., Sidiropoulos, K., Williams, M., Garapati, P., Jupe, S., Hermjakob, H., Jassal, B., May, B., Wu, G., Weiser, J., Rothfels, K., Milacic, M., Webber, M., Haw, R., McKay, S., Gillespie, M., Stein, L.,...D'Eustachio, P. (2015). The Reactome pathway Knowledgebase. *Nucleic Acids Research*, 44(D1), D481-D487. <https://doi.org/10.1093/nar/gkv1351>
- Fabregat, A., Sidiropoulos, K., Viteri, G., Forner, O., Marin-Garcia, P., Arnau, V., D'Eustachio, P., Stein, L., & Hermjakob, H. (2017). Reactome pathway analysis: a high-performance in-memory approach. *BMC Bioinformatics*, 18(1), 142. <https://doi.org/10.1186/s12859-017-1559-2>
- Farla, P., Hersmus, R., Trapman, J., & Houtsmuller, A. B. (2005). Antiandrogens prevent stable DNA-binding of the androgen receptor. *Journal of Cell Science*, 118(18), 4187-4198. <https://doi.org/10.1242/jcs.02546>
- Feng, Y., Spezia, M., Huang, S., Yuan, C., Zeng, Z., Zhang, L., Ji, X., Liu, W., Huang, B., Luo, W., Liu, B., Lei, Y., Du, S., Vuppalapati, A., Luu, H. H., Haydon, R. C., He, T.-C., & Ren, G. (2018). Breast cancer development and progression: Risk factors, cancer stem cells, signaling pathways,

- genomics, and molecular pathogenesis. *Genes & Diseases*, 5(2), 77-106. <https://doi.org/https://doi.org/10.1016/j.gendis.2018.05.001>
- Feoktistova, M., Geserick, P., & Leverkus, M. (2016). Crystal violet assay for determining viability of cultured cells. *Cold Spring Harb Protoc*, 2016(4), pdb. prot087379.
- Ferlay, J., Colombet, M., Soerjomataram, I., Parkin, D. M., Piñeros, M., Znaor, A., & Bray, F. (2021). Cancer statistics for the year 2020: An overview. *International Journal of Cancer*, 149(4), 778-789. <https://doi.org/https://doi.org/10.1002/ijc.33588>
- Fisher, M. B., Paine, M. F., Strelevitz, T. J., & Wrighton, S. A. (2001). The role of hepatic and extrahepatic UDP-glucuronosyltransferases in human drug metabolism. *Drug Metabolism Reviews*, 33(4), 273-297. <https://doi.org/10.1081/DMR-120000653>
- Fujiwara, R., Yokoi, T., & Nakajima, M. (2016). Structure and Protein–Protein Interactions of Human UDP-Glucuronosyltransferases [Review]. 7(388). <https://doi.org/10.3389/fphar.2016.00388>
- Gao, Y., Zhang, H., Lirussi, F., Garrido, C., Ye, X.-Y., & Xie, T. (2020). Dual inhibitors of histone deacetylases and other cancer-related targets: A pharmacological perspective. *Biochemical Pharmacology*, 182, 114224. <https://doi.org/https://doi.org/10.1016/j.bcp.2020.114224>
- Garvin, A. J., Khalaf, A. H. A., Rettino, A., Xicluna, J., Butler, L., Morris, J. R., Heery, D. M., & Clarke, N. M. (2019). GSK3 β -SCFFBXW7 α mediated phosphorylation and ubiquitination of IRF1 are required for its transcription-dependent turnover. *Nucleic Acids Research*, 47(9), 4476-4494. <https://doi.org/10.1093/nar/gkz163>
- Ge, S., Tu, Y., & Hu, M. (2016). Challenges and Opportunities with Predicting in Vivo Phase II Metabolism via Glucuronidation from in Vitro Data. *Curr Pharmacol Rep*, 2(6), 326-338. <https://doi.org/10.1007/s40495-016-0076-8>
- Germain, N., Dhayer, M., Boileau, M., Fovez, Q., Kluza, J., & Marchetti, P. (2020). Lipid Metabolism and Resistance to Anticancer Treatment. *Biology (Basel)*, 9(12). <https://doi.org/10.3390/biology9120474>
- Gilbert, Luke A., Horlbeck, Max A., Adamson, B., Villalta, Jacqueline E., Chen, Y., Whitehead, Evan H., Guimaraes, C., Panning, B., Ploegh, Hidde L., Bassik, Michael C., Qi, Lei S., Kampmann, M., & Weissman, Jonathan S. (2014). Genome-Scale CRISPR-Mediated Control of Gene Repression and Activation. *Cell*, 159(3), 647-661. <https://doi.org/https://doi.org/10.1016/j.cell.2014.09.029>
- Giovannelli, P., Di Donato, M., Auricchio, F., Castoria, G., & Migliaccio, A. (2019). Androgens Induce Invasiveness of Triple Negative Breast Cancer Cells Through AR/Src/PI3-K Complex Assembly. *Scientific Reports*, 9(1), 4490. <https://doi.org/10.1038/s41598-019-41016-4>
- Goldstein, J. L., DeBose-Boyd, R. A., & Brown, M. S. (2006). Protein sensors for membrane sterols. *Cell*, 124(1), 35-46.
- Gong, Y., Lee, J. N., Lee, P. C., Goldstein, J. L., Brown, M. S., & Ye, J. (2006). Sterol-regulated ubiquitination and degradation of Insig-1 creates a convergent mechanism for feedback control of cholesterol synthesis and uptake. *Cell Metabolism*, 3(1), 15-24.
- Gossen, M., & Bujard, H. (1992). Tight control of gene expression in mammalian cells by tetracycline-responsive promoters. *Proceedings of the National Academy of Sciences*, 89(12), 5547-5551.
- Gossen, M., Freundlieb, S., Bender, G., Müller, G., Hillen, W., & Bujard, H. (1995). Transcriptional activation by tetracyclines in mammalian cells. *Science*, 268(5218), 1766-1769.
- Grancharov, K., Naydenova, Z., Lozeva, S., & Golovinsky, E. (2001). Natural and synthetic inhibitors of UDP-glucuronosyltransferase. *Pharmacology & Therapeutics*, 89(2), 171-186. [https://doi.org/https://doi.org/10.1016/S0163-7258\(00\)00109-1](https://doi.org/https://doi.org/10.1016/S0163-7258(00)00109-1)
- Grant, D. J., Chen, Z., Howard, L. E., Wiggins, E., De Hoedt, A., Vidal, A. C., Carney, S. T., Squires, J., Magyar, C. E., Huang, J., & Freedland, S. J. (2017). UDP-glucuronosyltransferases and biochemical recurrence in prostate cancer progression. *BMC Cancer*, 17(1), 463. <https://doi.org/10.1186/s12885-017-3463-6>
- Grantham, R. (1974). Amino Acid Difference Formula to Help Explain Protein Evolution. *Science*, 185(4154), 862-864. <https://doi.org/10.1126/science.185.4154.862>

- Grimes, C. A., & Jope, R. S. (2001). The multifaceted roles of glycogen synthase kinase 3beta in cellular signaling. *Prog Neurobiol*, 65(4), 391-426. [https://doi.org/10.1016/s0301-0082\(01\)00011-9](https://doi.org/10.1016/s0301-0082(01)00011-9)
- Guillemette, C., Bélanger, A., & Lépine, J. (2004). Metabolic inactivation of estrogens in breast tissue by UDP-glucuronosyltransferase enzymes: an overview. *Breast cancer research : BCR*, 6(6), 246-254. <https://doi.org/10.1186/bcr936>
- Guillemette, C., Lévesque, E., Harvey, M., Bellemare, J., & Menard, V. (2010). UGT genomic diversity: beyond gene duplication AU - Guillemette, Chantal. *Drug Metabolism Reviews*, 42(1), 24-44. <https://doi.org/10.3109/03602530903210682>
- Guillemette, C., Lévesque, É., & Rouleau, M. (2014). Pharmacogenomics of Human Uridine Diphospho-Glucuronosyltransferases and Clinical Implications. *Clinical Pharmacology & Therapeutics*, 96(3), 324-339. <https://doi.org/10.1038/clpt.2014.126>
- Guo, G., Pinello, L., Han, X., Lai, S., Shen, L., Lin, T.-W., Zou, K., Yuan, G.-C., & Orkin, S. H. (2016). Serum-Based Culture Conditions Provoke Gene Expression Variability in Mouse Embryonic Stem Cells as Revealed by Single-Cell Analysis. *Cell Reports*, 14(4), 956-965. <https://doi.org/10.1016/j.celrep.2015.12.089>
- Gupta-Rossi, N., Le Bail, O., Gonen, H., Brou, C., Logeat, F., Six, E., Ciechanover, A., & Israël, A. (2001). Functional interaction between SEL-10, an F-box protein, and the nuclear form of activated Notch1 receptor. *Journal of Biological Chemistry*, 276(37), 34371-34378.
- Gutierrez, C., & Schiff, R. (2011). HER2: biology, detection, and clinical implications. *Arch Pathol Lab Med*, 135(1), 55-62. <https://doi.org/10.5858/2010-0454-rar.1>
- Haakensen, V. D., Biong, M., Lingjærde, O. C., Holmen, M. M., Frantzen, J. O., Chen, Y., Navjord, D., Romundstad, L., Lüders, T., Bukholm, I. K., Solvang, H. K., Kristensen, V. N., Ursin, G., Børresen-Dale, A.-L., & Helland, Å. (2010). Expression levels of uridine 5'-diphosphoglucuronosyltransferase genes in breast tissue from healthy women are associated with mammographic density. *Breast Cancer Research*, 12(4), R65. <https://doi.org/10.1186/bcr2632>
- Habibi, M., Mirfakhraie, R., Khani, M., Rakhshan, A., Azargashb, E., & Pouresmaeili, F. (2017). Genetic variations in UGT2B28, UGT2B17, UGT2B15 genes and the risk of prostate cancer: A case-control study. *Gene*, 634, 47-52. <https://doi.org/https://doi.org/10.1016/j.gene.2017.08.038>
- Han, W., Gao, S., Barrett, D., Ahmed, M., Han, D., Macoska, J. A., He, H. H., & Cai, C. (2017). Reactivation of androgen receptor-regulated lipid biosynthesis drives the progression of castration-resistant prostate cancer [Original Article]. *Oncogene*, 37, 710-721. <https://doi.org/10.1038/onc.2017.385>
- Hanahan, D., Jessee, J., & Bloom, F. R. (1991). Plasmid transformation of *Escherichia coli* and other bacteria. *Methods Enzymol*, 204, 63-113. [https://doi.org/10.1016/0076-6879\(91\)04006-a](https://doi.org/10.1016/0076-6879(91)04006-a)
- Hara, A., & Taketomi, T. (1982). Isolation and determination of cholesterol glucuronide in human liver. *Lipids*, 17(8), 515-518. <https://doi.org/https://doi.org/10.1007/BF02535377>
- Harris, L.-A. L. S., Skinner, J. R., & Wolins, N. E. (2013). Imaging of neutral lipids and neutral lipid associated proteins. *Methods in Cell Biology*, 116, 213-226. <https://doi.org/10.1016/B978-0-12-408051-5.00011-5>
- Harwood, A. J. (2001). Regulation of GSK-3: A Cellular Multiprocessor. *Cell*, 105(7), 821-824. [https://doi.org/10.1016/S0092-8674\(01\)00412-3](https://doi.org/10.1016/S0092-8674(01)00412-3)
- Hayashi, T., Hayashi, E., Fujimoto, M., Sprong, H., & Su, T.-P. (2012). The lifetime of UDP-galactose:ceramide galactosyltransferase is controlled by a distinct endoplasmic reticulum-associated degradation (ERAD) regulated by sigma-1 receptor chaperones. *The Journal of Biological Chemistry*, 287(51), 43156-43169. <https://doi.org/10.1074/jbc.M112.380444>
- Hayashi, T., & Su, T.-P. (2007). Sigma-1 receptor chaperones at the ER-mitochondrion interface regulate Ca²⁺ signaling and cell survival. *Cell*, 131(3), 596-610.
- He, L., Du, Z., Xiong, X., Ma, H., Zhu, Z., Gao, H., Cao, J., Li, T., Li, H., Yang, K., Chen, G., Richer, J. K., & Gu, H. (2017). Targeting Androgen Receptor in Treating HER2 Positive Breast Cancer. *Scientific Reports*, 7(1), 14584. <https://doi.org/10.1038/s41598-017-14607-2>

- He, Y., Liu, Y., Gong, J., Liu, C., Zhang, H., & Wu, H. (2019). Identification of key pathways and candidate genes in pancreatic ductal adenocarcinoma using bioinformatics analysis. *Oncology letters*, *17*(4), 3751-3764.
- Heemers, H., Heyns, W., Verhoeven, G., & Swinnen, J. V. (2005). Androgens stimulate the SREBP pathway in prostate cancer cells by inducing a shift in the SCAP-retention protein(s) balance. *Hormonal Carcinogenesis*, 357-363.
- Heemers, H., Maes, B., Fougelle, F., Heyns, W., Verhoeven, G., & Swinnen, J. V. (2001). Androgens stimulate lipogenic gene expression in prostate cancer cells by activation of the sterol regulatory element-binding protein cleavage activating protein/sterol regulatory element-binding protein pathway. *Molecular Endocrinology*, *15*(10), 1817-1828.
- Heemers, H., Verrijdt, G., Organe, S., Claessens, F., Heyns, W., Verhoeven, G., & Swinnen, J. V. (2004). Identification of an Androgen Response Element in Intron 8 of the Sterol Regulatory Element-binding Protein Cleavage-activating Protein Gene Allowing Direct Regulation by the Androgen Receptor *. *Journal of Biological Chemistry*, *279*(29), 30880-30887. <https://doi.org/10.1074/jbc.M401615200>
- Heemers, H. V., & Tindall, D. J. (2007). Androgen receptor (AR) coregulators: a diversity of functions converging on and regulating the AR transcriptional complex. *Endocrine reviews*, *28*(7), 778-808.
- Hegarty, B. D., Bobard, A., Hainault, I., Ferre, P., Bossard, P., & Fougelle, F. (2005). Distinct roles of insulin and liver X receptor in the induction and cleavage of sterol regulatory element-binding protein-1c. *Proceedings of the National Academy of Sciences of the USA*, *102*(3), 791-796. <https://doi.org/10.1073/pnas.0405067102>
- Hickey, T. E., Robinson, J. L., Carroll, J. S., & Tilley, W. D. (2012). Minireview: The androgen receptor in breast tissues: growth inhibitor, tumor suppressor, oncogene? *Mol Endocrinol*, *26*(8), 1252-1267. <https://doi.org/10.1210/me.2012-1107>
- Hirai, H., Tani, T., & Kikyo, N. (2010). Structure and functions of powerful transactivators: VP16, MyoD and FoxA. *Int J Dev Biol*, *54*(11-12), 1589-1596. <https://doi.org/10.1387/ijdb.103194hh>
- Hirano, Y., Yoshida, M., Shimizu, M., & Sato, R. (2001). Direct demonstration of rapid degradation of nuclear sterol regulatory element-binding proteins by the ubiquitin-proteasome pathway. *Journal of Biological Chemistry*, *276*(39), 36431-36437.
- Hobbs, S., Jitrapakdee, S., & Wallace, J. C. (1998). Development of a bicistronic vector driven by the human polypeptide chain elongation factor 1alpha promoter for creation of stable mammalian cell lines that express very high levels of recombinant proteins. *Biochemical and Biophysical Research Communications*, *252*(2), 368-372. <https://doi.org/10.1006/bbrc.1998.9646>
- Holliday, D. L., & Speirs, V. (2011). Choosing the right cell line for breast cancer research. *Breast cancer research : BCR*, *13*(4), 215-215. <https://doi.org/10.1186/bcr2889>
- Hölttä-Vuori, M., Uronen, R.-L., Repakova, J., Salonen, E., Vattulainen, I., Panula, P., Li, Z., Bittman, R., & Ikonen, E. (2008). BODIPY-Cholesterol: A New Tool to Visualize Sterol Trafficking in Living Cells and Organisms. *Traffic*, *9*(11), 1839-1849. <https://doi.org/10.1111/j.1600-0854.2008.00801.x>
- Horton, J. D., Goldstein, J. L., & Brown, M. (2002). SREBPs: activators of the complete program of cholesterol and fatty acid synthesis in the liver. *The Journal of clinical investigation*, *109*(9), 1125-1131.
- Hu, Selth, L. A., Tarulli, G. A., Meech, R., Wijayakumara, D., Chanawong, A., Russell, R., Caldas, C., Robinson, J. L., Carroll, J. S., Tilley, W. D., Mackenzie, P. I., & Hickey, T. E. (2016). Androgen and Estrogen Receptors in Breast Cancer Coregulate Human UDP-Glucuronosyltransferases 2B15 and 2B17. *Cancer Research*, *76*(19), 5881-5893. <https://doi.org/10.1158/0008-5472.Can-15-3372>
- Hu, D. G., Hulin, J.-A., Nair, P. C., Haines, A. Z., McKinnon, R. A., Mackenzie, P. I., & Meech, R. (2019). The UGTome: The expanding diversity of UDP glycosyltransferases and its impact on small

- molecule metabolism. *Pharmacology & Therapeutics*, 204, 107414. <https://doi.org/https://doi.org/10.1016/j.pharmthera.2019.107414>
- Hu, D. G., Mackenzie, P. I., McKinnon, R. A., & Meech, R. (2016B). Genetic polymorphisms of human UDP-glucuronosyltransferase (UGT) genes and cancer risk. *Drug Metabolism Reviews*, 48(1), 47-69. <https://doi.org/10.3109/03602532.2015.1131292>
- Hu, D. G., Mackenzie, P. I., Nair, P. C., McKinnon, R. A., & Meech, R. (2020). The Expression Profiles of ADME Genes in Human Cancers and Their Associations with Clinical Outcomes. *Cancers*, 12(11), 3369. <https://www.mdpi.com/2072-6694/12/11/3369>
- Hu, D. G., Marri, S., Hulin, J.-A., McKinnon, R. A., Mackenzie, P. I., & Meech, R. (2022). The Somatic Mutation Landscape of UDP-Glycosyltransferase (UGT) Genes in Human Cancers. *Cancers*, 14(22), 5708. <https://www.mdpi.com/2072-6694/14/22/5708>
- Hu, D. G., Marri, S., Mackenzie, P. I., Hulin, J. A., McKinnon, R. A., & Meech, R. (2021). The Expression Profiles and Deregulation of UDP-Glycosyltransferase (UGT) Genes in Human Cancers and Their Association with Clinical Outcomes. *Cancers (Basel)*, 13(17). <https://doi.org/10.3390/cancers13174491>
- Hu, D. G., Marri, S., McKinnon, R. A., Mackenzie, P. I., & Meech, R. (2019). Deregulation of the Genes that Are Involved in Drug Absorption, Distribution, Metabolism, and Excretion in Hepatocellular Carcinoma. *Journal of Pharmacology and Experimental Therapeutics*, 368(3), 363-374. <https://doi.org/10.1124/jpet.118.255018>
- Hu, D. G., Meech, R., McKinnon, R. A., & Mackenzie, P. I. (2014). Transcriptional regulation of human UDP-glucuronosyltransferase genes. *Drug Metabolism Reviews*, 46(4), 421-458. <https://doi.org/10.3109/03602532.2014.973037>
- Hu, L., Wu, Y., Guan, X., Liang, Y., Yao, X., Tan, D., Bai, Y., Xiong, G., & Yang, K. (2015). Germline copy number loss of UGT2B28 and gain of PLEC contribute to increased human esophageal squamous cell carcinoma risk in Southwest China. *Am J Cancer Res*, 5(10), 3056-3071.
- Hu, R., Dunn, T. A., Wei, S., Isharwal, S., Veltri, R. W., Humphreys, E., Han, M., Partin, A. W., Vessella, R. L., Isaacs, W. B., Bova, G. S., & Luo, J. (2009). Ligand-independent androgen receptor variants derived from splicing of cryptic exons signify hormone-refractory prostate cancer. *Cancer Res*, 69(1), 16-22. <https://doi.org/10.1158/0008-5472.Can-08-2764>
- Huang, S. Y., Huang, G. J., Wu, H. C., Kao, M. C., & Huang, W. C. (2018). Ganoderma tsugae Inhibits the SREBP-1/AR Axis Leading to Suppression of Cell Growth and Activation of Apoptosis in Prostate Cancer Cells. *Molecules*, 23(10), 1-12. <https://doi.org/10.3390/molecules23102539>
- Huang, W.-C., Li, X., Liu, J., Lin, J., & Chung, L. W. (2012). Activation of androgen receptor, lipogenesis, and oxidative stress converged by SREBP-1 is responsible for regulating growth and progression of prostate cancer cells. *Molecular Cancer Research*, 10(1), 133-142.
- Huang, W.-C., Zhau, H. E., & Chung, L. W. (2010). Androgen receptor survival signaling is blocked by anti- β 2-microglobulin monoclonal antibody via a MAPK/lipogenic pathway in human prostate cancer cells. *Journal of Biological Chemistry*, 285(11), 7947-7956.
- Hübner, S., Eam, J. E., Hübner, A., & Jans, D. A. (2006). Laminopathy-inducing lamin A mutants can induce redistribution of lamin binding proteins into nuclear aggregates. *Experimental Cell Research*, 312(2), 171-183. <https://doi.org/https://doi.org/10.1016/j.yexcr.2005.10.011>
- Iqbal, N., & Iqbal, N. (2014). Human Epidermal Growth Factor Receptor 2 (HER2) in Cancers: Overexpression and Therapeutic Implications. *Mol Biol Int*, 2014, 852748. <https://doi.org/10.1155/2014/852748>
- Irisawa, M., Inoue, J., Ozawa, N., Mori, K., & Sato, R. (2009). The sterol-sensing endoplasmic reticulum (ER) membrane protein TRC8 hampers ER to Golgi transport of sterol regulatory element-binding protein-2 (SREBP-2)/SREBP cleavage-activated protein and reduces SREBP-2 cleavage. *J Biol Chem*, 284(42), 28995-29004. <https://doi.org/10.1074/jbc.M109.041376>
- Iwase, M., Watanabe, K., Shimizu, M., Suzuki, T., Yamamoto, Y., Inoue, J., & Sato, R. (2019). Chrysin reduces the activity and protein level of mature forms of sterol regulatory element-binding

- proteins. *Bioscience, Biotechnology, and Biochemistry*, 83(9), 1740-1746. <https://doi.org/10.1080/09168451.2019.1608806>
- Jackson, A. L., Bartz, S. R., Schelter, J., Kobayashi, S. V., Burchard, J., Mao, M., Li, B., Cavet, G., & Linsley, P. S. (2003). Expression profiling reveals off-target gene regulation by RNAi. *Nature biotechnology*, 21(6), 635-637.
- Jancova, P., Anzenbacher, P., & Anzenbacherova, E. (2010). Phase II drug metabolizing enzymes. *Biomed Pap Med Fac Univ Palacky Olomouc Czech Repub*, 154(2), 103-116.
- Jeong, B.-C., Hong, C. Y., Chattopadhyay, S., Park, J. H., Gong, E.-Y., Kim, H.-J., Chun, S.-Y., & Lee, K. (2004). Androgen Receptor Corepressor-19 kDa (ARR19), a Leucine-Rich Protein that Represses the Transcriptional Activity of Androgen Receptor through Recruitment of Histone Deacetylase. *Molecular Endocrinology*, 18(1), 13-25. <https://doi.org/10.1210/me.2003-0065>
- Jeong, J., Lee, J., Lim, J., Shin, J., Yoo, K., Kim, J., Tanaka, Y., Tae, H. S., Kim, L. K., Park, I.-H., Wysolmerski, J., & Choi, J. (2024). FOXA1 is required for ErbB2 expression and luminal differentiation in HER2-positive breast cancer. *bioRxiv*, 2024.2004.2016.589460. <https://doi.org/10.1101/2024.04.16.589460>
- Ji, S., Qin, Y., Shi, S., Liu, X., Hu, H., Zhou, H., Gao, J., Zhang, B., Xu, W., Liu, J., Liang, D., Liu, L., Liu, C., Long, J., Zhou, H., Chiao, P. J., Xu, J., Ni, Q., Gao, D., & Yu, X. (2015). ERK kinase phosphorylates and destabilizes the tumor suppressor FBW7 in pancreatic cancer. *Cell Research*, 25(5), 561-573. <https://doi.org/10.1038/cr.2015.30>
- Jin, H., Meng, R., Li, C. S., CHAI, O. H., Lee, Y. H., Park, B.-H., Lee, J.-S., & Kim, S. M. (2024). HN1-mediated Activation of Lipogenesis Through AKT-SREBP Signaling Promotes Hepatocellular Carcinoma Cell Proliferation and Metastasis. *Cancer Gene Therapy*. <https://doi.org/https://doi.org/10.1038/s41417-024-00827-y>
- Joseph, D. P., Guengerich, P. F., & Miners, J. O. (2005). "Phase I and Phase II" drug metabolism: terminology that we should phase out? *Drug Metabolism Reviews*, 37(4), 575-580.
- Joshi, N., Johnson, L. L., Wei, W.-Q., Abnet, C. C., Dong, Z.-W., Taylor, P. R., Limburg, P. J., Dawsey, S. M., Hawk, E. T., Qiao, Y.-L., & Kirsch, I. R. (2006). Gene Expression Differences in Normal Esophageal Mucosa Associated with Regression and Progression of Mild and Moderate Squamous Dysplasia in a High-Risk Chinese Population. *Cancer Research*, 66(13), 6851-6860. <https://doi.org/10.1158/0008-5472.Can-06-0662>
- Ju, U.-I., Jeong, D.-W., Seo, J., Park, J. B., Park, J.-W., Suh, K.-S., Kim, J. B., & Chun, Y.-S. (2020). Neddylation of sterol regulatory element-binding protein 1c is a potential therapeutic target for nonalcoholic fatty liver treatment. *Cell Death & Disease*, 11(4), 283. <https://doi.org/10.1038/s41419-020-2472-6>
- Jude, A. R., Little, J. M., Czernik, P. J., Tephly, T. R., Grant, D. F., & Radominska-Pandya, A. (2001). Glucuronidation of Linoleic Acid Diols by Human Microsomal and Recombinant UDP-Glucuronosyltransferases: Identification of UGT2B7 as the Major Isoform Involved. *Archives of Biochemistry and Biophysics*, 389(2), 176-186. <https://doi.org/https://doi.org/10.1006/abbi.2001.2344>
- Kaivosari, S., Toivonen, P., Hesse, L. M., Koskinen, M., Court, M. H., & Finel, M. (2007). Nicotine Glucuronidation and the Human UDP-Glucuronosyltransferase UGT2B10. *Molecular Pharmacology*, 72(3), 761-768. <https://doi.org/10.1124/mol.107.037093>
- Kammoun, H. L., Chabanon, H., Hainault, I., Luquet, S., Magnan, C., Koike, T., Ferré, P., & Foufelle, F. (2009). GRP78 expression inhibits insulin and ER stress-induced SREBP-1c activation and reduces hepatic steatosis in mice. *J Clin Invest*, 119(5), 1201-1215. <https://doi.org/10.1172/jci37007>
- Kanayama, T., Arito, M., So, K., Hachimura, S., Inoue, J., & Sato, R. (2007). Interaction between sterol regulatory element-binding proteins and liver receptor homolog-1 reciprocally suppresses their transcriptional activities. *J Biol Chem*, 282(14), 10290-10298. <https://doi.org/10.1074/jbc.M700270200>
- Kaushik, A. K., Vareed, S. K., Basu, S., Putluri, V., Putluri, N., Panzitt, K., Brennan, C. A., Chinnaiyan, A. M., Vergara, I. A., & Erho, N. (2013). Metabolomic profiling identifies biochemical

- pathways associated with castration-resistant prostate cancer. *Journal of proteome research*, 13(2), 1088-1100.
- Kim, J. B., Wright, H. M., Wright, M., & Spiegelman, B. M. (1998). ADD1/SREBP1 activates PPARgamma through the production of endogenous ligand. *Proc Natl Acad Sci U S A*, 95(8), 4333-4337. <https://doi.org/10.1073/pnas.95.8.4333>
- Kim, Y.-R., Lee, E.-J., Shin, K.-O., Kim, M. H., Pewzner-Jung, Y., Lee, Y.-M., Park, J.-W., Futerman, A. H., & Park, W.-J. (2019). Hepatic triglyceride accumulation via endoplasmic reticulum stress-induced SREBP-1 activation is regulated by ceramide synthases. *Experimental & Molecular Medicine*, 51(11), 1-16. <https://doi.org/10.1038/s12276-019-0340-1>
- King, M.-C., Marks, J. H., & Mandell, J. B. (2003). Breast and Ovarian Cancer Risks Due to Inherited Mutations in BRCA1 and BRCA2. *Science*, 302(5645), 643-650. <https://doi.org/10.1126/science.1088759>
- Klenova, E., Chernukhin, I., Inoue, T., Shamsuddin, S., & Norton, J. (2002). Immunoprecipitation techniques for the analysis of transcription factor complexes. *Methods*, 26(3), 254-259. [https://doi.org/https://doi.org/10.1016/S1046-2023\(02\)00029-4](https://doi.org/https://doi.org/10.1016/S1046-2023(02)00029-4)
- Kober, D. L., Radhakrishnan, A., Goldstein, J. L., Brown, M. S., Clark, L. D., Bai, X.-c., & Rosenbaum, D. M. (2021). Scap structures highlight key role for rotation of intertwined luminal loops in cholesterol sensing. *Cell*, 184(14), 3689-3701.e3622. <https://doi.org/https://doi.org/10.1016/j.cell.2021.05.019>
- Kolvenbag, G. J. C. M., Blackledge, G. R. P., & Gotting-Smith, K. (1998). Bicalutamide (Casodex®) in the treatment of prostate cancer: History of clinical development. *The Prostate*, 34(1), 61-72. [https://doi.org/https://doi.org/10.1002/\(SICI\)1097-0045\(19980101\)34:1<61::AID-PROS8>3.0.CO;2-N](https://doi.org/https://doi.org/10.1002/(SICI)1097-0045(19980101)34:1<61::AID-PROS8>3.0.CO;2-N)
- Krycer, J. R., & Brown, A. J. (2011). Cross-talk between the Androgen Receptor and the Liver X Receptor implications for cholesterol homeostasis. *Journal of Biological Chemistry*, 286(23), 20637-20647.
- Krycer, J. R., Kristiana, I., & Brown, A. J. (2009). Cholesterol homeostasis in two commonly used human prostate cancer cell-lines, LNCaP and PC-3. *PLoS One*, 4(12), e8496.
- Krycer, James R., Phan, L., & Brown, Andrew J. (2012). A key regulator of cholesterol homeostasis, SREBP-2, can be targeted in prostate cancer cells with natural products. *Biochemical Journal*, 446(2), 191-201. <https://doi.org/10.1042/BJ20120545>
- Lacombe, L., Hovington, H., Brisson, H., Mehdi, S., Beillevaire, D., Émond, J.-P., Wagner, A., Villeneuve, L., Simonyan, D., Ouellet, V., Barrès, V., Latour, M., Aprikian, A., Bergeron, A., Castonguay, V., Couture, F., Chevalier, S., Brimo, F., Fazli, L.,...Lévesque, E. (2023). UGT2B28 accelerates prostate cancer progression through stabilization of the endocytic adaptor protein HIP1 regulating AR and EGFR pathways. *Cancer Letters*, 553, 215994. <https://doi.org/https://doi.org/10.1016/j.canlet.2022.215994>
- Lan, H., Tan, M., Zhang, Q., Yang, F., Wang, S., Li, H., Xiong, X., & Sun, Y. (2019). LSD1 destabilizes FBXW7 and abrogates FBXW7 functions independent of its demethylase activity. *Proceedings of the National Academy of Sciences*, 116(25), 12311-12320. <https://doi.org/doi:10.1073/pnas.1902012116>
- Le, P.-H., Kuo, C.-J., Hsieh, Y.-C., Chen, T.-H., Lin, C.-L., Yeh, C.-T., & Liang, K.-H. (2019). Ages of hepatocellular carcinoma occurrence and life expectancy are associated with a UGT2B28 genomic variation. *BMC Cancer*, 19(1), 1190. <https://doi.org/10.1186/s12885-019-6409-3>
- Lee, J. N., Kim, H., Yao, H., Chen, Y., Weng, K., & Ye, J. (2010). Identification of Ubx8 protein as a sensor for unsaturated fatty acids and regulator of triglyceride synthesis. *Proc Natl Acad Sci U S A*, 107(50), 21424-21429. <https://doi.org/10.1073/pnas.1011859107>
- Lee, J. N., Zhang, X., Feramisco, J. D., Gong, Y., & Ye, J. (2008). Unsaturated fatty acids inhibit proteasomal degradation of Insig-1 at a postubiquitination step. *J Biol Chem*, 283(48), 33772-33783. <https://doi.org/10.1074/jbc.M806108200>
- Lee, P. C., Sever, N., & Debose-Boyd, R. A. (2005). Isolation of sterol-resistant Chinese hamster ovary cells with genetic deficiencies in both Insig-1 and Insig-2. *J Biol Chem*, 280(26), 25242-25249. <https://doi.org/10.1074/jbc.M502989200>

- Lee, S.-R., Ahn, M.-H., Choi, Y. H., & Leem, S.-H. (2016). Influence of polymorphisms of UDP-glycosyltransferases (UGT) 2B family genes UGT2B15, UGT2B17 and UGT2B28 on the development of prostate cancer in Korean men. *Genes & Genomics*, *38*, 225-233.
- Lehmann-Che, J., Hamy, A. S., Porcher, R., Barritault, M., Bouhidel, F., Habuella, H., Leman-Detours, S., de Roquancourt, A., Cahen-Doidy, L., Bourstyn, E., de Cremoux, P., de Bazelaire, C., Albiter, M., Giacchetti, S., Cuvier, C., Janin, A., Espié, M., de Thé, H., & Bertheau, P. (2013). Molecular apocrine breast cancers are aggressive estrogen receptor negative tumors overexpressing either HER2 or GCDPF15. *Breast Cancer Res*, *15*(3), R37. <https://doi.org/10.1186/bcr3421>
- Lehmann, B. D., Bauer, J. A., Chen, X., Sanders, M. E., Chakravarthy, A. B., Shyr, Y., & Pietenpol, J. A. (2011). Identification of human triple-negative breast cancer subtypes and preclinical models for selection of targeted therapies. *J Clin Invest*, *121*(7), 2750-2767. <https://doi.org/10.1172/jci45014>
- Lévesque, E., Labriet, A., Hovington, H., Allain, É. P., Melo-Garcia, L., Rouleau, M., Brisson, H., Turcotte, V., Caron, P., Villeneuve, L., Leclercq, M., Droit, A., Audet-Walsh, E., Simonyan, D., Fradet, Y., Lacombe, L., & Guillemette, C. (2020). Alternative promoters control UGT2B17-dependent androgen catabolism in prostate cancer and its influence on progression. *British Journal of Cancer*, *122*(7), 1068-1076. <https://doi.org/10.1038/s41416-020-0749-2>
- Lévesque, É., Turgeon, D., Carrier, J.-S., Montminy, V., Beaulieu, M., & Bélanger, A. (2001). Isolation and Characterization of the UGT2B28 cDNA Encoding a Novel Human Steroid Conjugating UDP-Glucuronosyltransferase. *Biochemistry*, *40*(13), 3869-3881. <https://doi.org/10.1021/bi002607y>
- Lewis, B. C., Mackenzie, P. I., & Miners, J. O. (2011). Homodimerization of UDP-glucuronosyltransferase 2B7 (UGT2B7) and identification of a putative dimerization domain by protein homology modeling. *Biochemical Pharmacology*, *82*(12), 2016-2023.
- Li, H., Xie, N., Chen, R., Verreault, M., Fazli, L., Gleave, M. E., Barbier, O., & Dong, X. (2016). UGT2B17 Expedites Progression of Castration-Resistant Prostate Cancers by Promoting Ligand-Independent AR Signaling. *Cancer Research*, *76*(22), 6701. <https://doi.org/10.1158/0008-5472.CAN-16-1518>
- Liang, K., & Dai, J. Y. (2022). Progress of potential drugs targeted in lipid metabolism research. *Front Pharmacol*, *13*, 1067652. <https://doi.org/10.3389/fphar.2022.1067652>
- Liu, H., Wei, Z., Dominguez, A., Li, Y., Wang, X., & Qi, L. S. (2015). CRISPR-ERA: a comprehensive design tool for CRISPR-mediated gene editing, repression and activation. *Bioinformatics*, *31*(22), 3676-3678. <https://doi.org/10.1093/bioinformatics/btv423>
- Liu, L., Zhao, X., Zhao, L., Li, J., Yang, H., Zhu, Z., Liu, J., & Huang, G. (2016). Arginine Methylation of SREBP1a via PRMT5 Promotes De Novo Lipogenesis and Tumor Growth. *Cancer Research*, *76*(5), 1260-1272. <https://doi.org/10.1158/0008-5472.Can-15-1766>
- Liu, Y. (2006). Fatty acid oxidation is a dominant bioenergetic pathway in prostate cancer. *Prostate Cancer and Prostatic Diseases*, *9*(3), 230-234. <https://doi.org/10.1038/sj.pcan.4500879>
- Liu, Z., Liu, G., Ha, D. P., Wang, J., Xiong, M., & Lee, A. S. (2023). ER chaperone GRP78/BiP translocates to the nucleus under stress and acts as a transcriptional regulator. *Proc Natl Acad Sci U S A*, *120*(31), e2303448120. <https://doi.org/10.1073/pnas.2303448120>
- Livak, K. J., & Schmittgen, T. D. (2001). Analysis of relative gene expression data using real-time quantitative PCR and the 2(-Delta Delta C(T)) Method. *Methods*, *25*(4), 402-408. <https://doi.org/10.1006/meth.2001.1262>
- Lloyd, D. J., Trembath, R. C., & Shackleton, S. (2002). A novel interaction between lamin A and SREBP1: implications for partial lipodystrophy and other laminopathies. *Hum Mol Genet*, *11*(7), 769-777. <https://doi.org/10.1093/hmg/11.7.769>
- Lonergan, P. E., & Tindall, D. J. (2011). Androgen receptor signaling in prostate cancer development and progression. *J Carcinog*, *10*, 20. <https://doi.org/10.4103/1477-3163.83937>
- Lopez, D., Sanchez, M. D., Shea-Eaton, W., & McLean, M. P. (2002). Estrogen Activates the High-Density Lipoprotein Receptor Gene via Binding to Estrogen Response Elements and

- Interaction with Sterol Regulatory Element Binding Protein-1A. *Endocrinology*, 143(6), 2155-2168. <https://doi.org/10.1210/endo.143.6.8855>
- Lounis, M. A., Péant, B., Leclerc-Desaulniers, K., Ganguli, D., Daneault, C., Ruiz, M., Zoubeidi, A., Mes-Masson, A. M., & Saad, F. (2020). Modulation of de Novo Lipogenesis Improves Response to Enzalutamide Treatment in Prostate Cancer. *Cancers (Basel)*, 12(11). <https://doi.org/10.3390/cancers12113339>
- Mackenzie, P., Little, J. M., & Radomska-Pandya, A. (2003). Glucosidation of hyodeoxycholic acid by UDP-glucuronosyltransferase 2B7. *Biochemical Pharmacology*, 65(3), 417-421. [https://doi.org/https://doi.org/10.1016/S0006-2952\(02\)01522-8](https://doi.org/https://doi.org/10.1016/S0006-2952(02)01522-8)
- Mackenzie, P. I., Bock, K. W., Burchell, B., Guillemette, C., Ikushiro, S.-i., Iyanagi, T., Miners, J. O., Owens, I. S., Nebert, D. W. J. P., & genomics. (2005). Nomenclature update for the mammalian UDP glycosyltransferase (UGT) gene superfamily. 15(10), 677-685.
- Madeira, F., Park, Y. M., Lee, J., Buso, N., Gur, T., Madhusoodanan, N., Basutkar, P., Tivey, A. R. N., Potter, S. C., Finn, R. D., & Lopez, R. (2019). The EMBL-EBI search and sequence analysis tools APIs in 2019. *Nucleic Acids Research*, 47(1), 636-641. <https://doi.org/10.1093/nar/gkz268>
- Margaillan, G., Lévesque, É., & Guillemette, C. (2016). Epigenetic regulation of steroid inactivating UDP-glucuronosyltransferases by microRNAs in prostate cancer. *The Journal of Steroid Biochemistry and Molecular Biology*, 155, 85-93. <https://doi.org/https://doi.org/10.1016/j.jsbmb.2015.09.021>
- Marí, M., & Fernandez-Checa, J. C. (2014). Damage Mediated by Dysfunction of Organelles and Cellular Systems: Lysosomes. In L. M. McManus & R. N. Mitchell (Eds.), *Pathobiology of Human Disease* (pp. 97-107). Academic Press. <https://doi.org/https://doi.org/10.1016/B978-0-12-386456-7.01406-4>
- Marino, N., German, R., Rao, X., Simpson, E., Liu, S., Wan, J., Liu, Y., Sandusky, G., Jacobsen, M., Stoval, M., Cao, S., & Storniolo, A. M. V. (2020). Upregulation of lipid metabolism genes in the breast prior to cancer diagnosis. *npj Breast Cancer*, 6(1), 50. <https://doi.org/10.1038/s41523-020-00191-8>
- Mathur, B., Arif, W., Patton, M. E., Faiyaz, R., Liu, J., Yeh, J., Harpavat, S., Schoonjans, K., Kalsotra, A., Wheatley, A. M., & Anakk, S. (2020). Transcriptomic analysis across liver diseases reveals disease-modulating activation of constitutive androstane receptor in cholestasis. *JHEP Reports*, 2(5), 100140. <https://doi.org/https://doi.org/10.1016/j.jhepr.2020.100140>
- Maxfield, F. R., & Wüstner, D. (2012). Analysis of cholesterol trafficking with fluorescent probes. *Methods in Cell Biology*, 108, 367-393. <https://doi.org/10.1016/B978-0-12-386487-1.00017-1>
- McCarroll, S. A., Hadnott, T. N., Perry, G. H., Sabeti, P. C., Zody, M. C., Barrett, J. C., Dallaire, S., Gabriel, S. B., Lee, C., Daly, M. J., Altshuler, D. M., & The International HapMap, C. (2006). Common deletion polymorphisms in the human genome. *Nature Genetics*, 38, 86. <https://doi.org/10.1038/ng1696>
- <https://www.nature.com/articles/ng1696#supplementary-information>
- McCubrey, J. A., Steelman, L. S., Bertrand, F. E., Davis, N. M., Abrams, S. L., Montalto, G., D'Assoro, A. B., Libra, M., Nicoletti, F., Maestro, R., Basecke, J., Cocco, L., Cervello, M., & Martelli, A. M. (2014). Multifaceted roles of GSK-3 and Wnt/β-catenin in hematopoiesis and leukemogenesis: opportunities for therapeutic intervention. *Leukemia*, 28(1), 15-33. <https://doi.org/10.1038/leu.2013.184>
- McGranahan, N., & Swanton, C. (2017). Clonal heterogeneity and tumor evolution: past, present, and the future. *Cell*, 168(4), 613-628.
- Meech, R., Gomez, M., Woolley, C., Barro, M., Hulin, J.-A., Walcott, E. C., Delgado, J., & Makarenkova, H. P. (2010). The homeobox transcription factor Barx2 regulates plasticity of young primary myofibers. *PLoS One*, 5(7), e11612-e11612. <https://doi.org/10.1371/journal.pone.0011612>
- Meech, R., Hu, D. G., McKinnon, R. A., Mubarakah, S. N., Haines, A. Z., Nair, P. C., Rowland, A., & Mackenzie, P. I. (2019). The UDP-Glycosyltransferase (UGT) Superfamily: New Members,

- New Functions, and Novel Paradigms. *Physiological Reviews*, 99(2), 1153-1222. <https://doi.org/10.1152/physrev.00058.2017>
- Meech, R., Hu, D. G., Miners, J. O., & Mackenzie, P. I. (2018). 10.20 - UDP-Glycosyltransferases. In C. A. McQueen (Ed.), *Comprehensive Toxicology (Third Edition)* (pp. 468-496). Elsevier. <https://doi.org/https://doi.org/10.1016/B978-0-12-801238-3.65733-1>
- Meech, R., & Mackenzie, P. I. (1998). Determinants of UDP glucuronosyltransferase membrane association and residency in the endoplasmic reticulum. *Arch Biochem Biophys*, 356(1), 77-85. <https://doi.org/10.1006/abbi.1998.0750>
- Meech, R., Miners, J. O., Lewis, B. C., & Mackenzie, P. I. (2012). The glycosidation of xenobiotics and endogenous compounds: Versatility and redundancy in the UDP glycosyltransferase superfamily. *Pharmacology & Therapeutics*, 134(2), 200-218. <https://doi.org/https://doi.org/10.1016/j.pharmthera.2012.01.009>
- Meerbrey, K. L., Hu, G., Kessler, J. D., Roarty, K., Li, M. Z., Fang, J. E., Herschkowitz, J. I., Burrows, A. E., Ciccia, A., Sun, T., Schmitt, E. M., Bernardi, R. J., Fu, X., Bland, C. S., Cooper, T. A., Schiff, R., Rosen, J. M., Westbrook, T. F., & Elledge, S. J. (2011). The pINDUCER lentiviral toolkit for inducible RNA interference in vitro and in vivo. *Proc Natl Acad Sci U S A*, 108(9), 3665-3670. <https://doi.org/10.1073/pnas.1019736108>
- Melkonian, K. A., Ostermeyer, A. G., Chen, J. Z., Roth, M. G., & Brown, D. A. (1999). Role of lipid modifications in targeting proteins to detergent-resistant membrane rafts. Many raft proteins are acylated, while few are prenylated. *The Journal of Biological Chemistry*, 274(6), 3910-3917. <https://doi.org/10.1074/jbc.274.6.3910>
- Ménard, V., Collin, P., Margailan, G., & Guillemette, C. (2013). Modulation of the UGT2B7 Enzyme Activity by C-Terminally Truncated Proteins Derived from Alternative Splicing. *Drug Metabolism and Disposition*, 41(12), 2197-2205. <https://doi.org/10.1124/dmd.113.053876>
- Ménard, V., Eap, O., Harvey, M., Guillemette, C., & Lévesque, É. (2009). Copy-number variations (CNVs) of the human sex steroid metabolizing genes UGT2B17 and UGT2B28 and their associations with a UGT2B15 functional polymorphism. *Human Mutation*, 30(9), 1310-1319. <https://doi.org/10.1002/humu.21054>
- Menendez, J. A., & Lupu, R. (2007). Fatty acid synthase and the lipogenic phenotype in cancer pathogenesis [Review Article]. *Nature Reviews Cancer*, 7, 763-770. <https://doi.org/10.1038/nrc2222>
- Metallo, C. M., Gameiro, P. A., Bell, E. L., Mattaini, K. R., Yang, J., Hiller, K., Jewell, C. M., Johnson, Z. R., Irvine, D. J., Guarente, L., Kelleher, J. K., Vander Heiden, M. G., Iliopoulos, O., & Stephanopoulos, G. (2011). Reductive glutamine metabolism by IDH1 mediates lipogenesis under hypoxia. *Nature*, 481, 380-390. <https://doi.org/10.1038/nature10602>
- <https://www.nature.com/articles/nature10602#supplementary-information>
- Meyers, R. M., Bryan, J. G., McFarland, J. M., Weir, B. A., Sizemore, A. E., Xu, H., Dharia, N. V., Montgomery, P. G., Cowley, G. S., Pantel, S., Goodale, A., Lee, Y., Ali, L. D., Jiang, G., Lubonja, R., Harrington, W. F., Strickland, M., Wu, T., Hawes, D. C.,...Tsherniak, A. (2017). Computational correction of copy number effect improves specificity of CRISPR-Cas9 essentiality screens in cancer cells. *Nature Genetics*, 49(12), 1779-1784. <https://doi.org/10.1038/ng.3984>
- Miley, M. J., Zielinska, A. K., Keenan, J. E., Bratton, S. M., Radomska-Pandya, A., & Redinbo, M. R. (2007). Crystal Structure of the Cofactor-Binding Domain of the Human Phase II Drug-Metabolism Enzyme UDP-Glucuronosyltransferase 2B7. *Journal of Molecular Biology*, 369(2), 498-511. <https://doi.org/https://doi.org/10.1016/j.jmb.2007.03.066>
- Misawa, K., Horiba, T., Arimura, N., Hirano, Y., Inoue, J., Emoto, N., Shimano, H., Shimizu, M., & Sato, R. (2003). Sterol Regulatory Element-binding Protein-2 Interacts with Hepatocyte Nuclear Factor-4 to Enhance Sterol Isomerase Gene Expression in Hepatocytes *. *Journal of Biological Chemistry*, 278(38), 36176-36182. <https://doi.org/10.1074/jbc.M302387200>
- Miyauchi, Y., Kimura, S., Kimura, A., Kurohara, K., Hirota, Y., Fujimoto, K., Mackenzie, P. I., Tanaka, Y., & Ishii, Y. (2019). Investigation of the Endoplasmic Reticulum Localization of UDP-

- Glucuronosyltransferase 2B7 with Systematic Deletion Mutants. *Mol Pharmacol*, 95(5), 551-562. <https://doi.org/10.1124/mol.118.113902>
- Moore, N. L., Buchanan, G., Harris, J. M., Selth, L. A., Bianco-Miotto, T., Hanson, A. R., Birrell, S. N., Butler, L. M., Hickey, T. E., & Tilley, W. D. (2012). An androgen receptor mutation in the MDA-MB-453 cell line model of molecular apocrine breast cancer compromises receptor activity. *Endocrine related cancer*, 19(4), 599-603.
- Moore, N. L., Hanson, A. R., Ebrahimie, E., Hickey, T. E., & Tilley, W. D. (2020). Anti-proliferative transcriptional effects of medroxyprogesterone acetate in estrogen receptor positive breast cancer cells are predominantly mediated by the progesterone receptor. *The Journal of Steroid Biochemistry and Molecular Biology*, 199, 105548. <https://doi.org/https://doi.org/10.1016/j.jsbmb.2019.105548>
- Mostaghel, E. A., Solomon, K. R., Pelton, K., Freeman, M. R., & Montgomery, R. B. (2012). Impact of circulating cholesterol levels on growth and intratumoral androgen concentration of prostate tumors. *PLoS One*, 7(1), e30062. <https://doi.org/10.1371/journal.pone.0030062>
- Mullen, A. R., Wheaton, W. W., Jin, E. S., Chen, P.-H., Sullivan, L. B., Cheng, T., Yang, Y., Linehan, W. M., Chandel, N. S., & DeBerardinis, R. J. (2011). Reductive carboxylation supports growth in tumour cells with defective mitochondria. *Nature*, 481, 385-390. <https://doi.org/10.1038/nature10642>
- <https://www.nature.com/articles/nature10642#supplementary-information>
- Nadeau, G., Bellemare, J., Audet-Walsh, É., Flageole, C., Huang, S.-P., Bao, B.-Y., Douville, P., Caron, P., Fradet, Y., Lacombe, L., Guillemette, C., & Lévesque, E. (2011). Deletions of the Androgen-Metabolizing UGT2B Genes Have an Effect on Circulating Steroid Levels and Biochemical Recurrence after Radical Prostatectomy in Localized Prostate Cancer. *The Journal of Clinical Endocrinology & Metabolism*, 96(9), 1550-1557. <https://doi.org/10.1210/jc.2011-1049>
- Nair, P. C., Meech, R., Mackenzie, P. I., McKinnon, R. A., & Miners, J. O. (2015). Insights into the UDP-sugar selectivities of human UDP-glycosyltransferases (UGT): a molecular modeling perspective. *Drug Metabolism Reviews*, 47(3), 335-345. <https://doi.org/10.3109/03602532.2015.1071835>
- Naudí, A., Jové, M., Ayala, V., Portero-Otin, M., Barja, G., & Pamplona, R. (2013). Membrane lipid unsaturation as physiological adaptation to animal longevity [Review]. *Frontiers in Physiology*, 4(372). <https://doi.org/10.3389/fphys.2013.00372>
- Neumann, E., Riepl, B., Knedla, A., Lefèvre, S., Tarner, I. H., Grifka, J., Steinmeyer, J., Schölmerich, J., Gay, S., & Müller-Ladner, U. (2010). Cell culture and passaging alters gene expression pattern and proliferation rate in rheumatoid arthritis synovial fibroblasts. *Arthritis Research & Therapy*, 12(3), 83-84. <https://doi.org/10.1186/ar3010>
- Neuwirt, H., Bouchal, J., Kharaihvili, G., Ploner, C., Jöhrer, K., Pitterl, F., Weber, A., Klocker, H., & Eder, I. E. (2020). Cancer-associated fibroblasts promote prostate tumor growth and progression through upregulation of cholesterol and steroid biosynthesis. *Cell Communication and Signaling*, 18(1), 11. <https://doi.org/10.1186/s12964-019-0505-5>
- Ngan, S., Stronach, E. A., Photiou, A., Waxman, J., Ali, S., & Buluwela, L. (2009). Microarray coupled to quantitative RT-PCR analysis of androgen-regulated genes in human LNCaP prostate cancer cells [Oncogenomics]. *Oncogene*, 28, 2051. <https://doi.org/10.1038/onc.2009.68>
- <https://www.nature.com/articles/onc200968#supplementary-information>
- Ni, M., Chen, Y., Lim, E., Wimberly, H., Bailey, S. T., Imai, Y., Rimm, D. L., Liu, X. S., & Brown, M. (2011). Targeting androgen receptor in estrogen receptor-negative breast cancer. *Cancer cell*, 20(1), 119-131. <https://doi.org/10.1016/j.ccr.2011.05.026>
- Orrù, S., Pascariello, E., Sotgiu, G., Piras, D., Sadari, L., Muroli, M. R., Carru, C., Arru, C., Mocci, C., Pinna, G., Barbara, R., Cossu-Rocca, P., & De Miglio, M. R. (2022). Prognostic Role of Androgen Receptor Expression in HER2+ Breast Carcinoma Subtypes. *Biomedicines*, 10(1). <https://doi.org/10.3390/biomedicines10010164>

- Ouzzine, M., Antonio, L., Burchell, B., Netter, P., Fournel-Gigleux, S., & Magdalou, J. (2000). Importance of Histidine Residues for the Function of the Human Liver UDP-Glucuronosyltransferase UGT1A6: Evidence for the Catalytic Role of Histidine 370. *Molecular Pharmacology*, 58(6), 1609-1615. <https://doi.org/10.1124/mol.58.6.1609>
- Palmer, M. (2007). WatCut: An on-line tool for restriction analysis, silent mutation scanning, and SNP-RFLP analysis. *University of Waterloo*.
- Pan, J. A., Ullman, E., Dou, Z., & Zong, W. X. (2011). Inhibition of protein degradation induces apoptosis through a microtubule-associated protein 1 light chain 3-mediated activation of caspase-8 at intracellular membranes. *Mol Cell Biol*, 31(15), 3158-3170. <https://doi.org/10.1128/mcb.05460-11>
- Panda, A., Suvakov, M., Mariani, J., Drucker, K. L., Park, Y., Jang, Y., Kollmeyer, T. M., Sarkar, G., Bae, T., Kim, J. J., Yoon, W. H., Jenkins, R. B., Vaccarino, F. M., & Abyzov, A. (2023). Clonally Selected Lines After CRISPR-Cas Editing Are Not Isogenic. *The CRISPR Journal*, 6(2), 176-182. <https://doi.org/10.1089/crispr.2022.0050>
- Peppercorn, J., Perou, C. M., & Carey, L. A. (2008). Molecular Subtypes in Breast Cancer Evaluation and Management: Divide and Conquer. *Cancer Investigation*, 26(1), 1-10. <https://doi.org/10.1080/07357900701784238>
- Perlmutter, M. A., & Lopor, H. (2007). Androgen deprivation therapy in the treatment of advanced prostate cancer. *Rev Urol*, 9 Suppl 1(Suppl 1), S3-8.
- Prat, A., Adamo, B., Cheang, M. C. U., Anders, C. K., Carey, L. A., & Perou, C. M. (2013). Molecular Characterization of Basal-Like and Non-Basal-Like Triple-Negative Breast Cancer. *The Oncologist*, 18(2), 123-133. <https://doi.org/10.1634/theoncologist.2012-0397>
- Proverbs-Singh, T., Feldman, J. L., Morris, M. J., Autio, K. A., & Traina, T. A. (2015). Targeting the androgen receptor in prostate and breast cancer: several new agents in development. *Endocrine-Related Cancer*, 22(3), R87-R106. <https://doi.org/10.1530/ERC-14-0543>
- Punga, T., Bengoechea-Alonso, M. T., & Ericsson, J. (2006). Phosphorylation and Ubiquitination of the Transcription Factor Sterol Regulatory Element-binding Protein-1 in Response to DNA Binding*. *Journal of Biological Chemistry*, 281(35), 25278-25286. <https://doi.org/https://doi.org/10.1074/jbc.M604983200>
- Radomska-Pandya, A., Pokrovskaya, I. D., Xu, J., Little, J. M., Jude, A. R., Kurten, R. C., & Czernik, P. J. (2002). Nuclear UDP-Glucuronosyltransferases: Identification of UGT2B7 and UGT1A6 in Human Liver Nuclear Membranes. *Archives of Biochemistry and Biophysics*, 399(1), 37-48. <https://doi.org/https://doi.org/10.1006/abbi.2001.2743>
- Ran, F. A., Hsu, P. D., Wright, J., Agarwala, V., Scott, D. A., & Zhang, F. (2013). Genome engineering using the CRISPR-Cas9 system. *Nature Protocols*, 8(11), 2281-2308. <https://doi.org/10.1038/nprot.2013.143>
- Ravindran, A., Krieger, K. L., Kaushik, A. K., Hovington, H., Mehdi, S., Piyarathna, D. W. B., Putluri, V., Basil, P., Rasaily, U., Gu, F., Dang, T., Choi, J. M., Sonavane, R., Jung, S. Y., Wang, L., Mehra, R., Weigel, N. L., Putluri, N., Rowley, D. R.,...Sreekumar, A. (2022). Uridine Diphosphate Glucuronosyl Transferase 2B28 (UGT2B28) Promotes Tumor Progression and Is Elevated in African American Prostate Cancer Patients. *Cells*, 11(15). <https://doi.org/10.3390/cells11152329>
- Redmond, A. M., Omarjee, S., Chernukhin, I., Le Romancer, M., & Carroll, J. S. (2019). Analysis of HER2 genomic binding in breast cancer cells identifies a global role in direct gene regulation. *PLoS One*, 14(11), e0225180. <https://doi.org/10.1371/journal.pone.0225180>
- Rennie, P. S., Bruchofsky, N., Leco, K. J., Sheppard, P. C., McQueen, S. A., Cheng, H., Snoek, R., Hamel, A., Bock, M. E., MacDonald, B. S., Nickel, B. E., Chang, C., Liao, S., Cattini, P. A., & Matusik, R. J. (1993). Characterization of two cis-acting DNA elements involved in the androgen regulation of the probasin gene. *Molecular Endocrinology*, 7(1), 23-36. <https://doi.org/10.1210/mend.7.1.8446105>
- Rezen, T., Rozman, D., Pascussi, J.-M., & Monostory, K. (2011). Interplay between cholesterol and drug metabolism. *Biochimica et Biophysica Acta (BBA) - Proteins and Proteomics*, 1814(1), 146-160. <https://doi.org/https://doi.org/10.1016/j.bbapap.2010.05.014>

- Rodríguez-Paredes, M., & Esteller, M. (2011). Cancer epigenetics reaches mainstream oncology. *Nature medicine*, 17(3), 330-339.
- Rouleau, M., Collin, P., Bellemare, J., Harvey, M., & Guillemette, C. (2013). Protein–protein interactions between the bilirubin-conjugating UDPglucuronosyltransferase UGT1A1 and its shorter isoform 2 regulatory partner derived from alternative splicing. *Biochemical Journal*, 450(1), 107. <https://doi.org/10.1042/BJ20121594>
- Rouleau, M., Nguyen Van Long, F., Turcotte, V., Caron, P., Lacombe, L., Aprikian, A., Saad, F., Carmel, M., Chevalier, S., Lévesque, E., & Guillemette, C. (2022). Extensive metabolic consequences of human glycosyltransferase gene knockouts in prostate cancer. *British Journal of Cancer*. <https://doi.org/10.1038/s41416-022-02040-w>
- Rowland, A., Miners, J. O., & Mackenzie, P. I. (2013). The UDP-glucuronosyltransferases: Their role in drug metabolism and detoxification. *The International Journal of Biochemistry & Cell Biology*, 45(6), 1121-1132. <https://doi.org/https://doi.org/10.1016/j.biocel.2013.02.019>
- Rudalska, R., Harbig, J., Snaebjornsson, M. T., Klotz, S., Zwirner, S., Taranets, L., Heinzmann, F., Kronenberger, T., Forster, M., Cui, W., D'Artista, L., Einig, E., Hinterleitner, M., Schmitz, W., Dylawerska, A., Kang, T.-W., Poso, A., Rosenfeldt, M. T., Malek, N. P.,...Dauch, D. (2021). LXR α activation and Raf inhibition trigger lethal lipotoxicity in liver cancer. *Nature Cancer*, 2(2), 201-217. <https://doi.org/10.1038/s43018-020-00168-3>
- Rudalska, R., Zender, L., & Dauch, D. (2021). Exploiting lipotoxicity for the treatment of liver cancer. *British Journal of Cancer*, 125(11), 1459-1461. <https://doi.org/10.1038/s41416-021-01479-7>
- Russnes, H. G., Lingjærde, O. C., Børresen-Dale, A.-L., & Caldas, C. (2017). Breast Cancer Molecular Stratification: From Intrinsic Subtypes to Integrative Clusters. *The American journal of pathology*, 187(10), 2152-2162. <https://doi.org/https://doi.org/10.1016/j.ajpath.2017.04.022>
- Rysman, E., Brusselmans, K., Scheys, K., Timmermans, L., Derua, R., Munck, S., Van Veldhoven, P. P., Waltregny, D., Daniëls, V. W., Machiels, J., Vanderhoydonc, F., Smans, K., Waelkens, E., Verhoeven, G., & Swinnen, J. V. (2010). Lipogenesis Protects Cancer Cells from Free Radicals and Chemotherapeutics by Promoting Membrane Lipid Saturation. *Cancer Research*, 70(20), 8117-8124. <https://doi.org/10.1158/0008-5472.CAN-09-3871>
- Sakai, J., Duncan, E. A., Rawson, R. B., Hua, X., Brown, M. S., & Goldstein, J. L. (1996). Sterol-Regulated Release of SREBP-2 from Cell Membranes Requires Two Sequential Cleavages, One Within a Transmembrane Segment. *Cell*, 85(7), 1037-1046. [https://doi.org/https://doi.org/10.1016/S0092-8674\(00\)81304-5](https://doi.org/https://doi.org/10.1016/S0092-8674(00)81304-5)
- Sakai, J., Nohturfft, A., Goldstein, J. L., & Brown, M. S. (1998). Cleavage of Sterol Regulatory Element-binding Proteins (SREBPs) at Site-1 Requires Interaction with SREBP Cleavage-activating Protein: EVIDENCE FROM IN VIVO COMPETITION STUDIES. *Journal of Biological Chemistry*, 273(10), 5785-5793. <https://doi.org/10.1074/jbc.273.10.5785>
- Sano, R., & Reed, J. C. (2013). ER stress-induced cell death mechanisms. *Biochim Biophys Acta*, 1833(12), 3460-3470. <https://doi.org/10.1016/j.bbamcr.2013.06.028>
- Santos, C. R., & Schulze, A. (2012). Lipid metabolism in cancer. *The FEBS Journal*, 279(15), 2610-2623. <https://doi.org/10.1111/j.1742-4658.2012.08644.x>
- Schindelin, J., Arganda-Carreras, I., Frise, E., Kaynig, V., Longair, M., Pietzsch, T., Preibisch, S., Rueden, C., Saalfeld, S., Schmid, B., Tinevez, J.-Y., White, D. J., Hartenstein, V., Eliceiri, K., Tomancak, P., & Cardona, A. (2012). Fiji: an open-source platform for biological-image analysis. *Nature Methods*, 9(7), 676-682. <https://doi.org/10.1038/nmeth.2019>
- Scully, T., Ettela, A., Kase, N., LeRoith, D., & Gallagher, E. J. (2023). Unregulated LDL cholesterol uptake is detrimental to breast cancer cells. *Endocrine-Related Cancer*, 30(1), e220234. <https://doi.org/10.1530/erc-22-0234>
- Senafi, S. B., Clarke, D. J., & Burchell, B. (1994). Investigation of the substrate specificity of a cloned expressed human bilirubin UDP-glucuronosyltransferase: UDP-sugar specificity and involvement in steroid and xenobiotic glucuronidation. *Biochem J*, 303, 233-240. <https://doi.org/10.1042/bj3030233>

- Setlur, S. R., Chen, C. X., Hossain, R. R., Ha, J. S., Van Doren, V. E., Stenzel, B., Steiner, E., Oldridge, D., Kitabayashi, N., Banerjee, S., Chen, J. Y., Schäfer, G., Horninger, W., Lee, C., Rubin, M. A., Klocker, H., & Demichelis, F. (2010). Genetic Variation of Genes Involved in Dihydrotestosterone Metabolism and the Risk of Prostate Cancer. *Cancer Epidemiology, Biomarkers & Prevention*, *19*(1), 229-239. <https://doi.org/10.1158/1055-9965.Epi-09-1018>
- Setton, J., Zinda, M., Riaz, N., Durocher, D., Zimmermann, M., Koehler, M., Reis-Filho, J. S., & Powell, S. N. (2021). Synthetic Lethality in Cancer Therapeutics: The Next Generation. *Cancer Discovery*, *11*(7), 1626-1635. <https://doi.org/10.1158/2159-8290.Cd-20-1503>
- Sherbet, G. V. (2011). 20 - Oestrogens and Progesterone in Normal Physiology and Neoplasia. In G. V. Sherbet (Ed.), *Growth Factors and Their Receptors in Cell Differentiation, Cancer and Cancer Therapy* (pp. 229-235). Elsevier. <https://doi.org/https://doi.org/10.1016/B978-0-12-387819-9.00020-7>
- Sherry, S. T., Ward, M. H., Kholodov, M., Baker, J., Phan, L., Smigielski, E. M., & Sirotkin, K. (2001). dbSNP: the NCBI database of genetic variation. *Nucleic Acids Research*, *29*(1), 308-311. <https://doi.org/10.1093/nar/29.1.308>
- Shifera, A. S., & Hardin, J. A. (2010). Factors modulating expression of Renilla luciferase from control plasmids used in luciferase reporter gene assays. *Anal Biochem*, *396*(2), 167-172. <https://doi.org/10.1016/j.ab.2009.09.043>
- Shimano, H. (2001). Sterol regulatory element-binding proteins (SREBPs): transcriptional regulators of lipid synthetic genes. *Progress in Lipid Research*, *40*(6), 439-452. [https://doi.org/https://doi.org/10.1016/S0163-7827\(01\)00010-8](https://doi.org/https://doi.org/10.1016/S0163-7827(01)00010-8)
- Shuji, O., & Shizuo, N. (2011). Quantitative Analysis of UGT2B28 mRNA Expression by Real-Time RT-PCR and Application to Human Tissue Distribution Study. *Drug Metabolism Letters*, *5*(3), 202-208. <https://doi.org/http://dx.doi.org/10.2174/187231211796904955>
- Sigoillot, F. D., Lyman, S., Huckins, J. F., Adamson, B., Chung, E., Quattrochi, B., & King, R. W. (2012). A bioinformatics method identifies prominent off-targeted transcripts in RNAi screens. *Nature Methods*, *9*(4), 363-366.
- Simpson, P. T., Reis-Filho, J. S., Gale, T., & Lakhani, S. R. (2005). Molecular evolution of breast cancer. *The Journal of Pathology*, *205*(2), 248-254. <https://doi.org/10.1002/path.1691>
- Smith, A. D., Page, B. D. G., Collier, A. C., & Coughtrie, M. W. H. (2020). Homology Modeling of Human Uridine-5'-diphosphate-glucuronosyltransferase 1A6 Reveals Insights into Factors Influencing Substrate and Cosubstrate Binding. *ACS Omega*, *5*(12), 6872-6887. <https://doi.org/10.1021/acsomega.0c00205>
- Snapp, E. L., Sharma, A., Lippincott-Schwartz, J., & Hegde, R. S. (2006). Monitoring chaperone engagement of substrates in the endoplasmic reticulum of live cells. *Proceedings of the National Academy of Sciences*, *103*(17), 6536-6541. <https://doi.org/doi:10.1073/pnas.0510657103>
- Snoek, R., Rennie, P. S., Kasper, S., Matusik, R. J., & Bruchofsky, N. (1996). Induction of cell-free, in vitro transcription by recombinant androgen receptor peptides. *The Journal of Steroid Biochemistry and Molecular Biology*, *59*(3), 243-250. [https://doi.org/https://doi.org/10.1016/S0960-0760\(96\)00116-1](https://doi.org/https://doi.org/10.1016/S0960-0760(96)00116-1)
- Sripathy, S. P., Stevens, J., & Schultz, D. C. (2006). The KAP1 corepressor functions to coordinate the assembly of de novo HP1-demarcated microenvironments of heterochromatin required for KRAB zinc finger protein-mediated transcriptional repression. *Mol Cell Biol*, *26*(22), 8623-8638. <https://doi.org/10.1128/mcb.00487-06>
- Stanley, A., Ashrafi, G. H., Seddon, A. M., & Modjtahedi, H. (2017). Synergistic effects of various Her inhibitors in combination with IGF-1R, C-MET and Src targeting agents in breast cancer cell lines. *Sci Rep*, *7*(1), 3964. <https://doi.org/10.1038/s41598-017-04301-8>
- Stocco, D. M. (2001). StAR Protein and the Regulation of Steroid Hormone Biosynthesis. *Annual Review of Physiology*, *63*(1), 193-213. <https://doi.org/10.1146/annurev.physiol.63.1.193>
- Stojic, L., Lun, A. T. L., Mangei, J., Mascalchi, P., Quarantotti, V., Barr, A. R., Bakal, C., Marioni, J. C., Gergely, F., & Odom, D. T. (2018). Specificity of RNAi, LNA and CRISPRi as loss-of-function

- methods in transcriptional analysis. *Nucleic Acids Res*, 46(12), 5950-5966. <https://doi.org/10.1093/nar/gky437>
- Stoll, G. A., Pandiloski, N., Douse, C. H., & Modis, Y. (2022). Structure and functional mapping of the KRAB-KAP1 repressor complex. *The EMBO Journal*, 41(24), e111179. <https://doi.org/https://doi.org/10.15252/emboj.2022111179>
- Strauss, J. A., Shepherd, D. A., Macey, M., Jevons, E. F. P., & Shepherd, S. O. (2020). Divergence exists in the subcellular distribution of intramuscular triglyceride in human skeletal muscle dependent on the choice of lipid dye. *Histochemistry and Cell Biology*, 154(4), 369-382. <https://doi.org/10.1007/s00418-020-01898-2>
- Suh, J. H., Gong, E.-Y., Kim, J. B., Lee, I.-K., Choi, H.-S., & Lee, K. (2008). Sterol Regulatory Element-Binding Protein-1c Represses the Transactivation of Androgen Receptor and Androgen-Dependent Growth of Prostatic Cells. *Molecular Cancer Research*, 6(2), 314-324. <https://doi.org/10.1158/1541-7786.Mcr-07-0354>
- Sundqvist, A., Bengoechea-Alonso, M. T., Ye, X., Lukiyanchuk, V., Jin, J., Harper, J. W., & Ericsson, J. (2005). Control of lipid metabolism by phosphorylation-dependent degradation of the SREBP family of transcription factors by SCF(Fbw7). *Cell Metabolism*, 1(6), 379-391. <https://doi.org/10.1016/j.cmet.2005.04.010>
- Sundqvist, A., & Ericsson, J. (2003). Transcription-dependent degradation controls the stability of the SREBP family of transcription factors. *Proceedings of the National Academy of Sciences*, 100(24), 13833-13838. <https://doi.org/10.1073/pnas.2335135100>
- Suzuki, K., Bose, P., Leong-Quong, R. Y. Y., Fujita, D. J., & Riabowol, K. (2010). REAP: A two minute cell fractionation method. *BMC Research Notes*, 3(1), 294. <https://doi.org/10.1186/1756-0500-3-294>
- Sviridov, D., Mukhamedova, N., & Miller, Y. I. (2020). Lipid rafts as a therapeutic target: Thematic Review Series: Biology of Lipid Rafts. *Journal of lipid research*, 61(5), 687-695. <https://doi.org/https://doi.org/10.1194/jlr.TR120000658>
- Swinnen, J. V., Brusselmans, K., & Verhoeven, G. (2006). Increased lipogenesis in cancer cells: new players, novel targets. *Current Opinion in Clinical Nutrition & Metabolic Care*, 9(4), 358-365.
- Swinnen, J. V., Heemers, H., de Sande, T. V., Schrijver, E. D., Brusselmans, K., Heyns, W., & Verhoeven, G. (2004). Androgens, lipogenesis and prostate cancer. *The Journal of Steroid Biochemistry and Molecular Biology*, 92(4), 273-279. <https://doi.org/https://doi.org/10.1016/j.jsbmb.2004.10.013>
- Takahashi, A., Motomura, K., Kato, T., Yoshikawa, T., Nakagawa, Y., Yahagi, N., Sone, H., Suzuki, H., Toyoshima, H., Yamada, N., & Shimano, H. (2005). Transgenic Mice Overexpressing Nuclear SREBP-1c in Pancreatic β -Cells. *Diabetes*, 54(2), 492-499. <https://doi.org/10.2337/diabetes.54.2.492>
- Takahashi, Y., Shinoda, A., Furuya, N., Harada, E., Arimura, N., Ichi, I., Fujiwara, Y., Inoue, J., & Sato, R. (2013). Perilipin-mediated lipid droplet formation in adipocytes promotes sterol regulatory element-binding protein-1 processing and triacylglyceride accumulation. *PLoS One*, 8(5), e64605.
- Takashima, K., Saitoh, A., Funabashi, T., Hirose, S., Yagi, C., Nozaki, S., Sato, R., Shin, H.-W., & Nakayama, K. (2015). COPI-mediated retrieval of SCAP is crucial for regulating lipogenesis under basal and sterol-deficient conditions. *Journal of Cell Science*, 128(15), 2805-2815. <https://doi.org/10.1242/jcs.164137>
- Takeuchi, Y., Yahagi, N., Izumida, Y., Nishi, M., Kubota, M., Teraoka, Y., Yamamoto, T., Matsuzaka, T., Nakagawa, Y., Sekiya, M., Iizuka, Y., Ohashi, K., Osuga, J.-i., Gotoda, T., Ishibashi, S., Itaka, K., Kataoka, K., Nagai, R., Yamada, N.,...Shimano, H. (2010). Polyunsaturated fatty acids selectively suppress sterol regulatory element-binding protein-1 through proteolytic processing and autoloop regulatory circuit. *J Biol Chem*, 285(15), 11681-11691. <https://doi.org/10.1074/jbc.M109.096107>
- Taneja, S. S., Ha, S., Swenson, N. K., Torra, I. P., Rome, S., Walden, P. D., Huang, H. Y., Shapiro, E., Garabedian, M. J., & Logan, S. K. (2004). ART-27, an Androgen Receptor Coactivator

- Regulated in Prostate Development and Cancer*. *Journal of Biological Chemistry*, 279(14), 13944-13952. <https://doi.org/https://doi.org/10.1074/jbc.M306576200>
- Tang, Z., Kang, B., Li, C., Chen, T., & Zhang, Z. (2019). GEPIA2: an enhanced web server for large-scale expression profiling and interactive analysis. *Nucleic Acids Res*, 47(W1), W556-w560. <https://doi.org/10.1093/nar/gkz430>
- Tang, Z., Li, C., Kang, B., Gao, G., Li, C., & Zhang, Z. (2017). GEPIA: a web server for cancer and normal gene expression profiling and interactive analyses. *Nucleic Acids Res*, 45(W1), 98-102. <https://doi.org/10.1093/nar/gkx247>
- Taylor, B. S., Schultz, N., Hieronymus, H., Gopalan, A., Xiao, Y., Carver, B. S., Arora, V. K., Kaushik, P., Cerami, E., & Reva, B. (2010). Integrative genomic profiling of human prostate cancer. *Cancer cell*, 18(1), 11-22.
- Thareja, G., Evans, A. M., Wood, S. D., Stephan, N., Zaghlool, S., Halama, A., Kastenmüller, G., Belkadi, A., Albagha, O. M. E., Consortium, T. Q. G. P. R., & Suhre, K. (2022). Ratios of Acetaminophen Metabolites Identify New Loci of Pharmacogenetic Relevance in a Genome-Wide Association Study. *Metabolites*, 12(6), 496. <https://www.mdpi.com/2218-1989/12/6/496>
- Tirinato, L., Pagliari, F., Limongi, T., Marini, M., Falqui, A., Seco, J., Candeloro, P., Liberale, C., & Di Fabrizio, E. (2017). An Overview of Lipid Droplets in Cancer and Cancer Stem Cells. *Stem Cells International*, 2017, 1-17, Article 1656053. <https://doi.org/10.1155/2017/1656053>
- Tomczak, K., Czerwińska, P., & Wiznerowicz, M. (2015). The Cancer Genome Atlas (TCGA): an immeasurable source of knowledge. *Contemp Oncol (Pozn)*, 19(1a), A68-77. <https://doi.org/10.5114/wo.2014.47136>
- Tourancheau, A., Margaillan, G., Rouleau, M., Gilbert, I., Villeneuve, L., Lévesque, E., Droit, A., & Guillemette, C. (2016). Unravelling the transcriptomic landscape of the major phase II UDP-glucuronosyltransferase drug metabolizing pathway using targeted RNA sequencing. *The Pharmacogenomics Journal*, 16(1), 60-70. <https://doi.org/10.1038/tpj.2015.20>
- Tsoutsikos, P., Miners, J. O., Stapleton, A., Thomas, A., Sallustio, B. C., & Knights, K. M. (2004). Evidence that unsaturated fatty acids are potent inhibitors of renal UDP-glucuronosyltransferases (UGT): kinetic studies using human kidney cortical microsomes and recombinant UGT1A9 and UGT2B7. *Biochem Pharmacol*, 67(1), 191-199. <https://doi.org/10.1016/j.bcp.2003.08.025>
- Tukey, R. H., & Strassburg, C. P. (2000). Human UDP-Glucuronosyltransferases: Metabolism, Expression, and Disease. *Annual Review of Pharmacology and Toxicology*, 40(1), 581-616. <https://doi.org/10.1146/annurev.pharmtox.40.1.581>
- Turgeon, D., Chouinard, S., Bélanger, P., Picard, S., Labbé, J., Borgeat, P., & Bélanger, A. (2003). Glucuronidation of arachidonic and linoleic acid metabolites by human UDP-glucuronosyltransferases. *Journal of lipid research*, 44(6), 1182-1191. <http://www.jlr.org/content/44/6/1182.short>
- Turgeon, D., Hum, D. W., Lévesque, E. r., Carrier, J.-S. b., & Bélanger, A. (2001). Relative Enzymatic Activity, Protein Stability, and Tissue Distribution of Human Steroid-Metabolizing UGT2B Subfamily Members**This work was supported by the Medical Research Council of Canada, the Fonds de la Recherche en Santé du Québec, and Endorecherche. *Endocrinology*, 142(2), 778-787. <https://doi.org/10.1210/endo.142.2.7958>
- Vander Heiden, M. G., Cantley, L. C., & Thompson, C. B. (2009). Understanding the Warburg Effect: The Metabolic Requirements of Cell Proliferation. *Science*, 324(5930), 1029-1043. <https://doi.org/10.1126/science.1160809>
- Vogel, C., & Marcotte, E. M. (2012). Insights into the regulation of protein abundance from proteomic and transcriptomic analyses. *Nature Reviews Genetics*, 13(4), 227-232. <https://doi.org/10.1038/nrg3185>
- Walsh, C. A., Qin, L., Tien, J. C., Young, L. S., & Xu, J. (2012). The function of steroid receptor coactivator-1 in normal tissues and cancer. *Int J Biol Sci*, 8(4), 470-485. <https://doi.org/10.7150/ijbs.4125>

- Walther, T. C., & Farese, R. V. (2012). Lipid Droplets and Cellular Lipid Metabolism. *Annual Review of Biochemistry*, 81(1), 687-714. <https://doi.org/10.1146/annurev-biochem-061009-102430>
- Wang, J., Scholtens, D., Holko, M., Ivancic, D., Lee, O., Hu, H., Chatterton, R. T., Sullivan, M. E., Hansen, N., Bethke, K., Zalles, C. M., & Khan, S. A. (2013). Lipid Metabolism Genes in Contralateral Unaffected Breast and Estrogen Receptor Status of Breast Cancer. *Cancer Prevention Research*, 6(4), 3210-3330. <https://doi.org/10.1158/1940-6207.CAPR-12-0304>
- Wang, J., Shidfar, A., Ivancic, D., Ranjan, M., Liu, L., Choi, M.-R., Parimi, V., Gursel, D. B., Sullivan, M. E., Najor, M. S., Abukhdeir, A. M., Scholtens, D., & Khan, S. A. (2017). Overexpression of lipid metabolism genes and PBX1 in the contralateral breasts of women with estrogen receptor-negative breast cancer. *International Journal of Cancer*, 140(11), 2484-2497. <https://doi.org/10.1002/ijc.30680>
- Wang, L., Hsu, C. L., & Chang, C. (2005). Androgen receptor corepressors: an overview. *Prostate*, 63(2), 117-130. <https://doi.org/10.1002/pros.20170>
- Wang, Z., Wang, Y., Li, Z., Xue, W., Hu, S., & Kong, X. (2023). Lipid metabolism as a target for cancer drug resistance: progress and prospects. *Front Pharmacol*, 14, 1274335. <https://doi.org/10.3389/fphar.2023.1274335>
- Warnecke, D., Erdmann, R., Fahl, A., Hube, B., Müller, F., Zank, T., Zähringer, U., & Heinz, E. (1999). Cloning and functional expression of UGT genes encoding sterol glucosyltransferases from *Saccharomyces cerevisiae*, *Candida albicans*, *Pichia pastoris*, and *Dictyostelium discoideum*. *J Biol Chem*, 274(19), 13048-13059. <https://doi.org/10.1074/jbc.274.19.13048>
- Weber, L.-W., Boll, M., & Stampfl, A. (2004). Maintaining cholesterol homeostasis: sterol regulatory element-binding proteins. *World journal of gastroenterology*, 10(21), 3081-3087. <https://doi.org/10.3748/wjg.v10.i21.3081>
- Wijayakumara, D. D., Hu, D. G., Meech, R., McKinnon, R. A., & Mackenzie, P. I. (2015). Regulation of Human UGT2B15 and UGT2B17 by miR-376c in Prostate Cancer Cell Lines. *Journal of Pharmacology and Experimental Therapeutics*, 354(3), 417-425. <https://doi.org/10.1124/jpet.115.226118>
- Williams, J. A., Hyland, R., Jones, B. C., Smith, D. A., Hurst, S., Goosen, T. C., Peterkin, V., Koup, J. R., & Ball, S. E. (2004). Drug-drug interactions for UDP-glucuronosyltransferase substrates: a pharmacokinetic explanation for typically observed low exposure (AUC_i/AUC) ratios. *Drug Metab Dispos*, 32(11), 1201-1208. <https://doi.org/10.1124/dmd.104.000794>
- Wu, J., Sun, X., Wang, J., Cui, Y., Kato, F., Shirato, H., Ikeda, D. M., & Li, R. (2017). Identifying relations between imaging phenotypes and molecular subtypes of breast cancer: Model discovery and external validation. *J Magn Reson Imaging*, 46(4), 1017-1027. <https://doi.org/10.1002/jmri.25661>
- Xiaoping, Z., & Fajun, Y. (2012). Regulation of SREBP-Mediated Gene Expression. *Sheng Wu Wu Li Hsueh Bao*, 28(4), 287-294. <https://doi.org/10.3724/sp.J.1260.2012.20034>
- Xu, C., Li, C. Y., & Kong, A. N. (2005). Induction of phase I, II and III drug metabolism/transport by xenobiotics. *Arch Pharm Res*, 28(3), 249-268.
- Xu, S., Smothers, J. C., Rye, D., Endapally, S., Chen, H., Li, S., Liang, G., Kinnebrew, M., Rohatgi, R., Posner, B. A., & Radhakrishnan, A. (2024). A cholesterol-binding bacterial toxin provides a strategy for identifying a specific Scap inhibitor that blocks lipid synthesis in animal cells. *Proceedings of the National Academy of Sciences*, 121(7), e2318024121. <https://doi.org/doi:10.1073/pnas.2318024121>
- Yabe, D., Brown, M. S., & Goldstein, J. L. (2002). Insig-2, a second endoplasmic reticulum protein that binds SCAP and blocks export of sterol regulatory element-binding proteins. *Proceedings of the National Academy of Sciences of the USA*, 99(20), 12753-12758. <https://doi.org/10.1073/pnas.162488899>
- Yahagi, N., Shimano, H., Hasty, A. H., Matsuzaka, T., Ide, T., Yoshikawa, T., Amemiya-Kudo, M., Tomita, S., Okazaki, H., & Tamura, Y. (2002). Absence of sterol regulatory element-binding protein-1 (SREBP-1) ameliorates fatty livers but not obesity or insulin resistance in Lepob/Lepob mice. *Journal of Biological Chemistry*, 277(22), 19353-19357.

- Yam, C., Li, Z., Korkut, A., Ma, W., Kong, E., Hill, H. A., Abbas, H., Abouharb, S., Adrada, B., Arun, B. K., Barcenas, C. H., Bisen, A., Booser, D., Buzdar, A., Candelaria, R., Chen, J., Clayborn, A., Damodaran, S., Ding, Q.,...Tripathy, D. (2023). Abstract HER2-01: HER2-01 Clinical and Molecular Characteristics of HER2-low/zero Early Stage Triple-Negative Breast Cancer. *Cancer Research*, 83(5_Supplement), HER2-01-HER02-01. <https://doi.org/10.1158/1538-7445.Sabcs22-her2-01>
- Yamamoto, T., Shimano, H., Nakagawa, Y., Ide, T., Yahagi, N., Matsuzaka, T., Nakakuki, M., Takahashi, A., Suzuki, H., Sone, H., Toyoshima, H., Sato, R., & Yamada, N. (2004). SREBP-1 interacts with hepatocyte nuclear factor-4 alpha and interferes with PGC-1 recruitment to suppress hepatic gluconeogenic genes. *J Biol Chem*, 279(13), 12027-12035. <https://doi.org/10.1074/jbc.M310333200>
- Yan-qin, B., Hong-yan, C., Lu, L., Ming-yu, S., Dan, W., Zheng, W., Chao, W., Dong, X., & Jing-ru, S. (2022). Important roles of UGT2B28, FABP5, and CYP2C9 in the development of rat liver fibrosis induced by abnormal fatty acid metabolism. *Chinese Hepatology*, 27(9), 999-1003. http://www.hepatoday.org/EN/abstract/article_2941.shtml
- Yang, L., Zhang, F., Wang, X., Tsai, Y., Chuang, K. H., Keng, P. C., Lee, S. O., & Chen, Y. (2016). A FASN-TGF- β 1-FASN regulatory loop contributes to high EMT/metastatic potential of cisplatin-resistant non-small cell lung cancer. *Oncotarget*, 7(34), 55543-55554. <https://doi.org/10.18632/oncotarget.10837>
- Yang, T., Espenshade, P. J., Wright, M. E., Yabe, D., Gong, Y., Aebersold, R., Goldstein, J. L., & Brown, M. S. (2002). Crucial step in cholesterol homeostasis: sterols promote binding of SCAP to INSIG-1, a membrane protein that facilitates retention of SREBPs in ER. *Cell*, 110(4), 489-500. [https://doi.org/10.1016/s0092-8674\(02\)00872-3](https://doi.org/10.1016/s0092-8674(02)00872-3)
- Yang, T., Goldstein, J. L., & Brown, M. S. (2000). Overexpression of Membrane Domain of SCAP Prevents Sterols from Inhibiting SCAPSREBP Exit from Endoplasmic Reticulum *. *Journal of Biological Chemistry*, 275(38), 29881-29886. <https://doi.org/10.1074/jbc.M005439200>
- Ye, J. (2020). Transcription factors activated through RIP (regulated intramembrane proteolysis) and RAT (regulated alternative translocation). *Journal of Biological Chemistry*, 295(30), 10271-10280. <https://doi.org/https://doi.org/10.1074/jbc.REV120.012669>
- Ye, J., Coulouris, G., Zaretskaya, I., Cutcutache, I., Rozen, S., & Madden, T. L. (2012). Primer-BLAST: a tool to design target-specific primers for polymerase chain reaction. *BMC Bioinformatics*, 13, 134. <https://doi.org/10.1186/1471-2105-13-134>
- Yoshida, T., Kobayashi, T., Itoda, M., Muto, T., Miyaguchi, K., Mogushi, K., Shoji, S., Shimokawa, K., Iida, S., & Uetake, H. (2010). Clinical omics analysis of colorectal cancer incorporating copy number aberrations and gene expression data. *Cancer Informatics*, 9, 147-161.
- Yu, X., Zou, J., Ye, Z., Hammond, H., Chen, G., Tokunaga, A., Mali, P., Li, Y.-M., Civin, C., Gaiano, N., & Cheng, L. (2008). Notch signaling activation in human embryonic stem cells is required for embryonic, but not trophoblastic, lineage commitment. *Cell stem cell*, 2(5), 461-471. <https://doi.org/10.1016/j.stem.2008.03.001>
- Yuan, S., Chu, H., Chan, J. F.-W., Ye, Z.-W., Wen, L., Yan, B., Lai, P.-M., Tee, K.-M., Huang, J., Chen, D., Li, C., Zhao, X., Yang, D., Chiu, M. C., Yip, C., Poon, V. K.-M., Chan, C. C.-S., Sze, K.-H., Zhou, J.,...Yuen, K.-Y. (2019). SREBP-dependent lipidomic reprogramming as a broad-spectrum antiviral target. *Nature Communications*, 10(1), 120. <https://doi.org/10.1038/s41467-018-08015-x>
- Zaidi, N., Swinnen, J. V., & Smans, K. (2012). ATP-Citrate Lyase: A Key Player in Cancer Metabolism. *Cancer Research*, 72(15), 3709-3718. <https://doi.org/10.1158/0008-5472.CAN-11-4112>
- Zeković, M., Bumbaširević, U., Živković, M., & Pejčić, T. (2023). Alteration of Lipid Metabolism in Prostate Cancer: Multifaceted Oncologic Implications. *Int J Mol Sci*, 24(2). <https://doi.org/10.3390/ijms24021391>
- Zerenturk, E. J., Sharpe, L. J., & Brown, A. J. (2012). Sterols regulate 3 β -hydroxysterol Δ 24-reductase (DHCR24) via dual sterol regulatory elements: Cooperative induction of key enzymes in lipid synthesis by Sterol Regulatory Element Binding Proteins. *Biochimica et Biophysica Acta*

- (BBA) - *Molecular and Cell Biology of Lipids*, 1821(10), 1350-1360.
<https://doi.org/https://doi.org/10.1016/j.bbalip.2012.07.006>
- Zhang, Y., Motamed, M., Seemann, J., Brown, M. S., & Goldstein, J. L. (2013). Point mutation in luminal loop 7 of Scap protein blocks interaction with loop 1 and abolishes movement to Golgi. *J Biol Chem*, 288(20), 14059-14067. <https://doi.org/10.1074/jbc.M113.469528>
- Zheng, X. F., Huang, H. Y., & Wu, Q. (2019). Chromatin architectural protein CTCF regulates gene expression of the UGT1 cluster. *Yi Chuan*, 41(6), 509-523.
<https://doi.org/10.16288/j.ycz.19-072>
- Zhu, S., Jiang, L., Wang, L., Wang, L., Zhang, C., Ma, Y., & Huang, T. (2019). Identification of key genes and specific pathways potentially involved in androgen-independent, mitoxantrone-resistant prostate cancer. *Cancer Management and Research*, 11, 419-430.
<https://doi.org/10.2147/CMAR.S179467>